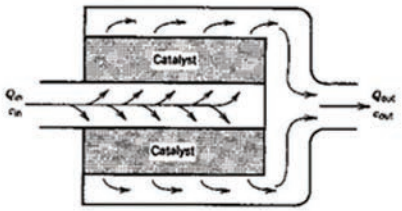

WILEY

CHEMICAL REACTOR DESIGN, OPTIMIZATION, AND SCALEUP

Second Edition

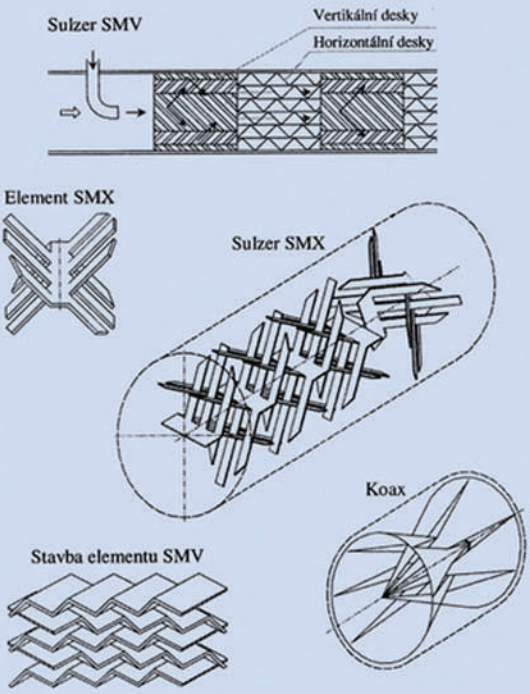

E. Bruce Nauman

Chemical Reactor Design, Optimization, and Scaleup

Second Edition

E. Bruce Nauman

Rensselaer Polytechnic Institute

A John Wiley & Sons, Inc., Publication

Chemical Reactor Design, Optimization, and Scaleup

Chemical Reactor Design, Optimization, and Scaleup

Second Edition

E. Bruce Nauman

Rensselaer Polytechnic Institute

A John Wiley & Sons, Inc., Publication

Copyright © 2008 by John Wiley & Sons, Inc. All rights reserved

Published by John Wiley & Sons, Inc., Hoboken, New Jersey
Published simultaneously in Canada

No part of this publication may be reproduced, stored in a retrieval system, or transmitted in any form or by any means, electronic, mechanical, photocopying, recording, scanning, or otherwise, except as permitted under Section 107 or 108 of the 1976 United States Copyright Act, without either the prior written permission of the Publisher, or authorization through payment of the appropriate per-copy fee to the Copyright Clearance Center, Inc., 222 Rosewood Drive, Danvers, MA 01923, (978) 750-8400, fax (978) 750-4470, or on the web at www.copyright.com. Requests to the Publisher for permission should be addressed to the Permissions Department, John Wiley & Sons, Inc., 111 River Street, Hoboken, NJ 07030, (201) 748-6011, fax (201) 748-6008, or online at http://www.wiley.com/go/permission.

Limit of Liability/Disclaimer of Warranty: While the publisher and author have used their best efforts in preparing this book, they make no representations or warranties with respect to the accuracy or completeness of the contents of this book and specifically disclaim any implied warranties of merchantability or fitness for a particular purpose. No warranty may be created or extended by sales representatives or written sales materials. The advice and strategies contained herein may not be suitable for your situation. You should consult with a professional where appropriate. Neither the publisher nor author shall be liable for any loss of profit or any other commercial damages, including but not limited to special, incidental, consequential, or other damages.

For general information on our other products and services or for technical support, please contact our Customer Care Department within the United States at (800) 762-2974, outside the United States at (317) 572-3993 or fax (317) 572-4002.

Wiley also publishes its books in a variety of electronic formats. Some content that appears in print may not be available in electronic formats. For more information about Wiley products, visit our web site at www.wiley.com.

Library of Congress Cataloging-in-Publication Data:

Library of Congress Cataloging-in-Publication Data
Nauman, E. B.
Chemical reactor design, optimization, and scaleup / E. Bruce Nauman. – 2nd ed.
p. cm.
Includes index.
ISBN 978-0-470-10525-2 (cloth)
1. Chemical reactors. I. Title.
TP157.N393 2008
660'.2832–dc22

2007051403

Printed in the United States of America

10 9 8 7 6 5 4 3 2 1

Contents

Preface to the Second Edition xiii
Symbols xv

1 Elementary Reactions in Ideal Reactors 1

1.1 Material Balances 1
1.1.1 Measures of Composition 4
1.1.2 Measures of Reaction Rate 5
1.2 Elementary Reactions 5
1.2.1 Kinetic Theory of Gases 6
1.2.2 Rate of Formation 6
1.2.3 First-Order Reactions 8
1.2.4 Second-Order Reactions with One Reactant 8
1.2.5 Second-Order Reactions with Two Reactants 9
1.2.6 Third-Order Reactions 9
1.3 Reaction Order and Mechanism 9
1.4 Ideal, Isothermal Reactors 12
1.4.1 Ideal Batch Reactors 12
1.4.2 Reactor Performance Measures 17
1.4.3 Piston Flow Reactors 19
1.4.4 Continuous Flow Stirred Tanks 24
1.5 Mixing Times and Scaleup 26
1.6 Dimensionless Variables and Numbers 31
1.7 Batch Versus Flow and Tank Versus Tube 33
Suggested Further Readings 36
Problems 37

2 Multiple Reactions in Batch Reactors 41

2.1 Multiple and Nonelementary Reactions 41
2.1.1 Reaction Mechanisms 42
2.1.2 Byproducts 43
2.2 Component Reaction Rates for Multiple Reactions 43
2.3 Multiple Reactions in Batch Reactors 44
2.4 Numerical Solutions to Sets of First-Order ODEs 46
2.5 Analytically Tractable Examples 52
2.5.1 The *n*th-Order Reaction 52
2.5.2 Consecutive First-Order Reactions, A→B→C→ ··· 53

2.5.3 Quasi-Steady Hypothesis 56
2.5.4 Autocatalytic Reactions 62
2.6 Variable-Volume Batch Reactors 65
2.6.1 Systems with Constant Mass 65
2.6.2 Fed-Batch Reactors 71
2.7 Scaleup of Batch Reactions 73
2.8 Stoichiometry and Reaction Coordinates 74
2.8.1 Matrix Formulation of Reaction Rates 74
2.8.2 Stoichiometry of Single Reactions 76
2.8.3 Stoichiometry of Multiple Reactions 77
Suggested Further Readings 78
Problems 79
Appendix 2.1 Numerical Solution of Ordinary Differential Equations 84

3 Isothermal Piston Flow Reactors 89

3.1 Piston Flow with Constant Mass Flow 90
3.1.1 Gas Phase Reactions 94
3.1.2 Liquid Phase Reactions 104
3.2 Scaleup Relationships for Tubular Reactors 107
3.2.1 Scaling Factors 107
3.2.2 Scaling Factors for Tubular Reactors 112
3.3 Scaleup Strategies for Tubular Reactors 113
3.3.1 Scaling in Parallel and Partial Parallel 113
3.3.2 Scaling in Series for Constant-Density Fluids 114
3.3.3 Scaling in Series for Gas Flows 116
3.3.4 Scaling with Geometric Similarity 117
3.3.5 Scaling with Constant Pressure Drop 119
3.4 Scaling Down 120
3.5 Transpired-Wall Reactors 122
Suggested Further Readings 124
Problems 124

4 Stirred Tanks and Reactor Combinations 129

4.1 Continuous Flow Stirred Tank Reactors 129
4.2 Method of False Transients 131
4.3 CSTRs with Variable Density 135
4.3.1 Liquid Phase CSTRs 136
4.3.2 Computational Scheme for Variable-Density CSTRs 137
4.3.3 Gas Phase CSTRs 138
4.4 Scaling Factors for Liquid Phase Stirred Tanks 143
4.5 Combinations of Reactors 145
4.5.1 Series and Parallel Connections 145
4.5.2 Tanks in Series 148

4.5.3 Recycle Loops 150
4.5.4 Maximum Production Rate 153
4.6 Imperfect Mixing 154
Suggested Further Readings 154
Problems 155
Appendix 4.1 Solution of Nonlinear Algebraic Equations 158

5 Thermal Effects and Energy Balances 163

5.1 Temperature Dependence of Reaction Rates 163
5.1.1 Arrhenius Temperature Dependence 163
5.1.2 Optimal Temperatures for Isothermal Reactors 166
5.2 Energy Balance 170
5.2.1 Nonisothermal Batch Reactors 172
5.2.2 Nonisothermal Piston Flow 175
5.2.3 Heat Balances for CSTRs 178
5.3 Scaleup of Nonisothermal Reactors 185
5.3.1 Avoiding Scaleup Problems 185
5.3.2 Heat Transfer to Jacketed Stirred Tanks 187
5.3.3 Scaling Up Stirred Tanks with Boiling 190
5.3.4 Scaling Up Tubular Reactors 191
Suggested Further Readings 194
Problems 195

6 Design and Optimization Studies 199

6.1 Consecutive Reaction Sequence 199
6.2 Competitive Reaction Sequence 216
Suggested Further Readings 218
Problems 218
Appendix 6.1 Numerical Optimization Techniques 220

7 Fitting Rate Data and Using Thermodynamics 225

7.1 Fitting Data to Models 225
7.1.1 Suggested Forms for Kinetic Models 226
7.1.2 Fitting CSTR Data 228
7.1.3 Fitting Batch and PFR Data 233
7.1.4 Design of Experiments and Model Discrimination 238
7.1.5 Material Balance Closure 239
7.1.6 Confounded Reactors 241
7.2 Thermodynamics of Chemical Reactions 244
7.2.1 Terms in the Energy Balance 244
7.2.2 Reaction Equilibria 252
Suggested Further Readings 269
Problems 269
Appendix 7.1 Linear Regression Analysis 274

8 Real Tubular Reactors in Laminar Flow **279**

8.1 Flow in Tubes with Negligible Diffusion 280
8.1.1 Criterion for Neglecting Radial Diffusion 281
8.1.2 Mixing-Cup Averages 282
8.1.3 Trapezoidal Rule 284
8.1.4 Preview of Residence Time Theory 287
8.2 Tube Flows with Diffusion 288
8.2.1 Convective Diffusion of Mass 288
8.2.2 Convective Diffusion of Heat 290
8.2.3 Use of Dimensionless Variables 290
8.2.4 Criterion for Neglecting Axial Diffusion 291
8.3 Method of Lines 292
8.3.1 Governing Equations for Cylindrical Coordinates 292
8.3.2 Solution by Euler's Method 294
8.3.3 Accuracy and Stability 295
8.3.4 Example Solutions 296
8.4 Effects of Variable Viscosity 301
8.4.1 Governing Equations for Axial Velocity 302
8.4.2 Calculation of Axial Velocities 303
8.4.3 Calculation of Radial Velocities 304
8.5 Comprehensive Models 307
8.6 Performance Optimization 307
8.6.1 Optimal Wall Temperatures 308
8.6.2 Static Mixers 308
8.6.3 Small Effective Diameters 310
8.7 Scaleup of Laminar Flow Reactors 311
8.7.1 Isothermal Laminar Flow 311
8.7.2 Nonisothermal Laminar Flow 312
Suggested Further Readings 312
Problems 313
Appendix 8.1 Convective Diffusion Equation 316
Appendix 8.2 External Resistance to Heat Transfer 317
Appendix 8.3 Finite-Difference Approximations 319

9 Packed Beds and Turbulent Tubes **323**

9.1 Packed-Bed Reactors 324
9.1.1 Incompressible Fluids 324
9.1.2 Compressible Fluids in Packed Beds 333
9.2 Turbulence 334
9.2.1 Turbulence Models 335
9.2.2 Computational Fluid Dynamics 336
9.3 Axial Dispersion Model 336
9.3.1 Danckwerts Boundary Conditions 339
9.3.2 First-Order Reactions 340

9.3.3 Utility of the Axial Dispersion Model 342
9.3.4 Nonisothermal Axial Dispersion 344
9.3.5 Shooting Solutions to Two-Point Boundary Value Problems 344
9.3.6 Axial Dispersion with Variable Density 352
9.4 Scaleup and Modeling Considerations 352
Suggested Further Readings 352
Problems 353

10 Heterogeneous Catalysis 355

10.1 Overview of Transport and Reaction Steps 357
10.2 Governing Equations for Transport and Reaction 358
10.3 Intrinsic Kinetics 360
10.3.1 Intrinsic Rate Expressions from Equality of Rates 361
10.3.2 Models Based on a Rate-Controlling Step 363
10.3.3 Recommended Models 367
10.4 Effectiveness Factors 368
10.4.1 Pore Diffusion 368
10.4.2 Film Mass Transfer 371
10.4.3 Nonisothermal Effectiveness 372
10.4.4 Deactivation 374
10.5 Experimental Determination of Intrinsic Kinetics 376
10.6 Unsteady Operation and Surface Inventories 380
Suggested Further Readings 381
Problems 382

11 Multiphase Reactors 385

11.1 Gas–Liquid and Liquid–Liquid Reactors 385
11.1.1 Two-Phase Stirred Tank Reactors 386
11.1.2 Measurement of Mass Transfer Coefficients 401
11.1.3 Fluid–Fluid Contacting in Piston Flow 404
11.1.4 Other Mixing Combinations 410
11.1.5 Prediction of Mass Transfer Coefficients 412
11.2 Three-Phase Reactors 415
11.3 Moving-Solids Reactors 417
11.3.1 Bubbling Fluidization 419
11.3.2 Fast Fluidization 420
11.3.3 Spouted Beds 420
11.3.4 Liquid-Fluidized Beds 421
11.4 Noncatalytic Fluid–Solid Reactions 421
11.5 Scaleup of Multiphase Reactors 427
11.5.1 Gas–Liquid Reactors 427
11.5.2 Gas-Moving Solids Reactors 429

Suggested Further Readings 429
Problems 430

12 Biochemical Reaction Engineering 433

12.1 Enzyme Catalysis 434
12.1.1 Michaelis–Menten Kinetics 434
12.1.2 Inhibition, Activation, and Deactivation 438
12.1.3 Immobilized Enzymes 439
12.1.4 Reactor Design for Enzyme Catalysis 440
12.2 Cell Culture 444
12.2.1 Growth Dynamics 446
12.2.2 Reactors for Freely Suspended Cells 450
12.2.3 Immobilized Cells 457
12.2.4 Tissue Culture 458
12.3 Combinatorial Chemistry 458
Suggested Further Readings 459
Problems 459

13 Polymer Reaction Engineering 461

13.1 Polymerization Reactions 461
13.1.1 Step Growth Polymerizations 462
13.1.2 Chain Growth Polymerizations 466
13.2 Molecular Weight Distributions 468
13.2.1 Distribution Functions and Moments 469
13.2.2 Addition Rules for Molecular Weight 470
13.2.3 Molecular Weight Measurements 470
13.3 Kinetics of Condensation Polymerizations 471
13.3.1 Conversion 471
13.3.2 Number- and Weight-Average Chain Lengths 472
13.3.3 Molecular Weight Distribution Functions 473
13.4 Kinetics of Addition Polymerizations 478
13.4.1 Living Polymers 479
13.4.2 Free-Radical Polymerizations 481
13.4.3 Transition Metal Catalysis 486
13.4.4 Vinyl Copolymerizations 486
13.5 Polymerization Reactors 490
13.5.1 Stirred Tanks with a Continuous Polymer Phase 492
13.5.2 Tubular Reactors with a Continuous Polymer Phase 495
13.5.3 Suspending-Phase Polymerizations 507
13.6 Scaleup Considerations 509
13.6.1 Binary Polycondensations 509
13.6.2 Self-Condensing Polycondensations 509
13.6.3 Living Addition Polymerizations 510
13.6.4 Vinyl Addition Polymerizations 510

Suggested Further Readings 511
Problems 511

14 Unsteady Reactors 513

14.1 Unsteady Stirred Tanks 513
14.1.1 Transients in Isothermal CSTRs 515
14.1.2 Nonisothermal Stirred Tank Reactors 523
14.2 Unsteady Piston Flow 526
14.3 Unsteady Convective Diffusion 529
Suggested Further Readings 530
Problems 530

15 Residence Time Distributions 535

15.1 Residence Time Theory 535
15.1.1 Inert Tracer Experiments 536
15.1.2 Means and Moments 539
15.2 Residence Time Models 540
15.2.1 Ideal Reactors and Reactor Combinations 540
15.2.2 Hydrodynamic Models 552
15.3 Reaction Yields 557
15.3.1 First-Order Reactions 557
15.3.2 Other Reactions 560
15.4 Extensions of Residence Time Theory 569
15.4.1 Unsteady Flow Systems 570
15.4.2 Contact Times 570
15.4.3 Thermal Times 571
15.5 Scaleup Considerations 571
Suggested Further Readings 572
Problems 572

16 Reactor Design at Meso-, Micro-, and Nanoscales 575

16.1 Mesoscale Reactors 577
16.1.1 Flow in Rectangular Geometries 578
16.1.2 False Transients Applied to PDEs 580
16.1.3 Jet Impingement Mixers 584
16.2 Microscale Reactors 584
16.2.1 Mixing Times 585
16.2.2 Radial or Cross-Channel Diffusion 586
16.2.3 False Transients Versus Method of Lines 587
16.2.4 Axial Diffusion in Microscale Ducts 587
16.2.5 Second-Order Reactions with Unmixed Feed 591
16.2.6 Microelectronics 594
16.2.7 Chemical Vapor Deposition 595

16.3 Nanoscale Reactors 596
16.3.1 Self-Assembly 597
16.3.2 Molecular Dynamics 598
16.4 Scaling, Up or Down 599
Suggested Further Readings 599
Problems 599

References 601
Index 603

Preface to the Second Edition

When I told a friend of mine who is not a chemical engineer that I was writing a new edition of my book, she said that I should include a murder mystery, as that would make the book more enjoyable. Now that was a challenge. How can a book called *Chemical Reactor Design, Optimization, and Scaleup*, second edition, include a murder mystery? Well, it doesn't, but it does have an evil assistant professor and a beautiful princess who is also an assistant professor. Their rather sophomoric adventures begin at Problem 1.13 and wander through Chapter 6.

This book can be considered a third edition since there was an earlier book, *Chemical Reactor Design*, John Wiley & Sons, 1987, that was followed by the first edition bearing the current title. The new title reflected an emphasis on optimization and particularly on scaleup, a topic rarely covered in detail in undergraduate or graduate education but of paramount importance to many practicing engineers. The treatment of biochemical and polymer reaction engineering is also more extensive than normal. There is a completely new chapter on meso-, micro-, and nanoreactors that includes such topics as axial diffusion in microreactors and self-assembly of nanostructures.

Practitioners are a major audience for the new book. Here, in one spot, you will find a reasonably comprehensive treatment of reactor design, optimization, and scaleup. Spend a few minutes becoming comfortable with the notation (anyone bothering to read a Preface obviously has the inclination), and you will find practical answers to many design problems.

The book is also used for undergraduate and graduate courses in chemical engineering. Some faults of the old book were eliminated. One fault was its level of difficulty. It was too hard for undergraduates at most U.S. universities. The new book is better. Known rough spots have been smoothed. However, the new book remains terse and somewhat more advanced in its level of treatment than is the current U.S. standard. Its goal is less to train students in the qualitative understanding of existing solutions than to prepare them for the solution of new problems. The reader should be prepared to work out the details of some examples rather than expect a complete solution.

There is a continuing emphasis on numerical solutions. Numerical solutions are needed for most practical problems in chemical reactor design, but sophisticated numerical techniques are rarely necessary given the speed of modern computers. Euler's method is routinely used to integrate sets of ordinary differential equations (ODEs). Random searches are used for optimization and least-squares analyses. These are appallingly inefficient but marvelously robust and easy to implement. The method of lines is used for solving the partial differential equations (PDEs) that govern real tubular reactors and packed beds. This technique is adequate for most problems in

reactor design, but the method of false transients is now introduced as well. The goal is to make the techniques understandable and easily accessible and to allow continued focus on the chemistry and physics of the problem. Computational elegance and efficiency are gladly sacrificed for simplicity.

Too many engineers are completely in the dark when faced with variable physical properties and tend to assume them away without full knowledge of whether the effects are important. They are often unimportant, but a real design problem, as opposed to an undergraduate exercise or preliminary process synthesis, deserves careful assembly of data and a rigorous solution. Thus the book gives simple but general techniques for dealing with varying physical properties in reactors of all types.

No CD ROM is supplied with the book. Many of the numerical problems can be solved with canned ODE and PDE solvers, but most of the solutions are quite simple to code. Creative engineers must occasionally write their own code to solve engineering problems. Due to their varied nature, the solutions require use of a general-purpose language rather than a specific program. Computational examples in the book are illustrated using Basic. This choice was made because Basic is indeed basic enough that it can be sight-read by anyone already familiar with another general-purpose language and because the ubiquitous spreadsheet, Excel, uses Basic macros. Excel provides input/output, plotting, and formatting routines as part of its structure so that coding efforts can be concentrated on the actual calculations. This makes it particularly well suited for students who have not yet become comfortable with another language. Those who prefer another language such as C or Fortran or a mathematical programming system such as Mathematica, Maple, Mathcad, or Matlab should be able to translate quite easily

I continue with a few eccentricities in notation, using *a, b, c, . . .* to denote molar concentrations of components A, B, C, ... Equations are numbered when the results are referenced or important enough to deserve some emphasis. The problems at the back of each chapter are generally arranged to follow the flow of the text rather than level of difficulty. I have tried to avoid acronyms and other abbreviations unless the usage is very common and there is a true economy of syllables. The abbreviations that did slip through include CSTR, PFR, ODE, PDE, MWD, PD, RTD, and CPU.

Troy, New York **E. Bruce Nauman**
May, 2008

Symbols

BASIC LANGUAGE CODES

Program segments and occasional variables within the text are set in a fixed-width font to indicate that they represent computer code.

SI UNITS

Some reaction rates and concentrations for biochemical reactions and polymerizations are normally in mass units rather than molar units.

Symbol	Definition	SI Units	Where Used*
A	Component A	—	1.9
A	A-type end group in condensation polymerization	—	Section 13.1
A	Amount of injected tracer	kg	Example 15.1
[A]	Concentration of component A	mol m^{-3}	1.8
A, B, C	Various constants	Varies	Various
A_b	Cross-sectional area associated with bubble phase	m^2	11.46
A_c	Cross-sectional area of tubular reactor	m^2	Table 1.1
A_e	Cross-sectional area of emulsion phase	m^2	11.45
A_{ext}	External surface area	m^2	5.13
A'_{ext}	External surface per unit length of reactor	m	5.22
A_g	Cross-sectional area of gas phase	m^2	11.28
A_i	Interfacial area per unit volume of reactor	m^{-1}	11.2
A'_i	Interfacial area per unit height of reactor	m	11.27
A_{inlet}	Cross-sectional area at reactor inlet	m^2	Problem 3.6
A_l	Cross-sectional area of liquid phase	m^2	11.27

* Refers to equation number, except as noted.

A_s	Cross-sectional area of solid phase in trickle bed	m^2	11.44
A_s	External surface area of catalyst per unit volume of gas phase	m^{-1}	10.2
[AS]	Surface concentration of A in adsorbed state	mol m^{-2}	10.5
Av	Avogadro's number	Dimensionless	1.11
a	Concentration of component A	mol m^{-3}	1.6
a	Vector of component concentrations $(N \times 1)$	mol m^{-3}	2.44
$a(0-)$	Concentration just before inlet to closed system	mol m^{-3}	Example 9.2
$a(0+)$	Concentration just after inlet to closed system	mol m^{-3}	Example 9.2
$a(L-)$	Concentration just before outlet of closed system	mol m^{-3}	Example 9.2
$a(L+)$	Concentration just after outlet of closed system	mol m^{-3}	Example 9.2
$a(t, z)$	Concentration in unsteady tubular reactor	mol m^{-3}	14.14
a'	Auxiliary variable, da/dz, used to convert second-order ODEs to set of first-order ODEs	mol m^{-3}	Example 9.5
a^*	Dimensionless concentration	Dimensionless	1.64
a_l^*	Liquid phase concentration at gas–liquid interface	mol m^{-3}	11.1
a_0	Initial concentration of component A	mol m^{-3}	1.24
a_b	Concentration of component A in bubble phase	mol m^{-3}	11.46
$a_{\text{batch}}(t)$	Concentration in batch reactor at time t	mol m^{-3}	8.16
a_c	Catalyst surface area per mass of catalyst	m^2 kg^{-1}	10.38
a_e	Gas phase concentration in emulsion phase	mol m^{-3}	11.45
a_{equil}	Concentration of component A at equilibrium	mol m^{-3}	Problem 1.15
a_{full}	Concentration when reactor becomes full during startup	mol m^{-3}	Example 14.3
a_g	Concentration of component A in gas phase	mol m^{-3}	11.2
a_g^*	Gas phase concentration at gas–liquid interface	mol m^{-3}	11.1
a_{in}	Inlet concentration of component A	mol m^{-3}	1.6

a_j	Concentration on jth tray of tray reactor	mol m^{-3}	Example 11.7
a_l	Concentration of component A in liquid phase	mol m^{-3}	11.2
$a_l(l)$	Concentration at position $l$within pore	mol m^{-3}	10.3
a_{mix}	Mixing-cup average concentration	mol m^{-3}	4.19, 8.5
a_{out}	Outlet concentration of component A	mol m^{-3}	1.6 Example 11.13
a_s	Concentration at surface of solid, e.g., solid catalyst	mol m^{-3}	10.2
a_{trans}	Concentration of transpired component	mol m^{-3}	3.48
$a(t, z)$	Concentration in unsteady PFR	mol m^{-3}	14.4
B	Component B	—	
B	B-type end group in condensation polymerization	—	Section 13.1
[B]	Concentration of component B	mol m^{-3}	1.9
[BS]	Surface concentration of B in adsorbed state	mol m^{-2}	10.5
b	Concentration of component B	mol m^{-3}	1.9
b_0	Initial concentration of component B	mol m^{-3}	1.32
b_l	Liquid phase concentration of component B	mol m^{-3}	Example 11.6
C	Component C	—	1.20
C	Constant in various equations	Varies	
C	Scaling exponent for equipment cost	Dimensionless	Problem 4.19
C	Concentration of inert tracer	mol m^{-3}	15.1
$C(t, z)$	Concentration of inert tracer in unsteady tubular reactor	mol m^{-3}	Example 15.4
C_0	Initial value for tracer concentration	mol m^{-3}	15.1
C_A	Capacity of ion exchange resin for component A	mol m^{-3}	11.49
C_{AB}	Collision rate between A and B molecules	m^{-3} s^{-1}	1.11
C_h	Constant in heat transfer correlation	Dimensionless	5.33
C_I	Specific heat of impeller	J kg^{-1}K^{-1}	Example 14.9
$C_{\text{out}}(t)$	Outlet concentration of inert tracer	mol m^{-3}	15.1
C_P	Heat capacity in mass units	J kg^{-1}K^{-1}	5.15
C_P	Heat capacity in molar units throughout Section 7.2	J mol^{-1}K^{-1}	7.43
CSTR	Continuous flow stirred tank reactor	Dimensionless	Section 1.4
c	Concentration of component C	mol m^{-3}	1.20

c_j	Gas concentration above jth tray in tray column	mol m^{-3}	Example 11.7
c_J	Gas concentration above last tray in tray column	mol m^{-3}	Example 11.8
c_l	Concentration of polymer chains having length l	chains m^{-3}	13.7
c_{polymer}	Summed concentration of all polymer chains	chains m^{-3}	13.7
D	Component D	—	
D	Axial dispersion coefficient	m^2 s^{-1}	11.9
D_A	Effective diffusivity in membrane	m^2 s^{-1}	9.18
$\mathscr{D}_A$	Diffusion coefficient for component A	m^2 s^{-1}	8.3
D_e	Axial dispersion coefficient in emulsion phase	m^2 s^{-1}	11.45
$\mathscr{D}_{\text{eff}}$	Effective diffusivity	m^2 s^{-1}	10.27
D_g	Axial dispersion coefficient for gas phase	m^2 s^{-1}	11.34
D_I	Impeller diameter	m	1.60
D_{in}	Axial dispersion coefficient in entrance region of open reactor	m^2 s^{-1}	Figure 9.2
$\mathscr{D}_K$	Knudsen diffusivity	m^2 s^{-1}	10.26
D_l	Axial dispersion coefficient for liquid phase	m^2 s^{-1}	11.33
D_{out}	Axial dispersion coefficient in exit region of open reactor	m^2 s^{-1}	Figure 9.2
$\mathscr{D}_P$	Diffusion coefficient of product P	m^2 s^{-1}	10.7
D_r	Radial dispersion coefficient in PDE models	m^2 s^{-1}	9.1, 16.11
D_z	Axial dispersion coefficient in PDE model	m^2 s^{-1}	16.11
d	Concentration of component D	mol m^{-3}	2.1
d_j	Liquid concentration on jth tray of tray column	mol m^{-3}	Example 11.7
d_p	Diameter of particle	m	3.21
d_{pore}	Diameter of pore	m	Section 10.4.1
d_t	Tube diameter	m	Sections 3.2, 9.6
d_{tank}	Tank diameter	m	Example 1.7
dw	Incremental mass of polymer being formed	kg	13.48
E	Component E	—	2.1
E	Axial dispersion coefficient for heat	m^2 s^{-1}	9.28
$\mathscr{E}$	Enhancement factor	Dimensionless	11.41

E_0	Concentration of active sites	sites m^{-2}	12.1
E_r	Radial dispersion coefficient for heat in packed bed	$m^2\ s^{-1}$	9.13
e	Concentration of component E	mol m^{-3}	Example 2.2
e	Epoxy concentration	mol m^{-3}	Example 14.9
F	Arbitrary function	Varies	Appendix 4.1
F	Constant value for F_j	$m^3\ s^{-1}$	Example 11.8
$F(t)$	Cumulative distribution of residence times	Dimensionless	15.4
$F(r)$	Cumulative distribution function expressed in terms of tube radius for monotonic velocity profile	Dimensionless	15.29
Fa	Fanning friction factor	Dimensionless	3.16
F_j	Volumetric flow of gas from jth tray	$m^3\ s^{-1}$	Example 11.7
f	Arbitrary function	Varies	Appendix 6.1
f	Initiator efficiency factor	Dimensionless	13.39
$f\ (l)$	Number fraction of polymer chains having length l	Dimensionless	13.8
$f(t)$	Differential distribution function for residence times	s^{-1}	15.6
$f(t)$	Differential distribution function for exposure times	s^{-1}	Section 11.1.5
f_-	Value of function at backward point	Varies	Appendix 8.3
f_+	Value of function at forward point	Varies	Appendix 8.3
f_0	Value of function at central point	Varies	Appendix 8.3
f_A°	Fugacity of pure component A	Pa	7.29
$\hat{f}_A$	Fugacity of component A in mixture	Pa	7.29
$f_c(t_c)$	Differential distribution of contact times	s^{-1}	15.52
$f_{\text{dead}}(l)$	Number fraction of terminated polymer chains having length l	Dimensionless	Section 13.4.2
$f_T(t_T)$	Differential distribution function for thermal times	s^{-1}	15.54
f_{in}, f_{out}	Material balance adjustment factors	Dimensionless	7.15
f_R	Collision efficiency factor	Dimensionless	1.10
G	Arbitrary function	Varies	Appendix 4.1
G_1	Integrals used in variable-viscosity calculations	$m^3\ kg\ s^{-1}$	8.45
G_2	Integrals used in variable-viscosity calculations	$m^5\ kg\ s^{-1}$	8.45
G_1, G_2	Growth limitation factors for substrates 1 and 2	Dimensionless	12.10

G_P	Growth limitation factor for product	Dimensionless	12.13
G_S	Growth limitation factor for substrate	Dimensionless	12.13
Gz	Graetz number	Dimensionless	5.36
g	Grass supply	kg m^{-2}	Section 2.5.4
g	Acceleration due to gravity	m s^{-2}	Section 4.4
$g(l)$	Weight fraction of polymer chains having length l	Dimensionless	13.11
$g(t)$	Impulse response function for open system	s^{-1}	15.41
$g(t)_{\text{rescaled}}$	Impulse response function for open system after rescaling so that mean is $\bar{t}$	s^{-1}	15.41
H	Enthalpy in mass units	J kg^{-1}	5.1
H	Enthalpy in molar units throughout Section 7.2	J mol^{-1}	7.42
H	Half-height of rectangular duct	m	16.1
H_A, H_B, H_I	Component enthaplies	J mol^{-1}	7.20
h	Heat transfer coefficient on jacket side	J m^{-2} s^{-1} K^{-1}	5.34
h	Hydrogen ion concentration	mol m^{-3}	Example 14.9
h_i	Interfacial heat transfer coefficient	J m^{-2} s^{-1} K^{-1}	11.19
h_r	Coefficient for heat transfer to wall of packed bed	J m^{-2} s^{-1} K^{-1}	9.4
I	Inert component I	—	3.13
I	System inventory	kg	1.2
I	Number of radial increments	Dimensionless	8.12
I–IV	Reactions I–IV	—	Section 2.2
I_0	Initiator concentration at $t = 0$	mol m^{-3}	13.31
[IX$_n$]	Concentration of growing polymer chains of length n that end with X group	chains m^{-3}	Section 13.4.4
[IY$_n$]	Concentration of growing polymer chains of length n that end with Y group	chains m^{-3}	Section 13.4.4
i	Concentration of inerts	mol m^{-3}	3.12
i	Index variable in radial direction	Dimensionless	8.12
i	Concentration of adsorbable inerts in gas phase	mol m^{-3}	10.14
J	Number of experimental data	Dimensionless	5.2
J	Number of axial increments	Dimensionless	Example 8.3
J	Number of trays	Dimensionless	Example 11.8

j	Index variable for axial direction	Dimensionless	Section 8.3.2
j	Index variable for data	Dimensionless	5.2
K_0, K_1, K_2, K_3	Factors for thermodynamic equilibrium constant	Dimensionless	7.35
K_1	Equilibrium constant	mol	Example 14.9
K_2	Various constants	Varies	12.3
K_a	Kinetic equilibrium constant for adsorption	$\text{mol}^{-1}\ \text{m}^3$	Example 10.4
K_d	Kinetic equilibrium constant for desorption	$\text{mol}\ \text{m}^{-3}$	Example 10.3
K_g	Mass transfer coefficient based on overall gas phase driving force	$\text{m}\ \text{s}^{-1}$	11.2
K_H	Henry's law constant	Varies	11.1
K_H^i	Liguid–gas equilibrium constant at interface	$\text{m}\ \text{s}^{-1}$	11.4
K_{kinetic}	Kinetic equilibrium constant	Varies	7.28
K_l	Mass transfer coefficient based on overall liquid phase driving force	$\text{m}\ \text{s}^{-1}$	11.3
K_m	Mass transfer coefficient between emulsion and bubble phases in gas-fluidized bed	$\text{m}\ \text{s}^{-1}$	11.45
K_M	Michaelis constant	$\text{mol}\ \text{m}^{-3}$	12.2
K_R	Kinetic equilibrium constant for surface reaction	Dimensionless	Example 10.3
K_{thermo}	Thermodynamic equilibrium constant	Dimensionless	7.29
k	Reaction rate constant	Varies	1.8
k'	Pseudo-first-order rate constant	s^{-1}	Section 1.3
k''	Linear burn rate	$\text{m}\ \text{s}^{-1}$	11.51
k^*	Rate constant	Dimensionless	1.64
k_0	Preexponential rate constant	Varies	5.1
k_a	Adsorption rate constant	$\text{site}^{-1}\ \text{s}^{-1}$	10.4
k_a^+	Forward rate constant for reversible adsorption step	$\text{site}^{-1}\ \text{s}^{-1}$	Example 10.2
k_a^-	Reverse rate constant for reversible adsorption step	$\text{mol}\ \text{m}^{-1}\text{site}^{-1}\ \text{s}^{-1}$	Example 10.2
k_A, k_B, ...	Denominator rate constant for component A	$\text{mol}^{-1}\text{m}^3$	7.5, 10.20
k_A, k_B, k_C	Rate constants for consecutive reactions	s^{-1}	2.20
k_{AB}	Second-order denominator constant	$\text{mol}^{-2}\ \text{m}^6$	12.5
k_c	Rate constant for termination by combination	$\text{mol}^{-1}\text{m}^3\ \text{s}^{-1}$	13.39
k_d	Rate constant for cell death	s^{-1}	12.17

k_d	Rate constant for termination by disproportionation	$\text{mol}^{-1}\text{m}^3\ \text{s}^{-1}$	13.39
k_d	Desorption rate constant	$\text{mol m}^{-1}\text{site}^{-1}\ \text{s}^{-1}$	10.6
k_d^+	Forward rate constant for reversible desorption step	$\text{mol m}^{-1}\text{site}^{-1}\ \text{s}^{-1}$	Example 10.2
k_d^-	Reverse rate constant for reversible desorption step	$\text{m}^2\ \text{site}^{-1}\ \text{s}^{-1}$	Example 10.2
k_D	Rate constant for catalyst deactivation	s^{-1}	10.35
k_f	Rate constant for forward reaction	Varies	1.15
k_g	Mass transfer coefficient based on gas phase driving force	m s^{-1}	11.6
k_i	Rate constant for chemical initiation	s^{-1}	13.39
k_I	Denominator rate constant for inerts I	$\text{mol}^{-1}\text{m}^3$	10.14
k_I, k_II	Rate constants for reactions I and II	$\text{mol}^{-1}\ \text{m}^3\ \text{s}^{-1}$	2.1
k_l	Mass transfer coefficient based on liquid phase driving force	m s^{-1}	11.5
k_p	Propagation rate constant	$\text{mol}^{-1}\text{m}^3\ \text{s}^{-1}$	13.31
k_r	Rate constant for reverse reaction		1.15
k_R	Rate constant for surface reaction	$\text{site}^{-1}\text{m}^2\ \text{s}^{-1}$	10.5
k_R^+	Forward rate constant for reversible surface reaction	s^{-1}	Example 10.2
k_R^-	Reverse rate constant for reversible surface reaction	s^{-1}	Example 10.2
k_s	Mass transfer coefficient	m s^{-1}	10.2
k_S	Rate constant for catalyst deactivation	$\text{site}^{-1}\text{m}^2\ \text{s}^{-1}$	Section 10.4.4
k_{SI}	Denominator constant for noncompetitive inhibition	$\text{mol}^{-2}\ \text{m}^6$	12.6
k_{XX}	Rate constant for monomer X reacting with polymer chain ending with X unit	$\text{mol}^{-1}\text{m}^3\ \text{s}^{-1}$	Section 13.4.4
k_{XY}	Rate constant for monomer Y reacting with polymer chain ending with X unit	$\text{mol}^{-1}\text{m}^3\ \text{s}^{-1}$	Section 13.4.4
k_{YX}	Rate constant for monomer X reacting with polymer chain ending with Y unit	$\text{mol}^{-1}\text{m}^3\ \text{s}^{-1}$	Section 13.4.4
k_{YY}	Rate constant for monomer Y reacting with polymer chain ending with Y unit	$\text{mol}^{-1}\text{m}^3\ \text{s}^{-1}$	Section 13.4.4

L	Length of tubular reactor	m	1.37
$\mathscr{L}$	Length of pore	m	Section 10.4.1
$L-$	Location just before reactor outlet	m	Example 9.3
$L+$	Location just after reactor outlet	m	Example 9.3
l	Lynx population	lynx m^{-2}	Section 2.5.4
l	Position within pore	m	10.3
l	Chain length of polymer	Dimensionless	13.1
l, m, p, q	Chain lengths for termination by combination	Dimensionless	Section 13.4.2
$\bar{l}_N$	Number-average chain length	Dimensionless	13.10
$\bar{l}_W$	Weight-average chain length	Dimensionless	13.12
M	Monomer	Dimensionless	13.1
M	Any molecule that serves as energy source	Dimensionless	Problem 7.7
M	Middle group in condensation polymerization	Dimensionless	Section 13.1
M	Number of simultaneous reactions	Dimensionless	2.9
M	Monomer concentration	mol m^{-3}	13.32
M_0	Monomer charged to system prior to initiation		13.31
M_A	Molecular weight of diffusing species	g mol^{-1}	10.26
M_0	Maintenance coefficient for oxygen		Table 12.1
M_S	Maintenance coefficient, mass of substrate per dry cell mass per time	s^{-1}	12.15
Mw	molecular weight	g mol^{-1}	Example 2.9
min	Function to select minimum		12.11
m	Reaction order exponent	Dimensionless	1.21
m	Exponent in Arrhenius equation	Dimensionless	5.1
m	Exponent on product limitation factor	Dimensionless	12.13
m	Chain length of polymer	Dimensionless	13.2
m, n, r, s	Parameters to be determined in regression analysis	Varies	7.48
m_A	Mass of A molecule	Da	1.11
m_I	Mass of impeller	kg	Example 14.9
$\mathbf{N}$	Vector of component moles ($N \times 1$)	mol	2.47

N	Middle group in condensation polymerization	Dimensionless	Section 13.1
N	Number of chemical components	Dimensionless	Section 2.3
N	Number of tanks in series	Dimensionless	4.16b
N_0	Moles initially present	mol	Example 7.15
N_A	Moles of component A	mol	2.45
$\dot{N}_A$	Molar flow rate of component A	mol s^{-1}	3.3
N_I	Rotational velocity of impeller	rev s^{-1}	1.59
N_{tubes}	Number of tubes in scaleup	Dimensionless	Section 3.3
Nu	Nusselt number	Dimensionless	5.33
N_{zones}	Number of zones used for temperature optimization	Dimensionless	Example 6.5
n	Reaction order exponent	Dimensionless	1.21
n	Index variable for number of tanks	Dimensionless	4.16b
n	Zone number	dimensionless	Example 6.5
n	Index for moments of distribution	Dimensionless	13.9, 15.11
O	Operator indicating order of magnitude	Dimensionless	Example 2.4
ODE	Ordinary differential equation	Dimensionless	
P	Product or polymer	Dimensionless	
P	Pressure	Pa	3.12
$P\bullet$	Concentration of growing chains summed over all lengths	chains	13.39
P_0	Standard pressure	Pa	7.30
PDE	Partial differential equation	Dimensionless	Section 8.2
Pe	Peclet number for PDE model, $\bar{u}_s d_p / D_r$	Dimensionless	Section 9.1.1
Pe	Peclet number for axial dispersion model, $\bar{u} L / D$	Dimensionless	9.19
PFR	Piston flow reactor	Dimensionless	Section 1.4
P_g	Agitator power while gas is being sparged	kw	Example 11.18
P_l	Polymer of chain length l	Dimensionless	13.1
Po	Power number	Dimensionless	1.60
Power	Agitator power	kw	1.60
Pr	Prandlt number	Dimensionless	Section 5.3.7
P_R	Probability that molecule will react	Dimensionless	Section 15.3.1
[PS]	Concentration of P in adsorbed state	mol m^{-2}	10.6
p	Concentration of product P	mol m^{-3}	
p	Parameter in analytical solution	Dimensionless	9.23
p_1, p_2	Optimization parameters	Varies	Appendix 6.1
p_l	Concentration of product P at location l within pore	mol m^{-3}	10.7

p_{max}	Growth-limiting value for product concentration	mol m^{-3}	12.13
p_{old}	Old or current value for optimization parameter	Varies	6.7
p_s	Concentration of product P at external surface of catalyst	mol m^{-3}	10.8
p_{trial}	Trial value for optimization parameter	Varies	6.7
Q	Component Q	Dimensionless	
Q	Volumetric flow rate	$m^3\ s^{-1}$	1.3
Q_0	Volumetric flow at initial steady state	$m^3\ s^{-1}$	14.9
Q_{full}	Volumetric flow rate at steady state	$m^3\ s^{-1}$	Example 14.4
Q_g	Gas volumetric flow rate	$m^3\ s^{-1}$	11.12
Q_{in}	Input volumetric flow rate	$m^3\ s^{-1}$	1.3
Q_l	Liquid volumetric flow rate	$m^3\ s^{-1}$	11.11
Q_l	Gas volumetric flow rate	$m^3\ s^{-1}$	11.11
Q_{mass}	Mass flow rate	$m^3\ s^{-1}$	1.2
Q_{out}	Discharge volumetric flow rate	$m^3\ s^{-1}$	1.6
q	Transpiration volumetric flow per unit length		3.48
q	Recycle rate	$m^3\ s^{-1}$	Section 4.5.3
q	Volumetric flow rate into side tank of side capacity model	$m^3\ s^{-1}$	Example 15.7
$q_{generated}$	Rate of heat generation		5.31
$q_{removed}$	Rate of heat removal		5.32
R	Component R	Dimensionless	
R	Radius of tubular reactor	m	8.55, Exp. 3.1
R	Ratio of monomer to polymer density	Dimensionless	4.7
$\mathscr{R}$	Vector of reaction rates (M × 1)	mol $m^{-3}\ s^{-1}$	2.42
$\bar{R}$	Average radius of surviving particles	m	11.55
$\mathscr{R}'$	Multicomponent, vector form of $\mathscr{R}'_A$	mol $m^{-3}\ s^{-1}$	3.9
R_0	Initial particle radius	m	11.52
$\mathscr{R}_A$	Rate of formation of component A	mol $m^{-3}\ s^{-1}$	1.6
$(\mathscr{R}_A)_g$	Rate of formation of component A in gas phase	mol $m^{-3}\ s^{-1}$	11.12
$(\mathscr{R}_A)_l$	Rate of formation of component A in liquid phase	mol $m^{-3}\ s^{-1}$	11.11
$\mathscr{R}_{data}$	Experimental values for reaction rate from CSTR data	mol $m^{-3}\ s^{-1}$	Section 7.1.1
Re	Reynolds number	Dimensionless	3.16
$(\mathbf{Re})_{impeller}$	Reynolds number based on impeller diameter	Dimensionless	4.11
$(\mathbf{Re})_p$	Reynolds number based on particle diameter	Dimensionless	3.21

R_g	Gas constant	J mol^{-1} K^{-1}	1.11
R_h	Radius of central hole in cylindrical catalyst particle	m	Problem 10.14
$\mathscr{R}_I$	Rate of reaction I, $I = 1, \ldots, M$	mol m^{-3} s^{-1}	2.8
$\mathscr{R}_{\max}$	Maximum growth rate	kg m^{-3} s^{-1}	12.2
$\mathscr{R}_{\text{model}}$	Reaction rate as predicted by model	mol m^{-3} s^{-1}	Section 7.1.1
RND	Random number	Dimensionless	6.7
R_p	Radius of a catalyst particle	mol m^{-3} s^{-1}	Problem 10.14
$\mathscr{R}_P$	Rate of formation of product P	mol m^{-3} s^{-1}	10.7
$\mathscr{R}_r$	Rate of reverse reaction	mol m^{-3} s^{-1}	Example 7.13
$\mathscr{R}_S$	Reaction rate for solid	mol m^{-3} s^{-1}	Example 11.16
$\mathscr{R}_S$	Reaction rate for substrate	kg m^{-3} s^{-1}	12.15
$\mathscr{R}_X$	Rate of formation of dry cell mass	kg m^{-3} s^{-1}	12.8
r	Radial coordinate	m	8.1
r	Rabbit population	rabbits m^{-2}	Section 2.5.4
$\varkappa$	Radius, r/R	Dimensionless	Table 8.1
r_1	Dummy variable of integration	m	8.41, 13.5
r_A	Radius of A molecule	m	1.11
r_B	Radius of B molecule	m	1.11
r_p	Radial coordinate for catalyst particle	m	10.32
r_X	Copolymer reactivity ratio	Dimensionless	13.41
r_Y	Copolymer reactivity ratio	Dimensionless	13.41
S	Component S	Dimensionless	1.13
S	Substrate in biological system	Dimensionless	Section 12.1.1
[S]	Concentration of vacant sites	sites m^{-2}	10.4
S	Scaling factor for scaleup with constant $\bar{t}$	Dimensionless	1.58
S	Concentration of tracer in side tank of side capacity model	mol m^{-3}	Example 15.7
S_0	Total concentration of sites, both occupied and vacant	sites m^{-2}	Example 10.1
S_1, S_2	Roots of quadratic equation		2.24
S_A	Root mean residual error for component A	Varies	7.10
S_{AB}	Stoichiometric ratio a_0/b_0 or of A end groups to B end groups at onset of reaction	Dimensionless	1.65, 13.3
Sc	Schmidt number, $\mu/(\rho\mathscr{D}_A)$	Dimensionless	Section 9.1.1
$S_{\text{inventory}}$	Scaling factor for inventory	Dimensionless	1.56
S_L	Scaleup factor for tube length	Dimensionless	Section 3.2.1
S_R	Scaleup factor for tube radius	Dimensionless	Section 3.2.1
SS^2	Sum-of-squares errors	Varies	5.2
SS_A^2, SS_B^2, SS_C^2	Sum of squares for individual components	Varies	7.14

SS^2_{residual}	Sum of squares after data fit	Varies	7.10
$S_{\text{throughput}}$	Scaling factor for throughput	Dimensionless	1.55
S_{volume}	Scaling factor for volume	Dimensionless	1.57
S_X	Scaling factor for property X	Dimensionless	Section 3.2.1
s	Root mean residual error	Varies	7.10
s	Substrate concentration	kg m^{-3} s^{-1}	12.1
s	Sulfate concentration	mol m^{-3}	Example 14.9
s	Laplace transform parameter	s^{-1}	Example 15.2
s_0	Initial substrate concentration		Example 12.5
$\mathscr{T}$	Dimensionless temperature	Dimensionless	Table 8.1
T_{burn}	Time required to burn particle	s	Section 11.17
T_{ext}	External temperature	K	5.13
T_g	Temperature in gas phase	K	Section 11.1.1
T_l	Temperature in liquid phase	K	Section 11.1.1
T_n	Temperature in nth zone	K	Example 6.5
T_{ref}	Reference temperature for enthalpy calculations	K	5.14
T_s	Temperature at external surface of catalyst particle	K	Section 10.4.3
T_{set}	Temperature set point	K	Example 14.8
t	Time	s	1.2
t	Residence time associated with streamline, $L/V_z(r)$	s	Section 8.1.4
$\bar{t}$	Mean residence time	s	1.40
t_1	Dummy variable of integration	s	11.49
t_0	Time at end of induction phase	s	12.9
$t_{1/2}$	Reaction half-life	s	1.28
t_b	Residence time for segregated group of molecules	s	Section 15.3.2
t_c	Contact time in heterogeneous reactor	s	15.52
t_{empty}	Time when reactor becomes empty	s	14.10
t_{first}	First appearance time when $W(t)$ first goes below 1	s	Section 15.2.1
t_{full}	Time to fill reactor	s	Example 14.3
t_{hold}	Holding time following fast fill	s	14.6
$\bar{t}_{\text{loop}}$	Mean residence time for single pass through loop	s	5.34
t_{mix}	Mixing time	s	Section 1.5
$\bar{t}_n$	Residence time in nth zone	s	Example 6.5
t_{s}	Time constant in packed bed, $L/\bar{u}_s$	s	9.9
t_T	Thermal time	s	15.53
U	Overall heat transfer coefficient	J m^{-2} s^{-1} K^{-1}	5.13

U'	Heat transfer group	s^{-1}	Example 7.8
$\bar{u}$	Average axial velocity	m s^{-1}	1.34
u_b	Gas velocity in bubble phase	m s^{-1}	11.46
u_e	Gas velocity in emulsion phase in fluidized bed	m s^{-1}	11.45
u_b	Gas velocity in bubble phase in fluidized bed	m s^{-1}	11.46
$\bar{u}_g$	Average gas velocity in gas–liquid PFR	m s^{-1}	11.28
$\bar{u}_l$	Average liquid velocity in gas–liquid PFR	m s^{-1}	11.27
$u_{\min}$	Minimum fluidization velocity	m s^{-1}	Section 11.3
$\bar{u}_s$	Superficial velocity in packed bed	m s^{-1}	3.21
$(\bar{u}_s)_g$	Superficial gas velocity, Q_g/A_c	m s^{-1}	Example 11.18
$\mathbf{V}$	Time-average velocity vector	m s^{-1}	9.16
V	Volume	m^3	1.3
V^0	Velocity at centerline	m s^{-1}	Problem 8.2
V_A	Molar volume of component A	$m^3 mol^{-1}$	7.32
V_{act}	Activation volume	m^3	Problem 5.4
V_{full}	Full volume of reactor	m^3	Example 14.3
V_g	Volume of gas phase	m^3	Section 11.1.1
V_l	Volume of liquid phase	m^3	Section 11.1.1
V_m	Volume of main tank in side capacity model	m^3	Example 15.7
V_r	Radial velocity	m s^{-1}	8.49
$\mathcal{V}_r$	Dimensionless radial velocity component, $V_r/\bar{u}$	Dimensionless	13.49
V_S	Volumetric consumption rate for solid		11.50
V_S	Volume of side tank in side capacity model	m^3	Example 15.7
V_z	Axial component of velocity	m s^{-1}	8.1
$\mathcal{V}_z$	Dimensionless axial velocity, $V_z/\bar{u}$	Dimensionless	Table 8.1
$V_z(r)$	Axial component of velocity in tube	m s^{-1}	8.1
$V_z(y)$	Axial velocity in slit flow	m s^{-1}	Example 16.3
$\mathbf{v}$	Velocity vector in turbulent flow	m s^{-1}	9.16
W	Mass flow rate	kg s^{-1}	Example 6.1
$W(t)$	Washout function	Dimensionless	15.2
$W(\theta, t)$	Washout function for unsteady system	Dimensionless	15.51
W_1, W_2	Randomly selected values for washout function	Dimensionless	Example 15.6
w_1, w_2	Weight of polymer aliquots	kg	13.14

w_A, w_B, w_C	Weighting factors for individual components	Dimensionless	Section 7.1.3
X	One monomer in vinyl copolymerization	Dimensionless	Section 13.4.4
X	Nonreactive or chain stopping end group	Dimensionless	Section 13.1
X	Dry cell mass per unit volume	kg m^{-3}	12.8
X_0	Initial cell mass per unit volume	kg m^{-3}	12.9
X_1, X_2, X_3	Independent variables in regression analysis	Varies	7.49
X_A	molar conversion of component A	Dimensionless	1.27
X_A	Conversion of limiting end group A	Dimensionless	13.16
x	Concentration of comonomer X		13.41
x_A	Mole fraction of component A	Dimensionless	Section 7.2
x_p	Concentration of X-type monomer in copolymer		13.41
Y	One monomer in vinyl copolymerization	Dimensionless	Section 13.4.4
Y_A	Molar fraction of component A that has not reacted	Dimensionless	1.26
Y_M	Fraction unreacted for monomer	Dimensionless	Example 4.3
Y'_M	Fraction unreacted if density did not change	Dimensionless	4.10
$Y_{P/S}$	Product mass produced per substrate mass	Dimensionless	12.14
$Y_{X/S}$	Dry cell mass produced per substrate mass	Dimensionless	12.14
$\hat{Y}_{X/S}$	Theoretical yield of dry cell mass per mass of substrate	Dimensionless	12.16
y	Coordinate in cross-flow direction	m	Section 16.1.1
y	Concentration of monomer Y		13.41
$\mathscr{y}$	Coordinate, y/Y	Dimensionless	16.13
y_A	Mole fraction of component A	Dimensionless	7.30
y_p	Mole fraction of Y-type monomer in copolymer	Dimensionless	13.41
z	Axial coordinate	m	1.34
$\mathscr{z}$	Dimensionless axial coordinate, z/L	Dimensionless	Table 8.1
z_R	Location of reaction front	m	11.51

GREEK

α	Time constant for lag phase	s	Problem 12.7
α	Thermal diffusivity, $\kappa/(\rho C_P)$	$m^2\ s^{-1}$	Table 8.1
α_{12}	Substrate limitation interaction parameter	Dimensionless	12.12
β	Constant in pressure drop equation	Pa m^{-1}	3.28
β	Volumetric coefficient of thermal expansion	K^{-1}	7.18
β	Heat generation number for nonisothermal effectiveness model	Dimensionless	Section 10.4.3
γ_A	Activity coefficient of component A	Dimensionless	7.32
δ	Thickness of stagnant film in film model	m	11.36
δ	Fractional increment in flow rate	Dimensionless	14.9
$\delta(t)$	Delta function	s^{-1}	15.9
ΔA_j	Interfacial area per tray	m^2	Example 11.7
ΔC_P	Difference in molar specific heats of reaction	J mol^{-1} K^{-1}	7.24
ΔE	Activation energy	J mol^{-1}	5.1
ΔE_f	Activation energy for forward reaction	J mol^{-1}	Section 5.1.2
ΔE_r	Activation energy for reverse reaction	J mol^{-1}	Section 5.1.2
ΔG_F°	Standard free energy of formation	J mol^{-1}	Table 7.2
ΔG_R	Free energy of reaction	J mol^{-1}	Example 7.12
ΔG_R°	Standard free energy of reaction	J mol^{-1}	7.29
ΔH_F°	Standard heat of formation	J mol^{-1}	Table 7.2
ΔH_R°	Standard heat of reaction	J mol^{-1}	7.35
$(\Delta H_R)_I$	Heat of reaction for reaction $I, I = 1, \ldots, M$	J mol^{-1}	5.16
$\mathbf{\Delta H_R}\mathscr{R}$	Implied summation of heats of reaction	J mol^{-1}	5.16
ΔP	Pressure drop	Pa	Section 3.1.1
ΔP_i	Difference in oxygen partial pressures across interface	Pa	Example 11.9
Δ_p	Range of random change	Varies	6.7
$\Delta\rho$	Density change upon reaction	kg m^3	Example 2.10
Δr	Radial step size	m	Table 8.2
ΔS_{mix}	Entropy of mixing	K^{-1}	Section 7.2
Δt	Time step for numerical integration	s	Section 2.4
ΔT	Temperature driving force	K	Table 4.1
$\Delta T_{\text{adiabatic}}$	Adiabatic temperature change	K	5.19
ΔV	Volume of liquid on tray	m^3	Example 11.7
ΔV_{act}	Activation volume	m^3	Problem 5.4
Δx	Thickness of membrane	m	11.9

Δz	Axial step size	m	8.36
$\Delta \mathcal{Z}_{max}$	Maximum axial increment for descretization stability	m	8.37
$\Delta \mathcal{Z}_{max}$	Maximum axial increment in Dimensionless form	m	8.39
ε	Void fraction in packed bed	Dimensionless	3.21
ε	Reaction coordinate for single reaction	mol	2.45
$\boldsymbol{\varepsilon}$	Reaction coordinate vector ($M \times 1$)	mol	2.47
$\varepsilon_{I,}$ $\varepsilon_{\mathrm{II},\cdots}$	Reaction coordinate for reactions I, II, ...	mol	2.48
ε_{total}	Void fraction including internal voids in catalyst particles	Dimensionless	10.38
η	Effectiveness factor	Dimensionless	10.23
η	Non-Newtonian flow index	Dimensionless	Problem 8.2
η	Effectiveness factor relative to enzyme in its native state	Dimensionless	12.7
η_0	Effectiveness factor ignoring film resistance	Dimensionless	10.31
η_{fresh}	Effective factor for fresh catalyst	Dimensionless	10.35
θ	Time catalytic or ion exchange reactor on stream	s	10.35
θ	Time variable for unsteady CSTR	s	15.51
κ	Thermal conductivity	J m^{-1} s^{-1} K^{-1}	8.56
κ_r	Effective thermal conductivity in radial direction	J m^{-1} s^{-1} K^{-1}	9.4
λ_{eff}	Effective thermal conductivity for catalyst particle	J m^{-1} s^{-1} K^{-1}	10.32
μ	Viscosity	kg m^{-1} s^{-1}, Pa s	3.18
μ	Growth rate for cell mass, cell mass formed per cell mass present per unit time	s^{-1}	12.8
μ_0	Viscosity before polymerization	kg m^{-1} s^{-1}, Pa s	Problem 8.15
μ_∞	Long-time value for maximum growth rate	s^{-1}	Problem 12.7
μ_{bulk}	Viscosity in main flow	kg m^{-1} s^{-1}, Pa s	5.36
μ_{max}	Maximum growth rate for cell mass	s^{-1}	12.8
μ_n	The nth moment of molecular weight distribution	Dimensionless, mol m^3	13.9
μ_{wall}	Viscosity at reactor wall	kg m^{-1} s^{-1}, Pa s	5.36
$\boldsymbol{\nu}$	The $N \times M$ matrix of stoichiometric coefficients	Dimensionless	2.41
ν	Change in number of moles upon reaction	Dimensionless	7.30

ν_A	Stoichiometric coefficient for component A	Dimensionless	1.13
$\nu_{A,\mathrm{I}}$	Stoichiometric coefficient for component A in reaction I	Dimensionless	2.8
ν_{I}	Change in number of moles upon reaction for reaction I	Dimensionless	7.47
ρ	Mass density	kg m^{-3}	1.3
$\bar{\rho}$	Density averaged with respect to flow rate	kg m^{-3}	8.42
ρ_∞	Mass density for complete reaction	kg m^{-3}	Example 2.10
ρ_c	Catalyst mass per total reactor volume	kg m^{-3}	10.38
ρ_{molar}	Molar density of reacting mixture	mol m^{-3}	3.12
ρ_{monomer}	Density of monomer	kg m^{-3}	4.9
ρ_{polymer}	Density of polymer	kg m^{-3}	4.9
σ^2	Dimensionless variance of residence time distribution	Dimensionless	15.17
σ_t^2	Variance of residence time distribution	s^2	15.15
τ	Dimensionless reaction time	Dimensionless	Example 2.10
τ	Dimensionless time	Dimensionless	5.30
τ	Mean exposure time		11.39
τ	Transformed time	Dimensionless	13.34
$\hat{\phi}_A$	Fugacity coefficient of component A	Dimensionless	7.30
Φ_A	Molar flux of component A	mol m^{-2} s^{-1}	3.6
$\mathbf{\Phi}$	Vector form of Φ_A	mol m^{-2} s^{-1}	3.9
ψ	Fluctuating velocity vector in turbulent flow	m s^{-1}	9.16
ω	Proportionality factor relating concentrations of consecutive chain lengths	Dimensionless	Section 13.4.2

Chapter 1

Elementary Reactions in Ideal Reactors

Material and energy balances are the heart of chemical engineering. Combine them with chemical kinetics, and they are the heart of chemical reaction engineering. Add transport phenomena and you have the intellectual basis for chemical reactor design. This chapter begins the study of chemical reactor design by combining material balances with kinetic expressions for elementary chemical reactions. The resulting equations are then solved for several simple but important types of chemical reactors. More complicated reactions and more complicated reactors are treated in subsequent chapters, but the real core of chemical reactor design is here in Chapter 1. Master it, and the rest will be easy.

1.1 MATERIAL BALANCES

Consider any region of space having a finite volume and prescribed boundaries that unambiguously separate the region from the rest of the universe. Such a region is called a ***control volume***, and the laws of conservation of mass and energy may be applied to it. We ignore nuclear processes so that there are separate conservation laws for mass and energy. For mass,

$$\begin{aligned}&\text{Rate at which mass enters the volume}\\&\quad=\text{rate at which mass leaves the volume}\\&\qquad+\text{rate at which mass accumulates within the volume}\end{aligned}\tag{1.1}$$

where "entering" and "leaving" apply to the flow of material across the boundaries. See Figure 1.1. Equation 1.1 is an ***overall mass balance*** that applies to the total mass within the control volume, as measured in kilograms or pounds. It can be written as

$$(Q_{\text{mass}})_{\text{in}} = (Q_{\text{mass}})_{\text{out}} + \frac{dI}{dt}\tag{1.2}$$

Chemical Reactor Design, Optimization, and Scaleup, Second Edition. By E. B. Nauman
Copyright © 2008 John Wiley & Sons, Inc.

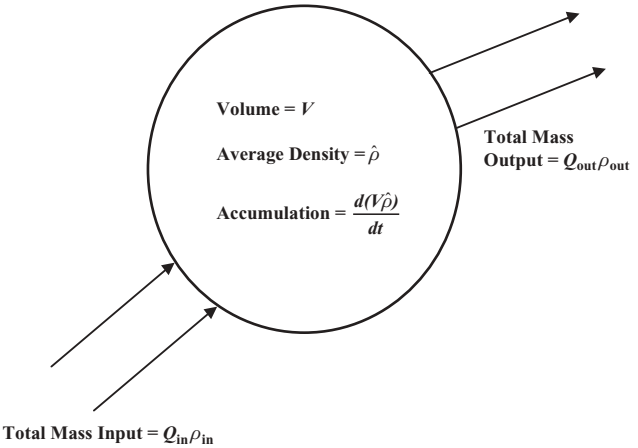

Figure 1.1 Control volume for total mass balance.

where Q_{mass} is the mass flow rate and I is the mass inventory in the system. We often write this equation using volumetric flow rates and volumes rather than mass flow rates and mass inventories.

$$Q_{\text{in}}\rho_{\text{in}} = Q_{\text{out}}\rho_{\text{out}} + \frac{d(\hat{\rho}V)}{dt} \tag{1.3}$$

where Q is the volumetric flow rate (volume per time) and ρ is the mass density (mass per volume). Note that $\hat{\rho}$ is the average mass density in the control volume so that $\hat{\rho}V = I$.

Equations 1.1–1.3 are different ways of expressing the overall mass balance for a flow system with variable inventory. In steady-state flow, the derivatives vanish, the total mass in the system is constant, and the overall mass balance simply states that input equals output. In batch systems, the flow terms are zero, the time derivative is zero, and the total mass in the system remains constant. We will return to the general form of Equation 1.3 when unsteady reactors are treated in Chapter 14. Until then, the overall mass balance merely serves as a consistency check on more detailed ***component balances*** that apply to individual substances.

In reactor design, we are interested in chemical reactions that transform one kind of mass into another. A material balance can be written for each component; but since chemical reactions are possible, the rate of formation of the component within the control volume must now be considered. The ***component balance*** for some substance A is

Rate at which component A enters the volume
+ net rate at which component A is formed by reaction
= rate at which component A leaves the volume
+ rate at which component A accumulates within the volume (1.4)

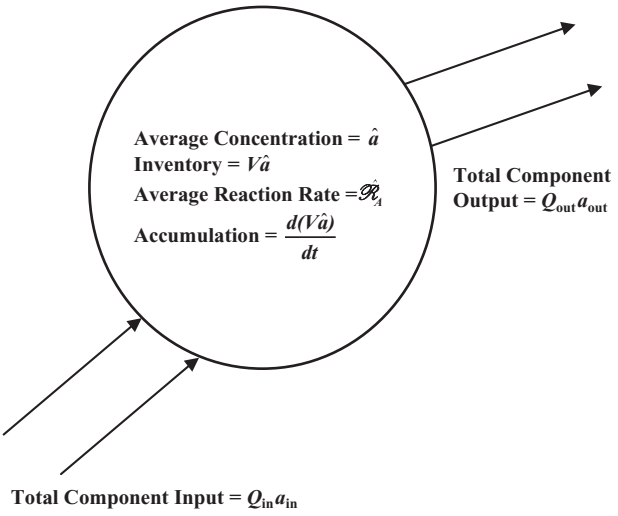

Figure 1.2 Control volumes for component balance.

More briefly,

$$\text{Input} + \text{formation} = \text{output} + \text{accumulation} \tag{1.5}$$

See Figure 1.2. A component balance can be expressed in mass units, and this is done for materials such as polymers that have an ill-defined molecular weight. Usually, however, component A will be a distinct molecular species, and it is more convenient to use molar units:

$$Q_{\text{in}}a_{\text{in}} + \hat{\mathscr{R}}_A V = Q_{\text{out}}a_{\text{out}} + \frac{d(V\hat{a})}{dt} \tag{1.6}$$

where a is the concentration or molar density of component A in moles per volume and $\hat{\mathscr{R}}_A$ is the volume-average rate of formation of component A in moles per volume per time.

There may be several chemical reactions occurring simultaneously, some of which generate A while others consume it. The net rate $\hat{\mathscr{R}}_A$ will be positive if there is net production of component A and negative if there is net consumption. Unless the system is very well mixed, concentrations and reaction rates will vary from point to point within the control volume. The component balance applies to the entire control volume so that $\hat{a}$ and $\hat{\mathscr{R}}_A$ denote spatial averages.

A version of Equation 1.4 can be written for each component, A, B, C. . . . If these equations are written in terms of mass and then summed over all components, the sum must equal Equation 1.1 since the net rate of mass formation must be zero. When written in molar units as in Equation 1.6, the sum need not be zero since chemical reactions can cause a net increase or decrease in the number of moles.

1.1.1 Measures of Composition

This book uses the term ***concentration*** to mean the molar density of a component, for example, moles of A per unit volume of the reacting mixture. In the International System of Units (SI) concentration is in moles per cubic meters where the moles are gram moles. ***Molarity*** is classically defined as moles per liter of solution and is a similar concentration measurement. ***Molality*** is classically defined as moles per kilogram of solvent (not of solution) and is thus not a standard measure of concentration. For gases at low pressure and moderate temperatures, partial pressures are sometimes used instead of concentrations since partial pressures are proportional to concentration for ideal gases.

Other measures of composition such as mole fraction and mass fraction are less commonly used to express chemical reaction rates. Weight measurements are frequently used to prepare solutions or fill reactors. The resulting composition will have a known ratio of moles and masses of the various components, but the numerical value for concentration requires that the density be known. Good practice is to prepare solutions in mass units and then convert to standard concentration units based on the known or observed density of the solution under reaction conditions. To avoid ambiguity, modern analytical chemists frequently define both molarity and molality in weight units as moles per kilogram of solution or moles per kilogram of solvent.

EXAMPLE 1.1

Sucrose, 342.3 g, is dissolved in one liter of water at "room temperature." Calculate the composition by various measures.

SOLUTION: The molecular weight of sucrose is 342.3 so the molality of the solution is approximately 1.0. It would be exactly 1.0 if molality were defined per liter of solvent rather than per kilogram of solvent. Room temperature in the scientific literature means 20–25°C, with 25°C being usual in the United States. The density of water at 25°C is 0.997 g cm^{-3} so that the solution used 0.997 kg of water, giving a molality of 1.003. The weight percent of sucrose is 25.56. The mole fraction of sucrose is 0.0177. The concentration of sucrose cannot be determined without knowing the density of the solution. It is about 1.10 g cm^{-3} at the experimental conditions. Thus the concentration of sucrose is $1/(997 + 342.3)/1.10 = 8.21 \times 10^{-4}$ mol $cm^{-3} = 821$ mol m^{-3}. The molarity is 0.821 mol L^{-1}.

A word of caution involves the definition of mole. As indicated above, SI moles are gram moles, the mass in grams of 6.02×10^{23} molecules. There is an inconsistency in the SI system of units that may cause problems when converting molar densities and molar flow rates to mass densities and mass flow rates. A point in the system with molar concentrations (i.e., molar densities) of a and b has a mass density of $\rho = aM_A + bM_B$, where M_A and M_B are the molecular weights of the two components.

The resulting units on ρ are grams per cubic meter and must be divided by 1000 to obtain conventional SI units of kilograms per cubic meter.

1.1.2 Measures of Reaction Rate

The SI units for reaction rate are moles per cubic meter per second, but other time units are frequently used and other volume units are sometimes used. It is obviously necessary to specify to what compound the reaction rate refers. This book makes the specification essentially automatic by defining a rate, $\mathscr{R}$, for the reaction as a whole. The reaction rate for component A is denoted $\mathscr{R}_A$ and is found from

$$\mathscr{R}_A = \nu_A \mathscr{R} \tag{1.7}$$

where ν_A is the stoichiometric coefficient for component A in the (single) reaction. The next section discusses this more fully, and Chapter 2 extends the treatment to multiple reactions. However, reaction rate expressions and data taken from other sources may not follow the convention and need careful scrutiny, particularly if the reaction is something like $4\text{Fe} + 3\text{O}_2 \rightarrow 2\text{Fe}_2\text{O}_3$.

To design a chemical reactor, the spatial-average concentrations $\hat{a}, \hat{b}, \hat{c}, \ldots$ must be found for a batch reactor and the outlet concentrations are needed for a flow reactor. Finding these concentrations is relatively easy for the single, elementary reactions and ideal reactors that are considered here in Chapter 1. We begin by discussing elementary reactions, of which there are just a few basic types.

1.2 ELEMENTARY REACTIONS

Consider the reaction of two chemical species according to the stoichiometric equation

$$\text{A} + \text{B} \rightarrow \text{P} \tag{1.8}$$

This reaction is said to be ***homogeneous*** if it occurs within a single phase. For the time being we are concerned only with reactions that take place in the gas phase or in a single liquid phase. These reactions are said to be ***elementary*** if they result from a single interaction (i.e., a collision) between the molecules appearing on the left-hand side of Equation 1.8. The rate at which collisions occur between A and B molecules should be proportional to their concentrations, a and b. Not all collisions cause a reaction, but at constant environmental conditions (e.g., temperature), some definite fraction should react. Thus we expect

$$\mathscr{R} = k[\text{A}][\text{B}] = kab \tag{1.9}$$

where k is a constant of proportionality known as the ***rate constant***.

1.2.1 Kinetic Theory of Gases

The kinetic theory of gases can be used to rationalize the functional form of Equation 1.9. Suppose that a collision between an A and B molecule is necessary but not sufficient for reaction to occur. Thus we expect

$$\mathscr{R} = \frac{C_{AB} f_R}{\mathrm{Av}} \tag{1.10}$$

where C_{AB} is the collision rate (collisions per volume per time) and f_R is the reaction efficiency. Avogadro's number, **Av**, has been included in Equation 1.10 so that $\mathscr{R}$ will have normal units, moles per cubic meter per second, rather than units of molecules per cubic meter per second. By hypothesis $0 < f_R < 1$.

Ideal gas theory treats the molecules as rigid spheres having radii r_A and r_B. They collide if they approach each other within a distance $r_A + r_B$. A result from kinetic theory is

$$C_{AB} = \left[\frac{8\pi R_g T(m_A + m_B)}{\mathbf{Av}\, m_A m_B}\right]^{1/2} (r_A + r_B)^2\, \mathbf{Av}^2\, ab \tag{1.11}$$

where R_g is the gas constant, T is the absolute temperature, and m_A and m_B are the molecular masses in kilograms per molecule. The collision rate is proportional to the product of the concentrations as postulated in Equation 1.9. The reaction rate constant is

$$k = \left[\frac{8\pi R_g T(m_A + m_B)}{\mathbf{Av}\, m_A m_B}\right]^{1/2} (r_A + r_B)^2\, \mathbf{Av}\, f_R \tag{1.12}$$

Collision theory is mute about the value of f_R. Typically $f_R \ll 1$ so that the number of molecules colliding is much greater than the number reacting. See Problem 1.2. Not all collisions have enough energy to produce a reaction. Steric effects may also be important. As will be discussed in Chapter 5, f_R is strongly dependent on temperature. This dependence usually overwhelms the $T^{1/2}$ dependence predicted for the collision rate.

1.2.2 Rate of Formation

Note that the rate constant k is positive so that $\mathscr{R}$ is positive. Here, $\mathscr{R}$ is defined as the ***rate of the reaction***, not the rate at which a particular component reacts or is formed. Components A and B are consumed by the reaction of Equation 1.8 and thus are "formed" at a negative rate:

$$\mathscr{R}_A = \mathscr{R}_B = -kab$$

while P is formed at a positive rate:

$$\mathscr{R}_P = +kab$$

The sign convention we have adopted is that the rate of a reaction is always positive. The ***rate of formation of a component*** is positive when the component is formed by the reaction and is negative when the component is consumed.

A general expression for any single reaction is

$$0_M \rightarrow \nu_A \mathrm{A} + \nu_B \mathrm{B} + \cdots + \nu_R \mathrm{R} + \nu_S \mathrm{S} + \cdots \tag{1.13}$$

As an example, the reaction $2H_2 + O_2 \rightarrow 2H_2O$ can be written as

$$0_M \rightarrow -2\mathrm{H}_2 - \mathrm{O}_2 + 2\mathrm{H}_2\mathrm{O}$$

This form is obtained by setting all participating species, whether products or reactants, on the right-hand side of the stoichiometric equation. The remaining term on the left is the ***zero molecule***, which is denoted by 0_M to avoid confusion with atomic oxygen. The ν_A, ν_B, ... are the ***stoichiometric coefficients*** for the reaction. They are positive for products and negative for reactants. The general relationship between the rate of the reaction and the rate of formation of component A is

$$\mathscr{R}_A = \nu_A \mathscr{R} \tag{1.14}$$

Stoichiometric coefficients can be fractions. However, for elementary reactions, they must be small integers, of magnitude 2, 1, or 0. If the reaction of Equation 1.13 were reversible and elementary, its rate would be

$$\mathscr{R} = k_f [\mathrm{A}]^{-\nu_A} [\mathrm{B}]^{-\nu_B} \cdots - k_r [\mathrm{R}]^{\nu_R} [\mathrm{S}]^{\nu_S} \tag{1.15}$$

where A, B, ... are reactants; R, S, ... are products; k_f is the rate constant for the forward reaction; and k_r is the rate constant for the reverse reaction.

The functional form of the reaction rate in Equation 1.15 is dictated by the reaction stoichiometry, Equation 1.13. Only the constants k_f and k_r can be adjusted to fit the specific reaction. This is the hallmark of an elementary reaction; its rate is consistent with the reaction stoichiometry and is given by Equation 1.15. However, reactions can have the form of Equation 1.15 without being elementary.

As a shorthand notation for indicating that a reaction is elementary, we shall include the rate constants in the stoichiometric equation by showing the rate constant above the arrow and, if reversible, below the arrow. Thus the reaction

$$\mathrm{A} + \mathrm{B} \underset{k_r}{\overset{k_f}{\rightleftharpoons}} 2\mathrm{C}$$

is elementary and reversible and has the following rate expression:

$$\mathscr{R} = k_f ab - k_r c^2$$

The relative magnitudes of k_f and k_r are constrained by an equilibrium constant. For this example, $\nu_A = \nu_B = -1$, $\nu_C = +2$, and the equilibrium constant is

$$K_{\text{kinetic}} = \frac{k_f}{k_r} = [\mathrm{A}]^{-1}[\mathrm{B}]^{-1}[\mathrm{C}]^2 = \frac{[\mathrm{C}]^2}{[\mathrm{A}][\mathrm{B}]} = \frac{c^2}{ab} \tag{1.16}$$

Reversible reactions and equilibrium constants are discussed at length in Section 7.2.

Chemical engineers deal with many reactions that are not elementary. Most industrially important reactions go through a complex kinetic mechanism before the final products are reached. The mechanism may give a rate expression far different than Equation 1.15 even though it involves only short-lived intermediates that never appear in conventional chemical analyses. Elementary reactions are generally limited to the following types: first order, second order unimolecular, and second order with two reactants. Third-order reactions exist but are rare.

1.2.3 First-Order Reactions

An irreversible first-order reaction involves only one reactant:

$$\mathrm{A} \xrightarrow{k} \text{products} \qquad \mathscr{R} = ka \tag{1.17}$$

Since $\mathscr{R}$ has units of moles per volume per time and a has units of moles per volume, the rate constant for a first-order reaction has units of reciprocal time, for example, reciprocal seconds. The best example of a truly first-order reaction is radioactive decay, for example,

$$^{238}\mathrm{U} \rightarrow {}^{234}\mathrm{Th} + {}^{4}\mathrm{He}$$

since it occurs spontaneously as a single-body event. Among strictly chemical reactions, thermal decompositions such as

$$\mathrm{CH_3OCH_3} \rightarrow \mathrm{CH_4} + \mathrm{CO} + \mathrm{H_2}$$

follow first-order kinetics at normal gas densities. The student of chemistry will recognize that the complete decomposition of dimethyl ether into methane, carbon monoxide, and hydrogen will not occur in a single step. Short-lived intermediates will exist, but since the reaction is irreversible, they will not affect the rate of the decomposition reaction since it is first order and has the form of Equation 1.17. The decomposition does require energy, and collisions between the reactant and other molecules are the usual mechanism for acquiring this energy. Thus a second-order dependence may be observed for the pure gas at very low densities since reactant molecules must collide with themselves to acquire energy.

1.2.4 Second-Order Reactions with One Reactant

The simplest example of a second-order reaction has one type of molecule reacting with itself:

$$2\mathrm{A} \xrightarrow{k} \text{products} \qquad \mathscr{R} = ka^2 \tag{1.18}$$

where k has units of cubic meters per mole per second. It is important to note that $\mathscr{R}_\mathrm{A} = -2ka^2$ according to the convention of Equation 1.14. Pesky factors of 2 are common in chemical kinetics. In using literature data, be sure to check the source to

see if the author defined the reaction rate as $\mathscr{R} = ka^2$ so that $\mathscr{R}_A = -2ka^2$. Another common possibility is to have $\mathscr{R}_A = -k_2 a^2$ where $k_2 = 2k$.

A gas phase reaction believed to be elementary and second order is

$$2\text{HI} \rightarrow \text{H}_2 + \text{I}_2$$

Here, collisions between two HI molecules supply energy and also supply the reactants needed to satisfy the observed stoichiometry.

1.2.5 Second-Order Reactions with Two Reactants

Second-order reactions with two reactants are common:

$$\text{A} + \text{B} \xrightarrow{k} \text{products} \qquad \mathscr{R} = kab \tag{1.19}$$

Liquid phase esterifications such as

$$\begin{array}{l} \\ \text{C}_2\text{H}_5\text{OH} + \text{CH}_3\overset{\displaystyle\text{O}}{\overset{\|}{\text{C}}}\text{OH} \rightarrow \text{C}_2\text{H}_5\text{O}\overset{\displaystyle\text{O}}{\overset{\|}{\text{C}}}\text{CH}_3 + \text{H}_2\text{O} \end{array}$$

typically follow second-order kinetics.

1.2.6 Third-Order Reactions

Elementary third-order reactions are vanishingly rare because they require a statistically improbable three-way collision. In principle there are three types of third-order reactions:

$$\begin{aligned} 3\text{A} &\xrightarrow{k} \text{products} \qquad \mathscr{R} = ka^3 \\ 2\text{A} + \text{B} &\xrightarrow{k} \text{products} \qquad \mathscr{R} = ka^2 b \\ \text{A} + \text{B} + \text{C} &\xrightarrow{k} \text{products} \qquad \mathscr{R} = kabc \end{aligned} \tag{1.20}$$

A homogeneous gas phase reaction that follows a third-order kinetic scheme is

$$2\text{NO} + \text{O}_2 \rightarrow 2\text{NO}_2 \qquad \mathscr{R} = k[\text{NO}]^2[\text{O}_2]$$

although the mechanism is believed to involve two steps (Tsukahara et al., 1999) and thus is not elementary. Reactions may approximate third-order and even higher order kinetics without being elementary.

1.3 REACTION ORDER AND MECHANISM

As suggested by these examples, the ***order*** of a reaction is the sum of the exponents $m, n, \ldots$ in

$$\mathscr{R} = ka^m b^n \ldots \qquad \text{Reaction order} = m + n + \cdots \tag{1.21}$$

This definition for reaction order is directly meaningful only for irreversible or forward reactions that have rate expressions in the form of Equation 1.21. If the reaction is reversible, the reverse reaction can have a different order. Thus

$$\mathrm{A} + \mathrm{B} \underset{k_r}{\overset{k_f}{\rightleftharpoons}} \mathrm{C} \qquad \mathscr{R} = k_f ab - k_r c$$

is second order for the forward reaction and first order for the reverse reaction.

Components A, B, . . . are consumed by the reaction and have negative stoichiometry coefficients so that $m = -\nu_A, n = -\nu_B, \ldots$ are positive (or zero). For elementary reactions, m and n must be integers of 2 or less and, practically speaking, must sum to 2 or less so that the only real possibilities for elementary reactions are first and second order.

Equation 1.21 is frequently used to correlate data from complex reactions. Complex reactions can give rise to rate expressions that have the form of Equation 1.21 but with fractional or even negative exponents. Complex reactions with observed orders of $\frac{1}{2}$ or $\frac{3}{2}$ can be explained theoretically based on mechanisms discussed in Chapter 2. Negative orders arise when a compound retards a reaction, say by competing for active sites in a heterogeneously catalyzed reaction or when the reaction is reversible. Observed reaction orders above 3 are occasionally reported. An example is the reaction of styrene with nitric acid where an overall order of 4 has been observed (Lewis and Moodie, 1997). The likely explanation is that the acid serves both as a catalyst and as a reactant. The reaction is far from elementary.

Complex reactions can be broken down into a number of series and parallel elementary steps, possibly involving short-lived intermediates such as free radicals. These individual reactions collectively constitute the ***mechanism*** of the complex reaction. The individual reactions are usually second order, and the number of reactions needed to explain an observed, complex reaction can be surprisingly large. For example, a good model burning methane such as

$$\mathrm{CH_4} + 2\mathrm{O_2} \rightarrow \mathrm{CO_2} + 2\mathrm{H_2O}$$

will involve 20 or more elementary reactions even assuming that the indicated products are the only ones formed in significant quantities. A detailed model for the oxidation of toluene involves 141 chemical species in 743 elementary reactions (Lindstedt and Maurice, 1996). A model for the creation of carbon nanotubes by the high-pressure carbon monoxide process (Dateo et al., 2002) involves 917 species and 1948 chemical reactions, although the experimental data are well explained by a simple model containing a mere 14 species and 22 reactions.

As a simpler example of a complex reaction, consider the nitration of toluene to give TNT, 2,4,6-trinitrotoluene (kindly do this abstractly, not experimentally like the evil professor in Problem 1.13). The reaction is

$$\mathrm{Toluene} + 3\mathrm{HNO_3} \rightarrow \mathrm{TNT} + 3\mathrm{H_2O}$$

or, in shorthand,

$$\mathrm{A} + 3\mathrm{B} \rightarrow \mathrm{C} + 3\mathrm{D}$$

This reaction cannot be elementary. We can hardly expect three nitric acid molecules to react at all three toluene sites (these are primarily the ortho and para sites; meta substitution is not favored) in a glorious, four-body collision. Thus the fourth-order rate expression $\mathscr{R} = kab^3$ is implausible. Instead, the mechanism of the TNT reaction involves at least seven steps (two reactions leading to *ortho*- or *para*-nitrotoluene, three reactions leading to 2,4- or 2,6-dinitrotoluene, and two reactions leading to 2,4,6-trinitrotoluene). Each step would require only a two-body collision, could be elementary, and could be governed by a second-order rate equation. Chapter 2 shows how the component balance equations can be solved for multiple reactions so that an assumed mechanism can be tested experimentally. For the toluene nitration, even the set of seven series and parallel reactions may not constitute an adequate mechanism since an experimental study (Chen et al., 1996) found the reaction to be 1.3 order in toluene and 1.2 order in nitric acid for an overall order of 2.5 rather than the expected value of 2. Furthermore, the reaction is not even homogeneous as it is normally conducted (Milllgan, 1986).

An irreversible, elementary reaction must have Equation 1.21 as its rate expression. A complex reaction may have an empirical rate equation with the form of Equation 1.21 and with integral values for n and m without being elementary. The classic example of this statement is a second-order reaction where one of the reactants is present in great excess. Consider the slow hydrolysis of an organic compound in water. A rate expression of the form

$$\mathscr{R} = k[\text{water}][\text{organic}]$$

is plausible, at least for the first step of a possibly complex mechanism. Suppose [organic] $\ll$ [water] so that the concentration of water does not change appreciably during the course of the reaction. Then the water concentration can be combined with k to give a composite rate constant. The rate expression appears to be first order in [organic]:

$$\mathscr{R} = k[\text{water}][\text{organic}] = k'[\text{organic}] = k'a$$

where $k' = k[\text{water}]$ is a ***pseudo-first-order rate constant***. From an experimental viewpoint, the reaction cannot be distinguished from first order even though the actual mechanism is second order. Gas phase reactions can appear first order when one reactant is dilute. Kinetic theory still predicts the collision rates of Equation 1.11, but the concentration of one species, call it B, remains approximately constant. The observed rate constant is

$$k' = \left[\frac{8\pi R_g T(m_A + m_B)}{\text{Av}\, m_A m_B}\right]^{1/2} (r_A + r_B)^2\, \mathbf{Av}\, f_R b$$

The only reactions which are strictly first order are radioactive decay. Among chemical reactions, thermal decompositions may seem first order, but an external energy source is generally required to excite the reaction. As noted earlier, this energy is usually acquired by intermolecular collisions. Thus the reaction rate could be written as

$$\mathscr{R} = k[\text{reactant molecules}]\ [\text{all molecules}]$$

The concentration of all molecules is normally much higher than the concentration of reactant molecules so that it remains essentially constant during the course of the reaction. Thus, what is truly a second-order reaction appears first order.

1.4 IDEAL, ISOTHERMAL REACTORS

Section 1.2 developed rate expressions for elementary reactions. These expressions are now combined with the material balances of Section 1.1 to develop reactor design equations, that is, equations to predict final concentrations in a batch reactor or outlet concentrations in a flow reactor. Since reaction rate expressions have units of concentration per time, it may seem that $\mathscr{R}_A$ is identical to da/dt. This is true only for an ideal batch reactor. In flow reactors, the concentration changes can be caused by any of convection, diffusion, and reaction.

There are four kinds of ideal reactors:

1. The batch reactor
2. The piston flow reactor (PFR)
3. The perfectly mixed continuous flow stirred tank reactor (CSTR)
4. The completely segregated continuous flow stirred tank.

This chapter discusses the first three types. These are overwhelmingly the most important. The fourth type is interesting theoretically but has limited practical importance. It is discussed in Chapter 15.

The batch reactor is an unsteady-state system. Reactants are charged to a vessel and the reaction proceeds in time. Piston flow and stirred tank reactors are normally designed to operate at a steady state where reactants are continuously charged and products continuously removed. Until Chapter 5, the reactors are assumed to be isothermal. This means that the operating temperature is known, is uniform throughout the reactor, and does not change with time in a batch reactor. Here in Chapter 1, we also assume that fluid properties and especially density are constant, independent of the extent of reaction. Finally, we assume that the system is homogeneous and that there is a single reaction that either is elementary or else has a rate expression identical to one of the elementary reactions. These various assumptions are realistic for some industrial reactors and grossly unrealistic for others. The simplified results in this chapter provide a starting point.

1.4.1 Ideal Batch Reactors

This is the classic reactor used by organic chemists. The typical volume in glassware is a few hundred milliliters. Reactants are charged to the system, rapidly mixed, and rapidly brought up to temperature so that operating conditions are well defined. Heating is done with an oil bath or an electric heating mantel. Mixing is done with a magnetic stirrer or a small mechanical agitator. Temperature is controlled by regulating the bath temperature or by allowing a solvent to reflux.

Batch reactors are the most common type of industrial reactor and may have volumes well in excess of 100,000 L. They tend to be used for small-volume, specialty products (e.g., an organic dye) rather than large-volume, commodity chemicals (e.g., ethylene oxide) that are normally reacted in continuous flow equipment. Industrial-scale batch reactors can be heated or cooled by external coils or a jacket, by internal coils, or by an external heat exchanger in a pump-around loop. Reactants are often preheated by passing them through heat exchangers as they are charged to the vessel. Heat generation due to the reaction can be significant in large vessels. Refluxing is one means for controlling the exotherm. Mixing in large batch vessels is usually done with a mechanical agitator, but is occasionally done with an external pump-around loop where the momentum of the returning fluid causes the mixing.

Heat and mass transfer limitations are rarely important in the laboratory but may emerge upon scaleup. Batch reactors with internal variations in temperature or composition are difficult to analyze and remain a challenge to the chemical reaction engineer. Tests for such problems are considered in Section 1.5. For now assume an ***ideal batch reactor*** with the following characteristics:

1. Reactants are quickly charged, mixed, and brought to temperature at the beginning of the reaction cycle.
2. The reaction mass constitutes a single, fluid phase.
3. Mixing and heat transfer are sufficient to assure that the batch remains completely uniform in temperature and composition throughout the reaction cycle.
4. The operating temperature is held constant.

A batch reactor has no input or output of mass after the initial charging. The amounts of individual components may change due to reaction but not due to flow into or out of the system. The component balance for component A, Equation 1.6, reduces to

$$\frac{d(Va)}{dt} = \mathscr{R}_A V \tag{1.22}$$

Together with similar equations for the other reactive components, Equation 1.22 constitutes the ***reactor design equation*** for an ideal batch reactor. Note that $\hat{a}$ and $\hat{\mathscr{R}}_A$ have been replaced with a and $\mathscr{R}_A$ due to the assumption of good mixing throughout the vessel. An ideal batch reactor has no temperature or concentration gradients within the system volume. The concentration will change with time due to the reaction, but at any time it is everywhere uniform. The temperature may also change with time, but this complication will be deferred until Chapter 5. The reaction rate will vary with time but is always uniform throughout the vessel. Here in Chapter 1, we make the additional assumption that the volume is constant. In a liquid phase reaction, this corresponds to assuming constant fluid density, an assumption that is usually reasonable for preliminary calculations. Industrial gas phase reactions are normally conducted in flow systems rather than batch systems. When batch reactors are used for a gas phase reaction, they are normally constant-volume devices so that the system pressure can vary during the batch cycle. Constant-pressure devices were used in early

kinetic studies and are occasionally found in industry. The constant pressure at which they operate is usually atmospheric pressure.

If the volume is constant, Equation 1.22 simplifies to

$$\frac{da}{dt} = \mathscr{R}_A \tag{1.23}$$

Equation 1.23 is an ordinary differential equation (ODE). Its solution requires an initial condition:

$$a = a_0 \quad \text{at } t = 0 \tag{1.24}$$

When $\mathscr{R}_A$ depends on a alone, the ODE is variable separable and can usually be solved analytically. If $\mathscr{R}_A$ depends on the concentration of several components (e.g., a second-order reaction of the two-reactant variety, $\mathscr{R}_A = -kab$), versions of Equations 1.23 and 1.24 can be written for each component and the resulting equations solved simultaneously. Alternatively, stoichiometric relations can be used to couple the concentrations, but this approach becomes awkward in multicomponent systems and is avoided by the methodology introduced in Chapter 2.

First-Order Batch Reactions

The reaction is

$$\mathrm{A} \xrightarrow{k} \text{products}$$

The rate constant over the reaction arrow indicates that the reaction is assumed to be elementary. Thus the rate equation is

$$\mathscr{R} = ka$$

and

$$\mathscr{R}_A = \nu_\mathrm{A}\mathscr{R} = -ka$$

Substituting into Equation 1.23 gives

$$\frac{da}{dt} + ka = 0$$

Solving this ODE and applying the initial condition of Equation 1.24 give

$$a = a_0 e^{-kt} \tag{1.25}$$

Equation 1.25 is arguably the most important result in chemical reaction engineering. It shows that the concentration of a reactant being consumed by a first-order batch reaction decreases exponentially. Dividing through by a_0 gives the ***fraction unreacted***,

$$Y_A = \frac{a}{a_0} = e^{-kt} \tag{1.26}$$

and

$$X_A = 1 - \frac{a}{a_0} = 1 - e^{-kt} \tag{1.27}$$

gives the ***conversion***. The ***half-life*** of the reaction is defined as the time necessary for a to fall to half its initial value:

$$t_{1/2} = 0.693/k \tag{1.28}$$

The half-life of a first-order reaction is independent of the initial concentration. Thus the time required for the reactant concentration to decrease from a_0 to $a_0/2$ is the same as the time required to decrease from $a_0/2$ to $a_0/4$. This is not true for reactions of order other than first.

Second-Order Batch Reactions with One Reactant

We now choose to write the stoichiometric equation as

$$2\mathrm{A} \xrightarrow{k/2} \text{products}$$

Compare this to Equation 1.18 and note the difference in rate constants. For the current formulation,

$$\mathscr{R} = \left(\tfrac{1}{2}k\right) a^2 \qquad \mathscr{R}_A = \nu_\mathrm{A}\mathscr{R} = -2\mathscr{R} = -ka^2$$

Substituting into Equation 1.22 gives

$$\frac{da}{dt} + ka^2 = 0$$

Solution gives

$$-a^{-1} + C = -kt$$

where C is a constant. Applying the initial condition gives $C = (a_0)^{-1}$ and

$$Y_A = \frac{a}{a_0} = \frac{1}{1 + a_0 kt} \tag{1.29}$$

The initial half-life of a second-order reaction corresponds to a decrease from a_0 to $a_0/2$ and is given by

$$t_{1/2} = \frac{1}{a_0 k} \tag{1.30}$$

The second half-life, corresponding to a decrease from $a_0/2$ to $a_0/4$, is twice the initial half-life.

Second-Order Batch Reactions with Two Reactants

The batch reaction is now

$$\mathrm{A} + \mathrm{B} \xrightarrow{k} \text{products}$$

$$\mathscr{R} = kab \qquad \mathscr{R}_\mathrm{A} = \nu_\mathrm{A}\mathscr{R} = -\mathscr{R} = -kab$$

Substituting into Equation 1.23 gives

$$\frac{da}{dt} + kab = 0$$

A similar equation can be written for component B:

$$\frac{db}{dt} + kab = 0$$

The pair can be solved simultaneously. A simple way to proceed is to note that

$$\frac{da}{dt} = \frac{db}{dt}$$

which is solved to give

$$a = b + C$$

where C is a constant of integration than can be determined from the initial conditions for a and b. The result is

$$a - a_0 = b - b_0 \tag{1.31}$$

which states that A and B are consumed in equal molar amounts as required by the reaction stoichiometry. Applying this result to the ODE for component A gives

$$\frac{da}{dt} + ka(a - a_0 + b_0) = 0$$

The equation is variable separable. Integrating and applying the initial condition give

$$\frac{a}{a_0} = \frac{b_0 - a_0}{b_0 \exp[(b_0 - a_0)kt] - a_0} \tag{1.32}$$

This is the general result for a second-order batch reaction. The mathematical form of the equation presents a problem when the initial stoichiometry is perfect, $a_0 = b_0$. Such problems are common with analytical solutions to ODEs. Special formulas are needed for special cases.

One way of treating a special case is to do a separate derivation. For the current problem, perfect initial stoichiometry means $b = a$ throughout the reaction. Substituting this into the ODE for component A gives

$$\frac{da}{dt} + ka^2 = 0$$

which is the same as that for the one-reactant case of a second-order reaction and the solution is Equation 1.29.

An alternative way to find a special formula for a special case is to apply L'Hospital's rule to the general case. When $b_0 \to a_0$, Equation 1.32 has an indeterminate form of the $0/0$ type. Differentiating the numerator and denominator with

respect to b_0 and then taking the limit give

$$\frac{a}{a_0} = \lim_{b_0 \to a_0} \left[\frac{1}{\exp[(b_0 - a_0)kt] + b_0 kt \ \exp[(b_0 - a_0)kt]} \right] = \frac{1}{1 + a_0 kt}$$

which is again identical to Equation 1.29.

Any Single Reaction in an Ideal Batch Reactor

The above results are directly useful when the batch reaction time t is known and $a(t)$ is sought. An alternative form is sometimes used when $a(t)$ is specified and the batch reaction time is sought. For this case, a general solution to Equation 1.23 is

$$t = \int_{a_0}^{a(t)} \frac{da_1}{\mathscr{R}_A(a_1)} \tag{1.33}$$

Here, a_1 is a dummy variable of integration that will be replaced by the upper and lower limits after the integral is evaluated. The results are equivalent to those obtained earlier, for example, Equations 1.26 and 1.29 depending on the reaction order, and all the restrictive assumptions still apply: a single reaction in a constant-volume, isothermal, perfectly mixed batch reactor. Note that Equation 1.33 becomes useless for the multiple reactions treated in Chapter 2.

1.4.2 Reactor Performance Measures

There are four common measures of reactor performance: fraction unreacted, conversion, yield, and selectivity. The fraction unreacted is the simplest and is usually found directly when solving the component balance equations. It is $a(t)/a_0$ for a batch reaction and $a_{\text{out}}/a_{\text{in}}$ for a flow reactor. The conversion is just 1 minus the fraction unreacted. The terms conversion and fraction unreacted refer to a specific reactant, usually the stoichiometrically limiting reactant. See Equations 1.26 and 1.27 for the first-order case.

For most reactions, a batch reactor give the lowest possible fraction unreacted, the highest possible conversion, the best yield, and the highest selectivity. Fraction unreacted and conversion refer to the reactants. Yield and selectivity refer to the desired products. The ***molar yield*** is the number of moles of a specified product that are made per mole of reactant charged. There is also a ***mass yield***. Either of these yields can be larger than 1 since one reactant may form more that 1 mol of product or there may be several reactants that contribute to the mass of a product. Thus A $\rightarrow$ 2B can have a molar yield of 2 if the reaction goes to completion. The yield of a reaction like A + B $\rightarrow$ C can be based on either A or B. The mass yield of this reaction depends on the extent of reaction and on the relative molecular weights of A and B. The ***theoretical yield*** is the amount of product that would be formed if all the reactant was converted to the desired product. This too can be expressed on either a molar or a mass basis and can be larger than 1. ***Selectivity*** is defined as the fractional amount of the converted portion of a reactant that is converted to the desired product. The selectivity will always be 100% when there is only one reaction even though the conversion may

be less than 100%. Selectivity is a trivial concept when there is only one reaction but becomes an important consideration when there are competing reactions. The following example illustrates a reaction with high conversion but low selectivity.

EXAMPLE 1.2

Suppose it is desired to make 1,4-dimethyl-2,3-dichlorobenzene by the direct chlorination of *para*-xylene. The desired reaction is

$$p\text{-Xylene} + Cl_2 \rightarrow \text{desired product} + 2\,HCl$$

But, there are many other reactions that can occur and it is implausible that the desired reaction will occur as a single, elementary step. A feed stream containing 40 mol % *p*-xylene and 60 mol % chlorine was fed to the reactor. The results of one experiment in a batch reactor gave the following results on a molar basis:

Component	Moles Output per Mole of Mixed Feed
p-Xylene	0.001
Chlorine	0.210
Monochloroxylene	0.032
1,4-Dimethyl-2,3-dichlorobenzene	0.131
Other dichloroxylenes	0.227
Trichloroxylene	0.009
Tetrachloroxylenes	0.001
Total	0.611

Compute various measures of reactor performance.

SOLUTION: Write the reaction as A + B → D + 2E where D is the desired dichlorobenzene. Some measures of performance based on xylene as the limiting component are

$$\text{Fraction unreacted} = \frac{a_{out}}{a_{in}} = \frac{0.001}{0.4} = 0.0025$$

$$\text{Conversion} = 1 - \frac{a_{out}}{a_{in}} = 1 - 0.0025 = 0.9975$$

$$\text{Yield} = \frac{d_{out}}{a_{in}} = \frac{0.131}{0.40} = 0.3275 \text{ moles of product per mole xylene charged}$$

$$\text{percent theoretical yield} = \frac{0.131}{0.4}(100) = 32.75\%$$

$$\text{Selectivity} = \frac{0.131}{(0.9975)(0.4)}(100) = 32.83\%$$

This example expresses all the performance measures on a molar basis. The mass yield of 1,4-dimethyl-2,3-dichlorobenzene sounds a bit better. It is 0.541 lb of the desired product per pound of xylene charged.

Note that the performance measures and definitions given here are the typical ones, but other terms and other definitions are sometimes used. Be sure to ask for the definition if there is any ambiguity.

1.4.3 Piston Flow Reactors

Continuous flow reactors are usually preferred for long production runs of high-volume chemicals. They tend to be easier to scale up; they are easier to control; the product is more uniform; material-handling problems are lessened; and the capital cost for the same annual capacity is lower.

There are two important types of ideal continuous flow reactors: the PFR and the CSTR. They behave very differently with respect to conversion and selectivity. The PFR behaves exactly like a batch reactor. It is usually visualized as a long tube, as illustrated in Figure 1.3. Consider a small clump of material that enters the reactor at time $t = 0$ and flows from the inlet to the outlet. We suppose there is no mixing between this particular clump and other clumps that enter at different times. The clump stays together, ages, and reacts as it flows down the tube. After it has been in the PFR for t seconds, the clump will have the same composition as if it had been in a batch reactor for t seconds. The composition of a batch reactor varies with time. The composition of a small clump flowing through a PFR varies with time in the same way. It also varies with position down the tube. The relationship between time and position is

$$t = \frac{z}{\bar{u}} \tag{1.34}$$

where z denotes distance measured from the inlet of the tube and $\bar{u}$ is the velocity of the fluid. Chapter 1 assumes steady-state operation so that the composition at point z is always the same. It also assumes constant fluid density and constant reactor cross section so that $\bar{u}$ is constant. The age of material at point z is t and the composition at this point is given by the constant-volume version of the component balance for a batch reaction, Equation 1.23. All that has to be done is to substitute $t = z/\bar{u}$. The result is

$$\bar{u}\frac{da}{dz} = \mathscr{R}_A \tag{1.35}$$

The initial condition is that

$$a = a_{\text{in}} \quad \text{at } z = 0 \tag{1.36}$$

Only the notation is different from the initial condition used for batch reactors. The subscripts "in" and "out" are used for flow reactors compared to a_0 and $a(t)$ for a batch reactor. The outlet concentration is found by setting $z = L$.

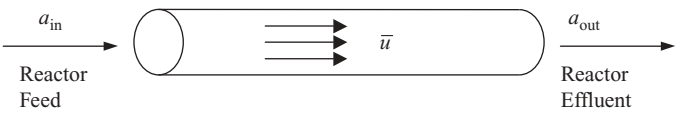

Figure 1.3 Piston flow reactor.

EXAMPLE 1.3

Find the outlet concentration of component A from a PFR assuming A is consumed by a first-order reaction.

SOLUTION: Equation 1.35 becomes

$$\bar{u}\frac{da}{dz} = -ka.$$

Integrating, applying the initial condition of Equation 1.36, and evaluating the result at $z = L$ give

$$a_{\text{out}} = a_{\text{in}} \exp\left(-\frac{kL}{\bar{u}}\right) \tag{1.37}$$

The quantity $L/\bar{u}$ has units of time and is the mean residence time $\bar{t}$. Thus, we can write Equation 1.37 as

$$a_{\text{out}} = a_{\text{in}} \exp(-k\bar{t}) \tag{1.38}$$

where

$$\bar{t} = \frac{L}{\bar{u}} \tag{1.39}$$

Equation 1.39 is a special case of a far more general result. The ***mean*** **residence time** $\bar{t}$ is the average amount of time that a material spends in a reactor. The concept of mean residence time is most useful for flow systems. In a steady-state flow system $\bar{t}$ is equal to the mass inventory of fluid in the system divided by the mass flow rate through the system:

$$\bar{t} = \frac{\text{mass inventory}}{\text{mass throughput}} = \frac{\hat{\rho}V}{\rho Q} \tag{1.40}$$

where $\rho Q = \rho_{\text{out}} Q_{\text{out}} = \rho_{\text{in}} Q_{\text{in}}$ is a consequence of steady-state operation. For the special case of a constant-density fluid,

$$\bar{t} = \frac{V}{Q} \tag{1.41}$$

where $Q = Q_{\text{in}} = Q_{\text{out}}$ when the system is at steady state and the mass density is constant. This reduces to

$$\bar{t} = \frac{L}{\bar{u}} \tag{1.42}$$

for a tubular reactor with constant fluid density and constant cross-sectional area. Piston flow is a still more special case where all molecules have the same velocity and the same residence time. We could write $\bar{t} = L/u$ for piston flow since the velocity is uniform across the tube but prefer to use Equation 1.42 for this case as well.

We now formalize the definition of piston flow. Denote position in the reactor using a cylindrical coordinate system (r, θ, z) so that the concentration at a point is denoted as $a(r, \theta, z)$. For the reactor to be a ***piston flow reactor*** (also called plug flow, slug flow, or ideal tubular reactor), three conditions must be satisfied:

(i) The axial velocity is independent of r and θ but may be a function of z, V_z $(r, \theta, z) = \bar{u}(z)$.

(ii) There is complete mixing across the reactor so that concentration is a function of z alone, that is, $a(r, \theta, z) = a(z)$.

(iii) There is no mixing in the axial direction.

Here in Chapter 1 we make the additional assumptions that the fluid has constant density, that the cross-sectional area of the tube is constant, and that the walls of the tube are impenetrable (i.e., no transpiration through the walls), but these assumptions are not required in the general definition of piston flow. In the general case, it is possible for $\bar{u}$, temperature, and pressure to vary as a function of z. The axis of the tube need not be straight. Helically coiled tubes usually approximate piston flow more closely than straight tubes because the coiling promotes cross-channel mixing. Reactors with square or triangular cross sections are occasionally used. However, in most of this book, we will assume that PFRs are circular tubes of length L and constant radius R.

Application of the general component balance, Equation 1.6, to a steady-state flow system gives

$$Q_{\text{in}}a_{\text{in}} + \hat{\mathscr{R}}_A V = Q_{\text{out}}a_{\text{out}}$$

While true, this result is not helpful. The derivation of Equation 1.6 used the entire reactor as the control volume and produced a result containing the average reaction rate $\hat{\mathscr{R}}_A$. In piston flow, a varies with z so that the local reaction rate also varies with z, and there is no simple way of calculating $\hat{\mathscr{R}}_A$. Equation 1.6 is an overall balance applicable to the entire system. It is also called an ***integral balance.*** It just states that, if more of a component leaves the reactor than enters, then the difference had to be formed inside the reactor.

A ***differential balance*** is written for a vanishingly small control volume within which $\mathscr{R}_A$ is approximately constant. Such a differential balance is needed to derive the design equation for a PFR. The differential volume element has volume ΔV, cross-sectional area A_c, and length Δz. See Figure 1.4. The general component balance applied to this differential volume gives

$$\text{Moles in} + \text{moles formed} = \text{moles out}$$

or

$$Qa(z) + \mathscr{R}_A\ \Delta V = Qa(z + \Delta z)$$

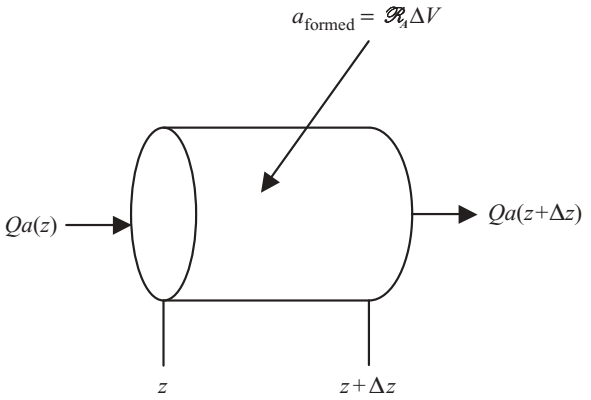

Figure 1.4 Differential element in a PFR.

Note that $Q = \bar{u}A_c$ and $\Delta V = A_c \Delta z$. Then

$$Q\frac{a(z+\Delta z)-a(z)}{\Delta V} = \bar{u}\frac{a(z+\Delta z)-a(z)}{\Delta z} = \mathscr{R}_A$$

Recall the definition of a derivative and take the limit as $\Delta z \to 0$:

$$\lim_{\Delta z \to 0}\left[\bar{u}\frac{a(z+\Delta z)-a(z)}{\Delta z}\right] = \bar{u}\frac{da}{dz} = \mathscr{R}_A \tag{1.43}$$

which agrees with Equation 1.35. Equation 1.35 was derived by applying a variable transformation to an unsteady batch reactor. Equation 1.43 was derived by applying a steady-state component balance to a differential flow reactor. Both methods work for this problem, but differential balances are the more general approach and can be extended to multiple dimensions where concentration can vary with radial and even tangential position. However, the strong correspondence between time in a batch reactor and position in a PFR is very important. The composition at time t in an ideal batch reactor is identical to the composition at position $z = \bar{u}t$ in an ideal PFR. This correspondence, which extends beyond the isothermal, constant-density case, is detailed in Table 1.1.

EXAMPLE 1.4

Determine the reactor design equations for the various elementary reactions in a PFR. Assume constant temperature, constant density, and constant reactor cross section. (Whether or not all these assumptions are needed will be explored in subsequent chapters.)

SOLUTION: Substitute the various rate equations into Equation 1.35 and integrate and apply the initial condition of Equation 1.36. Two versions of these equations can be used for a second-order reaction with two reactants. Another solution technique is to use the results obtained previously for a batch reactor and to replace t with $z/\bar{u}$ and a_0 with a_{in}. The result is $a(z)$ for the various reaction types.

For a first-order reaction,

$$\frac{a(z)}{a_{\text{in}}} = \exp\left(\frac{-kz}{\bar{u}}\right) \tag{1.44}$$

For second order with one reactant,

$$\frac{a(z)}{a_{\text{in}}} = \frac{1}{1 + a_{\text{in}} kz/\bar{u}} \tag{1.45}$$

For second order with two reactants,

$$\frac{a(z)}{a_{\text{in}}} = \frac{b_{\text{in}} - a_{\text{in}}}{b_{\text{in}} \exp[(b_{\text{in}} - a_{\text{in}})\, kz/\bar{u}] - a_{\text{in}}} \tag{1.46}$$

The outlet concentration is found by setting $z = L$. At the reactor outlet, $z/\bar{u} = L/\bar{u} = \bar{t}$.

Piston flow reactors and most other flow reactors have spatial variations in concentration such as $a = a(z)$. Such systems are called ***distributed.*** Their behavior is governed by an ODE when there is only one spatial variable and by a partial differential equation (PDE) when there are two or three spatial variables or when the system has a spatial variation and also varies with time. We turn now to a special type of flow reactor where the entire reactor volume is well mixed and has the same concentration, temperature, pressure, and so forth. There are no spatial variations in

Table 1.1 Relationships between batch and piston flow reactors

Batch Reactors	Piston Flow Reactors
Concentrations vary with time; composition is uniform at any time t	Concentrations vary with axial position; composition is uniform at any position z
Governing equation, 1.23	Governing equation, 1.43
Initial condition, a_0	Initial condition, a_{in}
Final condition, $a(t)$	Final condition, $a(L) = a_{\text{out}}$
Time equivalent to position in PFR, $t = z/\bar{u}$	Position equivalent to time in batch reactor, $z = \bar{u}t$
Variable density, $\rho(t)$	Variable density, $\rho(z)$
Variable temperature, $T(t)$	Variable temperature, $T(z)$
Heat transfer to wall, $dq = hA_{\text{wall}}(T - T_{\text{wall}})\, dt$	Heat transfer to wall, $dq = h(2\pi R)(T - T_{\text{wall}})\, dz$
Variable wall temperature, $T_{\text{wall}}(t)$	Variable wall temperature, $T_{\text{wall}}(z)$
Variable pressure, $P(t)$	Pressure drop, $P(z)$
Variable volume (e.g., constant-pressure reactor), $V(t)$	Variable cross section, $A_c(z)$
Fed-batch reactors, $Q_{\text{in}} \neq 0$	Transpired-wall reactors
Nonideal batch reactors may have spatial variations in concentration	Nonideal tubular reactors may have concentrations that vary in r and θ directions

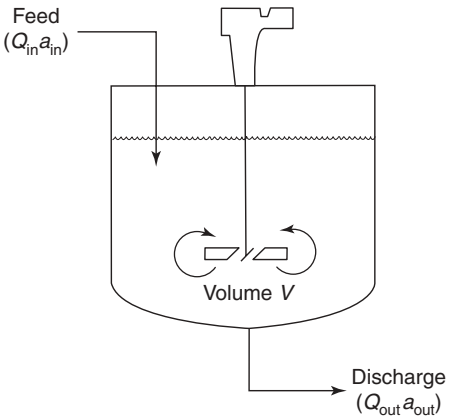

Figure 1.5 Classic CSTR: continuous flow stirred tank reactor with mechanical agitation.

these parameters. Such systems are called ***lumped*** and their behavior is governed by an algebraic equation when the system is at steady state and by an ODE when the system varies with time. The CSTR is the chemical engineer's favorite example of a lumped system. It has one lump, the entire reactor volume.

1.4.4 Continuous Flow Stirred Tanks

Figure 1.5 illustrates a flow reactor in which the contents are mechanically agitated. If mixing caused by the agitator is sufficiently fast, the entering feed will be quickly dispersed throughout the vessel and the composition at any point will approximate the average composition. Thus the reaction rate at any point will be approximately the same. Also, the outlet concentration will be identical to the internal composition, $a_{\text{out}} = \hat{a}$.

There are only two possible values for concentration in a CSTR. The inlet stream has concentration a_{in} and everywhere else has concentration a_{out}. The reaction rate will the same throughout the vessel and is evaluated at the outlet concentration, $\hat{\mathscr{R}}_A = \mathscr{R}_A(a_{\text{out}},\ b_{\text{out}}, \ldots)$. For the single reactions considered in this chapter, $\mathscr{R}_A$ continues to be related to $\mathscr{R}$ by the stoichiometric coefficient and Equation 1.14. With $\mathscr{R}_A$ known, the integral component balance, Equation 1.6, now gives useful information. For component A,

$$Qa_{\text{in}} + \mathscr{R}_A(a_{\text{out}},\ b_{\text{out}}, \ldots)V = Qa_{\text{out}} \tag{1.47}$$

Note that we have assumed steady-state operation and set $Q = Q_{\text{in}} = Q_{\text{out}}$, which assumes constant density. Dividing through by Q and setting $\bar{t} = V/Q$ gives

$$a_{\text{in}} + \mathscr{R}_A(a_{\text{out}},\ b_{\text{out}}, \ldots)\,\bar{t} = a_{\text{out}} \tag{1.48}$$

In the usual case, $\bar{t}$ and a_{in} will be known. Equation 1.48 is an algebraic equation that can be solved for a_{out}. If the reaction rate depends on the concentration of more than one component, versions of Equation 1.48 are written for each component and the resulting set of equations is solved simultaneously for the various outlet concentrations.

Even concentrations of components that do not affect the reaction rate can be found by writing versions of Equation 1.48 for them as well. As in the case of batch and piston flow reactors, the stoichiometric coefficient is used to relate the rate of formation of a component, say $\mathscr{R}_C$, to the rate of the reaction $\mathscr{R}$ using the stoichiometric coefficient for component C, ν_C, and Equation 1.14. After this, the stoichiometry takes care of itself.

A reactor with performance governed by Equation 1.48 is a steady-state, constant-density, perfectly mixed, continuous flow reactor. This mouthful is usually shortened in the chemical engineering literature to ***CSTR*** (for continuous flow stirred tank reactor). In subsequent chapters, we will relax the assumptions of steady state and constant density but will still call it a CSTR. It is also called an ideal mixer, a continuous flow perfect mixer, or a mixed flow reactor. This terminology is ambiguous in light of micromixing theory, discussed in Chapter 13, but is well entrenched. Unless otherwise qualified, we accept the term CSTR to mean that the reactor is perfectly mixed. Such a reactor is sometimes called a ***perfect mixer***. The term denotes instantaneous and complete mixing on the molecular scale. Obviously, no real reactor can achieve this ideal state just as no tubular reactor can achieve true piston flow. However, it is often possible to design reactors that very closely approach these limits.

EXAMPLE 1.5

Determine the reactor design equations for elementary reactions in a CSTR.

SOLUTION: The various rate equations for the elementary reactions are substituted into Equation 1.48, which is then solved for a_{out}.

For a first-order reaction, $\mathscr{R}_A = -ka$. Set $a = a_{\text{out}}$, substitute $\mathscr{R}_A$ into Equation 1.48, and solve for a_{out} to obtain

$$\frac{a_{\text{out}}}{a_{\text{in}}} = \frac{1}{1 + k\bar{t}} \tag{1.49}$$

For a second-order reaction with one reactant, $\mathscr{R}_A = -ka^2$, and Equation 1.48 becomes a quadratic in a_{out}. The solution is

$$\frac{a_{\text{out}}}{a_{\text{in}}} = \frac{-1 + \sqrt{1 + 4a_{\text{in}}k\bar{t}}}{2a_{\text{in}}k\bar{t}} \tag{1.50}$$

The negative root was rejected since $a_{\text{out}} \geq 0$.

For a second-order reaction with two reactants, $\mathscr{R}_A = \mathscr{R}_B = -kab$. Write two versions of Equation 1.48, one for a_{out} and one for b_{out}. Solve them simultaneously to give

$$\frac{a_{\text{out}}}{a_{\text{in}}} = \frac{-1 - (b_{\text{in}} - a_{\text{in}})k\bar{t} + \sqrt{[1 + (b_{\text{in}} - a_{\text{in}})k\bar{t}]^2 + 4a_{\text{in}}k\bar{t}}}{2a_{\text{in}}k\bar{t}} \tag{1.51}$$

Again, a negative root was rejected. The simultaneous solution also produces the stoichiometric relationship

$$b_{\text{in}} - b_{\text{out}} = a_{\text{in}} - a_{\text{out}} \tag{1.52}$$

Any Single Reaction in a CSTR

The above examples have assumed that a_{in} and $\bar{t}$ are known. The solution then gives a_{out}. The case where a_{in} is known and a desired value for a_{out} is specified can be easier to solve. The solution for $\bar{t}$ is

$$\bar{t} = \frac{a_{out} - a_{in}}{\mathscr{R}_A(a_{out}, b_{out,} \ldots)} \tag{1.53}$$

This result assumes constant density and is useful when the reaction rate depends on a single concentration or on multiple concentrations that are linked by a stoichiometric relationship such as Equation 1.52. It is not useful for the general case of multiple reactions.

EXAMPLE 1.6

Apply Equation 1.53 to calculate the mean residence time needed to achieve 90% conversion in a CSTR for (a) a first-order reaction and (b) a second-order reaction of the type A + B → products. The rate constant for a first-order reaction has units of reciprocal time. For the current example, assume $k = 0.1\ s^{-1}$. The rate constant for a second-order reaction has units of reciprocal time and reciprocal concentration. It is common practice to multiply a second-order rate constant by the initial or inlet concentration of the stoichiometrically limiting coefficient. This gives a rate constant with units of reciprocal time. For the second-order reaction suppose $a_{in}k = 0.1\ s^{-1}$.

SOLUTION: For the first-order reaction, $\mathscr{R}_A = -ka_{out} = -k(0.1\ a_{in})$. Equation 1.53 gives

$$\bar{t} = \frac{a_{out} - a_{in}}{-ka_{out}} = \frac{0.1a_{in} - a_{in}}{-k(0.1a_{in})} = \frac{9}{k} = 90\,s$$

For the second-order case, $\mathscr{R}_A = -ka_{out}b_{out}$. To use Equation 1.53, stoichiometry is needed to find the value for b_{out} that corresponds to a_{out}. Suppose, for example, that B is in 50% excess so that $b_{in} = 1.5a_{in}$. Then $b_{out} = 0.6a_{in}$ if $a_{out} = 0.1a_{in}$. Equation 1.53 gives

$$\bar{t} = \frac{a_{out} - a_{in}}{-ka_{out}b_{out}} = \frac{0.1a_{in} - a_{in}}{-k(0.1a_{in})(0.6a_{in})} = \frac{15}{ka_{in}} = 150\,s$$

Equation 1.53 is a beautifully simple way of designing a reactor for the few cases to which it applies. More commonly, the numerical methods introduced in Chapter 2 are needed.

1.5 MIXING TIMES AND SCALEUP

Suppose a homogeneous reaction is conducted in a pilot plant reactor that is equipped with a variable-speed agitator. Does changing the agitator speed (say by ±20%) change the outcome of the reaction? Does varying the addition rate of reactants change the selectivity? If so, there is a potential scaleup problem. The reaction is sensitive

to mixing. If the reaction is multiphase, the agitator speed can affect interphase mass transfer. See Chapter 11. If the reaction is single phase, the reaction is sensitive to the ***mixing time*** t_{mix}.

The mixing time in a batch stirred tank is easily measured. Add unmixed ingredients and determine how long it takes for the contents of the vessel to become uniform. For example, fill a vessel with plain water and start the agitator. At time $t = 0$, add a small quantity of a salt solution. Measure the concentration of salt at various points inside the vessel until it is constant within measurement error or by some other standard of near equality. Record the result as t_{mix}. A popular alternative is to start with a weak-acid solution that contains an indicator so that the solution is initially colored. An excess of concentrated base is added quickly at one point in the system. The mixing time t_{mix} corresponds to the disappearance of the last bit of color. The acid–base titration is very fast so that the color will disappear just as soon as the base is distributed throughout the vessel. This is an example where the reaction in the vessel is limited strictly by mixing. There is no kinetic limitation. For very fast reactions such as combustion or acid–base neutralization, no vessel will be perfectly mixed. The components must be transported from point to point in the vessel by fluid flow and diffusion, and these transport processes will be slower than the reaction. Whether a reactor can be considered to be perfectly mixed depends on the speed of the reaction. What is effectively perfect mixing is easy to achieve when the reaction is an esterification with a half-life of several hours. It is impossible to achieve in acid–base neutralizations that have half-lives of nanoseconds. One requirement for "perfect mixing" is that

$$t_{\text{mix}} \ll t_{1/2} \tag{1.54}$$

This requirement applies to batch reactors and to CSTRs. (For PFRs, we assume that the components are perfectly mixed when they enter the reactor.) When Equation 1.54 is satisfied, the conversion in the reactor will be limited by the reaction kinetics, not by the mixing rate. The assumption of perfect mixing is probably reasonable when $t_{1/2}$ is 8 times larger than t_{mix}.

What happens to t_{mix} upon scaleup? Mixing times in mechanically agitated vessels typically range from a few seconds in laboratory glassware to a few minutes in large industrial reactors. As the size of the vessel increases, t_{mix} will increase, and the increase will eventually limit the size at which the reactor is operable. No process is infinitely scaleable. Sooner or later, additional scaleup becomes impossible, and further increases in production cannot be achieved in ***single-train*** plants but must use units in parallel. Fortunately for the economics of the chemical industry, this size limit is often very large.

Plant sizes are usually characterized by their production capacity or throughput. Define the ***throughput scaleup factor*** as

$$S_{\text{throughput}} = \frac{\text{mass flow through full-scale unit}}{\text{mass flow through pilot unit}} = \frac{(\rho Q)_{\text{full scale}}}{(\rho Q)_{\text{pilot scale}}} \tag{1.55}$$

Assume that the pilot-scale and full-scale vessels operate with the same inlet density. Then ρ cancels in Equation 1.55 and

$$S_{\text{throughput}} = \frac{Q_{\text{full scale}}}{Q_{\text{pilot scale}}} \quad \text{(constant density)}$$

There is also an inventory scaleup factor defined as

$$S_{\text{inventory}} = \frac{\text{mass inventory in full-scale unit}}{\text{mass inventory in pilot unit}} = \frac{(\hat{\rho} V)_{\text{full scale}}}{(\hat{\rho} V)_{\text{pilot scale}}} \tag{1.56}$$

For successful scaleup we expect the volume-average density $\hat{\rho}$ to be the same in the large and small reactors. Thus, normally,

$$S_{\text{inventory}} = S_{\text{volume}} = \frac{V_{\text{full scale}}}{V_{\text{pilot scale}}} \tag{1.57}$$

This book deals with the scaleup of chemical reactors. The product from the scaled-up reactor should be the same as the product from the pilot reactor. The extent of reaction should be the same in the two reactors and thus the mean residence time $\bar{t}$ should held constant upon scaleup. According to Equation 1.40, inventory and throughput are increased by the same factor when $\bar{t}$ is held constant. Unless explicitly stated otherwise, it is understood that inventory, volume, and throughput all increase proportionately:

$$S_{\text{throughput}} = S_{\text{inventory}} = S_{\text{volume}} = S \tag{1.58}$$

Use of S without subscripts indicates that Equation 1.58 is satisfied. This is true for the great majority of reactor scaleups for both liquids and gases.

It is common practice to use ***geometric similarity*** in the scaleup of stirred tanks (but not tubular reactors). Geometric similarity means that the production-scale reactor will have the same shape as the pilot-scale reactor. All linear dimensions such as reactor diameter, impeller diameter, and liquid height will change by the same factor, $S^{1/3}$. Surface areas will scale as $S^{2/3}$. Now, what happens to t_{mix} upon scaleup? A classic correlation by Norwood and Metzner (1960) for turbine impellers in baffled vessels can be used to estimate t_{mix}. The full correlation shows t_{mix} to be a complex function of the Reynolds number, the Froude number, the ratio of tank to impeller diameter, and the ratio of tank diameter to liquid level. However, to a reasonable first approximation for geometrically similar vessels operating at high Reynolds numbers,

$$(N_I t_{\text{mix}})_{\text{large}} = \text{const} = (N_I t_{\text{mix}})_{\text{small}} \tag{1.59}$$

where N_I is the rotational velocity of the impeller. This means that scaleup with constant agitator speed will, to a reasonable approximation, give constant t_{mix}. The rub is that the power requirements for the agitator will increase sharply in the larger vessel. To a reasonable first approximation for geometrically similar vessels operating at high Reynolds numbers,

$$\left(\frac{P_I}{\rho N_I^3 D_I^5}\right)_{\text{large}} = \left(\frac{P_I}{\rho N_I^3 D_I^5}\right)_{\text{small}} = \mathbf{Po} \tag{1.60}$$

where P_I is the impeller power, D_I is the impeller diameter, and **Po** is a dimensionless group known as the ***power number***. If N_I is held constant, the impeller power will increase as D_I^5 and as $S^{5/3}$since D_I scales as $S^{1/3}$ using geometric similarity. A factor of 10 increase in the linear dimensions gives $S = 1000$ and allows a factor of 1000 increase in throughput. Unfortunately, it requires a factor of 100,000 increase in agitator power! The horsepower per unit volume must increase by a factor of 100 to maintain a constant t_{mix}. Let us hope that there is some latitude before the constraint of Equation 1.54 is seriously violated. Most scaleups are done with approximately constant power per unit volume, which causes N_I to decrease and t_{mix} to increase upon scaleup.

EXAMPLE 1.7

A factor of 10 scaleup in the linear dimensions of a CSTR, $S^{1/3} = 10$, requires a factor of 100,000 increase in total power and a factor of 100 increase in power per unit volume if t_{mix} is held constant. Such a scaleup would be absurd. A more reasonable scaleup rule is to maintain constant power per unit volume so that a 1000-fold increase in reactor volume requires a 1000-fold increase in power. What happens to t_{mix} in this case?

SOLUTION: Rearrange Equation 1.60 to give

$$\frac{(\text{Power})_{\text{large}}}{(\text{Power})_{\text{small}}} = \frac{\left(\rho N_I^3 D_I^5\right)_{\text{large}}}{\left(\rho N_I^3 D_I^5\right)_{\text{small}}}$$

Divide both sides by D_{tank}^3 to obtain power per unit volume:

$$\frac{(\text{Power per unit volume})_{\text{large}}}{(\text{Power per unit volume})_{\text{small}}} = \frac{\left(\rho N_I^3 D_I^5 / D_{\text{tank}}^3\right)_{\text{large}}}{\left(\rho N_I^3 D_I^5 / D_{\text{tank}}^3\right)_{\text{small}}}$$

Cancel out density, set the ratio of powers to 1, and note that D_I and D_{tank} scale by the same factor, $S^{1/3}$, for a geometrically similar scaleup. The result is

$$1 = \frac{\left(N_I^3 D_I^2\right)_{\text{large}}}{\left(N_I^3 D_I^2\right)_{\text{small}}} = \frac{\left(N_I^3\right)_{\text{large}}}{\left(N_I^3\right)_{\text{small}}} S^{2/3}$$

or

$$\frac{(N_I)_{\text{large}}}{(N_I)_{\text{small}}} = S^{-2/9}$$

For constant power per unit volume with a factor of 10 scaleup in linear dimensions, the agitator speed in the large reactor must be $10^{-2/9} = 0.6$ times that in the small reactor. If the small reactor operated at 100 revolutions per minute (RPM), the large reactor should operate at 60 RPM. What does this do to t_{mix}? Rearrange Equation 1.59 to obtain

$$\frac{(t_{\text{mix}})_{\text{large}}}{(t_{\text{mix}})_{\text{small}}} = \frac{(N_I)_{\text{small}}}{(N_I)_{\text{large}}}$$

For the case at hand, the mixing time increases by a factor of 1.67. Is Equation 1.54 still satisfied? Decreasing the speed of the pilot agitator to 60% of its initial value can experimentally test this.

Is the product still good? If so, scaleup should be possible from the viewpoint of mixing time. If not, a departure from geometric similarity, say by using multiple injection points for added ingredients, may solve the problem. The use of multiple injection points can be tested on the pilot scale. The logic assumes that the pilot reactor with a single injection point gave a good product. Determine t_{mix} for this original configuration. Then add injection points to the pilot reactor. Presumably, this will cause little change in product quality. Measure t_{mix} in the new configuration. Given simultaneous injection through all the ports, t_{mix} should be lower than the original value. Estimate what it will become upon scaleup, again using Equation 1.59. If the scaled value of t_{mix} remains smaller than the original t_{mix} (before adding injection points), then scaleup of the multiple-point design should be satisfactory. The reader will appreciate that scaleup is sometimes more engineering art than rigorous science.

Several caveats should be mentioned at this point. When there are multiple reactions, the half-life in Equation 1.54 is the shortest half-life that affects yield and selectivity. In complex reaction schemes, there may be some important fast reactions that are mixing dependent even thought the overall reaction is slow. An example is a catalyst that may react with itself if not rapidly diluted. Equations 1.59 and 1.60 are approximations that are reasonable for turbine agitators in stirred tanks at high Reynolds numbers. Many detailed correlations are available in the literature and should be used if the reaction is at all sensitive to mixing effects. This can be tested at the pilot scale by varying agitator speed. Mixing experts may recommend scaleups other than constant power per unit volume. Scaleup limitations other than mixing time are common. Heat transfer is a common limitation and is discussed in Chapter 5. The reader interested in agitator design should look at Problem 1.17 and then go to the cited literature.

In a batch vessel, the question of good mixing will arise at the start of the batch and whenever an ingredient is added to the batch. The component balance, Equation 1.22, assumes that uniform mixing is achieved before any appreciable reaction occurs. This will be true if Equation 1.54 is satisfied. Consider the same vessel being used as a CSTR. Now, the mixing time must be short compared to the mean residence time, else newly charged material could flow out of the reactor before being thoroughly mixed with the contents. A new condition to be satisfied is

$$t_{mix} \ll \bar{t} \tag{1.61}$$

In practice, Equation 1.61 will be satisfied if Equation 1.54 is satisfied since a CSTR will normally operate with $t_{1/2} \ll \bar{t}$.

The net flow though the reactor will be small compared to the circulating flow caused by the agitator. The existence of the throughput has little influence on the mixing time so that mixing time correlations for batch vessels can be used for CSTRs as well.

In summary, we have considered three characteristic times associated with a CSTR: t_{mix}, $t_{1/2}$, and $\bar{t}$. Treating the CSTR as a perfect mixer is reasonable provided t_{mix} is substantially shorter than the other characteristic times.

1.6 DIMENSIONLESS VARIABLES AND NUMBERS

Equation 1.35 governs the performance of an ideal PFR:

$$\bar{u}\frac{da}{dz} = \mathscr{R}_A \qquad a = a_{\text{in}} \quad \text{at } z = 0 \tag{1.62}$$

where for a circular tube $\bar{u} = Q/(\pi R^2)$ and for a first-order reaction $\mathscr{R}_A = -ka$. Reactor performance depends on many dimensioned parameters that can be manipulated by the designer or the experimentalist to change the response of the system, $a_{\text{out}} = a(L)$. The tube radius R and reactor length L would normally be considered ***design variables*** while the volumetric flow rate Q, rate constant k (which can be changed using temperature or catalyst concentration), and inlet concentration a_{in} (which can be changed with diluents) would be considered ***operating variables.*** The distinction between design and operating variable is not absolute. The operator of an industrial reactor may have no freedom to change the flow rate, but the operator of a pilot reactor may be able to quickly change the reactor length.

The response of the system, a_{out}, depends on at least five potentially manipulatable parameters (Q, R, L, k, a_{in}), and a plot showing the dependence of a_{out} would need an impossible six dimensions. However, the solution to Equation 1.62 can be written as

$$\frac{a_{\text{out}}}{a_{\text{in}}} = \exp(-k\bar{t}) \tag{1.63}$$

There are only two variables, $a_{\text{in}}/a_{\text{out}}$ and $k\bar{t}$, so an ordinary two-dimensional graph can be used.

A dramatic reduction in dimensionality is often possible by converting a design equation from dimensioned to dimensionless form. Equation 1.62 contains the dependent variable a and the independent variable z. The process begins by selecting characteristic values for these variables. By "characteristic value" we mean some known parameter that has the same dimensions as the variable and that characterizes the system. For a PFR, the variables are concentration and length. A characteristic value for concentration is a_{in} and a characteristic value for length is L. These are used to define the dimensionless variables $a^* = a/a_{\text{in}}$ and $\mathscr{z} = z/L$. The governing equation for a first-order reaction in an ideal PFR becomes

$$\frac{da^*}{d\mathscr{z}} = \frac{L}{\bar{u}}\mathscr{R}_A = \frac{-Lka}{\bar{u}a_{\text{in}}} = -k\bar{t}a^* = -k^*a^* \tag{1.64}$$

which is subject to the initial condition that $a^* = 1$ at $\mathscr{z} = 0$. The outlet concentration is found from the solution of Equation 1.64 evaluated at $\mathscr{z} = 1$. The result is identical to Equation 1.63. The product $k^* = k\bar{t}$ is the ***dimensionless first-order rate constant***. Here, $k^* = k\bar{t}$ can be changed by changing any of Q, R, L, or k, but it is only their composite value in the form of k^* that determines reactor performance as measured by the ***dimensionless outlet concentration***, $a_{\text{out}}/a_{\text{in}}$.

EXAMPLE 1.8

Find the equivalent to Equation 1.63 for second-order reactions.

SOLUTION: Begin with the case of one reactant, 2A → kC. The same variable transformations are used for a and z to give

$$\frac{da^*}{d\mathcal{Z}} = \frac{L}{\bar{u}}\mathscr{R}_A = \frac{-2k\bar{t}a^*}{a_{\text{in}}} = -2a_{\text{in}}k\bar{t}(a^*)^2 \qquad a' = 1 \quad \text{at } \mathcal{Z} = 0$$

The solution is

$$\frac{a_{\text{out}}}{a_{\text{in}}} = \frac{1}{1 + 2a_{\text{in}}\,k\bar{t}} = \frac{1}{1 + 2k^*}$$

where $k^* = a_{\text{in}}k\bar{t}$ is the dimensionless rate constant for a second-order reaction.

For the two-reactant case, A + B → kC, with perfect stoichiometry, the result is

$$\frac{a_{\text{out}}}{a_{\text{in}}} = \frac{1}{1 + a_{\text{in}}k\bar{t}} = \frac{1}{1 + k^*}$$

Note that the factor of 2 could have been included in the definition of k^* for the single-reactant case, but the results as given remind us that 2 moles of A are consumed to form each mole of C in the single-reactant case.

The other results for ideal flow reactors can be put into dimensionless form almost by inspection. For example, the results for a CSTR, Equations 1.49 and 1.50, are already in dimensionless form.

The conversion of the design equation for a batch reactor to dimensionless form is somewhat artificial since there is no natural time constant analogous to $\bar{t}$ that characterizes the reactor. A batch reaction can be continued indefinitely simply by running the reaction longer. A PFR has a natural time constant $\bar{t} = L/\bar{u}$, but there is nothing that prevents increasing the reactor length, thereby continuing the reaction. For a batch reactor, pick some arbitrary value for t_{batch} as a characteristic time. Then the treatment of batch reactors becomes identical to that for PFRs when kt_{batch} replaces $k\bar{t}$.

Consider now the more general rate equation

$$\mathscr{R} = ka^m b^n$$

The two concentration variables, a and b, are made dimensionless using the same characteristic value, a_{in}, so that $a^* = a/a_{\text{in}}$ and $b^* = b/a_{\text{in}}$. Choose A so that it is the stoichiometrically limiting reactant. If the reaction is A + B → products, then $a^* = 1$ and $b^* \geq 1$ at $t = 0$ or $z = 0$. The result of converting to dimensionless form is

$$\frac{\bar{t}\mathscr{R}}{a_{\text{in}}} = k\bar{t}a_{\text{in}}^{m+n-1}(a^*)^m(b^*)^n = k^*(a^*)^m(b^*)^n$$

where $k^* = k\bar{\imath}a_{\text{in}}^{m+n-1}$ is the dimensionless rate constant for this $(m + n)$-order reaction. The restriction that m and n be integers is removed in Chapter 2.

Table 1.2 summarizes the design equations for elementary reactions in ideal reactors. Note that component A is the only component or else is the stoichiometrically limiting component. Thus $a^* = a/a_0$ for batch reactions and $a^* = a/a_{\text{in}}$ for flow reactors and $Y_A = a^*$ in both cases. For the case of a second-order reaction with two reactants, the stoichiometric ratio is also needed:

$$S_{AB} = \frac{a_0}{b_0} \leq 1 \qquad \text{or} \qquad S_{AB} = \frac{a_{\text{in}}}{b_{\text{in}}} \leq 1 \tag{1.65}$$

1.7 BATCH VERSUS FLOW AND TANK VERSUS TUBE

Some questions that arise early in a design are: Should the reactor be batch or continuous? If continuous, is the goal to approach piston flow or perfect mixing?

For producing high-volume chemicals, flow reactors are usually preferred. The ideal PFR exactly duplicates the kinetic behavior of the ideal batch reactor, and the reasons for preferring one over the other involve secondary considerations such as heat and mass transfer, ease of scaleup, and the logistics of materials handling. For small-volume chemicals, the economics usually favor batch reactors. This is particularly true when general-purpose equipment can be shared between several products. Batch reactors are used for the greater number of products and produce products of higher economic value. Note that most pharmaceutical products are made in batch processes. Flow reactors are typically used for the commodity products of the petrochemical industry. They produce the overwhelmingly larger volume as measured in tons, but these tons have a lower economic value than the myriad specialty chemicals and pharmaceuticals made in batch processes.

Flow reactors are operated continuously, that is, at steady state with reactants continuously entering the vessel and with products continuously leaving. Batch reactors are operated discontinuously. A batch reaction cycle has periods for charging, reaction, and discharging. The continuous nature of a flow reactor lends itself to larger productivities and greater economies of scale than the cyclic operation of a batch reactor. The volume productivity (moles of product per unit volume of reactor) for batch systems is identical to that of PFRs and is higher than most real flow reactors. However, this volume productivity is achieved only when the reaction is actually occurring and not when the reactor is being charged or discharged, being cleaned, and so on. Within the class of flow reactors, piston flow is usually desired for reasons of productivity and selectivity. However, there are instances where a close approach to piston flow is infeasible or where a superior product results from the special reaction environment possible in stirred tanks.

Although they are both flow reactors, there are large differences in the behavior of PFRs and CSTRs. Reaction rates decrease as the reactants are consumed (autocatalytic reactions are an exception). In piston flow, the reactant concentration gradually declines with increasing axial position. The local rate is higher at the reactor inlet

Table 1.2 Design equations for elementary reactions in ideal reactors

Elementary Reaction	Dimensionless Rate Constant	Design Equation for Piston Flow or Batch Reactors	Design Equation for CSTR
First order: $A \xrightarrow{k} P$ $\mathscr{R}_A = -ka$	$k^* = k\bar{t}$ or $k^* = kt_{batch}$	$\frac{a_{out}}{a_{in}} = \exp(-k^*)$	$\frac{a_{out}}{a_{in}} = \frac{1}{1+k^*}$
Second order, one reactant: $2A \xrightarrow{k/2} P$ $\mathscr{R}_A = -ka^2$	$k^* = a_{in}k\bar{t}$ or $k^* = a_0 kt_{batch}$	$\frac{a_{out}}{a_{in}} = \frac{1}{1+k^*}$	$\frac{a_{out}}{a_{in}} = \frac{-1+\sqrt{1+4k^*}}{2k^*}$
Second order, two reactants: $A + B \xrightarrow{k} P$ $\mathscr{R}_A = -kab$	Same as second-order, one-reactant case but supplemented by stoichiometric ratio S_{AB}	$\frac{a_{out}}{a_{in}} = \frac{1-S_{AB}}{\exp[(1-S_{AB})k^*/S_{AB}] - S_{AB}}$ where $S_{AB} = \frac{a_{in}}{b_{in}}$ or $S_{AB} = \frac{a_0}{b_0}$	$\frac{a_{out}}{a_{in}} = \frac{-1-(1-S_{AB})k^*/S_{AB} + \sqrt{\left[1+(1-S_{AB})k^*/S_{AB}\right]^2 + 4k^*}}{2k^*}$
Third order, one reactant: $3A \xrightarrow{k/3} P$ $\mathscr{R}_A = -ka^3$	$k^* = a_{in}^2 k\bar{t}$ or $k^* = a_0^2 kt_{batch}$	$\frac{a_{out}}{a_{in}} = \frac{1}{\sqrt{1+2K}}$	There is an analytical solution to the cubic equation $k^*(a^*)^3 + a^* - 1 = 0$, but numerical solutions are easier to evaluate; See Chapter 2

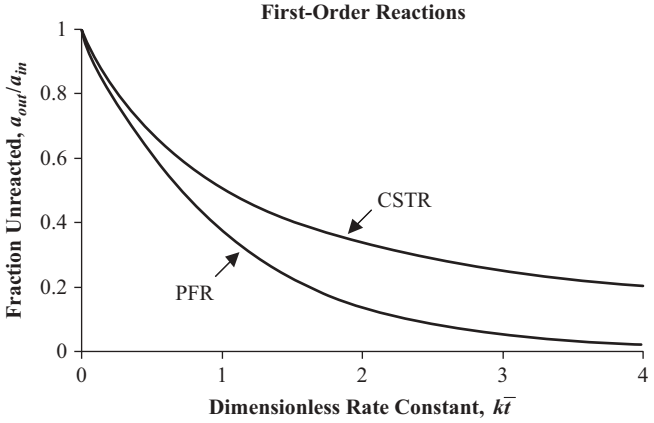

Figure 1.6 Relative performance of piston flow and continuous stirred tank reactors for first-order reactions.

than at the outlet, and the average rate for the entire reactor will correspond to some average composition that is between a_{in} and a_{out}. In contrast, the entire volume of a CSTR is at concentration a_{out}, and the reaction rate throughout the reactor is lower than that at any point in a PFR going to the same conversion.

Figures 1.6 and 1.7 display the conversion behavior for first- and second-order reactions in a CSTR and contrast the behavior to that of a PFR. It is apparent that a PFR is substantially better than the CSTR for obtaining high conversions. The comparison is even more dramatic when made in terms of the volume needed to achieve a given conversion (Fig. 1.8). The generalization that

Conversion in PFR > conversion in CSTR

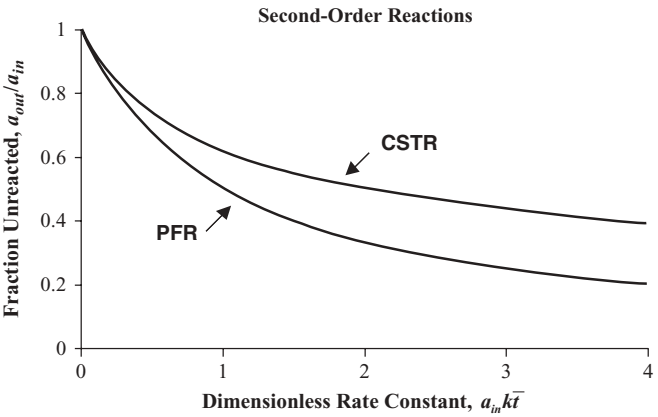

Figure 1.7 Relative performance of piston flow and continuous stirred tank reactors for second-order reactions.

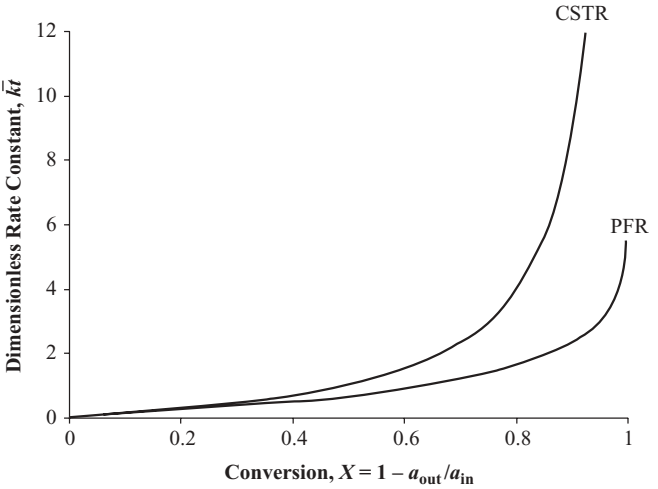

Figure 1.8 Comparison of reactor volume required for given conversion for a first-order reaction in PFR and CSTR.

is true for most kinetic schemes. The important exceptions to this rule, autocatalytic reactions, are discussed in Chapter 2. A second generalization is

$$\text{Selectivity in PFR} > \text{selectivity in CSTR}$$

which also has a few exceptions.

SUGGESTED FURTHER READINGS

There are many books on chemical engineering kinetics, and the reader may wish to browse through several of them to see how they introduce the subject. Most of them are intended for the introductory, undergraduate course. Here are two examples primarily aimed at the U.S. market:

O. Levenspiel, *Chemical Reaction Engineering*, 3rd ed., Wiley, New York, 1998.

L. D. Schmidt, *The Engineering of Chemical Reactions*, 2nd ed., Oxford University Press, New York, 2004.

Here is an example primarily aimed at the U.K. market:

M. B. King and M. B. Winterbottom, *Reactor Design for Chemical Engineers*, Chapman & Hall, London, 1998.

A relatively advanced book primarily used for graduate courses is:

F. Froment and K. B. Bischoff, *Chemical Reactor Analysis and Design*, 2nd ed., Wiley, New York, 1990.

An extended treatment of material balance equations with substantial emphasis on component balances in reacting systems is given in:

G. V. Reklaitis and D. R. Schneider, *Introduction to Material and Energy Balances*, Wiley, New York, 1983.

See also:

R. M. Felder and R. W. Rousseau, *Elementary Principles of Chemical Processes*, 3rd ed., Wiley, New York, 2000.

A general reference on mixing, especially in stirred tank reactors is:

E. L. Paul et al., *Handbook of Industrial Mixing*, Wiley, New York, 2003.

PROBLEMS

1.1 **(a)** Write the overall and component mass balances for an unsteady, perfectly mixed, continuous flow reactor.

(b) Simplify for the case of constant reactor volume and for constant-density, time-independent flow streams.

(c) Suppose there is no reaction but that the input concentration of some key component varies with time according to $C_{in} = C_0$, $t < 0$; $C_{in} = 0$, $t > 0$. Find $C_{out}(t)$.

(d) Repeat (c) for the case where the key component is consumed by a first-order reaction with rate constant k.

1.2 The homogeneous gas phase reaction

$$NO + NO_2Cl \rightarrow NO_2 + NOCl$$

is believed to be elementary with rate $\mathscr{R} = k[NO][NO_2Cl]$. Use the kinetic theory of gases to estimate f_R at 300 K. Assume $r_A + r_B = 3.5 \times 10^{-10}$ m. The experimentally observed rate constant at 300 K is $k = 8\ m^3\ mol^{-1}\ s^{-1}$.

1.3 Determine the initial half-life for an elementary, second-order reaction for which $a_0 < b_0$. Note that the half-life should be based on the stoichiometrically limiting component, A.

1.4 The data in Example 1.2 are in moles of the given component per mole of mixed feed. These are obviously calculated values. Check their consistency by using them to calculate the feed composition given that the feed contained only *para*-xylene and chlorine. Is your result consistent with the stated molar composition of 40% xylene and 60% chlorine?

1.5 Suppose that the following reactions are elementary. Write rate equations for the reaction and for each of the components:

(a) $2A \underset{k_r}{\overset{k_f}{\rightleftharpoons}} B + C$

(b) $2A \underset{k_r}{\overset{k_f/2}{\rightleftharpoons}} B + C$

(c) $B + C \underset{k_f}{\overset{k_r}{\rightleftharpoons}} 2A$

(d) $2A \xrightarrow{K_I} B + C$

$B + C \xrightarrow{K_{II}} 2A$

1.6 Determine $a(t)$ for a first-order, reversible reaction

$$\mathrm{A} \underset{k_r}{\overset{k_f}{\rightleftharpoons}} \mathrm{B}$$

in a batch reactor.

1.7 Compare $a(z)$ for a first- and second-order reaction in a PFR. Plot the profiles on the same graph and arrange the rate constants so that the initial and final concentrations are the same for the two reactions.

1.8 Equation 1.44 gives the spatial distribution of concentration, $a(z)$, in a PFR for a component that is consumed by a first-order reaction. The local concentration can be used to determine the local reaction rate $\mathscr{R}_A(z)$.

(a) Integrate the local reaction rate over the length of the reactor to determine $\hat{\mathscr{R}}_A$.

(b) Show that this $\hat{\mathscr{R}}_A$ is consistent with the general component balance, Equation 1.6.

(c) To what value of a does rate $\hat{\mathscr{R}}_A$ correspond?

(d) At what axial position does this average value occur?

(e) Now integrate a down the length of the tube. Is this spatial average the same as the average found in part (c)?

1.9 One type of (supposedly) third-order reaction is $2\mathrm{A} + \mathrm{B} \xrightarrow{k/2} \mathrm{C}$. Determine the fraction unreacted of component A in an ideal batch reactor.

1.10 Consider the reaction

$$\mathrm{A} + \mathrm{B} \xrightarrow{k} \mathrm{P}$$

with $k = 1\ \mathrm{m^3\ mol^{-1}\ s^{-1}}$. Suppose $b_{\mathrm{in}} = 10\ \mathrm{mol\ m^{-3}}$. It is desired to achieve $b_{\mathrm{out}} = 0.01\ \mathrm{mol\ m^{-3}}$.

(a) Find the mean residence time needed to achieve this assuming piston flow and $a_{\mathrm{in}} = \mathrm{b_{in}}$.

(b) Repeat (a) assuming that the reaction occurs in a CSTR.

(c) Repeat (a) and (b) assuming $a_{\mathrm{in}} = 10\ b_{\mathrm{in}}$.

1.11 The esterification reaction

$$\mathrm{RCOOH} + \mathrm{R'OH} \underset{k_r}{\overset{k_f}{\rightleftharpoons}} \mathrm{RCOOR'} + \mathrm{H_2O}$$

can be driven to completion by removing the water of condensation. This might be done continuously in a stirred tank reactor or in a horizontally compartmented, progressive flow reactor. This type of reactor gives a reasonable approximation to piston flow in the liquid phase while providing a vapor space for the removal of the byproduct water. Suppose it is desired to obtain an ester product containing not more than 1% (by mole) residual alcohol and 0.01% residual acid.

(a) What are the limits on initial stoichiometry if the product specifications are to be achieved?

(b) What value of $a_{\mathrm{out}} k\bar{t}$ is needed in a CSTR?

(c) What value of $a_{\mathrm{out}} k\bar{t}$ is needed in the progressive reactor?

(d) Discuss the suitability of a batch reactor for this situation.

1.12 Can an irreversible elementary reaction go to completion in a batch reactor in finite time?

1.13 An evil young professor was worried about getting tenure. He thought his chances would be better if he eliminated the competition, an untenured colleague who happened to be a beautiful princess who had a lab next to his and was arguably better at both research and teaching than the evil professor. The evil professor has heard about TNT and decided to make some and use it in diabolical ways. He began by writing a simplified but plausible reaction mechanism, including appropriate rate expressions, for the toluene nitration. He then charged toluene, nitric acid, and sulfuric acid (as a catalyst) to a small reactor and carefully monitored the results. He was surprised to observe that the rates of even the first nitration steps increased with increasing agitator speed. The mixing times in the vessel were very short compared to the reaction time even at the slowest agitator speed, and the reactor temperature was closely controlled. What is a plausible reaction mechanism and what is a reason for the evil professor's unexpected results? He asked his colleague, and she suggested he read at least the title of Chapter 11.

1.14 The reaction of trimethylamine with *n*-propyl bromide gives a quaternary ammonium salt:

$$N(CH_3)_3 + C_3H_7Br \rightarrow (CH_3)_3(C_3H_7)NBr$$

Suppose laboratory results at 110°C using toluene as a solvent show the reaction to be second order with rate constant $k = 5.6 \times 10^{-7}$ m^3 mol^{-1} s^{-1}. Suppose $[N(CH_3)_3]_0 = [C3H7Br]_0 = 80$ mol m^{-3}.

(a) Estimate the time required to achieve 99% conversion in a batch reactor.

(b) Estimate the volume required in a CSTR to achieve 99% conversion if a production rate of 100 kg h^{-1} of the salt is desired.

(c) Suggest means for increasing the productivity, that is, reducing the batch reaction time or the volume of the CSTR.

1.15 Ethyl acetate can be formed from dilute solutions of ethanol and acetic acid according to the reversible reaction

$$C_2H_5OH + CH_3COOH \rightarrow C_2H_5OOCCH_3 + H_2O$$

Ethyl acetate is somewhat easier to separate from water than either ethanol or acetic acid. For example, the relatively large acetate molecule has much lower permeability through a membrane ultrafilter. Thus esterification is sometimes proposed as an economical approach for recovering dilute fermentation products. Suppose fermentation effluents are available as separate streams containing 3% by weight acetic acid and 5% by weight ethanol. Devise a reaction scheme for generating ethyl acetate using the reactants in stoichiometric ratio. After reaction, the ethyl acetate concentration is increased first to 25% by weight using ultrafiltration and then to 99% by weight using distillation. The reactants must ultimately be heated for the distillation step. Thus we can suppose both the esterification and membrane separation to be conducted at 100°C. At this temperature,

$$k_f = 8.0 \times 10^{-9}\ \text{m}^3\ \text{mol}^{-1}\ \text{s}^{-1} \qquad k_r = 2.7 \times 10^{-9}\ \text{m}^3\ \text{mol}^{-1}\ \text{s}^{-1}$$

Determine $\bar{t}$ and a_{out} for a CSTR that approaches equilibrium within 5%, that is,

$$\frac{a_{\text{out}} - a_{\text{equil}}}{a_{\text{in}} - a_{\text{equil}}} = 0.05.$$

1.16 Rate expressions for gas phase reactions are sometimes based on partial pressures. Smith (1956, p. 131) gives $k = 1.1 \times 10^{-3}$ mol cm^{-3} atm^{-2} h^{-1} for the reaction of gaseous sulfur with methane at 873 K:

$$CH_4 + 2S_2 \rightarrow CS_2 + 2H_2S$$

where $\mathscr{R} = k P_{CH_4} P_{S_2}$, mol cm^{-3} h^{-1}. Determine k when the rate is based on concentrations: $\mathscr{R} = k[CH_4][S_2]$. Give k in SI units.

1.17 You have a flat-bottomed reactor with 1 m internal diameter that operates with a 1-m liquid level. It is agitated by a six-bladed, pitched turbine that is located 0.5 m above the reactor bottom. Paul et al. (2003) give $\mathbf{Po} = 1.3$ provided the vessel Reynolds number $\mathbf{Re} = \rho D_I^2 N_I / \mu$ is larger than about 500. The mixing time under these conditions is given by $\mathbf{Po}^{1/3} N_I t_{mix} (D_I / D_{tank})^2 = 5.2$, where d_t is the tank diameter. You wish to achieve a mixing time of 30 s with a waterlike liquid. What RPM should you use and how much power will be needed?

1.18 A second-order reaction of the type 2A→B reacts to 90% completion when the reactor in Problem 1.17 is operated with a batch reaction time of 1 h. It is proposed to operate it as a CSTR. What is the mean residence time needed to achieve 90% conversion in the continuous mode of operation?

Chapter 2

Multiple Reactions in Batch Reactors

Chapter 1 treated single, elementary reactions in ideal reactors. This chapter broadens the kinetics to include multiple and nonelementary reactions. Attention is restricted to batch reactors, but the method for formulating the kinetics of complex reactions will also be used for the flow reactors of Chapters 3 and 4 and for the nonisothermal reactors of Chapter 5.

The most important characteristic of an ideal batch reactor is that the contents are perfectly mixed. Corresponding to this assumption, the component balances are ODEs. The reactor operates at constant mass between filling and discharge steps. These steps are assumed to be fast compared to reaction half-lives and the batch reaction times. Chapter 1 made the further assumption of constant mass density, so that the working volume of the reactor was constant, but this chapter relaxes this assumption.

2.1 MULTIPLE AND NONELEMENTARY REACTIONS

Multiple reactions involve two or more stoichiometric equations, each with its own rate expression. An example of a ***consecutive*** reaction is

$$\begin{aligned} \mathrm{A} + \mathrm{B} &\xrightarrow{k_\mathrm{I}} \mathrm{C} \qquad \mathscr{R}_\mathrm{I} = k_\mathrm{I} ab \\ \mathrm{C} + \mathrm{D} &\xrightarrow{k_\mathrm{II}} \mathrm{E} \qquad \mathscr{R}_\mathrm{II} = k_\mathrm{II} cd \end{aligned} \tag{2.1}$$

Here, component C is formed by reaction I and consumed by reaction II.

An example of a ***competitive*** reaction is

$$\begin{aligned} \mathrm{A} + \mathrm{B} &\xrightarrow{k_\mathrm{I}} \mathrm{C} \qquad \mathscr{R}_\mathrm{I} = k_\mathrm{I} ab \\ \mathrm{A} + \mathrm{D} &\xrightarrow{k_\mathrm{II}} \mathrm{E} \qquad \mathscr{R}_\mathrm{II} = k_\mathrm{II} ad \end{aligned} \tag{2.2}$$

Component A is consumed by both reactions but the products are different. Typically, only one of the products is desired. The fraction unreacted for component A, $Y_A = a(t)/a_0$, provides no measure of selectivity. Instead, measures such as yield,

Chemical Reactor Design, Optimization, and Scaleup, Second Edition. By E. B. Nauman
Copyright © 2008 John Wiley & Sons, Inc.

$c(t)/a_0$, are needed, and the reaction engineer has the opportunity to optimize the reaction.

An example of ***completely independent*** reactions is

$$\begin{aligned} \mathrm{A} &\xrightarrow{k_\mathrm{I}} B & \mathscr{R}_\mathrm{I} &= k_\mathrm{I} a \\ \mathrm{C} + \mathrm{D} &\xrightarrow{k_\mathrm{II}} E & \mathscr{R}_\mathrm{II} &= k_\mathrm{II} cd \end{aligned} \tag{2.3}$$

Even ***reversible*** reactions can be regarded as multiple:

$$\begin{aligned} \mathrm{A} + \mathrm{B} &\xrightarrow{k_\mathrm{I}} \mathrm{C} & \mathscr{R}_\mathrm{I} &= k_\mathrm{I} ab \\ \mathrm{C} &\xrightarrow{k_\mathrm{II}} \mathrm{A} + \mathrm{B} & \mathscr{R}_\mathrm{II} &= k_\mathrm{II} c \end{aligned} \tag{2.4}$$

Note that the Roman numeral subscripts refer to numbered reactions and have nothing to do with iodine.

2.1.1 Reaction Mechanisms

All the examples in Equation 2.1–2.4 assumed the reactions to be elementary. Multiple reactions and apparently single but nonelementary reactions are called ***complex.*** Complex reactions, even when apparently single, consist of a number of elementary steps. These steps, some of which may be quite fast, constitute the ***mechanism*** of the observed, complex reaction. As an example, suppose

$$\begin{aligned} \mathrm{A} &\xrightarrow{k_\mathrm{I}} \mathrm{B} + \mathrm{C} & \mathscr{R}_\mathrm{I} &= k_\mathrm{I} a \\ \mathrm{B} &\xrightarrow{k_\mathrm{II}} \mathrm{D} & \mathscr{R}_\mathrm{II} &= k_\mathrm{II} b \end{aligned} \tag{2.5}$$

where $k_\mathrm{II} \gg k_\mathrm{I}$. Then the observed reaction will be

$$\mathrm{A} \rightarrow \mathrm{C} + \mathrm{D} \qquad \mathscr{R} = ka \tag{2.6}$$

This reaction is complex even though it has a stoichiometric equation and rate expression that could correspond to an elementary reaction. Agreement between the stoichiometry and reaction rate is a necessary but not sufficient condition that a reaction be elementary. Recall the convention used in this text: When a rate constant is written above the reaction arrow, the reaction is assumed to be elementary with a rate that is consistent with the stoichiometry according to Equation 1.15 or 1.21. The reactions in Equation 2.5 are examples. When the rate constant is missing, the reaction rate must be explicitly specified. The reaction in Equation 2.6 is an example. This reaction is complex since the mechanism involves a short-lived intermediate, B.

Knowledge of the reaction mechanism may not be critical to solving a problem in reactor design, but it is desirable. Two reasons are as follows:

1. Knowledge of the mechanism will allow fitting experimental data to a theoretical rate expression. This will presumably be more reliable on extrapolation or scaleup than an empirical fit.
2. Knowing the mechanism may suggest chemical modifications and optimization possibilities that would otherwise be missed.

The best way to find a reaction mechanism is to find a good chemist. Chemical insight can be used to hypothesize a mechanism, and the hypothesized mechanism can then be tested against experimental data. If inconsistent, the mechanism must be rejected. This is seldom the case. More typically, there are several mechanisms that will fit the data equally well. A truly definitive study of reaction mechanisms requires direct observation of all chemical species, including intermediates that may have low concentrations and short lives. Such studies are not always feasible. Working hypotheses for the reaction mechanisms must then be selected based on general chemical principles and on analogous systems that have been studied in detail. There is no substitute for understanding the chemistry or at least for having faith in the chemist.

2.1.2 Byproducts

A ***byproduct*** is something made in the course of making something else. The term is neutral, not pejorative, because byproducts can be valuable. A classic example in the chemical industry is the chlorination of benzene to produce monochlorobenzene:

$$C_6H_6 + Cl_2 \rightarrow C_6H_5\,Cl + HCl$$

In this reaction, HCl is a ***stoichiometrically determined byproduct***. For every mole of monochlorobenzene, there will be 1 mol of HCl. This mole of HCl cannot be avoided without changing the reaction. Depending on circumstances, HCl can be valuable or can be a disposal problem.

Monochlorobenzene readily chlorinates to give *para*- and *ortho*-dichlorobenzene. These are ***kinetically determined byproducts*** of monochlorobenzene production, and their relative amounts can be controlled through reaction engineering. For example, their production can be minimized by reacting with a large excess of benzene. However, the dichlorobenzenes are valuable to the extent that they are made intentionally, and this gives rise to trichlorobenzenes, and so on. Before chlorobenzenes became environmentally suspect, markets were found for all of them, and some major markets still exist. It was a wonderful exercise in reaction engineering to design a process optimized with respect to the relative production of the various chlorobenzenes.

2.2 COMPONENT REACTION RATES FOR MULTIPLE REACTIONS

The component balance for a batch reactor, $d(Va)/dt = V\mathscr{R}_A$, still holds when there are multiple reactions. However, the net rate of formation of component A may be the result of several different reactions. Thus

$$\mathscr{R}_A = \nu_{A,\mathrm{I}}\mathscr{R}_\mathrm{I} + \nu_{A,\mathrm{II}}\mathscr{R}_\mathrm{II} + \nu_{A,\mathrm{III}}\mathscr{R}_\mathrm{III} + \cdots \tag{2.7}$$

Here, we envision component A being formed by reactions I, II, III. . . , each of which has its own reaction rate and stoichiometric coefficients. Equivalent to Equation 2.7

we can write

$$\mathscr{R}_A = \sum_{\text{reactions}} \nu_{A,\mathrm{I}} \mathscr{R}_\mathrm{I} = \sum_{\mathrm{I}=1}^{M} \nu_{A,\mathrm{I}} \mathscr{R}_\mathrm{I} \tag{2.8}$$

Obviously, $\nu_{A,\mathrm{I}} = 0$ if component A does not participate in reaction I, and of course the rate of formation is negative for a reaction in which A is consumed.

EXAMPLE 2.1

Determine the overall reaction rate for each component in the following set of reactions:

$$\begin{aligned} \mathrm{A} + \mathrm{B} &\xrightarrow{K_\mathrm{I}} \mathrm{C} \\ \mathrm{C} &\xrightarrow{K_\mathrm{II}} 2\mathrm{E} \\ 2\mathrm{A} &\xrightarrow{K_\mathrm{III}/2} \mathrm{D} \end{aligned}$$

SOLUTION: We begin with the stoichiometric coefficients for each component for each reaction:

$$\begin{array}{lll} \nu_{A,\mathrm{I}} = -1 & \nu_{A,\mathrm{II}} = 0 & \nu_{A,\mathrm{III}} = -2 \\ \nu_{B,\mathrm{I}} = -1 & \nu_{B,\mathrm{II}} = 0 & \nu_{B,\mathrm{III}} = 0 \\ \nu_{C,\mathrm{I}} = +1 & \nu_{C,\mathrm{II}} = -1 & \nu_{C,\mathrm{III}} = 0 \\ \nu_{D,\mathrm{I}} = 0 & \nu_{D,\mathrm{II}} = 0 & \nu_{D,\mathrm{III}} = +1 \\ \nu_{E,\mathrm{I}} = 0 & \nu_{E,\mathrm{II}} = +2 & \nu_{E,\mathrm{III}} = 0 \end{array}$$

The various reactions are assumed to be elementary (as indicated by the rate constants over the arrows) so the rates are

$$\mathscr{R}_\mathrm{I} = k_\mathrm{I} ab \qquad \mathscr{R}_\mathrm{II} = k_\mathrm{II} c \qquad \mathscr{R}_\mathrm{III} = (\tfrac{1}{2} k_\mathrm{III}) a^2$$

Now apply Equation 2.7 or 2.8 to obtain

$$\begin{aligned} \mathscr{R}_A &= -k_\mathrm{I} ab - k_\mathrm{III} a^2 \\ \mathscr{R}_B &= -k_\mathrm{I} ab \\ \mathscr{R}_C &= +k_\mathrm{I} ab - k_\mathrm{II} c \\ \mathscr{R}_D &= (\tfrac{1}{2} k_\mathrm{III}) a^2 \\ \mathscr{R}_E &= +2k_\mathrm{II} c \end{aligned}$$

2.3 MULTIPLE REACTIONS IN BATCH REACTORS

Suppose there are N components involved in a set of M reactions. Then Equation 1.22 can be written for each component using the rate expressions of Equation 2.7 or 2.8.

The component balances for a batch reactor are

$$\begin{aligned}
\frac{d(Va)}{dt} &= V\mathscr{R}_A = V(\nu_{A,\mathrm{I}}\mathscr{R}_\mathrm{I} + \nu_{A,\mathrm{II}}\mathscr{R}_\mathrm{II} + \nu_{A,\mathrm{III}}\mathscr{R}_\mathrm{III} + \cdots + M \text{ terms}) \\
\frac{d(Vb)}{dt} &= V\mathscr{R}_B = V(\nu_{B,\mathrm{I}}\mathscr{R}_\mathrm{I} + \nu_{B,\mathrm{II}}\mathscr{R}_\mathrm{II} + \nu_{B,\mathrm{III}}\mathscr{R}_\mathrm{III} + \cdots + M \text{ terms}) \\
\frac{d(Vc)}{dt} &= V\mathscr{R}_C = V(\nu_{C,\mathrm{I}}\mathscr{R}_\mathrm{I} + \nu_{C,\mathrm{II}}\mathscr{R}_\mathrm{II} + \nu_{C,\mathrm{III}}\mathscr{R}_\mathrm{III} + \cdots + M \text{ terms})
\end{aligned} \tag{2.9}$$

This is a set of N ordinary differential equations, one for each component. The component reaction rates will have M terms, one for each reaction, although many of the terms may be zero. Equations 2.9 are subject to a set of N initial conditions of the form

$$\begin{aligned}
a &= a_0 \quad \text{at } t = 0 \\
a &= b_0 \quad \text{at } t = 0 \\
a &= c_0 \quad \text{at } t = 0
\end{aligned} \tag{2.10}$$

The number of simultaneous equations can usually be reduced to less than N using the methodology of Section 2.8. However, this reduction is typically more trouble than it is worth.

EXAMPLE 2.2

Derive the batch reactor design equations for the reaction set in Example 2.1. Assume a liquid phase system with constant density.

SOLUTION: The real work has already been done in Example 2.1, where $\mathscr{R}_A$, $\mathscr{R}_B$, $\mathscr{R}_C$, ... were found. When density is constant, volume is constant, and the V terms in Equations 2.9 cancel. Substituting the reaction rates from Example 2.1 gives

$$\begin{aligned}
\frac{da}{dt} &= -k_\mathrm{I}ab - k_\mathrm{III}a^2 & a &= a_0 \quad \text{at } t = 0 \\
\frac{db}{dt} &= -k_\mathrm{I}ab & b &= b_0 \quad \text{at } t = 0 \\
\frac{dc}{dt} &= +k_\mathrm{I}ab - k_\mathrm{II}c & c &= c_0 \quad \text{at } t = 0 \\
\frac{dd}{dt} &= \left(\frac{k_\mathrm{III}}{2}\right)a^2 & d &= d_0 \quad \text{at } t = 0 \\
\frac{de}{dt} &= +2k_\mathrm{II}c & e &= e_0 \quad \text{at } t = 0
\end{aligned}$$

This is a fairly simple set of first-order ODEs. The set is difficult to solve analytically, but numerical solutions are easy.

2.4 NUMERICAL SOLUTIONS TO SETS OF FIRST-ORDER ODEs

As shown by Equations 2.9 and 2.10, the design equations for batch reactors are sets of first-order ODEs of the type known as initial-value problems. Time t is the independent variable. The dependent variables are the component concentrations a, b, c, . . . and, in subsequent sections, the state variables of temperature and pressure. These ODEs all have the form

$$\frac{da}{dt} = F(a, b, c, \ldots, T, P)$$

with known initial values. Here, F is a function of the indicated dependent variables and occasionally of t. These sets of equations can sometimes be solved analytically. Important examples are given in Section 2.5. However, for realistic and industrially important kinetic schemes, the component balances soon become intractable from the viewpoint of obtaining analytical solutions. Fortunately, sets of first-order ODEs are easily solved numerically. There are sophisticated and computationally efficient methods, such as the popular Runge–Kutta method described in Appendix 2.1, that minimize computer time, and such methods can be used if the cost of computation becomes significant. However, computer costs will usually be inconsequential compared to the costs of the engineer's personal time. In this usual case, the use of a simple technique can save time and money by allowing the engineer to focus on the physics and chemistry of the problem rather than on the numerical mathematics. Another possible way to save engineering time is to use higher order mathematical programming systems such as Mathematica, Matlab, and Maple rather than the more fundamental programming languages such as Fortran, Basic, or C. There is some risk to this approach in that it may not be known when either the engineer or the system has made a mistake. This book illustrates numerical methods using the general-purpose language known as Basic. Basic was chosen because it can be sight-read by anyone familiar with computer programming, because it is widely available on personal computers, and because it is used as the programming component for the ubiquitous spreadsheet Excel.

The simplest possible method for solving a set of first-order ODEs, subject to given initial values, is ***Euler's method***, also called ***marching ahead.*** We suppose that all concentrations are known at time $t = 0$. This allows the initial reaction rates to be calculated, one for each component. Choose some time increment Δt which is so small that, given the calculated reaction rates, the concentrations will change very little during the time increment. Calculate these small changes in concentration assuming the reaction rates are constant. Use the new concentrations to revise the reaction rates. Pick another time increment and repeat the calculations. Continue until the specified reaction time has been reached. This is the tentative solution. It is tentative because you do not yet know whether the numerical solution has ***converged*** to the true solution with sufficient accuracy. Test for convergence by reducing Δt and repeating the calculation. Do you get the same results to, say, five decimal places? If so, you probably have an adequate solution. If not, reduce Δt again. Computers are

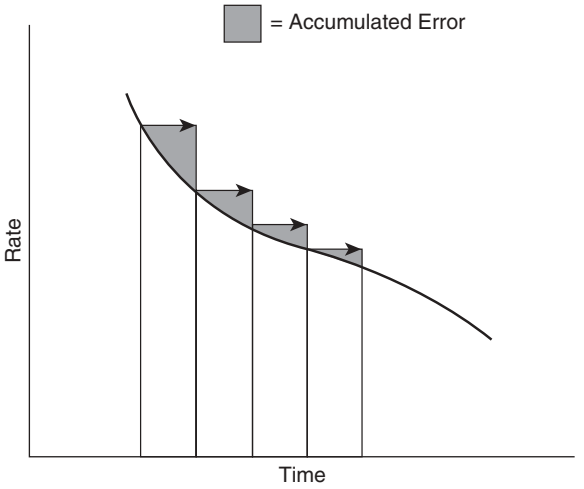

Figure 2.1 Systematic error of Euler integration.

so fast that this brute-force method of solving and testing for convergence will take only a few seconds for most of the problems in this book.

Euler's method can be illustrated by the simultaneous solution of

$$\frac{da}{dt} = \mathscr{R}_A(a, b) \qquad \frac{db}{dt} = \mathscr{R}_B(a, b) \tag{2.11}$$

The marching equations can be written as

$$\begin{aligned} a_{\text{new}} &= a_{\text{old}} + \mathscr{R}_A(a_{\text{old}}, b_{\text{old}})\,\Delta t \\ b_{\text{new}} &= b_{\text{old}} + \mathscr{R}_B(a_{\text{old}}, b_{\text{old}})\,\Delta t \\ t_{\text{new}} &= t_{\text{old}} + \Delta t \end{aligned} \tag{2.12}$$

The computation is begun by setting $a_{\text{old}} = a_0$, $b_{\text{old}} = b_0$, and $t_{\text{old}} = 0$. Rates are computed using the old concentrations and the marching equations are used to calculate the new concentrations. Old is then replaced by new and the march takes another step.

The marching-ahead technique systematically overestimates $\mathscr{R}_A$ when component A is a reactant since the rate is evaluated at the old concentrations where a and $\mathscr{R}_A$ are higher. This creates a systematic error similar to the numerical integration error shown in Figure 2.1. The error can be dramatically reduced by use of more sophisticated numerical techniques. It can also be reduced by the simple expedient of reducing Δt and repeating the calculation.

EXAMPLE 2.3

Solve the batch design equations for the reaction of Example 2.2. Use $k_{\text{I}} = 0.1$ mol^{-1} m^3 h^{-1}, $k_{\text{II}} = 1.2$ h^{-1}, and $k_{\text{III}} = 0.06$ mol^{-1} m^3 h^{-1}. The initial conditions are $a_0 = b_0 = 20$ mol m^{-3}. The reaction time is 1 h.

SOLUTION: Code for Example 2.3 is a complete program for performing the calculations. It is written in Basic as an Excel Macro. The output statements at the end of the program write the results to the cells of an Excel spreadsheet. The first column of the spreadsheet displays *dt*, the second column displays the corresponding values of *a* at the end of the batch reaction, and so on. The results are terrible for the largest *dt*, even calculating a negative concentration. However, as *dt* is decreased, the results begin to make sense and finally converge to at least

Code for Example 2.3

```
Sub Example2_3()

k1 = 0.1   'second order rate constant
k2 = 1.2   'first order rate constant
k3 = 0.06  'second order rate constant
tmax = 1   'batch reaction time
dt = 2

For N = 1 To 10 'This loop systematically reduces dt to show convergence
dt = dt / 4  'reduction of time step
a = 20   ' Initial values for each variable
b = 20
c = 0
d = 0
e = 0
t = 0

Do    'This starts the loop that advances t from 0 to tmax.
   RA = -k1 * a * b - k3 * a ^ 2 'Calculate the rate for each component
   RB = -k1 * a * b
   RC = k1 * a * b - k2 * c
   RD = k3 / 2 * a ^ 2
   RE = 2 * k2 * c
    a = a + dt * RA       'March ahead by one step in time
    b = b + dt * RB
    c = c + dt * RC
    d = d + dt * RD
    e = e + dt * RE
    t = t + dt
Loop While t < tmax  'This is the end of the "do" loop

Sum = a + b + c + d + e

' The following statements output the results to the Excel spreadsheet
Cells(N, 1) = dt
Cells(N, 2) = a
Cells(N, 3) = b
Cells(N, 4) = c
Cells(N, 5) = d
Cells(N, 6) = e
Cells(N, 7) = Sum

Next N    'This is the end of the "for" loop.

End Sub
```

five significant figures. The output statements need to be replaced with PRINT statements if you use a Basic compiler that writes directly to the screen.

Results from Code for Example 2.3 are shown below:

Δt	$a(t_{max})$	$b(t_{max})$	$c(t_{max})$	$d(t_{max})$	$e(t_{max})$	Sum
0.5	−16.3200	0.0000	8.0000	8.1600	24.0000	23.8400
0.125	2.8245	8.3687	5.1177	2.7721	13.0271	32.1102
0.03125	3.4367	8.6637	5.1313	2.6135	12.4101	32.2552
0.007813	3.5766	8.7381	5.1208	2.5808	12.2821	32.2984
0.001953	3.6110	8.7567	5.1176	2.5729	12.2513	32.3095
0.000488	3.6195	8.7614	5.1168	2.5709	12.2437	32.3123
0.000122	3.6217	8.7625	5.1166	2.5704	12.2418	32.3130
3.05×10^{-5}	3.6222	8.7628	5.1165	2.5703	12.2413	32.3131
7.63×10^{-6}	3.6223	8.7629	5.1165	2.5703	12.2412	32.3132
1.91×10^{-6}	3.6224	8.7629	5.1165	2.5703	12.2411	32.3132

These results have converged to at least five significant figures. The output required less than 3 s on what could be a slow PC by the time you read this.

EXAMPLE 2.4

Determine how the errors in the numerical solutions in Example 2.3 depend on the size of the time increment, Δt.

SOLUTION: Consider the values of $a(t_{max})$ versus Δt as shown below. The indicated errors are relative to the fully converged answer of 3.6224.

Δt	$a(t_{max})$	Error
0.5000000	−16.3200	19.9424
0.1250000	2.8245	−0.7972
0.0312500	3.4367	−0.1853
0.0078125	3.5766	−0.0458
0.0019531	3.6110	−0.0114
0.0004883	3.6195	−0.0029
0.0001221	3.6217	−0.0007
0.0000305	3.6222	−0.0002

The first result, for $\Delta t = 0.5$, shows a negative value for $a(t_{max})$. The time step is so large that the reaction goes beyond completion. For smaller Δt, the calculated values for $a(t_{max})$ are physically possible and the errors decrease by roughly a factor of 4 as the time step decreases by a factor of 4. Thus the error is proportional to Δt. Euler's method is said to ***converge order*** Δt, denoted $O(\Delta t)$.

Convergence order Δt for Euler's method is based on more than the empirical observation in Example 2.4. The order of convergence springs directly from the way in which the derivatives in Equations 2.11 are calculated. The simplest approximation of a first derivative is

$$\frac{da}{dt} \approx \frac{a_{\text{new}} - a_{\text{old}}}{\Delta t} \tag{2.13}$$

Substitution of this approximation into Equations 2.11 gives Equations 2.12. The limit of Equation 2.13 as $\Delta t \to 0$ is the usual definition of a derivative. It approximates the function $a(t)$, locally, as a straight line between $a_{\text{new}} - a_{\text{old}}$. A straight line is a first-order equation, and convergence $O(\Delta t)$ follows from this fact. Knowledge of the convergence order allows extrapolation and acceleration of convergence as discussed in Appendix 2.1. Runge–Kutta integration is also discussed in Appendix 2.1. The Runge–Kutta technique converges $O(\Delta t^5)$. Other things being equal, it is better to use a numerical method with a high order of convergence. However, such methods are usually more trouble to implement. Also, convergence is an ***asymptotic*** property. This means it only becomes true as Δt approaches zero. It may well be that the solution has already converged to adequate accuracy by the time the theoretical convergence order is reached.

The convergence of Euler's method to the true, analytical solution is assured for sets of linear ODEs. Just keep decreasing Δt. Occasionally, the word length of a computer becomes limiting. This text contains a few problems that cannot be solved in single precision (e.g., about seven decimal digits), and it is good practice to run double precision as a matter of course. This is automatic in Excel, but an explicit declaration may be needed in some versions of Basic. Most complex kinetic schemes give rise to nonlinear equations, and there is no absolute assurance of convergence. Fortunately, Euler's method behaves quite well for most nonlinear systems of engineering importance. Practical problems do arise in ***stiff*** sets of differential equations where some members of the set have characteristic times much smaller than other members. This occurs in reaction kinetics when some reactions have half-lives much shorter than others. In free-radical kinetics, reaction rates may differ by 6 orders of magnitude. The radioactive decay example in Section 2.5.2 has time constants that vary by 21 orders of magnitude. The allowable time step, Δt, must be set to accommodate the fastest reaction and may be too small to follow the overall course of the reaction even for modern computers. Special numerical methods have been devised to deal with stiff sets of differential equations. It is also possible to obtain highly accurate solutions to some stiff sets of equations through use of the ***quasi-steady-state hypothesis*** that is discussed in Section 2.5.3.

The need to use specific numerical values for the rate constants and initial conditions is a weakness of numerical solutions. If the specific values change, then the numerical solution must be repeated. Analytical solutions usually apply to all values of the input parameters, but special cases are sometimes needed. Recall the special case needed for $a_0 = b_0$ in Equation 1.32. Numerical solution techniques do not have this problem, and the problem of specificity with respect to numerical values can be minimized or overcome through the judicious use of ***dimensionless variables***, as

discussed in Section 1.6. Concentrations can be converted to dimensionless concentrations by dividing by an initial value, for example, $a* = a/a_0$, $b* = b/a_0$, and so on. The normal choice is to normalize using the initial concentration of the stoichiometrically limiting reactant. Time can be converted to a dimensionless variable by dividing by a characteristic time for the system. The mean residence time is usually used as the characteristic time of a flow system. In a batch system, the simplest possibility is to arbitrarily pick a "standard" batch reaction time, say, 1 h. Then time is scaled by t_{batch}, so that $t* = t/t_{\text{batch}}$ is dimensionless. The dimensionless rate constant is $k* = a_0^{n-1} k t_{\text{batch}}$, where n is the reaction order and k is an nth-order rate constant. When calculations are made, the dimensionless time needed to achieve the desired (dimensionless) concentration is readily converted to real time just by multiplying t^* by 1 h.

EXAMPLE 2.5

Consider the following competitive reactions in a constant-density batch reactor:

$$\begin{aligned} \text{A} + \text{B} &\rightarrow \text{P} \quad \text{(desired product)} & \mathcal{R}_{\text{I}} &= k_{\text{I}} ab \\ \text{A} &\rightarrow \text{Q} \quad \text{(undesired product)} & \mathcal{R}_{\text{II}} &= k_{\text{II}} a \end{aligned}$$

The selectivity based on component A is

$$\text{Selectivity} = \frac{\text{moles P produced}}{\text{moles A reacted}} = \frac{p}{a_0 - a} = \frac{p^*}{1 - a^*}$$

which ranges from 1 when only the desired product is made to 0 when only the undesired product is made. Components A and B have initial values a_0 and b_0. The other components have zero initial concentration. On how many parameters does the selectivity depend?

SOLUTION: On first inspection, it appears that four parameters are needed to determine selectivity as a function of reaction time. These are a_0, b_0, k_{I}, and k_{II}, but casting the governing equations into dimensionless form can reduce this number. Define $k_{\text{I}}^* = k_{\text{I}} t_{\text{batch}}$ and $k_{\text{II}}^* = a_0 k_{\text{II}} t_{\text{batch}}$ so that

$$\begin{aligned} \frac{da}{dt} &= -k_{\text{I}} ab - k_{\text{II}} a \quad \text{becomes} \quad \frac{da^*}{dt^*} = -a^* b^* k_{\text{I}}^* - k_{\text{II}}^* a^* \\ \frac{db}{dt} &= -k_{\text{I}} ab \quad \text{becomes} \quad \frac{db^*}{dt^*} = -a^* b^* k_{\text{I}}^* \\ \frac{dp}{dt} &= k_{\text{I}} ab \quad \text{becomes} \quad \frac{dp^*}{dt^*} = a^* b^* k_{\text{I}}^* \\ \frac{dq}{dt} &= k_{\text{II}} a \quad \text{becomes} \quad \frac{dq^*}{dt^*} = k_{\text{II}}^* a* \end{aligned}$$

where the dimensionless time is a multiple of the arbitrary chosen t_{batch}. The initial conditions are $a^* = 1$, $b^* = b_0/a_0$, $p^* = 0$, and $q^* = 0$ at $t^* = 0$. A plot of selectivity versus t^* depends on three parameters: a_0/b_0, k_{I}, and k_{II}.

A still further reduction is possible. Divide each of the dimensionless ODEs by k_I^* to obtain

$$\frac{da^*}{d\tau} = -a^*b^* - K_{II}a^*$$
$$\frac{db^*}{d\tau} = -a^*b^*$$
$$\frac{dp^*}{dt^*} = a^*b^*$$
$$\frac{dq^*}{d\tau} = K_{II}a^*$$

where $K_{II} = k_{II}^*/k_I^* = a_0k_{II}/k_I$ and $\tau = k_I^*t^* = k_It$. A plot of selectivity versusτ now depends only on b_0/a_0 and K_{II}. There are still too many parameters to conveniently plot the whole solution on a single graph, but partial results can easily be plotted. For example, plot the selectivity versus τ for a fixed value of b_0/a_0. There will be various curves corresponding to different values of the parameter K_{II}.

The dimensionless time τ in Example 2.5 does not depend on the arbitrarily chosen t_{batch}. Instead, t_{batch} cancels out in the conversion from t^* to τ so that t is scaled by a natural time constant for the system, k_1^{-1}. This effectively eliminates k_I as a parameter while scaling by t_{batch} does not. Whether the reactor is batch or continuous, it is always possible to use the reciprocal of a rate constant as a characteristic time. The quantity k_1^{-1} has units of time when k_1 is a first-order rate constant. Thus kt is a dimensionless reaction time. Similarly a_0k_2t is a dimensionless reaction time when k_2 is a second order rate constant. More generally, $(a_0^{\text{order}-1}k_{\text{order}})^{-1}$ will have units of time and $a_0^{\text{order}-1}k_{\text{order}}t$ will be dimensionless when k_{order} is the rate constant for a reaction of arbitrary order.

2.5 ANALYTICALLY TRACTABLE EXAMPLES

Relatively few kinetic schemes admit analytical solutions. The present section is concerned with the special cases that do and also with some cases where preliminary analytical work will ease the subsequent numerical studies. We begin with the ***n*th-order reaction.**

2.5.1 The *n*th-Order Reaction

$$\text{A} \rightarrow \text{products} \qquad \mathscr{R} = ka^n \tag{2.14}$$

This reaction can be elementary if $n = 1, 2$. More generally, it is complex. Noninteger values for n are often found when fitting rate data empirically, sometimes for sound kinetic reasons, as will be seen in Section 2.5.3. For an isothermal, constant-volume

batch reactor,

$$\frac{da}{dt} = -ka^n \qquad a = a_0 \quad \text{at } t = 0 \tag{2.15}$$

The first-order reaction is a special case mathematically. For $n = 1$, the solution has the exponential form of Equation 1.24:

$$\frac{a}{a_0} = e^{-kt} \tag{2.16}$$

For $n \neq 1$, the solution looks very different:

$$\frac{a}{a_0} = \left[1 + (n-1)a_0^{n-1}kt\right]^{1/(1-n)} \tag{2.17}$$

but see Problem 2.7. If $n > 1$, the term in square brackets is positive and the concentration gradually declines toward zero as the batch reaction time increases. Reactions with an order of 1 or greater never quite go to completion. In contrast, reactions with an order less than 1 can go to completion, at least mathematically. When $n < 1$, Equation 2.17 predicts $a = 0$ when

$$t = t_{\max} = \frac{a_0^{1-n}}{(1-n)k} \tag{2.18}$$

If the reaction order does not change, reactions with $n < 1$ will go to completion in the finite time $t_{\max}$. This is sometimes observed. Solid rocket propellants or firecracker fuses can burn at an essentially constant rate (a zero-order reaction) until all reactants are consumed. These are typically multiphase reactions limited by heat transfer and are discussed in Chapter 11. For single-phase systems, a reaction with $n < 1$ can be expected to slow and become first or second order in the limit of low concentration.

For $n < 1$, the reaction rate of Equation 2.14 should be supplemented by the condition that

$$\mathscr{R} = 0 \quad \text{if } a \leq 0 \tag{2.19}$$

Otherwise, the physics become unrealistic.

2.5.2 Consecutive First-Order Reactions, $\mathbf{A \rightarrow B \rightarrow C \rightarrow \cdots}$

Consider the following reaction sequence:

$$\mathrm{A} \xrightarrow{k_A} \mathrm{B} \xrightarrow{k_B} \mathrm{C} \xrightarrow{k_C} \mathrm{D} \xrightarrow{k_D} \cdots \tag{2.20}$$

These reactions could be elementary, first order, and without byproducts as indicated. For example, they could represent a sequence of isomerizations. More likely, there will be byproducts that do not influence the subsequent reaction steps and which were omitted in the shorthand notation of Equation 2.20. Thus the first member of the set could actually be

$$\mathrm{A} \xrightarrow{k_A} \mathrm{B} + \mathrm{P}$$

Table 2.1 Radioactive Decay Series for ^{238}U

Nuclear Species	Half-Life
^{238}U	4.5 billion years
^{234}Th	24 days
^{234}Pa	1.2 min
^{234}U	250,000 years
^{230}Th	80,000 years
^{226}Ra	1600 years
^{222}Rn	3.8 days
^{218}**Po**	3 min
^{214}Pb	27 min
^{214}Bi	20 min
^{214}**Po**	160 μs
^{210}Pb	22 years
^{210}Bi	5 days
^{210}**Po**	138 days
^{206}Pb	Stable

Radioactive decay provides splendid examples of first-order sequences of this type. The naturally occurring sequence beginning with ^{238}U and ending with ^{206}Pb has 14 consecutive reactions that generate alpha or beta particles as byproducts. The half-lives in Table 2.1—and the corresponding first-order rate constants, see Equation 1.28—differ by 21 orders of magnitude.

Within the strictly chemical realm, sequences of pseudo-first-order reactions are quite common. The usually cited examples are hydrations done in water and slow oxidations done in air where one of the reactants (e.g., water or oxygen) is present in great excess and hence does not change appreciably in concentration during the course of the reaction. These reactions are pseudo–first order and behave identically to those in Equation 2.20, although the rate constants over the arrows should be removed as a formality since the reactions are not elementary.

Any sequence of first-order reactions in a batch reactor can be solved analytically, although the algebra can become tedious if the number of reactions is large. The ODEs that correspond to Equation 2.20 are

$$\begin{aligned}
\frac{da}{dt} &= -k_A a \\
\frac{db}{dt} &= -k_B b + k_A a \\
\frac{dc}{dt} &= -k_C c + k_B b \\
\frac{dd}{dt} &= -k_D d + k_C c
\end{aligned} \tag{2.21}$$

Just as the reactions are consecutive, solutions to this set can be done consecutively. The equation for component A depends only on a and can be solved directly. The result is substituted into the equation for component B, which then depends only on b and t and can be solved. This procedure is repeated until the last, stable product is reached. Assuming component D is stable, the solutions to Equations 2.21 are

$$
\begin{aligned}
a &= a_0 e^{-k_A t} \\
b &= \left[b_0 - \frac{a_0 k_A}{k_B - k_A} \right] e^{-k_B t} + \left[\frac{a_0 k_A}{k_B - k_A} \right] e^{-k_A t} \\
c &= \left[c_0 - \frac{b_0 k_B}{k_C - k_B} + \frac{a_0 k_A k_B}{(k_C - k_A)(k_C - k_B)} \right] e^{-k_C t} \\
&\quad + \left[\frac{b_0 k_B}{k_C - k_B} - \frac{a_0 k_A k_B}{(k_C - k_B)(k_B - k_A)} \right] e^{-k_B t} + \left[\frac{a_0 k_A k_B}{(k_C - k_A)(k_B - k_A)} \right] e^{-k_A t} \\
d &= d_0 + (a_0 - a) + (b_0 - b) + (c_0 - c)
\end{aligned}
\tag{2.22}
$$

These results assume that all the rate constants are different. Special forms apply when some of the k values are identical, but the qualitative behavior of the solution remains the same. Figure 2.2 illustrates this behavior for the case of $b_0 = c_0 = d_0 = 0$. The concentrations of B and C start at zero, increase to maximums, and then decline back to zero. Typically, component B or C is the desired product whereas the others are undesired. If B is desired, the batch reaction time can be picked to maximize its

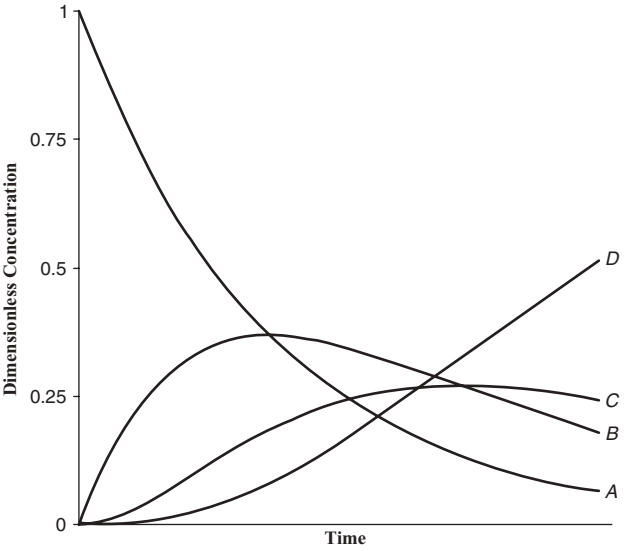

Figure 2.2 Consecutive reaction sequence, $A \rightarrow B \rightarrow C \rightarrow D$.

concentration. Setting $db/dt = 0$ and $b_0 = 0$ gives

$$t_{\max} = \frac{\ln(k_B/k_A)}{k_B - k_A} \tag{2.23}$$

Finding the optimal time for the production of C requires a numerical solution but remains conceptually straightforward.

Equations 2.22 and 2.23 become indeterminate if $k_B = k_A$. Special forms are needed for the analytical solution of a set of consecutive, first-order reactions whenever a rate constant is repeated. The derivation of the solution can be repeated for the special case or L'Hospital's rule can be applied to the general solution. Identical rate constants do exist. Examples include multifunctional molecules where reactions at physically different but chemically similar sites can have the same rate constant. Polymerizations are an important example of consecutive reactions where it is common to assume that reaction rates are independent of the length of the polymer chain. Unlike analytical solutions, numerical solutions to the governing set of simultaneous ODEs have no difficulty with repeated rate constants, but such solutions can become computationally challenging when the rate constants differ greatly in magnitude. Table 2.1 provides a dramatic example of reactions that lead to stiff equations. A method for finding analytical approximations to stiff equations is described in the next section.

2.5.3 Quasi-Steady Hypothesis

Many reactions involve short-lived intermediates that are so reactive that they never accumulate in large quantities and are difficult to detect. Their presence is important in the reaction mechanism and may dictate the functional form of the rate equation.

We begin with a reaction for which a full analytical solution is possible:

$$\mathrm{A} \underset{k_r}{\overset{k_f}{\rightleftharpoons}} \mathrm{B} \xrightarrow{k_B} \mathrm{C}$$

The governing ODEs for a constant-volume batch reactor are

$$\frac{da}{dt} = -k_f a + k_r b$$
$$\frac{db}{dt} = +k_f a - k_r b - k_B b$$

Assuming $b_0 = c_0 = 0$, the rigorous if complicated solution is

$$\begin{aligned} a &= \frac{k_f a_0}{S_1 - S_2}\left[\left(1 - \frac{k_B}{S_1}\right)e^{-S_1 t} - \left(1 - \frac{k_B}{S_2}\right)e^{-S_2 t}\right] \\ b &= \frac{k_f a_0}{S_1 - S_2}\left(e^{-S_2 t} - e^{-S_1 t}\right) \\ c &= a_0 - a - b \end{aligned} \tag{2.24}$$

where $S_1, S_2 = \frac{1}{2}[k_f + k_r + k_B \pm \sqrt{(k_f + k_r + k_B)^2 - 4k_f k_B}]$.

Now suppose that B is highly reactive. When formed, it rapidly reverts back to A or transforms into C. This implies $k_r \gg k_f$ or $k_B \gg k_f$. To apply the ***quasi-steady hypothesis*** to this batch reaction, set $db/dt = 0$. The ODE for B then becomes an algebraic equation and predicts that the concentration of B will be proportional to that of A:

$$b = \frac{k_f a}{k_r + k_B} \tag{2.25}$$

This is the quasi-steady result. The actual concentration of B is initially zero but rises quickly so that Equation 2.25 becomes a good approximation. From this point on, B is formed at nearly the same rate as it is consumed. It is actually consumed at a somewhat higher rate so that, after its initial rise, b will gradually decrease, maintaining near proportionality to a.

Substituting Equation 2.25 gives a simplified ODE for a that has the solution

$$a = a_0 \exp\left(\frac{-k_f k_B t}{k_f + k_B}\right) \tag{2.26}$$

After an initial startup period, Equation 2.25 and 2.26 become reasonable approximations of the true solution, Equation 2.24. See Figure 2.3 for the case of $k_r = k_B = 10k_f$. The approximation becomes better when there is a larger difference between k_f and the other two rate constants.

The general procedure for applying the quasi-steady hypothesis is the following:

1. Write down the assumed mechanism for the reaction.
2. Write rate equations for each species.
3. Divide the various components between short- and long-lived.
4. Set the reactions rates equal to zero for the short-lived components.

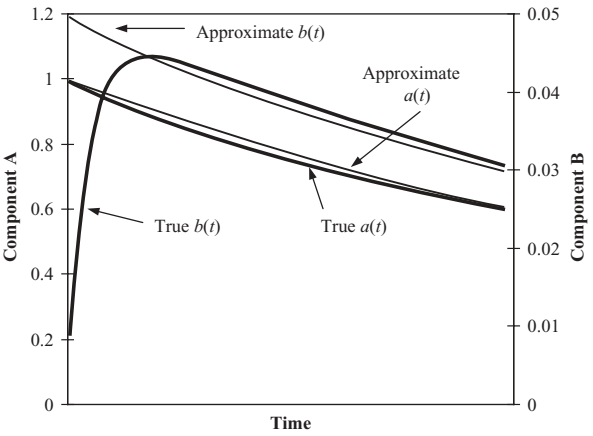

Figure 2.3 True solution versus approximation using the quasi-steady-state hypothesis.

5. Solve the resulting algebraic equations for the concentrations of the short-lived components.
6. Substitute these results into the rate equations for the long-lived components.

The result of this general procedure is a set of rate equations for the long-lived components that depend only on concentrations of the long-lived components. The resulting, simplified reaction rates can then be substituted in reactor design equations. The design equations can be for any type of reactor. The examples in this chapter will be for batch reactors.

The quasi-steady hypothesis is used when short-lived intermediates are formed as part of a relatively slow overall reaction. The short-lived molecules are hypothesized to achieve an approximate steady state in which they are created at nearly the same rate that they are consumed. Their concentration in this quasi–steady state is necessarily small. A typical use of the quasi-steady hypothesis is in ***chain reactions*** propagated by free radicals. Free radicals are molecules or atoms having an unpaired electron. Many common organic reactions such as thermal cracking and vinyl polymerization occur by free-radical processes. There are three steps to a typical free-radical reaction: ***initiation, propagation***, and ***termination.***

Initiation

Initiation creates one or more free radicals. The following mechanism has been postulated for the gas phase decomposition of acetaldehyde:

$$CH_3CHO \xrightarrow{k_I} CH_3\cdot + CHO\cdot$$

This is a spontaneous, thermal initiation that generates two free radicals by breaking a covalent bond. The methane radical is highly reactive; but rather than disappearing, most reactions regenerate it.

Propagation

Propagation preserves the number of free radicals. In essence they act as a catalyst. The postulated mechanism for the gas phase decomposition of acetaldehyde involves two propagation steps:

$$CH_3\cdot + CH_3CHO \xrightarrow{k_{II}} CH_4 + CH_3CO\cdot$$
$$CH_3CO\cdot \xrightarrow{k_{III}} CH_3\cdot + CO$$

These propagation reactions are circular. The first reaction consumes a methane radical but the second reaction regenerates it. In the process, another short-lived radical, $CH_3CO\cdot$, is formed and destroyed. There is no net consumption of free radicals, so a single initiation reaction can cause an indefinite number of propagation reactions, each one of which consumes an acetaldehyde molecule. Ignoring the relatively small concentrations of free radicals, the overall stoichiometry is found by adding the

propagation steps:

$$CH_3CHO \rightarrow CH_4 + CO$$

The methane radicals do not accumulate because of termination reactions. The concentration of radicals adjusts itself so that the initiation and termination rates are equal.

Termination

Termination reactions destroy free radicals. The major termination reaction postulated for the acetaldehyde decomposition is termination by combination:

$$2CH_3\cdot \xrightarrow{k_{IV}} C_2H_6$$

The assumption of a quasi–steady state is applied to the $CH_3\cdot$ and $CH_3CO\cdot$ radicals by setting their rate equations to zero:

$$\begin{aligned}\mathscr{R}_{CH_3\cdot} = {} & k_I[CH_3CHO] - k_{II}[CH_3CHO][CH_3\cdot] \\ & + k_{III}[CH_3CO\cdot] - 2k_{IV}[CH_3\cdot]^2 = 0\end{aligned}$$

and

$$\mathscr{R}_{CH_3\cdot CO} = k_{II}[CH_3CHO][CH_3\cdot] - k_{III}[CH_3CO\cdot] = 0$$

Note that the quasi-steady hypothesis is applied only to those short-lived species that appear in a rate equation. In this example, the concentration of $CHO\cdot$ does not appear in any rate equation and is ignored, but see Problem 2.16. Setting the rates to zero gives a set of algebraic equations that can be solved for the concentrations of the short-lived species. The solution expresses the concentrations of the short-lived species in terms of the (presumably measurable) concentrations of the long-lived species. For the current example, the solutions for the free-radical concentrations are

$$[CH_3\cdot] = \sqrt{\frac{k_I[CH_3CHO]}{2k_{IV}}}$$

and

$$[CH_3CO\cdot] = \left(\frac{k_{II}}{k_{III}}\right)\sqrt{\frac{k_I[CH_3CHO]^3}{2k_{IV}}}$$

The free-radical concentrations will be small—and the quasi-steady-state hypothesis will be justified—whenever the initiation reaction is slow compared to the termination reaction, $k_I \ll k_{IV}$.

Acetaldehyde is consumed by the initiation and propagation reactions:

$$\mathscr{R}_{CH_3CHO} = -k_I[CH_3CHO] - k_{II}[CH_3CHO][CH_3\cdot]$$

The quasi-steady hypothesis allows the difficult-to-measure free-radical concentrations to be replaced by the more easily measured concentrations of the long-lived

species. The result is

$$\mathscr{R}_{CH_3CHO} = -k_I[CH_3CHO] - \left(\frac{k_{II}^2 k_I}{2k_{IV}}\right)^{1/2} [CH_3CHO]^{3/2}$$

This result is still somewhat complicated but now depends only on the concentrations of long-lived species. The first term in the rate equation for CH3CHO is due to consumption by the initiation reaction and is presumed to be small compared to consumption by the propagation reactions. Thus the second term dominates, and the overall reaction has the form

$$A \rightarrow \text{products} \qquad \mathscr{R} = ka^{3/2}$$

This agrees with experimental findings (Boyer et al., 1952) on the decomposition of acetaldehyde. The appearance of the $\frac{3}{2}$ power is a wondrous result of the quasi-steady hypothesis. Half-integer kinetics are typical of free-radical systems. The next example describes a free-radical reaction with an apparent order of $\frac{1}{2}$, 1, or $\frac{3}{2}$ depending on the termination mechanism.

EXAMPLE 2.6

Apply the quasi-steady hypothesis to the monochlorination of a hydrocarbon. The initiation step is

$$Cl_2 \xrightarrow{k_I} 2Cl\cdot$$

The propagation reactions are

$$Cl\cdot + RH \xrightarrow{k_{II}} R\cdot + HCl$$
$$R\cdot + Cl_2 \xrightarrow{k_{III}} RCl + Cl\cdot$$

There are three possibilities for termination.

(a) $2Cl\cdot \xrightarrow{k_{IV}} Cl_2$

(b) $Cl\cdot + R\cdot \xrightarrow{k_V} RCl$

(c) $2R\cdot \xrightarrow{k_{VI}} R_2$

SOLUTION: The steps are the same as in the acetaldehyde example. The reaction rates for each of the free-radical species are set to zero. The resulting algebraic equations are then solved for the free-radical concentrations. These values are substituted into the rate equations for the long-lived species. The net, overall reaction is obtained by summing the propagation reactions:

$$HR + Cl_2 \xrightarrow{k_{III}} RCl + HCl$$

Depending on which termination mechanism is assumed, the rate for the overall reaction is given by one of the following:

(a) $\mathscr{R} = k[Cl_2]^{1/2}[RH]$

(b) $\mathscr{R} = k[Cl_2][RH]^{1/2}$

(c) $\mathscr{R} = k[Cl_2]^{3/2}$

If two or three termination reactions are simultaneously important, the algebra needed to find $\mathscr{R}$ is possible but bothersome. Laboratory results in such situations could probably be approximated as

$$\mathscr{R} = k[\mathrm{Cl}_2]^m[\mathrm{RH}]^n$$

where $\frac{1}{2} < m < \frac{3}{2}$ and $0 < n < 1$.

EXAMPLE 2.7

Apply the quasi-steady hypothesis to the consecutive reactions in Equation 2.20 assuming $k_A \ll k_B$ and $k_A \ll k_C$.

SOLUTION: The assumption of an approximate steady state is applied to components B and C. The batch reactor design equations are

$$\frac{da}{dt} = -k_A a$$
$$\frac{db}{dt} = -k_B b + k_A a = 0$$
$$\frac{dc}{dt} = -k_C c + k_B b = 0$$

The solutions are

$$a = a_0 e^{-k_A t} \qquad b = \frac{k_A a}{k_B} \qquad c = \frac{k_B b}{k_C}$$

This scheme can obviously be extended to larger sets of consecutive reactions provided all the intermediate species are short-lived compared to parent species A. See Problem 2.9

Our treatment of chain reactions has been confined to relatively simple situations where the number of participating species and their possible reactions have been sharply bounded. Most free-radical reactions of industrial importance involve many more species. The set of possible reactions is unbounded in polymerizations, and it is perhaps bounded but very large in processes such as naphtha cracking and combustion. The reactions can be postulated, but the rate constants are generally unknown. The quasi-steady hypothesis provides a functional form for the rate equations that can be used to fit experimental data.

The steps of initiation and propagation are common to all free-radical reactions and to many other types of catalysis. The termination step may be temporarily suppressed in some reactions. There are sometimes ***chain transfer reactions*** in which the catalytic site is switched from one molecule to another. See Problem 2.16 and Chapter 13 for examples.

2.5.4 Autocatalytic Reactions

The products of an autocatalytic reaction accelerate the rate of the reaction. For example, an acid-catalyzed reaction may produce additional acid. The rate of most reactions has an initial maximum and then decreases as reaction proceeds. Autocatalytic reactions have an initially increasing rate, although the rate must eventually decline as the reaction goes to completion. A model reaction frequently used to represent autocatalytic behavior is

$$\mathrm{A} \rightarrow \mathrm{B} + \mathrm{C}$$

with an assumed mechanism of

$$\mathrm{A} + \mathrm{B} \xrightarrow{k} 2\mathrm{B} + \mathrm{C} \tag{2.27}$$

For a batch system,

$$\frac{da}{dt} = -kab = -ka(b_0 + a_0 - a) \tag{2.28}$$

This ODE has the solution

$$\frac{a}{a_0} = \frac{[1 + (b_0/a_0)]\ \exp\{-[1 + (b_0/a_0)]a_0kt\}}{(b_0/a_o) + \exp\{-[1 + (b_0/a_0)]a_0kt\}} \tag{2.29}$$

Figure 2.4 illustrates the course of the reaction for various values of b_0/a_0. Inflection points and S-shaped curves are characteristic of autocatalytic behavior. The reaction rate is initially low because the concentration of the catalytic component, B, is low. Indeed, no reaction ever occurs if $b_0 = 0$. As B is formed, the rate accelerates and

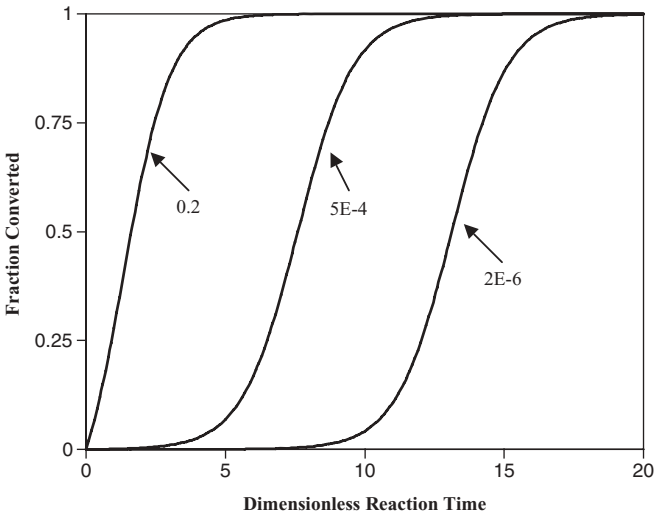

Figure 2.4 Conversion versus dimensionless time, a_0kt, for an autocatalytic batch reaction. The parameter is b_0/a_0.

continues to increase so long as the term *ab* in Equation 2.28 is growing. Eventually, however, this term must decrease as component A is depleted even though the concentration of B continues to increase. The inflection point is caused by depletion of component A.

Autocatalytic reactions often show higher conversions in a stirred tank than in a batch or piston flow reactor having the same holding time, $t_{\text{batch}} = \bar{t}$. Since $\hat{a} = a_{\text{out}}$ in a CSTR, the catalyst, B, is present at the same, high concentrations everywhere within the working volume of the reactor. In contrast, B may be quite low in concentration at early times in a batch reactor and only achieves its highest concentrations at the end of the reaction. Equivalently, the concentration of B is low near the inlet of a PFR and only achieves high values near the outlet. Thus the average reaction rate in the CSTR can be higher.

The qualitative behavior shown in Figure 2.4 is characteristic of many systems, particularly biological ones, even though the reaction mechanism does not agree with Equation 2.27. An inflection point is observed in most batch fermentations. Polymerizations of vinyl monomers such as methyl methacrylate and styrene also show autocatalytic behavior when the undiluted monomers react by free-radical mechanisms. A polymerization exotherm for a methyl methacrylate casting system is shown in Figure 2.5. The reaction was approximately adiabatic so that the reaction exotherm provides a good measure of the extent of polymerization. The autocatalytic behavior in this polymerization is caused partially by concentration effects (the "gel effect" is discussed in Section 13.4.2) and partially by the exothermic nature of the reaction (temperature effects are discussed in Chapter 5). Indeed, heat can be considered a reaction product that accelerates the reaction and is a common cause of autocatalytic behavior, typically giving inflection points with respect to both temperature and

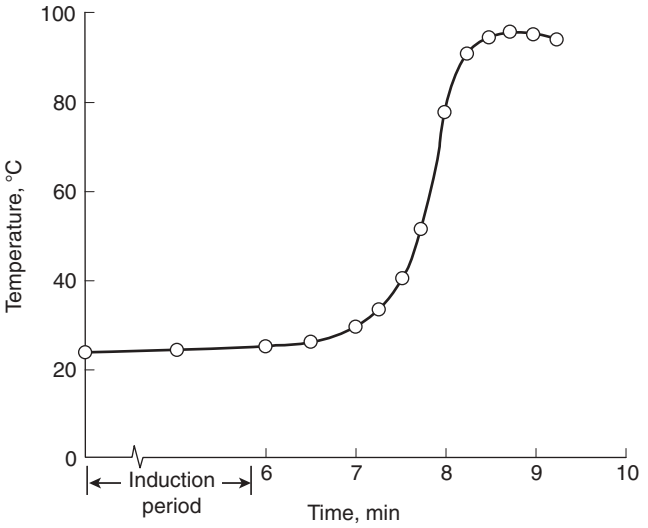

Figure 2.5 Reaction exotherm for a methyl methacrylate casting system.

composition. Autoacceleration also occurs in branching chain reactions where a single chain-propagating species can generate more than one new propagating species. Such reactions are obviously important in nuclear fission. They also occur in combustion processes. For example, the elementary reactions

$$H\cdot + O_2 \rightarrow HO\cdot + O\cdot \qquad H_2 + O\cdot \rightarrow HO\cdot + H\cdot$$

are believed important in the burning of hydrogen.

Autocatalysis can cause sustained oscillations in batch systems. This idea originally met with skepticism. Some chemists believed that sustained oscillations would violate the second law of thermodynamics, but this is not true. Oscillating batch systems certainly exist, although they must have some external energy source or else the oscillations will eventually subside. An important example of an oscillating system is the circadian rhythm in animals. A simple model of a ***chemical oscillator***, called the Lotka–Volterra reaction, has the assumed mechanism:

$$R + G \xrightarrow{k_I} 2R$$
$$L + R \xrightarrow{k_{II}} 2L$$
$$L \xrightarrow{k_{III}} D$$

Rabbits (R) eat grass (G) to form more rabbits. Lynx (L) eat rabbits to form more lynx. Lynx also die of old age to form dead lynx (D). The grass is assumed to be in constant supply and provides the energy needed to drive the oscillation. The set of ODEs that governs the batch reaction is

$$\frac{dr}{dt} = k_I g r - k_{II} l r \qquad \frac{dl}{dt} = k_{II} l r - k_{III} l$$

These equations are nonlinear and cannot be solved analytically. They are included in this section because they are autocatalytic and because this chapter discusses the numerical tools needed for their solution. Figure 2.6 illustrates one possible solution for the initial condition of 100 rabbits and 10 lynx. This model should not be taken

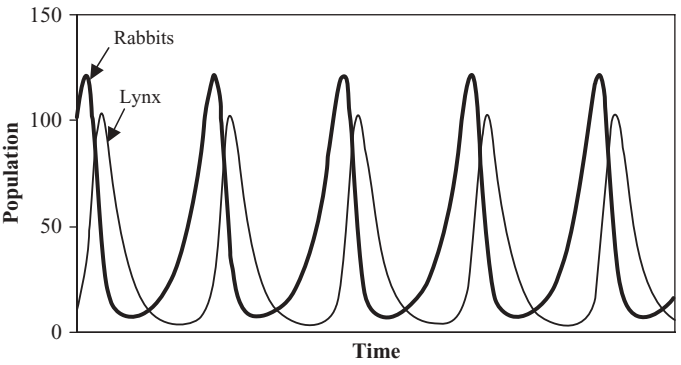

Figure 2.6 Population dynamics predicted by the Lotka–Volterra model for an initial population of 100 rabbits and 10 lynx.

too seriously since it represents no known chemistry or ecology. It does show that a relatively simple set of first-order ODEs can lead to oscillations. These oscillations are strictly periodic if the grass supply is not depleted. If the grass is consumed, albeit slowly, both the amplitude and the frequency of the oscillations will decline toward an eventual steady state of no grass and no lynx.

A conceptually similar reaction, known as the Prigogine–Lefver or Brusselator reaction, consists of the following steps:

$$\begin{aligned} A &\xrightarrow{k_{\mathrm{I}}} X \\ B + X &\xrightarrow{k_{\mathrm{II}}} Y + D \\ 2X + Y &\xrightarrow{k_{\mathrm{III}}} 3X \\ X &\xrightarrow{k_{\mathrm{IV}}} E \end{aligned}$$

This reaction can oscillate in a well-mixed system. In a quiescent system, diffusion–limited spatial patterns can develop, but these violate the assumption of perfect mixing that is made in this chapter. A well-known chemical oscillator that also develops complex spatial patterns is the Belousov–Zhabotinsky or BZ reaction. Flame fronts and detonations are other batch reactions that violate the assumption of perfect mixing. Their analysis requires treatment of mass or thermal diffusion or the propagation of shock waves. Such reactions are briefly touched upon in Chapter 11 but, by and large, are beyond the scope of this book.

2.6 VARIABLE-VOLUME BATCH REACTORS

This section considers two cases. The first is a reactor where the mass charged to the vessel is constant but the density changes so that the working volume of the vessel changes as the reaction proceeds. Performance of such a reactor is most easily determined by expressing the reactor contents in terms of total moles rather than concentration, that is, rather than moles per unit volume. An expression giving density as a function of composition is needed for anything but first-order reactions. The density function is empirical for liquid systems and is a gas law, for example, the ideal gas law, for gaseous systems.

The second case is a fed-batch reactor where the mass changes with time, typically increasing as new ingredients are added but decreasing if, for example, a reaction byproduct is removed to avoid an equilibrium limitation. If the addition or removal is done quickly and if the mixing time is short, such reactions can be treated as a sequence of ordinary, constant-mass batch reactions. If the addition or removal steps are slow, the methods of Chapter 14 are needed.

2.6.1 Systems with Constant Mass

The feed is charged all at once to a batch reactor, and the products are removed together, the mass in the system being held constant during the reaction step. Such

reactors usually operate at nearly constant volume. The reason for this is that most batch reactors are liquid phase, and liquid densities tend to be fairly constant. The batch reactors considered so far are perfectly mixed and isothermal and operate at constant density. We now relax the assumption of constant density but retain the other simplifying assumptions of perfect mixing and isothermal operation.

The component balance for a variable volume but otherwise ideal batch reactor can be written using moles rather than concentrations:

$$\frac{d(Va)}{dt} = \frac{dN_A}{dt} = V\mathscr{R}_A \tag{2.30}$$

where N_A is the number of moles of component A in the reactor. The initial condition associated with Equation 2.30 is that $N_A = (N_A)_0$ at $t = 0$. The case of a first-order reaction is especially simple:

$$\frac{dN_A}{dt} = -Vka = -kN_A$$

so that the solution is

$$N_A = (N_A)_0 e^{-kt} \tag{2.31}$$

This is a more general version of Equation 1.25. For a first-order reaction, the number of molecules of the reactive component decreases exponentially with time. This is true whether or not the density is constant. If the density happens to be constant, the concentration of the reactive component also decreases exponentially, as in Equation 1.25.

EXAMPLE 2.8

Most polymers have densities appreciably higher than their monomers. Consider a polymer having a density of 1040 kg m^{-3} that is formed from a monomer having a density of 900 kg m^{-3}. Suppose isothermal batch experiments require 2 h to reduce the monomer content to 20% by weight. What is the pseudo-first-order rate constant and what monomer content is predicted after 4 h?

SOLUTION: Use a reactor charge of 900 kg as a basis and apply Equation 2.31 to obtain

$$Y_A = \frac{N_A}{(N_A)_0} = \frac{0.2(900)/\text{Mw}}{900/\text{Mw}} = 0.2 = \exp(-2k)$$

This gives $k = 0.8047$ h^{-1}. The molecular weight of the monomer, Mw, is not actually needed for the calculation since the number of moles of this single component is proportional to its mass. Extrapolation of the first-order kinetics to a 4-h batch predicts there will be $900 \exp(-3.22) = 36$ kg or 4% by weight of monomer left unreacted. Note that the ***fraction unreacted***, Y_A, must be defined as a ratio of moles or mass rather than concentration whenever the density varies during the reaction.

WRONG SOLUTION: Assume that the concentration declines exponentially according to Equation 1.25. To calculate the concentration, we need the density. Assume it varies linearly with the weight fraction of monomer. Then $\rho = 1012$ kg m^{-3} at the end of the reaction. To

calculate the monomer concentrations, use a basis of 1 m^3 of reacting mass. This gives

$$\frac{a}{a_0} = \frac{0.2(1012)/\text{Mw}}{900/\text{Mw}} = 0.225 = \exp(-2k) \qquad \text{or} \qquad k = 0.746$$

The reason this result is wrong is that the concentration does not follow the simple exponential decay of first-order kinetics but also changes due to the density change. These changes are in opposite directions since a shrinking volume acts to increase concentration. The predicted rate constant is too low. If it were used erroneously, the predicted concentration would be 45.5/Mw kg mol m^{-3} at the end of the 4-h reaction. The predicted monomer content after 4 h is 4.4% rather than 4.0% as more properly calculated. The difference is small but could be significant for the design of the monomer recovery and recycling systems.

For reactions of order other than first, things are not so simple. For a second-order reaction,

$$\frac{dN_A}{dt} = -Vka^2 = -\frac{kN_A^2}{V} \tag{2.32}$$

A pesky factor of V has emerged. Unlike the first-order case, the volume dependency remains even though the composition is measured in terms of moles. Clearly, we must determine V or ρ as a function of composition. For liquid systems, it is generally easier to work with *intensive* variables like the fraction unreacted, Y_A, and the mass density, ρ, rather than *extensive* variables like N_A and V. Equation 2.32 can be converted to

$$\frac{dY_A}{dt} = -\frac{k(N_A)_0 Y_A^2 \rho}{V_0 \rho_0} = -ka_0 Y_A^2 \frac{\rho}{\rho_0} \tag{2.33}$$

EXAMPLE 2.9

Repeat Example 2.8 assuming that the polymerization is second order in monomer concentration. This assumption is appropriate for a binary polycondensation with good initial stoichiometry while the pseudo-first-order assumption of Example 2.8 is typical of an addition polymerization. As in Example 2.8, find the rate constant for the reaction assuming that the monomer content is reduced to 20% of its initial value after 2 h, now by second-order kinetics. Also determine the monomer content predicted after 4 h.

SOLUTION: The density varies from 900 to 1040 as Y_A ranges from 1 to 0. A simple expression for the density is

$$\rho = 1040 - 140Y$$

Substituting this into Equation 2.33 gives

$$\frac{dY}{dt} = -k^* Y^2 \left[\frac{1040 - 140Y}{900}\right]$$

where $k^* = k(N_A)_0/V_0 = ka_0$. The initial condition is $Y = 1$ at $t = 0$. An analytical solution to this ODE is possible but messy. A numerical solution integrates the ODE for various values of k^* until one is found that gives $Y = 0.2$ at $t = 2$. A program using manual guesses of k^* is given in Code for Example 2.9. The result is $k^* = 1.83$ with units of reciprocal hours. Continuing

the program for another 2 h of reaction time gives $Y = 0.109$ so that the monomer content is reduced from 20 to 10.9% by the extra 2 h of reaction.

Code for Example 2.9

```
Sub Example2_9 ()

dt = 0.0001
y = 1
K = Cells(1, 1).Value 'Reads value of K from cell A1 of the spreadsheet
Do While t < 2
   y = y - K * y * y * (1040 - 140 * y) / 900 * dt
   t = t + dt
Loop
Cells(1, 2) = y 'Outputs value of Y at t = 2 to cell B1 of the spreadsheet
Do While t < 4
   y = y - K * y * y * (1040 - 140 * y) / 900 * dt
   t = t + dt
Loop
Cells(1, 3) = y  'Outputs value of Y at t = 4 to cell C1 of the spreadsheet
End Sub
```

The next example treats the case of a liquid phase, second-order reaction in more general terms.

EXAMPLE 2.10

Suppose $2A \xrightarrow{k/2} B$ in the liquid phase and that the density changes from ρ_0 to $\rho_0 + \Delta\rho$ upon complete conversion. Derive the batch design equation and compare it to a hypothetical batch reactor in which the density is constant:

SOLUTION: For the constant density case, $\rho = \rho_0$ and Equation 2.33 becomes

$$\frac{dY'}{dt} = -k^* Y'^2 \quad \rho = \rho_0 \tag{2.34}$$

where $k^* = (N_A)_0 k / V_0 = a_0 k$ as in Example 2.9 and Y' is the fraction unreacted for this hypothetical case of no density change. The solution subject to the initial condition that $Y' = 1$ at $t = 0$ is

$$Y' = \frac{1}{1 + k^* t} \tag{2.35}$$

This is the expected result for a second reaction in a batch reactor.

Now define Y as the fraction unreacted for the variable-density case, and assume, as in Example 2.9, that the mass density is a linear function of Y:

$$\rho = \rho_0 + \Delta\rho - \Delta\rho\, Y$$

The governing ODE for the variable-density case is

$$\frac{dY}{dt} = \frac{-k^* Y^2 [\rho_0 + \Delta\rho - \Delta\rho\, Y]}{\rho_0} \tag{2.36}$$

At a given time and with the same value for k^*, we expect Y to be somewhat different from Y'. Divide Equation 2.34 by Equation 2.36. This eliminates time as an explicit variable and happens to eliminate k^* as well. The result is

$$\frac{dY'}{dY} = \frac{\rho_0 Y'^2}{[\rho_0 + \Delta\rho - \Delta\rho\, Y]\, Y^2} \tag{2.37}$$

Thus there is a unique relationship between Y and Y' that depends only on ρ_0 and $\Delta\rho$. The boundary condition associated with Equation 2.37 is $Y' = 1$ at $Y = 1$. An analytical solution is possible, but numerical integration of the ODE is easier. Euler's method works, but note that the independent variable, Y, starts at 1.0 and is decreased in small steps until the desired final value is reached. This means that the integration step, ΔY, in Euler's method is negative. Once Y' has been determined, k^*t can be found from Equation 2.35. The following table shows values for the case of $\rho_\infty = 1040$ and $\rho_0 = 900$:

Y (Variable ρ)	Y' (Constant ρ)	k^*t
1.000	1.000	0
0.700	0.705	0.418
0.500	0.512	0.953
0.200	0.214	3.15
0.100	0.110	8.09
0.010	0.011	89.9

The increase in density causes an increase in conversion (lower Y) because the working volume in the reactor is going down and this gives higher reactant concentrations. A decrease in density would show the opposite effect. The differences in conversion are small for the density changes typical of liquid phase systems and, as a practical matter, are likely to be masked by errors in the rate constants and operating conditions.

Industrial, gas phase reactions are common in flow reactors but rare in batch reactors. We will consider one example, a second-order reaction at constant pressure and temperature. Substituting the ideal gas law into Equation 2.32 gives

$$\frac{dN_A}{dt} = -\frac{kN_A^2}{V} = \frac{-kN_A^2 P}{[N_A + N_B + \cdots]R_g T} \tag{2.38}$$

Writing similar equations for N_B and any other components gives a set of ODEs than can be solved numerically. A more elegant approach is possible when there is only a single reaction. For an ideal gas mixture at constant pressure and temperature

$$\frac{V}{V_0} = \frac{N_{\text{total}}}{N_0}$$

and

$$\frac{dN_A}{dt} = -\frac{kN_A^2}{V} = \frac{-kN_0 N_A^2}{[N_A + N_B + \cdots]V_0}$$

For the case of only one reactant, it is generally possible to determine $N_{\text{total}} = N_A + N_B + \cdots$ as a function of N_A, giving an ODE that depends only on N_A.

EXAMPLE 2.11

Suppose initially pure A dimerizes, $2A \xrightarrow{k/2} B$, isothermally in the gas phase at a constant pressure of 1 atm. Find a solution to the batch design equation and compare the results to a hypothetical batch reactor in which the reaction is $2A \rightarrow B + C$ so that there is no volume change upon reaction.

SOLUTION: The unrealistic chemistry assumes no inerts and therefore maximizes the effect of the volume change. For the given reaction stoichiometry,

$$N_{\text{total}} = N_A + N_B = N_A + \tfrac{1}{2}[(N_A)_0 - N_A] = \tfrac{1}{2}[N_A + (N_A)_0]$$

This result can be substituted into Equation 2.38 to give an equation that can be integrated with N_A as the single dependent variable. A more elegant result can be obtained by converting to the intrinsic variable Y:

$$\frac{dY}{dt} = \frac{-2k^*Y^2}{1+Y}$$

Defining Y' as in Example 2.10 gives Equation 2.34 as before. Eliminating time gives

$$\frac{dY'}{dY} = \frac{Y+1}{2Y^2}Y'^2$$

As in Example 2.10, there is a unique relationship between Y and Y'. Results from a numerical solution are as follows:

Y (Variable ρ)	Y' (Constant ρ)	k^*t
1.000	1.000	0
0.700	0.718	0.393
0.500	0.542	0.847
0.200	0.263	2.80
0.100	0.150	5.65
0.050	0.083	11.0
0.020	0.036	26.5
0.010	0.019	51.8

The effect of the density change is larger than that for the liquid phase examples but is still not major. Note that most gaseous systems will have substantial amounts of inerts (e.g., nitrogen) that will mitigate volume changes at constant pressure and temperature.

The general conclusion is that density changes are of minor importance in liquid systems and of only moderate importance in gaseous systems at constant pressure and temperature. When they are important, the necessary calculations for a batch reactor are easier if compositions are expressed in terms of total moles [or the fraction unreacted, $Y = Y_A = N_A/(N_A)_0$] rather than molar concentrations.

We have considered volume changes resulting from density changes in liquid and gaseous systems. These volume changes were ***thermodynamically determined*** using an equation of state for the fluid that specifies volume or density as a function of composition, pressure, temperature, and any other state variable that may be important. This is the usual case in chemical engineering problems. In Example 2.10, the density depended only on the composition. In Example 2.11, the density depended on composition, pressure, and temperature, but only the composition was allowed to vary.

Volume changes also can be ***mechanically determined***, as in the combustion cycle of a piston engine. If $V = V(t)$ is an explicit function of time, Equations like 2.32 are then variable separable and relatively easy to integrate, either alone or simultaneously with other component balances. Note, however, that reaction rates can become dependent on pressure under extreme conditions. See Problem 5.4. Also, the results will not really apply to car engines since mixing of air and fuel is relatively slow, flame propagation is important, and the spatial distribution of the reaction must be considered. The combustion chamber is not perfectly mixed.

It is possible that the volume is determined by a combination of thermodynamics and mechanics. An example is reaction in an elastic balloon. See Problem 2.21.

The examples in this section have treated a single, second-order reaction, although the approach can be generalized to multiple reactions with arbitrary kinetics. Equation 2.30 can be written for each component:

$$\begin{aligned}\frac{d(Va)}{dt} &= \frac{dN_A}{dt} = V\mathscr{R}_A(a, b, \ldots) = V\mathscr{R}_A(N_A, N_B, \ldots, V)\\ \frac{d(Vb)}{dt} &= \frac{dN_B}{dt} = V\mathscr{R}_B(a, b, \ldots) = V\mathscr{R}_B(N_A, N_B, \ldots, V)\end{aligned} \tag{2.39}$$

and so on, for components C, D, ... An auxiliary equation is used to determine V. The auxiliary equation is normally an algebraic equation rather than an ODE. In chemical engineering problems, it will usually be an equation of state such as the ideal gas law. In any case, the set of ODEs can be integrated numerically starting with known initial conditions, and V can be calculated and updated as necessary. Using Euler's method, V is determined at each time step using the "old" values for $N_A, N_B, \ldots$. The integration of sets of ODEs with various auxiliary equations is discussed more fully in Chapter 3.

2.6.2 Fed-Batch Reactors

Many industrial reactors operate in the ***fed-batch*** mode. It is also called the ***semibatch*** mode. In this mode of operation, reactants are charged to the system at various times, and products are removed at various times. Occasionally, a ***heel*** of material from a previous batch is retained to start the new batch. There are a variety of reasons for operating in a semibatch mode. Some typical ones are as follows:

1. A starting material is subjected to several different reactions, one after the other. Each reaction is essentially independent, but it is convenient to use the

same vessel. The final reaction to trinitrotoluene in the evil professor's TNT process is an example. It requires a far different environment than normally used for the mono and dinitro reactions, but it could be conducted in the same vessel.

2. Appreciable reaction starts as soon as the reactants come into contact during the charging process. The initial reaction environment depends on whether the reactants are charged sequentially or simultaneously.
3. One reactant is charged to the reactor in small increments to control the composition distribution of the product. Vinyl copolymerizations discussed in Chapter 13 are typical examples. Incremental addition is also used to control reaction exotherms.
4. A byproduct comes out of solution or is intentionally removed to avoid an equilibrium limitation. Ethylene glycol removed during the polymerization of polyethylene terephthalate (PET) allows the formation of high-molecular-weight polymer.
5. One reactant is sparingly soluble in the reaction phase and would be depleted were it not added continuously. Oxygen used in an aerobic fermentation is a typical example.
6. The heel contains a biocatalyst (e.g., yeast cells) needed for the next batch. A fine Italian wine, Amarone, is an example.

All but the first of these has the chemical reaction occurring simultaneously with mixing or mass transfer. A general treatment requires the combination of transport equations with the chemical kinetics, and it becomes necessary to solve sets of PDEs rather than ODEs. Although this approach is becoming common in continuous flow systems, it remains difficult in batch systems. The central difficulty is in developing good models for the mixing and mass transfer steps. Programs for computational fluid dynamics (CFD) such as Fluent have recently been tuned to give good predictions for complex reactions in fed-batch reactors, but their use requires expert knowledge, validation remains necessary, and computation times can be many days.

The difficulty disappears when the mixing and mass transfer steps are fast compared to the reaction steps. The contents of the reactor remain perfectly mixed even while new ingredients are being added. Compositions and reaction rates will be spatially uniform, and a flow term is simply added to the mass balance. Instead of Equation 2.30, we write

$$\frac{dN_A}{dt} = (Qa)_{\text{in}} + V\mathscr{R}_A(N_A, N_B, \ldots, V) \tag{2.40}$$

where the term $(Qa)_{\text{in}}$ represents the molar flow rate of A into the reactor. A fed-batch reactor is an example of the unsteady, variable-volume CSTRs treated in Chapter 14, and solutions to Equation 2.40 are considered there. However, fed-batch reactors are amenable to the methods of this chapter if the charging and discharging steps are fast compared to reaction times. In this special case, the fed-batch reactor

becomes a sequence of ideal batch reactors that are reinitialized after each charging or discharging step

Many semibatch reactions involve more than one phase and are thus classified as ***heterogeneous.*** Examples are aerobic fermentations, where oxygen is supplied continuously to a liquid substrate, and chemical vapor deposition, where gaseous reactants are supplied continuously to a solid substrate. Typically, the overall reaction rate will be limited by the rate of interphase mass transfer. Such systems are treated using the methods of Chapters 10 and 11. Occasionally, the reaction will be kinetically limited so that the transferred component saturates the reaction phase. The system can then be treated as a batch reaction, with the concentration of the transferred component being dictated by its solubility. The early stages of batch fermentation will behave in this fashion with respect to oxygen content but will shift to a mass transfer limitation as the cell mass and thus the oxygen demand increase.

2.7 SCALEUP OF BATCH REACTIONS

Section 1.5 described one basic problem of scaling batch reactors. It is impossible to maintain a constant mixing time if the scaleup ratio is large. However, this is a problem for fed-batch reactors and does not pose a limitation if the reactants are premixed and preheated or if mixing occurs at a low initial temperature where reaction is negligible. A single-phase, isothermal or adiabatic batch reaction can be scaled indefinitely if the reactants are premixed and preheated before being charged. The restriction to single-phase systems avoids mass transfer limitations; the restriction to isothermal or adiabatic systems avoids heat transfer limitations; and the requirement for premixing eliminates concerns about mixing time. All the reactants are mixed initially, the reaction treats all molecules equally, and the agitator may as well be turned off. Thus, within the literal constraints of this chapter, scaleup is not a problem. It is often possible to preheat and premix the feed streams as they enter the reactor and, indeed, to fill the reactor in a time substantially less than the reaction half-life. Unfortunately, as we shall see in other chapters, real systems can be more complicated. Heat and mass transfer limitations are common. If there is an agitator on the reactor, it probably has a purpose.

One purpose of the agitator may be to mix the contents after they are charged rather than on the way in. When does this approach, which violates the strict assumptions of an ideal batch reactor, lead to practical scaleup problems? The simple answer is: whenever the mixing time, as described in Section 1.5, becomes commensurate with the reaction half-life. If the mixing time threatens to become limiting upon scaleup, try to accomplish the mixing in the transfer piping on the way into the reactor. Tee mixers and impinging jet mixers can be an effective way to do this.

Mixing, mass transfer, and heat transfer all become more difficult as size increases. To avoid limitations, avoid these steps. Use premixed feed with enough inerts so that the reaction stays single phase and the reactor can be operated adiabatically. This simplistic approach is occasionally possible and even economical. More sophisticated techniques for avoiding scaleup problems are discussed in Section 5.3.

Scaleup relationships for stirred tanks, both batch and continuous flow, are given in Section 4.4.

Early on in a laboratory program, it is necessary to determine if mixing effects are important. The reactor should be reasonably sized, say 1 L, and it should be agitated with an impeller of known and scaleable type. Good choices for moderate-viscosity systems are pitched-blade turbines and hydrofoil impellers. Little will be learned using magnetic stirrers and anchor or moon-type agitators, as these are rarely suited for commercial production. The small vessel should be baffled since commercial vessels are almost always baffled, and baffling can have a dramatic and usually beneficial effect on mass transfer. Vary the agitator speed over a wide range. Expect poor results at low speeds, but hope for a broad range of speeds in which the speed has little effect on yield and selectivity. For fed-batch systems, varying the feed rate and the location of the feed point will provide additional measures of sensitivity to mixing. If the laboratory reactor shows little or no sensitivity to mixing and if scaleup can be accomplished at constant power per unit volume, mass transfer should not be a problem in the large vessel. However, heat transfer may still be a problem. See Chapter 5.

2.8 STOICHIOMETRY AND REACTION COORDINATES

The reactor design equations in this book can be applied to all components in the system, even inerts. When the reaction rates are formulated using Equation 2.8, the solutions automatically account for the stoichiometry of the reaction. This is the simplest and preferred approach, but it has not always been followed in this book. Several examples have ignored product concentrations when they do not affect reactions rates and when they are easily found from the amount of reactants consumed. Also, some of the analytical solutions have used stoichiometry to ease the algebra. The present section formalizes the use of stoichiometric constraints. We begin with a matrix formulation for the reaction rates of the components in multiple reactions. The presentation is rather elegant from a mathematical viewpoint and does have some practical utility.

2.8.1 Matrix Formulation of Reaction Rates

Consider a system with N chemical components undergoing a set of M reactions. Define the $N \times M$ matrix of stoichiometric coefficients as

$$\boldsymbol{\nu} = \begin{pmatrix} \nu_{A,\mathrm{I}} & \nu_{A,\mathrm{II}} & \cdots \\ \nu_{B,\mathrm{I}} & \nu_{B,\mathrm{II}} & \\ \vdots & & \ddots \end{pmatrix} \tag{2.41}$$

There is a row in this matrix for each of the N components and a column for each of the M reactions. Multiply $\boldsymbol{\nu}$ by the vector ($M \times 1$ matrix) of reaction rates, $\mathscr{R}_{\mathrm{I}}$, to obtain the vector ($N \times 1$ matrix) of component reaction rates:

$$\mathscr{R}_A = \boldsymbol{\nu}\mathscr{R}_{\mathrm{I}} \tag{2.42}$$

In more explicit form,

$$\mathscr{R}_{\mathrm{I}} = \begin{pmatrix} \mathscr{R}_{\mathrm{I}} \\ \mathscr{R}_{\mathrm{II}} \\ \mathscr{R}_{\mathrm{III}} \\ \vdots \end{pmatrix} (M \times 1) \qquad \text{and} \qquad \mathscr{R}_A = \begin{pmatrix} \mathscr{R}_A \\ \mathscr{R}_B \\ \mathscr{R}_C \\ \vdots \end{pmatrix} (N \times 1) \tag{2.43}$$

Using this notation, we can write the design equations for a batch reactor in very compact form:

$$\frac{d(\mathbf{a}V)}{dt} = V\mathscr{R}_A \tag{2.44}$$

where $\mathbf{a}$ is the vector ($N \times 1$ matrix) of component concentrations.

EXAMPLE 2.12

Consider a constant-volume batch reaction with the following set of reactions:

$$\begin{array}{lll} \mathrm{A} + 2\mathrm{B} \rightarrow \mathrm{C} & & \mathscr{R}_{\mathrm{I}} = k_{\mathrm{I}}a \\ \mathrm{A} + \mathrm{C} \rightarrow \mathrm{D} & & \mathscr{R}_{\mathrm{II}} = k_{\mathrm{II}}ac \\ \mathrm{B} + \mathrm{C} \rightarrow \mathrm{E} & & \mathscr{R}_{\mathrm{III}} = k_{\mathrm{III}}c \end{array}$$

These reaction rates would be plausible if B were present in great excess, say as water in an aqueous reaction. Equation 2.44 can be written out as

$$\frac{d}{dt}\begin{pmatrix} a \\ b \\ c \\ d \\ e \end{pmatrix} = \begin{pmatrix} -1 & -1 & 0 \\ -2 & 0 & -1 \\ +1 & -1 & -1 \\ 0 & +1 & 0 \\ 0 & 0 & +1 \end{pmatrix} \begin{pmatrix} k_{\mathrm{I}}a \\ k_{\mathrm{II}}ac \\ k_{\mathrm{III}}c \end{pmatrix}$$

Expanding this result gives the following set of ODEs:

$$\begin{aligned} \frac{da}{dt} &= -k_{\mathrm{I}}a - k_{\mathrm{II}}ac \\ \frac{db}{dt} &= -2k_{\mathrm{I}}a - k_{\mathrm{III}}c \\ \frac{dc}{dt} &= +k_{\mathrm{I}}a - k_{\mathrm{II}}ac - k_{\mathrm{III}}c \\ \frac{dd}{dt} &= k_{\mathrm{II}}ac \\ \frac{de}{dt} &= +k_{\mathrm{III}}c \end{aligned}$$

There are five equations in five unknown concentrations. The set is easily solved by numerical methods, and the stoichiometry has already been incorporated. However, it is not the smallest set of ODEs that can be solved to determine the five concentrations. The first and third equations contain only a and c as unknowns and can thus be solved without recourse to the other two equations. However, this solution does not enable the concentrations of D and E to be calculated. A third equation, say for the concentration of D, must be solved. The effective dimensionality of the set is actually 3.

The dimensionality of a set of design equations can always be reduced to the number of ***independent*** chemical reactions. A set of reactions is independent if no member of the set can be obtained by adding or subtracting multiples of the other members. The set will be independent if each reaction contains one species not present in any other reaction, but this is not a necessary condition and is frequently violated (e.g., Example 2.12). The student of linear algebra will understand that the ***rank*** of $\boldsymbol{\nu}$ will equal M when the reactions are independent. Then, no more than M reactor design equations need to be solved to determine all N concentrations. When the reactions are independent, $M < N$, so that fewer equations need to be solved. Years ago, this fact was useful since numerical solutions to ODEs required substantial computer time. Large sets of ODEs can now be solved in literally the blink of an eye, and there is little incentive to reduce dimensionality in sets of ODEs. However, the theory used to reduce dimensionality also gives global stoichiometric equations that can be useful in thermodynamic calculations and in overall material balances. These are discussed in Section 7.2.

2.8.2 Stoichiometry of Single Reactions

The general stoichiometric relationships for a single reaction in a batch reactor are

$$\frac{N_A - (N_A)_0}{\nu_A} = \frac{N_B - (N_B)_0}{\nu_B} = \frac{N_C - (N_C)_0}{\nu_C} = \cdots = \varepsilon \tag{2.45}$$

where N_A is the number of moles of A in the system at any time and ε is the ***extent of reaction*** or ***reaction coordinate***. Here, ε has units of moles and provides a standardized measure of the extent of reaction. When $\varepsilon = 1$, one mole of a material having a stoichiometric coefficient of $+1$ will have been formed by the reaction. This definition applies even if no reactant has a stoichiometric coefficient of $+1$. For the reaction A $\rightarrow$ 2B, a value of $\varepsilon = 1$means that 1 mol of A will have been consumed and 2 mol of B will have been produced.

Equation 2.45 applies at every instant of time in a batch reactor. Whether or not there are spatial variations within the reactor makes no difference. All batch reactors satisfy the ***global stoichiometry*** of Equation 2.45

Equation 2.45 is frequently used to close the material balance for components that do not affect the reaction rate. A second use of Equation 2.45 is to eliminate some of the composition variables from rate expressions. Divide Equation 2.45 by V

to obtain

$$\frac{a-(N_A)_0/V}{\nu_A}=\frac{b-(N_B)_0/V}{\nu_B}=\cdots=\varepsilon \tag{2.46}$$

where $(N_A)_0/V = a_0$when the volume is constant. These stoichiometric relationships between a and the concentrations of the other components can be used to convert $\mathscr{R}_A(a, b, c, ...)$ to $\mathscr{R}_A(a)$ if Equation 2.46 can be applied to each and every point in the reactor. Reactors for which this is possible are said to ***preserve local stoichiometry***. It does not apply to real reactors if there are internal mixing or separation processes such as molecular diffusion that distinguish between types of molecules. It does not apply to multiple reactions, although this restriction can be relaxed through use of the reaction coordinate method described in the next section.

2.8.3 Stoichiometry of Multiple Reactions

Multiple reactions have an extent of reaction, ε_{I}, for each reaction. If there are N components and M reactions,

$$\mathbf{N}-\mathbf{N}_0=\boldsymbol{\nu}\boldsymbol{\varepsilon} \tag{2.47}$$

where $\mathbf{N}$ and $\mathbf{N}_0$ are column vectors ($N \times 1$ matrices) giving the final and initial number of moles of each component and $\boldsymbol{\varepsilon}$ is the reaction coordinate vector ($M \times 1$ matrix). In more explicit form,

$$\begin{pmatrix} N_A \\ N_B \\ \vdots \end{pmatrix} - \begin{pmatrix} N_A \\ N_B \\ \vdots \end{pmatrix}_0 = \begin{pmatrix} \nu_{A,\mathrm{I}} & \nu_{A,\mathrm{II}} & \cdots \\ \nu_{B,\mathrm{I}} & \nu_{B,\mathrm{II}} & \\ \vdots & & \ddots \end{pmatrix} \begin{pmatrix} \varepsilon_{\mathrm{I}} \\ \varepsilon_{\mathrm{II}} \\ \vdots \end{pmatrix} \tag{2.48}$$

Equation 2.48 is a generalization to M reactions of the stoichiometric constraints of Equation 2.45. If the vector $\boldsymbol{\varepsilon}$ is known, the amounts of all N components that are consumed or formed by the reaction can be calculated.

The vector $\boldsymbol{\varepsilon}$ is found by solving

$$\frac{d\boldsymbol{\varepsilon}}{dt}=V\boldsymbol{\mathscr{R}}_{\mathrm{I}} \quad \text{where } \boldsymbol{\varepsilon}=0 \text{ at } t=0. \tag{2.49}$$

In this formulation, $\boldsymbol{\mathscr{R}}_{\mathrm{I}}$ is the $M \times 1$ vector of reaction rates. See Equation 2.43. The conversion from $\boldsymbol{\mathscr{R}}_{\mathrm{I}}(N_A, N_B, \ldots, V)$ to $\boldsymbol{\mathscr{R}}_{\mathrm{I}}(\varepsilon_{\mathrm{I}}, \varepsilon_{\mathrm{II}}, \ldots, V)$is done using the algebraic equations obtained from Equation 2.48. The initial condition associated with Equation 2.49 is $\boldsymbol{\varepsilon}=0$ at $t=0$.

Equation 2.49 represents a set of M ODEs in M independent variables, $\varepsilon_{\mathrm{I}}, \varepsilon_{\mathrm{II}}, \ldots$. Numerical solutions are usually necessary. Once solved, the values for $\boldsymbol{\varepsilon}$ can be used to calculate the N composition variables using Equation 2.48. These compositions can in turn be used in an equation of state to calculate the volume for variable-volume problems.

EXAMPLE 2.13

Apply the reaction coordinate method to the reactions in Example 2.12.

SOLUTION: Equation 2.42 for this set is

$$\frac{d}{dt}\begin{pmatrix}\varepsilon_{\mathrm{I}}\\ \varepsilon_{\mathrm{II}}\\ \varepsilon_{\mathrm{III}}\end{pmatrix} = V\begin{pmatrix}k_{\mathrm{I}}a\\ k_{\mathrm{II}}ac\\ k_{\mathrm{III}}c\end{pmatrix} = \begin{pmatrix}k_{\mathrm{I}}N_A\\ \dfrac{k_{\mathrm{I}}N_AN_C}{V}\\ k_{\mathrm{III}}N_C\end{pmatrix} \tag{2.50}$$

Equation 2.48 can be written out for this reaction set to give

$$\begin{aligned}
N_A - (N_A)_0 &= -\varepsilon_{\mathrm{I}} - \varepsilon_{\mathrm{II}}\\
N_B - (N_B)_0 &= -2\varepsilon_{\mathrm{I}} - \varepsilon_{\mathrm{III}}\\
N_C - (N_C)_0 &= +\varepsilon_{\mathrm{I}} - \varepsilon_{\mathrm{II}} - \varepsilon_{\mathrm{III}}\\
N_D - (N_D)_0 &= +\varepsilon_{\mathrm{II}}\\
N_E - (N_E)_0 &= +\varepsilon_{\mathrm{III}}
\end{aligned} \tag{2.51}$$

The first three of these equations are used to eliminate N_A, N_B, and N_C from the reaction rate vector. The result is

$$\begin{aligned}
\frac{d\varepsilon_{\mathrm{I}}}{dt} &= k_{\mathrm{I}}[(N_A)_0 - \varepsilon_{\mathrm{I}} - \varepsilon_{\mathrm{II}}]\\
\frac{d\varepsilon_{\mathrm{II}}}{dt} &= \frac{k_{\mathrm{II}}}{V}[(N_A)_0 - \varepsilon_{\mathrm{I}} - \varepsilon_{\mathrm{II}}][(N_C)_0 + \varepsilon_{\mathrm{I}} - \varepsilon_{\mathrm{II}} - \varepsilon_{\mathrm{III}}]\\
\frac{d\varepsilon_{\mathrm{III}}}{dt} &= k_{\mathrm{III}}[(N_C)_0 + \varepsilon_{\mathrm{I}} - \varepsilon_{\mathrm{II}} - \varepsilon_{\mathrm{III}}]
\end{aligned}$$

Integrate these out to time t_{batch} and then use Equations 2.51 to evaluate $N_A \ldots, N_E$. Note, however, that the equation for $\varepsilon_{\mathrm{II}}$ contains volume as an ancillary variable that will physically depend on the component concentrations, not on the ε. This is an awkwardness that can be overcome but that is likely to eliminate the computation advantages of the reaction coordinate. It is also likely that the reader will dislike the algebra needed for this example.

Using concentration or the number of moles as the dependent variable allows better physical insight than using reaction coordinates. A substantial objection to the reaction coordinate method is that the minimal set of M independent chemical reactions is likely to be nonsense in terms of mechanism. See Problem 2.24.

SUGGESTED FURTHER READINGS

Most undergraduate texts on physical chemistry give a survey of chemical kinetics and reaction mechanisms. A comprehensive treatment is provided in:

S. W. Benson, *Foundations of Chemical Kinetics,* McGraw-Hill, New York, 1960.

A briefer and more recent description is:

J. H. Espenson (Ed.), *Chemical Kinetics and Reaction Mechanisms,* McGraw-Hill, New York, 1995.

A comprehensive treatment of chemical oscillators and assorted reaction esoterica is given in:

I. R. Epstein, I. R., and J. A. Pojman (Ed.), *An Introduction to Nonlinear Chemical Dynamics: Oscillations, Waves, Patterns, and Chaos*, Oxford University Press, New York, 1998.

A mathematically oriented work that is far more elegant than Section 2.8 has been reprinted as a paperback:

R. Aris, *Elementary Chemical Reactor Analysis*, Dover, Mineola, NY, 2000.

An account of the reaction coordinate method as applied to chemical equilibrium is given in Chapter 14 of:

J. M. Smith, H. C. Van Ness, and M. M. Abbott, *Introduction to Chemical Engineering Thermodynamics,* 7th ed., McGraw-Hill, New York, 2004.

The Internet has become a wonderful source of (sometimes free) software for numerical analysis. Browse through it, and you will soon see that Fortran remains the programming language for serious computation. One excellent book is:

W. H. Press, S. A. Teukolsky, W. T. Vetterling, and B. P. Flannery, *Numerical Recipes in Fortran 77: The Art of Scientific Computing*, Vol. 1, 2nd ed., Cambridge University Press, New York, 1992.

This book describes and gives Fortran subroutines for a wide variety of ODE solvers. Indeed, it gives numerical recipes for practically anything you will ever need to compute. There is a Volume 2 that discusses Fortran 90 in the context of parallel computing. Versions of Volume I for C, Pascal, and Basic are also available.

PROBLEMS

2.1 The following reactions are occurring in a constant-volume, isothermal batch reactor:

$$\begin{aligned} \mathrm{A} + \mathrm{B} &\xrightarrow{k_1} \mathrm{C} \\ \mathrm{B} + \mathrm{C} &\xrightarrow{k_2} \mathrm{D} \end{aligned}$$

Parameters for the reactions are $a_0 = b_0 = 10$ mol m^{-3}, $c_0 = d_0 = 0$, $k_1 = k_2 = 0.01$ m^3 mol^{-1} h^{-1}, and $t_{\text{batch}} = 4$ h.

(a) Find the concentration of C at the end of the batch cycle.

(b) Find a general relationship between the concentrations of A and C when that of C is at a maximum.

2.2 The following kinetic scheme is postulated for a batch reaction:

$$\begin{aligned} \mathrm{A} + \mathrm{B} &\rightarrow C \qquad \mathscr{R}_{\mathrm{I}} = k_{\mathrm{I}} a^{1/2} b \\ \mathrm{B} + \mathrm{C} &\rightarrow \mathrm{D} \qquad \mathscr{R}_{\mathrm{II}} = k_{\mathrm{II}} c^{1/2} b \end{aligned}$$

Determine a, b, c, and d as functions of time. Continue your calculations until the limiting reagent is 90% consumed given $a_0 = 10$ mol m^{-3}, $b_0 = 2$ mol m^{-3}, $c_0 = d_0 = 0$, and $k_{\mathrm{I}} = k_{\mathrm{II}} = 0.02$ m$^{3/2}$ mol$^{-1/2}$ s^{-1}.

2.3 Refer to Example 2.4. Prepare the plot referred to in the last sentence of that example. Assume $k_{\mathrm{II}}/k_{\mathrm{I}} = 0.1$.

2.4 Dimethyl ether thermally decomposes at temperatures above 450°C. The predominant reaction is

$$\mathrm{CH_3OCH_3} \rightarrow \mathrm{CH_4} + \mathrm{H_2} + \mathrm{CO}$$

Suppose a homogeneous, gas phase reaction occurs in a constant-volume batch reactor. Assume ideal gas behavior and suppose pure A is charged to the reactor.

(a) Show how the reaction rate can be determined from pressure measurements. Specifically, relate $\mathscr{R}$ to dP/dt.

(b) Determine $P(t)$ assuming the decomposition is first-order.

2.5 The first step in manufacturing PET is to react terephthalic acid with a large excess of ethylene glycol to form diglycol terephthalate:

$$\begin{aligned}&\text{HOOC-}\phi\text{-COOH} + 2\text{HOCH}_2\text{CH}_2\text{OH}\\ &\quad\rightarrow \text{HOCH}_2\text{CH}_2\text{OOC-}\phi\text{-COOCH}_2\text{CH}_2\text{OH} + 2\text{H}_2\text{O}\end{aligned}$$

Derive a plausible kinetic model for this reaction. Be sure your model reflects the need for the large excess of glycol. This need is inherent in the chemistry if you wish to avoid byproducts.

2.6 Consider the liquid phase reaction of a diacid with a diol, the first reaction step being

$$\text{HO-R-OH} + \text{HOOC-R}' - \text{COOH} \rightarrow \text{HO-ROOCR}'\text{-COOH} + \text{H}_2\text{O}$$

Suppose the desired product is the single-step mixed acidol as shown above. A large excess of the diol is used, and batch reactions are conducted to experimentally determine the reaction time $t_{\max}$, which maximizes the yield of acidol. Devise a kinetic model for the system and explain how the parameters in this model can be fit to the experimental data.

2.7 The exponential function can be defined as a limit:

$$\lim_{m\rightarrow\infty}\left(1+\frac{z}{m}\right)^m = e^z$$

Use this fact to show that Equation 2.17 becomes Equation 2.16 in the limit as $n \rightarrow \infty$.

2.8 Determine the maximum batch reactor yield of B for a reversible, first-order reaction

$$\text{A} \underset{k_r}{\overset{k_f}{\rightleftharpoons}} \text{B}$$

Do not assume $b_0 = 0$. Instead, your answer will depend on the amount of B initially present.

2.9 Refer to Table 2.1. Start with 1 mol of ^{238}U and let it age for 10 billion years or so. What is the maximum number of atoms of ^{214}**Po** that will ever exist? Warning! This problem is monstrously difficult to solve by brute-force methods. A long but straightforward analytical solution is possible. See also Section 2.5.3 for a shortcut method.

2.10 Consider the consecutive reactions

$$\text{A} \xrightarrow{k} \text{B} \xrightarrow{k} \text{C}$$

Suppose the two reactions have equal rate constants. Find $b(t)$for a batch reactor.

2.11 Find the batch reaction time that maximizes the concentration of component B in Problem 2.10. You may begin with the solution of Problem 2.10 or with Equation 2.23.

2.12 Find $c(t)$ for the consecutive, first-order reactions of Equation 2.20 given that $k_B = k_C$.

2.13 Determine the batch reaction time that maximizes the concentration of component C in Equation 2.20 given that $k_A = 1\ \text{h}^{-1}$, $k_B = 0.5\ \text{h}^{-1}$, $k_C = 0.25\ \text{h}^{-1}$, and $k_D = 0.125\ \text{h}^{-1}$.

2.14 Consider the sequential reactions of Equation 2.20 and suppose $b_0 = c_0 = d_0 = 0$, $k_{\mathrm{I}} = 3\ \mathrm{h}^{-1}$, $k_{\mathrm{II}} = 2\ \mathrm{h}^{-1}$, and $k_{\mathrm{III}} = 4\ \mathrm{h}^{-1}$. Determine the ratios a/a_0, b/a_0, c/a_0, and d/a_0 when the batch reaction time is chosen such that:

(a) The final concentration of A is maximized.

(b) The final concentration of B is maximized.

(c) The final concentration of C is maximized.

(d) The final concentration of D is maximized.

2.15 Find the value of the dimensionless batch reaction time, $k_f t_{\mathrm{batch}}$, that maximizes the concentration of B for the following set of reactions:

$$\mathrm{A} \underset{k_r}{\overset{k_f}{\rightleftarrows}} \mathrm{B} \xrightarrow{k_B} \mathrm{C}$$

Compare this maximum value for b to the value for b obtained using the quasi-steady hypothesis. Try several cases: (a) $k_r = k_B = 10k_f$, (b) $k_r = k_B = 20k_f$, (c) $k_r = 2k_B = 10k_f$.

2.16 The acetaldehyde decomposition discussed in Section 2.5.3 is observed to produce minor amounts of ethane as expected from the proposed termination mechanism. Minor amounts of hydrogen are also observed. A postulated mechanism adds two chain transfer reactions to account for the hydrogen:

$$\mathrm{CHO}\cdot \xrightarrow{k_{\mathrm{V}}} \mathrm{CO} + \mathrm{H}\cdot$$
$$\mathrm{H}\cdot + \mathrm{CH_3CHO} \xrightarrow{k_{\mathrm{VI}}} \mathrm{CH_3CO}\cdot + \mathrm{H_2}$$

The previous result for the observed reaction rate had the form

$$\mathscr{R}_{\mathrm{CH_3CHO}} = k[\mathrm{CH_3CHO}]^{3/2}$$

What does this become when the two new reactions are considered?

2.17 The bromine–hydrogen reaction

$$\mathrm{Br_2} + \mathrm{H_2} \rightarrow 2\mathrm{HBr}$$

is believed to proceed by the following elementary reactions:

$$\mathrm{Br_2} + \mathrm{M} \underset{k_{\mathrm{II}}}{\overset{k_{\mathrm{I}}}{\rightleftarrows}} 2\mathrm{Br}\cdot + \mathrm{M} \qquad \text{(I)}$$

$$\mathrm{Br}\cdot + \mathrm{H_2} \underset{k_{\mathrm{III}}}{\overset{k_{\mathrm{II}}}{\rightleftarrows}} \mathrm{HBr} + \mathrm{H}\cdot \qquad \text{(II)}$$

$$\mathrm{H}\cdot + \mathrm{Br_2} \xrightarrow{k_{\mathrm{III}}} \mathrm{HBr} + \mathrm{Br}\cdot \qquad \text{(III)}$$

The initiation step, reaction I, represents the thermal dissociation of bromine, which is brought about by collision with any other molecule, denoted by M.

(a) A postulated termination reaction is the reverse of the initiation step and is third order. Apply the quasi-steady hypothesis to [Br·] and [H·] to obtain

$$\mathscr{R} = \frac{k[\mathrm{H_2}][\mathrm{Br_2}]^{3/2}}{[\mathrm{Br_2}] + k'[\mathrm{HBr}]}$$

(b) What is the result if the reverse reaction (I) does not exist and termination is second order, $2\mathrm{Br}\cdot \rightarrow \mathrm{Br_2}$?

2.18 A proposed mechanism for the thermal cracking of ethane is

$$\begin{aligned} C_2H_6 + M &\xrightarrow{k_I} 2CH_3\cdot + M \\ CH_3\cdot + C_2H_6 &\xrightarrow{k_{II}} CH_4 + C_2H_5\cdot \\ C_2H_5\cdot &\xrightarrow{k_{III}} C_2H_4 + H\cdot \\ H\cdot + C_2H_6 &\xrightarrow{k_{IV}} H_2 + C_2H_5\cdot \\ 2C_2H_5\cdot &\xrightarrow{k_V} C_4H_{10} \end{aligned}$$

The overall reaction has variable stoichiometry:

$$\begin{aligned} C_2H_6 \rightarrow\ & \nu_B C_2H_4 + \nu_C C_4H_{10} + (2 - 2\nu_B - 4\nu_C)CH_4 \\ & + (-1 + 2\nu_B + 3\nu_C)H_2 \end{aligned}$$

The free-radical concentrations are small and are ignored in this equation for the overall reaction.

(a) Apply the quasi-steady hypothesis to obtain an expression for the disappearance of ethane.

(b) What does the quasi-steady hypothesis predict for ν_B *and* ν_B?

(c) Ethylene is the desired product. Which is better for this gas phase reaction, high or low pressure?

2.19 The Lotka–Volterra reaction described in Section 2.5.4 has three initial conditions, one each for grass, rabbits, and lynx, all of which must be positive. There are three rate constants assuming the supply of grass is not depleted. Use dimensionless variables to reduce the number of independent parameters to four. Pick values for these that lead to a sustained oscillation. Then, vary the parameter governing the grass supply and determine how this affects the period and amplitude of the solution.

2.20 It is proposed to study the hydrogenation of ethylene,

$$C_2H_4 + H_2 \rightarrow C_2H_6$$

in a constant-pressure, gas phase batch reactor. Derive an expression for the reactor volume as a function of time assuming second-order kinetics, ideal gas behavior, perfect stoichiometry, and 50% inerts by volume at $t = 0$.

2.21 Suppose a rubber balloon is filled with a gas mixture and that one of the following reactions occurs:

$$\begin{aligned} 2A &\xrightarrow{k} B \\ A + B &\xrightarrow{k} C \\ A &\xrightarrow{k} B + C \end{aligned}$$

Determine $V(t)$. *Hint 1*: The pressure difference between the inside and the outside of the balloon must be balanced by the stress in the fabric of the balloon so that $\pi R^2 \Delta P = 2\pi Rh\sigma$, where h is the thickness of the fabric and σ is the stress. *Hint 2*: assume the density of the fabric is constant so that $4\pi R^2 h = 4\pi R_0^2 h_0$. *Hint 3*: Assume the fabric is perfectly elastic so that stress is proportional to strain (Hooke's law). *Hint 4*: The ideal gas law applies.

2.22 A numerical integration scheme has produced the following results:

Δz	Integral
1.0	0.23749
0.5	0.20108
0.25	0.19298
0.125	0.19104
0.0625	0.19056

(a) What is the apparent order of convergence?

(b) Extrapolate the results to $\Delta z = 0$. (*Note:* Such extrapolation should not be done unless the integration scheme has a theoretical order of convergence that agrees with the apparent order. Assume it does.)

(c) What value for the integral would you expect at $\Delta z = \frac{1}{32}$?

2.23 See Example 2.14 in Appendix 2.1. (a) Write chemical equations which will give the ODEs of that example. (b) Rumor has it that there is an error in the Runge–Kutta calculations for the case of $\Delta t = 0.5$. Write or acquire the necessary computer code and confirm or deny the rumor.

2.24 The usual method of testing for convergence and of extrapolating to zero step size assumes that the step size is halved in successive calculations. Example 2.4 quartered the step size. Develop an extrapolation technique for this procedure. Test it using the data in Example 2.15 in Appendix 2.1.

2.25 Consider molecules A, B, and C reacting in the gas phase. The observed reaction is $A + B \rightleftarrows C$. Assume all reactions occur by bimolecular collisions so that the first-order reaction $C \rightarrow A + C$ does not occur. Also, A and B are not self-reactive. A postulated mechanism for the observed reaction involves all pairs of reactants except for A with A and B with B:

$$\begin{aligned} A + B &\rightarrow C \\ A + C &\rightarrow 2A + B \\ B + C &\rightarrow A + 2B \\ 2C &\rightarrow C + A + B \end{aligned}$$

Is this a possible mechanism for a real chemical system? How many independent reactions are there? What are they?

2.26 The evil assistant professor continues the pursuit of TNT that he started in Problem 1.13. He is much better at chemical analysis than chemical kinetics, let alone reactor design. Still, he has now read Chapter 2 and has learned that even the mononitration of toluene needs to be modeled as a set of reactions rather than a single reaction in order to explain his results. The mononitration gave the following distribution of isomers: ortho 62%, meta 4%, para 34%. Only small amounts of dinitrotoluene were formed. The reaction at 0°C and with HNO_3 in great excess was fast, with 98% of the toluene converted after 20 min. The evil professor has the audacity to ask the beautiful princess for help in developing a kinetic model. Unaware of his possibly nefarious use of the ultimate product, she quickly produced a reasonable model that considered only the organic phase. What was it?

2.27 The evil professor was disappointed by the low yield of dinitrotoluene and the almost complete absence of trinitrotoluene. He increased the temperature and the concentration of the sulfuric acid and, with the continued large excess of nitric acid, succeeded in driving the reaction to almost complete conversion of the toluene to dinitrotoluenes. Again, there was negligible yield of trinitrotoluene. Assuming the same relative reactivity of the ortho, meta, and para positions as in Problem 2.26, what was the distribution of the dinitro products?

2.28 The evil professor has now read about fed-batch reactors and checked an authoritative source (Wikipedia!) to learn that the reaction of dinitrotoluene to TNT uses fuming sulfuric acid as a catalyst. He added this in the fed-batch mode and reacted to near completion. The major product was 2,4,6-trinitrotoluene, as desired. What other isomers are possible. Quesstimate their relative concentrations, again based on the same relative reactivity of the ortho, meta, and para positions as in Problem 2.26.

APPENDIX 2.1 NUMERICAL SOLUTION OF ORDINARY DIFFERENTIAL EQUATIONS

Chapter 2 described Euler's method for solving sets of ODEs. The method is extremely simple from a conceptual and programming viewpoint. It is computationally inefficient in the sense that a great many arithmetic operations are necessary to produce accurate solutions. More efficient techniques should be used when the same set of equations is to be solved many times as in optimization studies. One such technique, ***fourth-order Runge–Kutta,*** has proved very popular and can be generally recommended for all but stiff sets of first-order ODEs. The set of equations to be solved is

$$\frac{da}{dt} = \mathscr{R}_A(a, b, \ldots, t) \qquad \frac{db}{dt} = \mathscr{R}_B(a, b, \ldots, t) \tag{2.52}$$

A value of Δt is selected, and values for Δa, Δb, ... are calculated by evaluating the functions $\mathscr{R}_A, \mathscr{R}_B, \ldots$. In Euler's method, this evaluation is done at the initial point $(a_0, b_0, \ldots, t_0)$ so that the estimate for Δa is just $\Delta t\, \mathscr{R}_A(a_0, b_0, \ldots, t_0) = \Delta t(\mathscr{R}_A)_0$. In fourth order Runge–Kutta, the evaluation is done at four points and the estimates for Δa, Δb,... are based on weighted averages of the $\mathscr{R}_A$, $\mathscr{R}_B$, ... at these four points:

$$\begin{aligned} \Delta a &= \Delta t \frac{(\mathscr{R}_A)_0 + 2(\mathscr{R}_A)_1 + 2(\mathscr{R}_A)_2 + (\mathscr{R}_A)_3}{6} \\ \Delta b &= \Delta t \frac{(\mathscr{R}_B)_0 + 2(\mathscr{R}_B)_1 + 2(\mathscr{R}_B)_2 + (\mathscr{R}_B)_3}{6} \end{aligned} \tag{2.53}$$

where the various $\mathscr{R}$'s are evaluated at the points

$$\begin{aligned} a_1 &= a_0 + \tfrac{1}{2}\Delta t(\mathscr{R}_A)_0 \\ a_2 &= a_0 + \tfrac{1}{2}\Delta t(\mathscr{R}_A)_1 \\ a_3 &= a_0 + \Delta t(\mathscr{R}_A)_2 \end{aligned} \tag{2.54}$$

with similar equations for b_1, b_2,b_3, and so on. Time rarely appears explicitly in $\mathscr{R}$, but should it appear,

$$\begin{aligned} t_1 &= t_0 + \Delta t\ 2 \\ t_2 &= t_1 \\ t_3 &= t_0 + \Delta t \end{aligned} \tag{2.55}$$

EXAMPLE 2.14

Use fourth–order Runge–Kutta integration to solve the following set of ODEs.

$$\begin{aligned} \frac{da}{dt} &= -k_1 a^2 \\ \frac{db}{dt} &= +k_1 a^2 - k_2 bc \\ \frac{dc}{dt} &= -k_2 bc \end{aligned}$$

Use $a_0 = c_0 = 30$, $b_0 = = 0$, $k_1 = 0.01$, and $k_2 = 0.02$. Find a, b, c for $t = 1$.

SOLUTION: The coding is left to the reader, but if you really need a worked example of the Runga–Kutta integration, check out Example 6.4. Following are detailed results for $\Delta t = 1.0$ which means only one step was taken to reach the answer.

i	a_i	b_i	c_i	$(\mathscr{R}_A)_\mathrm{I}$	$(\mathscr{R}_B)_i$	$(\mathscr{R}_C)_i$
0	30.000	0	30.000	−18.000	9.000	0
1	21.000	4.500	30.000	−8.820	1.710	−2.700
2	25.590	0.855	28.650	−13.097	6.059	−0.490
3	16.903	6.059	29.510	−5.714	−0.719	−3.576
	Final:		18.742	3.970	28.341	

For $\Delta t = 0.5$, the results for *a, b,* and *c* are

Final:		18.740	4.069	28.445

Results accurate to three places after the decimal are obtained with $\Delta t = 0.25$.

Final:		18.750	4.072	28.448

The fourth–order Runge–Kutta method converges $O(\Delta t^5)$. Thus, halving the step size decreases the error by a factor of 32. By comparison, Euler's method converges $O(\Delta t)$ so that halving the step size decreases the error by a factor of only 2. These remarks apply only in the limit as $\Delta t \to 0$, and either method can give anomalous behavior if Δt is large. If you can confirm that the data are converging according to the theoretical order of convergence, the convergence order can be used to extrapolate calculations to the limit as $\Delta t \to 0$.

EXAMPLE 2.15

Develop an extrapolation technique suitable for the first-order convergence of Euler integration. Test it for the set of ODEs in Examples 2.3.

SOLUTION: Repeat the calculations in Example 2.3 but now reduce Δt by a factor of 2 for each successive calculation rather than by the factor of 4 used in the examples. Calculate the corresponding changes in $a(t_{max})$ and denote these changes by Δ. Then Δ should decrease by a factor of two for each calculation of $a(t_{max})$. (The reader interested in rigor will note that the error is halved and will do some algebra to prove that the Δ are halved as well.) If Δ was the change that just occurred, then we would expect the next change to be $\Delta/2$, the one after that to be $\Delta/4$, and so on. The total change yet to come is thus $\Delta/2 + \Delta/4 + \Delta/8 + \cdots$. This is a geometric series that converges to Δ. Using Euler's method, the cumulative change yet to come is equal to the single change that just occurred. Thus, the extrapolated value for $a(t_{max})$ is the value just calculated plus the Δ just calculated. The extrapolation scheme is illustrated for the ODEs in Examples 2.3 in the following table:

Number of Steps	$a(t_{max})$	Δ	Extrapolated $a(t_{max})$
2	−16.3200		
4	1.5392	17.8591	19.3938
8	2.8245	1.2854	4.1099
16	3.2436	0.4191	3.6626
32	3.4367	0.1931	3.6298
64	3.5304	0.0937	3.6241
128	3.5766	0.0462	3.6228
256	3.5995	0.0229	3.6225
512	3.6110	0.0114	3.6224
1,024	3.6167	0.0057	3.6224
2,048	3.6195	0.0029	3.6224
4,096	3.6210	0.0014	3.6224
8,192	3.6217	0.0007	3.6224
16,384	3.6220	0.0004	3.6224
32,768	3.6222	0.0002	3.6224
65,536	3.6223	0.0001	3.6224
131,072	3.6223	0.0000	3.6224

Extrapolation can reduce computational effort by a large factor, but computation is cheap. The value of the computational reduction will be trivial for most problems. Convergence acceleration can be useful for complex problems or for the inside loops in optimization studies. For such cases you should also consider more sophisticated integration schemes such as Runge–Kutta. It too can be extrapolated although the extrapolation rule is different. The extrapolated factor for Runge–Kutta integration is based on the series

$$1/32 + 1/32^2 + 1/32^3 + \cdots = 0.03226$$

Thus the total change yet to come is about 3% of the change that just occurred. As a practical matter, your calculations will probably achieve the required accuracy by the time you confirm that successive changes in the integral really are decreasing by a factor of 32 each time. With modern computers and Runge–Kutta integration, extrapolation is seldom needed for the solution of ODE's. It may still be useful in the solution of the second-order PDEs treated in Chapters 8 and 9. The ODE solvers are often used as part of the solution technique for PDEs. Extrapolation is used in some highly efficient ODE solvers. A variety of sophisticated integration techniques are available both as freeware and as commercial packages. Their use may be justified for design and optimization studies where the same set of equations must be solved repetitively or when the equations are exceptionally stiff. The casual user need go no further than Runge–Kutta, possibly with adaptive step sizes where Δt is varied from step to step in the calculations based on error estimates. See Press et al. (1992), for a usable example of Runge–Kutta integration with adaptive step sizes.

Chapter 3

Isothermal Piston Flow Reactors

Chapter 2 developed a methodology for treating multiple and complex reactions in batch reactors. The methodology is now applied to PFRs. The reactors considered in this chapter are single phase and isothermal, but some of the design and scaleup methods can be applied to nonisothermal systems as well. This chapter generalizes the design equations for piston flow to include variable density, variable velocity, and even variable cross-sectional area. The key assumptions of piston flow remain intact: There must be complete mixing in the direction perpendicular to flow and no mixing in the direction of flow. Most reactors that reasonably approximate piston flow are long, circular tubes. Accordingly, we will refer to the direction perpendicular to the flow as the radial direction and the direction of flow as the axial direction. However, noncircular cross sections and cross sections that vary with axial position are sometimes used.

Chapter 1 treated PFRs with constant axial velocity. The design equations for this type of PFR are directly analogous to the design equations for a constant-density batch reactor. What happens in time in the batch reactor happens in space in the PFR, and the transformation $t = z/\bar{u}$ converts one design equation to the other. For component A,

$$\bar{u}\frac{da}{dz} = \mathscr{R}_A \qquad \text{where } a = a_{\text{in}} \quad \text{at } z = 0 \tag{3.1}$$

All the results obtained for isothermal, constant-density batch reactors apply to isothermal, constant-density (and constant-cross-section) PFRs. Just replace t with $z/\bar{u}$, and evaluate the outlet concentration at $z = L$. Equivalently, leave the result in the time domain and evaluate the outlet composition at time $\bar{t} = L/\bar{u}$. For example, the solution for component B in the competitive reaction sequence

$$\text{A} \xrightarrow{k_A} \text{B} \xrightarrow{k_B} \text{C} \xrightarrow{k_C} \text{D} \xrightarrow{k_D} \cdots$$

Chemical Reactor Design, Optimization, and Scaleup, Second Edition. By E. B. Nauman
Copyright © 2008 John Wiley & Sons, Inc.

is given by Equation 2.22 for a batch reactor:

$$b_{\text{batch}}(t) = \left[b_0 - \frac{a_0 k_A}{k_B - k_A}\right] e^{-k_B t} + \left[\frac{a_0 k_A}{k_B - k_A}\right] e^{-k_A t}$$

The solution for the same reaction sequence run in a PFR is

$$b_{\text{PFR}}(z) = \left[b_{\text{in}} - \frac{a_{\text{in}} k_A}{k_B - k_A}\right] e^{-k_B z/\bar{u}} + \left[\frac{a_{\text{in}} k_A}{k_B - k_A}\right] e^{-k_A z/\bar{u}}$$

The extension to multiple reactions is done by writing Equation 3.1 (or the more complicated versions of Equation 3.1 that will soon be developed) for each of the N components. The component reaction rates are found from Equation 2.8 in exactly the same ways as in a batch reactor. The result is an ***initial-value problem*** consisting of N simultaneous, first-order ODEs that can be solved using your favorite ODE solver. The same kind of problem was solved in Chapter 2, but the independent variable is now z rather than t.

An emphasis in this chapter is on the generalization of piston flow to situations other than constant velocity down the tube. Real reactors can closely approximate PFRs, yet show many complications compared to the constant-density and constant-cross-section case considered in Chapter 1. Gas phase tubular reactors may have appreciable density differences between the inlet and outlet. The mass density and thus the velocity down the tube can vary at constant pressure if there is a change in the number of moles upon reaction. The pressure drop due to skin friction can cause even larger changes in the density and velocity of the gas. Reactors are sometimes designed to have variable cross sections, and this too can change the density and velocity. Despite these complications, PFRs remain closely akin to batch reactors. There is a one-to-one correspondence between time in a batch and position in a tube, but the general relationship is no longer as simple as $z = \bar{u}t$.

3.1 PISTON FLOW WITH CONSTANT MASS FLOW

Most of this chapter assumes that the mass flow rate down the tube is constant, that is, the tube wall is impermeable. The reactor cross-sectional area A_c is allowed to vary as a function of axial position, $A_c = A_c(z)$. Figure 3.1 shows the system and indicates the nomenclature. An overall mass balance gives

$$Q\rho = Q_{\text{in}}\rho_{\text{in}} = A_c \bar{u} \rho = (A_c)_{\text{in}} \bar{u}_{\text{in}} \rho_{\text{in}} = \text{const} \tag{3.2}$$

where ρ is the mass density which is assumed uniform over the cross section of the reactor but which may change as a function of z. The counterpart for Equation 3.2 in a batch system is that ρV is constant.

The component balance will be based on the molar flow rate:

$$\dot{N}_A = Qa \tag{3.3}$$

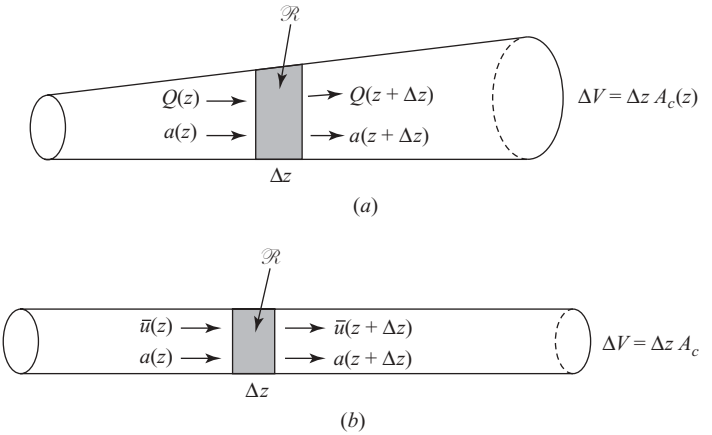

Figure 3.1 Differential volume elements in PFRs: (*a*) variable cross section; (*b*) constant cross section.

Unlike $Q\rho$, $\dot{N}_A$ is not a conserved quantity and varies down the length of the tube. Consider a small volume element of length Δz and volume $\Delta z A_c$. The molar flow entering the element is $\dot{N}_A(z)$ and that leaving the element is $\dot{N}_A(z + \Delta z)$, the difference being due to reaction within the volume element. A balance on component A gives

$$\dot{N}_A(z) + A_c\, \Delta z\, \mathscr{R}_A = \dot{N}_A(z + \Delta z)$$

or

$$\frac{\dot{N}_A(z + \Delta z) - \dot{N}_A(z)}{A_c\, \Delta z} = \mathscr{R}_A$$

Taking the limit as $\Delta z \to 0$ gives

$$\frac{1}{A_c}\frac{d(\dot{N}_A)}{dz} = \frac{1}{A_c}\frac{d(Qa)}{dz} = \frac{1}{A_c}\frac{d(A_c\bar{u}a)}{dz} = \mathscr{R}_A \tag{3.4}$$

This is the piston flow analog of the variable-volume batch reactor, Equation 2.30. Note that Equation 3.4 reduces to Equation 3.1 when A_c and $\bar{u}$ are constant.

The derivative in Equation 3.4 can be expanded into three separate terms:

$$\frac{1}{A_c}\frac{d(A_c\bar{u}a)}{dz} = \bar{u}\frac{da}{dz} + a\frac{d\bar{u}}{dz} + \frac{\bar{u}a}{A_c}\frac{dA_c}{dz} \tag{3.5}$$

The first of the three terms must be retained since A is a reactive component and thus varies in the z direction. The second term must be retained if either the mass density or the reactor cross-sectional area varies with z. The last term is needed for reactors with variable cross sections. Figure 3.2 illustrates an annular flow reactor that is an industrially relevant reason for including this term.

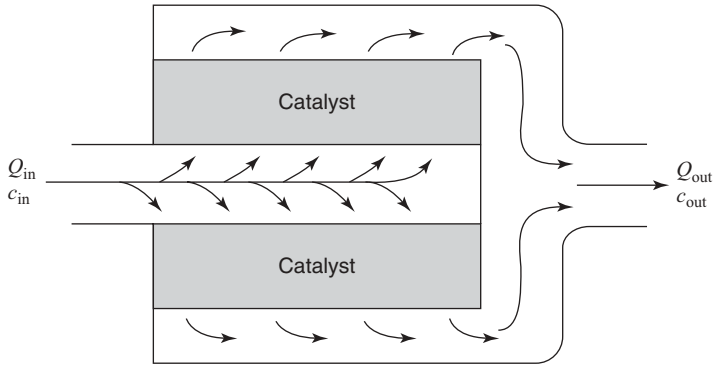

Figure 3.2 Annular packed-bed reactor used for adiabatic reactions favored by low pressure.

Most problems involving variable-density PFRs require numerical solutions, and for these it is better to avoid expanding Equation 3.4 into separate derivatives for a and $\bar{u}$. We could continue to use the molar flow rate $\dot{N}_A$ as the dependent variable but prefer to use the flow counterpart of an intrinsic variable, the molar flux,

$$\Phi_A = \bar{u}a \tag{3.6}$$

The units on Φ_A are moles per square meter per second. This is the ***convective flux***. The student of mass transfer will recognize that a diffusion term like $-\mathscr{D}_A da/dz$ is usually included in the flux. This term is the ***diffusive flux*** and is zero for piston flow. The design equation for a variable-density, variable-cross-section PFR is

$$\frac{d\Phi_A}{dz} = \mathscr{R}_A - \frac{\Phi_A}{A_c}\frac{dA_c}{dz} \qquad \text{where } \Phi_A = (\Phi_A)_{\text{in}} \quad \text{at } z = 0 \tag{3.7}$$

The dA_c/dz term is usually zero since most tubular reactors have a constant diameter. For the exceptional case, we suppose that $A_c(z)$ is known, say from the design drawings of the reactor. It must be a smooth (meaning differentiable) and slowly varying function of z or else the assumption of piston flow will run into hydrodynamic as well as mathematical difficulties. Abrupt changes in A_c will create secondary flows that invalidate the assumptions of piston flow. Thus reactors shaped like a megaphone are acceptable; those with an abrupt change in diameter are not.

We can define a new rate expression $\mathscr{R}'_A$ that includes the dA_c/dz term within it. The design equation becomes

$$\frac{d\Phi_A}{dz} = \mathscr{R}_A - \frac{\Phi_A}{A_c}\frac{dA_c}{dz} = \mathscr{R}'_A = \mathscr{R}'_A(a, b, \ldots, z) \tag{3.8}$$

where $\mathscr{R}'_A$ has an explicit dependence on z when the cross section is variable. and where $\mathscr{R}'_A = \mathscr{R}_A$ for the usual case of constant cross section. The explicit dependence on z causes no problem in numerical integration. In Euler's method, the old value of the independent variable, z, is used to evaluate the right-hand side of the marching-ahead equations in the same way that the old values of the dependent variables are used. Equation 2.55 shows how an explicit dependence on the independent variable is treated in Runge–Kutta integration.

EXAMPLE 3.1

Given $\mathscr{R}_A$, find $\mathscr{R}'_A$ for the megaphone reactor shown in Figure 3.1*a*.

SOLUTION: The cross section is circular, so $A_c = \pi R^2$, $dA_c/dz = 2\pi R\, dR/dz$, and

$$\frac{\Phi_A}{A_c}\frac{dA_c}{dz} = \frac{2\Phi_A}{R}\frac{dR}{dz}$$

The radius of the megaphone varies linearly with z according to the equation

$$R = R_{\text{in}} + \frac{(R_{\text{out}} - R_{\text{in}})z}{L} \qquad \text{and} \qquad \frac{dR}{dz} = \frac{R_{\text{out}} - R_{\text{in}}}{L}$$

Thus

$$\frac{d\Phi_A}{dz} = \mathscr{R}'_A = \mathscr{R}_A - \frac{2\Phi_A(R_{\text{out}} - R_{\text{in}})}{R_{\text{in}}L + (R_{\text{out}} - R_{\text{in}})z}$$

Although somewhat messy, a numerical solution causes no special problems.

If there are M reactions involving N components,

$$\frac{d\boldsymbol{\Phi}}{dz} = \boldsymbol{\nu}\mathscr{R}'_A \qquad \text{where } \boldsymbol{\Phi} = \boldsymbol{\Phi}_{\text{in}} \quad \text{at } z = 0 \tag{3.9}$$

where $\boldsymbol{\Phi}$ and $\boldsymbol{\Phi}_{\text{in}}$ are $N \times 1$ column vectors of the component fluxes, $\boldsymbol{\nu}$ is the $N \times M$ matrix of stoichiometric coefficients, and $\mathscr{R}'_A$ is an $M \times 1$ column vector of reaction rates which includes the effects of varying the reactor cross section. Equation 3.9 represents a set of first-order ODEs and is the flow analog of Equation 2.44. The dimensionality of the set can be limited to the number of independent reactions using the reaction coordinate method discussed in Section 2.8, but there is little point in doing so. The reduction provides no significant help in either numerical or analytical solutions. Even the case of one reactant going to one product is difficult to solve analytically when the density or cross section varies with axial position. A reason for this difficulty is illustrated in Example 3.2.

EXAMPLE 3.2

Find the fraction unreacted for a first-order reaction in a variable-density, variable-cross-section PFR.

SOLUTION: It is easy to begin the solution. In piston flow, molecules that enter together leave together and have the same residence time in the reactor, $\bar{t}$. When the kinetics are first order, the probability that a molecule reacts depends only on its residence time. The probability that a particular molecule will leave the system without reacting is $\exp(-k\bar{t})$. For the entire collection of molecules, the probability becomes a deterministic fraction. The ***fraction unreacted*** for a first-order reaction in any PFR is

$$Y_A = \frac{(\dot{N}_A)_{\text{out}}}{(\dot{N}_A)_{\text{in}}} = \frac{(Qa)_{\text{out}}}{(Qa)_{\text{in}}} = \frac{(A_c\bar{u}a)_{\text{out}}}{(A_c\bar{u}a)_{\text{in}}} = e^{-k\bar{t}} \tag{3.10}$$

The solution for Y_A is simple, even elegant, but what is the value of $\bar{t}$? It is equal to the mass holdup divided by the mass throughput, Equation 1.40, but there is no simple formula for the holdup when the density is variable. The same reactor will give different conversions for A when the reactions are A → 2B and A → B even though it is operated at the same temperature and pressure and the first-order rate constants are identical.

Fortunately, it is possible to develop a general-purpose technique for the numerical solution of Equation 3.9 even when the density varies down the tube. It is first necessary to convert the component reaction rates from their normal dependence on concentration to a dependence on the molar fluxes. This is done simply by replacing a by $\Phi_A/\bar{u}$ and so on for the various components. The reaction rate now explicitly depends on $\bar{u}$ and the design equation is

$$\frac{d\Phi_A}{dz} = \mathscr{R}'_A = \mathscr{R}'_A(a, b, \ldots, z) = \mathscr{R}'_A(\Phi_A, \Phi_B, \ldots, \bar{u}, z) \tag{3.11}$$

Two examples follow: If $\mathscr{R}(a) = ka$, then $\mathscr{R}(\Phi_A, \bar{u}) = k\Phi_A/\bar{u}$. If $\mathscr{R}(a, b, c, d) = k_f ab - k_r cd$, then $\mathscr{R}(\Phi_A, \Phi_B, \Phi_C, \Phi_D, \bar{u}) = (k_f \Phi_A \Phi_B - k_r \Phi_C \Phi_D)/\bar{u}^2$.

As usual, in solving initial-value problems, we assume that all variables are known at the reactor inlet so that $(A_c)_{\text{in}}\bar{u}_{\text{in}}\rho_{\text{in}}$ will be known. An ancillary equation is needed to update $\bar{u}$ after each step. Equation 3.2 can be used to calculate $\bar{u}$ at a downstream location if ρ is known. An equation of state will give ρ but requires knowledge of state variables such as composition, pressure, and temperature. To find these, we will need still more equations, but a closed set can eventually be achieved, and the calculations can proceed in a stepwise fashion down the tube.

3.1.1 Gas Phase Reactions

For gas phase reactions, the molar density is more useful than the mass density. Determining the equation of state for a nonideal gas mixture can be a difficult problem in thermodynamics. For illustrative purposes and for a great many industrial problems, the ideal gas law is sufficient. Here it is in a form suitable for flow reactors:

$$\frac{P}{R_g T} = \rho_{\text{molar}} = a + b + c + \cdots + i \tag{3.12}$$

where i represents the concentration (molar density) of inerts. Note that Equation 3.9 should include inerts as one of the components when the reaction is gas phase. The stoichiometric coefficient is zero for an inert so that $\mathscr{R}_I = 0$, but if A_c varies with z, $\mathscr{R}'_I \neq 0$.

Multiply Equation 3.12 by $\bar{u}$ to obtain

$$\frac{P\bar{u}}{R_g T} = \bar{u}a + \bar{u}b + \bar{u}c + \cdots + \bar{u}i = \Phi_A + \Phi_B + \Phi_C + \cdots + \Phi_I \tag{3.13}$$

If the reactor operates isothermally and if the pressure drop is sufficiently low, we have achieved closure where Equations 3.11 and 3.13 together allow a marching-ahead

solution. An analytical solution to a variable-density problem is rarely possible, even when the pressure is assumed to be constant. The following example is an exception that illustrates the solution technique first in analytical form and then in numerical form.

EXAMPLE 3.3

Consider the reaction $2A \xrightarrow{k} B$. Derive an analytical expression for the fraction unreacted in a gas phase, isothermal PFR of length L. The pressure drop in the reactor is negligible. The reactor cross section is constant. There are no inerts. The feed is pure A and the gases are ideal. Test your mathematics with a numerical solution.

SOLUTION: The design equations for the two components are

$$\frac{d(\bar{u}a)}{dz} = \frac{d\Phi_A}{dz} = -2ka^2 = -2k\frac{\Phi_A^2}{\bar{u}^2}$$
$$\frac{d(\bar{u}b)}{dz} = \frac{d\Phi_B}{dz} = ka^2 = k\frac{\Phi_A^2}{\bar{u}^2}$$

Applying the ideal gas law

$$\frac{P}{R_g T} = \rho_{\text{molar}} = a + b$$

Multiplying by $\bar{u}$ gives

$$\frac{P\bar{u}}{R_g T} = \bar{u}\bar{\rho}_{\text{molar}} = \bar{u}(a+b) = \Phi_A + \Phi_B$$

Since the pressure drop is small, $P = P_{\text{in}}$, and

$$\bar{u} = \frac{\Phi_A + \Phi_B}{a+b} = \frac{\Phi_A + \Phi_B}{a_{\text{in}}} \tag{3.14}$$

The ODEs governing the system become

$$\frac{d\Phi_A}{dz} = -2k\frac{a_{\text{in}}^2\Phi_A^2}{(\Phi_A + \Phi_B)^2} \tag{3.15}$$
$$\frac{d\Phi_B}{dz} = k\frac{a_{\text{in}}^2\Phi_A^2}{(\Phi_A + \Phi_B)^2} \tag{3.16}$$

These equations are the starting point for both the analytical and the numerical solutions.

ANALYTICAL SOLUTION: A stoichiometric relationship can be used to eliminate Φ_B. Combine Equations 3.15 and 3.16 to obtain

$$-\frac{1}{2}(d\Phi_A) = d\Phi_B$$

The initial condition is that $\Phi_A = \Phi_{\text{in}}$ when $\Phi_B = 0$. Thus,

$$\Phi_B = \frac{1}{2}(\Phi_{\text{in}} - \Phi_A) \tag{3.17}$$

Substitute this into Equation 3.15 to obtain a single ODE,

$$\frac{d\Phi_A}{dz} = \frac{-8ka_{\text{in}}^2\Phi_A^2}{(\Phi_A + \Phi_{\text{in}})^2}$$

that is variable separable. Thus,

$$\int_{\Phi_{\text{in}}}^{\Phi_A} \frac{(\Phi_A + \Phi_{\text{in}})^2}{\Phi_A^2} d\Phi_A = -\int_0^z 8ka_{\text{in}}^2\, dz$$

A table of integrals (and a variable substitution, $s = \Phi_A + \Phi_{\text{in}}$) gives

$$\frac{\Phi_A}{\Phi_{\text{in}}} - \frac{\Phi_{\text{in}}}{\Phi_A} - 2\ln\frac{\Phi_{\text{in}}}{\Phi_A} = \frac{-8ka_{\text{in}}^2 z}{\Phi_{\text{in}}}$$

Since A_c is constant in this example, $Y_A = (\Phi_A)_{\text{out}}/\Phi_{\text{in}}$. Setting $z = L$ and some algebra give

$$Y_A - \frac{1}{Y_A} + 2\ln Y_A = -\frac{8ka_{\text{in}}L}{u_{\text{in}}}$$

where $ka_{\text{in}}L/\bar{u}_{\text{in}}$ is a dimensionless, second-order rate constant. Note that $L/\bar{u}_{\text{in}}$ is not the mean residence time $\bar{t}$. It is what the mean residence time would be if the velocity stayed at its inlet value, $\bar{u}_{\text{in}}$. Instead, $\bar{u} = \bar{u}(z)$ decreases down the tube because the number of moles of gas decreases due to reaction. As an example, suppose $Y_A = 0.5$. Then $ka_{\text{in}}L/\bar{u}_{\text{in}} = 0.3608$. Equations 3.17 and 3.14 give

$$\frac{(\Phi_B)_{\text{out}}}{\Phi_{\text{in}}} = \frac{1 - Y_A}{2} = 0.25$$

$$\frac{\bar{u}_{\text{out}}}{\bar{u}_{\text{in}}} = \frac{(\Phi_A + \Phi_B)_{\text{out}}}{\bar{u}_{\text{in}}a_{\text{in}}} = Y_A + \frac{(\Phi_B)_{\text{out}}}{\Phi_{\text{in}}} = 0.75$$

and

$$\frac{a_{\text{out}}}{a_{\text{in}}} = Y_A\frac{\bar{u}_{\text{in}}}{\bar{u}_{\text{out}}} = 0.6667$$

The solution to the constant-density case is

$$Y_A = \frac{(\Phi_A)_{\text{out}}}{\Phi_{\text{in}}} = \frac{a_{\text{out}}}{a_{\text{in}}} = \frac{1}{1 + 2ka_{\text{in}}L/\bar{u}_{\text{in}}}$$

The constant-density case for $Y_A = 0.5$ gives $ka_{\text{in}}L/\bar{u}_{\text{in}} = 0.5$, $\bar{u}_{\text{out}}/\bar{u}_{\text{in}} = 1$, and $a_{\text{out}}/a_{\text{in}} = 0.5$. The constant-density case fails to account for the reduction in $\bar{u}$ as the reaction proceeds and thus underestimates the residence time.

Numerical Solution: The problem statement does not give any specific units for concentration, length, or time. It is possible to choose special units such that $a_{\text{in}} = 1$, $\bar{u}_{\text{in}} = 1$, and $k = 1$. In these special units, the value of z that gives $Y_A = 0.5$ is also the value of the dimensionless rate constant, $ka_{\text{in}}z/\bar{u}_{\text{in}}$, that will give $Y_A = 0.5$. The program is given in Code for Example 3.3.

The output, rounded to four places, is $z = 0.3608$, $u = 0.7500$, and $a = 0.6666$, in agreement with the analytical solution (and a lot easier for most of us).

We turn now to the case of a gas phase, tubular reactor in which the pressure drop is significant. An ODE for pressure must be added to those for the component

Code for Example 3.3

```
Sub Example3_3()

a = 1
b = 0
u = 1
k = 1
dz = 0.0001
z = 0
PAold = u * a
PBold = 0

Do
       PAnew = PAold - 2 * k * PAold ^ 2 / u ^ 2 * dz
       PBnew = PBold + k * PAold ^ 2 / u ^ 2 * dz
       u = PAnew + PBnew
       PAold = PAnew
       PBold = PBnew
       z = z + dz
Loop While PAold > 0.5

Cells(1, 1) = z
Cells(2, 1) = u
a = PAnew / u
Cells(3, 1) = a

End Sub
```

fluxes. The specific form of the ODE depends on whether the reactor is an open tube with laminar flow, an open tube with turbulent flow or a packed bed.

For ***laminar flow*** in a circular tube, the pressure gradient is given by a differential form of the Hagen–Poiseuille equation:

$$\frac{dP}{dz} = -\frac{8\mu\bar{u}}{R^2} \tag{3.18}$$

where μ is the viscosity. In the general case, $\bar{u}$, μ, and R will all vary as a function of z and Equation 3.18 must be integrated numerically. The reader may wonder if piston flow is a reasonable assumption for a laminar flow system since laminar flow has a pronounced velocity profile. The answer is, not really, but there are exceptions. See Chapters 8 and 9 for more suitable design methods and to understand the exceptional—and generally unscaleable—case where piston flow is a reasonable approximation to laminar flow.

For ***turbulent flow***, the pressure drop is calculated from

$$\frac{dP}{dz} = -\frac{\mathbf{Fa}\,\rho\bar{u}^2}{R} \tag{3.19}$$

where the Fanning friction factor **Fa** can be approximated as

$$\mathbf{Fa} = \frac{0.079}{\mathbf{Re}^{1/4}} \tag{3.20}$$

More accurate correlations that take factors like wall roughness into account are readily available, but the form used here is adequate for most purposes. It has a simple, analytical form that lends itself to conceptual thinking and scaleup calculations. Detailed design calculations can use more accurate values of the friction factor.

For ***packed beds*** in either turbulent or laminar flow, the Ergun equation is often satisfactory:

$$\frac{dP}{dz} = -\frac{\rho \bar{u}_s^2}{d_p}\frac{1-\varepsilon}{\varepsilon^3}\left[\frac{150(1-\varepsilon)\mu}{d_p \rho \bar{u}_s} + 1.75\right] = -\frac{\rho \bar{u}_s^2}{d_p}\frac{1-\varepsilon}{\varepsilon^3}\left[\frac{150(1-\varepsilon)}{(\mathbf{Re})_p} + 1.75\right] \tag{3.21}$$

where ε (not to be confused with the reaction coordinate) is the void fraction of the bed, $(\mathbf{Re})_p$ is the particle Reynolds number, and d_p is the diameter of the packing. For nonspherical packing, use six times the ratio of volume to surface area of the packing as an effective d_p. Note that $\bar{u}_s$ is the superficial velocity, this being the velocity the fluid would have if the tube were empty.

For ***rectangular and other noncircular ducts*** in turbulent flow, the standard procedure is to replace R with the hydraulic radius

$$R_H = \frac{2A_c}{\text{wetted perimeter}} \tag{3.22}$$

For circular pipes, $R_H = R$. The reader is cautioned that some definitions of R_H omit the factor of 2 shown in Equation 3.22 so that the result must be multiplied by 2 for use in equations such as 3.18 and 3.19. The use of R_H is not recommended for laminar flow, but alternatives are available in the literature. Also, the method of false transients applied to PDEs in Chapter 16 can be used to calculate laminar velocity profiles in ducts with noncircular cross sections. For turbulent, low-pressure gas flows in rectangular ducts, the American Society of Heating, Refrigerating and Air Conditioning Engineers recommends use of an equivalent diameter defined as

$$D_{\text{Equivalent}} = \frac{1.3(hw)^{5/8}}{(h+w)^{1/4}} \tag{3.23}$$

where w and h are the width and height of the duct. Circular ducts are the most efficient way of moving fluids in terms of pressure drop and the amount of metal needed for fabrication, but noncircular geometries are occasionally used. Figure 3.2 shows an example of an annular packed bed where the flow is in the positive r direction. Microreactors and specialized heat exchangers often have rectangular ducts and slits. See Chapter 16.

Including inerts among the Ncomponents, there are N ODEs that have the Φ as dependent variables and one ODE that has pressure as the dependent variable. There is also an equation of state such as Equation 3.13 that relates P, T, and Φ.

The marching-ahead technique assumes that all variables are known at the reactor inlet. Pressure may be an exception since the discharge pressure is usually specified, and the inlet pressure has whatever value is needed to achieve the desired flow rate. Pressure may be treated as an initially known variable by assuming a value for P_{in}, doing the calculations, then adjusting the assumed value for P_{in} until the specified value for P_{out} is obtained.

Computational Scheme for Gas Phase PFRs

A general procedure for solving the reactor design equations for a PFR using the marching-ahead technique (Euler's method) has seven steps. Note that this general procedure allows for variable temperature as well as variable pressure. The necessary ODE for temperature is given in Chapter 5.

1. Pick a step size, Δz.
2. Calculate initial values for all variables including a guess for P_{in}. Initial values are needed for $a, b, c, \ldots, i, \bar{u}, \Phi_A, \Phi_B, \Phi_C, \ldots, \Phi_I, P, T$ plus physical properties such as μ that are used in the ancillary equations.
3. Take one step, calculating new values for $\Phi_A, \Phi_B, \Phi_C, \ldots, \Phi_I, P, T$ at the new axial location, $z + \Delta z$. The marching-ahead equations for the molar fluxes have the form

$$(\Phi_A)_{\text{new}} = (\Phi_A)_{\text{old}} + \Delta z \, \mathscr{R}'_A[(\Phi_A)_{\text{old}}, (\Phi_B)_{\text{old}}, \ldots, (\Phi_I)_{\text{old}}, z] \tag{3.24}$$

   The right-hand sides of these equations are evaluated using the old values that correspond to position z. A similar Euler-type solution is used for one of Equations 3.14, 3.15, or 3.17 to calculate P_{new}, and an ODE from Chapter 5 is solved in the same way to calculate T_{new}.
4. Update $\bar{u}$ using

$$\bar{u}_{\text{new}} = \frac{R_g T_{\text{new}} (\Phi_A + \Phi_B + \Phi_C + \cdots + \Phi_I)_{\text{new}}}{P_{\text{new}}} \tag{3.25}$$

   Note that this step uses the ideal gas law. Other equations of state could be substituted.
5. Update all physical property values to the new conditions. The component concentrations are updated using

$$a_{\text{new}} = \frac{(\Phi_A)_{\text{new}}}{\bar{u}_{\text{new}}}, \quad b_{\text{new}} = \frac{(\Phi_B)_{\text{new}}}{\bar{u}_{\text{new}}}, \quad \text{etc.} \tag{3.26}$$

6. If $z < L$, go to step 3. If $z \geq L$, is P_{out} correct? If not, go to step 2 and guess another value for P_{in}.
7. Decrease Δz by a factor of 2 and go to step 1. Repeat until the results converge to four or five significant figures.

The next example applies this general procedure to a packed-bed reactor.

EXAMPLE 3.4

Fixed-bed reactors are used for the catalytic dehydrogenation of ethylbenzene to form styrene:

$$C_8H_{10} \rightleftarrows C_8H_8 + H_2 \quad (A \rightleftarrows B + C)$$

The reaction is endothermic, but large amounts of steam are used to minimize the temperature drop and, by way of the water–gas shift reaction, to prevent accumulation of coke on the catalyst. Ignore the reverse and competitive reactions and suppose that a proprietary catalyst in the form of 3-mm spheres gives a first-order rate constant of 15 s^{-1} at 625°C.

The molar ratio of steam to ethylbenzene at the inlet is 9 : 1. The bed is 1 m in length and the void fraction is 0.5. The inlet pressure is set at 1 atm and the outlet pressure is adjusted to give a superficial velocity of 9 m s^{-1} at the tube inlet. (The real design problem would specify the downstream pressure and the mass flow rate.) The particle Reynolds number is 100 based on the inlet conditions ($\mu \approx 4 \times 10^{-5}$ Pa s). Find the conversion, pressure, and velocity at the tube outlet assuming isothermal operation.

SOLUTION: This is a variable-velocity problem with $\bar{u}$ changing because of the reaction stoichiometry and the pressure drop. The flux marching equations for the various components are

$$\begin{aligned}
(\Phi_A)_{j+1} &= (\Phi_A)_j - ka\,\Delta z = (\Phi_A)_j - k\frac{(\Phi_A)_j}{\bar{u}}\Delta z \\
(\Phi_B)_{j+1} &= (\Phi_B)_j + ka\,\Delta z = (\Phi_B)_j + k\frac{(\Phi_A)_j}{\bar{u}}\Delta z \\
(\Phi_C)_{j+1} &= (\Phi_C)_j + ka\,\Delta z = (\Phi_C)_j + k\frac{(\Phi_A)_j}{\bar{u}}\Delta z \\
(\Phi_D)_{j+1} &= (\Phi_D)_j
\end{aligned}$$

where D represents the inerts. There is one equation for each component. It is perfectly feasible to retain each of these equations and to solve them simultaneously. Indeed, this is necessary if there is a complex reaction network or if molecular diffusion destroys local stoichiometry. For the current example, the stoichiometry is so simple it may as well be used. At any step j,

$$\Phi_C = \Phi_B = (\Phi_A)_{\text{in}} - \Phi_A$$

Thus we need retain only the flux marching equation for component A.

The pressure is also given by an ODE. The Ergun equation 3.21 applies to a packed bed:

$$P_{j+1} = P_j - \frac{\rho\bar{u}_s^2}{d_p}\frac{1-\varepsilon}{\varepsilon^3}\left[\frac{150(1-\varepsilon)}{\mathbf{Re}_p} + 1.75\right]\Delta z$$

where $\mathbf{Re}_p = d_p\rho\bar{u}_s/\mu$ is the particle Reynolds number. The viscosity is approximately constant since μ is a function of temperature alone for low-density gases. Also, $\rho\bar{u}_s$ is constant because the mass flow is constant in a tube of constant cross section. These facts justify the assumption that $\mathbf{Re}_p$ is constant. Since $\rho\bar{u}_s$ is constant, the $\rho\bar{u}_s^2$ term in the Ergun equation is equal to $(\rho\bar{u}_s)_{\text{in}}\bar{u}_s$.

The marching equations for flux and pressure contain the superficial velocity $\bar{u}_s$. The ideal gas law in the form of Equation 3.13 is used to relate it to the flux:

$$(\bar{u}_s)_j = \frac{R_g T}{P_j}(\Phi_A + \Phi_B + \Phi_C + \Phi_D) = \frac{R_g T}{P_j}[2(\Phi_A)_{\text{in}} - \Phi_A + \Phi_D]$$

The computational scheme marches flux and pressure ahead one step and then updates $\bar{u}_s$.

The various inlet conditions are calculated using the ideal gas law. They are $a_{\text{in}} = 1.36\,\text{mol m}^{-3}$, $b_{\text{in}} = c_{\text{in}} = 0$, $d_{\text{in}} = 12.2\,\text{mol m}^{-3}$, $(\rho\bar{u}_s)_{\text{in}} = 1.23\,\text{kg m}^{-2}\,\text{s}^{-1}$, $(\Phi_A)_{\text{in}} = 12.2\,\text{mol m}^{-2}\,\text{s}^{-1}$, and $\Phi_D = 110\,\text{mol m}^{-2}\text{s}^{-1}$. Substituting known values and being careful with the units gives

$$\begin{aligned}(\Phi_A)_{j+1} &= (\Phi_A)_j\left[1 - \frac{15\,\Delta z}{(\bar{u}_s)_j}\right]\\ P_{j+1} &= P_j - 0.041(\bar{u}_s)_j\,\Delta z\\ (\bar{u}_s)_{j+1} &= \frac{0.08}{P_{j+1}}[134 - \Phi_A]_{j+1}\end{aligned}$$

These equations are solved, starting with the known initial conditions and proceeding step by step down the reactor until the outlet is reached. The solution is

$$X = 1 - \frac{(\Phi_A)_{\text{out}}}{(\Phi_A)_{\text{in}}} = 0.67 \quad (67\%\ \text{conversion})$$

with $P_{\text{out}} = 0.4$ atm and $(\bar{u})_{\text{out}} = 26\ \text{m s}^{-1}$.

The selectivity is 100% in this simple example, but do not believe it. Many things happen at 625°C, and the actual effluent contains substantial amounts of carbon dioxide, benzene, toluene, methane, and ethylene in addition to styrene, ethylbenzene, and hydrogen. It contains small but troublesome amounts of diethyl benzene, divinyl benzene, and phenyl acetylene. The actual selectivity is about 90%. A good kinetic model would account for all the important byproducts and would even reflect the age of the catalyst. A good reactor model would, at a minimum, include the temperature change due to reaction.

Mean Residence Time in Gas Phase Tubular Reactor

Examples such as 3.4 show that numerical solutions to the design equations are conceptually straightforward if a bit cumbersome. The problem with numerical solutions is that they are difficult to generalize. Analytical solutions can provide much greater insight. The next example addresses a very general problem that was raised in Example 3.1. What is the pressure profile and mean residence time $\bar{t}$ in an isothermal, gas phase tubular reactor? If $\bar{t}$ is known, even approximately, Equations like 3.10 suddenly become useful. The results that follow in Example 3.5 apply to any gas phase, tubular reactor, whether it approximates piston flow or not, provided that the change in moles upon reaction is negligible. This assumption is valid when the reaction stoichiometry gives no change in volume, when inerts are present in large quantities, or when the change in density due to the pressure drop is large compared to the change caused by the reaction. Many gas phase reactors satisfy at least one of these conditions.

EXAMPLE 3.5

Find the mean residence time in an isothermal, gas phase, tubular reactor. Assume that the reactor has a circular cross section of constant radius. Assume ideal gas behavior and ignore any change in the number of moles upon reaction.

SOLUTION: Begin with laminar flow and Equation 3.18:

$$\frac{dP}{dz} = -\frac{8\mu\bar{u}}{R^2}$$

To integrate this, $\bar{u}$ is needed. When there is no change in the number of moles upon reaction, Equation 3.2 applies to the total molar density as well as to the mass density. Thus, for constant A_c,

$$\bar{u}\rho_{\text{molar}} = \bar{u}(a + b + \cdots) = \text{const} = \bar{u}_{\text{in}}(\rho_{\text{molar}})_{\text{in}}$$

and

$$\frac{\bar{u}(z)}{\bar{u}_{\text{in}}} = \frac{\rho_{\text{in}}}{\rho(z)} = \frac{(\rho_{\text{molar}})_{\text{in}}}{\rho_{\text{molar}}} = \frac{P_{\text{in}}}{P(z)}$$

These relationships result from assuming ideal gas behavior and no change in the number of moles upon reaction. Substituting $\bar{u}$ into the ODE for pressure gives

$$\frac{dP}{dz} = \frac{-\beta}{2P} \tag{3.27}$$

where β is a constant. The same result but with a different value for β is obtained for turbulent flow when Equation 3.19 is used instead of Equation 3.18. The values for β are

$$\beta = \frac{16\mu P_{\text{in}}\bar{u}_{\text{in}}}{R^2} = \frac{16\mu P_{\text{out}}\bar{u}_{\text{out}}}{R^2} \quad \text{(laminar flow)} \tag{3.28}$$

and

$$\beta = \frac{0.13\mu^{.25}P_{\text{in}}(\rho_{\text{in}}\bar{u}_{\text{in}})^{1.75}}{\rho_{\text{in}}R^{1.25}} = \frac{0.13\mu^{.25}P_{\text{out}}(\rho_{\text{out}}\bar{u}_{\text{out}})^{1.75}}{\rho_{\text{out}}R^{1.25}} \quad \text{(turbulent flow)} \tag{3.29}$$

Integrating Equation 3.27 and applying the inlet boundary condition give

$$P^2 - P_{\text{out}}^2 = \beta(L - z)$$

Observe that $P = P_{\text{in}}$ when $z = 0$. Thus

$$\beta L = P_{\text{in}}^2 - P_{\text{out}}^2 \tag{3.30}$$

for both laminar and turbulent flow.

We are now ready to calculate the mean residence time. According to Equation 1.40, $\bar{t}$ is the ratio of mass inventory to mass throughput. When the number of moles does not change, $\bar{t}$ is also the ratio of molar inventory to molar throughput. Denote the molar inventory (i.e., the total number of moles in the tube) as N_{actual}. Then

$$N_{\text{actual}} = \int_0^L A_c\rho_{\text{molar}}\,dz = \frac{A_c(\rho_{\text{molar}})_{\text{in}}}{P_{\text{in}}}\int_0^L P\,dz = \frac{A_c(\rho_{\text{molar}})_{\text{in}}}{P_{\text{in}}}\int_0^L \left[P_{\text{out}}^2 + \beta(L - z)\right]^{1/2} dz$$

Integration gives

$$\frac{N_{\text{actual}}}{N_{\text{inlet}}} = \frac{2[P_{\text{in}}^3 - P_{\text{out}}^3]}{3\beta L P_{\text{in}}} = \frac{2[P_{\text{in}}^3 - P_{\text{out}}^3]}{3(P_{\text{in}}^2 - P_{\text{out}}^2)P_{\text{in}}} \tag{3.31}$$

where $N_{\text{inlet}} = A_c(\rho_{\text{molar}})_{\text{in}}L$ is the number of moles that the tube would contain if its entire length were at pressure P_{in}. When the pressure drop is low, $P_{\text{in}} \to P_{\text{out}}, \beta \to 0$, and the inventory approaches N_{inlet}. When the pressure drop is high, $P_{\text{in}} \to \infty, \beta \to \infty$, and the inventory is two-thirds of N_{inlet}.

The mean residence time is

$$\bar{t} = \frac{N_{\text{actual}}}{A_c(\rho_{\text{molar}})_{\text{in}}\bar{u}_{\text{in}}} = \frac{2[P_{\text{in}}^3 - P_{\text{out}}^3]}{3\beta L P_{\text{in}}}\left[\frac{L}{\bar{u}_{\text{in}}}\right] = \frac{2[P_{\text{in}}^3 - P_{\text{out}}^3]}{3(P_{\text{in}}^2 - P_{\text{out}}^2)P_{\text{in}}}\left[\frac{L}{\bar{u}_{\text{in}}}\right] \tag{3.32}$$

The term $[L/\bar{u}_{\text{in}}]$ is what the residence time would be if the entire reactor were at the inlet pressure. The factor multiplying it ranges from $\frac{2}{3}$ to 1 as the pressure drop ranges from large to small and as β ranges from infinity to zero.

The terms ***space–time*** and ***space–velocity*** are antiques of petroleum refining but have some utility in this example. The space–time is defined as V/Q_{in}, which is what $\bar{t}$ would be if the fluid remained at its inlet density. The space–time in a tubular reactor with constant cross section is $[L/\bar{u}_{\text{in}}]$. The space–velocity is the inverse of the space–time. The mean residence time $\bar{t}$ is $V\hat{\rho}/(Q\rho)$, where $\hat{\rho}$ is the average density and ρQ is a constant (because the mass flow is constant) that can be evaluated at any point in the reactor. The mean residence time ranges from the space–time to two-thirds the space–time in a gas phase, tubular reactor when the gas obeys the ideal gas law and there is no change in the number of moles upon reaction.

Equation 3.32 determined the mean residence time in terms of variables measured at the reactor inlet. Outlet values can also be used to obtain the same final result:

$$\bar{t} = \frac{N_{\text{actual}}}{A_c(\rho_{\text{molar}})_{\text{out}}\bar{u}_{\text{out}}} = \frac{2[P_{\text{in}}^3 - P_{\text{out}}^3]}{3\beta L P_{\text{out}}}\left[\frac{L}{\bar{u}_{\text{out}}}\right] = \frac{2[P_{\text{in}}^3 - P_{\text{out}}^3]}{3(P_{\text{in}}^2 - P_{\text{out}}^2)P_{\text{out}}}\left[\frac{L}{\bar{u}_{\text{out}}}\right] \tag{3.33}$$

The actual residence time for an ideal gas will always be higher than $[L/\bar{u}_{\text{out}}]$, and it will always be lower than $[L/\bar{u}_{\text{in}}]$.

EXAMPLE 3.6

A 1-in. internal diameter (ID) coiled tube, 57 m long, is being used as a tubular reactor. The operating temperature is 973 K. The inlet pressure is 1.068 atm. The outlet pressure is 1 atm. The outlet velocity has been measured to be 9.96 m s^{-1}. The fluid is mainly steam, but it contains small amounts of an organic compound that decomposes according to first-order kinetics with a half-life of 2.1 s at 973 K. Determine the mean residence time and the fractional conversion of the organic.

SOLUTION: The first-order rate constant is $0.693/2.1 = 0.33$ s^{-1} so that the fractional conversion for a first-order reaction will be $1 - \exp(-0.22\bar{t})$, where $\bar{t}$ is in seconds. The inlet and outlet pressures are known so Equation 3.33 can be used to find $\bar{t}$ given that $[L/\bar{u}_{\text{out}}] = 57/9.96 = 5.72$ s. The result is $\bar{t} = 5.91$ s, which is 3.4% higher than what would be expected based on the outlet conditions. The conversion of the organic compound is 86%.

The ideal gas law can be used to find $[L/\bar{u}_{\text{in}}]$ given $[L/\bar{u}_{\text{out}}]$. The result is $[L/\bar{u}_{\text{in}}] = 6.11$ s. The pressure factor in Equation 3.32 is 0.967, again giving $\bar{t} = 5.91$ s.

Note that the answers do not depend on the tube diameter, the temperature, or the properties of the fluid other than it is an ideal gas.

Although Example 3.6 shows only a modest effect, density changes can be important for gas phase reactions. Kinetic measurements made on a flow reactor are likely to be confounded by the density change. In principle, a kinetic model can still be fit to the data, but this is more difficult than when the measurements are made on a batch system where the reaction times are directly measured. When kinetics measurements are made using a flow reactor, $\bar{t}$ will not be known a priori if the density change upon reaction is appreciable. It can be calculated as part of the data-fitting process. The equation of state must be known along with the inlet and outlet pressures. The calculations follow the general scheme for gas phase PFRs given above. Chapter 7 discusses methods for determining kinetic constants using data from a reactor with complications such as variable density. As stated there, it is better to avoid confounding effects. Batch or CSTR experiments are far easier to analyze.

3.1.2 Liquid Phase Reactions

Solution of the design equations for liquid phase PFRs is usually easier than for gas phase reactors because pressure typically has little effect on the fluid density or the reaction kinetics. Extreme pressures are an exception that theoretically can be handled by the same methods used for gas phase systems. The difficulty will be finding an equation of state. For ordinary pressures, the mass density can usually be estimated as a simple function of composition. This leads to easy and direct use of Equation 3.2.

Computational Scheme for Liquid Phase PFRs

Following is a procedure for solving the reactor design equations for a moderate-pressure, liquid phase PFR using the marching-ahead technique (Euler's method). Note that the general procedure allows for variable temperature but the pressure variation is unimportant in that pressure is assumed to have no effect on the reaction rate or on fluid properties.

1. Pick a step size, Δz.
2. Calculate initial values for all variables. Initial values are needed for $a, b, c, \ldots, i, \rho, \bar{u}, \Phi_A, \Phi_B, \Phi_C, \ldots, \Phi_I, T$. The pressure can be included if desired but does not affect the reaction calculations.
3. Take one step, calculating new values for $\Phi_A, \Phi_B, \Phi_C, \ldots, \Phi_I$ at the new axial location, $z + \Delta z$. The current chapter considers only isothermal reactors, but the general case includes an ODE for temperature. The marching-ahead equations have the form

$$(\Phi_A)_{\text{new}} = (\Phi_A)_{\text{old}} + \Delta z\, \mathscr{R}'_A[(\Phi_A)_{\text{old}}, (\Phi_B)_{\text{old}}, \ldots, (\Phi_I)_{\text{old}}, z] \tag{3.34}$$

The right-hand sides of these equations are evaluated using the old values, which correspond to position z.

4. Update the component concentrations using

$$a_{\text{new}} = \frac{(\Phi_A)_{\text{new}}}{\bar{u}_{\text{old}}}, \qquad b_{\text{new}} = \frac{(\Phi_B)_{\text{new}}}{\bar{u}_{\text{old}}}, \qquad \text{etc.} \tag{3.35}$$

5. Use these new concentrations to update the physical properties that appear in ancillary equations. One property that must be updated is the mass density ρ.

6. Use the new value for ρ to update $\bar{u}$:

$$\bar{u}_{\text{new}} = \frac{\bar{u}_{\text{in}}\rho_{\text{in}}(A_c)_{\text{in}}}{\rho_{\text{new}}A_c} \tag{3.36}$$

7. If $z < L$, go to step 3. If $z \geq L$, decrease Δz by a factor of 2 and go to step 1. Repeat until the results converge to three or four significant figures.

Note that step 4 in this procedure uses the old value for $\bar{u}$ since the new value is not yet known. As a general rule, the exact sequence of calculations is unimportant in marching schemes. What is necessary is that each variable be updated once during each Δz step. Then, taking the numerical limit as $\Delta z \to 0$ removes the discretization error.

EXAMPLE 3.7

The isothermal batch polymerization in Example 2.8 converted 80% of the monomer in 2 h. You want to do the same thing in a meso–pilot plant using a capillary tube. (If the tube diameter is small enough, assumptions of piston flow and isothermal operation may be reasonable even for laminar flow. Criteria are given in Chapters 8 and 16.) The tube has an ID of 0.0015 m and it is 1 m long. The monomer density is 900 kg m^{-3} and the polymer density is 1040 kg m^{-3}. The pseudo-first-order rate constant is 0.8047 h^{-1} and the residence time needed to achieve 80% conversion is $\bar{t} = 2$ h. What flow rate should be used?

SOLUTION: The required flow rate is the mass inventory in the system divided by the mean residence time:

$$Q\rho = \frac{\pi R^2 L\hat{\rho}}{\bar{t}}$$

where the composite quantity $Q\rho$ is the mass flow rate and is constant. It is what we want to find. Its value is easily bounded since $\hat{\rho}$ must lie somewhere between the inlet and outlet densities. Using the inlet density,

$$Q\rho = \frac{1}{2}\left[\pi(0.0015)^2(1)(900)\right] = 0.00318 \text{ kg h}^{-1}$$

The outlet density is calculated assuming the mass density varies linearly with conversion to polymer as in Example 2.8: $\rho_{\text{out}} = 1012$ kg m^{-3}. The estimate for $Q\rho$ based on the outlet density is

$$Q\rho = \frac{1}{2}\left[\pi(0.0015)^2(1)(1012)\right] = 0.00358 \text{ kg h}^{-1}$$

Thus we can make a reasonably accurate initial guess for $Q\rho$. This guess is used to calculate the conversion in a tubular reactor of the given dimensions. When the right guess is made, the mean residence time will be 2 h and the fraction unreacted will be 20%. The computer code used to solve this problem follows the general procedure for liquid phase PFRs as outlined above. The fraction unreacted is calculated as the ratio of $\Phi_A/(\Phi_A)_{\text{in}}$, which is denoted as Phi/PhiIn in **Code for Example 3.7.** A trial-and-error-search gives $Q\rho = 0.003426$ kg h^{-1} for the specified residence time of 2 h and a fraction unreacted of 80%. The calculated outlet density is 1012 kg m^{-3}.

Code for Example 3.7

```
Sub Example3_7()

Qp=Cells(1,1).value  'Input guess from spreadsheet
dz = .00001
R = .0015
L = 1
Pi = 3.14159
k = .8047

rhoin = 900              'Inlet value
Qin = Qp / rhoin         'Inlet value
uin = Qin / (Pi * R ^ 2) 'Inlet value
ain = 1                  'Inlet value
PhiIn = uin * ain        'Inlet value

z = 0    'Starting value for integration
a = ain       'Will vary with z
u = uin       'Will vary with z
Phi = PhiIn   'Will vary with z
t = 0         'Will vary with z

DO
  Phinew = Phi - k * Phi / u * dz
  anew = Phinew / u
  rho = 1040 - 140 * Phinew / PhiIn
  unew = uin * rhoin / rho
  z = z + dz
  t = t + dz / unew
  Phi = Phinew
  u = unew
LOOP WHILE z < L  'End of tube?

Cells(2,1) = t            'Desired value = 2
Cells(2,2) = Phi / PhiIn  'Desired value = 0.8
Cells(2,3) = rho          'Average density


End Sub
```

As noted in Chapter 2, density changes tend to be of secondary importance for liquid phase reactions. They are frequently ignored but can make a large enough difference to justify their inclusion in detailed design calculations. They can cause error in kinetic measurements (e.g., by using the space–time rather than the mean residence time when fitting the data to a kinetic model). As in the case of gas phase reactions, it is preferred to use a batch reactor or a CSTR for kinetic measurements even though the final design will be a tubular reactor.

This chapter is restricted to homogeneous, single-phase reactions, but the restriction can sometimes be relaxed. The formation of a second phase as a consequence of an irreversible reaction will not affect the kinetics except for a possible density change. If the second phase is solid or liquid, the density change will be moderate. If the new phase is a gas, its formation can have a major effect. Specialized models are needed. Two-phase flows of air–water and steam–water in tubes have been extensively studied, but few data are available for chemically reactive systems.

3.2 SCALEUP RELATIONSHIPS FOR TUBULAR REACTORS

We begin a discussion of scaleup relationships and strategies for tubular reactors. Results are restricted to tubes with a constant cross-sectional area. Chapter 3 discusses only isothermal or adiabatic reactors, but the relationships in Tables 3.1–3.3 include scaleup factors for the nonisothermal reactors that are discussed in Chapter 5. These results assume constant density, but Tables 3.4 and 3.5 give some specialized results for ideal gases when the pressure drop down the tube is significant.

3.2.1 Scaling Factors

Scaling factors are ratios. Suppose X is any design or operating variable of a chemical reactor. Then the scaling factor with respect to X is defined as the ratio of X in the full-scale plant to that in the pilot plant:

$$S_X = \frac{X_{\text{full scale}}}{X_{\text{pilot scale}}} = \frac{X_2}{X_1}$$

Chapter 1 introduced throughput and inventory scaling factors, $S_{\text{throughput}}$ and $S_{\text{inventory}}$, in the context of stirred tank reactors, but the defining ratios of mass flow rate and mass inventory given in Chapter 1 can be used for any flow reactor. If density is constant, the scaling factor for inventory is identical to that for volume.

Some scaling factors depend on the specific type of reactor. For tubular reactors, there are scaling factors for the radius and length that together give the scaling factor for volume:

$$S_V = \frac{V_2}{V_1} = \frac{\pi R_2^2 L_2}{\pi R_1^2 L_1} = \left(\frac{R_2}{R_1}\right)^2 \left(\frac{L_2}{L_1}\right) = S_R^2 S_L$$

Table 3.1 Scaleup Factors for Tubular Reactors Operating with Constant Physical Properties: Laminar Flow with Low Graetz Numbers

Laminar Flow in the Asymptotic Region for Heat Transfer[a]	Unconstrained with Arbitrary $\bar{t}$,	Scaleups with Constant $\bar{t}$, $S_{\text{throughput}} = S = S_R^2 S_L$		Scaleup Strategies with Constant $\bar{t}$			
	General Scaleup Factors	S and S_R Specified	S and S_L Specified	Series Scaleup	Geometric Similarity	Constant Pressure Drop	Constant Heat Transfer[b]
Diameter scaling factor	S_R	S_R	$S^{1/2} S_L^{-1/2}$	1	$S^{1/3}$	$S^{1/3}$	1
Length scaling factor	S_L	$S S_R^{-2}$	S_L	S	$S^{1/3}$	$S^{1/3}$	S
Length-to-diameter ratio	$S_L S_R^{-1}$	$S S_R^3$	$S^{-1/2} S_L^{3/2}$	S	1	1	S
Velocity, $\bar{u}$	$S_{\text{throughput}} S_R^{-2}$	$S S_R^{-2}$	S_L	S	$S^{1/3}$	$S^{1/3}$	S
Pressure scaling factor, ΔP	$S_{\text{throughput}} S_R^{-4} S_L$	$S^2 S_R^{-6}$	$S^{-1} S_L^3$	S^2	1	1	S^2
Heat transfer area, A_{ext}	$S_R S_L$	$S S_R^{-1}$	$S^{1/2} S_L^{1/2}$	S	$S^{2/3}$	$S^{2/3}$	S
Inside coefficient, h	S_R^{-1}	S_R^{-1}	$S^{-1/2} S_L^{1/2}$	1	$S^{-1/3}$	$S^{-1/3}$	1
Coefficient times area, hA_{ext}	S_L	$S S_R^{-2}$	S_L	S	$S^{1/3}$	$S^{1/3}$	S
Driving force,[c] ΔT	$S_{\text{throughput}} S_L^{-1}$	S_R^2	$S S_L^{-1}$	1	$S^{2/3}$	$S^{2/3}$	1

[a] See Equations 3.18 and 5.35.
[b] Heat transferred per unit mass is held constant without changing the driving force, ΔT.
[c] Change in driving force, ΔT, needed to achieve the same amount of heat transferred per unit mass.

Table 3.2 Scaleup Factors for Tubular Reactors Operating with Constant Physical Properties: Laminar Flow with High Graetz Numbers

Laminar Flow in the Entrance Region for Heat Transfer[a]	Unconstrained with Arbitrary $\bar{t}$,	Scaleups with Constant $\bar{t}$, $S_{\text{throughput}} = S = S_R^2 S_L$		Scaleup Strategies with Constant $\bar{t}$			
	General Scaleup Factors	S and S_R Specified	S and S_L Specified	Series Scaleup	Geometric Similarity	Constant Pressure Drop	Constant Heat Transfer[b]
Diameter scaling factor	S_R	S_R	$S^{1/2} S_L^{-1/2}$	1	$S^{1/3}$	$S^{1/3}$	1
Length scaling factor	S_L	$S S_R^{-2}$	S_L	S	$S^{1/3}$	$S^{1/3}$	S
Length-to-diameter ratio	$S_L S_R^{-1}$	$S S_R^{3}$	$S^{-1/2} S_L^{3/2}$	S	1	1	S
Velocity, $\bar{u}$	$S_{\text{throughput}} S_R^{-2}$	$S S_R^{-2}$	S_L	S	$S^{1/3}$	$S^{1/3}$	S
Pressure scaling factor, ΔP	$S_{\text{throughput}} S_R^{-4} S_L$	$S^2 S_R^{-6}$	$S^{-1} S_L^{3}$	S^2	1	1	S^2
Heat transfer area, A_{ext}	$S_R S_L$	$S S_R^{-1}$	$S^{1/2} S_L^{1/2}$	S	$S^{2/3}$		S
Inside coefficient, h	$S^{1/3} S_R^{-1} S_L^{-1/3}$	$S_R^{-1/3}$	$S^{-1/6} S_L^{1/6}$	1	$S^{-1/9}$	$S^{-1/9}$	1
Coefficient times area, hA_{ext}	$S_{\text{throughput}}^{1/3} S_L^{2/3}$	$S S_R^{-4/3}$	$S^{1/3} S_L^{2/3}$	S	$S^{5/9}$	$S^{5/9}$	S
Driving force,[c] ΔT	$S_{\text{throughput}}^{2/3} S_L^{-2/3}$	$S_R^{4/3}$	$S^{2/3} S_L^{-2/3}$	1	$S^{4/9}$	$S^{4/9}$	1

[a] See Equations 3.18 and 5.36.

[b] Heat transferred per unit mass is held constant without changing the driving force, ΔT.

[c] Change in driving force, ΔT, needed to achieve the same amount of heat transferred per unit mass.

Table 3.3 Scaleup Factors for Tubular Reactors Operating with Constant Physical Properties: Fully Turbulent Flow for Ordinary Fluids in Long Tubes. See the restrictions on Equation 5.37

	Unconstrained with Arbitrary $\bar{t}$	Scaleups with Constant $\bar{t}$, $S_{\text{Throughput}} = S = S_R^2 S_L$		Scaleup Strategies with Constant $\bar{t}$			
Fully Turbulent Flow[a]	General Scaleup Factors	S and S_R Specified	S and S_L Specified	Series Scaleup	Geometric Similarity	Constant Pressure Drop	Constant Heat Transfer[b]
Diameter scaling factor	S_R	S_R	$S^{1/2} S_L^{-1/2}$	1	$S^{1/3}$	$S^{11/27}$	$S^{2/7}$
Length scaling factor	S_L	$S S_R^{-2}$	S_L	S	$S^{1/3}$	$S^{5/27}$	$S^{3/7}$
Length-to-diameter ratio	$S_L S_R^{-1}$	$S S_R^{3}$	$S^{-1/2} S_L^{3/2}$	S	1	$S^{-2/9}$	$S^{1/7}$
Velocity, $\bar{u}$	$S_{\text{Throughput}} S_R^{-2}$	$S S_R^{-2}$	S_L	S	$S^{1/3}$	$S^{5/27}$	$S^{1/7}$
Pressure scaling factor, ΔP	$S_{\text{Throughput}}^{1.75} S_R^{-4.75} S_L$	$S^{2.75} S_R^{-6.75}$	$S^{5/8} S_L^{27/8}$	$S^{2.75}$	$S^{1/2}$	1	$S^{22/7}$
Heat transfer area, A_{ext}	$S_R S_L$	$S S_R^{-1}$	$S^{1/2} S_L^{1/2}$	S	$S^{2/3}$	$S^{0.59}$	$S^{3/7}$
Inside coefficient, h	$S_{\text{Throughput}}^{0.8} S_R^{-1.8}$	$S^{0.8} S_R^{-1.8}$	$S^{-0.1} S_L^{0.9}$	$S^{0.8}$	$S^{0.2}$	$S^{0.067}$	1
Coefficient times area, hA_{ext}	$S_{\text{Throughput}}^{0.8} S_R^{-0.8} S_L$	$S^{1.8} S_R^{-2.8}$	$S^{0.4} S_L^{1.4}$	$S^{1.8}$	$S^{0.867}$	$S^{0.659}$	S
Driving force,[c] ΔT	$S_{\text{Throughput}}^{0.2} S_R^{0.8} S_L^{-1}$	$S^{-0.8} S_R^{2.8}$	$S^{0.8} S_L^{-1.4}$	$S^{-0.8}$	$S^{2.13}$	$S^{2.34}$	1

[a] See Equations 3.18 and 5.37.
[b] Heat transferred per unit mass is held constant without changing the driving force, ΔT.
[c] Change in driving force, ΔT, needed to achieve the same amount of heat transferred per unit mass.

Table 3.4 Series Scaleup of Gas Phase Reactors in Turbulent Flow

$S_{\text{Throughput}}$	$(P_{\text{in}}/P_{\text{out}})_1$	$(P_{\text{in}}/P_{\text{out}})_2$	L_2/L_1	$\Delta P_2/\Delta P_1$
2	100	189	1.06	1.90
	10	18.9	1.07	1.99
	2	3.6	1.21	2.64
	1.1	1.48	1.68	4.78
100	100	6813	1.47	68.8
	10	681	1.48	75.6
	2	130	1.79	129
	1.1	47.1	3.34	461

where $S_R = R_2/R_1$ and $S_L = L_2/L_1$. Some scaling factors contain a ratio of linear velocities, $\bar{u}_2/\bar{u}_1$. These can be replaced by the scaling factors for volumetric flow rate and radius:

$$S_{\bar{u}} = \frac{\bar{u}_2}{\bar{u}_1} = \frac{(Q/\pi R^2)_1}{(Q/\pi R^2)_2} = S_Q S_R^{-2}$$

If the small and large reactors have the same density, $S_Q = S_{\text{throughput}}$.

The product $\rho\bar{u}$ appears naturally in some equations so that an assumption of constant density is not required. An example of this is the Reynolds number:

$$S_{\mathbf{Re}} = \frac{\mathbf{Re}_2}{\mathbf{Re}_1} = \frac{R_2\rho_2\bar{u}_2/\mu_2}{R_1\rho_2\bar{u}_{21}/\mu_1} = \left[\frac{R_2}{R_1}\right]^{-1}\left[\frac{\pi R_2^2\rho_2\bar{u}_2}{\pi R_1^2\rho_1\bar{u}_1}\right] = S_R^{-1}S_{\text{throughput}} \tag{3.37}$$

The ratios were rearranged so that the mass flow rate $\pi R^2\rho\bar{u}$ appeared as a ratio, giving the $S_{\text{throughput}}$ term.

Scaling factors are most useful when the equation for X is a multiplicative form. This allows S_X to be expressed as a product of other scaling factors such as S_R and S_L. The reduction to products of scaling factors is possible in the Reynolds number example but is not possible when there is an additive term. Consider the scaling factor

Table 3.5 Series Scaleup of Gas Phase Reactors in Laminar Flow

$S_{\text{Throughput}}$	$(P_{\text{in}}/P_{\text{out}})_1$	$(P_{\text{in}}/P_{\text{out}})_2$	L_2/L_1	$\Delta P_2/\Delta P_1$
2	100	159	1.26	1.90
	10	15.9	1.27	1.99
	2	3.1	1.41	2.64
	1.1	1.3	1.80	4.78
100	100	2154	4.64	21.8
	10	215	4.69	23.6
	2	41.2	5.66	40.2
	1.1	14.9	10.5	139

for the area of a cylinder:

$$S_{\text{area}} = \left[\frac{2\pi R_2^2 + 2\pi R_2 L_2}{2\pi R_1^2 + 2\pi R_1 L_1}\right] = \left[\frac{R_2^2 + R_2 L_2}{R_1^2 + R_1 L_1}\right]$$

Only R and L appear in this equation, but S_{area} for this case cannot be reduced to a form containing only the scaling factors S_R and S_L. The desired, simple form is obtained in two limits. If the cylinder is very short, $S_{\text{area}} \to S_R^2$, and if the cylinder is very long, $S_{\text{area}} \to S_R S_L$.

3.2.2 Scaling Factors for Tubular Reactors

We suppose that $S_{\text{throughput}}$ is known. Typically it has a value assigned by management: This is the size of plant we wish to build. The design of a chemical reactor may specify several tubes in parallel, but $S_{\text{throughput}}$ refers to the scaleup factor for a single tube. After the single tube is scaled up, its output is multiplied by N_{tube} to get the desired total scaleup. For a scaleup completely in parallel, $S_{\text{throughput}} = 1$.

The scaleup factor for inventory is the same as that for volume when the density is constant:

$$S_{\text{inventory}} = S_R^2 S_L \quad \text{(constant density)} \tag{3.38}$$

For an ideal gas, the results of Example 3.5 give an inventory scaling factor that depends on inlet and outlet pressures:

$$S_{\text{inventory}} = S_R^2 S_L \frac{[P_{\text{in}}^3 - P_{\text{out}}^3]_2 [P_{\text{in}}^2 - P_{\text{out}}^2]_1}{[P_{\text{in}}^3 - P_{\text{out}}^3]_1 [P_{\text{in}}^2 - P_{\text{out}}^2]_2} \quad \text{(ideal gas)} \tag{3.39}$$

Tables 3.1–3.3 summarize approximate scaling behavior of tubular reactors operating with fluids having constant physical properties. Many of the factors are merely ratios of geometric formulas. Those for pressure drop are based on Equation 3.18 for laminar flow and Equation 3.19 for turbulent flow. Results for heat transfer are included for convenience. Tables 3.1 and 3.2 are both for laminar flow and are identical except for the heat transfer correlations that are discussed in Chapter 5. Table 3.3 is for turbulent flow. Scaling in parallel is not shown since the scaling factors for a single tube would all be 1.

The general scaleup factors in Tables 3.1–3.3 treat $S_{\text{throughput}}$, S_R, and S_L as independent variables. These factors can be used without regard to the extent of reaction. For example, the scaling factor for pressure drop in the laminar regime is $S_{\text{throughput}} S_R^{-4} S_L$. Doubling the flow rate doubles the pressure drop, but increasing the tube diameter by a factor of $\sqrt[4]{2}$ returns ΔP to its original value. The general scaleup factors allow $\bar{t}$ to vary upon scaleup.

Constraining scaleup factors to have a constant value for the mean residence time is appropriate to reactor scaleups. The general scaleup factors are then subject to the constraints that $S_{\text{throughput}} = S$ and $S = S_R^2 S_L$. Imposing a constant value for $\bar{t}$ means that there are only two independent variables. We treat S as one of them. Then either

S_R or S_L can be chosen as the other. Tables 3.1–3.3 give both options. Choosing a specific value for either of S_R or S_L is a matter of ***scaleup strategy.***

The reader is reminded of the usual caveat**:** Detailed calculations are needed to confirm any design. The scaling exponents are approximate. They are used for conceptual studies and to focus attention on the most promising options for scaleup. Pick a promising strategy and then do accurate calculations to confirm the choice.

3.3 SCALEUP STRATEGIES FOR TUBULAR REACTORS

There are several ways of increasing the capacity of a tubular reactor.

1. Add identical reactors in parallel. This sets $S_R = S_L = 1$ for each reactor. The number of reactors is $N_{\text{tube}} = S_{\text{throughput}}$. The shell-and-tube design used for heat exchangers is a common and inexpensive way of increasing capacity by scaling in parallel.
2. Make the tube longer. For a constant-density fluid, this strategy sets $S_R = 1$ and $S_L = S$. Adding tube length is not a common way to increase capacity, but it is done. Single-tube reactors exist that are several miles long.
3. Increase the tube diameter while keeping constant length, $S_R = S^{1/2}$ and $S_L = 1$. This method is typically used for adiabatic and gas phase reactors.
4. Increase both the length and diameter. This sets $S_R > 1$ and $S_L > 1$ subject to the constraint of a fixed total volume. An example of this scaleup strategy is geometric similarity, which for a tube means keeping the same length-to-diameter ratio, L/d_t or L/R.

One way ***not*** to scale up is to keep a constant Reynolds number. To see the folly of scaling at constant **Re**, use Equation 3.37 and set $S_{\mathbf{Re}} = S_R^{-1} S = 1$. This gives $S_R = S$ for the constant-density case. Applying the constraint that $S = S_R^2 S_L$ gives $S_L = S^{-1}$. Upon scaleup, the reactor becomes fatter but shorter, a scaleup strategy that has nothing to recommend it. As a practical matter, the Reynolds number will increase upon scaleup. This is usually advantageous when the small reactor is turbulent, because the scaled-up reactor will even more closely approximate piston flow and will have a higher heat transfer coefficient to the wall.

3.3.1 Scaling in Parallel and Partial Parallel

Scaling in parallel gives an exact duplication of reaction conditions and is the most common way to scaleup tubular reactors. The number of tubes increases in direct proportion to the desired increase in throughput.

There are three, somewhat similar, concerns about scaling in parallel. The first concern applies mainly to viscous fluids in unpacked tubes. The second applies mainly to packed tubes.

(a) Will the feed distribute itself evenly between the tubes? This is a concern when there is a large change in viscosity due to reaction. The resulting stability problem is discussed in Chapter 13. Feed distribution can also be a concern with very large tube bundles when the pressure drop down the tube is small.

(b) Will a single tube in a pilot plant adequately represent the range of behaviors in a multitubular design? This question arises in heterogeneous reactors using large-diameter catalyst particles in small-diameter tubes. The concern is that random variations in the void fraction will cause significant tube-to-tube variations. One suggested solution is to pilot with a minimum of three tubes in parallel. Replicate runs, repacking a single tube between runs, can also be used.

(c) Will the distribution of flow on the shell side be uniform enough to give the same heat transfer coefficient for all the tubes?

Subject to resolution of these concerns, scaling in parallel has no obvious limit. Multitubular reactors with 10,000 tubes have been built, for example, for phthalic anhydride production.

A usual goal of scaleup is to maintain a ***single-train*** process. This means that the process will consist of a single line of equipment with a single control system and a single operating crew. Single-train processes give the greatest economies of scale and are generally preferred for high-volume chemicals. Shell-and-tube designs are not single train in a strict sense, but they are cheap to fabricate and operate when all the tubes are fed from a single source and discharge into a common receiver. Thus, shell-and-tube reactors and heat exchangers are acceptable within the usual definition of a single-train process.

A scaleup in partial parallel is occasionally useful. A single tube is scaled up as far as possible given the constraints of a conservative design that produces a satisfactory product. The result is a tube with a larger volume that, by itself, will produce S times more product. As many of these larger tubes as necessary are installed in parallel to satisfy the desired output for the plant. In cases where tube-to-tube distribution problems are feared, a separate feed pump can be used for each of the larger tubes.

3.3.2 Scaling in Series for Constant-Density Fluids

Scaling in series—meaning keeping the same tube diameter and increasing the tube length—is somewhat unusual but is a conservative way of scaling when the fluid is incompressible. It obviously maintains a single-train process. If the length is doubled, the flow rate can be doubled while keeping the same residence time. As will be quantified in subsequent chapters, a liquid phase, tubular reactor that works well in the pilot plant will probably work even better in a production unit that is 100 times longer and has 100 times the output. The rub, of course, is the pressure drop. Also, even a liquid will show some compressibility if the pressure is high enough. However, single tubes that are several miles long do exist, and a 25% capacity increase

at a high-pressure polyethylene plant was once achieved by adding an extra mile to the length of the reactor!

The general scaleup relationships in Tables 3.1–3.3 are made specific for scaling in series by setting $S_R = 1$ and $S_L = S$. The results are $S_{\mathbf{Re}} = S$ for Reynolds number, $S_{\Delta P} = S^{2.75}$ for a turbulent pressure drop, and $S_{\Delta P} = S^2$ for a laminar pressure drop.

For ***turbulent flow*** in tubes, a series scaleup by a factor of 2 at constant $\bar{t}$ increases both $\bar{u}$ and L by a factor of 2, but the pressure drop increases by a factor of $2^{2.75} = 6.73$. A factor of 100 scaleup increases the pressure drop by a factor of 316,000! The external area of the reactor, $2\pi RL$, increases as S, apace with the heat generated by the reaction. The Reynolds number also increases as S, and the inside heat transfer coefficient increases by $S^{0.8}$ (see Chapter 5). There should be no problem with heat transfer if the pressure drop is acceptable. The input of power by the pump, $Q\,\Delta P$, increases dramatically upon series scaleup, as $S^{3.75}$. The power per unit volume of fluid increases by the same factor as the pressure drop, $S^{2.75}$. In turbulent flow, part of this extra energy buys something. It increases eddy diffusion and improves heat transfer and mixing.

For ***laminar flow*** in tubes, the increase in pumping energy is smaller than for turbulent flow but is still large. The total power input increases by a factor of S^3 and the power input to a unit volume of fluid increases by a factor of S^2. Alas, the increase in energy only buys an increase in fluid velocity unless the Reynolds number—which scales as S—increases enough to cause turbulence. If the flow remains laminar, heat transfer and mixing will remain similar to that observed in the pilot unit. Scaleup should give satisfactory results if the pressure drop can be tolerated. One approach sometimes used in polymer plants is to install booster bumps at intermediate points. If the fluid has the very high viscosity typical of a molten polymer, heating by viscous dissipation can become important and may limit the scaleup.

For ***packed-bed*** reactors, the Ergun equation 3.21 says that the pressure drop depends on the packing diameter but is independent of the tube diameter. This is reasonable for packing that is small compared to the tube diameter. The case where the packing is large compared to the tube diameter is briefly discussed in Chapter 9. This situation is mainly encountered in heterogeneous catalysis with large reaction exotherms and small-diameter tubes. Such reactors are almost always scaled in parallel. For now, assume that the same packing is used in both large and small reactors and that it is small compared to the tube diameter even in the small reactor.

To study the series scaleup of a packed bed, take ratios for the large and small reactors of Equation 3.21. Due to the additive term, there is no simple scaleup relationship, but simple relationships emerge in the limits of high and low particle Reynolds numbers. Set $S_R = 1$ and $S_L = S$ for a series scaleup to obtain

$$S_{\Delta P} = \frac{\Delta P_2}{\Delta P_1} = S^2 \qquad (\mathbf{Re}_p \to 0) \tag{3.40}$$

$$S_{\Delta P} = \frac{\Delta P_2}{\Delta P_1} = S^3 \qquad (\mathbf{Re}_p \to \infty) \tag{3.41}$$

The pressure drop across a packed bed in laminar flow scales like the pressure drop across an open tube in laminar flow. In the turbulent limit, the Ergun equation predicts

that the pressure drop increases faster in a packed bed than in an open tube, as S^3 rather than $S^{2.75}$. Wall effects become progressively less important in open-tube flows as the diameter of the tube increases. In the Ergun equation, wall effects have already been neglected. Note that there is no dependence on the tube diameter in Equation 3.21.

3.3.3 Scaling in Series for Gas Flows

It is usually infeasible to use a series scaleup for a gas phase reaction. The exception is a reaction that can tolerate an adiabatic temperature change. The pressure factor in Equation 3.32 causes the inventory to increase much faster than the surface area so there is little possibility for heat transfer. A series scaleup for a compressible fluid continues to set $S_R = 1$, but now $S_L < S_{\text{throughput}}$. If the reactor length is increased and the exhaust pressure held constant, the holdup within the reactor will increase more than proportionately because the increased length will force a higher inlet pressure and thus a higher average density. When scaling with constant residence time, the throughput increases much faster than length, and the scaled-up reactors are remarkably short. They will be highly turbulent when the small reactor is turbulent because the Reynolds number increases as $S_{\text{throughput}}$.

The series scaleup of a gas phase reactor requires two ancillary equations that can be deduced from Example 3.5. The form of the equations depends on whether the flow is turbulent or laminar:
For turbulent flow,

$$\frac{(P_{\text{in}}^3)_2 - (P_{\text{out}}^3)_2}{(P_{\text{in}}^3)_1 - (P_{\text{out}}^3)_1} = S_{\text{throughput}}^{2.75} S_R^{-6.75} \tag{3.42}$$

$$\frac{(P_{\text{in}}^2)_2 - (P_{\text{out}}^2)_2}{(P_{\text{in}}^2)_1 - (P_{\text{out}}^2)_1} = S_{\text{throughput}}^{1.75} S_R^{-4.75} S_L \tag{3.43}$$

For laminar flow,

$$\frac{(P_{\text{in}}^3)_2 - (P_{\text{out}}^3)_2}{(P_{\text{in}}^3)_1 - (P_{\text{out}}^3)_1} = S_{\text{throughput}}^{2} S_R^{-6} \tag{3.44}$$

$$\frac{(P_{\text{in}}^2)_2 - (P_{\text{out}}^2)_2}{(P_{\text{in}}^2)_1 - (P_{\text{out}}^2)_1} = S_{\text{throughput}} S_R^{-4} S_L \tag{3.45}$$

These results assume ideal gas behavior and scaling with a constant value of $\bar{t}$. Set $S_R = 1$ for scaleup in series. It is assumed that P_{in} and P_{out} are known for the pilot unit and that a desired outlet pressure has been selected for the full-scale plant. Typically this will be the same outlet pressure as used in the pilot plant. Assume $S_{\text{throughput}}$ is known. Then the only unknowns are $(P_{\text{in}})_2$ and S_L. Solve Equation 3.42 (turbulent flow) or 3.44 (laminar flow) for $(P_{\text{in}})_2$. Then solve Equation 3.43 or 3.45 for S_L. Example results are given in Table 3.4 for turbulent flow and in Table 3.5 for laminar flow.

At first glance, these results seem fantastic. Look at the turbulent flow case with $S_{\text{throughput}} = 100$. When the pressure drop across the pilot reactor is large, a mere 47% increase in length gives a 100-fold increase in inventory! The pressure and the density

increase by a factor of about 69. Multiply the pressure increase by the length increase, and the factor of 100 in inventory has been found. The reactor volume increases by a factor of only 1.47. The inventory and throughput scale together. Because the gas density increases with pressure, the scaling factor for volume is much lower, 1.47 instead of 100 as it would be with constant density. Results for the laminar flow case are only slightly less dramatic. Scaling in series could make sense for an adiabatic, gas phase reaction with no change in the number of moles upon reaction. It would also make sense when the number of moles decreases upon reaction since the high pressures caused by this form of scaleup will favor the forward reaction. The designs are obviously unsuitable if the reaction requires transfer of heat through the tube walls or if low pressure is required to avoid an equilibrium limitation.

3.3.4 Scaling with Geometric Similarity

Scaling in parallel keeps a constant ΔP upon scaleup, but multitubular designs are not always the best choice. Scaling in series uses a single tube but keeps the same diameter and increases the pressure to potentially excessive levels. If there is some latitude on heat transfer, it may be preferable to increase the tube diameter in order to limit the pressure in the full-scale plant. One way to do this is to scale with geometric similarity, which is a normal scaleup method for stirred tank reactors but is less common for tubes. For tubes it means increasing the diameter as required to achieve the desired throughput while keeping the same aspect ratio, L/d_t or L/R. For incompressible fluids, the volume and throughput scale together, $S = S_V = S_{\text{throughput}}$ so that $S_R = S_L = S^{1/3}$. The Reynolds number scales as $S^{2/3}$.

The case of a compressible fluid is more complicated since it is the inventory and not the volume that must scale with $S_{\text{throughput}}$ in order to keep a constant value for $\bar{t}$. Laminar flow is the simplest case and is the one where scaling with geometric similarity makes the most sense.

Geometrically Similar Scaleups for Laminar Flow in a Tube

Table 3.1 gives the general scaling factor for pressure drop as $S_{\text{throughput}} S_R^{-4} S_L$. Inserting $S_{\text{throughput}} = S$ and $S_R = S_L = S^{1/3}$ gives

$$\frac{\Delta P_2}{\Delta P_1} = S S_L S_R^{-4} = S^0 = 1$$

so that the pressure drop remains constant upon scaleup. The same result is obtained when the fluid is compressible. Thus, using geometric similarity to scale isothermal, laminar flows gives constant pressure drop provided the flow remains laminar upon scaleup. The large and small reactors will have the same inlet pressure and the same average density if they are operated at the same outlet pressure. Throughput, inventory, and volume all scale as S.

The external area scales as $S^{2/3}$ so that this design has the usual problem of surface area rising more slowly than heat generation. Thus, large scaleups using

geometric similarity are limited to reactors that are adiabatic or nearly so. There is another problem associated with laminar flow in tubes. Although piston flow may be a reasonable approximation for a small-diameter pilot reactor, it will cease to be a reasonable assumption upon scaleup. As described in Chapter 8, radial diffusion of mass and heat gives beneficial effects in small tubes that will decline upon scaleup. Geometrically similar scaleups of laminar flow in tubes cannot be recommended unless radial diffusion was negligible in the pilot-scale reactor. Chapter 8 gives criteria and design methods.

Geometrically Similar Scaleups for Turbulent Flow in a Tube

Table 3.3 gives the general scaling factor for pressure drop in turbulent flow as $S_{\text{throughput}}^{1.75} S_R^{-4.75} S_L$. If density is constant, $S_{\text{throughput}} = S$. Then inserting $S_R = S_L = S^{1/3}$ gives

$$\frac{\Delta P_2}{\Delta P_1} = \frac{S^{1.75} S_L}{S_R^{4.75}} = S^{1/2} \tag{3.46}$$

In laminar flow, the pressure drop is constant when scaleup is done by geometric similarity. In turbulent flow, it increases as the square root of throughput. There is extra pumping energy per unit volume of throughput, which gives somewhat better mixing and heat transfer. The surface area and Reynolds number both scale as $S^{2/3}$. We shall see in Chapter 5 that the increase in heat transfer coefficient is insufficient to overcome the relative loss in surface area. The reactor will become adiabatic if the scaleup factor is large.

Turning to the case where the working fluid is an ideal gas, substituting $S_R = S_L = S_{\text{throughput}}^{1/3}$ into Equations 3.42 and 3.43 gives $S_{\text{throughput}}^{1/2}$ as the scaling factor for both pressure ratios. This looks neat, but there is no solution to the scaling equations if both the large and small reactors have the same discharge pressure. What happens is that the larger reactor has too much inventory to satisfy the condition of constant $\bar{t}$. Geometrically similar scaleups for gases in turbulent flow require that the discharge pressure be lower in the large unit than the small one. This can be accomplished using a backpressure value on the small unit. It is doubtful that such a scaleup has ever been attempted.

Geometrically Similar Scaleups for Packed Beds

As was the case for scaling packed beds in series, the way packed beds scale with geometric similarity depends on the particle Reynolds number. The results are somewhat different than those for empty tubes because the bed radius does not appear in the Ergun equation. The asymptotic behavior for the incompressible case is

$$\frac{\Delta P_2}{\Delta P_1} \to S^2 S_L S_R^{-4} = S \quad \text{as } (\mathbf{Re})_p \to \infty$$

Note that S_R appears here even though it is missing from the Ergun equation. It arises because throughput is proportional to $R^2 \bar{u}$.

The other limiting value is

$$\frac{\Delta P_2}{\Delta P_1} \rightarrow S S_L S_R^{-2} = S^{2/3} \text{as}(\mathbf{Re})_\text{p} \rightarrow 0$$

These asymptotic forms may be useful for conceptual studies, but the real design calculations must be based on the full Ergun equation. Turning to the case of compressible fluids, a scaleup using geometric similarity with $S_R = S_L = S^{1/3}$ is generally infeasible. Simply stated, the reactors are just too long and have too much inventory. Note that the pressure drop in a packed bed increases more than the equivalent scaleup using an open tube.

3.3.5 Scaling with Constant Pressure Drop

Scaleup of tubes using geometric similarity gives the same pressure drop when the tube is open and in laminar flow but higher pressure drops in turbulent flow and packed beds. To achieve the same pressure drop, the tubes need to be shorter and fatter. This section considers how single tubes can be scaled up to achieve higher capacity at the same residence time and pressure drop. In contrast to the previous section, these scaleups are usually feasible, even for gas phase reactions, although they have the common failing of losing heat transfer area relative to throughput.

Constant-Pressure Scaleups for Laminar Flow in a Tube

As shown in the previous section, scaling with geometric similarity, $S_R = S_L = S^{1/3}$, gives constant pressure drop when the flow is laminar and remains laminar upon scaleup. This is true for both liquids and gases. The Reynolds number and the external area increase as $S^{2/3}$. Piston flow is a poor assumption for laminar flow in anything but small tubes. Conversion and selectivity of the reaction is likely to worsen upon scaleup unless the pilot reactor is already so large that molecular and thermal diffusion are negligible on the pilot scale. Ways to avoid unpleasant surprises are discussed in Chapter 8

Constant-Pressure Scaleups for Turbulent Flow in a Tube

Table 3.3 gives the general scaling factor for pressure drop in turbulent flow as $S_\text{throughput}^{1.75} S_R^{-4.75} S_L$. Set $\Delta P_2 = \Delta P_1$ to obtain $1 = S^{1.75} S_L S_R^{-4.75}$. Also set $S = S_L S_R^2$. There are two equations and two unknowns. Simultaneous solution gives

$$S_R = S^{11/27} \qquad \text{and} \qquad S_L = S^{5/27} \tag{3.47}$$

This version of scaleup gives a shorter, fatter tube than scaling by geometric similarity. The same results are obtained from Equations 3.42 and 3.43 that apply to the turbulent flow of ideal gases. Thus tube radius and length scale in the same way for turbulent liquids and gases when the pressure drop is constant. For the gas case, it is supposed that the large and small reactors have the same discharge pressure.

The reactor volume scales as S, and the aspect ratio of the tube decreases upon scaleup. The external surface area scales as $S_R S_L = S^{16/27}$ compared to $S^{2/3}$ for the case with geometric similarity. The Reynolds number also scales as $S^{16/27}$.

Constant-Pressure Scaleups for Packed Beds

A scaleup with constant pressure drop can be achieved in a packed bed just by increasing the diameter while maintaining the same superficial velocity, $\bar{u}_s$. This form of scaleup has

$$S_R = S^{1/2} \qquad \text{and} \qquad S_L = 1$$

Obviously, the ability to transfer heat through the walls drops dramatically when scaling in this fashion, but it is certainly a straightforward and normal method for scaling adiabatic reactors. A potential limit arises when the bed diameter becomes so large that even distribution of the entering fluid becomes a problem. Large packed beds are the preferred reactor for heterogeneous catalysis if the reaction (and the catalyst) can tolerate the adiabatic temperature change.

Scaleup of Noncircular Ducts

Pressure scaleup factors for noncircular ducts are identical to those for circular ducts provided the shape of the duct (e.g., the width-to-height ratio for a rectangular duct) is not changed. Set $S_h = S_w$ for a rectangular duct. This conclusion is based on the use of the hydraulic radius, Equation 3.22, but it also applies to other equivalents such as the equivalent diameter of Equation 3.23. The pressure scaleup relationships are the same as those for S_R in circular tubes.

3.4 SCALING DOWN

There are two reasons for scaling down a chemical reactor:

1. A large reactor exists. A smaller version is desired for more convenient experimentation.
2. The desired reactor is very small indeed. A larger version is desired for more convenient experimentation.

Small versions of production facilities are sometimes used for product development, particularly in the polymer industries. Single-train plants producing 20 to 100 metric tons per hour are common for major volume plastics such as polyethylene, polypropylene, and polystyrene. These plastics are made in many grades, and the optimization of product properties is a means of finding competitive advantage in what would otherwise be a strictly commodity market. Important property changes can result from subtle changes in raw materials, catalysts, and operating conditions.

Multiply the production rate by the selling price and you will understand management's reluctance to conduct product development experiments in the plant. The

cost can easily exceed $1,000,000 for a day of experimentation. Pilot plants, built and operated after the fact of the production line, are fairly common. Some process licensors include the design of a pilot plant in their technology package for a full-scale plant. The purpose of these pilot plants is to duplicate the performance of the full-scale line at a fraction of the production rate. The scaledown factor between the two plants will typically be in the range 100–1000. This would be considered highly ambitious for a scaleup. There is less risk when scaling down, but it may be necessary to adjust the heating and mixing characteristics of the pilot plant to make them as bad as they are in the full-scale facility.

A very different reason for scaling down arises in fields such as biotechnology, microelectronics, and nanotechnology. We are interested in building, altering, or just plain understanding very small reactors but find it difficult or impossible to do the necessary experiments on the small scale. Measurements made on the "pilot plant" will ultimately be scaled down to the "production plant." One generalization is that the small unit will probably be in laminar flow and close to isothermal in operation. Chapter 16 discusses meso-, micro-, and nanoscale reactors in detail. One point worth making here is that flow in very small channels does not necessarily require high pressures. Take the integrated form of the Hagen–Poiseuille equation and replace $\bar{u}$ with $L/\bar{t}$ to obtain

$$\Delta P = \frac{8\mu\bar{u}L}{R^2} = \frac{8\mu}{\bar{t}}\left(\frac{L}{R}\right)^2$$

Thus the pressure drop is independent of tube size, depending only on μ, $\bar{t}$, and L/R. Of these, μ and $\bar{t}$ should be the same in the large and small units. However, L/R will vary with the form of scaledown but will be constant and thus will give the same pressure drop if the scaledown is done by geometric similarity.

The scaling methods in this chapter work about as well or as poorly when $S < 1$ as when $S > 1$. Scaling down in parallel works until there is only a single tube. Other ways of scaling down cause a decrease in Reynolds number that may cause a transition to laminar flow. This will substantially change the mixing mechanisms in the reactor. Scaling down in series may lead to unfeasibly small L/R ratios. Scaling by geometric similarity tends to work better going down than going up. The surface area and Reynolds number both decrease, but they decrease only by $S^{2/3}$ while throughput decreases by S. Thus heat transfer will be better on the small scale. Scaling an open tube at constant pressure drop is the same as scaling by geometric similarity if the flow is laminar. If the small reactor is turbulent, scaling down at constant pressure drop will increase the length-to-diameter ratio in the smaller unit. Packed beds can be scaled down just by decreasing the bed diameter as long as the ratio of bed diameter to packing diameter is reasonable, although values as low as 3 are sometimes used. The correlations in Section 9.1 include the effects of packing diameter although the range of the experimental data on which these correlations are based is limited.

As a general rule, scaled-down reactors will have better radial mixing and a closer approach to isothermal operation. However, there is an awkward size range for mesoreactors in which the transition to laminar flow hurts radial mixing, and there is

a smaller, microscale size where axial mixing caused by molecular diffusion becomes important. Details are provided in Chapter 16.

3.5 TRANSPIRED-WALL REACTORS

Tubular reactors sometimes have side entrance points for downstream injection. Like the case of fed-batch reactors, this raises the question of how quickly the new ingredients are mixed. Mixing in the radial direction is the dominant concern. If radial mixing is fast, the assumption of piston flow may be reasonable and the addition of new ingredients merely reinitializes the problem. The equivalent phenomenon was discussed in Section 2.6.2 for fed-batch reactors.

The present section considers the case where the tube has a porous wall so that reactants or inerts can be fed gradually. ***Transpiration*** is used to cool the walls in high-temperature combustion. In this application there is usually a change of phase, from liquid to gas, so that the cooling benefits from the heat of vaporization. However, we use the term transpiration to include transfer through a porous wall without a phase change. It can provide chemical protection of the wall in extremely reactive systems such as direct fluorinations. There may be selectivity advantages for complex reactions. Example 3.8 suggests this possibility.

Assume that radial mixing is fast so that the composition is always uniform in the radial direction. The transpiration rate per unit length of tube is $q = q(z)$ with units of square meters per second. Transpiration will increase the average velocity and the concentration of the transpired components. Suppose component A has concentration $a_{\text{trans}} = a_{\text{trans}}(z)$ in the transpired stream. The component balance 3.4 now becomes

$$\frac{1}{A_c}\frac{d(\dot{N}_A)}{dz} = \frac{1}{A_c}\frac{d(Qa)}{dz} = \frac{1}{A_c}\frac{d(A_c\bar{u}a)}{dz} = \frac{a_{\text{trans}}q}{A_c} + \mathscr{R}_A \tag{3.48}$$

We also need a total mass balance. The general form is

$$Qp = Q_{\text{in}}\rho_{\text{in}} + \int_0^z q\rho_{\text{trans}}\,dz \tag{3.49}$$

Analytical solutions are possible in special cases. It is apparent that transpiration will lower the conversion of the injected component. It is less apparent but true that transpired-wall reactors can be made to approach the performance of a CSTR with respect to a transpired component while providing an environment similar to piston flow for components that are present only in the initial feed.

EXAMPLE 3.8

Solve Equation 3.48 for the case of a first-order reaction where ρ, q, and a_{trans} are constant. Then take limits as $Q_{\text{in}} \to 0$ and see what happens. Also take the limit as $q \to 0$.

SOLUTION: With constant density, Equation 3.49 becomes

$$Q = Q_{\text{in}} + qz$$

Substitute this into the Qa version of Equation 3.48 to obtain a variable-separable ODE. Integrate it subject to the initial condition that $a = a_{\text{in}}$ at $z = 0$. The result is

$$a(z) = \frac{qa_{\text{trans}}}{A_c k + q} - \frac{[qa_{\text{trans}}/(A_c k + q) - a_{\text{in}}]}{[1 + qz/Q_{\text{in}}]^{(A_c k+q)/q}} \tag{3.50}$$

Taking the limit as $Q_{\text{in}} \to 0$ gives

$$a = \frac{qa_{\text{trans}}}{A_c k + q} = \frac{a_{\text{trans}}}{A_c Lk/Q_{\text{out}}} + 1$$

The z dependence has disappeared! The reactor is well mixed and behaves like a CSTR with respect to component A. Noting that $Q_{\text{out}} = qL$ gives

$$a_{\text{out}} = \frac{a_{\text{trans}}}{1 + Vk/Q_{\text{out}}} = \frac{a_{\text{trans}}}{1 + k\bar{t}}$$

which is exactly the behavior of a CSTR. When a transpired-wall reactor has no initial feed and a constant transpiration rate, the tube behaves like a stirred tank. When $Q_{\text{in}} > 0$ but $a_{\text{in}} = 0$, it will still have a fairly uniform concentration of A inside the reactor while behaving much like a PFR for component B, which has $b_{\text{in}} > 0$ but $b_{\text{trans}} = 0$. For this component B,

$$b(z) = \frac{b_{\text{in}}}{[1 + qz/Q_{\text{in}}]^{(A_c k+q)/q}}$$

Physical insight should tell you what this becomes in the limit as $q \to 0$. Problem 2.7 shows the mathematics of the limit.

Example 3.8 suggests a method for making otherwise unachievable products through the use of transpired-wall reactors. By feeding the more reactive component through the wall, a desired stoichiometry can be maintained. In copolymerizations, the two monomers often polymerize at different rates, but a uniform product is desired. For the specific case of an anionic polymerization, transpiration of the more reactive monomer could give a chemically uniform copolymer while maintaining a narrow molecular weight distribution. See Section 13.4.4 for the background to this statement. Transpired-wall reactors are used for water purification on U.S. naval vessels. Organic contaminants are oxidized at temperatures above the critical point of water, the transpiration being used to ease materials of construction problems. Bermejo et al. (2005) give a model and comparison with experimental results.

Membrane reactors, whether batch or continuous, offer the possibility of selective transpiration. They can be operated in the reverse mode so that some products are selectively removed from the reaction mixture in order to avoid an equilibrium limitation. Membrane reactors can be used to separate cell mass from fermentation products. See Section 12.2.2.

SUGGESTED FURTHER READINGS

Realistic examples of variable-property piston flow models, usually nonisothermal, are given in:

G. F. Froment and K. B. Bischoff, *Chemical Reactor Analysis and Design,* 2nd ed., Wiley, New York, 1990.

Scaleup techniques are discussed in:

A. Bisio and R. L. Kabel, *Scaleup of Chemical Processes*, Wiley, New York, 1985.

PROBLEMS

3.1 The first-order sequence

$$\mathrm{A} \xrightarrow{k_\mathrm{I}} \mathrm{B} \xrightarrow{k_\mathrm{II}} \mathrm{C}$$

is occurring in a constant-density PFR. The residence time is $\bar{t}$.

(a) Determine b_{out} and c_{out} given that $b_{\text{in}} = c_{\text{in}} = 0$ and that $k_\mathrm{I} = k_\mathrm{II}$.

(b) Find a real chemical example, not radioactive decay, where the assumption that $k_\mathrm{I} = k_\mathrm{II}$ is plausible. As a last resort, you may consider reactions that are only pseudo–first order.

3.2 Suppose

$$\boldsymbol{\nu} = \begin{bmatrix} -1 & 0 \\ -1 & -1 \\ 1 & -1 \\ 0 & 0 \end{bmatrix}$$

gives the stoichiometric coefficients for a set of elementary reactions.

(a) Determine the elementary reactions and the vector of reaction rates that corresponds to $\boldsymbol{\nu}$.

(b) Write the component balances applicable to these reactions in a PFR with an exponentially increasing reactor cross section $A_c = A_c = A_{\text{inlet}} \exp(\alpha z)$.

3.3 Equation 3.10 can be applied to an incompressible fluid just by setting $\bar{t} = V/Q$. Show that you get the same result by integrating Equation 3.8 for a first-order reaction with arbitrary $A_c = A_c(z)$.

3.4 Consider the reaction

$$B \xrightarrow{k} 2\mathrm{A}$$

in the gas phase. Use a numerical solution to determine the length of an isothermal PFR that achieves 50% conversion of B. The pressure drop in the reactor is negligible. The reactor cross section is constant. There are no inerts. The feed is pure B and the gases are ideal. Assume $b_{\text{in}} = 1$, $a_{\text{in}} = 0$, $\bar{u}_{\text{in}} = 1$, and $k = 1$ in some system of units.

3.5 Solve Problem 3.4 analytically rather than numerically.

3.6 Repeat the numerical solution in Example 3.3 for a reactor with a circular cross section that varies as $A_c = A_{\text{in}} \exp(\alpha\, z)$. Using the numerical values in that example, plot the length

needed to obtain 50% conversion versus α for $-1 < \alpha < 1$ (e.g., $z = 0.3608$ for $\alpha = 0$ as determined in Example 3.3). Also plot the reactor volume V versus α assuming $A_{\text{inlet}} = 1$.

3.7 Some nasty person, perhaps the evil professor, has deleted the code used to solve Example 3.4. Write an Excel Macro that (presumably) reproduces the results in Example 3.4. Now rework the example considering reversibility of the reaction. Assume

$$K_{\text{kinetic}} = \frac{P_{\text{STY}} P_{\text{H}_2}}{P_{\text{EB}}} = 0.61 \text{ atm at } 700^\circ\text{C}$$

3.8 Annular flow reactors, such as that illustrated in Figure 3.2, are sometimes used for reversible, adiabatic, solid-catalyzed reactions where pressure near the end of the reactor must be minimized to achieve a favorable equilibrium. Ethylbenzene dehyrogenation fits this situation. Repeat Problem 3.7 but substitute an annular reactor for the tube. The inside (inlet) radius of the annulus is 0.1 m and the outside (outlet) radius is 1.1 m.

3.9 Suppose A $\rightarrow$ B + C in an isothermal, gas phase, tubular reactor that operates at atmospheric pressure with negligible pressure drop. The molecular weights are 100, 48, and 52 for A, B, and C, respectively. The input gas velocity is 10 m s^{-1}. The reactor is 10 m long. The entering gas is pure A. The temperature is 700°C. The reaction is first order with a rate constant of 2 s^{-1}. Determine Y_A, a_{out}, and u_{out}.

3.10 The gas phase decomposition A $\rightarrow$ B + C is occurring in an isothermal tubular reactor. The tube ID is 1 in. There is no packing. The pressure drop is 0.3 psi with the outlet at atmospheric pressure. The inlet gas flow rate is 0.05 Standard Cubic Feet/s (1 atm, 60°F). The molecular weights of B and C are 48 and 52. The entering gas contains 50% A and 50% inerts (nitrogen) by volume. The operating temperature is 700°C. The cracking reaction is first order with a rate constant of 0.93 s^{-1}. How long is the tube and what is the conversion? Use $\mu = 5 \times 10^{-5}$ Pa s.

3.11 Suppose

$$\text{B} \xrightarrow{k} 2\text{A}$$

in the liquid phase and that the density changes from 1000 to 900 kg m^{-3} upon complete conversion. Find a solution to the design equation for a PFR and compare the results to a hypothetical PFR in which the density is constant.

3.12 A pilot-scale, liquid phase esterification with near-zero heat of reaction is being conduced in a small tubular reactor. The chemist thinks the reaction should be reversible, but the byproduct water is sparingly soluble in the reaction mixture and you are not removing it. The conversion is 85%. Your job is to design a 100× scaleup. The pilot reactor is a 31.8-mm-ID tube, 4 m long, constructed from 12 British Wire Gauge (BWG) (2.769 mm) 316 stainless steel. The feed is preheated to 80°C and the reactor is jacketed with tempered water at 80°C. The material begins to discolor if higher temperatures are used. The flow rate is 50 kg h^{-1} and the upstream gauge pressure is 1.2 psi. The density of the mixture is around 860 kg m^{-3}. The viscosity of the material has not been measured under reaction conditions but is believed to be substantially independent of conversion. The pilot plant discharges at atmospheric pressure.

(a) Propose alternative designs based on scaling in parallel, in series, by geometric similarity, and by constant pressure drop. Estimate the Reynolds number and pressure drop for each case.

(b) Estimate the total weight of metal needed for the reactor in each of the designs. Do not include the metal needed for the water jacket in your weight estimates. Is the 12 BWG tube strong enough for all the designs?

(c) Suppose the full-scale reactor is to discharge directly into a finishing reactor that operates at 100 torr. Could this affect your design? What precautions might you take?

(d) Suppose you learn that the viscosity of the fluid in Problem 3.9 is far from constant. The starting raw material has a viscosity of 0.0009 Pa s at 80°C. You still have no measurements of the viscosity after reaction, but the fluid is obviously quite viscous. What influence will this have on the various forms of scaleup?

3.13 A pilot-scale, turbulent, gas phase reactor performs well when operated with a inlet pressure of 1.02 bar and an outlet pressure of 0.99 bar. Is it possible to do a geometrically similar scaleup by a factor of 10 in throughput while maintaining the same mean residence time? Assume ideal gas behavior and ignore any change in the number of moles due to reaction. If necessary, the discharge pressure on the large reactor can be something other than 0.99 bar.

3.14 Refer to the results in Example 3.5. Suppose that the tube is suddenly capped. Determine the equilibrium pressures in the tube assuming $P_{\text{out}} = 1$ and

(a) $(P_{\text{in}}/P_{\text{out}})_1 = 100$

(b) $(P_{\text{in}}/P_{\text{out}})_1 = 10$

(c) $(P_{\text{in}}/P_{\text{out}})_1 = 2$

(d) $(P_{\text{in}}/P_{\text{out}})_1 = 1.1$

What assumptions must be made about the gas?

3.15 An alternative to Equation 3.20 is $\mathbf{Fa} = 0.04\ \mathbf{Re}^{-0.16}$. It is more conservative in the sense that it predicts higher pressure drops at the same Reynolds number. Use it to recalculate the scaling exponents in Section 3.2 for pressure drop. Specifically, determine the exponents for ΔP when scaling in series and with geometric similarity for an incompressible fluid in turbulent flow. Also, use it to calculate the scaling factors for S_R and S_L when scaling at constant pressure.

3.16 An integral form of Equation 3.19 was used to derive the pressure ratio for scaleup in series of a turbulent liquid phase reactor, $S_{\Delta P} = S^{2.75}$. The integration apparently requires μ to be constant. Consider the case where μ varies down the length of the reactor. Define an average viscosity as

$$\hat{\mu} = \tfrac{1}{L} \int_0^L \mu(z)\, dz$$

Show that the same scaleup factor for pressure is valid if the large and small reactors have the same value for $\hat{\mu}$ and that this will be true for an isothermal or adiabatic PFR being scaled up in series.

3.17 Suppose an inert material is transpired into a tubular reactor in an attempt to achieve isothermal operation. Suppose the transpiration rate q is independent of z and that $qL = Q_{\text{trans}}$. Assume all fluid densities to be constant and equal. Find the fraction unreacted for a first-order reaction. Express your final answer as a function of the two dimensionless parameters $Q_{\text{trans}}/Q_{\text{in}}$ and kV/Q_{in}, where k is the rate constant and Q_{in} is the volumetric flow rate at $z = 0$ (i.e., $Q_{\text{out}} = Q_{\text{in}} + Q_{\text{trans}}$). *Hint*: The correct formula gives $a_{\text{out}}/a_{\text{in}} = 0.25$ when $Q_{\text{trans}}/Q_{\text{in}} = 1$ and $kV/Q_{\text{in}} = 1$.

3.18 Repeat Problem 3.17 for a second-order reaction of the type

$$2A \xrightarrow{k/2} B$$

The dimensionless parameters are now Q_{trans}/Q_{in} and $ka_{in}V/Q_{in}$.

3.19 The evil professor of Problem 1.13 learned that the industrial process for making TNT is continuous and decides to try a two-stage tubular reactor. The feed is toluene and the mixed acids. He keeps the feed composition, residence time, and temperature the same as in the batch reactor and gets a similar yield of dinitrotoluenes. Chuckling in an evil manner, he adds a tee and another length of tube and feeds fuming sulfuric acid into the tee. The starting composition, temperature, and residence time in the second portion of the tube is nearly the same as in the second stage of the batch process, but this time the yield of trinitrotoluene is very low. He seeks advice from a colleague who happens to be the beautiful princess. What do you think she suggested as the likely cause?

3.20 Show that Equation 3.31 applies to a packed bed. What is β is this case?

Chapter 4

Stirred Tanks and Reactor Combinations

Chapter 2 treated multiple and complex reactions in an ideal batch reactor. The reactor is ideal in the sense that mixing is assumed to be instantaneous and complete throughout the vessel. Real batch reactors will approximate ideal behavior when the characteristic time for mixing is short compared to the reaction half-life. Industrial batch reactors have inlet and outlet ports, pumps, and an agitation system. The same hardware is easily converted to continuous operation. Just feed and discharge continuously. If the reactor is well mixed in the batch mode, it is likely to remain well mixed in the continuous mode, at least for the same reaction. The assumption of instantaneous and perfect mixing remains a reasonable approximation, but the batch reactor has become a CSTR.

This chapter develops the techniques needed to analyze multiple and complex reactions in CSTRs. Physical properties may be variable. Also treated is the common industrial practice of using reactor combinations, such as a stirred tank in series with a tubular reactor, to accomplish the overall reaction.

4.1 CONTINUOUS FLOW STIRRED TANK REACTORS

Perfectly mixed stirred tank reactors have no spatial variations in composition or physical properties within the reactor or in the exit from it. Everything inside the system is uniform except at the very entrance. Molecules experience a step change in environment immediately upon entering. A perfectly mixed CSTR has only two environments, one at the inlet and the other inside the reactor and at the outlet. These environments are specified by a set of compositions and operating conditions which have only two values: either a_{in}, b_{in}, . . . , P_{in}, T_{in} or a_{out}, b_{out}, . . . , P_{out}, T_{out}. When the reactor is at a steady state, the inlet and outlet properties are related by algebraic equations. In contrast, PFRs show a gradual change from inlet to outlet, and the inlet and outlet properties are related by differential equations rather than algebraic equations.

Chemical Reactor Design, Optimization, and Scaleup, Second Edition. By E. B. Nauman
Copyright © 2008 John Wiley & Sons, Inc.

The component material balances for an ideal CSTR are the following set of algebraic equations:

$$\begin{aligned} Q_{\text{in}}a_{\text{in}} + V\mathscr{R}_A(a_{\text{out}}, b_{\text{out}}, \ldots, P_{\text{out}}, T_{\text{out}}) &= Q_{\text{out}}a_{\text{out}} \\ Q_{\text{in}}b_{\text{in}} + V\mathscr{R}_B(a_{\text{out}}, b_{\text{out}}, \ldots, P_{\text{out}}, T_{\text{out}}) &= Q_{\text{out}}b_{\text{out}} \\ &\vdots \end{aligned} \tag{4.1}$$

These equations follow directly from the steady-state version of the general component balance, Equation 1.6. The reaction terms are evaluated at the outlet concentrations since everything inside the reactor has this composition. The set of component balances can be summarized as

$$Q_{\text{in}}\mathbf{a}_{\text{in}} + V\mathscr{R}_A = Q_{\text{out}}\mathbf{a}_{\text{out}} \tag{4.2}$$

where $\mathscr{R}_A$ is the column vector ($N \times 1$ matrix) of component reaction rates and $\mathbf{a}_{\text{in}}$ and $\mathbf{a}_{\text{out}}$ are column vectors of the component concentrations. See Section 2.8.1.

For now, we assume that all operating conditions are known. This specifically includes P_{out} and T_{out} which correspond to conditions within the vessel. Suppose also that the inlet concentrations $a_{\text{in}}, b_{\text{in}}, \ldots,$ volumetric flow rate Q_{in}, and working volume V are all known. Then Equations 4.1 or 4.2 are a set of N simultaneous, algebraic equations in $N + 1$ unknowns, the unknowns being the N outlet concentrations $a_{\text{out}}, b_{\text{out}}, \ldots$ and the one volumetric flow rate Q_{out}. Note that Q_{out} is evaluated at the conditions within the reactor. If the mass density of the fluid is constant, as is approximately true for liquid systems, then $Q_{\text{out}} = Q_{\text{in}}$. This allows Equations 4.1 to be solved for the outlet compositions. If Q_{out} is unknown, then the component balances must be supplemented by an equation of state for the system. Perhaps surprisingly, the algebraic equations governing the steady-state performance of a CSTR are usually more difficult to solve than the sets of simultaneous, first-order ODEs encountered in Chapters 2 and 3. We start with an example that is easy but important.

EXAMPLE 4.1

Suppose a liquid phase CSTR is used for consecutive, first-order reactions:

$$\text{A} \xrightarrow{k_A} \text{B} \xrightarrow{k_B} \text{C} \xrightarrow{k_C} \text{D}$$

Determine all outlet concentrations assuming constant density.

SOLUTION: When density is constant, $Q_{\text{out}} = Q_{\text{in}} = Q$ and $\bar{t} = V/Q$. Equations 4.1 become

$$\begin{aligned} a_{\text{in}} - k_A\bar{t}a_{\text{out}} &= a_{\text{out}} \\ b_{\text{in}} + k_A\bar{t}a_{\text{out}} - k_B\bar{t}b_{\text{out}} &= b_{\text{out}} \\ c_{\text{in}} + k_B\bar{t}b_{\text{out}} - k_C\bar{t}c_{\text{out}} &= c_{\text{out}} \\ d_{\text{in}} + k_C\bar{t}c_{\text{out}} &= c_{\text{out}} \end{aligned}$$

These equations can be solved sequentially to give

$$
\begin{aligned}
a_{\text{out}} &= \frac{a_{\text{in}}}{1 + k_A \bar{t}} \\
b_{\text{out}} &= \frac{b_{\text{in}}}{1 + k_B \bar{t}} + \frac{k_A \bar{t} a_{\text{in}}}{(1 + k_A \bar{t})(1 + k_B \bar{t})} \\
c_{\text{out}} &= \frac{c_{\text{in}}}{a + k_C \bar{t}} + \frac{k_B \bar{t} b_{\text{in}}}{(1 + k_B \bar{t})(1 + k_C \bar{t})} + \frac{k_A k_B \bar{t}^2 a_{\text{in}}}{(1 + k_A \bar{t})(1 + k_B \bar{t})(1 + k_C \bar{t})} \\
d_{\text{out}} &= d_{\text{in}} + (a_{\text{in}} - a_{\text{out}}) + (b_{\text{in}} - b_{\text{out}}) + (c_{\text{in}} - c_{\text{out}})
\end{aligned}
\tag{4.3}
$$

Compare these results to those of Equation 2.22 for the same reactions in a batch reactor. The CSTR solutions do not require special forms when some of the rate constants are equal. Intermediate components B and C will exhibit maximum concentration at particular values of $\bar{t}$, and a plot of outlet concentrations versus $\bar{t}$ is qualitatively similar to the behavior shown in Figure 2.2. However, the value for $\bar{t}$ that gives a maximum in a CSTR will be different than the value of $\bar{t}$ that gives a maximum in a PFR. For the normal case of $b_{\text{in}} = 0$, the value of $\bar{t}$ that maximizes b_{out} is a root mean, $\bar{t}_{\max} = 1/\sqrt{k_A k_B}$, rather than the log mean of Equation 2.23. The best possible yield of B is lower in a CSTR than in a PFR or batch reactor. Continuous flow stirred tank reactors are almost always worse in terms of selectivity because the entire reactor operates under conditions that favor production of undesired byproducts.

Competitive first-order reactions and a few other simple cases can be solved analytically, but any reasonably complex kinetic scheme will require a numerical solution. Mathematics programs such as Mathematica, Mathcad, and Matlab offer nearly automatic solvers for sets of algebraic equations. They usually work. Those of you who wish to understand the inner workings of a solution technique are referred to Appendix 4.1 where a multidimensional version of Newton's method is described. It converges quickly provided your initial guesses for the unknowns are good but will take you to never-never land when your initial guesses are poor. A more robust method of solving the design equations for multiple reactions in a CSTR is to convert the algebraic equations to differential equations.

4.2 METHOD OF FALSE TRANSIENTS

The method of false transients converts a steady-state problem into a time-dependent problem. Equations 4.1 govern the steady-state performance of a CSTR. How does a reactor reach the steady state? There must be a startup transient that eventually evolves into the steady state, and a simulation of that transient will also evolve to the steady state. The simulation need not be physically exact. Any startup trajectory that is mathematically convenient can be used even if it does not duplicate the actual startup. It is in this sense that the transient can be false. Suppose at time $t = 0$ the reactor is instantaneously filled with fluid of initial concentrations $a_0, b_0, \ldots$. The initial concentrations are usually set equal to the inlet concentrations, $a_{\text{in}}, b_{\text{in}}, \ldots$, but other values can be used. The simulation begins with Q_{in} set to its steady-state value. For constant-density cases, Q_{out} is set to the same value, and V is constant. The variable-density case is treated in Section 4.3.

Hold volume constant and set $\hat{a} = a_{\text{out}}$ in Equation 1.6 to obtain the ODEs governing an unsteady CSTR:

$$\begin{aligned} V\frac{d(a_{\text{out}})}{dt} &= Q_{\text{in}}a_{\text{in}} + \mathscr{R}_A(a_{\text{out}}, b_{\text{out}}, \ldots, P_{\text{out}}, T_{\text{out}})V - Q_{\text{out}}a_{\text{out}} \\ V\frac{d(b_{\text{out}})}{dt} &= Q_{\text{in}}b_{\text{in}} + \mathscr{R}_B(a_{\text{out}}, b_{\text{out}}, \ldots, P_{\text{out}}, T_{\text{out}})V - Q_{\text{out}}b_{\text{out}} \\ &\vdots \end{aligned} \tag{4.4}$$

This set of first-order ODEs is easier to solve numerically than the algebraic equations that result from setting all the time derivatives to zero. The initial conditions are $a_{\text{out}} = a_0$, $b_{\text{out}} = b_0, \ldots$ at $t = 0$. The long-time solution to the ODEs will satisfy Equations 4.1 provided that a steady-state solution exits and is accessible from the initial conditions. As discussed in Chapter 5, some CSTRs have multiple steady states and the achieved steady state depends on the initial conditions. There may be no steady state. Recall the chemical oscillators of Chapter 2. Stirred tank reactors can exhibit oscillations or even a semirandom behavior known as chaos. The method of false transients will then fail to achieve a steady state. Another possibility is a metastable steady state. Operation at a metastable steady state requires a control system and cannot be reached by the method of false transients. Metastable steady states arise mainly in nonisothermal systems and are discussed in Chapter 5.

EXAMPLE 4.2

Suppose the competing, elementary reactions

$$\text{A} + \text{B} \xrightarrow{k_{\text{I}}} \text{C} \qquad \text{A} \xrightarrow{k_{\text{II}}} \text{D}$$

occur in a CSTR. Assume density is constant and use the method of false transients to determine the steady-state outlet composition. Suppose $k_{\text{I}}a_{\text{in}}\bar{t} = 4$, $k_{\text{II}}\bar{t} = 1$, $b_{\text{in}} = 1.5\ a_{\text{in}}$, $c_{\text{in}} = 0.1\ a_{\text{in}}$, and $d_{\text{in}} = 0.1\ a_{\text{in}}$.

SOLUTION: Write a version of Equation 4.4 for each component. Divide through by Q and substitute the appropriate reaction rates to obtain

$$\begin{aligned} \bar{t}\frac{da_{\text{out}}}{dt} &= a_{\text{in}} - a_{\text{out}} - k_{\text{I}}\bar{t}a_{\text{out}}b_{\text{out}} - k_{\text{II}}\bar{t}a_{\text{out}} \\ \bar{t}\frac{db_{\text{out}}}{dt} &= b_{\text{in}} - b_{\text{out}} - k_{\text{I}}\bar{t}a_{\text{out}}b_{\text{out}} \\ \bar{t}\frac{dc_{\text{out}}}{dt} &= c_{\text{in}} - c_{\text{out}} + k_{\text{I}}\bar{t}a_{\text{out}}b_{\text{out}} \\ \bar{t}\frac{dd_{\text{out}}}{dt} &= d_{\text{in}} - d_{\text{out}} + k_{\text{II}}\bar{t}a_{\text{out}} \end{aligned}$$

These equations are directly suitable for solution by Euler's method. Use a first-order difference approximation for the time derivatives, for example,

$$\frac{da}{dt} \approx \frac{a_{\text{new}} - a_{\text{old}}}{\Delta t}$$

The equations for Euler's method are

$$\left(\frac{a}{a_{\text{in}}}\right)_{\text{new}} = \left(\frac{a}{a_{\text{in}}}\right)_{\text{old}} + \left[1 - (1 + k_{\text{II}}\bar{t})\left(\frac{a}{a_{\text{in}}}\right)_{\text{old}} - k_{\text{I}}a_{\text{in}}\bar{t}\left(\frac{a}{a_{\text{in}}}\right)_{\text{old}}\left(\frac{b}{a_{\text{in}}}\right)_{\text{old}}\right]\Delta\tau$$

$$\left(\frac{b}{a_{\text{in}}}\right)_{\text{new}} = \left(\frac{b}{a_{\text{in}}}\right)_{\text{old}} + \left[\left(\frac{b_{\text{in}}}{a_{\text{in}}}\right) - \left(\frac{b}{a_{\text{in}}}\right)_{\text{old}} - k_{\text{I}}a_{\text{in}}\bar{t}\left(\frac{a}{a_{\text{in}}}\right)_{\text{old}}\left(\frac{b}{a_{\text{in}}}\right)_{\text{old}}\right]\Delta\tau$$

$$\left(\frac{c}{a_{\text{in}}}\right)_{\text{new}} = \left(\frac{c}{a_{\text{in}}}\right)_{\text{old}} + \left[\left(\frac{c_{\text{in}}}{a_{\text{in}}}\right) - \left(\frac{c}{a_{\text{in}}}\right)_{\text{old}} + k_{\text{I}}a_{\text{in}}\bar{t}\left(\frac{a}{a_{\text{in}}}\right)_{\text{old}}\left(\frac{b}{a_{\text{in}}}\right)_{\text{old}}\right]\Delta\tau$$

$$\left(\frac{d}{a_{\text{in}}}\right)_{\text{new}} = \left(\frac{d}{a_{\text{in}}}\right)_{\text{old}} + \left[\left(\frac{d_{\text{in}}}{a_{\text{in}}}\right) - \left(\frac{d}{a_{\text{in}}}\right)_{\text{old}} + k_{\text{II}}\bar{t}\left(\frac{a}{a_{\text{in}}}\right)\right]\Delta\tau$$

where $\tau = t/\bar{t}$ is dimensionless time. The set can be written more compactly as

$$a^*_{\text{new}} = a^*_{\text{old}} + [1 - 2a^*_{\text{old}} - 4a^*_{\text{old}}b^*_{\text{old}}]\,\Delta\tau$$
$$b^*_{\text{new}} = b^*_{\text{old}} + [1.5 - b^*_{\text{old}} - 4a^*_{\text{old}}b^*_{\text{old}}]\,\Delta\tau$$
$$c^*_{\text{new}} = c^*_{\text{old}} + [0.1 - c^*_{\text{old}} + 4a^*_{\text{old}}b^*_{\text{old}}]\,\Delta\tau$$
$$d^*_{\text{new}} = d^*_{\text{old}} + [0.1 - d^*_{\text{old}} + a^*_{\text{old}}]\,\Delta\tau$$

where the various concentrations have been normalized by a_{in} and numerical values have been substituted for the rate constants. Suitable initial conditions are $a^*_0 = 1$, $b^*_0 = 1.5$, $c^*_0 = 0.1$, and $d^*_0 = 0.1$. Figure 4.1 shows the transient approach to steady state. Numerical values for the long-time, asymptotic solutions are also shown in Figure 4.1. The code used for this solution is shown in Code for Example 4.2.

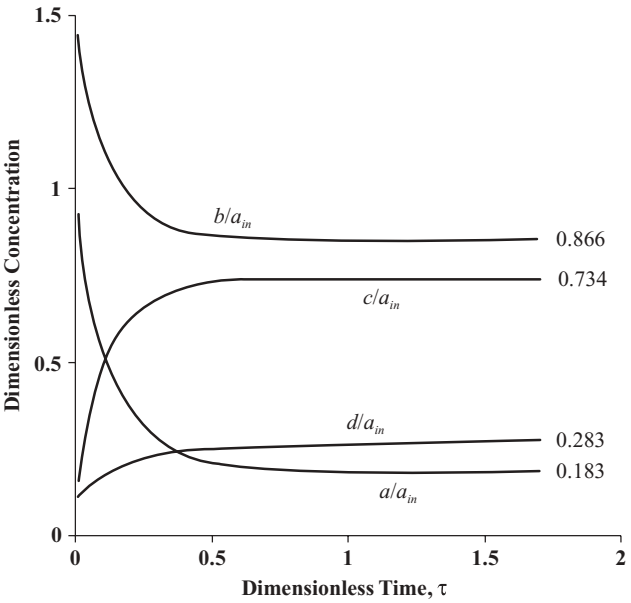

Figure 4.1 Transient approaches to a stable steady state in a CSTR.

Code for Example 4.2

```
Sub Example4_2()

aold = 1
Bold = 1.5
cold = 0.1
dold = 0.1
dtau = 0.05

Do

   n = n + 1
   Cells(n, 1) = tau
   Cells(n, 2) = anew
   Cells(n, 3) = bnew
   Cells(n, 4) = cnew
   Cells(n, 5) = dnew

   anew = aold + (1 - 2 * aold - 4 * aold * Bold) * dtau
   bnew = Bold + (1.5 - Bold - 4 * aold * Bold) * dtau
   cnew = cold + (0.1 - cold + 4 * aold * Bold) * dtau
   dnew = dold + (0.1 - dold + aold) * dtau
   tau = tau + dtau

   aold = anew
   Bold = bnew
   cold = cnew
   dold = dnew

Loop While tau < 10

End Sub
```

Solving the ODEs out to about $\tau = 10$ is adequate. The steady-state solutions can be found by setting the accumulation terms to zero and solving the following set of algebraic equations:

$$0 = 1 - 2a^*_{\text{out}} - 4a^*_{\text{out}}b^*_{\text{out}}$$
$$0 = 1.5 - b^*_{\text{out}} - 4a^*_{\text{out}}b^*_{\text{out}}$$
$$0 = 0.1 - c^*_{\text{out}} + 4a^*_{\text{out}}b^*_{\text{out}}$$
$$0 = 0.1 - d^*_{\text{out}} + a^*_{\text{out}}$$

The method of false transients is one way to solve these equations.

Analytical solutions are desirable because they explicitly show the functional dependence of the solution on the operating variables. Unfortunately, they are difficult or impossible for complex kinetic schemes and are almost always impossible for the nonisothermal reactors considered in Chapter 5. All numerical solutions have the disadvantage of being case specific, but this disadvantage can be alleviated

through the judicious use of dimensionless variables. Direct algebraic solutions to Equations 4.1 will, in principle, give all the steady states, both stable and metastable. On the other hand, when a solution is obtained using the method of false transients, the steady state is known to be stable and achievable from the assumed initial conditions.

Example 4.2 applied the method of false transients to a CSTR to find the steady-state output. A set of algebraic equations was converted to a set of ODEs. Chapter 16 shows how the method can be applied to PDEs by converting them to sets of ODEs. The method of false transients can also be used to find the equilibrium concentrations resulting from a set of batch chemical reactions. Formulate the ODEs for a batch reactor and integrate until the concentrations stop changing. Irreversible reactions go to completion. Reversible reactions reach equilibrium concentrations. This is illustrated in Problem 4.6(b). Section 11.1.1 shows how the method of false transients can be used to determine physical or chemical equilibria in multiphase systems.

4.3 CSTRs WITH VARIABLE DENSITY

The design equations for a CSTR, Equations 4.1, do not require that the reacting mixture have constant physical properties or that operating conditions such as temperature and pressure be the same for the inlet and outlet environments.

They do require knowledge of Q_{in}, Q_{out}, and V, and determination of these quantities is not immediate when the density of the reacting mixture varies with composition. The inlet temperature and the inlet and outlet pressures in a CSTR are usually determined or controlled independently of the extent of reaction. The outlet temperature can be set arbitrarily in small laboratory equipment because of excellent heat transfer at the small scale. It is sometimes possible to predetermine the temperature in industrial-scale reactors, for example, if the heat of reaction is small or if the contents are boiling. Chapter 5 discusses the case where the outlet temperature is found from a heat balance. The design equations do not depend on P_{in} and T_{in}, and we assume Q_{in} is known. This chapter considers the case where both P_{out} and T_{out} are known. The outlet density ρ_{out} will vary with composition and is determined from an equation of state. The volumetric flow rate at the outlet, Q_{out}, is found from a steady-state material balance:

$$\rho_{\text{in}} Q_{\text{in}} = \rho_{\text{out}} Q_{\text{out}} \tag{4.5}$$

The fraction unreacted for the general case of any flow reactor is

$$Y_A = \frac{Q_{\text{out}} a_{\text{out}}}{Q_{\text{in}} a_{\text{in}}} \tag{4.6}$$

Note that Y_A is a ratio of moles, and will be a ratio of concentrations only if density is constant.

4.3.1 Liquid Phase CSTRs

This chapter treats reactions within a single phase. Multiphase CSTRs are treated in Chapter 11. For the single-phase case, there is no essential difference between liquid and gas reactors except for the equation of state. Density changes in liquid systems tend to be small, and the density is usually assumed to be a linear function of concentration. Liquid phase CSTRs can be hydraulically full but frequently operate with a fixed level and have a free surface in contact with a vapor phase. Occasionally they are mounted on load cells or use radiation-level detectors and operate with a fixed mass.

EXAMPLE 4.3

Suppose a pure monomer polymerizes in a CSTR with pseudo-first-order kinetics. The reactor volume is constant. The monomer and polymer have different densities. Assume a linear relationship based on the monomer concentration. Then determine the fraction unreacted.

SOLUTION: The reaction is

$$\mathrm{M} \longrightarrow \mathrm{P} \qquad \mathscr{R} = kM$$

The reactor design equation for the monomer is

$$0 = M_{\text{in}} Q_{\text{in}} - VkM_{\text{out}} - M_{\text{out}} Q_{\text{out}} \tag{4.7}$$

where the unknowns are

$$\frac{M_{\text{out}}}{M_{\text{in}}} = \frac{Q_{\text{in}}}{Q_{\text{out}} + kV} \tag{4.8}$$

This gives the standard result $Y' = M_{\text{out}}/M_{\text{in}} = 1/(1 + k\bar{t})$ when $Q_{\text{out}} = Q_{\text{in}}$. Otherwise, a somewhat different result is obtained that depends on the relative densities of the inlet and outlet streams.

A relationship between density and composition is needed for the variable-density case. One that serves the purpose is

$$\rho = \rho_{\text{polymer}} - (\rho_{\text{polymer}} - \rho_{\text{monomer}}) \left(\frac{M}{M_{\text{in}}} \right) \tag{4.9}$$

The procedure from this point is straightforward if algebraically messy. Set $M = M_{\text{out}}$ in Equation 4.9 to obtain ρ_{out}. Substitute ρ_{out} into Equation 4.5 to obtain Q_{out} and then substitute Q_{out} into Equation 4.7 so that m_{out} becomes the only unknown. The solution for m_{out} is

$$\frac{M_{\text{out}}}{M_{\text{in}}} = \frac{1 - \sqrt{1 - 4(1 - \rho_{\text{monomer}}/\rho_{\text{polymer}}) Y'_M (1 - Y'_M)}}{2(1 - \rho_{\text{monomer}}/\rho_{\text{polymer}})(1 - Y'_M)} \tag{4.10}$$

where Y'_M is the fraction unreacted that would be calculated if the density change were ignored, $Y' = Q_{\text{in}}/(Q_{\text{in}} + kV)$.

As a numerical example, suppose $Y'_M = 0.5$ and $\rho_{\text{monomer}}/\rho_{\text{polymer}} = 0.9$. Then Equation 4.10 gives $M_{\text{out}}/M_{\text{in}} = 0.513$. This result may seem strange at first. The density increases upon polymerization so that the reactor has a greater mass inventory when filled with the polymerizing mass than when filled with monomer. More material means a higher residence

time, yet M_{out}/M_{in} is higher, suggesting less reaction. The answer is that M_{out}/M_{in} is not the fraction unreacted when there is a density change. For the problem at hand,

$$\frac{Q_{out}}{Q_{in}} = \frac{\rho_{in}}{\rho_{out}} = \frac{r}{1 + (1 - r)M_{out}/M_{in}}$$

For the numerical example, $Q_{out}/Q_{in} = 0.949$ and the fraction unreacted is

$$Y_M = \frac{Q_{out}M_{out}}{Q_{in}M_{in}} = 0.487$$

This compares to 0.5 for the constant-density case. Thus the density change causes a modest increase in conversion.

4.3.2 Computational Scheme for Variable-Density CSTRs

Example 4.3 represents the simplest possible example of a variable-density CSTR. The reaction is isothermal, first order, and irreversible and the density is a linear function of reactant concentration. This simplest system is about the most complicated one for which an analytical solution is possible. Realistic variable-density problems, whether in liquid or gas systems, require numerical solutions. These numerical solutions use the method of false transients and involve sets of first-order ODEs with various auxiliary functions. The solution methodology is similar to but simpler than that used for PFRs in Chapter 3. Temperature is known and constant in this chapter. An equation for temperature will be added in Chapter 5 and is conceptually incorporated in the methodology that follows.

Method of False Transients for a CSTR

The method of false transients begins with the inlet stream set to its steady-state values of Q_{in}, T_{in}, ρ_{in}, a_{in}, b_{in}, ... The reactor volume is fixed at V and is full of material having concentrations a_0, b_0, ...

0. Pick the initial values a_0, b_0, ... Use the equation of state to calculate an initial value for ρ_{out} and determine the initial value for Q_{out} from $Q_{out} = \rho_{in}Q_{in}/\rho_{out}$.

1. Pick a step size, Δt.

2. Set a_{out}, b_{out}, ..., T_{out}, Q_{out} to the initial values determined in Step 0.

3. Take one step, calculating new values for a_{out}, b_{out}, ..., T_{out} at the new time $t + \Delta t$. The marching-ahead equations have the form

$$(a_{out})_{new} = (a_{out})_{old} + \frac{[Q_{in}a_{in} + \mathscr{R}_A(a_{out}, b_{out}, \ldots, P_{out}, T_{out})V - Q_{out}a_{out}]\Delta t}{V} \tag{4.11}$$

4. Use the equation of state to calculate ρ_{out}.

5. Calculate $Q_{out} = \rho_{in}Q_{in}/\rho_{out}$.

6. Check if$(a_{\text{out}})_{\text{new}} \cong (a_{\text{out}})_{\text{old}}$. If not, go to Step 3.
7. Decrease Δt by a factor of 2 and go to Step 1. Repeat until the results converge to four or five significant figures.

For the case where the reacting mass, $\rho_{\text{out}} V$, is held constant rather than the reacting volume, a value of V is guessed initially and is updated whenever ρ_{out} is updated. Note that it is not necessary to include V inside the derivatives in Equations 4.4 since this is the method of *false* transients rather than real transients. Note also that an accurate solution is not required for the early portions of the trajectory, and Euler's method is the perfect integration routine. A large step size can be used provided the solution remains stable. As steady state is approached, the quantity in square brackets in Equation 4.11 goes to zero. This allows an accurate solution at the end of the trajectory even thought the step size is large. Convergence is achieved very easily, and Step 7 is included as a matter of good computing practice or if it is desired to model an actual transient. Actual startup transients—as opposed to a false transient used to get steady-state values—are discussed in Chapter 14.

EXAMPLE 4.4

Solve Example 4.3 numerically.

SOLUTION: The individual values for k, V, and Q_{in} are combined into the dimensionless group $k\bar{t}_{\text{in}} = kV/Q_{\text{in}}$. This group determines the performance of a constant-density reactor and is one of the two parameters needed for the variable-density case. The other parameter is the density ratio $r = \rho_{\text{monomer}}/\rho_{\text{polymer}}$. The individual values for k, V, and Q_{in} can be assigned as convenient provided the composite value for $k\bar{t}_{\text{in}}$ is retained, $k\bar{t}_{\text{in}} = 1$ in this example. The individual values for ρ_{monomer} and ρ_{polymer} can also be assigned as convenient provided their ratio is set, 0.9 in the example. Executing Code for Example 4.4 gives the same results as found in Example 4.3 but with less work. The long-time results to three decimal places are mnew $= 0.513 = m_{\text{out}}$, Qout $= 0.949 = Q_{\text{out}}/Q_{\text{in}}$, and Qout * mnew $= 0.487 = Y_M$.

4.3.3 Gas Phase CSTRs

Strictly gas phase CSTRs are rare. Two-phase gas–liquid CSTRs are common and are treated in Chapter 11. Two-phase gas–solid CSTRs are often used to study heterogeneous catalysis. When the solid is a catalyst, the use of ***pseudohomogeneous kinetics*** allows these two-phase systems to be treated as though only the fluid phase were present. All concentration measurements are made in the gas phase, and the rate expression is fitted to the gas phase concentrations. The present section outlines a method for fitting pseudohomogeneous kinetics using measurements made in a CSTR. A more general treatment is given in Chapter 10. Here we consider a recycle loop reactor containing a small bed of finely ground catalyst through which the gas is circulated at a high rate. See Figure 4.2. The high flow rate gives good heat transfer

Code for Example 4.4

```
Sub Example4_4()

dt = 0.1
Qin = 1
k = 1
V = 1
Min = 1

rhom = 0.9
rhop = 1
rhoin = rhom
Qout = Qin
mold = Min

Do
       mnew = mold + (Qin * Min - k * V * mold - Qout * mold) * dt/V
       rhoout = rhop - (rhop - rhom) * mnew/Min
       Qout = Qin * rhoin/rhoout
       mold = mnew
       Cells(1, 1) = mnew
       Cells(1, 2) = Qout
       Cells(1, 3) = Qout * mnew
       t = t + dt
Loop While t < 10

End Sub
```

and eliminates gas phase resistance to mass transfer. The net throughput is relatively small since most of the gas exiting from the catalyst bed is recycled. The per-pass conversion is low, but the overall conversion is high enough that a chemical analysis can be reasonably accurate. Recycle loops behave as CSTR's when the recycle ratio is high. This fact is intuitively reasonable since the external pump causes circulation similar to that caused by the agitator in a conventional stirred tank reactor. A variant of the loop reactor puts the catalyst in a basket and then rotates the basket at high speed within the gas mixture. This more closely resembles the tank-plus-agitator design of a conventional stirred tank, but the kinetic result is the same. Section 4.5.3 shows the mathematical justification for treating a loop reactor as a CSTR.

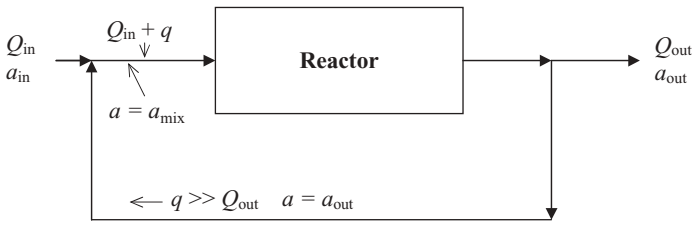

Figure 4.2 Reactor in a recycle loop.

A gas phase CSTR with prescribed values for P_{out} and T_{out} is relatively simple when ideal gas behavior can be assumed. The molar density in the reactor will be known and independent of composition.

EXAMPLE 4.5

Suppose the recycle reactor in Figure 4.2 is used to evaluate a catalyst for the manufacture of sulfuric acid. The catalytic step is the gas phase oxidation of sulfur dioxide:

$$SO_2 + \tfrac{1}{2}\,O_2 \rightarrow SO_3$$

Studies on similar catalysts have suggested a rate expression of the form

$$\mathscr{R} = \frac{k[SO_2][O_2]}{1 + k_C[SO_3]} = \frac{kab}{1 + k_C c}$$

where $a = [SO_2]$, $b = [O_2]$, and $c = [SO_3]$. The object is to determine k and k_C for this catalyst. In practice, many runs should be made at various values of a_{in}, b_{in}, and c_{in}, and the model should be fit to the data using the nonlinear least-squares techniques of Section 7.1. The present example treats the case of just two runs where k and k_C are fit exactly. The following compositions have been measured:

	Inlet Concentration (mol %)		Outlet Concentration (mol %)	
	Run 1	Run 2	Run 1	Run 2
SO_2	10	5	4.1	2.0
O_2	10	10	7.1	8.6
SO_3	0	5	6.3	8.1
Inerts	80	80	82.5	81.3

The operating conditions for these runs were $Q_{in} = 0.000268$ m^3 s^{-1}, $P_{in} = 2.04$ atm, $P_{out} = 1.0$ atm, $T_{in} = 40^\circ$C, $T_{out} = 300^\circ$C, and $V = 0.0005$ m^3.

SOLUTION: The analysis could be done using mole fractions as the composition variable, but this would restrict applicability to the specific conditions of the experiment. Greater generality is possible by converting to concentration units. The results will then apply to somewhat different pressures. The "somewhat" recognizes the fact that the reaction mechanism and even the equation of state may change at extreme pressures. The results will not apply at different temperatures since k and k_C will be functions of temperature. The temperature dependence of rate constants is considered in Chapter 5.

Converting to standard concentrations units, moles per cubic meter, gives the following molar concentrations:

	Inlet Concentration		Outlet Concentration	
	Run 1	Run 2	Run 1	Run 2
SO_2	7.94	3.97	0.87	0.43
O_2	7.94	7.94	1.51	1.83
SO_3	0	3.97	1.34	1.72
Inerts	63.51	63.51	17.54	17.28
ρ_{molar}	79.38	79.39	21.26	21.26

The outlet flow rate Q_{out}, is required. The easiest way to get it is by a molar balance on the inerts:

$$Q_{\text{in}} d_{\text{in}} = Q_{\text{out}} d_{\text{out}}$$

which gives $Q_{\text{out}} = (0.000268)(63.51)/(17.54) = 0.000970\ \text{m}^3\ \text{s}^{-1}$ for run 1 and 0.000985 for run 2. These results allow the molar flow rates to be calculated:

	Inlet Molar Flow Rate		Outlet Molar Flow Rate	
	Run 1	Run 2	Run 1	Run 2
SO_2	0.00213	0.00106	0.00085	0.00042
O_2	0.00213	0.00213	0.00146	0.00180
SO_3	0	0.00106	0.00130	0.00169
Inerts	0.01702	0.01704	0.01702	0.01702
Total moles	0.02128	0.02128	0.02063	0.02093

The reader may wish to check these results against the reaction stoichiometry for internal consistency. They are certainly as good as warranted by the two-place precision of the analytical results.

The reactor design equation for SO_3 is

$$0 = c_{\text{in}} Q_{\text{in}} + \frac{V k a_{\text{out}} b_{\text{out}}}{1 + k_C c_{\text{out}}} - c_{\text{out}} Q_{\text{out}}$$

Everything in this equation is known but the two rate constants. Substituting the known quantities for each run gives a pair of simultaneous equations:

$$0.00130 + 0.00174 k_C = 0.000658k$$
$$0.00063 + 0.00109 k_C = 0.000389k$$

Solution gives k = 8.0 mol m^{-3} s^{-1} and k_C = 2.3 mol^{-1} m^3. Be warned that this problem is ***ill-conditioned***. Small differences in the input data or rounding errors can lead to major differences in the calculated values for k and k_C. The numerical values in this problem were calculated using greater precision than indicated in the above tables. Also, the values for k and

k_C will depend on which component was picked for the component balance. The example used component C, but A or B could have been chosen. Despite this numerical sensitivity, predictions of performance using the fitted values for the rate constants will closely agree within the range of the experimental results. The estimates for k and k_C are ***correlated*** so that a high value for one will lead to a compensating high value for the other. Further discussion of data fitting is given in Chapter 7.

EXAMPLE 4.6

Use the kinetic model of Example 4.5 to determine the outlet concentration for the loop reactor if the operating conditions are the same as in run 1.

SOLUTION: Example 4.5 was a ***reverse problem*** where measured reactor performance was used to determine constants in the rate equation. We now treat the ***forward problem*** where the kinetics are known and the reactor performance is desired. Obviously, the results of run 1 should be closely duplicated. The solution uses the method of false transients for a variable-density system. The ideal gas law is used at the equation of state. The ODEs are

$$\frac{da_{\text{out}}}{dt} = \frac{a_{\text{in}}Q_{\text{in}}}{V} - \frac{ka_{\text{out}}b_{\text{out}}}{1+k'c_{\text{out}}} - \frac{a_{\text{out}}Q_{\text{out}}}{V}$$
$$\frac{db_{\text{out}}}{dt} = \frac{b_{\text{in}}Q_{\text{in}}}{V} - \frac{ka_{\text{out}}b_{\text{out}}}{2(1+k'c_{\text{out}})} - \frac{b_{\text{out}}Q_{\text{out}}}{V}$$
$$\frac{dc_{\text{out}}}{dt} = \frac{c_{\text{in}}Q_{\text{in}}}{V} + \frac{ka_{\text{out}}b_{\text{out}}}{1+k'c_{\text{out}}} - \frac{c_{\text{out}}Q_{\text{out}}}{V}$$
$$\frac{dd_{\text{out}}}{dt} = \frac{d_{\text{in}}Q_{\text{in}}}{V} - \frac{d_{\text{out}}Q_{\text{out}}}{V}$$

Add all these together, noting that the sum of the component concentrations is the molar density:

$$\frac{d(\rho_{\text{molar}})_{\text{out}}}{dt} = \frac{(\rho_{\text{molar}})_{\text{in}}Q_{\text{in}}}{V} - \frac{ka_{\text{out}}b_{\text{out}}}{2(1+k'c_{\text{out}})} - \frac{(\rho_{\text{molar}})_{\text{out}}Q_{\text{out}}}{V}$$

The ideal gas law says that the molar density is determined by pressure and temperature and is thus known and constant in the reactor. Setting the time derivative of molar density to zero gives an expression for Q_{out} at steady state. The result is

$$Q_{\text{out}} = \frac{(\rho_{\text{molar}})_{\text{in}}Q_{\text{in}}}{(\rho_{\text{molar}})_{\text{out}}} - \left(\frac{1}{2}\right)\frac{Vka_{\text{out}}b_{\text{out}}}{(\rho_{\text{molar}})_{\text{out}}(1+k_Cc_{\text{out}})}$$

For the numerical solution, the ODEs for the three reactive components are solved in the usual manner and Q_{out} is updated after each time step. If desired, d_{out} is found from

$$d_{\text{out}} = \rho_{\text{molar}} - a_{\text{out}} - b_{\text{out}} - c_{\text{out}}$$

The results for the conditions of run 1 are $a_{\text{out}} = 0.87$, $b_{\text{out}} = 1.55$, $c_{\text{out}} = 1.37$, and $d_{\text{out}} = 17.47$. The agreement with Example 4.5 is less than perfect because the values for k and k' were rounded to two places. Better precision is unrealistic.

4.4 SCALING FACTORS FOR LIQUID PHASE STIRRED TANKS

This section treats both batch and continuous flow stirred tank reactors but is restricted to single-phase liquid systems. Two-phase behavior resulting from boiling is discussed in Chapter 5 and multiphase reactions are discussed in Chapter 11. Scaleups of liquid phase stirred tanks are usually based on geometric similarity and, for flow reactors, a constant value for the mean residence time. Possible density differences between the large and small reactors are ignored. Thus there is a single scaling factor, S, for throughput, inventory, and volume. See Equation 1.58. Mechanically agitated vessels have an additional scaling factor, S_N, which is the ratio of impeller speeds in the large compared to the small vessel. The normal case is for the impeller speed to decrease upon scaleup so $S_N < 1$ is usual.

The most common problem in scaling up stirred tank reactors is the difficulty in maintaining the desired operating temperature. The current section assumes this is possible. Techniques for maintaining a desired energy balance are deferred to Chapter 5.

When scaling with geometric similarity, all linear dimensions—for example, the impeller diameter and blade width, the tank diameter, the distance that the impeller is off the bottom, the height of the liquid in the reactor, and the width of the baffles—scale as $S^{1/3}$. The scaleup relations are comparatively simple when scaling with geometric similarity and when the small-scale vessel is fully turbulent. The Reynolds number for a mechanically agitated vessel is defined as

$$(\mathbf{Re})_{\text{impeller}} = \frac{\rho N_{\text{I}} D_{\text{I}}^2}{\mu} \tag{4.12}$$

where N_I is the rotational speed of the impeller in revolutions per second and D_I is the diameter of the impeller, not of the tank. The velocity term in the Reynolds number is the tip velocity of the impeller, $N_I D_I$. The transition from laminar flow occurs when the impeller Reynolds number is about 100, and the vessel is highly turbulent by $(\mathbf{Re})_{\text{impeller}} = 1000$. These statements are true for commercial examples of turbine and paddle agitators. Most industrial stirred tanks operate in the fully turbulent regime. The exceptions are typically polymerization reactors. They often use special types of agitators: anchors, helical ribbons, and large-diameter pitched-blade turbines.

Taking ratios of Equation 4.12 for large and small vessels gives

$$S_{\mathbf{Re}} = \frac{\left[\rho N_I D_I^2/\mu\right]_2}{\left[\rho N_I D_I^2/\mu\right]_1} = S_N S^{2/3}.$$

The mixing time scales as S_N^{-1}; the pumping capacity of the impellor scales as $S_N S$; and the power to the impeller scales as $S_N^3 S^{5/3}$. As discussed in Section 1.5, it is impractical to maintain a constant mixing time upon scaleup since the power requirements increase too dramatically. However, the increase in t_{mix} is usually moderate when scaling with constant power per unit volume. Although experts in agitator design are loath to admit using such a simplistic rule, most scaleups of conventionally agitated vessels are done

at or near constant power per unit volume. The consequences of scaling in this fashion are explored in Example 4.7.

EXAMPLE 4.7

A fully turbulent, baffled vessel is to be scaled up by a factor of 512 in volume while maintaining constant power per unit volume. Determine the effects of the scaleup on the impeller speed and mixing time.

SOLUTION: At high **Re**, agitator power is proportional to $N_I^3 D_I^5$. Thus the scaling relationship for power is $S_N^3 S^{5/3}$, and power per unit volume scales as $S_N^3 S^{2/3}$. To maintain constant power per unit volume, N_I must decrease upon scaleup. Specifically, N_I must be proportional to $D_I^{-2/3}$ and thus scale as $S^{-2/9}$. The mixing time is proportional to N_I^{-1} and thus scales as $S^{2/9}$. Results for these and other design and operating variables are shown in Table 4.1.

A volumetric scaleup by a factor of 512 is quite large, and the question arises as to whether the large vessel will remain well mixed on the large scale. The concern is the fact that the mixing time increases by a factor of 4. Does it remain true that $t_{\text{mix}} \ll t_{1/2}$ and for a CSTR that $t_{\text{mix}} \ll \bar{t}$? If so, the assumption that the large vessel will behave as a CSTR is probably justified. The ratio of internal circulation to net throughput—which is the internal recycle ratio—scales as the inverse of the mixing time and will thus decrease by a factor of 4. The decrease may appear worrisome, but if the increase in mixing time can be tolerated, it is likely that the decrease in internal recycle ratio is also acceptable since the two are causally related.

Table 4.1 Scaleup Factors for Geometrically Similar Stirred Tanks

	General Scaling Factor	Scaling Factor for Constant Power per Unit Volume	Numerical Scaling Factor for S = 512
Vessel diameter	$S^{1/3}$	$S^{1/3}$	8
Impeller diameter	$S^{1/3}$	$S^{1/3}$	8
Vessel volume	S	S	512
Throughput	S	S	512
Residence time	1	1	1
Reynolds number	$S_N S^{2/3}$	$S^{4/9}$	8
Froude number	$S_N^2 S^{1/3}$	$S^{-1/9}$	0.5
Agitator speed	S_N	$S^{-2/9}$	0.25
Power	$S_N^3 S^{5/3}$	S	512
Power per volume	$S_N^3 S^{2/3}$	1.0	1
Mixing time	S_N^{-1}	$S^{2/9}$	4
Circulation rate	$S_N S$	$S^{7/9}$	128
Circulation rate/throughput	S_N	$S^{-2/9}$	0.25
Heat transfer area, A_{ext}	$S^{2/3}$	$S^{2/3}$	64
Inside coefficient, h	$S_N^{2/3} S^{1/9}$	$S^{-1/27}$	0.79
Coefficient times area, hA_{ext}	$S_N^{2/3} S^{7/9}$	$S^{17/27}$	50.8
Driving Force, ΔT	$S_N^{-2/3} S^{2/9}$	$S^{10/27}$	10.1

Table 4.1 includes the Froude number, $N_I^2 D_I/g$, where g is the acceleration due to gravity. This dimensionless group governs the extent of swirling and vortexing in an unbaffled stirred tank. Turbulent stirred tanks are normally baffled so that the power from the agitator causes turbulence rather than mere circular motion. Intentional vortexing is occasionally used as a means for rapidly engulfing a feed stream. Table 4.1 shows that the extent of vortexing will decrease for scaleups at constant power per unit volume. Unbaffled tanks will draw somewhat less power than baffled tanks.

Most of the factors in Table 4.1 apply equally to batch and flow vessels. The throughput in a well-designed CSTR is small compared to the internal circulation and does not affect quantities such as power, mixing time, and heat transfer to the jacket. The heat transfer factors in Table 4.1 are discussed in Chapter 5.

4.5 COMBINATIONS OF REACTORS

We have considered two types of ideal flow reactor: piston flow and the perfectly mixed CSTR. These two ideal types can be connected together in a variety of series and parallel arrangements to give composite reactors that are generally intermediate in performance compared to the ideal reactors. Sometimes the composite reactor is only conceptual. It is used to model a real reactor that is intermediate in performance compared to the ideal reactors. Sometimes the composite reactors are actually built. There are many good reasons for building reactor combinations. Temperature control is a major motivation. The use of standard designs is sometimes a factor as is the ability to continue operating a plant while adding capacity. Series and parallel scaleups of tubular reactors were considered in Chapter 3. Parallel scaleups of CSTRs are uncommon, but they are sometimes used to gain capacity. Series installations are more common. The series combinations of a stirred tank followed by a tube is also common. This section begins the analysis of composite reactors while retaining the assumption of isothermal operation, at least within a single reactor. Different reactors in the composite system may operate at different temperatures and thus have different rate constants.

4.5.1 Series and Parallel Connections

When reactors are connected in series, the output from one serves as the input for the other. For ***reactors in series***,

$$(a_{\text{in}})_2 = (a_{\text{out}})_1 \tag{4.13}$$

The design equations for reactor 1 are solved and used as the input to reactor 2.

EXAMPLE 4.8

Find the yield for a first-order reaction in a composite reactor that consists of a CSTR followed by a PFR. Assume that the mean residence time is $\bar{t}_1$ in the CSTR and $\bar{t}_2$ in the PFR.

SOLUTION: The exit concentration from the perfect mixer is

$$(a_{\text{out}})_1 = \frac{a_{\text{in}}}{1 + k\bar{t}_1}$$

and that for the PFR is

$$a_{\text{out}} = (a_{\text{in}})_2 \exp(-k\bar{t}_2)$$

Using Equation 4.13 to combine these results gives

$$a_{\text{out}} = \frac{a_{\text{in}} \exp(-k\bar{t}_2)}{1 + k\bar{t}_1}$$

Compare the outlet concentration of the composite reactor to that from a single CSTR and to a PFR having the same mean residence time:

$$\bar{t} = \frac{V}{Q} = \frac{V_1 + V_2}{Q} = \bar{t}_1 + \bar{t}_2$$

The following inequality is true for physically realistic (meaning positive) values of k, $\bar{t}_1$, and $\bar{t}_2$:

$$\frac{1}{1 + k(\bar{t}_1 + \bar{t}_2)} \geq \frac{\exp(-k\bar{t}_2)}{1 + k\bar{t}_1} \geq \exp[-k(\bar{t}_1 + \bar{t}_2)]$$

Thus the combination reactor gives intermediate performance. There will be less conversion than for a PFR with $\bar{t} = \bar{t}_1 + \bar{t}_2$ but more conversion than for a single CSTR with $\bar{t} = \bar{t}_1 + \bar{t}_2$.

For two ***reactors in parallel***, the output streams are averaged based on flow rate:

$$a_{\text{out}} = \frac{Q_1(a_{\text{out}})_1 + Q_2(a_{\text{out}})_2}{Q_1 + Q_2} \tag{4.14}$$

EXAMPLE 4.9

Find the conversion for a first-order reaction in a composite system that consists of a perfect mixer and a PFR in parallel.

SOLUTION: Using Equation 4.14,

$$a_{\text{out}} = \frac{a_{\text{in}}}{Q_1 + Q_2}\left(\frac{Q_1}{1 + k\bar{t}_1} + Q_2 \exp(-k\bar{t}_2)\right)$$

A parallel reactor system has an extra degree of freedom compared to a series system. The total volume and flow rate can be arbitrarily divided between the parallel elements. For reactors in series, only the volume can be divided since the two reactors must operate at the same flow rate. Despite this extra variable, there are

no performance advantages compared to a single reactor having the same total V and Q, provided the parallel reactors are at the same temperature. When significant amounts of heat must be transferred to or from the reactants, identical small reactors in parallel may be preferred because the desired operating temperature is easier to achieve.

The general rule is that combinations of isothermal reactors provide intermediate levels of performance compared to single PFRs and CSTRs having the same total volume and flow rate. The second general rule is that a single PFR will give higher conversion and better selectivity than a CSTR. Autocatalytic reactions provide the exception to both these statements.

EXAMPLE 4.10

Consider a reactor train consisting of a CSTR followed by a PFR. The total volume and flow rate are fixed. Can a series combination give a performance advantage compared to a single reactor if the reaction is autocatalytic? The reaction is

$$\mathrm{A} + \mathrm{B} \xrightarrow{k} 2\mathrm{B}$$

Treat the semipathological case where $b_{\text{in}} = 0$.

SOLUTION: With $b_{\text{in}} = 0$, a reaction will never start in a PFR, but a steady-state reaction is possible in a CSTR if the reactor is initially spiked with component B. An analytical solution can be found for this problem, but a numerical solution is easier. The design equations in a form suitable for the method of false transients are

$$\frac{d(a_{\text{out}})_1}{dt} = (a_{\text{in}})_1 - k\bar{t}_1(a_{\text{out}})_1(b_{\text{out}})_1 - (a_{\text{out}})_1$$
$$\frac{d(b_{\text{out}})_1}{dt} = (b_{\text{in}})_1 + k\bar{t}_1(a_{\text{out}})_1(b_{\text{out}})_1 - (b_{\text{out}})_1$$

The long-time solution to these ODEs gives $(a_{\text{out}})_1$ and $(b_{\text{out}})_1$, which are the inlet concentrations for the piston flow portion of the system. The design equations for the PFR are

$$\frac{da_2}{dt} = -ka_2b_2 \qquad \frac{db_2}{dt} = ka_2b_2$$

A simple numerical example sets $a_{\text{in}} = 1$, $b_{\text{in}} = 0$, and $k = 5$. Suitable initial conditions for the method of false transients are $a_0 = 0$ and $b_0 = 1$. Suppose the residence time for the composite system is $\bar{t}_1 + \bar{t}_2 = 1$. The question is how this total time should be divided. The following results were obtained:

$\bar{t}_1$	$\bar{t}_2$	$(a_{out})_1$	$(b_{out})_1$	$(a_{out})_2$	$(b_{out})_2$
1.0	0	0.2000	0.8000	0.2000	0.8000
0.9	0.1	0.2222	0.7778	0.1477	0.8523
0.8	0.2	0.2500	0.7500	0.1092	0.8908
0.7	0.3	0.2857	0.7143	0.0819	0.9181
0.6	0.4	0.3333	0.6667	0.0634	0.9366
0.5	0.5	0.4000	0.6000	0.0519	0.9481
0.4	0.6	0.5000	0.5000	0.0474	0.9526
0.3	0.7	0.6667	0.3333	0.0570	0.9430
0.2	0.8	1	0	1	0
0.1	0.9	1	0	1	0
0.0	1.0	1	0	1	0

There is an interior optimum. In this numerical example it occurs when 40% of the reactor volume is in the initial CSTR and 60% is in the downstream PFR. The model reaction is chemically unrealistic but illustrates behavior that can arise with real reactions. An excellent process for the bulk polymerization of styrene consists of a CSTR followed by a tubular postreactor.

The autocatalytic reaction in this example demonstrates a phenomenon known as ***washout***. Washout occurs in the example calculations for $\bar{t}_1 < 0.2$. If $\bar{t}_1$ is too small, a steady-state reaction cannot be sustained even with initial spiking of component B. A continuous fermentation process will have a minimum residence time below which the initial inoculum of cells will be washed out of the system. At lower flow rates, the cells reproduce fast enough to achieve and hold a steady state. Although not studied in this example, there is also a minimum inoculum size. If too few cells are charged to the CSTR at startup, washout will occur even though $\bar{t}_1$ is large enough to sustain cell growth.

4.5.2 Tanks in Series

For the great majority of reaction schemes, piston flow is optimal. Thus the reactor designer normally wants to build a tubular reactor and to operate it at high Reynolds numbers so that piston flow is closely approximated. This may not be possible. There are many situations where a tubular reactor is infeasible and where CSTRs are used instead. Typical examples are reactions involving suspended solids and autorefrigerated reactors where the reaction mass is held at its boiling point.

It is common to use several CSTRs in series. When there is only one CSTR, the entire reactor volume is at the lowest concentration, a_{out}, and the reaction rate will be low. Distributing the same total volume over several vessels means that some of the volume will be at higher concentrations and thus higher rates. Of course, the capital cost of the series arrangement will be higher. See Problems 4.19 and 4.20.

EXAMPLE 4.11

Determine the fraction unreacted for a second-order reaction, $2A \xrightarrow{k} B$, in a composite reactor consisting of two equal-volume CSTRs in series. The rate constant is the same for each reactor

and $k\bar{t}_1 a_{in} = 0.5$ where $\bar{t}_1 = V_1/Q$ is the mean residence time in a single vessel. Compare your result to the fraction unreacted in a single CSTR having the same volume as the series combination, $V = 2V_1$. Assume constant mass density.

SOLUTION: Begin by considering the first CSTR. The rate of formation of A is $\mathscr{R}_A = -2ka^2$. For constant ρ, $Q_{in} = Q_{out} = Q$ and the design equation for component A is

$$0 = a_{in} - 2k\bar{t}_1(a_{out}^2)_1 - (a_{out})_1$$

The solution is

$$\frac{(a_{out})_1}{a_{in}} = \frac{-1 + \sqrt{1 + 8k\bar{t}_1 a_{in}}}{4k\bar{t}_1 a_{in}} \tag{4.15}$$

Set $a_{in} = 1$ for convenience. When $k\bar{t}_1 a_{in} = 0.5$, Equation 4.15 gives

$$(a_{out})_1 = (a_{in})_2 = 0.618 a_{in}$$

The second CSTR has the same rate constant and residence time, but the dimensionless rate constant is now based on $(a_{in})_2 = 0.618 a_{in}$ rather than on a_{in}. Inserting $k\bar{t}_2(a_{in})_2 = k\bar{t}_2 a_{in}(a_{in})_2 = (0.5)(0.618) = 0.309$ into Equation 4.15 gives

$$a_{out} = (a_{out})_2 = (0.698)(a_{in})_2 = 0.432 a_{in}$$

Thus $a_{out}/a_{in} = 0.432$ for the series combination. A single CSTR with twice the volume has $k\bar{t}_1 a_{in} = 1$. Equation 4.15 gives $a_{out}/a_{in} = 0.5$ so that the composite reactor with two tanks in series gives the higher conversion.

Numerical calculations are the easiest way to determine the performance of CSTRs in series. Simply analyze them one at a time beginning at the inlet. However, there is a neat analytical solution for the special case of first-order reactions. The outlet concentration from the nth reactor in the series of CSTRs is

$$(a_{out})_n = \frac{(a_{in})_n}{1 + k_n \bar{t}_n} \tag{4.16}$$

where k_n is the rate constant and $\bar{t}_n$ is the mean residence time, $n = 1, 2, \ldots, N$. Applying Equation 4.13 repeatedly gives the outlet concentration for the entire train of reactors:

$$a_{out} = \frac{a_{in}}{(1 + k_1\bar{t}_1)(1 + k_2\bar{t}_2)\cdots(1 + k_N\bar{t}_N)} = a_{in}\prod_{n=1}^{N}(1 + k_n\bar{t}_n)^{-1} \tag{4.16a}$$

When all the k_n are equal (i.e. the reactors are at the same temperature) and all the t_n are equal (i.e., the reactors are the same size),

$$a_{out} = \frac{a_{in}}{(1 + k\bar{t}/N)^N} \tag{4.17}$$

where $\bar{t}$ is the mean residence time for the entire system. In the limit of many tanks in series,

$$\lim_{N\to\infty} \frac{a_{out}}{a_{in}} = e^{-k\bar{t}} \tag{4.18}$$

Thus the limit gives the same result as a PFR with mean residence time $\bar{t}$. Putting tanks in series is one way to combine the advantages of CSTRs with the better yield of a PFR. In practice, good improvements in yield are possible for fairly small N.

EXAMPLE 4.12

Suppose the concentration of a toxic substance must be reduced by a factor of 1000. Assuming the substance decomposes with first-order kinetics, compare the total volume requirements when several stirred tanks are placed in series to the volume needed in a PFR to achieve the same factor-of-1000 reduction.

SOLUTION: The comparisons will be made at the same k and same throughput (i.e., the same Q). Rearrange Equation 4.17 and take the Nth root to obtain

$$k\bar{t} = N\left(-1 + \sqrt[N]{\frac{a_{\text{in}}}{a_{\text{out}}}}\right) = N\left(-1 + \sqrt[N]{1000}\right)$$

where $k\bar{t}$ is proportional to the volume of the system. Some results are as follows:

Number of Tanks in Series, N	Value of $k\bar{t}$ to Achieve a 1000-Fold Reduction in Concentration	Volume of the Composite Reactor Relative to a PFR
1	999	144.6
2	61.2	8.8
3	27	3.9
4	18.5	2.7
⋮	⋮	⋮
∞	6.9	1

Thus a single CSTR requires 144.6 times the volume of a single PFR, and the inefficiency of using a CSTR to achieve high conversions is dramatically illustrated. The volume disadvantage drops fairly quickly when CSTRs are put in series, but the economic disadvantage remains great.

4.5.3 Recycle Loops

Most reaction systems have a separation step after the reactor. Products and unreacted raw materials are separated, and the unreacted raw materials are recycled to ultimate extinction. Figure 4.2 shows a different situation. It is a loop reactor where some of the reaction mass is returned to the inlet without separation. Internal recycle exists in every stirred tank reactor. An external recycle loop as shown in Figure 4.2 is less common but is used, particularly in large plants where a conventional stirred tank would have heat transfer limitations. The net throughput for the system is Q_{in}, but an

amount q is recycled back to the reactor inlet so that the flow through the reactor is $Q_{in} + q$. Performance of this loop reactor system depends on the ***recycle ratio*** q/Q_{in} and on the type of reactor that is in the loop. ***Fast external recycle*** has no effect on the performance of a CSTR but will affect the performance of other reactors. By fast recycle, we mean that no appreciable reaction occurs in the recycle line. The CSTR already has enough internal recycle to justify the assumption of perfect mixing so that fast external recycle does nothing more. If the reactor in the loop is a PFR, the external recycle has a dramatic effect. At high q/Q_{in}, the loop reactor will approach the performance of a CSTR.

Refer to Figure 4.2. A material balance about the mixing point gives

$$a_{mix} = \frac{Q_{in}a_{in} + qa_{out}}{Q_{in} + q} \tag{4.19}$$

The feed to the reactor inside the recycle loop is a_{mix}, and the exit concentration is a_{out}. The relationship between a_{mix} and a_{out} is determined in the usual manner for a single-pass reactor operating at a flow rate of $Q_{in} + q$. In the general case, this single-pass solution must be obtained numerically. Then the overall solution is iterative. One guesses a_{mix} and solves numerically for a_{out}. Equation 4.19 is then used to calculate a_{mix} for comparison with the original guess. Any good root finder will work. The function to be zeroed is

$$a_{mix} - \frac{Q_{in}a_{in} + qa_{out}}{Q_{in} + q} = 0$$

where a_{out} denotes the solution of the single-pass reactor design problem. When a_{out} is known analytically, an analytical solution to the recycle reactor problem is usually possible.

EXAMPLE 4.13

Determine the outlet concentration from a loop reactor as a function of Q_{in} and q when the reactor element is a PFR and the reaction is first order. Assume constant density and isothermal operation.

SOLUTION: The single-pass solution is

$$a_{out} = a_{mix} \exp\left(\frac{-kV}{Q_{in} + q}\right)$$

Note that $V/(Q_{in} + q)$ is the per-pass residence time and is far different from the mean residence time for the system, $\bar{t} = V/Q_{in}$. Equation 4.19 gives

$$a_{mix} = \frac{a_{in}Q_{in}}{Q_{in} + q - q\exp\left[-kV/(Q_{in} + q)\right]}$$

and the solution for a_{out} is

$$a_{out} = \frac{a_{in}Q_{in}}{(Q_{in} + q)\exp\left[kV/(Q_{in} + q)\right] - q} \tag{4.20}$$

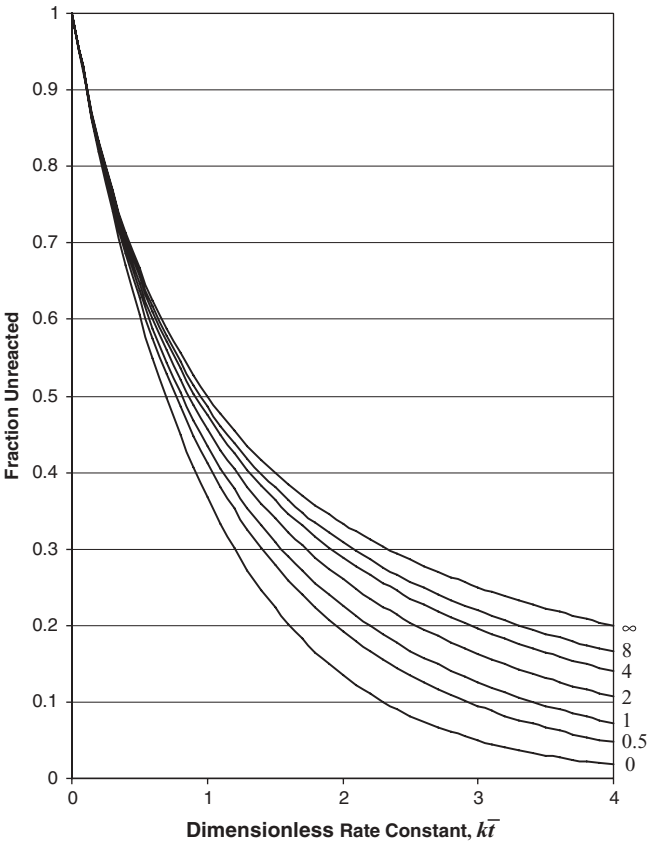

Figure 4.3 Effect of recycle rate on the performance of a loop reactor. The dimensionless rate constant is based on the system residence time $\bar{t} = V/Q_{\text{in}}$. The parameter is q/Q_{in}.

Figures 4.3 and 4.4 show how a loop reactor approaches the performance of a CSTR as the recycle rate is increased. Two things happen as $q \to \infty$: $a_{\text{out}} \to a_{\text{in}}Q_{\text{in}}/(Q_{\text{in}} + kV)$ and $a_{\text{mix}} \to a_{\text{out}}$. The specific results in Figures 4.3 and 4.4 apply to a first-order reaction with a PFR in the recycle loop, but the general concept applies to almost any type of reaction and reactor. High recycle rates mean that perfect mixing will be closely approached. There are two provisos: The mixing point must do a good job of mixing the recycle with the incoming feed and all the volume in the reactor must be accessible to the increased throughput. A rule of thumb is that $q/Q_{\text{in}} > 8$ will give performance equivalent to a conventionally agitated vessel. This may seem belied by the figures since there is still appreciable difference between the loop performance at $q/Q_{\text{in}} = 8$ and a CSTR. However, the difference will be smaller when a real reactor is put in a recycle loop since, unlike the idealization of piston flow, the real reactor will already have some internal mixing.

The loop reactor is sometimes used to model conventionally agitated stirred tanks. The ratio of internal circulation to net throughput in a large, internally agitated vessel

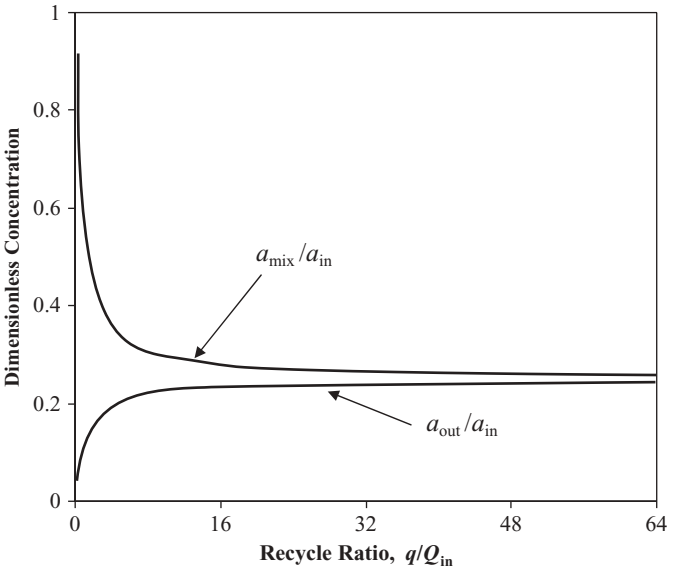

Figure 4.4 Extreme concentrations a_{mix} and a_{out} within a loop reactor. The case shown is for $k\bar{t} = 3$.

can be as low as 8. The mixing inside the vessel is far from perfect, but assuming that the vessel behaves as a CSTR may still be adequate for design purposes. Alternatively, the conventionally agitated vessel could be modeled as a PFR or composite reactor installed in a recycle loop in order to explore sensitivity of the system to the details of mixing.

4.5.4 Maximum Production Rate

With few exceptions, reaction rates decline as reactant concentrations decline. This provides an easy method for determining the maximum production rate possible with a flow reactor. Maximum production occurs when the entire reactor is filled with the entering composition. Suppose A → P. Then the ***maximum production rate*** of P is

$$\text{Maximum production} = \max(Qp_{out}) = V\mathscr{R}_A(a_{in}) \tag{4.21}$$

Maximum production is achieved by feeding the reactor at a high rate, $Q \to \infty$. This high productivity is obtained at the price of very low conversion, $a_{out} \to a_{in}$; a low outlet concentration of the product, $p_{out} \to 0$; and a large separation system. In contrast, maximum conversion, $a_{out} \to 0$, is achieved when $Q \to 0$, $p_{out} \to a_{in}$, and productivity is zero, $Qp_{out} \to 0$.

Equation 4.21 applies to almost any type of reactor and almost any type of single reaction. The exceptions with regard to type of reactor are generally pathological. There must be some portions of the reactor that are flow restricted so that these portions are unaffected by increases in Q and thus have some volume with concentrations

less than a_{in} even at very high flow rates. In such cases, the maximum productivity will be less than $V\mathscr{R}_A(a_{in})$. The exceptions with respect to type of reaction are autocatalytic reactions and some of the site competition models discussed in Chapters 10 and 12. These cases achieve maximum productivity at intermediate values for Q and p_{out}.

4.6 IMPERFECT MIXING

The usual assumption, made throughout most of this book and in essentially all books on chemical reactor design, is that single-phase stirred tank reactors are perfectly mixed. Section 1.1.1 justifies this assumption for slow reactions on the basis that the reaction half-life is much longer that the mixing time in the vessel. The assumption is obviously untrue for fast reactions, but it may not make a difference with respect to reactor performance. Consider a CSTR with two feed streams, one acidic and one basic. Acid–base titrations are fast so that $t_{1/2} \ll t_{mix}$. Indeed, acid–base titrations are commonly used to measure mixing times. However, if $\bar{t} \gg t_{mix}$, the neutralization reaction will go to completion and the reactor output will be chemically uniform at the neutralized concentration just as if feed to the reactor was premixed. A concurrent reaction with a half-life much longer than t_{mix} will proceed in the neutralized environment just as if the reactor were perfectly mixed.

There are "mixing-time sensitive" reactions where $t_{1/2} \ll t_{mix}$ will cause a difference in selectivity. A widely studied example is the Bourne reaction

$$\begin{aligned} A + B &\xrightarrow{k_1} R \\ R + B &\xrightarrow{k_2} S \end{aligned}$$

where $k_1 \gg k_2$. Suppose that A and B are fed separately at flow rates $Q/2$ with concentrations $a_{in} = b_{in}$. If A and B are mixed quickly, the reaction gives mainly R with little S. If mixing is slow, some A is transported to regions rich in B. Reaction at these locations would give R, but in a B-rich environment so that S would be formed. The result of slow mixing compared to fast mixing would be more S and more unreacted A. Modeling the case of slow mixing is difficult, and good design methods have not yet emerged. See Chapter 13 of Paul et al. (2003) for a recent review.

SUGGESTED FURTHER READINGS

Reactor models consisting of series and parallel combinations of ideal reactors are discussed at length in:

O. Levenspiel, *Chemical Reaction Engineering*, 3rd ed., Wiley, NewYork, 1998.

The reaction coordinate ε is also call the ***molar extent*** or ***degree of advancement***. It is applied to CSTRs in:

R. Aris, *Elementary Chemical Reactor Analysis*, Dover, Mineola, NY, 2000.

PROBLEMS

4.1 Observed kinetics for the reaction A + B $\longrightarrow$ 2C are $\mathscr{R} = 0.43ab^{0.8}$, mol m^{-3} h^{-1}. Suppose the reactor is run in a constant-density CSTR with $a_{in} = 15$ mol m^{-3}, $b_{in} = 20$ mol m^{-3}, $V = 3.5$ m^{-3}, and $Q = 125$ m^{-3} h^{-1}. Determine the exit concentration of C.

4.2 Find the analytical solution to the steady-state problem in Example 4.2.

4.3 Use Newton's method to solve the algebraic equations in Example 4.2. Note that the first two equations can be solved independently of the second two so that only a two-dimensional version of Newton's method is required.

4.4 Repeat the false-transient solution in Example 4.2 using a variety of initial conditions. Specifically include the case where the initial concentrations are all zero and the cases where the reactor is initially full of pure A, pure B, and so on. What do you conclude from these results?

4.5 Suppose the following reaction network is occurring in a constant-density CSTR:

$$\begin{aligned} \mathrm{A} &\rightleftarrows \mathrm{B} & \mathscr{R}_{\mathrm{I}} &= k_{\mathrm{I}} a^{1/2} - k'_{\mathrm{I}} b \\ \mathrm{B} &\longrightarrow \mathrm{C} & \mathscr{R}_{\mathrm{II}} &= k_{\mathrm{II}} b^2 \\ \mathrm{B} + \mathrm{D} &\longrightarrow \mathrm{E} & \mathscr{R}_{\mathrm{III}} &= k_{\mathrm{III}} bd \end{aligned}$$

The rate constants are $k_{\mathrm{I}} = 3.0 \times 10^{-2}$ mol$^{1/2}$ m$^{-3/2}$ h^{-1}, $k'_{\mathrm{I}} = 0.4$ h^{-1}, $k_{\mathrm{II}} = 5.0 \times 10^{-4}$ mol^{-1} m^3 h^{-1}, and $k_{\mathrm{III}} = 3.0 \times 10^{-4}$ mol^{-1} m^3 h^{-1}. The feed is pure A with $a_{in} = 100$ mol m^{-3}.

(a) Formulate a solution via the method of false transients. Use dimensionless time $\tau = t/\bar{t}$ and dimensionless rate constants, for example, $K_{\mathrm{III}} = k_{\mathrm{III}} a_{in} \bar{t}$.

(b) Solve the set of ODEs for sufficiently long times to closely approximate steady state. Use $a_0 = 3$ mol m^{-3}, $d_0 = 3$ mol m^{-3}, $b_0 = c_0 = e_0 = 0$, and $\bar{t} = 1$ h. Do vary $\Delta\tau$ to confirm that your solution has converged.

4.6 A more complicated version of Problem 4.5 treats all the reactions as being reversible:

$$\begin{aligned} A &\rightleftarrows B & \mathscr{R}_{\mathrm{I}} &= k_{\mathrm{I}} a^{1/2} - k'_{\mathrm{I}} b \\ B &\rightleftarrows C & \mathscr{R}_{\mathrm{II}} &= k_{\mathrm{II}} b^2 - k'_{\mathrm{II}} c \\ B + D &\rightleftarrows E & \mathscr{R}_{\mathrm{III}} &= k_{\mathrm{III}} bd - k'_{\mathrm{III}} e \end{aligned}$$

Suppose $k'_{\mathrm{II}} = 0.08$ h^{-1} and $k'_{\mathrm{III}} = 0.05$ h^{-1}.

(a) Work Problem 4.5(b) for this revised reaction network.

(b) Suppose the reactor is filled but the feed and discharge pumps are never turned on. The reaction proceeds in batch and eventually reaches an equilibrium composition. Simulate the batch reaction going to completion to determine the equilibrium concentrations.

4.7 Equation 4.8 appears to be the solution to a quadratic equation. Why was the negative root chosen?

4.8 Are the kinetic constants determined in Example 4.5 accurate? Address this question by doing the following:

(a) Repeat Example 4.5 choosing component A (sulfur dioxide) as the key component rather than component C (sulfur trioxide).

(b) Use these new values for k and k_C to solve the forward problem in Example 4.6.

(c) Suppose a revised compositional analysis for run I gave $(y_C)_{out} = 0.062$ rather than the original value of 0.063. The inerts change to 0.826. Repeat the example calculation of k and k_C using these new values.

(d) Suppose a repeat of run 2 gave the following analysis at the outlet:

SO_2	2.2%
O_2	8.7%
SO_3	7.9%
Inerts	81.2%

Find k and k_C.

4.9 The ODE for the inerts was used to calculate Q_{out} in Example 4.6. How would you work the problem if there were no inerts? Use your method to predict reactor performance for the case where the feed contains 67% SO_2 and 33% O_2 by volume.

4.10 A 100-gal pilot plant reactor is agitated with a six-blade pitched turbine 6 in. in diameter that consumes 0.35 kw at 300 RPM. Experiments with acid–base titrations showed that the mixing time in the vessel is 2 min. Scaleup to a 1000-gal vessel with the same mixing time is desired.

(a) Estimate the impeller size, motor size, and RPM for the larger reactor.

(b) What would be the mixing time if the scaleup were done at constant power per unit volume rather than constant mixing time?

4.11 Solve Example 4.10 algebraically and confirm the numerical example. For $b_{in} = 0$ you should find that the system has two steady states: one with $a_{out} = a_{in}$ that is always possible and one with

$$\frac{a_{out}}{a_{in}} = \frac{1}{1 + (kt_1 a_{in} - 1)\exp(kt_2 a_{in})}$$

that is possible only when $kt_1 > 1$. You should also conclude that the interior optimum occurs when $t_1 = 2/ka_{in}$.

4.12 Remove the PFR from Example 4.10. What is the maximum production rate and what are the concentrations in the reactor at this rate?

4.13 Example 4.10 used the initial conditions that $a_0 = 0$ and $b_0 = 1$. Will smaller values for b_0 work? How much smaller?

4.14 Consider two CSTRs in series with a combined volume of V. How should this volume be divided between the two reactors in order to achieve maximum conversion for a first-order reaction?

4.15 Suppose you have two identical CSTRs and you want to make as much product as possible. The reaction is pseudo–first order and the product recovery system requires a minimum conversion of 93.75%. Do you install the reactors in series or parallel? Would it affect your decision if the minimum conversion could be lowered?

4.16 Suppose you have two identical PFRs and you want to make as much product as possible. The reaction is pseudo–first order and the product recovery system requires a minimum conversion of 93.75%. Assume constant density. Do you install the reactors in series or parallel? Would it affect your decision if the minimum conversion could be lowered?

4.17 Example 4.12 used N stirred tanks in series to achieve a 1000-fold reduction in the concentration of a reactant that decomposes by first-order kinetics. Show how much worse would the CSTRs be if the 1000-fold reduction had to be achieved by dimerization, that is, by a second order of the single reactant type. The reaction is irreversible and density is constant.

4.18 Suppose you have two CSTRs, one with a volume of 2 m^2 and one with a volume of 4 m^3. You have decided to install them in series and to operate them at the same temperature. Which goes first if you want to maximize production subject to a minimum conversion constraint? Consider the following cases:

(a) The reaction is first order.

(b) The reaction is second order of the form $2A \rightarrow P$.

(c) The reaction is half order.

4.19 Equipment costs are sometimes estimated using a scaling rule

$$\frac{\text{Cost of large unit}}{\text{Cost of small unit}} = S^C$$

where C is the scaling exponent. If $C = 1$, twice the size (volume or throughput) means twice the cost and there is no economy of scale. The installed cost of chemical process equipment typically scales as $C = 0.6$ to $C = 0.75$. Suppose the installed cost of stirred tank reactors varies as $V^{0.75}$. Determine the optimum number of tanks in series for a first-order reaction going to 99.9% completion.

4.20 Repeat Problem 4.19 for $C = 0.6$. Note that more reactors will affect more than just the capital costs. Additional equipment will lower system reliability and increase operating costs. Which value of C is the more conservative? Is this value of C also the more conservative when estimating the installed cost of an entire plant based on the cost of a smaller plant?

4.21 Example 4.13 treated the case of a PFR inside a recycle loop. Replace the PFR with two equal-volume stirred tanks in series. The reaction remains first order, irreversible, and constant density.

(a) Derive algebraic equations for a_{mix} and a_{out} for the composite system.

(b) Reproduce Figures 4.3 and 4.4 for this case.

4.22 Work Example 4.13 for the case where the reaction is second order of the single-reactant type. It is irreversible and density is constant. The reactor element inside the loop is a PFR.

4.23 Find the limit of Equations 4.19 and 4.20 as $q \rightarrow \infty$ with Q_{in} fixed. Why would you expect these results?

4.24 The material balance around the mixing point of a loop reactor is given by Equation 4.19 for the case of constant fluid density. How would you work a recycle problem with variable density? Specifically, write the variable-density counterpart of Equation 4.19 and explain how you would use it.

4.25 Refer to the model reactions in Section 4.6. Determine the yields of R and S, expressed as r_{out}/b_{in} and s_{out}/b_{in} for a CSTR and a PFR. Discuss your results in reference to those in Table 13.1 of Paul et al. (2003).

4.26 The evil professor of Problem 1.13 felt he was having some success in making TNT, but the cost of chemicals was beginning to challenge his budget. He thought that a two-stage CSTR process could save money by recycling some of the spent acids back to the first stage of the process. The feed to the first stage has a molar ratio of 1 toluene to 4 nitric acid and also 1:4 with respect to sulfuric acid. The first CSTR converts essentially all the

toluene to dinitrotoluene. The reactor effluent is decanted and the organic phase is sent to the second CSTR together with fresh nitric acid and fuming sulfuric acid, now with a 2:1 molar ratio of dinitrotoluene to each of the two acids. Suppose the intermediate separation step is completely efficient and the second CSTR gives complete conversion to trinitrotoluene. Develop a material balance for this reaction system.

Devise a recycle scheme that minimizes the combined amounts of nitric and sulfuric acids that must be discarded subject to the constraint that the combined acid concentration in the aqueous phase in the first CSTR must be at least 25 wt %. The nitric acid comes as a 68 wt % solution. The sulfuric acid comes as a 98 wt. % solution, and the fuming sulfuric acid is the equivalent of 114%.

APPENDIX 4.1 SOLUTION OF NONLINEAR ALGEBRAIC EQUATIONS

Consider a set of N algebraic equations of the form

$$\begin{aligned} F(a, b, \ldots) &= 0 \\ G(a, b, \ldots) &= 0 \\ &\vdots \end{aligned} \tag{4.22}$$

where $a, b, \ldots$ represent the N unknowns. We suppose none of these equations is easily solvable for any of the unknowns. If an original equation were solvable for an unknown, that unknown could be eliminated and the dimensionality of the set reduced by 1. Such eliminations are usually worth the algebra when they are possible.

Binary Searches

A binary search is a robust and easily implemented method for finding a root T of a single equation $F(T) = 0$. It is necessary to know bounds $T_{\min} \leq T \leq T_{\max}$ within which the root exists. If $F(T_{\min})$ and $F(T_{\max})$ differ in sign, there will be an odd number of roots within the bounds and a binary search will find one of them to a specified level of accuracy. It does so by calculating F at the midpoint of the interval, that is, at $T = (T_{\min} + T_{\max})/2$. The sign of F will be the same as at one of the endpoints. Discard that endpoint and replace it with the midpoint. The sign of F at the two new endpoints will differ, so that the range in which the solution must lie has been halved. This procedure can obviously be repeated i times to reduce the range in which a solution must lie to 2^{-i} of the original range. The accuracy is set in advance by choosing i:

$$i = \ln \frac{[(T_{\max} - T_{\min})/\varepsilon]}{\ln 2}$$

where ε is the allowable uncertainty in the answer.

EXAMPLE 4.14

Use the binary-search technique to find a zero of a function.

SOLUTION: Code for Example 4.14 works for any arbitrary function, Func (T), of the single variable T provided a range on T can be specified in which there is a single zero. The Func (T) used as an example in the code finds a root of an energy balance used in Example 5.7:

$$F(T) = T_{\text{in}} - T + \frac{\Delta T_{\text{adiabatic}} k\bar{t}}{1 + k\bar{t}} = 0 \qquad \text{where } k = k_0 \exp(-T_{act}/T)$$

Code for Example 4.14

```
Sub Example4_14 ()

Tmax = 450 'User supplied value
Tmin = 350 'User supplied value
er = 0.0000005 'User supplied value

x = Log((Tmax - Tmin) / er) / Log(2)
i = x + 0.5 'Rounds up

'Test that there is a root within the range
If Func(Tmax)*Func(Tmin)>= 0 Then Stop 'No root or even number of roots

For j = 1 To i
        Tmid = (Tmax + Tmin) / 2
        If Func(Tmid) * Func(Tmin) > 0 Then
           Tmin = Tmid
        Else
           Tmax = Tmid
        End If
Next j
T = Tmid

End Sub

Function Func(T)
      ktbar = 20000000000{\#} * Exp(-10000 / T)
      Func = 300 - T + 400 * ktbar / (1 + ktbar)
End Function
```

For the input range $350 < T < 450$, the code locates a root at $T = 403.7$. This function has two other roots.

Multidimensional Newton Method

We return to the general problem of solving Equation 4.22. Consider some point $(a_0, b_0, \ldots)$ within the region of definition of the functions $F, G, \ldots$ and suppose the

functions can be represented by an multidimensional Taylor series about this point. Truncating the series after the first-order derivatives gives

$$F(a, b, \ldots) = F(a_0, b_0, \ldots) + \left[\frac{\partial F}{\partial a}\right]_0 (a - a_0) + \left[\frac{\partial F}{\partial b}\right]_0 (b - b_0) + \cdots$$
$$G(a, b, \ldots) = G(a_0, b_0, \ldots) + \left[\frac{\partial G}{\partial a}\right]_0 (a - a_0) + \left[\frac{\partial G}{\partial b}\right]_0 (b - b_0) + \cdots$$
$$\vdots$$

where there are as many equations as there are unknowns. In matrix form,

$$\begin{bmatrix} \left[\frac{\partial F}{\partial a}\right]_0 & \left[\frac{\partial F}{\partial b}\right]_0 & \cdots \\ \left[\frac{\partial G}{\partial a}\right]_0 & \left[\frac{\partial G}{\partial b}\right]_0 & \cdots \\ \vdots & \vdots & \end{bmatrix} \begin{bmatrix} a - a_0 \\ b - b_0 \\ \vdots \end{bmatrix} = \begin{bmatrix} F - F_0 \\ G - G_0 \\ \vdots \end{bmatrix}$$

We seek values for $a, b, \ldots$ which give $F = G = \cdots = 0$. Setting $F = G = \cdots = 0$ and solving for $a, b, \ldots$ give

$$\begin{bmatrix} a \\ b \\ \vdots \end{bmatrix} = \begin{bmatrix} a_0 \\ b_0 \\ \vdots \end{bmatrix} - \begin{bmatrix} \left[\frac{\partial F}{\partial a}\right]_0 & \left[\frac{\partial F}{\partial b}\right]_0 & \cdots \\ \left[\frac{\partial G}{\partial a}\right]_0 & \left[\frac{\partial G}{\partial b}\right]_0 & \cdots \\ \vdots & \vdots & \end{bmatrix}^{-1} \begin{bmatrix} F_0 \\ G_0 \\ \vdots \end{bmatrix}$$

For the special case of one unknown,

$$a = a_0 - \frac{F_0}{[dF/da]_0}$$

which is Newton's method for finding the roots of a single equation. For two unknowns,

$$a = a_0 - \frac{F_0 [\partial G/\partial a]_0 - G_0 [\partial F/\partial a]_0}{[\partial F/\partial a]_0 [\partial G/\partial b]_0 - [\partial F/\partial b]_0 [\partial G/\partial a]_0}$$
$$b = b_0 - \frac{-F_0 [\partial G/\partial b]_0 + G_0 [\partial F/\partial b]_0}{[\partial F/\partial a]_0 [\partial G/\partial b]_0 - [\partial F/\partial b]_0 [\partial G/\partial a]_0}$$

which is a two-dimensional generalization of Newton's method.

The above technique can be used to solve large sets of algebraic equations; but, like the ordinary one-dimensional form of Newton's method, the algorithm may diverge unless the initial guess $(a_0, b_0, \ldots)$ is quite close to the final solution. Thus it might be considered as a method for rapidly improving a good initial guess, with other techniques being necessary to obtain the initial guess.

For the one-dimensional case, *dF/da* can usually be estimated using values of F determined at previous guesses. Thus

$$a = a_0 - \frac{F_0}{[(F_0 - F_{-1})/(a_0 - a_{-1})]}$$

where $F_0 = F(a_0)$ is the value of F obtained one iteration ago when the guess was a_0 and $F_{-1} = F(a_{-1})$ is the value obtained two iterations ago when the guess was a_{-1}.

For two- and higher dimensional solutions, it is probably best to estimate the first partial derivatives by a formula such as

$$\left[\frac{\partial F}{\partial a}\right]_0 \approx \frac{F(a_0, b_0, \ldots) - F(\gamma a_0, b_0, \ldots)}{a_0 - \gamma a_0}$$

where γ is a constant close to 1.0.

Chapter 5

Thermal Effects and Energy Balances

This chapter treats the effects of temperature on the three ideal reactors: batch, piston flow, and continuous flow stirred tank. Three major questions in reactor design are addressed. What is the optimal temperature for a reaction? How can this temperature be achieved or at least approximated in practice? How can results from the laboratory or pilot plant be scaled up?

5.1 TEMPERATURE DEPENDENCE OF REACTION RATES

Most reaction rates are sensitive to temperature, and most laboratory studies regard temperature as an important means of improving reaction yield or selectivity. Our treatment has so far ignored this point. The reactors have been isothermal, and the operating temperature, as reflected by the rate constant, has been arbitrarily assigned. In reality, temperature effects should be considered even for isothermal reactors since the operating temperature must be specified as part of the design. For nonisothermal reactors, where the temperature varies from point to point within the reactor, the temperature dependence directly enters the design calculations.

5.1.1 Arrhenius Temperature Dependence

The rate constant for elementary reactions is almost always expressed as

$$k = k_0 T^m \exp\left(\frac{-\Delta E}{R_g T}\right) = k_0 T^m \exp\left(\frac{-T_{\text{act}}}{T}\right) \tag{5.1}$$

where $m = 0, \frac{1}{2}, 1$ depending on the specific theoretical model being used. The quantity ΔE is the ***activation energy*** although the specific theories interpret this energy term in different ways. The quantity $T_{\text{act}} = \Delta E / R_g$ has units of temperature

Chemical Reactor Design, Optimization, and Scaleup, Second Edition. By E. B. Nauman
Copyright © 2008 John Wiley & Sons, Inc.

(invariably kelvin) and is called the ***activation temperature***. The activation temperature has no physical interpretation as a temperature. It is just a convenient way of expressing the composite quantity $\Delta E/R_g$.

The case of $m = 0$ corresponds to classical Arrhenius theory, $m = 1/2$ is derived from the collision theory of bimolecular gas phase reactions, and $m = 1$ corresponds to activated complex or transition state theory. None of these theories is sufficiently well developed to predict reaction rates from first principles, and it is practically impossible to choose between them based on experimental measurements. The relatively small variation in rate constant due to the preexponential temperature dependence T^m is overwhelmed by the exponential dependence $\exp(-T_{\text{act}}/T)$. For many reactions, a plot of $\ln(k)$ versus T^{-1} will be approximately linear, and the slope of this line can be used to calculate E. Plots of $\ln(k/T^m)$ versus T^{-1} for the same reactions will also be approximately linear as well, which shows the futility of determining m by this approach.

EXAMPLE 5.1

The bimolecular reaction

$$NO + ClNO_2 \rightarrow NO_2 + ClNO$$

is thought to be elementary. The following rate data are available (Treiling et al., 1952):

T, K	300	311	323	334	344
k, m^3 mol^{-1} s^{-1}	0.79	1.25	1.64	2.56	3.40

Fit Equation 5.1 to these data for $m = 0, 0.5, 1$.

SOLUTION: The classic way of fitting these data is to plot $\ln(k/T^m)$ versus T^{-1} and to extract k_0 and T_{act} from the slope and intercept of the resulting (nearly) straight line. Special graph paper with a logarithmic y axis and a $1/T$ x axis was made for this purpose. The currently preferred method is to use nonlinear regression to fit the data. The object is to find values for k_0 and T_{act} that minimize the sum of squares:

$$SS^2 = \sum_{\text{Data}} [\text{experiment-model}]^2 = \sum_{j=1}^{J} \left[k_j - k_0 T_j^m \exp\left(\frac{-T_{\text{act}}}{T_j} \right) \right]^2 \tag{5.2}$$

where $J = 5$ for the data at hand. Here, k_j is the experimentally determined rate constant that was measured at temperature T_j. The goal is to find values for k_0 and T_{act} that minimize SS^2. Automatic methods for performing minimizations are described in Chapter 6 and the general topic of nonlinear regression is discussed in Chapter 7. However, with only two unknowns, even a manual search will produce the answers in reasonable time. The results of this fitting procedure are as follows:

T	k Experimental	k As Fitted			
		$m = 0$	$m = 0.5$	$m = 1$	Exponential Fit
300	0.79	0.771	0.772	0.774	0.819
311	1.25	1.165	1.165	1.166	1.174
323	1.64	1.770	1.769	1.768	1.739
334	2.56	2.529	2.528	2.527	2.493
344	3.44	3.429	3.430	3.430	3.458
	Root mean error (see Section 7.1)	0.0714	0.0711	0.0708	0.0652
	k_0, $m^3\,mol^{-1}s^{-1}\,K^{-m}$	89,676	3,335	100.8	4.434×10^{-5}
	T_{act}, K	3,499	3,007	3,172	$\alpha = 0.03274$, K^{-1}

The predictions for the various forms of the Arrhenius model are essentially identical. The minimization procedure automatically adjusts the values for k_0 and T_{act} to account for the different values of m. The predictions are good but imperfect. The lack of complete accuracy is due to experimental errors and perhaps due to inadequacies of the Arrhenius models. For the data of this example, an exponential model $k = k_0 \exp(\alpha T)$ happens to give a marginally better fit than any of the Arrhenius models, but the latter have a century of theoretical underpinnings and widespread acceptance that justifies their use. There is clearly nothing to choose between the various Arrhenius models. For simplicity and to conform to general practice, we will use the Arrhenius form with $m = 0$. However, a great many reactions, even reactions thought to be elementary, show non-Arrhenius behavior. The engineer then must use a form that fits the data.

Figure 5.1 shows an Arrhenius plot for the reaction $O + N_2 \rightarrow NO + N$ which is linear over an experimental temperature range of 1500 K. Note that the rate constant is expressed per molecule rather than per mole. This method for expressing k is favored by some chemical kineticists. It differs by a factor of Avogadro's number from the more usual k.

Few reactions have been studied over the enormous range indicated in Figure 5.1. Even so, they will often show curvature in an Arrhenius plot of $\ln(k)$ versus T^{-1}. The usual reason for curvature is that the reaction is complex with several elementary steps and with different values of E for each step. The overall temperature behavior may be quite different from the simple Arrhenius behavior expected for an elementary reaction. However, a linear Arrhenius plot is neither necessary nor sufficient to prove that a reaction is elementary. It is not sufficient because complex reactions may have one dominant activation energy or several steps with similar activation energies that lead to an overall temperature dependence of the Arrhenius sort. Arrhenius behavior is not necessary since some low-pressure, gas phase, bimolecular reactions exhibit distinctly non-Arrhenius behavior even though the reactions are believed to

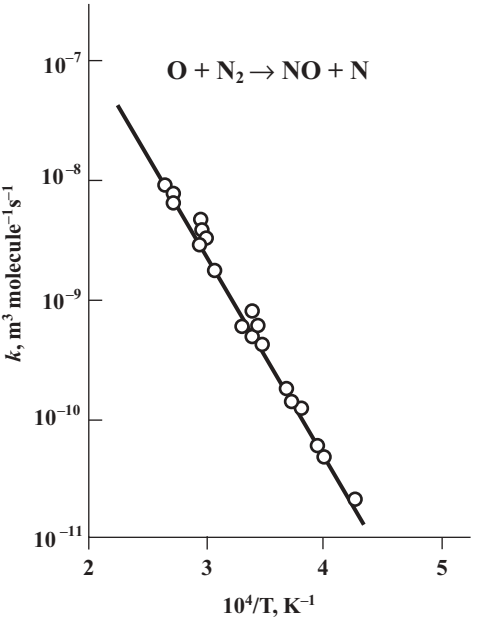

Figure 5.1 Arrhenius behavior over a large temperature range. (Adapted from J. P. Monat, R. K. Hanson, and C. H. Kruger, *Seventeenth Symposium (International) on Combustion*, The Combustion Institute, Pittsburgh, PA 1979, p. 543.)

be elementary. Any experimental study should consider the possibility that k_0 and T_{act} are functions of temperature. A strong dependence on temperature usually signals a change in reaction mechanism, for example, a shift from a kinetic limitation to a mass transfer limitation.

You may recall the rule of thumb that reaction rates double for each 10°C increase in temperature. Doubling when going from 20 to 30°C means $E = 51.2$ kJ mol^{-1} or $T_{act} = 6160$ K. Doubling when going from 100 to 110°C means $E = 82.4$ kJ mol^{-1} or $T_{act} = 9910$ K. Activation temperatures in the range from 5000 to 15,000 K are typical of homogeneous reactions, but activation temperatures above 40,000 K are known. The higher the activation energy, the more the reaction rate is sensitive to temperature. Biological systems typically have high activation energies. An activation temperature below about 2000 K usually indicates that the reaction is limited by a mass transfer step (diffusion) rather than chemical reaction. Such limitations are common in heterogeneous systems.

5.1.2 Optimal Temperatures for Isothermal Reactors

Reaction rates usually increase with temperature. Thus the best temperature for a single, ***irreversible*** reaction, whether elementary or complex, is the highest possible temperature. Practical reactor designs must consider materials of construction

limitations and economic trade-offs between heating costs and yield, but there is no optimal temperature from a strictly kinetic viewpoint. Of course, at sufficiently high temperatures, a competitive reaction or reversibility will emerge.

Multiple reactions, and reversible reactions since these are a special form of a multiple reaction, usually exhibit an optimal temperature with respect to the yield of a desired product. The reaction energetics are not trivial even if the reactor is approximately isothermal. One must specify the isotherm at which to operate. Consider the elementary, reversible reaction

$$\mathrm{A} \underset{k_r}{\overset{k_f}{\rightleftharpoons}} \mathrm{B} \tag{5.3}$$

Suppose this reaction is occurring in a CSTR of fixed volume and throughput. It is desired to find the reaction temperature that maximizes the yield of product B. Suppose $\Delta E_f > \Delta E_r$. Then the forward reaction is favored by increasing temperature. The equilibrium shifts in the desirable direction, and the reaction rate increases. The best temperature is the highest possible temperature and there is no interior optimum. For $\Delta E_f < \Delta E_r$, increasing the temperature shifts the equilibrium in the wrong direction, but the forward reaction rate still increases with increasing temperature. There is an optimum temperature for this case. A high reaction temperature hurts selectivity but improves conversion. A low reaction temperature helps selectivity but hurts conversion.

The outlet concentration from the stirred tank, assuming constant physical properties and $b_{\text{in}} = 0$, is given by

$$b_{\text{out}} = \frac{k_f a_{\text{in}} \bar{t}}{1 + k_f \bar{t} + k_r \bar{t}} \tag{5.4}$$

We assume the forward and reverse reactions have Arrhenius temperature dependences with $\Delta E_f < \Delta E_r$. Setting $db_{\text{out}}/dT = 0$ gives

$$T_{\text{optimal}} = \frac{\Delta E_r}{R_g \ln[(\Delta E_r - \Delta E_f)(k_0)_r \bar{t} \big/ \Delta E_f]} \tag{5.5}$$

as the kinetically determined optimum temperature.

The reader who duplicates the algebra needed for this analytical solution will soon appreciate that a CSTR is the most complicated reactor and Equation 5.3 is the most complicated reaction for which an analytical solution for T_{optimal} is likely. The same reaction occurring in a PFR with $b_{\text{in}} = 0$ leads to

$$b_{\text{out}} = \frac{a_{\text{in}} k_f \{1 - \exp[-(k_f + k_r)\bar{t}]\}}{k_f + k_r} \tag{5.6}$$

Differentiation and setting $db_{\text{out}}/dT = 0$ gives a transcendental equation in T_{optimal} that cannot be solved in closed form. The optimal temperature must be found numerically.

EXAMPLE 5.2

Suppose the rate constants in Equation 5.3 are $k_f = 10^8 \exp(-5000/T)$ and $k_r = 10^{15} \exp(-10000/T)$ in reciprocal hours. Find the temperature that maximizes the concentration of B for reaction in a CSTR with $\bar{t} = 2$ h and in a PFR with $\bar{t} = 2$ h. Assume constant density and a feed of pure A. Also calculate the equilibrium concentration at both values for T_{optimal}.

SOLUTION: Equation 5.5 can be applied directly to the CSTR case. The result is $T_{\text{optimal}} = 283.8$ K for which $b_{\text{out}}/a_{\text{in}} = 0.691$. The equilibrium concentration is found from

$$K = \frac{k_f}{k_r} = \frac{b_{\text{equil}}}{a_{\text{equil}}} = \frac{b_{\text{equil}}}{a_{\text{in}} - b_{\text{equil}}} \tag{5.7}$$

which gives $b_{\text{equil}}/a_{\text{in}} = 0.817$ at 283.8 K.

The PFR reactor gives a better result at the same temperature. Equation 5.6 gives $b_{\text{out}}/a_{\text{in}} = 0.814$ for the PFR at 283.8 K. However, this is not the optimum, as a better temperature exists. With only one optimization variable, a trial-and-error search is probably the fastest way to determine that $T_{\text{optimal}} = 277.5$ K and $b_{\text{out}}/a_{\text{in}} = 0.842$ for the PFR. The equilibrium concentration at 277.5 K is $b_{\text{equil}}/a_{\text{in}} = 0.870$.

The CSTR operates at a higher temperature in order to compensate for its inherently lower conversion. The higher temperature shifts the equilibrium concentration in an unfavorable direction, but the higher temperature is still worthwhile for the CSTR because equilibrium is not closely approached.

The results of Example 5.2 apply to a ***reversible*** reaction with a fixed reaction time, $\bar{t}$ or t_{batch}. Equation 5.5 shows that the optimal temperature in a CSTR decreases as the mean residence time increases. This is also true for a PFR or a batch reactor. There is no interior optimum with respect to reaction time for a single reversible reaction. When $\Delta E_f < \Delta E_r$, the best yield is obtained in a large reactor operating at low temperature. Obviously, the kinetic model ceases to apply when the reactants freeze. More realistically, capital and operating costs impose constraints on the design.

The above examples maximized the concentration of component B, but this does not maximize the production rate of B in a flow system. See Section 4.5.4. The production rate of B is $b_{\text{out}} Q_{\text{out}}$. Total production can normally be increased by increasing the flow rate and thus decreasing the reaction time. The reactor operates nearer to the feed composition so that the average reaction rate is higher. More product is made, but it is dilute. This imposes a larger burden on the downstream separation and recovery facilities. The design is dictated by capital and operating costs. Reactor optimization cannot be done without considering the process as a whole. The one-variable-at-a-time optimizations considered in this chapter are done as preludes to the more comprehensive optimizations in Chapter 6.

EXAMPLE 5.3

Suppose

$$\mathrm{A} \xrightarrow{k_\mathrm{I}} \mathrm{B} \xrightarrow{k_\mathrm{II}} \mathrm{C} \tag{5.8}$$

with $k_\mathrm{I} = 10^8 \exp(-5000/T)$ and $k_\mathrm{II} = 10^{15} \exp(-10000/T)$ in reciprocal hours. Find the temperature that maximizes b_out for a CSTR with $\bar{t} = 2$ and for a PFR with the same 2-h residence time. Assume constant density with $b_\mathrm{in} = c_\mathrm{in} = 0$.

SOLUTION: Use Equation 4.3 with $b_\mathrm{in} = 0$ for the CSTR to obtain

$$b_\mathrm{out} = \frac{k_\mathrm{I} a_\mathrm{in} \bar{t}}{(1 + k_\mathrm{I}\bar{t})(1 + k_\mathrm{II}\bar{t})} \tag{5.9}$$

A one-dimensional search gives $T_\mathrm{optimal} = 271.4$ K and $b_\mathrm{out} = 0.556 a_\mathrm{in}$.

Convert Equation 2.22 to the PFR form and set $b_\mathrm{in} = 0$ to obtain

$$b_\mathrm{out} = \frac{k_\mathrm{I} a_\mathrm{in}[\exp(-k_\mathrm{I}\bar{t}) - \exp(-k_\mathrm{II}\bar{t})]}{k_\mathrm{II} - k_\mathrm{I}} \tag{5.10}$$

Numerical optimization gives $T_\mathrm{optimal} = 271.7$ and $b = 0.760 a_\mathrm{in}$.

At a fixed temperature, a single reversible reaction $\mathrm{A} \rightleftharpoons \mathrm{B}$ has no interior optimum with respect to reaction time. (We ignore the trivial case where $b_\mathrm{in} > b_\mathrm{equil}$.) A very large flow reactor or a very long batch reaction is best since it will give a close approach to equilibrium. In contrast, there will always be an interior optimum with respect to reaction time at a fixed temperature when an intermediate product in a set of ***consecutive*** reactions is desired. (We ignore the trivial exception where $b_\mathrm{in} > a_\mathrm{in}$.) A very small reactor forms no B and a very large reactor destroys whatever B is formed. Thus there will be an interior optimum with respect to reaction time.

Example 5.3 asked the question: If reaction time is fixed, what is the best temperature? Example 5.4 asks a related but different question: If the temperature is fixed, what is the best reaction time? Both examples address maximization of product concentration, not total production rate.

EXAMPLE 5.4

Determine the optimum reaction time for the consecutive reactions of Example 5.3 for the case where the operating temperature is specified. Consider both a CSTR and a PFR.

SOLUTION: Analytical solutions are possible for this problem. For the CSTR, differentiate Equation 5.9 with respect to $\bar{t}$ and set the result to zero. Solving for $\bar{t}$ gives

$$\bar{t}_\mathrm{optimal} = \sqrt{\frac{1}{k_\mathrm{I} k_\mathrm{II}}} \tag{5.11}$$

Suppose $T = 271.4$ as for the CSTR case in Example 5.3. Using Equation 5.11 and the same rate constants as in Example 5.3 gives $\bar{t}_{\text{optimal}} = 3.17$ h. The corresponding value for b_{out} is $0.578a_{\text{in}}$. Recall that Example 5.3 used $\bar{t} = 2$ h and gave $b_{\text{out}}/a_{\text{in}} = 0.556$. Thus the temperature that is best for a fixed volume and the volume that is best for a fixed temperature do not correspond.

For a PFR, use Equation 5.10 and set $db_{\text{out}}/d\bar{t} = 0$ to obtain

$$\bar{t}_{\text{optimal}} = \frac{\ln(k_{\text{I}}/k_{\text{II}})}{k_{\text{I}} - k_{\text{II}}} \tag{5.12}$$

Suppose $T = 271.7$ as for the PFR (or batch) case in Example 5.3. Using Equation 5.12 and the same rate constants as in Example 5.3 gives $\bar{t}_{\text{optimal}} = 2.50$ h. The corresponding value for b_{out} is $0.772a_{\text{in}}$. Recall that Example 5.3 used $\bar{t} = 2$ h and gave $b_{\text{out}}/a_{\text{in}} = 0.760$. Again, the temperature that is best for a fixed volume does not correspond to the volume that is best for a fixed temperature.

The ***competitive*** reactions

$$\text{A} \xrightarrow{k_{\text{I}}} \text{B} \qquad \text{A} \xrightarrow{k_{\text{II}}} \text{C}$$

will have an interior optimum for B only if $\Delta E_{\text{I}} < \Delta E_{\text{II}}$ and will have an intermediate optimum for C only if $\Delta E_{\text{I}} > \Delta E_{\text{II}}$. Otherwise, the yield of the desired product is maximized at high temperatures: If $\Delta E_{\text{I}} > \Delta E_{\text{II}}$, high temperatures maximize the yield of B. If $\Delta E_{\text{I}} < \Delta E_{\text{II}}$, high temperatures maximize the yield of C.

The reader will appreciate that the rules for what maximizes what can be quite complicated to deduce and even to express. The safe way is to write the reactor design equations for the given set of reactions and then to numerically determine the best values for reaction time and temperature. An interior optimum may not exist. When one does exist, it provides a good starting point for the more comprehensive optimization studies discussed in Chapter 6.

5.2 ENERGY BALANCE

A reasonably general energy balance for a flow reactor can be written in English as

Enthalpy of input streams − enthalpy of output streams
+ heat generated by reaction + heat input from impellers and pumps
− heat transferred to the environment
= accumulation of energy

and in mathematics as

$$Q_{\text{in}}\rho_{\text{in}}H_{\text{in}} - Q_{\text{out}}\rho_{\text{out}}H_{\text{out}} - V\boldsymbol{\Delta}\mathbf{H_R}\hat{\mathscr{R}} + P_{\text{I}} + \hat{U}A_{\text{ext}}(T_{\text{ext}} - \hat{T}) = \frac{d(V\hat{\rho}\hat{H})}{dt} \tag{5.13}$$

This is an integral balance written for the whole system. Each of the additive terms has units of power, joules per second or watts. The various terms deserve discussion.

The ***enthalpies*** are relative to some reference temperature T_{ref}. Standard tabulations of thermodynamic data (see Chapter 7) make it convenient to choose $T_{\text{ref}} =$ 298 K, but choices of $T_{\text{ref}} = 0$ K or $T_{\text{ref}} = 0°\text{C}$ are also common. The enthalpy terms will normally be replaced by temperature using

$$H = \int_{T_{\text{ref}}}^{T} C_P \, dT \tag{5.14}$$

For many purposes, the heat capacity will be approximately constant over the range of temperatures in the system. Then

$$H = C_P(T - T_{\text{ref}}) \tag{5.15}$$

where C_P is the average value for the entire reactant mixture including any inerts. It may be a function of composition as well as temperature. An additional term (e.g., a heat of vaporization) must be added to Equations 5.14 and 5.15 if any of the components undergo a phase change. Also, the equations must be modified if there is a large pressure change during the course of the reaction. See Section 7.2.1.

The ***heat generated by the reaction*** is given by the $-V\,\boldsymbol{\Delta H_R}\hat{\mathscr{R}}$ term. By (perverse) thermodynamic convention, $\Delta H_R < 0$ for exothermic reactions, so a negative sign is attached to this term. When there are multiple reactions, the heat generation term refers to the net effect of all reactions. Thus, the $\boldsymbol{\Delta H_R}\mathscr{R}$ term is an implicit summation over all M reactions that may be occurring:

$$\boldsymbol{\Delta H_R}\mathscr{R} = \sum_{\text{Reactions}} (\Delta H_R)_{\text{I}} \mathscr{R}_{\text{I}} = \sum_{I=1}^{M} (\Delta H_R)_{\text{I}} \mathscr{R}_{\text{I}} \tag{5.16}$$

The reaction rates in Equation 5.16 are positive and apply to "the reaction" rather than to a particular component. Alternatively, they are the rates of formation of a possibly hypothetical component with a stoichiometric coefficient of +1. Similarly, the heats of reaction are per mole of the same component. Some care is needed in using literature values.

Chapter 7 provides a review of chemical thermodynamics useful for estimating specific heats, heats of reaction, and reaction equilibria. The examples here in Chapter 5 assume constant physical properties. This allows simpler illustrations of principles and techniques. Example 7.16 gives a detailed treatment of a reversible, gas phase reaction where there is a change in the number of moles upon reaction and where the equilibrium composition, heat capacities, and reactions rates all vary with temperature. Such rigorous treatments are complicated but should be used for final design calculations. It is better engineering practice to include phenomena than to argue on qualitative grounds that the phenomena are unimportant. Similarly, high numerical precision should be used in the calculations even though the accuracy of the data may be quite limited. The object is to eliminate sources of error, either physical or numerical, that can be eliminated with reasonable effort. A sensitivity analysis can then be confined to the remaining sources of error that are difficult to eliminate. As a practical matter, few reactor design calculations will have absolute accuracies

better than two decimal places. Relative accuracies between similar calculations can be much better and can provide justification for citing values to four or more decimal places, but citing values to full computational precision is a sign of naiveté.

The ***power input from impellers and pumps*** represents viscous dissipation in the fluid of mechanical energy. This can be the dominant form of energy input when processing polymers and is significant in many industrial processes involving even low-viscosity fluids.

The ***heat transfer term*** $\hat{U}\,A_{\text{ext}}(T_{\text{ext}} - \hat{T})$ envisions convection to an external surface, and U is an overall heat transfer coefficient. The heat transfer area could be the reactor jacket, coils inside the reactor, cooled baffles, or an external heat exchanger. Other forms of heat transfer or heat generation can be added to this term, for example, radiative heat transfer. The reactor is ***adiabatic*** when $\hat{U} = 0$.

The accumulation term is zero for steady-state processes. The accumulation term is needed for batch reactors and to solve steady-state problems by the method of false transients.

In practice, the integral formulation of Equation 5.13 is directly useful only when the reactor is a stirred tank with good internal mixing. When there are temperature gradients inside the reactor, as there will be in the axial direction in a nonisothermal PFR, the integral balance remains true but is not especially useful. Instead, a differential energy balance is needed. The situation is exactly analogous to the integral and differential component balances used for the ideal reactors in Chapter 1.

5.2.1 Nonisothermal Batch Reactors

The ideal batch reactor is internally uniform in both composition and temperature. The flow and mixing patterns that are assumed to eliminate concentration gradients will eliminate temperature gradients as well. Homogeneity on a scale approaching molecular dimensions requires diffusion. Both heat and mass diffuse, but thermal diffusivities tend to be orders-of-magnitude higher than molecular diffusivities. Thus, if one is willing to assume compositional uniformity, it is reasonable to assume thermal uniformity as well.

For a perfectly mixed batch reactor, the energy balance is

$$\frac{d(V\rho H)}{dt} = -V\,\mathbf{\Delta H_R}\mathscr{R} + P_{\text{I}} + \hat{U}\,A_{\text{ext}}(T_{\text{ext}} - \hat{T}) \tag{5.17}$$

For constant volume and physical properties,

$$\frac{dT}{dt} = \frac{-\mathbf{\Delta H_R}\mathscr{R}}{\rho C_P} + \frac{P_{\text{I}}}{V\rho C_P} + \frac{\hat{U}\,A_{\text{ext}}(T_{\text{ext}} - \hat{T})}{V\rho C_P} \tag{5.18}$$

Suppose that there is only one reaction and that component A is the limiting reactant. Then the quantity

$$\Delta T_{\text{adiabatic}} = \frac{-\Delta H_R\,\mathscr{R}_A}{\rho C_P} \tag{5.19}$$

gives the ***adiabatic temperature change*** for the reaction. This is the temperature the batch would reach if the physical properties really were constant, if there were no change in the reaction mechanism, and if there were no heat transfer with the environment. Despite all these usually incorrect assumptions, $\Delta T_{\text{adiabatic}}$ provides a rough measure of the difficulty in thermal management of a reaction. If $\Delta T_{\text{adiabatic}} = 10$ K, the reaction is a pussycat. If $\Delta T_{\text{adiabatic}} = 1000$ K, it is a tiger. When there are multiple reactions, $\boldsymbol{\Delta \mathbf{H}_\mathbf{R}} \mathscr{R}$ is a sum according to Equation 5.16, and the adiabatic temperature change is most easily found by setting $U = 0$ and solving Equation 5.18 simultaneously with the component balance equations.

The N component balances are unchanged from those in Chapter 2 although the reaction rates are now understood to be functions of temperature. In matrix form,

$$\frac{d(\mathbf{a}V)}{dt} = \boldsymbol{\nu} \mathscr{R} V \tag{5.20}$$

The design equations for a nonisothermal batch reactor include $N + 1$ ODEs, one for each component and one for energy. These ODEs are coupled by the temperature and compositional dependence of $\mathscr{R}$. They may also be weakly coupled through the temperature and compositional dependence of physical properties such as density and heat capacity, but the strong coupling is through the reaction rate.

EXAMPLE 5.5

Ingredients are quickly charged to a jacketed batch reactor at an initial temperature of 25°C. The jacket temperature is 80°C. A pseudo-first-order reaction occurs. Determine the reaction temperature and the fraction unreacted as a function of time. The following data are available:

$$V = 1.2\,\text{m}^3 \qquad A_{\text{ext}} = 4.68\,\text{m}^2 \qquad U = 1100\,\text{J m}^{-2}\,\text{s}^{-1}\text{K}^{-1} \qquad \rho = 820\,\text{kg m}^{-3}$$

$$C_P = 3400\,\text{J kg}^{-1}\,\text{K}^{-1} \qquad k = 3.7 \times 10^8 \exp\left(\frac{-6000}{T}\right)\text{s}^{-1} \qquad \Delta H_R = -108{,}000\,\text{J mol}^{-1}$$

$$a_{\text{in}} = 1900.0\,\text{mol m}^{-3} \qquad P_{\text{I}} = 10\,\text{kW}$$

Physical properties may be assumed constant.

SOLUTION: The component balance for A is

$$\frac{da}{dt} = -ka$$

and the energy balance is

$$\begin{aligned}\frac{dT}{dt} &= \frac{-\boldsymbol{\Delta \mathbf{H}_\mathbf{R}} \mathscr{R}}{\rho C_P} + \frac{P_{\text{I}}}{V \rho C_P} + \frac{UA_{\text{ext}}(T_{\text{ext}} - T)}{V \rho C_P} \\ &= \Delta T_{\text{adiabatic}} \left(\frac{ka}{a_{\text{in}}}\right) + \frac{P_{\text{I}}}{V \rho C_P} + \frac{UA_{\text{ext}}(T_{\text{ext}} - T)}{V \rho C_P}\end{aligned}$$

where $\Delta T_{\text{adiabatic}} = 73.6$ K for the subject reaction. The initial conditions are $a = 1900$ and $T = 298$ at $t = 0$. The Arrhenius temperature dependence prevents an analytical solution. All the dimensioned quantities are in consistent units so they can be substituted directly into the ODEs. A numerical solution gives the results shown in Figure 5.2. The results are fairly typical

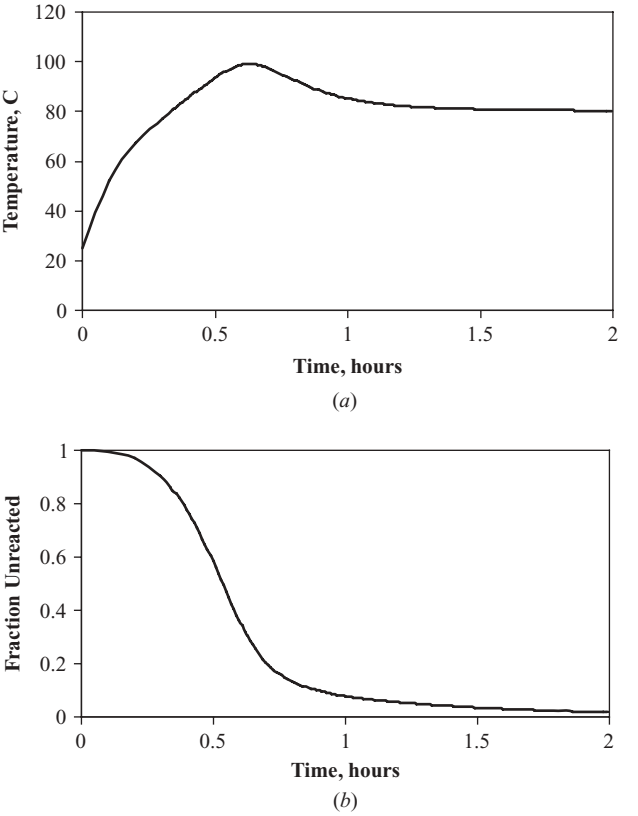

Figure 5.2 (*a*) Temperature and (*b*) fraction unreacted in a nonisothermal batch reactor with jacket cooling.

of an exothermic reaction in a reactor of limited heat transfer. The temperature temporarily overshoots the jacket temperature. This is due to the heat of reaction and is loosely called an ***exotherm***. The exotherm is moderate in Example 5.5, but exotherms become larger and perhaps uncontrollable upon scaleup. Ways of managing an exotherm during scaleup are discussed in Section 5.3. When the reaction is complete, the contents return to the jacket temperature with about a 2°C offset that is due to power from the agitator.

Advice on Debugging and Verifying Computer Programs

The computer programs needed so far have been relatively simple. Most of the problems can be solved using canned ODE packages, although learning how to use the solvers may take more work than writing the code from scratch. Even if you use canned packages, there are many opportunities for error. You have to specify the functional forms for the equations, supply the data, and supply any ancillary functions such as equations of state and physical property relationships. Few programs work correctly

the first time. You will need to debug them and confirm that the output is plausible. A key to doing this for physically motivated problems like those in reactor design is simplification. You may wish to write the code all at once, but don't try to debug it all at once. For the nonisothermal problems encountered in this chapter, start by running an isothermal and isobaric case. Set T and P to constant values and see if the reactant concentrations are calculated correctly. If the reaction network is complex, you may need to simplify it, say by dropping some side reactions, until you find a case that you know is giving the right results. When the calculated solution for an isothermal and isobaric reaction makes sense, put the ODEs for temperature or pressure back into the program and see what happens. You may wish to test the adiabatic case by setting $U = 0$ and to retest the isothermal case by setting U to some large value. Complications like variable physical properties and variable reactor cross sections are best postponed until you have a solid base case that works. If something goes wrong when you add a complication, revert to a simpler case to help pinpoint the source of the problem.

The energy balance in Example 5.5 has three additive terms: the reaction exotherm, the agitator power, and heat transfer from the jacket. Delete two of these and see what the remaining term does by itself. Is the sign correct and is the magnitude reasonable? In Example 5.5, the jacket by itself will raise the contents to 80°C within an hour. The agitator by itself will raise the contents to 47°C in 2 h. By itself, the reaction does very little within 2 h. However, increase the initial temperature 60°C and the full adiabatic temperature rise will be reached within 1 h. Put all three together to get the results in Figure 5.2.

Debugging by simplifying before complicating is even more important for the optimization problems in Chapter 6 and the nonideal reactor design problems in Chapters 8 and 9. When the reactor design problem is embedded as a subroutine inside an optimization routine, be sure that the subroutine will work for any parameter values that the optimization routine is likely to give it. Having trouble with an axial dispersion problem in Chapter 9? Throw out the axial dispersion terms for heat and mass and confirm that you get the right results for a nonisothermal (or even isothermal) PFR. Having trouble with the velocity profile in a laminar flow reactor? Get the reactor program to work with a parabolic or even a flat profile. Separately test the subroutine for calculating the axial velocity profile by sending it a known viscosity profile. Put it back into the main program only after it works on its own. Additional complications like radial velocity components are added still later.

Long programs will take hours and even days to write and test. A systematic approach to debugging and verification will reduce this time to a minimum. It will also give you confidence that the numbers are right when they finally are produced.

5.2.2 Nonisothermal Piston Flow

Steady-state temperatures along the length of a PFR are governed by an ODE. Figure 5.3 illustrates the differential energy balance for a PFR. The terms in the energy balance are the same as in Equation 5.13, but the reactor is assumed to be at

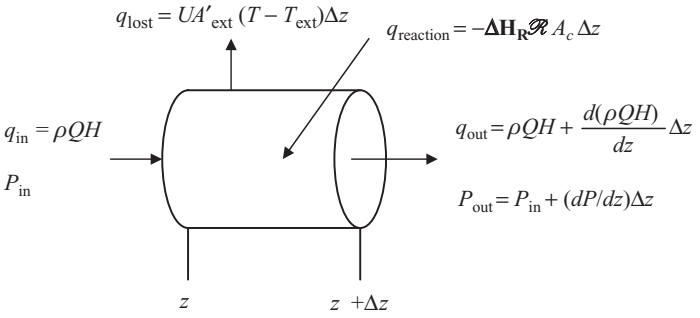

Figure 5.3 Differential element in a nonisothermal PFR.

steady state and differential quantities are now used. The ρQH terms cancel and Δz factors out to give

$$\frac{d(\rho QH)}{dz} = \rho Q\frac{dH}{dz} = \rho A_c\bar{u}\frac{dH}{dz} = -\mathbf{\Delta H_R}\mathscr{R}A_c + Q\frac{dP}{dz} + UA'_{\text{ext}}(T_{\text{ext}} - T) \tag{5.21}$$

Unlike a molar flow rate (e.g., aQ), the mass flow rate ρQ is constant and can be brought outside the differential. Note that $Q = \bar{u}A_c$ and that A'_{ext} is the external surface area per unit length of tube. Equation 5.21 can be written as

$$\frac{dH}{dz} = \frac{-\mathbf{\Delta H_R}\mathscr{R}}{\rho\bar{u}} + \frac{1}{\rho}\frac{dP}{dz} + \frac{UA'_{\text{ext}}}{\rho\bar{u}A_c}(T_{\text{ext}} - T) \tag{5.22}$$

This equation is coupled to the component balances of Equation 3.9 and with an equation for the pressure, for example, one of Equations 3.18, 3.19, or 3.21. There are $N + 2$ equations and some auxiliary algebraic equations that need to be solved simultaneously. Numerical solution techniques are similar to those used in Section 3.1 for variable-density PFRs. The dependent variables are the component fluxes $\mathbf{\Phi}$, the enthalpy H, and the pressure P. A necessary auxiliary equation is the thermodynamic relationship that gives enthalpy as a function of temperature, pressure, and composition. Equation 5.15 with $T_{\text{ref}} = 0$ is the simplest example of this relationship and is usually adequate for preliminary calculations.

With a constant, circular cross section, $A'_{\text{ext}} = 2\pi R$ (although the concept of piston flow is not restricted to circular tubes). If C_P is constant,

$$\frac{dT}{dz} = \frac{-\mathbf{\Delta H_R}\mathscr{R}}{\bar{u}\rho C_P} + \frac{1}{\rho C_P}\frac{dP}{dz} + \frac{2U}{\bar{u}\rho C_P R}(T_{\text{ext}} - T) \tag{5.23}$$

This is the form of the energy balance that is usually used for preliminary calculations. Equation 5.23 does not require that $\bar{u}$ be constant, but if it is constant, we can set $dz = \bar{u}\,dt$ and $2/R = A_{\text{ext}}/A_c$ to make Equation 5.23 similar to Equation 5.18. A PFR with constant velocity and constant physical properties behaves like a batch reactor with constant volume and constant physical properties. The curves in Figure 5.2 could apply to a PFR as well as to the batch reactor analyzed in Example 5.5.

However, Equation 5.22 is the appropriate version of the energy balance when the reactor cross section or physical properties are variable.

The solution of the energy and component balances is more straightforward when temperature and the component concentrations can be used directly as the dependent variables rather that enthalpy and the component fluxes. In any case, however, the initial values T_{in}, P_{in}, a_{in}, b_{in}, ... must be known at $z = 0$. Reaction rates and physical properties can then be calculated at $z = 0$ so that the right-hand side of Equation 5.22 or 5.23 can be evaluated. This gives ΔT, and thus $T(z + \Delta z)$, directly in the case of Equation 5.23 and implicitly via the enthalpy in the case of Equation 5.22. The component equations are evaluated similarly to give $a(z + \Delta z)$, $b(z + \Delta z)$, ... either directly or via the concentration fluxes as described in Section 3.1. The pressure equation is evaluated to give $P(z + \Delta z)$. The various auxiliary equations are used as necessary to determine quantities such as $\bar{u}$ and A_c at the new axial location. Thus $T, a, b, \ldots$ and other necessary variables are determined at the next axial position along the tubular reactor. The axial position variable z can then be incremented and the entire procedure repeated to give temperatures and compositions at the next point. Thus we march down the tube.

EXAMPLE 5.6

Hydrocarbon cracking reactions are endothermic, and many different techniques are used to supply heat to the system. The maximum inlet temperature is limited by materials of construction or by undesirable side reactions such as coking. If the reactor is adiabatic with inlet temperature T_{in}, the temperature will gradually decline as the reaction proceeds. This decrease, with the consequent reduction in reaction rate, can be minimized by using a high proportion of inerts in the feed stream. Suppose the reaction rate $\mathscr{R} = \left[10^{14} \exp(-24000/T)\right] a$, where a is in grams per cubic meter. The reaction is conducted in an adiabatic tubular reactor having a mean residence time of 1 s. The crackable component and its products have a heat capacity of 0.4 cal g^{-1} K^{-1}, and the inerts have a heat capacity of 0.5 cal g^{-1} K^{-1}; the entering concentration of crackable component is 132 g m^{-3} and the concentration of inerts is 270 g m^{-3}; $T_{\text{in}} = 525^{\circ}$C. Calculate the exit concentration of A given $\Delta H_R = 203$ cal g^{-1}. Physical properties may be assumed constant. Repeat the calculation in the absence of inerts.

SOLUTION: Aside from the temperature calculations, this example illustrates the systematic use of mass rather than molar concentrations for reactor calculations. This is common practice for mixtures having ill-defined molecular weights. The energy balance for the adiabatic reactor gives

$$\frac{dT}{dt} = \frac{-\Delta H_R \mathscr{R}_A}{\rho C_P} = \Delta T_{\text{adiabatic}} \left(\frac{ka}{a_{\text{in}}}\right)$$

Note that ρ and C_P are properties of the reaction mixture. Thus $\rho = 132 + 270 = 402$ g m^{-3} and $C_P = [0.4(132) + 0.5(270)]/402 = 0.467$ cal g^{-1} K^{-1}. This gives $\Delta T_{\text{adiabatic}} = -142.7$ K. If the inerts are removed, $\rho = 132$ g m^{-3}, $C_P = 0.4$ cal $g^{-1}K^{-1}$, and $\Delta T_{\text{adiabatic}} = -507.5$ K.

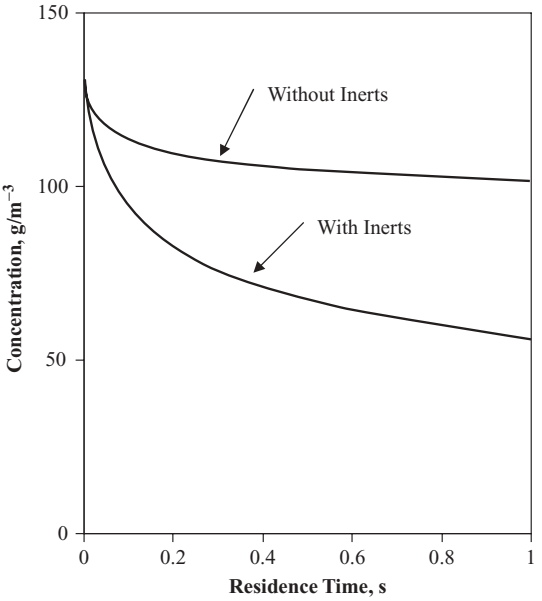

Figure 5.4 Concentration profiles for endothermic reaction in an adiabatic reactor.

Figure 5.4 displays the solution. The results are $a_{out} = 57.9$ g m^{-3} and $T_{out} = 464.3°$C for the case with inerts and $a_{out} = 107.8$ g m^{-3} and $T_{out} = 431.9°$C. It is apparent that inerts can have a remarkably beneficial effect on the course of the reaction.

In the general case of a PFR, one must solve a fairly small set of simultaneous ODEs. In theory, one equation is needed for each independent reaction. In practice, numerical solutions are somewhat easier to implement if a separate equation is written for each component. This ensures that the stoichiometry is correct and keeps the physics and chemistry of the problem rather more transparent than when the reaction coordinate method is used to obtain the smallest possible set of differential equations. Computational speed is rarely important in solving design problems of this type. The work involved in understanding the problem, the assembling the data, writing any necessary code, debugging the code, and verifying the results takes much more time than the computation.

5.2.3 Heat Balances for CSTRs

Setting $\hat{T} = T_{out}$, $\hat{H} = H_{out}$, and so on, specializes the integral energy balance of Equation 5.13 to a perfectly mixed, continuous flow stirred tank:

$$\frac{d(V\rho_{out}H_{out})}{dt} = Q_{in}\,\rho_{in}\,H_{in} - Q_{out}\,\rho_{out}\,H_{out} - V\boldsymbol{\Delta H_R}\,\mathscr{R} + P_I + UA_{ext}(T_{ext} - T_{out}) \tag{5.24}$$

where $\boldsymbol{\Delta H_R}\,\mathscr{R}$ denotes the implied summation of Equation 5.16.

The corresponding component balance for component A is

$$\frac{d(Va)}{dt} = Q_{\text{in}}\, a_{\text{in}} - Q_{\text{out}}\, a_{\text{out}} + V\mathscr{R}_A \tag{5.25}$$

which also has an implied summation

$$\mathscr{R}_A = \nu_{A,\text{I}}\,\mathscr{R}_\text{I} + \nu_{A,\text{II}}\mathscr{R}_\text{II} + \cdots \tag{5.26}$$

The simplest, nontrivial version of these equations is obtained when all physical properties (e.g., ρ and C_P) and process parameters (e.g. Q_{in}, a_{in}, and T_{in}) are constant. The energy balance for this simplest but still reasonably general case is

$$\bar{t}\frac{dT_{\text{out}}}{dt} = T_{\text{in}} - T_{\text{out}} - \frac{\mathbf{\Delta H_R}\,\mathscr{R}\bar{t}}{\rho C_P} + \frac{P_\text{I}}{V\rho C_P} + \frac{UA_{\text{ext}}(T_{\text{ext}} - T_{\text{out}})\bar{t}}{V\rho C_p} \tag{5.27}$$

The time derivative is zero at steady state, but it is included so that the method of false transients can be used. The computational procedure in Section 4.3.2 applies directly when the energy balance is given by Equation 5.27. The same basic procedure can be used for Equation 5.24. The enthalpy rather than the temperature is marched ahead as the dependent variable, and then T_{out} is calculated from H_{out} after each time step. The examples that follow assume constant physical properties and use Equation 5.27. Their purpose is to explore nonisothermal reaction phenomena rather than to present detailed design calculations.

EXAMPLE 5.7

A CSTR is commonly used for the bulk polymerization of styrene. Assume a mean residence time of 2 h, cold monomer feed (300 K), adiabatic operation ($UA_{\text{ext}} = 0$), and a pseudo-first-order reaction with rate constant $k = 10^{10}\exp(-10000/T)$ h^{-1} where T is in kelvin. The adiabatic temperature rise for complete conversion is approximately 400 K. Assume constant physical properties and ignore power input form the agitator.

SOLUTION: The component balance for styrene for a first-order reaction in a constant-volume, constant-density CSTR is

$$\bar{t}\frac{ds_{\text{out}}}{dt} = s_{\text{in}} - s_{\text{out}} - k\bar{t}s_{\text{out}}$$

or

$$\bar{t}\frac{dY_S}{dt} = \frac{dY_S}{d\tau} = 1 - Y_S - k\bar{t}Y_S \tag{5.28}$$

where Y_S is the fraction unreacted and where $\tau = t/\bar{t}$ is a dimensionless time. The temperature balance for the adiabatic case is

$$\frac{dT_{\text{out}}}{d\tau} = T_{\text{in}} - T_{\text{out}} - \frac{\Delta H_R\mathscr{R}\bar{t}}{\rho C_P} = T_{\text{in}} - T_{\text{out}} + \Delta T_{\text{adiabatic}}\, k\bar{t}Y_S \tag{5.29}$$

Equations 5.28 and 5.29 must be solved simultaneously. There are three parameters: T_{in}, $\Delta T_{\text{adiabatic}}$ and the dimensionless (but temperature-dependent) rate constant $k\bar{t}$. The initial conditions associated with Equations 5.28 and 5.29 are $Y_S = 1$ and $T_{\text{out}} = T_0$ at $\tau = 0$. Solutions for a feed of pure styrene and various values for T_0 are shown in Figure 5.5.

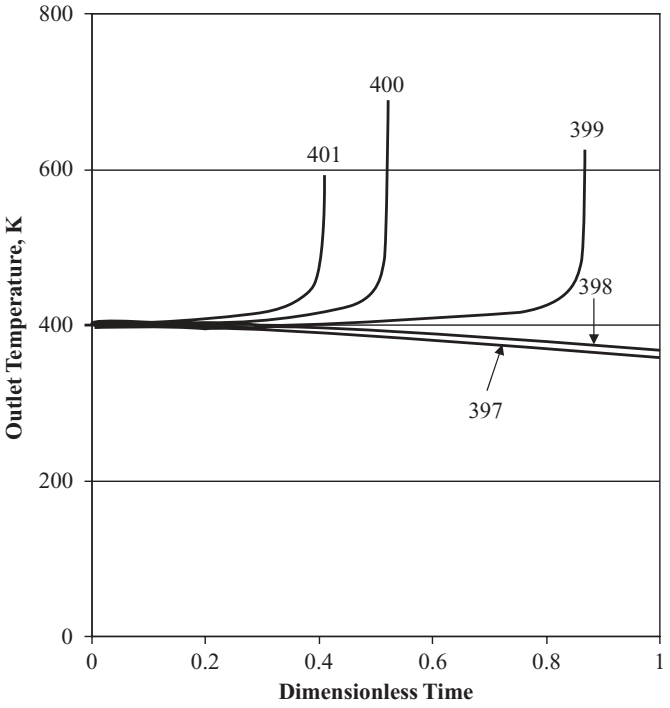

Figure 5.5 Method of false transients applied to a system having two stable steady states. The parameter is the initial temperature T_0.

The behavior shown in Figure 5.5 is typical of systems having two stable steady states. The realized steady state depends on the initial conditions. For this example, the upper steady state is reached if T_0 is greater than about 398 K, and the lower steady state is reached if T_0 is less than about 398 K. At the lower steady state, the CSTR acts as a styrene monomer storage vessel with $T_{out} \approx T_{in}$ and there is no significant reaction. The upper steady state is a runaway where the reaction goes to near completion with $T_{out} \approx T_{in} + \Delta T_{adiabatic}$. (In actuality, the styrene polymerization has a ceiling temperature of about 625 K due to reversibility and thermal degradation.)

There is a middle steady state, but it is metastable. The reaction will tend toward either the upper or lower steady states, and a control system is needed to maintain operation around the metastable point. For the styrene polymerization, a common industrial practice is to operate at the metastable point, with temperature control achieved by boiling. A combination of feed preheating and jacket heating ensures a positive heat balance so that the uncontrolled reaction would tend toward the upper, runaway condition. However, the reactor pressure is set so that the system boils when the desired operating temperature is reached. The latent heat of vaporization plus the return of subcooled condensate maintains the temperature at the boiling point.

The method of false transients cannot be used to find a metastable steady state. Instead, the time derivatives in Equations 5.28 and 5.29 are set to zero and the resultant algebraic equations are solved simultaneously. This is easy in the current example since Equation 5.28

(with $dY_A/d\tau = 0$) can be solved for Y_A. The result is substituted into Equation 5.29 (with $dT_{out}/d\tau = 0$) to obtain a single equation in a single unknown:

$$0 = T_{in} - T_{out} + \frac{\Delta T_{adiabatic}\, k\bar{t}}{1 + k\bar{t}}$$

where $k = k_0 \exp(-T_{act}/T)$. A binary search can be used to locate the zeros of this equation. This is done in Code for Example 4.14. The three solutions can be found by varying the temperature range over which the search is performed:

T_{out}, K	$Y_A = s_{out}/s_{in}$
300.03	0.99993
403.7	0.741
699.97	0.00008

The existence of three steady states, two stable and one metastable, is common for exothermic reactions in a CSTR. Also common is the existence of only one steady state. For the styrene polymerization example, three steady states exist for a limited range of the process variables. For example, if T_{in} is sufficiently low, any reaction that is occurring at $t = 0$ will be quenched, and only a lower steady state is possible. The external heat transfer term, $UA_{ext}(T_{ext} - T_{out})$, in Equation 5.27 can also be used to vary the location and number of steady states,

EXAMPLE 5.8

Suppose that, to achieve a desired molecular weight, the styrene polymerization must be conducted at 413 K. Use external heat transfer to achieve this temperature as the single steady state in a stirred tank.

SOLUTION: Equation 5.27 is unchanged. An external heat transfer term is added to Equation 5.29 to give

$$\frac{dT_{out}}{d\tau} = T_{in} - T_{out} + \Delta T_{adiabatic}\, k\bar{t} Y_S + \frac{UA_{ext}}{\rho Q C_P}(T_{ext} - T_{out}) \tag{5.30}$$

We consider T_{ext} to be an ***operating variable*** that can be manipulated to achieve $T_{out} = 413$ K. The dimensionless heat transfer group $UA_{ext}/\rho Q C_P$ is considered a ***design variable***.It must be large enough that a single steady state can be imposed on the system. In small equipment with good heat transfer, one simply sets $T_{ext} \approx T_{out}$ to achieve the desired steady state. In larger vessels, $UA_{ext}/\rho Q C_P$ is finite, and one must find set $T_{ext} < T_{out}$ such that the steady state is 413 K.

Since the external heat exchange is supposed to stabilize the steady state, the method of false transients could be used for the simultaneous solution of Equations 5.28 and 5.30. However, the ease of solving Equation 5.28 for a first-order reaction makes the algebraic

approach simpler. Whichever method is used, a value for $UA_{ext}/\rho QC_P$ is assumed and then a value for T_{ext} found that gives 413 K as the single steady state. Some results are

$UA_{ext}/\rho QC_P$	T_{ext} that gives $T_{out} = 413$ K
100	412.6
50	412.3
20	411.1
10	409.1
5	405.3
4	No solution

Thus the minimum value for $UA_{ext}/\rho QC_P$ is about 5. If the heat transfer group is any smaller than this, stable operation at $T_{out} = 413$ K by manipulation of T_{est} is no longer possible because the temperature driving force, $\Delta T = T_{out} - T_{ext}$, becomes impossibly large. As will be seen in Section 5.3.2, the quantity $UA_{ext}/\rho QC_P$ normally declines on scaleup.

At a steady state, the amount of heat generated by the reaction must exactly equal the amount of heat removed by flow plus heat transfer to the environment: $q_{generated} = q_{removedl}$. The heat generated by the reaction is

$$q_{generated} = -V\Delta H_R \mathscr{R} \tag{5.31}$$

This generation term will be an S-shaped curve when plotted against T_{out}. When T_{out} is low, reaction rates are low, and little heat is generated. When T_{out} is high, the reaction goes to completion, the entire exotherm is released, and T_{out} reaches a maximum. A typical curve for the rate of heat generation is plotted in Figure 5.6(a). The shape of the curve can be varied by changing the reaction mechanism and rate constant.

The rate of heat removal is given by

$$q_{removed} = -Q_{in}\rho_{in}H_{in} + Q_{out}\rho_{out}H_{out} + UA_{ext}(T_{out} - T_{ext}) \tag{5.32}$$

As shown in Figure 5.6*b*, the rate of heat removal is a linear function of T_{out} when physical properties are constant:

$$\begin{aligned} q_{removed} &= \rho QC_P(T_{out} - T_{in}) + UA_{ext}(T_{out} - T_{ext}) \\ &= -(\rho QC_P T_{in} + UA_{ext}T_{ext}) + (\rho QC_P + UA_{ext})T_{out} = C_0 + C_1 T_{out} \end{aligned}$$

where C_0 and C_1 are the slope and intercept of the heat absorption line. They can be manipulated by changing either the design or operating variables.

Setting Equation 5.31 equal to Equation 5.32 gives the general heat balance for a steady-state system. Figure 5.6*c* shows the superposition of the heat generation and removal curves. The intersection points are steady states. There are three in the illustrated case, but Figure 5.6*d* includes cases having only one steady state.

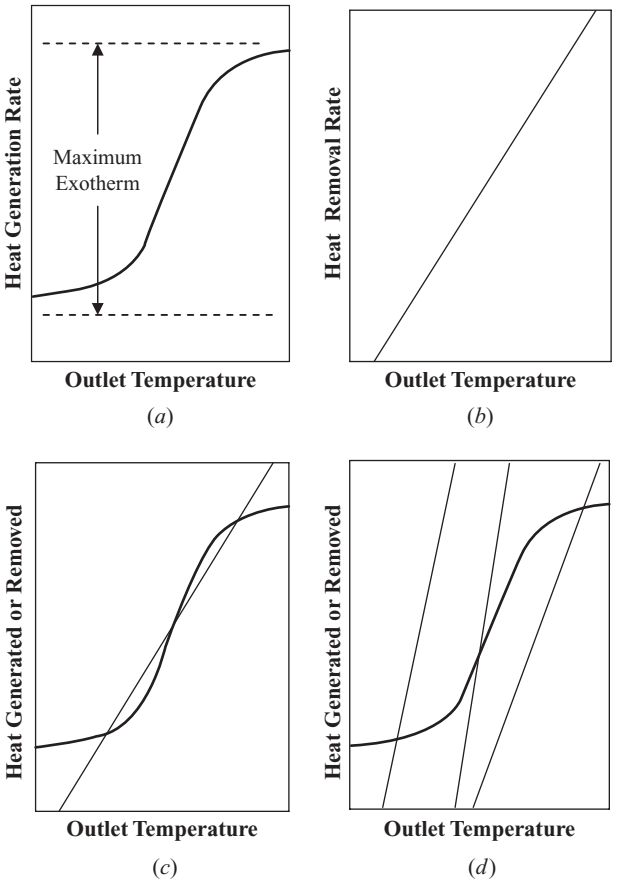

Figure 5.6 Heat balance in a CSTR: (*a*) heat generated by reaction; (*b*) heat removed by flow and transfer to the environment; (*c*) superposition of generation and removal curves. The intersection points are steady states. (*d*) Superposition of alternative heat removal curves that give only one steady state.

More than three steady states are sometimes possible. Consider the reaction sequence

$$\mathrm{A} + \mathrm{B} \rightarrow \mathrm{C} \qquad \text{(I)}$$

$$\mathrm{A} \rightarrow \mathrm{D} \qquad \text{(II)}$$

where reaction I occurs at a lower temperature than reaction II. It is possible that reaction I will go to near completion, consuming all the B, while still at temperatures below the point where reaction II becomes significant. This situation can generate up to five steady states, as illustrated in Figure 5.7. A practical example is styrene polymerization using component B as an initiator at low temperatures, $<120^{\circ}$C, and with spontaneous (thermal) initiation at higher temperatures. The lower S-shaped

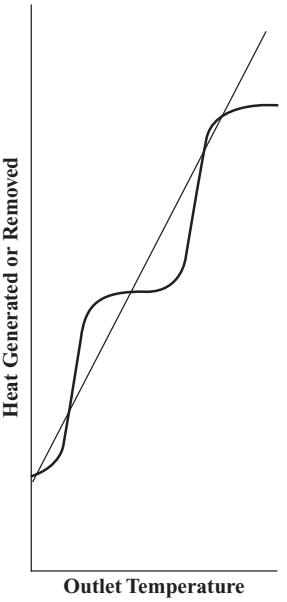

Figure 5.7 Consecutive reactions with five steady states.

portion of the heat generation curve consumes all the initiator, B; but there is still unreacted styrene, A. The higher S-shaped portion consumes the remaining styrene.

To learn whether a particular steady state is stable, it is necessary to consider small deviations in operating conditions. Do they decline and damp out or do they lead to larger deviations? Return to Figure 5.6*c* and suppose that the reactor has somehow achieved a value for T_{out} that is higher than the upper steady state. In this region, the heat removal line is above the heat generation line so that the reactor will tend to cool, approaching the steady state from above. Suppose, on the other hand, that the reactor becomes cooler than the upper steady state but remains hotter than the central, metastable state. In this region the heat removal line is below the heat generation line so that the temperature will increase, heading back to the upper steady state. Thus the upper steady state is stable when subject to small disturbances, either positive or negative. The same reasoning can be applied to the lower steady state. However, the middle steady state is unstable. A small positive disturbance will send the system toward the upper steady state and a small negative disturbance will send the system toward the lower steady state. Applying this reasoning to the system in Figure 5.7 with five steady states shows that three of them are stable. These are the lower, middle, and upper ones that can be numbered 1, 3, and 5. The two even-numbered steady states, 2 and 4, are metastable.

The dynamic behavior of nonisothermal CSTRs is extremely complex and has received much academic study. Systems exist that have only a metastable state and no stable steady states. Included in this class are some ***chemical oscillators*** that operate in a reproducible limit cycle about their metastable state. ***Chaotic*** systems have discernible average values and long-term patterns but have short-term temperature–composition trajectories that appear essentially random. Occasionally, such dynamic

behavior is of practical importance for industrial reactor design. A classic situation of a sustained oscillation occurs in emulsion polymerizations. These are complex reactions involving both kinetic and mass transfer limitations, and a stable steady state is difficult or impossible to achieve in a single CSTR. It was reasoned that, if enough CSTRs were put in series, results would average out so that effectively stable, high conversions could be achieved. For a synthetic rubber process built during wartime emergency, enough stirred tanks turned out to be 25–40. Full-scale production units were actually built in this configuration! More elegant solutions to continuous emulsion polymerizations are now available.

5.3 SCALEUP OF NONISOTHERMAL REACTORS

Thermal effects are often the key concern in reactor scaleup. The generation of heat is proportional to the volume of the reactor. Note the factor of V in Equation 5.31. For a scaleup that maintains geometric similarity, the surface area increases only as $V^{2/3}$. Sooner or later, temperature can no longer be controlled by external heat transfer, and the reactor will approach adiabatic operation. There are relatively few reactions where the full adiabatic temperature change can be tolerated. Endothermic reactions will have poor yields. Exothermic reactions will have thermal runaways giving undesired byproducts. It is the reactor designer's job to avoid limitations of scale or at least to understand them so that a desired product will result. There are many options. The best process and the best equipment at the laboratory scale are rarely the best for scaleup. Put another way, a process that is less than perfect at a small scale may be better for scaleup precisely because it is scaleable.

5.3.1 Avoiding Scaleup Problems

Scaleup problems are sometimes avoidable. A few simple possibilities are as follows:

Use enough diluents so that the adiabatic temperature change is acceptable.

Scale in parallel, for example, shell-and tube designs.

Depart from geometric similarity so that V and A_{ext} both increase in direct proportion to the throughput scaling factor S. Scaling a tubular reactor by adding length is a possibility for an incompressible fluid.

Use temperature control techniques that inherently scale as S, for example, cold feed to a CSTR or autorefrigeration (boiling).

Intentionally degrade the performance of the small unit so that the same performance and product quality can be achieved upon scaleup.

1. Use diluents: In a gas system, inerts such as nitrogen, carbon dioxide, or steam can be used to mitigate the reaction exotherm. In a liquid system, a solvent can be used. Another possibility is to introduce a second liquid phase that has the function of absorbing and transferring heat, that is, water in an emulsion or suspension polymerization. Adding an extraneous material will increase cost, but the increase may be acceptable if it allows scaleup. Solvents have a deservedly bad name in open,

unconfined applications, but these are largely eliminated in modern practice. In a closed environment, solvent losses are small and the cost of confining the solvent is often borne by the necessary cost of confining the reactants.

2. Scale in parallel: This common scaling technique was discussed in Section 3.2.1. Subject to possible tube-to-tube distribution problems, it is an inexpensive way of gaining capacity.

3. Depart from geometric similarity: Adding length to a tubular reactor while keeping the diameter constant allows both volume and external area to scale as S if the liquid is incompressible. Scaling in this manner gives poor results for gas phase reactions. The quantitative aspects of such scaleups are discussed in Section 5.3.4. Another possibility is to add stirred tanks or, indeed, any type of reactor in series. Two reactors in series give twice the volume, have twice the external surface area, and give a closer approach to piston flow than a single geometrically similar reactor that has twice the volume but only 1.59 times the surface area of the smaller reactor. Designs with several reactors in series are quite common. Multiple pumps are sometimes used to avoid high pressures. The apparent cost disadvantage of using many small reactors rather than one large one can be partially offset by standardizing the design of the small reactors.

If a single large CSTR is desired, internal heating coils or an external pump-around loop can be added. This is another way of departing from geometric similarity and is discussed in Section 5.3.2.

4. Use scaleable heat transfer: The feed flow rate scales as S and a cold-feed stream removes heat from the reaction in direct proportion to the flow rate. If the energy needed to heat the feed from T_{in} to T_{out} can absorb the reaction exotherm, the heat balance for the reactor can be scaled indefinitely. Cooling costs may be an issue, but there are large-volume industrial processes that have $T_{in} \approx -40°C$ and $T_{out} \approx 200°C$. Obviously, cold feed to a PFR will not work since the reaction will not start at low temperatures. Injection of cold reactants at intermediate points along the length of a PFR is a possibility but lowers conversion. In the limiting case of many injections, this will reduce reactor performance to that of a CSTR. See Section 3.5 on transpired-wall reactors.

Autorefrigeration or boiling is another example of heat transfer that scales as S. The chemist calls it refluxing and routinely uses it as a method of temperature control. Laboratory glassware is usually operated at atmospheric pressure so the temperature is set by the normal boiling point of the reaction mix. Chemists often choose solvents based on boiling point. Process equipment can operate at a regulated pressure so the boiling point can be adjusted. On the basis of boiling point, toluene at a reduced pressure of about 0.4 atm can replace benzene. The elevation of boiling point with pressure does impose a scaleup limitation. A tall reactor will have a temperature difference between top and bottom due to the liquid head. Special problems with the scaleup of boiling reactors are discussed is Section 5.3.3.

5. Use diplomatic scaleup: This possibility is called diplomatic scaleup because it may require careful negotiations to implement. The idea is that thermal effects are likely to change the distribution of byproducts or the product properties upon scaleup. The economics of the scaled process may be perfectly good and the product may be completely satisfactory, but it will be different than what the chemist could achieve in

glassware. Setting appropriate and scaleable expectations for product properties can avoid surprises and the cost of requalifying the good but somewhat different product that is made in the larger reactor. Diplomacy may be needed to convince the chemist to change the laboratory or bench-scale process to lower its performance with respect to heat transfer. A recycle loop reactor is one way of doing this in a controlled fashion.

5.3.2 Heat Transfer to Jacketed Stirred Tanks

This section is concerned with the $UA_{\text{ext}}(T_{\text{ext}} - T)$ term in the energy balance for a stirred tank. The usual and simplest case is heat transfer, typically cooling, from a jacket. Then A_{ext} refers to the inside surface area of the tank that is jacketed on the outside and in contact with the fluid on the inside. The temperature difference $T_{\text{ext}} - T$ is between the bulk fluid in the tank and the heat transfer medium in the jacket. The overall heat transfer coefficient includes contributions from wall resistance and jacket-side coefficient, but the inside coefficient is normally limiting. A correlation applicable to tanks with turbine, paddle, and propeller agitators is

$$\mathbf{Nu} = \frac{hD_{\text{I}}}{\kappa} = C_h \left(\frac{D_{\text{I}}^2 N_{\text{I}} \rho}{\mu} \right)^{2/3} \left(\frac{\mu}{\mu_{\text{wall}}} \right)^{0.14} \tag{5.33}$$

where **Nu** is the Nusselt number and κ is the thermal conductivity. The value for C_h is needed for detailed design calculations but factors out in a scaling analysis; $C_h \approx 0.5$ for turbines and propellers. For a scaleup that maintains constant fluid properties,

$$\frac{(hD_{\text{I}})_{\text{large}}}{(hD_{\text{I}})_{\text{small}}} = \left[\frac{\left(D_{\text{I}}^2 N_{\text{I}}\right)_{\text{large}}}{\left(D_{\text{I}}^2 N_{\text{I}}\right)_{\text{small}}} \right]^{2/3}$$

Assuming geometric similarity and recalling that D_{I} scales as $S^{1/3}$ gives

$$\frac{h_{\text{large}}}{h_{\text{small}}} = \left[\frac{\left(D_{\text{I}} N_{\text{I}}^2\right)_{\text{large}}}{\left(D_{\text{I}} N_{\text{I}}^2\right)_{\text{small}}} \right]^{1/3} = S^{1/9} S_N^{2/3}$$

For a scaleup with constant power per unit volume, Table 4.1 shows that S_N scales as $S^{-2/9}$. Thus,

$$\frac{h_{\text{large}}}{h_{\text{small}}} = S^{1/9} (S^{-2/9})^{2/3} = S^{-1/27}$$

and h decreases slightly upon scaleup. Assuming h controls the overall coefficient,

$$\frac{(UA_{\text{ext}})_{\text{large}}}{(UA_{\text{ext}})_{\text{small}}} = S^{-1/27} D_{\text{I}}^2 = S^{17/27}$$

If we want $UA_{\text{ext}}(T_{\text{ext}} - T)$ to scale as S, the driving force for heat transfer must be increased.

$$\frac{(T_{\text{ext}} - T)_{\text{large}}}{(T_{\text{ext}} - T)_{\text{small}}} = S^{10/27}$$

These results are summarized in the last four rows of Table 4.1. Scaling the volume by a factor of 512 causes a large loss in hA_{ext} per unit volume. An increase in the temperature driving force by a factor of 10 (e.g., by reducing T_{ext} if the reactor is being cooled) could compensate, but such a large increase is unlikely to be possible. Also, with cooling at the walls, the viscosity correction term in Equation 5.33 will become important and will decrease hA_{ext} still more.

This analysis has been done for a batch reactor, but it applies equally well to a CSTR. The heat transfer coefficient is the same because the agitator dominates the flow inside the vessel with little contribution from the net throughput. The analysis also applies to heat transfer using internal coils or baffles. The equations for the heat transfer coefficients are similar in form to Equation 5.33. Experimental results for the exponent on the impeller Reynolds number vary from 0.62 to 0.67 and are thus close to the semi-theoretical value of 2/3 used in Equation 5.33. The results in Table 4.1 are generally restricted to turbulent flow. The heat transfer coefficient in laminar flow systems scales with impeller Reynolds number to the $\frac{1}{2}$ power. This causes an even greater loss in heat transfer capability upon scaleup than in a turbulent system, although a transition to turbulence will occur if S is large enough. Close-clearance impellers such as anchors and helical ribbons are frequently used in laminar systems. So are pitched-blade turbines with large ratios of the impeller to tank diameter. This improves the absolute values for h but has a minor effect on the scaling relationships. Several correlations for **Nu** in laminar flow show a dependence on **Re** to the 0.5 power rather than the 0.67 power.

It is sometimes proposed to increase A_{ext} by adding internal coils or increasing the number of coils upon scaleup. This is a departure from geometric similarity that will alter flow within the vessel and reduce the heat transfer coefficient for the jacket. It can be done within reason; but to be safe, the coil design should be tested on the small scale using dummy coils or by keeping a low value for $T_{ext} - T$. A better approach to maintaining good heat transfer upon scaleup is to use a heat exchanger in an external loop as shown in Figure 5.8. The illustrated case is for a CSTR, but the concept can also be used for a batch reactor. The per-pass residence time in the loop should be small compared to $\bar{t}$ for the reactor as a whole. A rule of thumb for a CSTR is

$$\bar{t}_{loop} = \frac{\text{volume of loop}}{\text{flow rate through loop}} < \bar{t}/10 \tag{5.34}$$

where $\bar{t}$ is the mean residence time for the entire system of loop plus tank. Reaction occurs in the loop as well as in the stirred tank, and it is possible to eliminate the stirred tank so that the reactor volume consists entirely of the heat exchanger and piping. This approach is used for very large CSTR's.

Equation 5.34 is similar to the rule-of-thumb discussed in Section 4.5.3 that a recycle loop reactor approximate a CSTR. The reader may wonder why the rule-of-thumb proposed a minimum recycle ratio of 8 in Chapter 4 but 10 here. Thumbs vary in size. More conservative designers have proposed a minimum recycle ratio of 16, and loop reactors with recycle ratios above 100 are known. The real issue is how much conversion per pass can be tolerated in the more-or-less piston flow environment of the heat exchanger. The same issue arises in the stirred tank reactor itself since the

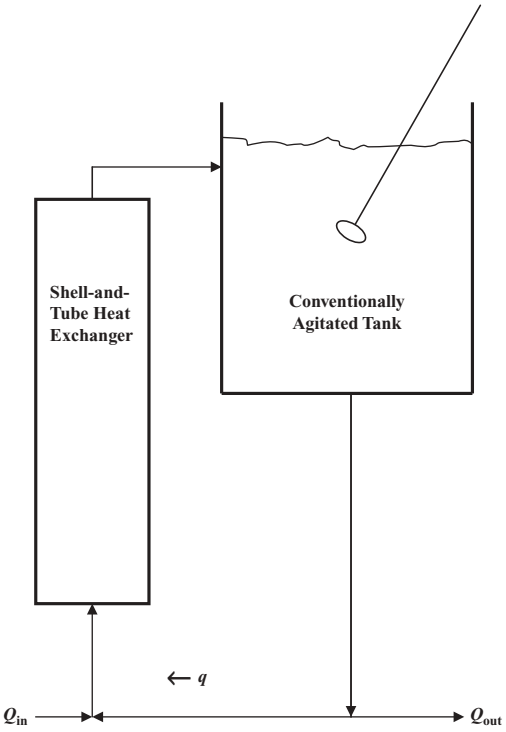

Figure 5.8 CSTR that includes external heat exchange.

internal pumping rate is finite and intense mixing occurs only in the region of the impeller. In a loop reactor, the recirculation pump acts as the impeller and provides a local zone of intense mixing.

EXAMPLE 5.9

This is a consultant's war story. A company had a brand-name product for which they purchased a polymer additive. They decided to create their own proprietary additive, and assigned the task to a synthetic chemist who soon created a fine polymer in a 300 ml flask. Scaleup was assigned to engineers who translated the chemistry to a 10 gallon, steel reactor. The resulting polymer was almost as good as what the chemist had made. Enough polymer was made in the 10 gallon reactor for expensive qualification trials. The trials were a success. Management was happy and told the engineers to design a 1000 gallon vessel.

Now the story turns bad. The engineers were not rash enough to attempt a direct scaleup with $S = 100$, but first went to a 100 gallon vessel for a test with $S = 10$. There they noted a significant exotherm and found that the polymer had a broader molecular weight distribution than on the small scale. The product was probably acceptable but was different from what had been so carefully tested. Looking back at the data from the 10 gallon runs, yes there was a small exotherm but it had seemed insignificant. Looking ahead to a 1000 gallon reactor and

(finally) doing the necessary calculations, the exotherm would clearly become intolerable. A mixing problem had also emerged. One ingredient in the fed-batch recipe was reacting with itself rather than with the target molecule. Still, the engineers designed a 2000 gallon reactor that might have handled the heat load. The reactor volume was 2000 gallons rather that 1000 to accommodate the great mass of cooling coils. Obviously, these coils would significantly change the flow in the vessel so that the standard correlation for heat transfer to internal coils could not be trusted. The consultant was asked what to do?

SOLUTION: There were several possibilities, but the easiest to design and implement with confidence was a shell-and-tube heat exchanger in an external loop. Switching the feed point for the troublesome ingredient to the loop also allowed its rapid and controlled dilution even though the overall mixing time in the vessel was not significantly changed by the loop.

There is one significant difference between batch and continuous stirred tanks. The heat balance for a CSTR depends on the inlet temperature, and T_{in} can be adjusted to achieve a desired steady state. As discussed in Section 5.3.1, this is a very scaleable approach to reactor design.

5.3.3 Scaling Up Stirred Tanks with Boiling

We distinguish three situations where boiling occurs in a stirred tank:

1. The bulk fluid is below the boiling point, agitation is moderate, and the vessel is heated through the jacket. Nucleate boiling gives bubbles at the metal surface but they rapidly collapse when they leave the surface. There is little change in overall density due to the bubble volume, and what change there is decreases upon scaleup, as does the amount of heat that can be transferred. This form of heat transfer scales at $S^{2/3}$ just like sensible heat transfer to the vessel contents.
2. The bulk fluid at its boiling point but agitation is good and few bubbles form on the metal surfaces. Instead, homogeneous nucleation occurs near the surface of the liquid where the temperature exceeds the boiling point. The liquid head suppresses boiling deep within the vessel, and the bubble volume is typically a few percent of the liquid volume. This form of heat transfer also scales as $S^{2/3}$.
3. An exothermic reaction generates heat throughout the vessel, and boiling occurs by homogeneous nucleation. There will be temperature differences due to liquid head, but boiling will occur throughout the vessel with a consequent reduction in average density. Heat is removed by way of the heat of vaporization, and this form of heat transfer scales approximately as S^1. Vapor disengagement at the liquid surface will become limiting in very large vessels since the surface area scale only as $S^{2/3}$. Also, temperature differences between the top and bottom of the liquid could adversely affect reaction

selectivity. There is obviously a limit beyond which further scaleup is infeasible. However, this limit can be very large since some boiling reactor processes behave similarly with reactor volumes that vary by a factor of 100,000. Detailed models of how liquid density and reaction temperature vary with liquid height in reaction-heated stirred tanks have not been reported, but history has shown that incremental scaleup with modest value of S is possible.

In some chemical systems, boiling can create relatively stable foams. Foams can also result from the release of a gaseous byproduct. Such problems are usually apparent on the small scale. Anti-foaming agents are sometimes effective.

5.3.4 Scaling Up Tubular Reactors

Convective heat transfer to fluid inside circular tubes depends on three dimensionless groups: the Reynolds number, $\mathbf{Re} = \rho d_t \bar{u}/\mu$, the Prandtl number, $\mathbf{Pr} = C_P \mu/\kappa$ where κ is the thermal conductivity, and the length-to-diameter ratio, L/d_t. These groups can be combined into the Graetz number, $\mathbf{Gz} = \mathbf{RePr}\, d_t/L = d_t^2/(\alpha \bar{t})$ where $\alpha = \kappa/(\rho C_P)$ is the thermal diffusivity. Commonly used correlations for the inside heat transfer coefficient are

$$\frac{h d_t}{\kappa} = 3.66 + \frac{0.085\mathbf{Gz}}{1 + 0.047\mathbf{Gz}^{2/3}} \left(\frac{\mu_{\text{bulk}}}{\mu_{\text{wall}}}\right)^{0.14} \quad \text{(deep laminar)} \tag{5.35}$$

for laminar flow and $\mathbf{Gz} < 75$,

$$\frac{h d_t}{\kappa} = 1.86\mathbf{Gz}^{1/3} \left(\frac{\mu_{\text{bulk}}}{\mu_{\text{wall}}}\right)^{0.14} \quad \text{(laminar)} \tag{5.36}$$

for laminar flow and $\mathbf{Gz} > 75$ and

$$\frac{h d_t}{\kappa} = 0.023\mathbf{Re}^{0.8}\mathbf{Pr}^{1/3} \left(\frac{\mu_{\text{bulk}}}{\mu_{\text{wall}}}\right)^{0.14} \quad \text{(fully turbulent)} \tag{5.37}$$

for $\mathbf{Re} > 10,000$, $0.7 < \mathbf{Pr} < 700$ and $L/d_t > 60$.

These equations apply to ordinary fluids (not liquid metals) and ignore radiative transfer. Equation 5.35 is rarely used and applies to very low **Re** or very long tubes. No correlation is available for the transition region, but Equation 5.36 should provide a lower limit on $h d_t/\kappa$ in the transition region. The dimensionless number, $h d_t/\kappa$, is the Nusselt number, **Nu**.

Approximate scaling behavior for incompressible fluids based on Equations 5.35–5.37 is included in Tables 3.1–3.3 together with pressure drop and other scaling relationships. Scaling in parallel is not shown since the scaling factors for a single tube would all be 1. The results in these tables apply to incompressible fluids, although some of the results may be used for gases when the pressure drop is low.

The reader is reminded of the usual caveat**:** detailed calculations are needed to confirm any design. The scaling exponents are approximate. They are used for

conceptual studies and to focus attention on the most promising options for scaleup. The results in Tables 3.1–3.3 ignore the 0.14 power correction terms for viscosity in Equations 5.35–5.37. This correction becomes larger, and decreases heat transfer, if the driving force, ΔT, is increased in magnitude when cooling. For the deep laminar region, the range on Nusselt number predicted by Equation 5.36 is small, $3.66 < \mathbf{Nu} = h d_t/\kappa < 7.13$. The scalup factors in Table 3.1 apply to the lower limit, $\mathbf{Gz} \rightarrow 0$. The factors for the driving force, ΔT, set the heat transfer rate proportional to the throughput

EXAMPLE 5.10

A liquid phase, pilot plant reactor uses a 12-foot tube with a 1.049-inch ID. The working fluid has a density of 860 kg/m^3, the residence time in the reactor is 10.2 seconds, and the Reynolds number is 8500. The pressure drop in the pilot plant has not been accurately measured, but is known to be less than 1 psi. The entering feed is preheated and premixed. The inlet temperature is 60°C and the outlet temperature is 64°C. Tempered water at 55°C is used for cooling. Management loves the product and wants you to design a plant that is a factor of 128 scaleup over the pilot plant. Propose scaleup alternatives and explore their thermal consequences.

SOLUTION: Table 3.3 provides the scaling relationships. The desired throughput and volume scaling factor is $S = 128$. Some alternatives for the large plant are:

Parallel: Put 128 identical tubes in parallel using a shell-and-tube design. The total length of tubes will be 1536 feet, but they are compactly packaged. All operating conditions are identical on a per-tube basis to those used in the pilot plant.

Series : Build a reactor that is 1536 feet long. Use U-bends or coiling to make a reasonable package. The length-to-diameter ratio increases to $137S = 17{,}600$. The Reynolds number increases to $8500S = 1.1 \times 10^6$, and the pressure drop will be $S^{2.75} = 623{,}000$ times greater than it was in the pilot plant. The temperature driving force changes by a factor of $S^{-0.8} = 0.021$, decreasing from 7°C to 0.14°C. The production unit would have to restrict the water flow rate to hold this low a ΔT. Note that the driving force for turbulent flow should be based on the log-mean ΔT. The difference is minor, and approximations can be justified in a scaling study. When a reasonable scaleup is found, more accurate estimates can be made. The current calculations are accurate enough to show that a series scaleup is unreasonable based on pressure drop and packaging concerns.

Geometric similarity: Build a reactor that is nominally $12S^{1/3} = 61$ feet long and $1.049S^{1/3} = 5.3$ inches in diameter. Use U-bends to give a reasonable footprint. Correct to a standard pipe size in the detailed design phase. The length-to-diameter ratio is unchanged in a geometrically similar scaleup. The Reynolds number increases to $8500S^{2/3} = 216{,}000$, and the pressure drop increases by factor of $S^{1/2} = 11.2$. The temperature driving force will increase by a factor of $S^{0.13} = 1.9$ to about 13°C so that the jacket temperature would be about 49°C. This design seems reasonable.

Constant pressure: Build a reactor that is nominally $12S^{5/27} = 29$ feet long and $1.049S^{11/27} = 7.6$ inches in diameter. The length-to-diameter ratio decreases by a factor of $S^{-2/9}$ to 47. The Reynolds number increases to $8500S^{16/27} = 151{,}000$. The

temperature driving force must increase by a factor of $S^{0.34} = 5.2$ to about 36°C so that the jacket temperature would be about 26°C. This design is also reasonable, but the jacket temperature is a bit lower than is normally possible without a chiller.

There is no unique solution to this or most other design problems. Any design using a single tube with an ID of about 7.5 inches or less and with a volume scaled by S will probably function from a reaction engineering viewpoint. The shell-and-tube heat exchanger will also work and is likely to be the most cost effective design.

EXAMPLE 5.11

The turbulent scaling factors in Table 3.3 suggest that scaling a tubular reactor with ***constant heat transfer*** per unit volume and unit throughput at constant $\bar{t}$ is possible even with the further restriction that the temperature driving force be the same in the large and small units. Find the various scaling factors for this form of scaleup for turbulent liquids and apply them to the pilot reactor in Example 5.10.

SOLUTION: Since the fluid is incompressible, $S_{\text{throughput}} = S$, and Table 3.3 gives the driving force scaling factor as $S^{0.2}S_R^{0.8}S_L^{-1}$. This is set to 1. Setting $S_R^2 S_L = S$ imposes a constant residence time. There are two equations and two unknowns, S_R and S_L. The solution is $S_R = S^{0.28}$ and $S_L = S^{0.44}$. The length-to-diameter ratio scales as $S^{0.16}$. The scaling factor for pressure drop is $S^{0.86}$. The Reynolds number scales as $S/S_R = S^{0.72}$

Applying these factors to the $S = 128$ scaleup in Example 5.10 gives a tube that is nominally $12S^{0.44} = 101$ feet long and $1.049S^{0.28} = 4.1$ inches in diameter. The length-to-diameter ratio increases to 298. The Reynolds number increases to $8500S^{0.72} = 278{,}000$. The pressure drop would increase by a factor of $S^{0.86} = 65$. The temperature driving force would remain constant at 7°C so that the jacket temperature would remain 55°C. This too would be a reasonable design.

EXAMPLE 5.12

Repeat Examples 5.10 and 5.11 for $T_{\text{in}} = 160$°C and $T_{\text{out}} = 164$°C. The coolant temperature remains at 55°C,

SOLUTION: Now, $\Delta T = 107$°C. Scaling with geometric similarity would force the temperature driving force to increase by $S^{0.13} = 1.9$ as before, but the scaled up value for ΔT is now 201°C so that the coolant temperature would drop to −39°C, technically feasible but undesirable. Scaling with constant pressure forces an even lower coolant temperature. A scaleup using a shell-and-tube reactor is feasible but scaling with constant heat transfer should be considered.

These examples show that the ease of scaling up of tubular reactors depends on the heat load. With moderate heat loads, single tube scaleups are possible. Multitubular scaleups become attractive for when the heat load is high, although it may not be necessary to go to full parallel scaling with $N_{\text{tube}} = S$. The easiest way to apply the scaling relations in Tables 3.1–3.3 to multitubular reactors is to assume a number of tubes and to divide S by that number. Just regard the quotient as the volumetric and throughput scaling factor per tube.

EXAMPLE 5.13

An existing shell-and-tube heat exchanger is available for the process in Example 5.10. It has 20 tubes, each 2 inches ID and 18 feet long. How will it perform?

SOLUTION: The volume of the existing heat exchanger is 7.85 ft^3. The volume of the pilot reactor is 0.072 ft^3. Thus, at constant $\bar{t}$, the scaleup is limited to a factor of 109 rather than the desired 128. The per-tube scaling factor is $S = 109/20 = 5.45$. $S_R = 1.91$ and $S_L = 1.5$. The general scaling factor for pressure drop in turbulent, incompressible flow is $S^{1.75} S_R^{-4.75} S_L = 1.35$ so that the upstream pressure increases modestly. The scaling factor for ΔT is $S^{0.2} S_R^{0.8} S_L^{-1} = 1.57$ so $\Delta T = 11^\circ$C and the coolant temperature will be 51°C. What about the deficiency in capacity? Few marketing estimates are that accurate. If the factor of 109 scaleup becomes inadequate, a second or third shift can be added. If operation on a 24/7 basis is already planned – as is common in the chemical industry – the operators may nudge the temperatures a bit in an attempt to gain capacity. Presumably, the operating temperature was already optimized in the pilot plant, but it is a rare process that cannot be pushed a bit further.

This section has based scaleups on pressure drops and temperature driving forces. Any consideration of mixing, and particularly the closeness of approach to piston flow, has been ignored. Mixing effects in tubular reactors are discussed in Chapters 8 and 9. If the flow is turbulent and if the Reynolds number increases upon scaleup (as is normal), and if the length-to-diameter ratio does not decrease upon scaleup, then the reactor will approach piston more closely upon scaleup. Substantiation for this statement can be found by applying the axial dispersion model discussed in Section 9.3. All the scaleups discussed in Examples 5.10–5.13 should be reasonable from a mixing viewpoint since the scaled up reactors will approach piston flow more closely.

SUGGESTED FURTHER READINGS

Chemical theoreticians would like to determine reaction rates, including temperature dependence, by ab initio calculations (i.e., from first principles). This remains an exercise for the future. See:

E. Pollak and P. Talkner, "Reaction rate theory: What it was, where is it today, and where is it going?" *Chaos*, **15,** 026116 (2005).

For design calculations, scaleup methods, and a wealth of practical know how related to stirred tanks, the best reference is:

E. L. Paul et al., *Handbook of Industrial Mixing*, Wiley, New York, 2003.

A reasonable starting point for design equations relevant to tubular reactors (pressure drop, heat transfer coefficients, standard pipe and tubing sizes) remains:

Perry's Handbook, 7th ed., McGraw-Hill, New York, 1997.

Another useful design reference is:

A. K. Coker, *Ludwig's Applied Process Design for Chemical and Petrochemical Plants*, 4th ed., Gulf Professional Publishing, 2007.

Use it or other detailed sources after preliminary scaling calculations have been made. Similar information, including canned programs, is becoming available on the Internet.

PROBLEMS

5.1 A reaction takes one hour to complete at 60°C and 50 minutes at 65°C. Estimate the activation energy. What assumptions were necessary for your estimate?

5.2 Dilute acetic acid is to be made by the hydrolysis of acetic anhydride at 25°C. Pseudo-first order rate constants are available at 10°C and 40°C. They are $k = 3.40\ \text{hr}^{-1}$ and $22.8\ \text{hr}^{-1}$, respectively. Estimate k at 25°C.

5.3 Calculate $b_{\text{out}}/a_{\text{in}}$ for the reversible reaction in Example 5.2 in a CSTR at 280 K and 285 K with $\bar{t} = 2$ hr. Suppose these results were actual measurements and that you did not realize the reaction was reversible. Fit a first order model to the data to find the apparent activation energy. Discuss your results.

5.4 At extreme pressures, liquid phase reactions exhibit pressure effects. A suggested means for correlation is the ***activation volume***, ΔV_{act}:

$$k = k_0 \exp\left(\frac{-\Delta E}{R_g T}\right) \exp\left(\frac{-\Delta V_{\text{act}} P}{R_g T}\right)$$

Di-t-butyl peroxide is a commonly used free-radical initiator that decomposes according to first order kinetics. Use the following data (Walling and Metzger, 1959) to estimate ΔV_{act} for the decomposition in toluene at 120°C.

P, kg cm^{-2}	k, s^{-1}
1	13.4×10^{-6}
2040	9.5×10^{-6}
2900	8.0×10^{-6}
4480	6.6×10^{-6}
5270	5.7×10^{-6}

5.5 Consider the consecutive reactions, $A \xrightarrow{k_I} B \xrightarrow{k_{II}} C$, with rate constants of $k_I = 10^{15} \exp(-10000/T)$ and $k_{II} = 10^8 \exp(-5000/T)$. Find the temperature that maximizes b_{out} for a CSTR with $\bar{t} = 2$ and for a batch reactor with a reaction time of 2 hours. Assume constant density with $b_{\text{in}} = c_{\text{in}} = 0$.

5.6 Find the temperature that maximizes b_{out} for the competitive reactions $A \xrightarrow{k_I} B$ and $A \xrightarrow{k_{II}} C$. Do this for a CSTR with $\bar{t} = 2$ and for a batch reactor with a reaction time of 2 hours. Assume constant density with $b_{\text{in}} = c_{\text{in}} = 0$. The rate constants are $k_I = 10^8 \exp(-5000/T)$ and $k_{II} = 10^{15} \exp(-10000/T)$.

5.7 The reaction $A \xrightarrow{k_I} B \xrightarrow{k_{II}} C$ is occurring in an isothermal, piston flow reactor having a mean residence time of 2 min. Assume constant cross section and physical properties and

$$k_I = 1.2 \times 10^{15} \exp(-12{,}000/T),\ \text{min}^{-1}$$
$$k_{II} = 9.4 \times 10^{15} \exp(-14{,}700/T),\ \text{min}^{-1}$$

(a) Find the operating temperature that maximizes b_{out} given $b_{in} = 0$.

(b) The laboratory data were confused: k_I was interchanged with k_{II}. Revise your answer accordingly.

5.8 (a) A CSTR is mechanically agitated using a 200-kW motor. The throughput is 25,000 kg/hr of a liquid that has a specific heat of 1900 J kg^{-1} K^{-1}. Assume operation at full load and ignore bearing, gear and seal losses. What is the temperature increase due to the agitator power?

(b) Suppose the throughput is stopped. How fast will the temperature increase if the vessel volume is 25 m^3? Ignore heat losses to the environment.

5.9 Repeat the analysis of hydrocarbon cracking in Example 5.6 with $a_{in} = 100$ gm/ m^3.

5.10 Repeat the analysis of hydrocarbon cracking in Example 5.6 for the case where there is external heat exchange. Suppose the reaction is conducted in tubes 0.012 m in diameter and 3 m long. The inside heat transfer coefficient is 9.5 cal K^{-1} m^{-2} s^{-1} and the wall temperature is 525°C. The inerts are present.

5.11 For the styrene polymerization in Example 5.7, determine that value of T_{in} below which only the lower steady state is possible. Also determine that value of T_{in} above which only the upper steady state is possible.

5.12 For the styrene polymerization in Example 5.7, determine those values of the mean residence time that give one, two, or three steady states

5.13 The pressure drop was not measured in the pilot plant in Example 5.10, but the viscosity must be known since the Reynolds number is given. Use it to calculate the pressure drop. Does your answer change the feasibility of any of the scaleups in Examples 5.10–5.13?

5.14 Determine the reactor length, diameter, Reynolds number and scaling factor for pressure drop for the scaleup with constant heat transfer in Example 5.11.

5.15 Your company is developing a highly proprietary new product. The chemistry is complicated, but the last reaction step is a dimerization:

$$2A \xrightarrow{k} B$$

Laboratory kinetic studies gave $a_0 k = 1.7 \times 10^{13} \exp(-14000/T)$, s^{-1}. The reaction was then translated to the pilot plant and reacted in a 10-liter batch reactor according to the following schedule:

Time from Start of Batch (mins)	Action
0	Begin charging raw materials
15	Seal vessel; turn on jacket heat (140°C steam)
90	Vessel reaches 100°C and reflux starts
180	Reaction terminated; vessel discharge begins
195	Vessel empty; washdown begins
210	Reactor clean, empty, and cool

Management likes the product and has begun to sell it enthusiastically. The pilot plant vessel is being operated around the clock and produces two batches per shift for a total

of 42 batches per week. It is desired to increase production by a factor of 1000, and the engineer assigned to the job ordered a geometrically similar vessel that has a working capacity of 10,000 liters.

(a) What production rate will actually be realized in the larger unit? Assume the heat of reaction is negligible.

(b) You have replaced the original engineer and been told to achieve the forecast production rate of 1000 times the pilot rate. What might you do to achieve this? (You might think the engineer was fired. More likely, he was promoted based on the commercial success of the pilot plant work, is now your boss, and will expect you to deliver planned capacity from the reactor he ordered).

5.16 A liquid phase, pilot plant reactor uses a 0.1-m^3 CSTR with cooling at the walls. The working fluid has waterlike physical properties. The residence time in the reactor is 3.2 h. The entering feed is preheated and premixed. The inlet temperature is 60°C and the outlet temperature is 64°C. Tempered water at 55°C is used for cooling. The agitator speed is 600 RPM. Management loves the product and wants you to scale up by a modest factor of 20. However, for reasons obscure to you, they insist that you maintain the same agitator tip speed. Thus the scaleup will use a geometrically similar vessel with $N_I D$ held constant.

(a) Assuming highly turbulent flow, by what factor will the total power to the agitator increase in the larger, 2 m^3 reactor?

(b) What should be the temperature of the cooling water temperature to keep the same inlet and outlet temperatures for the reactants?

Chapter 6

Design and Optimization Studies

The goal of this chapter is to provide semirealistic design and optimization exercises. Design is a creative endeavor that combines elements of art and science. It is hoped that the examples presented here will provide some appreciation of the creative process.

The chapter introduces several optimization techniques. The emphasis is on robustness and ease of use rather than computational efficiency.

6.1 CONSECUTIVE REACTION SEQUENCE

The first consideration in any design and optimization problem is to determine the boundaries of "the system." A reactor can rarely be optimized without considering the upstream and downstream processes connected to it. This chapter attempts to integrate the reactor design concepts of Chapters 1–5 with process economics. The goal is an optimized process design that includes the costs of product recovery, recycling, and byproduct disposition. The reactions are

$$\mathrm{A} \xrightarrow{k_{\mathrm{I}}} \mathrm{B} \xrightarrow{k_{\mathrm{II}}} \mathrm{C} \tag{6.1}$$

where A is the raw material, B is the desired product, and C an undesired byproduct. The process flow diagram is given in Figure 6.1. For simplicity, the recovery system is assumed able to make a clean separation of the three components without material loss.

Note that the production of C is not stoichiometrically determined. Varying the reaction conditions will change the relative amounts of B and C. Had C been stoichiometrically determined, as in the production of byproduct HCl when hydrocarbons are directly chlorinated, there is nothing that can be done short of very fundamental changes to the chemistry, for example, using ClO_2 rather than Cl_2. Philosophically at least, this is a problem for a chemist rather than a chemical engineer. In the present example, component C is a secondary or side product such as a disubstituted compound when monosubstitution is desired. The chemical reaction engineer has many options for improving performance without changing the basic chemistry.

Chemical Reactor Design, Optimization, and Scaleup, Second Edition. By E. B. Nauman
Copyright © 2008 John Wiley & Sons, Inc.

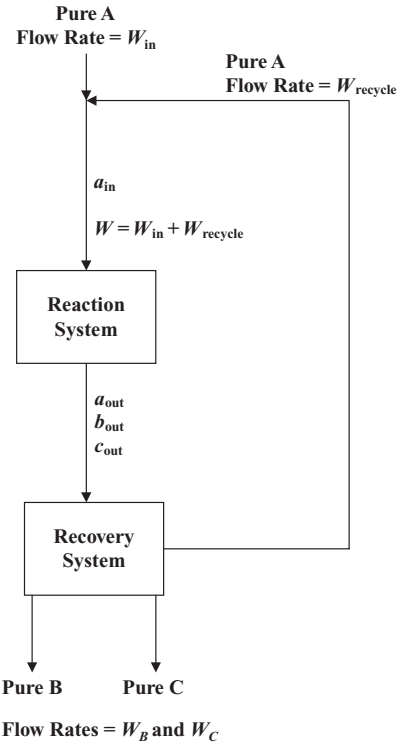

Figure 6.1 Simplified process flow diagram for a consecutive reaction process.

Few reactions are completely clean in the sense of giving only the desired product. There are some cases where the side products have commensurate value with the main products, but these cases are becoming increasingly rare even in the traditional chemical industry and are essentially nonexistent in fields like pharmaceuticals. Sometimes, C is a hazardous waste and has a large, negative value.

The structure of the reactions in Equation 6.1 is typical of an immense class of industrially important reactions. It makes little difference if the reactions are all second order. Thus, the reaction set

$$A_1 + A_2 \rightarrow B_1 + B_2 \rightarrow C_1 + C_2 \tag{6.2}$$

has essentially the same structure. The A's can be lumped as the raw material, the B's can be lumped as product even though only one may be useful (the other is stoichiometrically determined), and the C's can be lumped as undesired. The reaction mechanism and the kinetics are different in detail, but the optimization methodology and economic analysis will be very similar

EXAMPLE 6.1

Show by example that it is generally necessary to include the cost of recovering the product and recycling unused reactants in the reactor design optimization.

SOLUTION: Suppose component C in Equation 6.1 is less valuable than A. Then, if the cost of the recovery step is ignored, the optimal design is a high-throughput reactor that operates at high concentrations of A, low concentrations of B, and even lower concentrations of C. Component B is recovered (at zero cost!), component C is discarded at cost but in negligible amounts, and component A is recycled. Essentially all the incoming A will be converted to B or recycled. Thus, the reaction end of the process will consist of a cheap reactor with nearly 100% raw material efficiency after recycling. Of course, huge quantities of reactor effluent must be separated in order to recover the miniscule amounts of products, B and C, and the huge amounts of A to be recycled, but that is the problem of the separations engineer.

In fairness, processes do exist where the cost of the recovery step has little influence on the reactor design, but they are the exceptions.

The rest of this chapter is a series of examples and problems built around semirealistic scenarios of reaction characteristics, reactor costs, and recovery costs. The object is not to reach general conclusions but to demonstrate a method of approaching such problems and to provide an introduction to optimization techniques.

Assume for now that the reactions in Equation 6.1 are first order with rate constants

$$k_1 = 4.5 \times 10^{11} \exp\left(-\frac{10,000}{T}\right) \text{h}^{-1}$$
$$k_2 = 4.2 \times 10^{20} \exp\left(-\frac{19,000}{T}\right) \text{h}^{-1} \tag{6.3}$$

Table 6.1 illustrates the behavior of the rate constants as a function of absolute temperature.

Low temperatures favor the desired, primary reaction, but the rate is low. If reactor volume were free, you could run at low temperatures and achieve a reasonable yield of B with very little C. Raise the rate enough to give a reasonable reactor volume and the undesired, secondary reaction becomes significant. For any reactor volume, there will be an interior optimum with respect to temperature.

Table 6.1 Effect of Temperature on Rate Constants

T, K	k_1, h^{-1}	k_1/k_2
300	0.002	11,450
310	0.004	4,350
320	0.012	1,756
330	0.031	749
340	0.076	336
350	0.176	158
360	0.389	77
370	0.823	39
380	1.677	21
390	3.292	11
400	6.250	6

Both reactions are endothermic:

$$\frac{(\Delta H_R)_{\mathrm{I}} a_{\mathrm{in}}}{\rho C_P} = \frac{(\Delta H_R)_{\mathrm{II}} a_{\mathrm{in}}}{\rho C_P} = 30\,\mathrm{K} \tag{6.4}$$

Recall the negative convention on ΔH_R imposed by mechanical engineers and history. Thus if the reaction went to completion in an adiabatic reactor with all A converted to C, the temperature would decrease by 60 K.

Following are some data applicable to a desired plant to manufacture component B of Equation 6.1:

All three components, A, B, and C, have a molecular weight of 200.

Required production rate is 50,000 tons y^{-1} (metric tons) = 6250 kg h^{-1}.

Cost of raw material A is \$1.50 kg^{-1}.

Value of side product C is \$0.30 kg^{-1}.

Note that 8000 h is a commonly used standard "year" for continuous processes. The remainder of the time is for scheduled and random maintenance. In a good year when demand is high, production personnel have the opportunity to exceed their planned output.

You can expect the cost of A and the value of C to be fairly accurate. The required production rate is a marketing guess. So is the selling price of B, which is not shown above. For now, assume it is high enough to justify the project. Your job is the conceptual design of a reactor to produce the required product at minimum total cost.

Following are capital and operating cost estimates for the process:

Reactor capital costs: $\$8{,}000{,}000V^{0.6}$

Reactor operating costs (excluding raw materials): \$0.07 kg^{-1} of reactor throughput

Recovery system capital cost: $\$210W^{0.6}$

Recovery system operating costs \$0.20 kg^{-1} of recovery system throughput

where V is the reactor volume in cubic meters and W is the total mass flow rate of A into the reactor (virgin + recycle) in kilograms per year. Options in reactor design can include CSTRs, shell-and-tube reactors, and single-tube reactors, particularly a single adiabatic tube. The cost of these different reactors may all scale similarly, for example, as $V^{0.6}$, but the base-case cost, say at $V = 1$, will be different. The CSTRs are more expensive than shell-and-tube reactors, which are more expensive than adiabatic single tubes. However, in what follows, the same capital cost will be used for all reactor types in order to emphasize inherent kinetic differences. This will bias the results toward CSTRs and shell-and-tube reactors over most single-tube designs.

Why are the CSTRs worth considering at all? They are more expensive per unit volume and less efficient as chemical reactors (except for autocatalysis). The CSTRs are useful for some multiphase reactions, but that is not the situation here. A potential justification is to remove the heat of reaction by boiling, but the example reactions are endothermic. Boiling (autorefrigerated) reactors can still be used

for precise temperature control. The shell-and-tube reactors cost less but offer less effective temperature control. Adiabatic reactors have no control at all except for T_{in}.

As shown in Figure 6.1, the separation step has been assumed to give clean splits, pure A being recycled back to the reactor. As a practical matter, the B and C streams must be clean enough to sell. Any C in the recycle stream will act as an inert (or it may react to some component D). Any B in the recycle stream invites the production of undesired C. A final design analysis would have the recovery system costs vary as a function of purity of the recycle stream, but we avoid this complication for now.

The operating costs are based on total throughput for the process. Their main components are utilities and maintenance costs along with associated overheads. Some costs like labor will be more or less independent of throughput in a typical chemical plant. There may be differences in operating costs for the various reactor types, but we will worry about them, like the difference in capital costs, only if the choice is a close call. The total process may include operations other than reaction and recovery and will usually have some shared equipment such as the control system. These costs are ignored since the task at hand is to design the best reaction and recovery process and not to justify the overall project. That may come later. The dominant uncertainty in justifying most capacity expansions or new product introductions is marketing. How much can be sold at what price?

Some of the costs are for capital and some are operating costs. How to convert apples to oranges? The proper annualization of capital costs is a difficult subject. Economists, accountants, and corporate managers may have very different viewpoints. Your company may have a cast-in-stone rule. Engineers tend to favor precision and have invented a complicated, time-dependent scheme (***net present value***, or ***NPV***, analysis) that has its place (on a Fundamentals of Engineering exam among other places) but can impede understanding of cause and effect. We will adopt the simple rule that the annual cost associated with a capital investment is 25% of the investment. This accounts for depreciation plus a return on fixed capital investment. Working capital items (cash, inventory, accounts receivable) will be ignored on the grounds that they will be similar for all the options under consideration.

EXAMPLE 6.2

Cost out a process governed by Equation 6.1 that uses a single CSTR for the reaction. Ignore the energy balance and assume that any desired temperature can be imposed on the reactor.

SOLUTION: The reactor design equations are very simple:

$$\begin{aligned} a_{out} &= \frac{a_{in}}{1 + k_1\bar{t}} \\ b_{out} &= \frac{b_{in} + k_1\bar{t}(a_{in} + b_{in})}{(1 + k_1\bar{t})(1 + k_2\bar{t})} \\ c_{out} &= c_{in} + a_{in} - a_{out} + b_{in} - b_{out} \end{aligned} \tag{6.5}$$

The total product demand is fixed. The adjustable parameters are the reactor volume V and the temperature T_{out}. These are the variables that determine the reactor performance, but the

calculation of yield is complicated because the throughput is not specified. Instead, the output of B is specified and the necessary input of A must be found. We suppose that the temperature in the CSTR, T_{out}, can be set arbitrarily. Pick values for T_{out} and V. Then guess a value for the total flow rate W, which is the sum of virgin A flow, W_{in}, and the recycle flow, $W_{recycle}$. All these streams are pure A. The amount of B in the reactor effluent is calculated and compared to the required value of 6250 kg h^{-1}. The guessed value for W is then adjusted. The Basic program in Code for Example 6.2 uses a *binary search* to adjust the guess. A simple example of a binary search is given in Code for Example 4.14.

Code for Example 6.2

```
Private MwA, MwB, MwC, rho, ain, hr1, hr2, k10, k20, AT1, AT2
Private V, Tin, Tout, Q, Win, tbar, aout, bout, cout

Sub Example6_2()
'Code for Example 6.2

V = 100
Tout = 350
Call GetData
Call Balance
Call Cost(UnitCost)
Cells(1, 1) = UnitCost

End Sub  'End of main routine

Sub GetData()
'This subroutine is used to input data

MwA = 200          'kg/kg moles
MwB = 200
MwC = 200
rho = 900          'kg/m^3
ain = rho / MwA    'kg-mol/m^3
rho = 900          'kg/m^3
ain = rho / MwA    'kg-moles/m^3
hr1 = 30 / ain     'heat of reaction, K
hr2 = 30 / ain
k10 = 450000000000#
AT1 = 10000
k20 = 4.2E+20
AT2 = 19000

End Sub
_____________________________________________________________
Sub Balance()
'This subroutine uses a binary search to close the material balance.

Wmin = 6250    'lower bound, kg/hr
Wmax = 1000000  'upper bound
For I = 1 To 24
   W = (Wmin + Wmax) / 2
   Q = W / rho
```

```
   tbar = V / Q
   Call Reactor
   WB = bout * Q * MwB
   If WB > 6250 Then
      Wmax = W
   Else
      Wmin = W
   End If
Next I
Waout = Q * aout * MwA


WC = Q * cout * MwC
Win = WB + WC

End Sub
```

```
Sub Reactor()
'This reactor subroutine is for a single CSTR

   k1 = k10 * Exp(AT1 / Tout)
   k2 = k20 * Exp(AT2 / Tout)

   aout = ain / (1 + k1 * tbar)
   bout = (k1 * tbar * ain) / (1 + k1 * tbar) / (1 + k2 * tbar)
   cout = ain - aout - bout

End Sub
```

```
Sub Cost(UnitCost)
'The unit cost of production is calculated

   WB = bout * Q * MwB
   WC = cout * Q * MwC
   Win = WB + WC
   W = Q * rho
   RMCost = Win * 1.5 * 8000
   ByproductCredit = WC * 0.3 * 8000
   ThroughputCost = W * (0.2 + 0.07) * 8000
   ReactorCapital = 8000000 * V ^ 0.6
   SeparationCapital = 210 * (W * 8000) ^ 0.6
   Capital = ReactorCapital + SeparationCapital
   Annualized = 0.25 * Capital
   TotalCost = RMCost - ByproductCredit + ThroughputCost + Annualized
   UnitCost = TotalCost / WB / 8000
   Stop 'Allows all cost variables to be examined in the debug mode

End Sub
```

The original design concept was to use a large reactor operating at a relatively low temperature in order to minimize byproduct production. The maximum size of a vessel that can be shipped to a plant site via rail or road is about 100 m^3. The width is the limiting dimension. It is on the order of 14.5 ft and this restricts prefabricated vessel sizes to about 100 m^3unless there is water access to the site. Larger vessels can be field erected but at substantially higher cost. The results for a single CSTR operating at $T = T_{out} = 350$ K and $V = 100$ m^3 are as follows:

Feed rate, pure A	6310	kg h^{-1}
Product rate, component B	6250	kg h^{-1}
Byproduct rate, component C	60	kg h^{-1}
Raw materials cost	76	MM$ yr^{-1}
Byproduct credit	0.1	MM$ yr^{-1}
Throughput cost	23	MM$ yr^{-1}
Reactor capital cost	127	MM$
Separation capital cost	12	MM$
Annualized capital cost	35	MM$ yr^{-1}
Total annual cost	133	MM$ yr^{-1}
Unit cost of product	2.66	$ kg^{-1}

Note that MM$ or $MM are commonly used shorthand for millions of dollars. Marketing cringes at the $2.66 cost per kilogram and the reactor cost (even installed with a control system and all ancillary services) is outrageous. Engineering needs to come up with something better.

This example found the reactor throughput that would give the required annual production of product B. For prescribed values of the design variables T and V there may not be a solution. If there is a solution, it is unique. The program uses a binary search to find the answer, but another ***root finder*** could be used instead. For the same accuracy, Newton's method (see Appendix 4.1) requires about 3 times fewer function evaluations (i.e., calls to the Reactor subroutine). The saving in computation time is trivial in the current example but could be important if the reactor model is a complicated, distributed parameter model such as those in Chapters 8 and 9.

The next phase of the problem is to find those values for T, and V that will give the lowest product cost. This is a problem in ***optimization*** rather than root finding. Numerical methods for optimization are described in Appendix 6.1. The present example of consecutive, mildly endothermic reactions provides exercises for these optimization methods.

EXAMPLE 6.3

Find the values of T and V that give the lowest production cost for the consecutive reactions of Example 6.2.

SOLUTION: The most straightforward way to optimize a function is by a brute-force search. Code for Example 6.3 does this using subroutines developed in Code for Example 6.2. Results from such a search are shown in Table 6.2. The example reaction sequence shows a board range of values for T and V that give close to the minimum cost. The engineer should rejoice. Since the cost is relatively insensitive to the design choices, decisions should be reasonable despite model error.

Table 6.2 Annualized Unit Costs for Single CSTR Process

	V, m^3						
T, K	6	8	10	12	14	16	18
374	11.38	3.10	2.53	2.39	2.33	2.31	2.31
375	10.73	2.82	2.46	2.35	2.32	**2.30**	2.31
376	5.06	2.65	2.40	2.33	2.31	**2.30**	2.31
377	3.67	2.54	2.37	2.31	**2.30**	**2.30**	2.32
378	3.12	2.46	2.34	**2.30**	**2.30**	2.31	2.33
379	2.84	2.41	2.32	**2.30**	2.31	2.32	2.34
380	2.67	2.37	2.31	**2.30**	2.31	2.34	2.36
381	2.55	2.34	**2.30**	2.31	2.33	2.35	2.39
382	2.47	2.33	**2.30**	2.32	2.34	2.38	2.41
383	2.42	2.32	2.31	2.33	2.36	2.40	2.44
384	2.38	2.31	2.32	2.35	2.39	2.43	2.48

Code for Example 6.3

```
Private MwA, MwB, MwC, rho, ain, hr1, hr2, k10, k20, AT1, AT2
Private V, Tin, Tout, Q, Win, tbar, aout, bout, cout

Sub Example6_3()

Call GetData 'See Code for Example 6.2

For Ivol = 0 To 8
For ITemp = 0 To 15
   Tout = 342 + 1 * ITemp
   V = 90 + 40 * Ivol
   Cells(ITemp + 2, 1) = Tout
   Cells(1, Ivol + 2) = V
   Call Balance  'See Code for Example 6.2

   Call Cost(UnitCost) 'See Code for Example 6.2

   Cells(ITemp + 2, Ivol + 2) = UnitCost

Next ITemp
Next Ivol

End Sub  'End of main routine
```

Table 6.3 Capital Costs in $MM for Single CSTR Process.

	V, m^3						
T, K	6	8	10	12	14	16	18
374							
375						54.35	
376						54.15	
377				48.37	51.15	53.99	
378				48.08	50.96		
379				47.84			
380				47.65			
381			44.42				
382			44.22				
383							
384							

Note: The unit cost for the various cases is approximately equal at about \$2.30 kg^{-1}.

It turns out that the 100-m^3 reactor is grossly oversized. The boldface values in Table 6.2 show a valley in the $V - T$ plane where the annualized unit cost rounds to \$2.30 kg^{-1}. Marketing is somewhat relieved. A more detailed search shows what appears to be a minimum at $V = 12$ m^3 and $T = 379$ K with an associated cost of \$2.3001 kg^{-1}. Within the boldface area, the maximum cost difference is about \$0.005 kg^{-1}. At a production rate of 50,000,000 kg y^{-1}, the annual cost difference would be \$250,000. However, do not take this number too seriously. An economic prediction accurate to \$0.005 kg^{-1} is unrealistic for anything but an operating plant. There is model error, and there are other factors to consider before a design choice is made.

One consideration is risk capital. The marketing people may not be right. Management understands this and tends to be risk adverse. Table 6.3 shows the capital costs for the boldface region in Table 6.2.

A major factor in investment decisions is the amount of capital at risk. There is a reduction of about \$3MM in capital investment at the low-V, high-T end of the boldface region compared to the "optimum" at $V = 12$ m^3 and $T = 379$ K. Many companies would take this lower capital option in order to spend the \$3MM on another project or just to lower the amount of capital at risk.

More or less automatic ways of finding an optimum are described in Appendix 6.1. The simplest of these by far is the ***random-search*** method. It can be used for any number of optimization variables. It is extremely inefficient from the viewpoint of the computer but is joyously simple to implement. The time needed to reach an optimum depends on the initial guesses for variables and the range over which subsequent guesses are allowed to vary. The program is very fast for the single CSTR optimization. The final result is $V = 13.0$ m^3 and $T = 378$ K with a

Table 6.4 Spurious Local Optimum

	10	12	14
378	2.3384	2.3040	2.3006
379	2.3199	**2.3001**	2.3052
380	2.3088	2.3014	2.3140

unit cost of \$2.2996 kg^{-1}. We cite results to unrealistic precisions for purposes of comparison.

Compare the new minimum to the previously cited minimum at $V = 12$ and $T = 379$. The difference is inconsequential given uncertainties in the model. Even so, the interested reader may ask why the brute-force search technique of Example 6.3 failed to find the true optimum. One reason is obvious: The grid was too large. Another reason is more subtle and does not vanish just because the grid is small. Table 6.4 illustrates a problem that arises when optimizing a function by making one-at-a-time guesses.

The cost at $V = 12$ m^3 and $T = 379$ K is not the minimum but is lower than the entries above and below it, on either side of it, or even diagonally above or below it. Think about a stream that runs northeast to southwest through a valley. You are standing in the stream. Look straight north. It is uphill. Look straight south. It is uphill. Straight east is uphill. Straight west is uphill. Travel in any principal direction leads uphill, yet the stream flows downhill. Great care must be taken to avoid false optima. This is tedious to do manually even with only two variables and quickly becomes unmanageable as the number of variables increases.

The random-search method changes all variables at once to avoid this kind of trap. The technique requires a great many function evaluations, but the design equations for the CSTR are simple algebraic equations so the optimum is quickly found. More complicated reactions in a CSTR may need the method of false transients, and any reaction in a nonisothermal PFR will require the solution of simultaneous ODEs. Computing times may become annoyingly long if crude numerical methods continue to be used. However, crude methods are probably best when starting a complex program. Get them working; get a feel for the system, and then upgrade them.

The general rule in speeding up a computation is to start by improving the innermost loops. For the example problem, the subroutine Reactor cannot be significantly improved for the case of a single CSTR, but Runge–Kutta integration is better than Euler integration for PFR cases when ODEs must be solved to high precision. The next level of code is the overall material balance used to calculate the reactor throughput and residence time. Some form of Newton's method can be used instead of the binary search once you have a feel for the problem and know what are reasonable initial guesses. Also, physical reasoning may avoid infeasible regions. Finally, tackle the outer loop that comprises the optimization routine.

The next example treats isothermal and adiabatic PFRs.

EXAMPLE 6.4

Find the best combination of inlet temperature and reactor volume for the example reaction in an isothermal PFR and an adiabatic PFR.

SOLUTION: A program for evaluating the adiabatic reactor is given in Code for Example 6.4. The Reactor subroutine solves simultaneous ODEs for a_{out}, b_{out}, and $T(z)$. The example uses Runge–Kutta integration (see Appendix 2.1) for illustrative purposes, although Euler integration could have been used instead. The equation for temperature includes contributions from both reactions according to the methods of Section 5.2. Energy input from pumping is ignored. Newton's method is used to close the material balance. This is about four times faster than the binary search used in Example 6.2. The outermost loop is the optimization loop. It uses the random-search method to find optimal values for V and T_{in}.

As shown, Code for Example 6.4 treats the adiabatic case, but setting the heats of reaction to zero gives the isothermal case.

The computation is quite fast. Results for the three ideal reactor types are shown in Table 6.5. The CSTR is clearly out of the running, but the isothermal and adiabatic PFRs are a dead heat. Any reasonable shell-and-tube design would work. A few large-diameter tubes in parallel would be fine, but a single adiabatic reactor would probably be the best choice.

The CSTR is isothermal but selectivity in a CSTR is inherently poor when the desired product is an intermediate in a consecutive reaction scheme. An isothermal PFR is much better for selectivity and can be approximated in a shell-and-tube design by using many small tubes. Before worrying about the details of the shell-and–tube design, calculate the performance of a truly isothermal PFR and compare it to that of a CSTR and an adiabatic reactor. If the isothermal design gives a significant advantage, then tube size and number can be selected as a separate design exercise.

The results in Table 6.5 show that isothermal piston flow is not always the best environment for consecutive reactions. The adiabatic reactor gives marginally better results, and its capital cost will probably be lower. However, both reactors as modeled here assume preheated feed. The adiabatic reactor would require a feed preheater. A shell-and-tube reactor might be used for both the preheating and the reaction, although the reactor would no longer be isothermal. This is a point for detailed design calculations.

Table 6.5 Comparisons of Ideal Reactors for Consecutive, Endothermic Reactions

	Single CSTR	Isothermal PFR	Adiabatic PFR
T_{in}, K	378.3	381.6	399.2
T_{out}, K	378.3	381.6	382.6
V, m^3	13.0	7.45	7.82
W, kg h^{-1}	6687	6590	6583
Unit cost, $/kg	2.2996	2.1119	2.1079

Code for Example 6.4

```
Private MwA, MwB, MwC, rho, ain, hr1, hr2, k10, k20, AT1, AT2
Private V, Tin, Tout, Q, Win, tbar, aout, bout, cout

Sub Example6_4()

GetData  'See Code for Example 6.2

BestUnitCost = 100000  'an arbitrary high value
BestT = 381.6          'Initial guess
BestV = 7.45           'Initial guess
Tin = BestT
V = BestV
x = Timer

Do
   Call Balance2
   Call Cost(UnitCost)
   If UnitCost < BestUnitCost Then
             BestUnitCost = UnitCost
             BestT = Tin
             BestV = V
     Cells(1, 1) = BestT
     Cells(1, 2) = Tout
     Cells(1, 3) = BestV
     Cells(1, 4) = Win
     Cells(1, 5) = Ntrials
     Cells(1, 6) = BestUnitCost
       End If
       Tin = BestT + 0.5 * (0.5 - Rnd)
       V = BestV + 0.1 * (0.5 - Rnd)
       Ntrials = Ntrials + 1

Loop  'Observe results on spreadsheet.  Stop program manually.


End Sub

Sub Balance2()
'This version of Balance uses Newton's method to find Win

   Win = 6250    'lower bound, kg/hr
   Q = Win / rho
   tbar = V / Q
   Call Reactor2
   WB = bout * Q * MwB
   WAin = 2 * 6250  'Used for numerical differentiation
   Q = WAin / rho
   tbar = V / Q
   Call Reactor2
   WBout = bout * Q * MwB
     Do
      Del = WAin - Win
```

```
      If Abs(WBout - 6250) < 0.001 Then Exit Do
      Win = WAin
      WAin = WAin - (WBout - 6250) / (WBout - WB) * Del
      WB = WBout
      Q = WAin / rho
      tbar = V / Q
      Call Reactor2
      WBout = bout * Q * MwB
   Loop

End Sub
```

```
Sub Reactor2()
'Adiabatic PFR version
Integration is by Runge-Kutta

N = 256
dtau = tbar / N
a = ain
T = Tin
For I = 1 To N
   k1 = k10 * Exp(-AT1 / T)
   k2 = k20 * Exp(-AT2 / T)
   RA0 = -k1 * a
   RB0 = k1 * a - k2 * b
   RT0 = -k1 * a * hr1 - k2 * b * hr2
   a1 = a + dtau * RA0 / 2
   b1 = b + dtau * RB0 / 2
   T1 = T + dtau * RT0 / 2
   k1 = k10 * Exp(-AT1 / T1)
   k2 = k20 * Exp(-AT2 / T1)
   RA1 = -k1 * a1
   RB1 = k1 * a1 - k2 * b1
   RT1 = -k1 * a1 * hr1 - k2 * b1 * hr2
   a2 = a + dtau * RA1 / 2
   b2 = b + dtau * RB1 / 2
   T2 = T + dtau * RT1 / 2
   k1 = k10 * Exp(-AT1 / T2)
   k2 = k20 * Exp(-AT2 / T2)
   RA2 = -k1 * a2
   RB2 = k1 * a2 - k2 * b2
   RT2 = -k1 * a2 * hr1 - k2 * b2 * hr2
   a3 = a + dtau * RA2
   b3 = b + dtau * RB2
   T3 = T + dtau * RT2 / 2
   k1 = k10 * Exp(-AT1 / T3)
   k2 = k20 * Exp(-AT2 / T3)
   RA3 = -k1 * a3
   RB3 = k1 * a3 - k2 * b3
   RT3 = -k1 * a3 * hr1 - k2 * b3 * hr2
   a = a + dtau * (RA0 + 2 * RA1 + 2 * RA2 + RA3) / 6
   b = b + dtau * (RB0 + 2 * RB1 + 2 * RB2 + RB3) / 6
   T = T + dtau * (RT0 + 2 * RT1 + 2 * RT2 + RT3) / 6
```

```
Next
aout = a
bout = b
cout = ain - aout - bout
Tout = T

End Sub
```

There is no reason to suppose that the temperature profile in an adiabatic reactor is the best possible profile. Finding the best temperature profile is a problem in ***functional optimization.***

EXAMPLE 6.5

The mean residence time for the optimized PFR reactors in Example 6.4 is about 0.8 h and b_{out} is about 3.4 kg mol m^{-3}. Find the optimal temperature profile $T(z)$ that maximizes the concentration of component B in the competitive reaction sequence of Equation 6.1 for a PFR subject to the constraint that $\bar{t} = 0.8$ h. Assume $a_{in} = 4.5$ kg mol m^{-3}.

SOLUTION: The problem statement envisions a PFR operating at a fixed flow rate. We suppose that the PFR has been installed and is now producing about 6250 kg h^{-1}. Marketing has been successful and the plant is sold out. Smart engineers say they are able to modify the temperature profile $T(z)$. Asking how is a good question, but we will defer that. What temperature profile maximizes b_{out}? Material balance closure is not an issue. If b_{out} is increased, less A will be recycled and additional A will be fed as required to maintain $t = 0.8$ hr.

The problem is best solved in the time domain, $t = z/\bar{u}$, since the results will then be independent of tube diameter and flow rate. Divide the reactor into N_{zones} equal length zones each with residence time $\bar{t}/N_{zones}$. Treat each zone as an isothermal reactor operating at temperature T_n, $n = 1, 2, \ldots N_{zones}$. The problem in functional optimization has been converted to a problem in parameter optimization, the parameters being the various T_n. The profile for 10-zone optimization is shown in Figure 6.2*a*. These results were generated by the Code for Example 6.5 in less than a minute.

Figure 6.2*b* displays the temperature profile for a 100-zone case that is a tour de force for the optimization routine. The results took less than 20 min of computing time, but the difference in b_{out} between the 10- and 100-zone cases is negligible. These multizone designs give $b_{out} = 3.61$ compared to 3.59 for the best adiabatic reactor with $\bar{t} = 0.8$ h, but multizone reactors would be very expensive to build. Problems 6.11–6.13 suggest practical approaches to achieving a desirable temperature profile.

EXAMPLE 6.6

Suppose the reactions in Equation 6.1 are exothermic rather than endothermic. Specifically, reverse the sign on the heat of reaction terms so that the adiabatic temperature rise for complete conversion of A to B (but no C) is +30 K rather than −30 K. How does this change the results of Examples 6.2–6.5?

Code for Example 6.5

```
Private MwA, MwB, MwC, rho, ain, hr1, hr2, k10, k20, AT1, AT2
Private V, Tin, Tout, Q, Win, tbar, aout, bout, cout

Sub Example6_5()

Dim Tzone(100), BestT(100)

Call GetData 'See Code for Example 6.2

Randomize (Timer)  'Changes sequence of random numbers

Nzones = 10
For nz = 1 To Nzones
     BestT(nz) = 381.6
     Tzone(nz) = BestT(nz)
Next

tbar = 0.8 / Nzones

Do  'Main Loop
aout = ain
bout = 0

For nz = 1 To Nzones
    Tin = Tzone(nz)
    Call Reactor3
Next nz

If bout > BestB Then

   BestB = bout
   For nz = 1 To Nzones
       BestT(nz) = Tzone(nz)
       Cells(nz, 6) = BestT(nz)
   Next nz
   Cells(1, 1) = aout
   Cells(1, 2) = bout
   Cells(1, 3) = cout
   Cells(1, 4) = ntrials
   Cells(2, 4) = Timer - tt

End If

For nz = 1 To Nzones
   Tzone(nz) = BestT(nz) + 0.1 * (0.5 - Rnd)  'Changes each Tzone randomly
Next
ntrials = ntrials + 1
Loop  'Observe spreadsheet and end manually when satisfied
End Sub
```

```
Sub Reactor3()
'Isothermal PFR version
'Runge-Kutta integration is used

      N = 256
      dtau = tbar / N
      a = aout
      b = bout
      k1 = k10 * Exp(-AE1 / Tin)
      k2 = k20 * Exp(-AE2 / Tin)
      For I = 1 To N
        RA0 = -k1 * a
        RB0 = k1 * a - k2 * b
        a1 = a + dtau * RA0 / 2
        b1 = b + dtau * RB0 / 2
        RA1 = -k1 * a1
        RB1 = k1 * a1 - k2 * b1
        a2 = a + dtau * RA1 / 2
        b2 = b + dtau * RB1 / 2
        RA2 = -k1 * a2
        RB2 = k1 * a2 - k2 * b2
        a3 = a + dtau * RA2
        b3 = b + dtau * RB2
        RA3 = -k1 * a3
        RB3 = k1 * a3 - k2 * b3
        a = a + dtau * (RA0 + 2 * RA1 + 2 * RA2 + RA3) / 6
        b = b + dtau * (RB0 + 2 * RB1 + 2 * RB2 + RB3) / 6
     Next
     aout = a
     bout = b

End Sub
```

SOLUTION: The temperature dependence of the reaction rates is unchanged. When temperatures can be imposed on the system, as for the CSTR and isothermal reactor examples, the results are unchanged from the endothermic case. The optimal profile results in Example 6.5 are identical for the same reason. The only calculation that changes is that for an adiabatic reactor.

Code for Example 6.4 can be changed by setting hr1 and hr2 to -30 rather than $+30$. The material balance subroutine, Balance2 requires some tweaking, and it is easier to switch to the more robust binary search, Balance. The adiabatic temperature profile is increasing rather than decreasing, and this hurts selectivity. The production cost for an adiabatic reactor would be substantially higher than that for an isothermal reactor. Thus, a shell-and-tube design that approximates isothermal operation or one that imposes a decreasing temperature profile is the logical choice for the process. The required volume for this reactor will be on the order of 7 m^3. The specific choice of number of tubes, tube length, and tube diameter depends on the fluid properties, the cost of heat exchangers, and possibly even the prejudgment of plant management regarding minimum tube diameters.

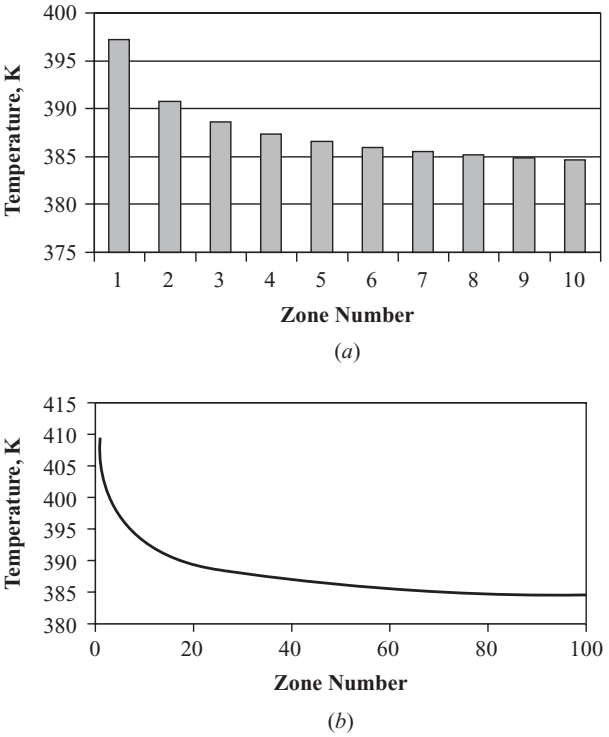

Figure 6.2 Piecewise-constant approximation to the optimal terperature profile for consecutive reactions: (*a*) 10-zone optimization; (*b*) 100-zone optimization.

6.2 COMPETITIVE REACTION SEQUENCE

Suppose the reactions are elementary, competitive, and of the form

$$\mathrm{A} \xrightarrow{k_{\mathrm{I}}} \mathrm{B} \qquad \mathrm{A} \xrightarrow{k_{\mathrm{II}}} \mathrm{C} \tag{6.6}$$

Equation 6.3 gives the rate constants, and both reactions are endothermic per Equation 6.4. The flow diagram is identical to that in Figure 6.1, and all cost factors are the same as for the consecutive reaction examples. Table 6.1 also applies, and there is an interior optimum for any of the ideal reactor types.

EXAMPLE 6.7

Determine optimal reactor volumes and operating temperatures for the three ideal reactors: a single CSTR, an isothermal PFR, and an adiabatic PFR.

SOLUTION: The computer programs used for the consecutive reaction examples can be used. All that is needed is to modify the reactor subroutines.

Table 6.6 Comparison of Ideal Reactors for Competitive, Endothermic Reactions

	Single CSTR	Isothermal PFR	Adiabatic PFR
T_{in}, K	387	385	398
T_{out}, K	387	385	372
V, m^3	12.0	8.6	10.2
W, kg h^{-1}	6721	6649	6707
Unit cost, \$/kg	2.19	2.08	2.13

All other things being equal, as they are in this contrived example, the competitive reaction sequence of Equation 6.6 is superior for the manufacture of B than the consecutive sequence of Equation 6.1. The CSTR remains a doubtful choice, but the isothermal PFR is now better than the adiabatic PFR. This is because the optimal temperature profile is increasing rather decreasing. See Table 6.6 for comparisons.

EXAMPLE 6.8

Find the optimal temperature profile $T(t)$ that maximizes the concentration of component B in the consecutive reaction sequence of Equation 6.6 for a PFR subject to the constraint that $\bar{t} = 0.8$ h.

SOLUTION: The computer program used for Example 6.5 will work with minor changes. It is a good idea to start with a small number of zones until you get some feel for the shape of the profile. This allows you to input a reasonable starting estimate for the profile and greatly speed convergence when the number of zones is large. It also ensures that you converge to a local optimum and miss a better, global optimum that, under quite rare circumstances, may be lurking somewhere.

Results are shown in Figure 6.3.

The optimal profile for the competitive reaction pair is an increasing function of t (or z). An adiabatic temperature profile is a decreasing function when the reactions are endothermic, so it is obviously worse than the constant–temperature, isothermal case. However, reverse the signs on the heats of reactions, and the adiabatic profile is preferred although still suboptimal.

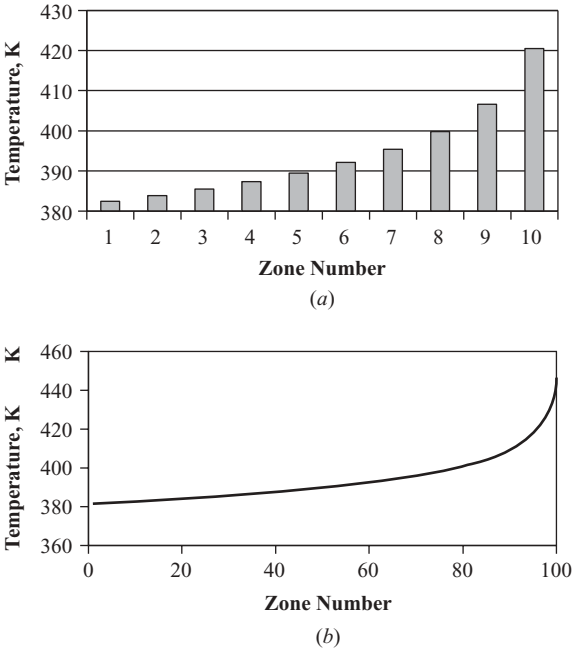

Figure 6.3 Piecewise-constant approximations to the optimal temperature profile for competitive reactions: (*a*) 10-zone optimization; (*b*) 100-zone optimization.

SUGGESTED FURTHER READINGS

A good place to begin a more comprehensive study of chemical engineering optimization is:

T. F. Edgar and D. M. Himmelblau, *Optimization of Chemical Processes*, 2nd ed., McGraw-Hill, New York, 2001.

Two books with a broader engineering focus that have also survived the test of time are:

R. Fletcher, *Practical Methods of Optimization,* 2nd ed., Wiley, New York, 2000.

S. S. Rao*, Engineering Optimization: Theory and Practice*, 3rd ed., Wiley, New York, 1996.

The bible of numerical methods remains:

W. H. Press, S. A. Teukolsky, W. T. Vetterling, and B. P. Flannery, *Numerical Recipes in Fortran 77: The Art of Scientific Computing,* Vol. 1, 2nd ed., Cambridge University Press, New York, 1992.

Versions of Volume I exist for C, Basic, and Pascal. Matlab enthusiasts will find some coverage of optimization (and nonlinear regression) techniques in:

A. Constantinides and N. Mostoufi, *Numerical Methods for Chemical Engineers with Matlab Applications*, Prentice-Hall, Upper Saddle River, NJ, 1999.

Mathematica fans may consult:

M. A. Bhatti, *Practical Optimization Methods with Mathematica Applications*, Springer-Verlag, New York, 1999.

PROBLEMS

6.0 Use the random optimization technique to find extreme values for the following functions. Determine all extreme values of f and the value of the independent variables at which the extremes occur.

(a) $f(x, y) = xy \sin(x) \sin(y),\ 0 < x < \pi,\ 0 < y < \pi$

(b) $f(x, y) = xy \sin(x) \sin(y),\ 0 < x < 2\pi,\ 0 < y < 2\pi$

(c) $b_{\text{out}} = \frac{k_f a_{\text{in}} \bar{t}}{(1+k_f \bar{t}+k_r \bar{t})}$ where $\bar{t} = 3$, $k_f = 10^8 \exp(-5000/T)$, and $k_r = 10^{15} \exp(-10,000/T)$

(d) $b_{\text{out}} = \frac{k_f a_{\text{in}} \bar{t}}{(1+k_f \bar{t}+k_r \bar{t})}$ where $\bar{t} = 3$, $k_f = 10^{15} \exp(-10,000/T)$, and

$$k_r = 10^8 \exp(-5000/T)$$

6.1 For the reaction sequence of Equation 6.1, what is an absolute lower bound on the volume of an isothermal reactor that can be used to achieve the desired throughput of 6250 kg h^{-1}? In determining this lower bound, ignore the second reaction, B → C. Your answer should depend on the operating temperature but should not depend on the type of reactor being used.

6.2 Determine the minimum operating cost for the process of Example 6.2 when the reactor consists of two equal-volume CSTRs in series. The capital cost per reactor is $\$8{,}000{,}000V^{0.6}$.

6.3 Add a parameter to Problem 6.2 and study the case where the CSTRs can have different volumes.

6.4 The following sets of rate constants give nearly the same values for k_{I} and k_{II} at 360 K:

k_{I}	k_{II}
$4.2 \times 10^5 \exp(-5000/T)$	$1.04 \times 10^5 \exp(-6000/T)$
$4.5 \times 10^{11} \exp(-10{,}000/T)$	$1.8 \times 10^{12} \exp(-12{,}000/T)$
$5.2 \times 10^{23} \exp(-20{,}000/T)$	$5.4 \times 10^{26} \exp(-24{,}000/T)$

There are nine possible combinations of rate constants. Pick (or be assigned) a combination other than the base case of Equation 6.3 that was used in the worked examples. For the new combination:

(a) Do a comprehensive search similar to that shown in Table 6.2 for the case of a single CSTR. Find the volume and temperature that minimizes the total cost. Compare the relative flatness or steepness of the minimum to that of the base case.

(b) Repeat the comparison of reactor types as in Example 6.4.

(c) Determine the optimum set of temperatures for a 10-zone reactor as in Example 6.4. Discuss the shape of the profile compared to that of the base case. Computer heroes may duplicate the 100-zone case instead.

6.5 For the process of Example 6.5, determine the optimum temperatures and volumes for the three-parameter problem consisting of two isothermal zones but with variable zone lengths and with $\bar{t}$ fixed at 0.8 h.

6.6 Work the five-parameter problem consisting of three variable-length zones with $\bar{t}$ fixed at 0.8 h.

6.7 Repeat Example 6.5 using 10 zones of equal length but impose the constraint that no zone temperature can exceed 390 K.

6.8 Determine the best value for T_{in} for an adiabatic reactor for the exothermic case of the competitive reactions in Equation 6.6.

6.9 Compare the (unconstrained) optimal temperature profiles of 10-zone PFRs for the following cases:
- **(a)** The reactions are consecutive per Equation 6.1 and endothermic.
- **(b)** The reactions are consecutive and exothermic.
- **(c)** The reactions are competitive per Equation 6.6 and endothermic.
- **(d)** The reactions are competitive and exothermic.

6.10 Determine the best two-zone PFR strategy for the competitive, endothermic reactions of Equation 6.6.

6.11 Design a shell-and-tube reactor to approximate the isothermal case in Example 6.3. Fix $T_{in} = 381.6$ K, $V = 7.45$ m^3, $W_{in} = 6590$ kg h^{-1}. Use tubes with an ID of 0 .0254 m and a length of 5 m. Assume components A, B, C all have a specific heat of 1.9 kJ kg^{-1} K^{-1} and a thermal conductivity of 0.15 W m^{-1} K^{-1}. Run the reaction on the tube side and assume that the shell-side temperature is constant (e.g., use condensing steam). Do the consecutive, endothermic case.

6.12 Revise the heat exchanger design in Problem 6.11 to accommodate cold feed, $T_{in} = 298$ K.

6.13 It is time to find a near-optimal solution to the technical and social problems of the evil professor who, as it turns out, is only marginally evil. Even this marginal evilness can be explained by his frustration at being assigned to a chemical engineering department. His Ph.D. was in history. Devise an optimal solution to this mess. One possible solution is that he was reassigned to the history department where he was quickly awarded tenure for his historical study of the manufacture of high explosives; he courted and married the beautiful princess who even more quickly was awarded tenure in chemical engineering; and they lived happily ever after. However, this leaves unresolved the question of the TNT that was cooking away in the hot oil bath. Find some semiplausible solution that saves the laboratories.

APPENDIX 6.1 NUMERICAL OPTIMIZATION TECHNIQUES

Optimization is a complex and sometimes difficult topic. Many books and countless research papers have been written about it. This appendix discusses ***parameter optimization***. There is a function $F(p_1, p_2, \ldots)$ called the ***objective function*** that depends on the parameters $p_1, p_2, \ldots$. The goal is to determine the best values for the parameters, best in the sense that these values will maximize or minimize F. For the reactors in Example 6.4, the parameters are T and V and the objective function is the unit cost of production. The parameters must be positive, but there are no other restrictions, and the optimization is ***unconstrained***. Suppose that the reactor has a limit on operating temperature, say 500 K. The problem becomes a ***constrained*** optimization, but the constraint has no effect on the result. The constraint is not ***active***. Lower the temperature limit to 390 K and it becomes active for the adiabatic PFR, forcing a lower inlet temperature and poorer economic performance. Multidimensional optimization problems often have some active constraints.

Numerical optimization techniques find local optima. They will find the top of a hill or the bottom of a valley. In constrained optimizations, they may take you to

a boundary of the parameter space. At a local optimum, the objective function gets worse when moving a small distance in any direction. However, there may be a higher hill or a deeper valley or even a better boundary. There can be no guarantee that the global minimum will be found unless $F(p_1, p_2, \dots)$ belongs to a restricted class of functions. If $F(p_1, p_2, \dots)$ is linear in its parameters, there are no interior optima, no hills or valleys but just slopes. Linear programming techniques will then find the global optimum which will be at an intersection of constraints. However, problems in reactor design can be aggressively nonlinear, and interior optima are fairly common.

Random Searches

The random search technique can be applied to constrained or unconstrained optimization problems involving any number of parameters.

The concept is the following:

1. Start with a feasible set of values for the optimization variables.
2. Evaluate the objective function.
3. Apply a random change to each of the optimization variables. *Note:* Change all the variables at once.
4. Evaluate the objective function.
5. If the new value is better, replace the previous best result and all the optimization variables with the new, better values. Otherwise, keep all the old values.
6. Go to step 3 to continue the search.

The random-search method will always go to a local optimum. If the size of the random changes are large enough, the search algorithm will eventually go to the global optimum.

EXAMPLE 6.9

Use the random optimization technique to determine the maximum value for the function $f(x, y) = \exp[-(x-2)^2 - (y+3)^2]$. The starting guesses are $x = 0$ and $y = 0$.

SOLUTION: The optimization code is given in Code for Example 6.9. The outer loop of this program has no end. Given a very slow computer, you could watch the program run and terminate it when the value of the objective function ceases to change. On a modern computer it almost instantly reaches $x \approx 0$ and $y \approx 3$ with the value of the function approximately 1.0. The Basic function Rnd as implemented in Excel 2003 has a resolution of about 1 part in 10^8. This limits the accuracy of x and y in this example to about 1 part in 10^6. Better random number generators do exist but are rarely needed.

The key to the method is the step that sets the new trial values for the parameters:

$$p_{\text{trial}} = p_{\text{best}} + \Delta_p(0.5 - \text{Rnd}) \tag{6.7}$$

Rnd is a random number uniformly distributed over the range 0–1.0. Similar functions exist in all major programming languages. Equation 6.7 generates values of p_{trial} in the range $p_{\text{best}} \pm \Delta_p/2$. Large values of Δ_p are desirable early in the search. If the range of guesses is large enough to span the feasible space, the program will eventually find the global optimum. Small values of Δ_p will generally give faster convergence to an optimum, but it may be a local optimum. Repeated numerical experiments with different initial values can be used to search for other local optima.

Code for Example 6.9

```
Sub Example6_9()

xbest = 0
ybest = 0
fbest = Exp(-(x - 2) ^ 2 - (y + 3) ^ 2)

Do
   x = xbest + 0.5 * (0.5 - Rnd)        change x randomly
   y = ybest + 0.5 * (0.5 - Rnd)        change y randomly
   f = Exp(-(x - 2) ^ 2 - (y + 3) ^ 2)  calculate result
   If f > fbest Then  if new result the best so far, update everything
      xbest = x
      ybest = y
      fbest = f
      Cells(1, 1) = xbest
      Cells(1, 2) = ybest
      Cells(1, 3) = fbest
   End If
Loop  'Observe results on spreadsheet.  Stop when output stops changing

End Sub
```

Golden Section Search

The golden section search is the optimization analog of a binary search. It is used for functions of a single variable, $F(a)$. It is faster than a random search, but the difference in computing time will be trivial unless the objective function is extremely hard to evaluate.

To know that a minimum exists, we must find three points $a_{\min} < a_{\text{int}} < a_{\max}$ such that such that $F(a_{\text{int}})$ is less than either $F(a_{\min})$ or $F(a_{\max})$. Suppose this has been done. Now choose another point $a_{\min} < a_{\text{new}} < a_{\max}$ and evaluate $F(a_{\text{new}})$. If $F(a_{\text{new}}) < F(a_{\text{int}})$, then a_{new} becomes the new interior point. Otherwise a_{new} will become one of the new endpoints. Whichever the outcome, the result is a set of three points with an interior minimum and with a smaller distance between the endpoints than before. This procedure continues until the distance between $a_{\min}$ and $a_{\max}$ has been narrowed to an acceptable extent. The way of choosing a_{new} is not of critical importance, but

the range narrows fastest if a_{new} is chosen to be at 0.38197 of the distance between the interior point and the more distant of the endpoints, a_{min} and a_{max}.

Sophisticated Methods of Parameter Optimization

If the objective function is very complex or if the optimization must be repeated a great many times, the random-search method should be replaced with something more efficient computationally. For a minimization problem, all the methods search for a way downhill. One group of methods uses nothing but function evaluations to find the way. Another group combines function evaluations with derivative calculations, for example, $\partial F/\partial a$, to speed the search. All these methods are complicated. The easiest to implement is the simplex method of Nelder and Mead. (It is different than the simplex algorithm used to solve linear programming problems.) A subroutine is given by Press et al. (1992). Other sources and codes for other languages are available on the Web and in some versions of commercial packages (e.g., Matlab). More efficient but more complicated, gradient-based methods are available from the same sources.

Functional Optimization

A function $f(x)$ starts with a number x, performs mathematical operations, and produces another number f. It transforms one number into another. A ***functional*** starts with a function, performs mathematical operations, and produces a number. It transforms an entire function into a single number. The simplest and most common example of a functional is a definite integral. The goal in Example 6.5 was to maximize the integral

$$b_{out} - b_{in} = \int_0^L \mathscr{R}_B(a, b, T)\, dz \tag{6.8}$$

Equation 6.8 is a functional. There are several functions, $a(z)$, $b(z)$, $T(z)$, that contribute to the integral, but $T(z)$ is the one function directly available to the reactor designer as a manipulated variable. Function optimization is used to determine the best function $T(z)$. Specification of this function requires that $T(z)$ be known at every point within the interval $0 < z < L$.

Some problems in functional optimization can be solved analytically. A topic known as the ***calculus of variations*** is included in most courses in advanced calculus. It provides ground rules for optimizing integral functionals. The ground rules are necessary conditions analogous to the derivative conditions (i.e., $df/dx = 0$) used in the optimization of ordinary functions. In principle, they allow an exact solution, but the solution may only be implicit or not in a useful form. For problems involving Arrhenius temperature dependence, a numerical solution will be needed sooner or later.

Example 6.5 converted the functional optimization problem to a parameter optimization problem. The function $T(t)$ was assumed to be piecewise constant. There were N pieces, the nth piece was at temperature T_n, and these N temperatures became

the optimization parameters. There are other techniques for numerical functional optimization, including some gradient methods, but conversion to parameter optimization is by far the easiest to implement and most reliable. In the limit as N grows large, the numerical solution will presumably converge to the true solution. In Example 6.5, no constraints were imposed on the temperature, and the parameter optimization appears to be converging to a smooth function with a high temperature spike at the inlet. In constrained optimizations, the optimal solution may be at one of the constraints and then suddenly shift to the opposite constraint. This is called ***bang-bang control*** and is studied in courses in advanced process control. The best strategy for a constrained optimization may be to have a small number of different-length zones with the temperature in each zone being at either one constraint or the other. This possibility is easily explored using parameter optimization.

Chapter 7

Fitting Rate Data and Using Thermodynamics

Chapter 7 has two goals. The first is to show how reaction rate expressions $\mathscr{R}(a, b, \ldots, T)$ are obtained from experimental data. The second is to review the thermodynamic underpinnings for calculating reaction equilibria, heats of reactions, and heat capacities needed for the rigorous design of chemical reactors.

7.1 FITTING DATA TO MODELS

Excellent kinetic models can be found in the literature, but they rarely meet the needs of new product or process development activities. Finding a kinetic model that has the right chemistry, the right catalyst, and the right operating conditions is a normal part of research and development. Model development begins by postulating a mathematical model that contains one or more adjustable parameters. An optimization routine is then used to adjust the parameters to obtain a good fit to a set of experimental measurements. The usual approach is to minimize a sum of squares:

$$\mathrm{SS}^2 = \sum_{\text{Data}} [\text{experiment} - \text{model}]^2 \tag{7.1}$$

Here, "experiment" refers to a measurement, typically of a concentration or reaction rate, made in laboratory, pilot scale, and sometimes even plant scale equipment. The "model" refers to predictions of the concentrations or rates calculated from an assumed kinetic model.

The simplest case is when the experiments are performed in a constant-density CSTR. Then the measured inlet and outlet concentration give the reaction rate directly:

$$\left[\frac{a_{\text{out}} - a_{\text{in}}}{\bar{t}}\right]_{\text{data}} = \left[\mathscr{R}_A\right]_{\text{data}}$$

Chemical Reactor Design, Optimization, and Scaleup, Second Edition. By E. B. Nauman
Copyright © 2008 John Wiley & Sons, Inc.

For a simple reaction like A → B, the postulated rate equation might be

$$\left[\mathscr{R}_A\right]_{\text{model}} = k_0 \exp\left(-\frac{T_{\text{act}}}{T}\right) a^n$$

The sum of squares has the form

$$\text{SS}^2 = \sum_{j=1}^{J} \left[\mathscr{R}_{\text{data}} - \mathscr{R}_{\text{model}}\right]^2 = \sum_{j=1}^{J} \left[\left(\frac{a_{\text{out}} - a_{\text{in}}}{\bar{t}}\right)_{\text{data}} - k_0 \exp\left(-\frac{T_{\text{act}}}{T}\right) a^n\right]^2$$

where J is the number of data and k_0, T_{act}, and n are model parameters to be determined by the fitting routine.

The situation is a bit more complex when the experiments are done in a batch reactor. Here, typical data will consist of concentrations $a(t)$ for various times within a run and for various temperatures between runs. Equation 7.1 takes the form

$$\text{SS}^2 = \sum_{j=1}^{J} \left[[a(t)]_{\text{data}} - [a(t)]_{\text{model}}\right]^2$$

For A → B, the model equations could be Equations 2.16 and 2.17:

$$\text{SS}^2 = \sum_{j=1}^{J} \left[a(t)_{\text{data}} - a_0 \exp\left[-k_0 t \ \exp\left(-\frac{T_{\text{act}}}{T}\right)\right]\right]^2 \qquad \text{for } n = 1$$

$$= \sum_{j=1}^{J} \left[a(t)_{\text{data}} - \left[1 + (n-1)a_0^{n-1} k_0 t \ \exp\left(-\frac{T_{\text{act}}}{T}\right)\right]^{1/(1-n)}\right]^2 \qquad \text{for } n \neq 1$$

Do not be tempted to differentiate batch reactor data to determine the rate. Numerical differentiation is a noisy process and will give inferior results. Instead, assume a functional form for the rate equation, substitute it into the batch design equation, and integrate. The integration may be numerical. The result will be a prediction of $a(t)$ that can be compared directly to the experimental results.

7.1.1 Suggested Forms for Kinetic Models

With two adjustable constants, you can fit a straight line. With six, you can fit an elephant. With eight, you can fit a running elephant or a cosmological model of the universe (Hogan, 2000).

The general reaction is

$$\nu_A \text{A} + \nu_B \text{B} + \cdots \rightleftarrows \nu_R \text{R} + \nu_S \text{S} + \cdots$$

If the reaction is elementary, then

$$\mathscr{R} = k_f [\text{A}]^{-\nu_A} [\text{B}]^{-\nu_B} \cdots - k_r [\text{R}]^{\nu_R} [\text{S}]^{\nu_S} \cdots \tag{7.2}$$

where the stoichiometric coefficients are known small integers. Experimental data will be used to determine the rate constants k_f and k_r. It may be that the reaction is irreversible or that the equilibrium constant is known. Then there is only one adjustable constant, k_f. See Section 7.2.2.

A more general form for the rate expression is

$$\mathscr{R} = k_f[\mathrm{A}]^m[\mathrm{B}]^n \cdots - k_r[\mathrm{R}]^r[\mathrm{S}]^s \cdots \tag{7.3}$$

where $m, n, \ldots, r, s, \ldots$ are empirical constants that may or may not be integers and that must be determined from the data. An alternative form that may fit the data reasonably well is

$$\mathscr{R} = k[\mathrm{A}]^m[\mathrm{B}]^n[\mathrm{R}]^r[\mathrm{S}]^s \cdots \tag{7.4}$$

where some of the exponents (e.g., $r, s, \ldots$) can be negative. The virtue of this form is that it has one fewer empirical constant than Equation 7.3. Its fault is that it lacks the mechanistic basis of Equations 7.3 and will not perform as well near the equilibrium point of a reversible reaction.

For enzymatic and other heterogeneously catalyzed reactions, there is competition for active sites. This leads to rate expressions with forms such as

$$\mathscr{R} = \frac{k_f[\mathrm{A}]^m[\mathrm{B}]^n \cdots - k_r[\mathrm{R}]^r[\mathrm{S}]^s \cdots}{(1 + k_A[\mathrm{A}] + k_B[\mathrm{B}] + k_R[\mathrm{R}] + k_S[\mathrm{S}] + \cdots)} \tag{7.5}$$

or

$$\mathscr{R} = \frac{k[\mathrm{A}]^m[\mathrm{B}]^n[R]^r[\mathrm{S}]^s \cdots}{(1 + k_A[\mathrm{A}] + k_B[\mathrm{B}] + k_R[\mathrm{R}] + k_S[\mathrm{S}] + \cdots)} \tag{7.6}$$

All the rate constants should be positive so the denominator in this expression will always retard the reaction. The same denominator can be used with Equation 7.3 to model reversible heterogeneous reactions. Although the dimensions of the numerator rate constant k depend on the overall reaction order, all the denominator rate constants have dimensions of inverse concentration.

More complicated rate expressions are possible. For example, the denominator may be squared or square roots can be inserted here and there based on theoretical considerations. The denominator may include a term, $k_I[I]$, to account for compounds that are nominally inert and do not appear in Equation 7.1 but occupy active sites on the catalyst and thus retard the rate. The various rate constants will be functions of temperature and are usually modeled using an Arrhenius form. This doubles the number of adjustable parameters. The more complex kinetic models have enough adjustable parameters to fit a stampede of elephants. Careful analysis is needed to avoid being crushed underfoot.

7.1.2 Fitting CSTR Data

The goal is to determine a function $\mathscr{R}(a, b, \ldots, T)$ that can be used to design reactors. Suppose the reaction is A → B and that the CSTR measurements are all done at the same temperature. Then $\mathscr{R}_A = \nu_A \mathscr{R}$ should be a function of a and possibly of b. Referring to Equations 7.2–7.6, here are some choices that contain no more than three adjustable constants:

$$\mathscr{R} = k a_{\text{out}}^n \quad \text{or} \quad \mathscr{R} = \frac{k a_{\text{out}}^n}{1 + k_A a_{\text{out}}} \quad \text{or} \quad \mathscr{R} = k a_{\text{out}}^n b_{\text{out}}^r \quad \text{or} \quad \mathscr{R} = \frac{k a_{\text{out}}^n}{1 + k_B b_{\text{out}}} \tag{7.7}$$

Models with more constants will give better fits, but this does not justify their use. Statistical tests can help avoid "overfitting" data, but there may be simpler physical tests: Is there any reason to believe that site competition is important? Is the reaction essentially irreversible? It may be that $n = -\nu_A$ provides a good fit to the data so that n ceases to be an adjustable constant. Most importantly, is the residual sum of squares, SS^2, low enough to represent experimental error?

The choice of a model that contains one, two, or more adjustable constants is a matter of physical judgment combined with mathematics. The mathematical portion is the minimization of the sum of squares:

$$\text{SS}^2 = \sum_{j=1}^{J} [\mathscr{R}_{\text{data}} - \mathscr{R}_{\text{model}}]^2 \tag{7.8}$$

where $\mathscr{R}_{\text{data}}$ is the set of J experimental rate measurements. For a variable-density CSTR, the experimental rate is calculated from

$$\left[\mathscr{R}_A\right]_{\text{data}} = \left[\frac{Q_{\text{out}} a_{\text{out}} - Q_{\text{in}} a_{\text{in}}}{V}\right]_{\text{data}} \tag{7.9}$$

The predicted rate $\mathscr{R}_{\text{model}}$ is calculated by substituting the measured concentrations for a_{out} and b_{out} into one of Equations 7.7 with assumed values for the model parameters, for example, k, n, and k_A. The optimization methods of Chapter 6 are then used to adjust the parameter values in order to minimize SS^2. There will be some residual error:

$$s = \sqrt{\frac{\text{SS}^2_{\text{residual}}}{J}} \tag{7.10}$$

is a root mean error that combines experimental error and fitting error. The physical judgment in fitting a model is the decision that the root mean error is a reasonable estimate of experimental error and that the model itself is adequate. Introduction of additional constants would reduce the root mean error but would be overfitting. Remember that a fit can be perfect if there are as many constants as data, but the turns and the kinks in such a fit can be physically meaningless.

EXAMPLE 7.1

The following measurements have been made for a reaction A → B at one temperature using a CSTR with $\bar{t} = 2$ h. The fluid density was constant.

Run Number	a_{in}	a_{out}	$\mathscr{R}_A = \frac{a_{out} - a_{in}}{\bar{t}}$
1	0.200	0.088	−0.0560
2	0.400	0.191	−0.1045
3	0.600	0.307	−0.1654
4	0.800	0.390	−0.2050
5	1.000	0.493	−0.2535

Fit these data to the kinetic model

$$\mathscr{R} = -\mathscr{R}_A = \frac{k a_{out}^n}{1 + k_A a_{out}}$$

SOLUTION: Equation 7.8 becomes

$$SS^2 == \sum_{j=1}^{J} [\mathscr{R}_{data} - \mathscr{R}_{model}]^2 = \sum_{j=1}^{J} \left[(\mathscr{R}_{data})_j + \left(\frac{k a_{out}^n}{1 + k_A a_{out}} \right)_j \right]^2 \tag{7.11}$$

The $(\mathscr{R}_{Data})_j$ terms in the summation have been calculated as part of the problem statement. The outlet concentrations, also given as part of the problem statement, are substituted into the kinetic model. Then the model parameters k, n, and k_A are adjusted to minimize SS^2. Specials cases that force $k_A = 0$ and $n = 1, 2$ will be considered. Code for Example 7.1 uses the random-search method to determine best values for the model parameters.

Code for Example 7.1

```
Sub Example7_1()
Dim ain(10), aout(10), Rate(10)
Dim Ntrials As Long

'Data
ain(1) = 0.2: aout(1) = 0.088
ain(2) = 0.4: aout(2) = 0.191
ain(3) = 0.6: aout(3) = 0.307
ain(4) = 0.8: aout(4) = 0.39
ain(5) = 1#:  aout(5) = 0.493

tbar = 2
Ndata = 5

For i = 1 To Ndata
   Rate(i) = (ain(i) - aout(i)) / tbar
Next i
```

```
bestss = 100
k = 1
kA = 0
n = 1

Ntrials = 200000
For j = 1 To Ntrials
   ss = 0
   For i = 1 To Ndata
      ss = ss + (Rate(i) - k * aout(i) ^ n / (1 + kA * aout(i))) ^ 2
   Next i
   If ss < bestss Then
       bestk = k
       bestn = n
       bestkA = kA
       bestss = ss
       Cells(1, 1) = k
       Cells(1, 2) = n
       Cells(1, 3) = kA
       Cells(1, 4) = Sqr(ss / Ndata)
       Cells(1, 5) = j

    End If
    'kA = bestkA + 0.05 * (0.5 - Rnd)      'adjusts kA randomly
    'n = bestn + 0.05 * (0.5 - Rnd)        'adjusts n randomly
     k = bestk + 0.05 * (0.5 - Rnd)        'adjusts k randomly
Next j

End Sub
```

As given above, the program adjusts only k and n. The code for adjusting k_A has been "commented out" so that it remains at its initial value of zero. The following cases were run by adjusting the initial values and comments in the code:

Case	k	n	k_A	Root Mean Error
1	0.515	1	0	0.0078
2	0.490	0.947	0.000	0.0073
3	0.274	0.680	−0.686	0.0055
4	1.199	2	0.000	0.0423
5	0.535	1	0.098	0.0076

Case 1 forces $n = 1$ and $k_A = 0$. It is the simplest model and provides a reasonably good fit of the data. Most chemists and chemicals engineers would prefer this model. Case 2 provides a better fit by allowing n to vary, but there is no mechanistic reason to suspect a reaction order of 0.947, and the reduction in root mean error compared to $n = 1$ is small. Case 3 improves the fit substantially, but the negative value for k_A

is physically unrealistic. Case 4 clearly shows the reaction is not second order. Case 5 provides an insignificant improvement over case 1. Exactly first order with $k_A = 0$, case 1 is probably the best choice for the model, particularly if it must be extrapolated to values of a_{in} that are outside the experimental range.

EXAMPLE 7.2

It happens that the product concentrations were also measured during the experiments of Example 7.1. The data are as follows

Run Number	b_{out}
1	0.088
2	0.206
3	0.291
4	0.400
5	0.506

Use these data to test for the possibility of reversibility by the reaction.

SOLUTION: Since B is a product, its concentration should affect the reaction rate only if the reaction is reversible. A test for this is to fit $\mathscr{R}_{\text{model}} = ka^n b^r$ to the experimental data and check whether r is negative.

Case	k	n	r	Root Mean Error
1	0.515	1	0	0.0078
6	0.496	1	−0.040	0.0075
7	0.478	−0.086	1.025	0.0042

Case 6 provides a partial test; r is slightly negative, but the reduction in root mean error is small. The reaction is essentially irreversible within the experimental range.

Case 7 illustrates a weakness of statistic analysis: Correlation does not imply causation. Case 7 is obtained by minimizing the sum of squares when k, n, and r are all allowed to vary. It gives the lowest root mean error and shows that the reaction rate correlates better with the product concentrations than the reactant concentrations! The reason for the spurious fit and corresponding physical absurdity is that a_{out} and b_{out} are strongly correlated. The experiments were run at a fixed value for $\bar{t}$ and with no B in the feed. Under these conditions, higher values for a_{in} necessarily give higher values for both a_{out} and b_{out}. Including the product concentration in the model does not improve the analysis. The conclusion, based on a mixture of physical insight and statistical analysis, is that $\mathscr{R} = 0.515a$ is close to the truth, but further experiments can be run. A more complete experimental design would vary $\bar{t}$ and b_{in} .

EXAMPLE 7.3

The nagging concern that the reaction of Examples 7.1 and 7.2 may somehow depend on the product concentration prompted the following additional runs. These runs add product to the feed in order to destroy the correlation between a_{out} and b_{out}:

Run Number	a_{in}	b_{in}	a_{out}	b_{out}
6	0.500	0.200	0.248	0.430
7	0.500	0.400	0.246	0.669
8	0.500	0.600	0.239	0.854
9	0.500	0.800	0.248	1.052
10	0.500	1.000	0.247	1.233

SOLUTION: The new data show that adding B to the feed has little if any real effect on a_{out}, reinforcing the conclusion that the reaction is essentially irreversible. This is confirmed by adding the new data to the computer program and rerunning the model, $\mathscr{R}_{model} = ka^n b^r$. The results are as follows:

Case	k	n	r	Root Mean Error
8	0.516	1	0	0.0060
9	0.504	1	−0.029	0.0059
10	0.328	0	1	0.0503

Most chemical engineers would choose case 8, which is the same as case 1 but with the extended data set. The new data have slightly revised the value of k(from 0.515 to 0.516). The root mean error is lower than before, but this only means that the revised model fits the new points, all with $a_{in} = 0.5$, quite well. The fit for other values of a_{in} will be slightly worse due to the changed value for k. Case 9 confirms that the reaction is irreversible over the experimental range, and the high error in case 10 confirms that the new data have eliminated the spurious correlation between rate and product concentration.

For the regression analysis, the experimental data are fixed and the model parameters are varied to minimize SS^2 using any of the optimization techniques discussed in Chapter 6. An analytical solution to the minimization problem is possible when the model has a linear form such as $\mathscr{R}_{model} = ka$. The fitting process is then known as ***linear regression analysis*** and is summarized in Appendix 7.1. Unfortunately, the more complex rate expressions are nonlinear. It is sometimes possible to transform the model to a linear form, but the transformation causes a bias so that some portions of the operating space will be better fit than other portions. This book

emphasizes ***nonlinear regression*** because it is generally more suitable for fitting kinetic data.

7.1.3 Fitting Batch and PFR Data

When kinetic measurements are made in batch or piston flow reactors, the reaction rate is not directly determined. Instead, an integral of the rate is measured, and the rate itself must be inferred. All the parameters of the model must be specified, for example, $\mathscr{R}_{\text{model}}(k, m, n, r, s, \ldots, k_0, T_{\text{act}})$, but this will be done by the optimization routine. The integration can be done analytically in simple cases or numerically in more complicated cases. For a batch reactor,

$$\left[\frac{d(V a)}{dt} = V\,\mathscr{R}_A\right]_{\text{model}} \tag{7.12}$$

EXAMPLE 7.4

An irreversible reaction A → B is occurring in an isothermal, constant-volume batch reactor. The concentration has been measured at various times. Find an objective function (i.e., SS^2) that is suitable for fitting the model $\mathscr{R}_A = -ka^n$.

SOLUTION: This has already been done in the beginning of the chapter. Analytical integrals of Equation 7.12 (e.g., Equations 2.16 and 2.17) can be used for this *n*th-order reaction, but recall that $n = 1$ is a special case and that reactions with $n < 1$ can go to completion. Thus,

$$\text{SS}^2 = \sum_{j=1}^{J}\left[a_{\text{data}}(t_j) - a_{\text{model}}(t_j)\right]^2$$

where

$$a_{\text{model}} = \begin{cases} a_0\left[1 + (n-1)a_0^{n-1}kt\right]1/(n-1) & \text{if } n \neq 1 \qquad a > 0 \\ 0 & \text{if } a \leq 0 \\ a_0 \exp(-kt) & \text{if } n = 1 \end{cases}$$

Numerical integration of the rate equation with $\mathscr{R}_A = -ka^n$ is simple and works for all values of k and t, although large values of k will force small values of Δt to ensure convergence.

EXAMPLE 7.5

The following data have been obtained in a constant-volume, isothermal reactor for a reaction with known stoichiometry: A → B + C. The initial concentration of component A was 2200 mol m^{-3}. No B or C was charged to the reactor. Find a good kinetic model.

Sample Number, i	Time, t (min)	Fraction Unreacted, Y_A
1	0.4	0.683
2	0.6	0.590
3	0.8	0.513
4	1.0	0.445
5	1.2	0.381

SOLUTION: The model parameters are n and k. Results for various values of n, forced and fitted, are given below and are plotted in Figure 7.1:

Reaction Order, n	Rate Constant, $a_0^{n-1}k$	Root-Mean Error
0	0.572	0.0599
1	0.846	0.0181
1.53	1.024	0.0058
2	1.220	0.0140

The fit with $n = 1.53$ is quite good. The results for the fits with $n = 1$ and $n = 2$ show systematic deviations between the data and the fitted model. The reaction order is approximately 1.5, and this value could be used instead of $n = 1.53$ with essentially the same goodness of fit. A result so close to 1.5 should motivate a search for a mechanism that predicts this order. See Section 2.5.3. Absent such a mechanism, the best-fit value of 1.53 may as well be retained.

The curves in Figure 7.1 plot the natural variable, $a(t)/a_0$, versus time. Although this accurately portrays the goodness of fit, there is a classical technique for plotting batch data that is more sensitive to reaction order for irreversible nth-order reactions. The reaction order

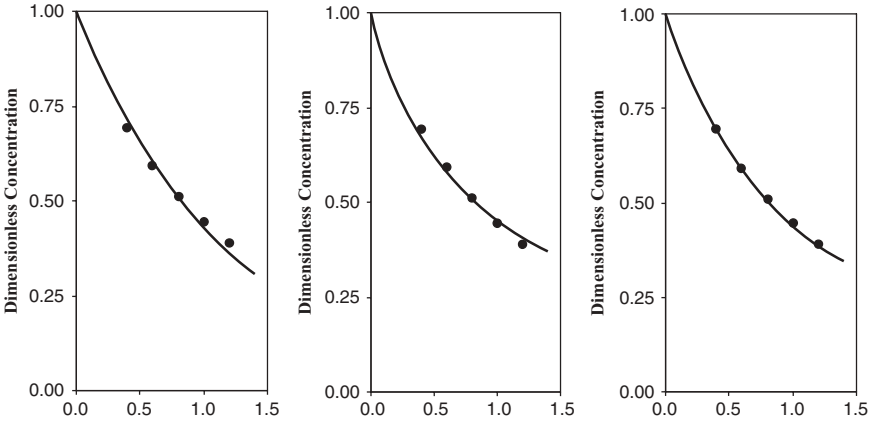

Figure 7.1 Experiment versus fitted batch reaction data.

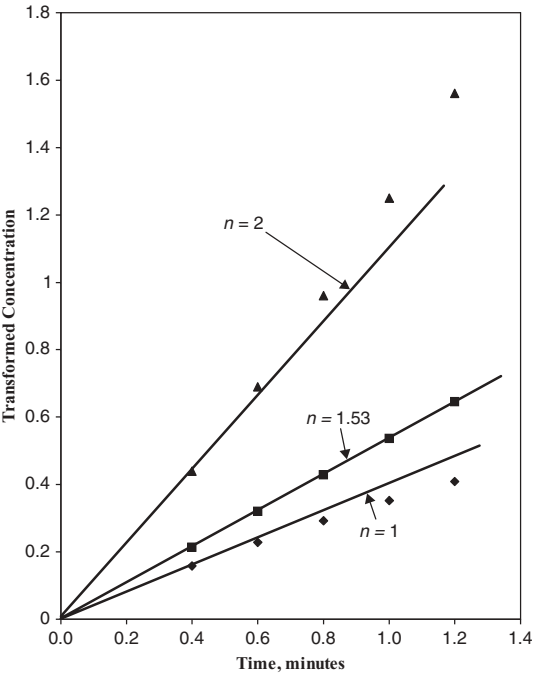

Figure 7.2 Classical graphical test for reaction order.

is assumed and the experimental data are transformed to one of the following forms:

$$\left[\frac{a(t)}{a_0}\right]^{1-n} - 1 \quad \text{for} \quad n \neq 1 \qquad -\ln\left[\frac{a(t)}{a_0}\right] \quad \text{for } n = 1 \tag{7.13}$$

Plot the transformed variable versus time. A straight line is a visually appealing demonstration that the correct value of n has been found. Figure 7.2 shows these plots for the data of Example 7.5. The central line in Figure 7.2 is for $n = 1.53$. The upper line shows the curvature in the data that results from assuming an incorrect order of $n = 2$, and the lower line is for $n = 1$.

The 1.53-order reaction of Example 7.5 is not elementary and could involve short-lived intermediates, but it was treated as a single reaction. We turn now to the problem of fitting kinetic data to multiple reactions. The multiple reactions listed in Section 2.1 are consecutive, competitive, independent, and reversible. Of these, the consecutive and competitive types, and combinations of them, pose special problems with respect to kinetic studies. They will be discussed in the context of integral reactors, although the concepts are also applicable to the CSTRs of Section 7.1.1 and to the confounded reactors of Section 7.1.6.

Consecutive Reactions

The prototypical reaction is A $\rightarrow$ B $\rightarrow$ C although reactions like Equation 6.2 can be treated in the same fashion. It may be that the first reaction is independent of the

second. This is the normal case when the first reaction is irreversible and homogeneous (so that components B and C do not occupy active sites and thus retard the primary reaction). A kinetic study can then measure just the initial and final concentrations of component A (or of A_1 and A_2 per Equation 6.2), and these data can be used to fit the rate expression as in Example 7.1. It is sometimes possible to measure the kinetics of the second reaction independently of the first reaction by reacting pure B, but there are many situations where pure B is not available.

If the reactions cannot be separated, it is not immediately clear as to what sum of squares should be minimized to fit the data. Define

$$SS_A^2 = \sum_{\text{data}} [a_{\text{experiment}} - a_{\text{model}}]^2 \tag{7.14}$$

with similar equations for SS_B^2 and SS_C^2. If only b_{out} has been measured, there is no choice but to use SS_B^2 to fit both reactions. If both a_{out} and b_{out} have been measured, SS_A^2 can be used to find $\mathscr{R}$ for the first reaction. The fitted rate expression becomes part of the model used to calculate b_{out}. The other part of the model is the assumed rate expression for the second reaction, the parameters of which are found by minimizing SS_B^2.

EXAMPLE 7.6

Suppose the consecutive reactions $2A \rightarrow B \rightarrow C$ are elementary. Determine the rate constants from the following experimental data obtained with an isothermal, constant-volume batch reactor:

Time, min	$a(t)$	$b(t)$	c(t) as Calculated from Stoichiometry
0	2.000	0	0
5	1.242	0.302	0.077
10	0.906	0.356	0.191
15	0.722	0.308	0.331
20	0.608	0.261	0.435
25	0.488	0.224	0.532
30	0.452	0.184	0.590

The concentrations shown are dimensionless. Actual concentrations have been divided by $a_0/2$ so that the initial conditions are $a = 2$, $b = 0$, and $c = 0$ at $t = 0$. The long-time value for $c(t)$ is 1.0.

SOLUTION: Since the reactions are assumed to be elementary, the batch reactor design equations are

$$\frac{da}{dt} = -2k_{\text{I}}a^2$$

and

$$\frac{db}{dt} = k_{\text{I}}a^2 - k_{\text{II}}b$$

Values for k_{I} and k_{II} are assumed and the above equations are integrated subject to the initial conditions. The random-search technique is then used to determine optimal values for the rate constants. Following are results for three different minimization strategies:

Minimization Method	k_{I}	k_{II}	s_A	s_B	s_C
Minimize S_A^2 and then S_B^2	2.98	7.56	0.0123	0.0070	0.0072
Minimize S_B^2 alone	3.01	7.58	0.0133	0.0069	0.0080
Minimize S_C^2 alone	2.10	10.33	0.15518	0.0785	0.0059

The first method begins by ignoring the data for b and c and uses just the data for a to determine the second-order rate constant k_{I} by minimizing S_A^2. This will obviously give the lowest possible value of s_A, which is the root mean error corresponding to the residual value of SS_A^2. With the resulting value for k_{I} fixed (i.e., $k_{\mathrm{I}} = 2.98$), S_B^2 is minimized to obtain k_{II}.

The second method uses the minimization of S_B^2 to simultaneously determine both k_{I} and k_{II}. This method gives the lowest value for ε_B. There is little difference between the first two methods in the current example since the data are of high quality. However, the sequential approach of first minimizing S_A^2 and then minimizing S_B^2 is somewhat better for this example and is preferred in general. Figure 7.3 shows the correlation.

The third method fits k_{I} and k_{II} by minimizing S_C^2. This approach gives the lowest value for s_C but at the expense of major errors in the predictions for a and b. The lesson from this is that reaction rates are best fit using data for the reactants and not the products.

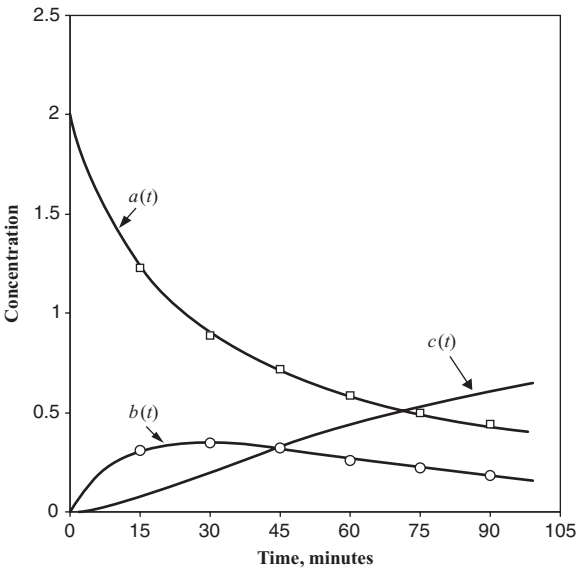

Figure 7.3 Combined data fit for consecutive reactions.

Competitive Reactions

The prototypical reactions are A → B and A → C. At least two of the three component concentrations should be measured and the material balance closed (see Section 7.1.5). Functional forms for the two reaction rates are assumed, and the parameters contained within these functional forms are estimated by minimizing an objective function of the form $w_A S_A^2 + w_B S_B^2 + w_B S_C^2$ where w_A, w_B, and w_C are positive weights that sum to 1. Weighting the three sums of squares equally gives good results when the rates for the two reactions are similar in magnitude.

7.1.4 Design of Experiments and Model Discrimination

The most import consideration is the design of the reactor that is used to collect kinetic data. A CSTR (called a chemostat in the biological field) is ideal because a significant volume is at a uniform composition and temperature and gives a significant extent of reaction so that chemical analysis is easy. Operation at steady state allows measurements to be repeated, further improving experimental accuracy.

Continuous flow stirred tank reactors are wonderful for kinetic experiments since they allow a direct determination of the reaction rate at known concentrations of the reactants. One other type of reactor allows this in principle. ***Differential reactors*** have such a small volume that concentrations and temperatures do not change appreciably from their inlet values. However, the small change in concentration makes it very hard to determine an accurate rate. The use of differential reactors is akin to numerical differentiation and is not recommended. If a CSTR cannot be used, a batch or piston flow reactor is preferred over a differential reactor even though the reaction rate is not measured directly but must be inferred from measured outlet concentrations. See also Sections 4.3.3 and 4.5.3, which describe a common technique for converting a differential reactor to a CSTR through the use of recycle.

Despite the theoretical advantages of a CSTR, most kinetic experiments are run in batch reactors for one simple reason: They are the easiest reactor to operate at a laboratory scale. Mixing is fast and temperatures are easily controlled in typical glassware, but it is difficult to operate at anything but atmospheric pressure. Kinetic measurements are sometimes conducted in small, sealed ampoules. These can withstand significant pressure, but sample sizes are small. The possibility of operating at pressure or under vacuum is one reason why engineers generally prefer metal reactors, whether batch or continuous.

Turn now to the selection of operating conditions. The most important consideration in picking an experimental design is that the range of variables used to fit the model should be larger than the range of variables that will be encountered in the use of the model. Run a few interaction experiments outside the expected operating space to avoid unpleasant surprises. To develop a comprehensive model, it is often necessary to add components to the feed in amounts that would not normally be present. For A → B, the concentration of B is correlated to that of A: $a_{\text{in}} - a = b - b_{\text{in}}$. Varying b_{in} will lessen the correlation and will help distinguish between competing rate expressions such as $\mathscr{R} = ka$, $\mathscr{R} = k_f a - k_r b$, and $\mathscr{R} = ka/(1 + k_B b)$.

Courses and books on the ***design of experiments*** can provide guidance, although our need for formalized techniques is less than that in the social and biological sciences, where experiments are more difficult to control and reproduce. A common experimental design is a two-level factorial where each operating variable is run at two levels, one high and one low, and the various combinations of these levels are also run. With two variables, experiments are run at the four corners of a square: low–low, low–high, high–low, and high–high. With three variables, experiments are run at the eight vertices of a cube (e.g., at low–low–low, low–low–high, and so on). With four variables, the experiments are done at the 16 vertices of a hypercube. Factorial designs are a good way to discover interactions between variables, but they are not optimal for fitting constants in a process model. Multilevel experiments on key variables such as catalyst concentrations and temperatures, particularly at conditions that will track the time or position in a real or anticipated reactor, will give more accurate constants for a given number of experiments. A good model is consistent with physical phenomena (i.e., $\mathscr{R}$ has a physically plausible form) and reduces the root mean error to plausible experimental error using as few adjustable parameters as possible. There is a philosophical principle known as Occam's razor that is particularly appropriate to statistical data analysis: When two theories can explain the data, the simpler theory is preferred. As seen in Section 5.1 on the various forms of Arrhenius temperature dependence, it is usually impossible to distinguish between mechanisms based on goodness of fit. The choice of the simplest form of Arrhenius behavior ($m = 0$) can be justified by Occam's razor. The same situation arises in complex reactions, particularly heterogeneous reactions, where several models may fit the data equally well.

7.1.5 Material Balance Closure

Material balance closure is a serious and sometimes difficult issue. Material balances can be made to appear perfect when some of the flow rates and concentrations are unmeasured. Simply assume values for the unmeasured quantities that close the material balance. However, no process can be commercialized without a reasonably accurate material balance. The keen experimenter in Examples 7.1–7.3 measured the outlet concentration of both components and consequently obtained a less than perfect balance. Should the measured concentrations be adjusted to achieve closure and, if so, how should the adjustment be done? The general advice is that a material balance should be closed if it is reasonably possible to do so. Methods for doing so can be fairly complicated. Here we treat a simple example of a partial balance about a chemical reactor.

It is necessary to know the number of inlet and outlet flow streams and the various components in those streams. Example 7.3 has one inlet stream, one outlet stream, and three components. The components are A, B, and I, where I represents all inerts. Closure normally begins by satisfying the overall mass balance, that is, by equating the input and outlet mass flow rates for a steady-state system. For the present case, the outlet flow was measured. The inlet flow was unmeasured so it must be assumed equal to the outlet flow. We suppose that A and B are the only reactive components. Then, for a constant-density system, it must be that $a_{\text{in}} + b_{\text{in}} = a_{\text{out}} + b_{\text{out}}$. This balance

is not quite satisfied by the experimental data, so an adjustment is needed. Define material balance fudge factors by

$$f_{\text{in}} f_{\text{out}} = \left[\frac{a_{\text{in}} + b_{\text{in}}}{a_{\text{out}} + b_{\text{out}}} \right]_{\text{measured}} \tag{7.15}$$

and then adjust the component concentrations using

$$\begin{aligned} [a_{\text{out}}]_{\text{adjusted}} &= f_{\text{out}} [a_{\text{out}}]_{\text{measured}} \\ [a_{\text{in}}]_{\text{adjusted}} &= \frac{[a_{\text{in}}]_{\text{measured}}}{f_{\text{in}}} \end{aligned} \tag{7.16}$$

with similar adjustments for component B. When the adjustments are made, $a_{\text{in}} + b_{\text{in}} = a_{\text{out}} + b_{\text{out}}$ will be satisfied. The apportionment of the total imbalance between the inlet and outlet streams is based on judgment regarding the relative accuracy of the measurements. Equation 7.15 merely specifies the product of the two fudge factors. If the inlet measurements are very accurate, that is, when the feed stream is prepared using batch weigh vessels or well-calibrated proportioning pumps, set $f_{\text{in}} = 1$ and let f_{out} absorb the whole error. If the errors are similar, the two factors are equal to the square root of the concentration ratio in Equation 7.15.

EXAMPLE 7.7

Close the material balance and repeat Example 7.3.

SOLUTION: Suppose $f_{\text{in}} = 1$ so that f_{out} is equal to the concentration ratio in Equation 7.15. Equations 7.16 are applied to each experimental run using the value of f_{out} appropriate to that run. The added code is:

```
For i = 1 To Ndata
     fudgeout=(ain(i)+bin(i))/(aout(i)+bout(i))
     aout(i) = fudgeout*aout(i)
     bout(i) = fudgeout*bout(i)
Next i
```

Following are the results for the combined data of Examples 7.1–7.3:

Case	k	n	r	Root Mean Error
11	0.509	1	0	0.0057
12	0.516	1.002	0.018	0.0055

The changes are small, but the results show that closing the material balance improves the fit. The recommended fit is now $\mathscr{R} = 0.509a$. It is shown in Figure 7.4. As a safeguard against elephant stampedes and other hazards of statistical analysis, a ***graphical view of a correlation*** is always recommended. However, graphical techniques are not recommended for the fitting process.

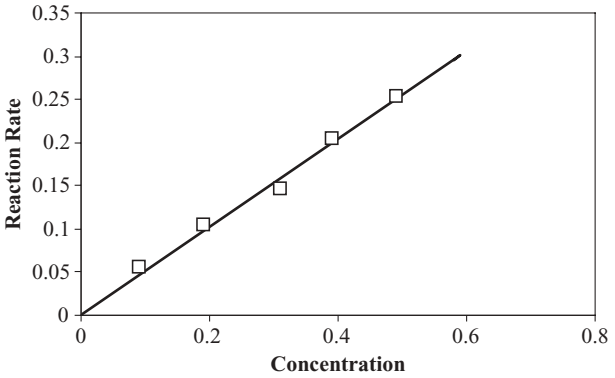

Figure 7.4 Final correlation for $\mathscr{R}(a)$.

All these examples have treated kinetic data taken at a single temperature. Most kinetic studies will include a variety of temperatures so that two parameters, k_0 and $\Delta E/R_g = T_{\text{act}}$, can be determined for each rate constant. The question now arises as to whether all the data should be pooled in one glorious minimization or if you should conduct separate analyses at each temperature and then fit the resulting rate constants to the Arrhenius form. The latter approach was used in Example 5.1, although the preliminary work needed to find the rate constants was not shown. This sequential approach has a major advantage over the combined approach. Suppose Equation 7.4 is being fit to the data. Are the exponents $m, n, \ldots$ the same at each temperature? If not, the reaction mechanism is changing and the possibility of consecutive or competitive reactions should be explored. If the exponents are the same within reasonable fitting accuracy, the data can be pooled or kept separate as desired. Pooling will give the best overall fit, but a better fit in some regions of the experimental space might be desirable for scaleup.

7.1.6 Confounded Reactors

The general approach of Equation 7.1 is applicable to any type of system:

1. Conduct kinetic experiments and ***measure*** some response of the system. Call this "experiment."
2. Pick a model for the system and assume values for the model's parameters. Solve the model to ***predict*** the response. Call this "model."
3. Adjust the parameters to minimize the sum of squares in Equation 7.1.

There is no requirement that the model represent a simple reactor such as a CSTR or isothermal PFR. If necessary, the model can represent a nonisothermal PFR with variable physical properties. It can be one of the distributed parameter models in Chapters 8 or 9. The model parameters can include the kinetic parameters in Equations

7.2–7.6 together with unknown transport properties such as a heat transfer coefficient. However, the simpler the better, and the extraction of rate data can be difficult if the model is confounded by heat and mass transfer effects.

There are many attempts to extract kinetic information from pilot plant or plant data. This may sound good to parsimonious management, but it is seldom a good alternative to doing the kinetic measurements under controlled conditions in the laboratory. Laboratory studies can usually approximate isothermal operation of an ideal reactor while measurements on larger equipment will be confounded by heat transfer and mixing effects. The laboratory studies can cover a broader rate of the experimental variables than is possible on the larger scale. An idealized process development sequence has the following steps:

1. Determine physical property and kinetic data from the literature or laboratory studies.
2. Combine these data with estimates of the transport parameters to model the desired full-scale plant.
3. Scale down the model to design a pilot plant that is scaleable upward and that will address the most significant uncertainties in the model of the full-scale facility.
4. Operate the pilot plant to determine the uncertain parameters. These will usually involve mixing and heat transfer, not basic kinetics.
5. Revise the model and build the full-scale plant.

Ideally, measurements on a pilot scale or plant scale are used to supplement rather than determine the reaction kinetics. If the kinetics are unknown, experimental limitations will usually prevent their accurate determination. The following section describes how to make the best of a less than ideal situation.

A relatively simple example of a confounded reactor is a nonisothermal batch reactor where the assumption of perfect mixing is reasonable but the temperature varies with time. The experimental data are fit to a model by minimizing Equation 7.1, but the prediction now requires a heat balance to be solved simultaneously with the component balances. For a batch reactor,

$$\frac{d(V\rho H)}{dt} = -V\,\Delta H_R\,\mathscr{R}_1 - UA_{\text{ext}}(T - T_{\text{ext}}) \tag{7.17}$$

Equation 7.17 introduces a number of new parameters, although physical properties such as the heats of reaction should be available. If all the parameters are all known with good accuracy, then the introduction of a heat balance merely requires that two parameters, k_0 and $\Delta E/R_g = T_{\text{act}}$, be used in place of each rate constant. Unfortunately, parameters such as UA_{ext} have $\pm 20\%$ error when calculated from standard correlations, and such errors are large enough to confound the kinetics experiments. As a practical mater, T_{out} should be measured as an experimental response that is used to help determine UA_{ext}. Even so, fitting the data can be extremely difficult. The sum

of squares may have such a shallow minimum that essentially identical fits can be achieved over a broad range of parameter values or there may be a systematic error that is difficult to identify.

EXAMPLE 7.8

Suppose a liquid–solid, heterogeneously catalyzed reaction is conducted in a jacketed, batch vessel. The reaction is A → B. The reactants are in the liquid phase, and the catalyst is present as a slurry. The adiabatic temperature rise for complete conversion is 50 K. The reactants are charged to the vessel at 298 K. The jacket temperature is held constant at 343 K throughout the reaction. The following data were measured:

t, h	$a(t)$	$T(t)$, K
0.4	0.972	313
0.8	0.901	326
1.0	0.842	332
1.2	0.759	339
1.4	0.623	346
1.6	0.487	350
1.8	0.302	360
2.2	0.081	361

where $a(t) = [\mathrm{A}]/[\mathrm{A}]_0$. Use these data to fit a rate expression of the form $\mathscr{R} = ka/(1 + k_A a)$.

SOLUTION: The equations to be solved are

$$\frac{da}{dt} = -\mathscr{R} = -\frac{k_0 \exp(-T_{\mathrm{act}}/T)a}{1 + k_A a}$$

and

$$\frac{dT}{dt} = 50\mathscr{R} - U'(T - T_{\mathrm{ext}})$$

We suppose that only the primary rate constant $k = k_0 \exp(-T_{\mathrm{act}}/T)$ is a function of temperature. Thus there are four adjustable constants, k_0, T_{act}, k_A, and U'. A least-squares minimization can be based on S_A^2, S_T^2 or a combination of the two, such as $S_C^2 = (100^* S_A^2 + S_T^2)/101$. The following table, although perhaps not showing the absolute minima, is representative of the fits that result from the various minimization criteria. The data in this example are artificial and were derived by adding random noise to a model with the parameters shown as "actual" in the table. The actual values for the root mean errors reflect the added random noise that simulates experimental error.

Minimize	k_0	T_{act}	k_A	U'	s_A	s_T	s_C
S_A^2	9.108×10^9	7817	0.2012	0.9402	0.0057	1.436	0.14330
S_T^2	5.054×10^9	7585	0.2686	0.9429	0.0302	1.068	0.1104
S_C^2	1.319×10^{10}	7947	0.1366	0.9654	0.0208	1.078	0.1092
Actual	4.000×10^9	7500	0.5000	1.000	0.0062	1.254	0.1249

All the fits are good with physically plausible values for the parameters and with root mean errors that are reasonable compared to the "experimental" error. If the data were from a real reactor, any of the fitted values would be judged as reasonable. The parameter values differ significantly between the cases and some are quite different from the actual values. The conclusion is that any of the fits can reproduce the data but none give accurate estimates of the actual parameter values.

Confounded reactors are likely to stay confounded. Data correlations can produce excellent fits and can be useful for predicting the response of the system to modest changes in operating conditions. Their predictive utility is largely limited to the system on which the measurements were made. Such fits are unlikely to produce any fundamental information regarding the reaction rate and have very limited utility in scaleup calculations.

7.2 THERMODYNAMICS OF CHEMICAL REACTIONS

Thermodynamics is a fundamental engineering science that has many applications to chemical reactor design. Here we give a summary of two important topics: determination of heat capacities and heats of reaction for inclusion in energy balances and determination of free energies of reaction to calculate equilibrium compositions and to aid in the determination of reverse reaction rates. The treatment is brief and is intended as a review. Details are available in any standard textbook on chemical engineering thermodynamics, (e.g., Smith et al. 2004). Tables 7.1 and 7.2 provide selected thermodynamic data for use in the examples and for general use in reaction engineering. Note that enthalpies, free energies, and heat capacities used in most thermodynamics books and in this section are expressed in molar units rather than mass units.

7.2.1 Terms in the Energy Balance

The design equations for a chemical reactor contain several parameters that are functions of temperature. Equation 7.17 applies to a nonisothermal batch reactor and is exemplary of the physical property variations that can be important even for ideal types of reactor. Note that the word "ideal" has three uses in this chapter. In connection with reactors, ideal refers to the quality of mixing in the vessel. Ideal batch reactors and CSTRs have perfect internal mixing. Ideal PFRs are perfectly mixed in the

Table 7.1 Heat Capacities at Low Pressures

	T_{max}	Standard	A	B	C	D
Gaseous Alkanes						
Methane, CH_4	1500	4.217	1.702	9.081	−2.164	
Ethane, C_2H_6	1500	6.369	1.131	19.225	−5.561	
ropane, C_3H_8	1500	9.001	1.213	28.785	−8.824	
n-Butane, C_4H_{10}	1500	11.928	1.935	36.915	−11.402	
iso-Butane, C_4H_{10}	1500	11.901	1.677	37.853	−11.945	
n-Pentane, C_5H_{12}	1500	14.731	2.464	45.351	−14.111	
n-Hexane, C_6H_{14}	1500	17.550	3.025	53.722	−16.791	
n-Heptane, C_7H_{16}	1500	20.361	3.570	62.127	−19.486	
n-Octane, C_8H_{18}	1500	23.174	4.108	70.567	−22.208	
Gaseous Alkenes						
Ethylene, C_2H_4	1500	5.325	1.424	14.394	−4.392	
Propylene, C_3H_6	1500	7.792	1.637	22.706	−6.915	
1-Butene, C_4H_8	1500	10.520	1.967	31.630	−9.873	
1-Pentene, C_5H_{10}	1500	13.437	2.691	39.753	−12.447	
1-Hexene, C_6H_{12}	1500	16.240	3.220	48.189	−15.157	
1-Heptene, C_7H_{14}	1500	19.053	3.768	56.588	−17.847	
1-Octene, C_8H_{16}	1500	21.868	4.324	64.960	−20.521	
Organic Gases						
Acetaldehyde, C_2H_4O	1000	6.506	1.693	17.978	−6.158	
Acetylene, C_2H_2	1500	5.253	6.132	1.952	−1.299	
Benzene, C_6H_6	1500	10.259	−0.206	39.064	−13.301	
1,3-Butadiene, C_4H_6	1500	10.720	2.734	26.786	−8.882	
Cyclohexane, C_6H_{12}	1500	13.121	3.876	63.249	−20.928	
Ethanol, C_2H_6O	1500	8.948	3.518	20.001	−6.002	
Ethylbenzene, C_8H_{10}	1500	15.993	1.124	55.380	−18.476	
Ethylene oxide, C_2H_4O	1000	5.784	0.385	23.463	−9.296	
Formaldehyde, CH_2O	1500	4.191	2.264	7.022	−1.877	
Methanol, CH_4O	1500	5.547	2.211	12.216	−3.450	
Styrene, C_8H_8	1500	15.534	2.050	50.192	−16.662	
Toluene, C_7H_8	1500	12.922	0.290	47.052	−15.716	
Inorganic Gases						
Air	2000	3.509	3.355	0.575		−0.016
Ammonia, NH_3	1800	4.269	3.578	3.020		−0.186
Bromine, Br2	3000	4.337	4.493	0.056		−0.154
Carbon monoxide, CO	2500	3.507	3.376	0.557		−0.031
Carbon dioxide, CO_2	2000	4.467	5.457	1.045		−1.157
Carbon disulfide, CS_2	1800	5.532	6.311	0.805		−0.906
Chlorine, Cl_2	3000	4.082	4.442	0.089		−0.344
Hydrogen, H_2	3000	3.468	3.249	0.422		0.083
Hydrogen sulfide, H_2S	2300	4.114	3.931	1.490		−0.232
Hydrogen chloride, HCl	2000	3.512	3.156	0.623		−0.151

(*Continued*)

Table 7.1 Heat Capacities at Low Pressures (*Continued*)

	T_{max}	Stdandard	A	B	C	D
Inorganic Gases						
Hydrogen cyanide, HCN	2500	4.326	4.736	1.359		−0.725
Nitrogen, N_2	2000	3.502	3.280	0.593		− 0.040
Nitrous oxide, N_2O	2000	4.646	5.328	1.214		−0.928
Nitric oxide, NO	2000	3.590	3.387	0.629		−0.014
Nitrogen dioxide, NO_2	2000	4.447	4.982	1.195		−0.792
Dinitrogen tetroxide, N_2O_4	2000	9.198	11.660	2.257		− 2.787
Oxygen, O_2	2000	3.535	3.639	0.506		−0.227
Sulfur dioxide, SO_2	2000	4.796	5.699	0.801		− 1.015
Sulfur trioxide, SO_3	2000	6.094	8.060	1.056		− 2.028
Water, H_2O	2000	4.038	3.470	1.450		0.121
Liquids						
Ammonia, NH_3	373	9.718	22.626	−100.75	192.71	
Aniline, C_6H_7N	373	23.070	15.819	29.03	−15.80	
Benzene, C_6H_6	373	16.157	−0.747	67.96	−37.78	
1,3-Butadiene, C_4H_6	373	14.779	22.711	−87.96	205.79	
Carbon tetrachloride, CCl_4	373	15.751	21.155	−48.28	101.14	
Chlorobenzene, C_6H_5Cl	373	18.240	11.278	32.86	−31.90	
Chloroform, $CHCl_3$	373	13.806	19.215	−42.89	83.01	
Cyclohexane, C_6H_{12}	373	18.737	−9.048	141.38	−161.62	
Ethanol, C_2H_6O	373	13.444	33.866	−172.60	349.17	
Ethylene oxide, C_2H_4O	373	10.590	21.039	−86.41	172.28	
Methanol, CH_4O	373	9.798	13.431	−51.28	131.13	
n-Propanol, C_3H_8O	373	16.921	41.653	−210.32	427.20	
Sulfur trioxide, SO_3	373	30.408	−2.930	137.08	−84.73	
Toluene, C_7H_8	373	18.611	15.133	6.79	16.35	
Water, H_2O	373	9.069	8.712	1.25	−0.18	
Solids						
Carbon(graphite), C	2000	1.026	1.771	0.771		−0.867
Sulfur (rhombic), S	368	3.748	4.114	−1.728		−0.783

Note: This table provides data for calculating molar heat capacities at low pressures according to the empirical formula

$$\frac{C_P}{R_g} = A + \frac{BT}{10^3} + \frac{CT^2}{10^6} + \frac{10^5 D}{T^2}$$

The column marked "Standard" shows the calculated value of C_P/R_g at 298.15 K.
Source: Data from Smith et al. (2001).

radial direction and have no mixing in the axial direction. These ideal reactors may be nonisothermal and may have physical properties that vary with temperature, pressure, and composition.

Ideal gases obey the ideal gas law, $P\rho_{\text{molar}} = R_g T$, and have internal energies that are a function of temperature alone. Ideal solutions have no enthalpy change upon

Table 7.2 Standard Enthalpies and Gibbs Free Energies of Formation in Joules per Mole of Substance Formed

	ΔH_F°	ΔG_F°
Gaseous Alkanes		
Methane, CH_4	−74,520	−50,460
Ethane, C_2H_6	−83,820	−31,855
Propane, C_3H_8	−104,680	−24,290
n-Butane, C_4H_{10}	−125,790	−16,570
n-Pentane, C_5H_{12}	−146,760	−8,650
n-Hexane, C_6H_{14}	−166,920	150
n-Heptane, C_7H_{16}	−187,780	8,260
n-Octane, C_8H_{18}	−208,750	16,260
Gaseous Alkenes		
Ethylene, C_2H_4	52,510	68,460
Propylene, C_3H_6	19,710	62,205
1-Butene, C_4H_8	−540	70,340
1-Pentene, C_5H_{10}	−21,820	78,410
1-Hexene, C_6H_{12}	−41,950	86,830
Other Organic Gases,		
Acetaldehyde, C_2H_4O	−166,190	−128,860
Acetylene, C_2H_2	227,480	209,970
Benzene, C_6H_6	82,930	129,665
1,3-Butadiene, C_4H_6	109,240	149,795
Cyclohexane, C_6H_{12}	−123,140	31,920
Ethanol, C_2H_6O	−235,100	−168,490
Ethylbenzene, C_8H_{10}	29,920	130,890
Ethylene oxide, C_2H_4O	−52,630	−13,010
Formaldehyde, CH_2O	−108,570	−102,530
Methanol, CH_4O	−200,660	−161,960
Methylcyclohexane, C_7H_{14}	−154,770	27,480
Styrene, C_8H_8	147,360	213,900
Toluene, C_7H_8	50,170	122,050
Inorganic Gases		
Ammonia, NH_3	−46,110	−16,450
Carbon dioxide, CO2	−393,509	−394,359
Carbon monoxide, CO	−110,525	−137,169
Hydrogen chloride, HCl	−92,307	−95,299
Hydrogen cyanide, HCN	135,100	124,700
Hydrogen sulfide, H_2S	−20,630	−33,560
Nitrous oxide, N_2O	82,050	104,200
Nitric oxide, NO	90,250	86,550
Nitrogen dioxide, NO_2	33,180	51,310
Nitrogen tetroxide, N_2O_4	9,160	97,540
Sulfur dioxide, SO_2	−296,830	−300,194

(*Continued*)

Table 7.2 Standard Enthalpies and Gibbs Free Energies of Formation in Joules per Mole of Substance Formed (*Continued*)

	ΔH_F°	ΔG_F°
Sulfur trioxide, SO_3	−395,720	−371,060
Water, H_2O	−241,818	−228,572
Acetic acid, $C_2H_4O_2$	−484,500	−389,900
Benzene, C_6H_6	49,080	124,520
Cyclohexane, C_6H_{12}	−156,230	26,850
Ethanol, C_2H_6O	−277,690	−174,780
Ethylene glycol, $C_2H_6O_2$	−454,800	−323,080
Ethylene oxide, C_2H_4O	−52,630	−13,010
Methanol, CH_4O	−238,660	−166,270
Methylcyclohexane ,C_7H_{14}	−190,160	20,560
Toluene, C_7H_8	12,180	113,630
Other Liquids		
Nitric Acid, HNO_3	−174,100	−80,710
Sulfuric acid, H_2SO_4	−813,989	−690,003
Water, H_2O	−285,830	−237,129

Source: Data from Smith et al. (2004).

mixing and have a special form for the entropy change upon mixing, $\Delta S_{\text{mix}} = R_g \Sigma x_A \ln x_A$, where x_A is the mole fraction of component A. Ideal gases form ideal solutions. Some liquid mixtures approximate ideal solutions, but this is relatively uncommon.

Enthalpy

Enthalpy is calculated relative to a standard state that is normally chosen as $T_0 = 298.15\text{K} = 25^\circ\text{C}$ and $P_0 = 1$ bar pressure. The change in enthalpy with pressure can usually be ignored. For extreme changes in pressure, changes due to pressure can be calculated using

$$\left(\frac{\partial H}{\partial P}\right)_T = V - T\left(\frac{\partial V}{\partial T}\right)_P = V(1 - \beta T) \tag{7.18}$$

where β is the volumetric coefficient of thermal expansion and can be evaluated from the equation of state for the material and is zero for an ideal gas. The standard state for gases is actually that for a hypothetical ideal gas. Real gases are not perfectly ideal at 1 bar. Thus H for a real gas at 298.15 K and 1 bar will not be exactly zero. The difference is usually negligible.

The change in enthalpy with respect to temperature is not negligible. It can be calculated for a pure component using the specific heat correlations like those in Table 7.1:

$$H = \int_{T_0}^{T} C_P \, dt = R_g \left[AT + \frac{BT^2}{2 \times 10^3} + \frac{CT^3}{3 \times 10^6} - \frac{10^5 D}{T} \right]_{T_0}^{T} \tag{7.19}$$

where the constants are given in Table 7.1. Note that these are molar heat capacities. For reactions involving a change of phase, Equation 7.19 must be modified to include the heat associated with the phase transition (e.g., a heat of vaporization). The enthalpy term in the heat balance applies to the entire reacting mixture, and thus heats of mixing may warrant inclusion. However, they are usually small compared to the heats of reaction and are generally ignored in reaction engineering calculations. The normal assumption is that

$$H = aH_A + bH_B + \cdots + iH_I = \sum_{\text{species}} aH_A \tag{7.20}$$

where the summation extends over all reactants and inerts.

Heats of Reaction

Chemical reactions absorb or liberate energy, usually in the form of heat. The heat of reaction, ΔH_R, is defined as the amount of energy absorbed or liberated if the reaction goes to completion at a fixed temperature and pressure. When $\Delta H_R > 0$, energy is absorbed and the reaction is said to be ***endothermic***. When $\Delta H_R < 0$, energy is liberated and the reaction is said to be ***exothermic***. The magnitude of ΔH_R depends on the temperature and pressure of the reaction and on the phases (e.g., gas, liquid, solid) of the various components. It also depends on an arbitrary constant multiplier in the stoichiometric equation.

EXAMPLE 7.9

The reaction of hydrogen and oxygen is highly exothermic. At 298.15 K and 1 bar,

$$H_2(g) + \tfrac{1}{2}O_2(g) \rightarrow H_2O(g) \qquad \Delta H_R = -241{,}818 \text{ J} \tag{I}$$

Alternatively,

$$2H_2(g) + O_2(g) \rightarrow 2H_2O(g) \qquad \Delta H_R = -483{,}636 \text{ J} \tag{II}$$

The reverse reaction, the decomposition of water, is highly endothermic:

$$H_2O(g) \rightarrow H_2(g) + \tfrac{1}{2}O_2(g) \qquad \Delta H_R = +241{,}818 \text{ J} \tag{III}$$

$$H_2O(g) \rightarrow 2H_2(g) + O_2(g) \qquad \Delta H_R = +483{,}636 \text{ J} \tag{IV}$$

These equations differ by constant factors, but all the heats of reaction become equal when expressed in joules per mole of water formed, −241,818. They are also equal when expressed in joules per mole of oxygen formed, +483,636, or in joules per mole of hydrogen formed, +241,818. Any of these values can be used provided $\mathscr{R}$ is the rate at which a reaction product with a stoichiometric coefficient of +1 is being produced. Thus, $\mathscr{R}_{\text{I}}$ should be the rate at which water is being formed; $\mathscr{R}_{\text{II}}$ should be the rate at which hydrogen is being produced; and $\mathscr{R}_{\text{IV}}$ should be the rate at which oxygen is being produced. Even $\mathscr{R}_{\text{III}}$ can be made to fit the scheme, but it must be the rate at which a hypothetical component is being formed.

Suppose ΔH_R for reaction I was measured in a calorimeter. Hydrogen and oxygen were charged at 298.15 K and 1 bar. The reaction occurred, the system was restored to 298.15 K and 1 bar, but the product water was not condensed. This gives the heat of reaction for reaction I. Had the water been condensed, the measured exothermicity would have been larger:

$$H_2(g) + \tfrac{1}{2}O_2(g) \rightarrow H_2O(l) \qquad \Delta H_R = -285{,}830 \text{ J} \tag{V}$$

Reactions I and V differ by the heat of vaporization:

$$H_2O(g) \rightarrow H_2O(l) \qquad \Delta H_R = +44{,}012J \tag{VI}$$

Reactions V and VI can obviously be summed to give reaction I.

The heats of reaction associated with stoichiometric equations are additive just as the equations themselves are additive. Some authors illustrate this fact by treating the evolved heat as the product of the reaction. Thus, they write

$$H_2(g) + \tfrac{1}{2}O_2(g) \rightarrow H_2O(g) + 241{,}818 \text{ J}$$

This is beautifully correct in terms of the physics and is a very useful way to include heats of reaction when summing chemical equations. It is confused by the thermodynamic convention that heat is positive when absorbed by the system. The convention may have been logical for mechanical engineers concerned with heat engines, but chemists and chemical engineers would have chosen the opposite convention. Once a convention is adopted, it is almost impossible to change. Electrical engineers still pretend that current flows from positive to negative.

The additive nature of stoichiometric equations and heats of reactions allows the tabulation of ΔH_R for a relatively few canonical reactions that can be algebraically summed to give ΔH_R for a reaction of interest. The canonical reactions represent the formation of compounds directly from their elements. The participating species in these reactions are the elements as reactants and a single chemical compound as the product. The heats of reactions for these mainly hypothetical reactions are called ***heats of formation***. Table 7.2 gives ***standard heats of formation***, ΔH_F°, for a variety of compounds. The reacting elements and the product compound are all assumed to be at standard conditions of $T_0 = 298.15$ K and $P_0 = 1$ bar. In addition to directly tabulated data, heats of formation can be calculated from heats of combustion and can be estimated using group contribution theory.

EXAMPLE 7.10

Determine ΔH_R for the dehydrogenation of ethylbenzene to styrene at 298.15 K and 1 bar.

SOLUTION: Table 7.2 gives ΔH_F° for styrene at 298.15 K. The formation reaction is

$$8C(\text{graphite}) + 4H_2(g) \rightarrow \text{styrene}(g) \qquad \Delta H_R = 147,360 \text{ J} \tag{7.21}$$

For ethylbenzene, $\Delta H_F^\circ = 29{,}920$ J, but we write the stoichiometric equation using a multiplier of -1 . Thus

$$-8\text{C(graphite)} - 5\text{H}_2\text{(g)} \rightarrow -\text{ethylbenzene(g)} \qquad \Delta H_R = -29{,}920 \text{ J} \tag{7.22}$$

The stoichiometry and heats of reaction in Equations 7.21 and 7.22 are algebraically summed to give

$$\text{Ethylbenzene(g)} \rightarrow \text{styrene(g)} + \text{H}_2\text{(g)} \qquad \Delta H_R = 117{,}440 \text{ J} \tag{7.23}$$

so that $\Delta H_R = 117{,}440$ J per mole of styrene produced. Note that the species participating in Equation 7.23 are in their standard states since standard heats of formation were used in Equations 7.21 and 7.22. Thus we have obtained the ***standard heat of reaction***, ΔH_R°, at $T_0 = 298.15$ K and $P_0 = 1$ bar.

It does not matter that there is no known catalyst that can accomplish the reaction in Equation 7.21 directly. Heats of reaction, including heats of formation, depend on conditions before and after the reaction but not on the specific reaction path. Thus one might imagine a very complicated chemistry that starts at standard conditions, goes through an arbitrary trajectory of temperature and pressure, returns to standard conditions, and has Equation 7.21 as its overall effect. Here, $\Delta H_F^\circ = +147{,}360$ J per mole of styrene formed is the net heat effect associated with this overall reaction.

The reaction in Equation 7.23 is feasible as written but certainly not at temperatures as low as 25°C, and it must be adjusted for more realistic conditions. The adjustment for temperature uses

$$\left(\frac{\partial \Delta H_R}{\partial T}\right)_P = \sum_{\text{species}} \nu_A \left[\left(\frac{\partial H}{\partial T}\right)_P\right]_A = \sum_{\text{species}} \nu_A (C_P)_A = \Delta C_P \tag{7.24}$$

So that the corrected heat of reaction is

$$\Delta H_R = \Delta H_R^\circ + \int_{T_0}^{T} \Delta C_P \, dT = \Delta H_R^\circ + \sum_{\text{species}} \nu_A H_A \tag{7.25}$$

The summations in these equations include only those chemical species that directly participate in the reaction, and the weighting is by the stoichiometric coefficient. Compare this to Equation 7.20 where the summation includes everything in the reactor and the weighting is by concentration. Equation 7.25 is used to determine the heat generated by the reaction. Equation 7.20 is used to determine how the generated heat affects the entire reacting mass.

A pressure adjustment to the heat of reaction may be needed at high pressures. The adjustment is based on

$$\left(\frac{\partial \Delta H_R}{\partial P}\right)_T = \sum_{\text{species}} \nu_A \left[\left(\frac{\partial H}{\partial P}\right)_T\right]_A = \Delta \left(\frac{\partial H}{\partial P}\right)_T \tag{7.26}$$

See Equation 7.18 to evaluate this expression.

EXAMPLE 7.11

Determine ΔH_R for the ethylbenzene dehydrogenation reaction at 973 K and 0.5 atm.

SOLUTION: From Example 7.10, $\Delta H_R = 117,440$ J at $T_0 = 298.15$ K. We need to calculate ΔC_P. Using Equation 7.24

$$\Delta C_P = (C_P)_{\text{styrene}} + (C_P)_{\text{hydrogen}} - (C_P)_{\text{ethylbenzene}} \tag{7.27}$$

The data of Table 7.1 give

$$\frac{\Delta C_P}{R_g} = 4.175 - \frac{4.766T}{10^3} + \frac{1.814T^2}{10^6} + \frac{8300}{T^2}$$

From this,

$$\Delta H_R = \Delta H_R^\circ + \int_{T_0}^{T} \Delta C_P \, dT = 117{,}440 + 8.314 \left[4.175T - \frac{4.766T^2}{2 \times 10^3} + \frac{1.814T^3}{3 \times 10^6} - \frac{8300}{T}\right]_{T_0}^{T}$$

Setting $T = 973$ K gives $\Delta H_R = 117{,}440 + 11{,}090 = 128{,}530$ J. The temperature is high and the pressure is low relative to critical conditions for all three components. Thus an ideal gas assumption is reasonable, and the pressure change from 1 bar to 0.5 atm does not affect the heat of reaction.

7.2.2 Reaction Equilibria

Many reactions show appreciable reversibility. This section introduces thermodynamic methods for estimating equilibrium compositions from free energies of reaction and relates these methods to the kinetic approach where the equilibrium composition is found by equating the forward and reverse reaction rates.

Equilibrium Constants

We begin with the kinetic approach. Refer to Equation 1.15 and set the rate of the reaction to zero:

$$K_{\text{kinetic}} = \frac{k_f}{k_r} = \frac{[\text{R}]^{\nu_R}[\text{S}]^{\nu_S}}{[\text{A}]^{-\nu_A}[\text{B}]^{-\nu_B}} = \prod_{\text{species}} a^{\nu_A} \tag{7.28}$$

This is the expected form of the ***kinetic equilibrium constant*** for elementary reactions; K_{kinetic} is a function of the temperature and pressure at which the reaction is conducted. Note that K_{kinetic} is dimensionless only when there is no change in the number of moles upon reaction, $\nu = \sum \nu_A = 0$.

In principle, K_{kinetic} is found by determining the rates of the forward and reverse reactions and then equating them. In practice, the usual method for determining K_{kinetic} is to run batch reactions to completion. If different starting concentrations give the same value for K_{kinetic}, the functional form for Equation 7.28 is justified. Values for

chemical equilibrium constants are routinely reported in the literature for specific reactions but are seldom compiled because they are hard to generalize.

The reactant mixture may be so nonideal that Equation 7.28 is inadequate. The rigorous thermodynamic approach is to replace the concentrations in Equation 7.28 with fugacities. This leads to the ***thermodynamic equilibrium constant:***

$$K_{\text{thermo}} = \prod_{\text{species}} \left[\frac{\hat{f}_A}{f_A^\circ} \right]^{\nu_A} = \exp\left(\frac{-\Delta G_R^\circ}{R_g T} \right) \tag{7.29}$$

where $\hat{f}_A$ is the fugacity of component A in the mixture, f_A° is the fugacity of pure component A at the temperature and pressure of the mixture, and ΔG_R° is the ***standard free energy of reaction***, at the temperature of the mixture. The right-hand side of Equation 7.29 is used to determine a numerical value for K_{thermo} based on the ***standard free energy of formation***, ΔG_F°. Values for ΔG_F° are given in Table 7.2. They can be algebraically summed just like heats of formation to obtain ΔG_R° for reactions of interest.

EXAMPLE 7.12

Determine ΔG_R° for the dehydrogenation of ethylbenzene to styrene at 298.15 K.

SOLUTION: Table 7.2 gives ΔG_F° for styrene at 298.15 K. The formation reaction is

$$8\text{C(graphite)} + 4\text{H}_2\text{(g)} \rightarrow \text{styrene(g)} \qquad \Delta G_R = 213{,}900 \text{ J}$$

For ethylbenzene,

$$-8\text{C(graphite)} - 5\text{H}_2\text{(g)} \rightarrow -\text{ethylbenzene(g)} \qquad \Delta G_R = -130{,}890 \text{ J}$$

These equations are summed to give

$$\text{Ethylbenzene(g)} \rightarrow \text{styrene(g)} + \text{H}_2\text{(g)} \qquad \Delta G_R = 83,010 \text{ J}$$

so that $\Delta G_R = 83{,}010$ J per mole of styrene produced. Since the species are in their standard states, we have obtained ΔG_R°.

We now turn to the calculation of compositions. The fugacities in Equation 7.29 may be related to partial pressures or mole fractions. A form of Equation 7.29 suitable for gases is

$$K_{\text{thermo}} = \left[\frac{P}{P_0} \right]^{\nu} \prod_{\text{species}} [y_A \hat{\phi}_A]^{\nu_A} \tag{7.30}$$

where $\nu = \sum \nu_A$; y_A is the mole fraction of component A, $\hat{\phi}_A$ is its fugacity coefficient, and P_0 is the pressure used to determine ΔG_R°. The fugacity coefficients in Equation 7.30 can be calculated from PVT (pressure, volume, temperature) data for the mixture or from generalized correlations. It is frequently possible to assume ideal gas behavior

so that $\hat{\phi}_A = 1$ for each component. Then Equation 7.30 becomes

$$K_{\text{thermo}} = \left[\frac{P}{P_0}\right]^{\nu} \prod_{\text{species}} [y_A]^{\nu_A} \tag{7.31}$$

For liquids or solids, the counterpart to Equation 7.30 is

$$K_{\text{thermo}} = \exp\left[\frac{P - P_0}{R_g T} \sum_{\text{species}} \nu_A V_A\right] \prod_{\text{species}} [x_A \gamma_A]^{\nu_A} \tag{7.32}$$

where x_A is the mole fraction of component A, V_A is its molar volume, and γ_A is its activity coefficient in the mixture. For incompressible materials, the exponential term is 1.0. If the mixture is an ideal solution, $\gamma_A = 1$ and

$$K_{\text{thermo}} = \prod_{\text{species}} [x_A]^{\nu_A} = \exp\left(\frac{-\Delta G_R^{\circ}}{R_g T}\right) \tag{7.33}$$

The equilibrium constant is independent of pressure as is ΔG_R°. Equation 7.33 applies to ideal solutions of incompressible materials and has no pressure dependence. Equation 7.31 applies to ideal gas mixtures and has the explicit pressure dependence of the P/P_0 term when there is a change in the number of moles upon reaction, $\nu \neq 0$. The temperature dependence of the thermodynamic equilibrium constant is given by

$$\frac{d \ln K_{\text{thermo}}}{dT} = \frac{\Delta H_R}{R_g T^2} \tag{7.34}$$

This can be integrated to give

$$K_{\text{thermo}} = K_0 K_1 K_2 K_3 = \exp\left(\frac{-\Delta G_R^{\circ}}{R_g T_0}\right) \exp\left[\frac{\Delta H_R^{\circ}}{R_g T_0}\left(1 - \frac{T_0}{T}\right)\right] \times \exp\left[-\frac{1}{T}\int_{T_0}^{T} \frac{\Delta C_P}{R_g} dT\right] \exp\left[\int_{T_0}^{T} \frac{\Delta C_P \, dT}{R_g T}\right] \tag{7.35}$$

Equation 7.35 is used to find K_{thermo} as a function of reaction temperature T. Only the first two factors are important when $\Delta C_P^{\circ} \approx 0$, as is frequently the case. Then $\ln(K_{\text{thermo}})$ will be a linear function of T^{-1}. This fact justifies Figure 7.5, which plots the equilibrium constant as a linear function of temperature for some gas phase reactions.

Reconciliation of Equilibrium Constants

The two approaches to determining equilibrium constants are consistent for ideal gases and ideal solutions of incompressible materials. For a reaction involving ideal

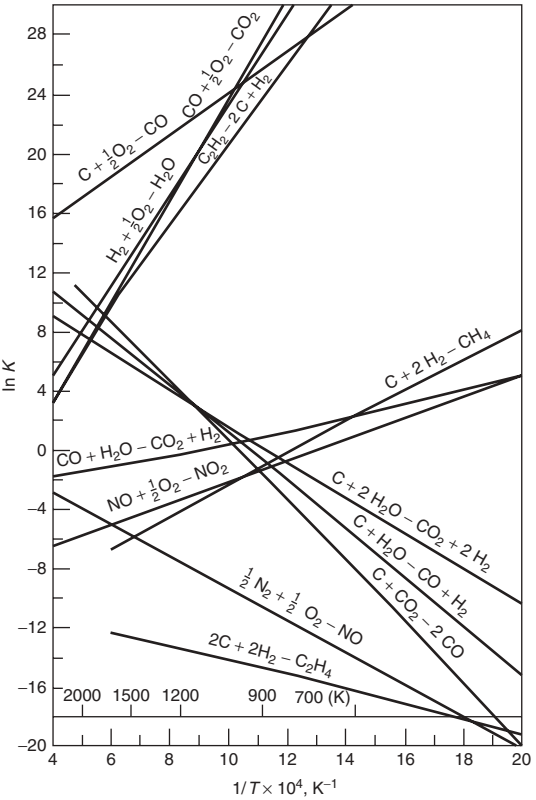

Figure 7.5 Thermodynamic equilibrium constants for gas phase reactions. From J. M. Smith, and H. C. Van Ness, *Introduction to Chemical Engineering Thermodynamics*, 4th ed., McGraw-Hill, New York, 1986.

gases, Equation 7.29 becomes

$$K_{\text{thermo}} = \left[\frac{P}{P_0}\right]^{\nu} \rho_{\text{molar}}^{-\nu} \prod_{\text{species}} [A]^{\nu_A} = \left[\frac{P}{P_0}\right]^{\nu} \rho_{\text{molar}}^{-\nu} K_{\text{kinetic}} = \left[\frac{R_g T}{P_0}\right]^{\nu} K_{\text{kinetic}} \tag{7.36}$$

and the explicit pressure dependence vanishes. Since K_{thermo} is independent of pressure, so is K_{kinetic} for an ideal gas mixture.

For ideal solutions of incompressible materials,

$$K_{\text{thermo}} = \rho_{\text{molar}}^{-\nu} \prod_{\text{species}} [A]^{\nu_A} = \rho_{\text{molar}}^{-\nu} K_{\text{kinetic}} = \exp\left(\frac{-\Delta G_R^{\circ}}{R_g T}\right) \tag{7.37}$$

which is also independent of pressure.

For nonideal solutions, the thermodynamic equilibrium constant, as given by Equations 7.29, is fundamental and K_{kinetic} should be reconciled to it even though the exponents in Equation 7.28 may be different than the stoichiometric coefficients. As

a practical matter, the equilibrium composition of nonideal solutions is usually found by running reactions to completion rather than by thermodynamic calculations, but they can also be predicted using generalized correlations.

Reverse Reaction Rates

Suppose that the kinetic equilibrium constant is known in terms of both its numerical value and the exponents in Equation 7.28. If the solution is ideal and the reaction is elementary, then the exponents in the reaction rate, that is, the exponents in Equation 1.15, should be the stoichiometric coefficients for the reaction, and K_{kinetic} should be the ratio of forward to reverse rate constants as in Equation 1.15. If the reaction is complex, the kinetic equilibrium constant may still have the ideal form of Equation 7.28. The appropriateness of Equation 7.28 is based on the ideality of the mixture at equilibrium and not on the kinetic path by which equilibrium was reached. However, the forward and reverse reaction rates must still be equal at equilibrium, and this fact dictates the functional form of the rate expression near the equilibrium point.

EXAMPLE 7.13

Suppose A $\rightleftarrows$ B + C at high temperatures and low pressures in the gas phase. The reaction rate is assumed to have the form

$$\mathscr{R} = k_f a^n - \mathscr{R}_r$$

where the various constants are to be determined experimentally. Suppose the kinetic equilibrium constant as defined by Equation 7.28 is

$$K_{\text{kinetic}} = \frac{bc}{a}$$

and has been measured to be 50 mol m^{-3} at 1 atm pressure and 550 K. Find the appropriate functional form for the overall rate equation in the vicinity of the equilibrium point as a function of temperature, pressure, and composition

SOLUTION: Assume the reverse reaction has the form $\mathscr{R}_r = k_r a^m b^r c^s$. Setting the overall reaction rate equal to zero at the equilibrium point gives a second expression for K_{kinetic}:

$$K_{\text{kinetic}} = \frac{k_f}{k_r} = \frac{a^m b^r c^s}{a^n}$$

Equating the two expressions for K_{kinetic} gives $m = n - 1$ and $r = s = 1$. Also, $k_r = k_f K_{\text{kinetic}}$. Thus,

$$\mathscr{R} = k_f \left[a^n - \frac{a^{n-1} bc}{K_{\text{kinetic}}} \right]$$

This is the required form with $K_{\text{kinetic}} = 50$ mol m^{-3} at 1 atm and 550 K. According to Equation 7.36, K_{kinetic} is a function of temperature but not of pressure. (This does not mean that the equilibrium composition is independent of pressure. See Example 7.14.) To evaluate the

temperature dependence, it is useful to replace K_{kinetic} with K_{thermo}. For $\nu = 1$,

$$\mathscr{R} = k_f \left[a^n - \frac{R_g T}{P_o K_{\text{thermo}}} a^{n-1} bc \right] \tag{7.38}$$

Equation 7.35 is used to find K_{thermo} as a function of temperature. Since K_{kinetic} was given and K_{thermo} can be calculated from it, Equation 7.38 contains only n and k_f as adjustable constants, although k_f can be divided between k_0 and T_{act} if measurements are made at several temperatures.

Example 7.13 showed how reaction rates can be adjusted to account for reversibility. The method uses a single constant, K_{kinetic} or K_{thermo}, and is rigorous for both the forward and reverse rates when the reactions are elementary. For complex reactions with fitted rate equations, the method should produce good results provided the reaction always starts on the same side of equilibrium. A separate fitting exercise and a separate rate expression are needed for reactions starting on the other side of equilibrium.

Equation 7.28 may not provide a good fit for the equilibrium data if the equilibrium mixture is nonideal. Suppose that the proper form is determined through extensive experimentation or by using thermodynamic correlations. It could be a version of Equation 7.28 with exponents different from the stoichiometric coefficients or it may be a different functional form. Whatever the form, it is possible to force the reverse rate to be consistent with the equilibrium constant, and this is recommended whenever the reaction shows appreciable reversibility.

Equilibrium Compositions for Single Reactions

We turn now to the problem of calculating the equilibrium composition for a single homogeneous reaction. The most direct way of estimating equilibrium compositions is by simulating the reaction. Set the desired initial conditions and simulate an isothermal, constant-pressure batch reaction. If the simulation is accurate, a real reaction could follow the same trajectory of composition versus time to approach equilibrium, but an accurate simulation is unnecessary. The solution can use the method of false transients. The rate equation must have a functional form consistent with the functional form of K_{kinetic}, for example, Equation 7.28. The time scale is unimportant and even the functional forms for the forward and reverse reactions have some latitude, as will be illustrated in the following example.

EXAMPLE 7.14

Use the method of false transients to determine equilibrium concentrations for the reaction of Example 7.13. Specifically, determine the equilibrium mole fraction of component A at $T = 550$ K as a function of pressure given that the reaction begins with pure A.

SOLUTION: The obvious way to solve this problem is to choose a pressure, calculate a_0 using the ideal gas law, and then conduct a batch reaction at constant T and P. Equation 7.38

gives the reaction rate. Any reasonable values for n and k_f can be used. Since there is a change in the number of moles upon reaction, a variable-volume reactor is needed. A straightforward but messy approach uses the methodology of Section 2.6 and solves component balances in terms of the number of moles, N_A, N_B, and N_C.

A simpler method arbitrarily picks values for a_0 and reacts this material in a batch reactor at constant V and T. When the reaction is complete, P is calculated from the molar density of the equilibrium mixture. As an example, set $a_0 = 22.2$ ($P = 1$ atm) and react to completion. The long-time results from integrating the constant-volume batch equations are $a = 5.53$, $b = c = 16.63$, $\rho_{\text{molar}} = 38.79$ mol m^{-3} and $y_A = 0.143$. The pressure at equilibrium is 1.75 atm.

Whichever method is used produces the curve in Figure 7.6. The curve is independent of n and k_f in Equation 7.38.

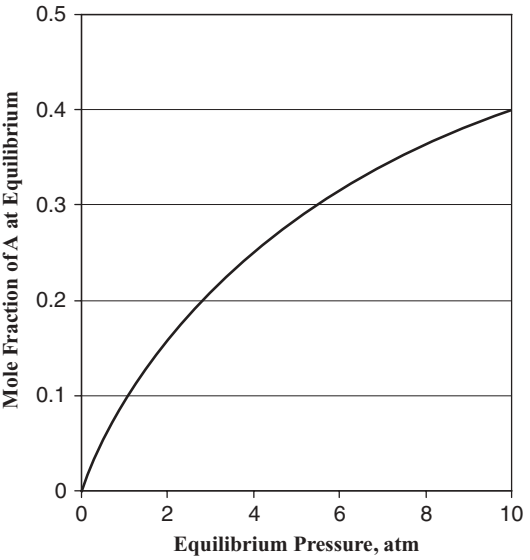

Figure 7.6 Equilibrium concentrations calculated by the method of false transients for a non-elementary reaction.

The reaction coordinate defined in Section 2.8 provides an algebraic method for calculating equilibrium concentrations. For a single reaction,

$$N_A = (N_A)_0 + \nu_A \varepsilon \tag{7.39}$$

and mole fractions are given by

$$y_A = \frac{N_A}{N_0 + \nu\varepsilon} = \frac{(N_A)_0 + \nu_A\varepsilon}{N_0 + \nu\varepsilon} \tag{7.40}$$

Suppose the numerical value of the thermodynamic equilibrium constant is known, say from the free energy of formation. Then Equation 7.40 is substituted into Equation 7.31 and the result is solved for ε.

EXAMPLE 7.15

Use the reaction coordinate method to determine equilibrium concentrations for the reaction of Example 7.11. Specifically, determine the equilibrium mole fraction of component A at $T = 550\,\text{K}$ as a function of pressure given that the reaction begins with pure A.

SOLUTION: The kinetic equilibrium constant is 50 mol m^{-3}. It is converted to mole fraction form using

$$\prod_{\text{species}} [y_A]^{\nu_A} = \rho_{\text{molar}}^{-\nu} K_{\text{kinetic}} = \frac{\prod_{\text{species}} [a]^{\nu_A}}{[P/(R_g T)]^{\nu}} \tag{7.41}$$

For the reaction at hand,

$$\frac{y_B y_C}{y_A} = \frac{[(N_B)_0 + \varepsilon]\,[(N_C)_0 + \varepsilon]}{[(N_A)_0 - \varepsilon]\,[N_0 + \varepsilon]} = \frac{50 \times 8.205 \times 10^{-5} \times 550}{P} = \frac{2.256}{P}$$

where P is in atmospheres. This equation is a quadratic in ε that has only one root in the physically realistic range of $-1 \le \varepsilon \le 1$. The root depends on the pressure and the relative values for N_A, N_B, and N_C. For a feed of pure A, set $N_A = 1$ and $N_B = N_C = 0$. Solution gives

$$\varepsilon = \sqrt{\frac{2.256}{P + 2.256}}$$

Set $P = 1.75$ atm. Then $\varepsilon = 0.750$ and $y_A = 0.143$, in agreement with Example 7.14.

Examples 7.14 and 7.15 treated the case where the kinetic equilibrium constant had been determined experimentally. The next two examples illustrate the case where the thermodynamic equilibrium constant is estimated from tabulated data.

EXAMPLE 7.16

Estimate the equilibrium composition of the ethylbenzene dehydrogenation reaction at 298.15 K and 0.5 atm. Consider two cases:

(a) The initial composition is pure ethylbenzene.

(b) The initial composition is 1 mol each of ethylbenzene and styrene and 0.5 mol of hydrogen.

SOLUTION: Example 7.12 found $\Delta G_R = 83,010$ J. Equation 7.29 gives $K_{\text{thermo}} = 2.8 \times 10^{-15}$ so that equilibrium at 298.15 K overwhelmingly favors ethylbenzene. Suppose the ideal gas assumption is not too bad even at this low temperature ($T_c = 617$ K for ethylbenzene). The pressure is 0.5066 bar and $\nu = 1$. The reaction has the form A $\rightarrow$ B + C so the reaction coordinate formulation is similar to that in Example 7.15. When the feed is pure ethylbenzene, Equation 7.31 becomes

$$2.86 \times 10^{-15} = \left[\frac{0.5066}{1}\right] \frac{y_{\text{H}_2}\, y_{\text{styrene}}}{y_{\text{ethylbenzene}}} = 0.5066 \frac{\varepsilon^2}{(1-\varepsilon)(1+\varepsilon)}$$

Solution gives $\varepsilon = 7.5 \times 10^{-8}$. The equilibrium mole fractions are $y_{\text{ethylbenzene}} \approx 1$ and $y_{\text{styrene}} = y_{\text{hydrogen}} = 7.5 \times 10^{-8}$.

The solution for part (b) is obtained from

$$2.8 \times 10^{-15} = \left[\frac{0.5066}{1}\right] \frac{y_{H_2}\, y_{\text{styrene}}}{y_{\text{ethylbenzene}}} = 0.5066 \frac{(1+\varepsilon)(0.5+\varepsilon)}{(1-\varepsilon)(2.5+\varepsilon)}$$

Solution of the quadratic gives $\varepsilon \approx -0.5$ so that $y_{\text{ethylbenzene}} \approx 0.75$, $y_{\text{styrene}} \approx 0.25$, and $y_{\text{hydrogen}} \approx 0$. The equilibrium is shifted so strongly toward ethylbenzene that essentially all the hydrogen is used to hydrogenate styrene.

EXAMPLE 7.17

Estimate the equilibrium composition from the ethylbenzene dehydrogenation reaction at 973 K and 0.5 atm. The starting composition is pure ethylbenzene.

SOLUTION: This problem illustrates the adjustment of K_{thermo} for temperature. Equation 7.35 expresses it as the product of four factors. The results in Examples 7.12 and 7.13 are used to evaluate these factors.

$$K_0 = \exp\left(\frac{-\Delta G_R^o}{R_g T_0}\right) = \exp\left(\frac{-83{,}010}{8.314 T_0}\right) = 2.86 \times 10^{-15}$$

$$K_1 = \exp\left[\frac{\Delta H_R^o}{R_g T_0}\left(1 - \frac{T_0}{T}\right)\right] = \exp\left[\frac{117{,}440}{8.314 T_0}\left(1 - \frac{T_0}{T}\right)\right] = 1.87 \times 10^{14}$$

$$K_2 = \exp\left[-\frac{1}{R_g T}\int_{T_0}^{T} \Delta C_P\, dt\right] = \exp\left[\frac{\Delta H_R^0 - \Delta H_R}{8.314 T}\right] = 0.264$$

$$K_3 = \exp\left[\int_{T_0}^{T} \frac{\Delta C_P\, dT}{R_g T}\right] = \exp\left[4.175 \ln T - \frac{4.766 T}{10^3} + \frac{1.814 T^2}{2 \times 10^6} - \frac{8300}{2T^2}\right]_{T_0}^{T} = 12.7$$

and $K_{\text{thermo}} = K_0 K_1 K_2 K_3 = 1.72$. Proceeding as in Example 7.16(a)

$$1.72 = \left[\frac{0.5066}{1}\right] \frac{y_{\text{H}_2}\, y_{\text{styrene}}}{y_{\text{ethylbenzene}}} = 0.5066 \frac{\varepsilon^2}{(1-\varepsilon)(1+\varepsilon)}$$

Solution gives $\varepsilon = 0.879$. The equilibrium mole fractions are $y_{\text{ethylbenzene}} = 0.064$ and $y_{\text{styrene}} = y_{\text{hydrogen}} = 0.468$.

EXAMPLE 7.18

Pure ethylbenzene is contacted at 973 K with a 9:1 molar ratio of steam and a small amount of a dehydrogenation catalyst. The reaction rate has the form

$$A \underset{k_r}{\overset{k_f}{\rightleftarrows}} B + C \text{ where } k_f = k_0 \exp\left(-\frac{T_{\text{act}}}{T}\right) = 160{,}000 \exp\left(-\frac{9000}{T}\right) s^{-1}$$

and k_r is determined from the equilibrium relationship according to Equation 7.38. The mixture is charged at an initial pressure of 0.1 bar to an adiabatic, constant-volume batch reactor. The

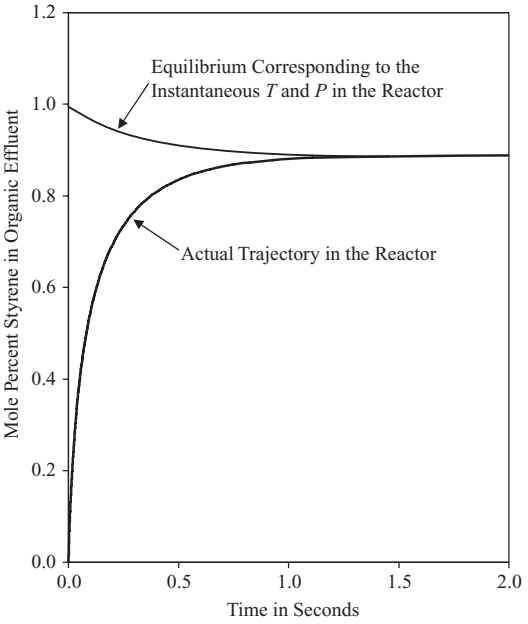

Figure 7.7 Batch reaction trajectory for ethylbenzene dehydrogenation.

steam is inert and the thermal mass of the catalyst can be neglected. Calculate the reaction trajectory. Do not assume constant physical properties.

SOLUTION: A rigorous treatment of a reversible reaction with variable physical properties is quite complicated, as will be seen by the code. The present example involves just two ODEs, one for composition and one for enthalpy. Pressure is a dependent variable. If the rate constants are accurate, the solution will give the actual reaction trajectory (temperature, pressure, and composition as a function of time). If k_0 and T_{act} are wrong, the long-time solution will still approach equilibrium. The solution is then an application of the method of false transients.

Results from Code for Example 7.18 are shown in Figure 7.7. The macro is specific to the example reaction with $\nu = +1$ but can be generalized to other reactions. Components of the macro illustrate many of the previous examples. Specific heats and enthalpies are calculated analytically using the functional form of Equation 7.19 and the data in Tables 7.1 and 7.2. The main computational loop begins with the estimation of K_{thermo} using the methodology of Example 7.17.

The equilibrium composition corresponding to instantaneous values of T and P is estimated using the methodology of Example 7.15. These calculations are included as a point of interest. They are not needed to find the reaction trajectory. Results are reported as the mole fraction of styrene in the organic mixture of styrene plus ethylbenzene. The initial value, corresponding to $T = 973$ and $P = 0.1$ bar, is 0.995. This equilibrium value gradually declines, primarily due to the change in temperature. The final value is 0.888, which is closely approximated by the long-time solution. The kinetic equilibrium constant is estimated from the thermodynamic equilibrium constant using Equation 7.36. The reaction rate is calculated and compositions are marched ahead by one time step. The energy balance is then used to march

Code for Example 7.18

```
Dim conc(4), yinit(4)
Public A(5), B(5), C(5), D(5), y(4)
Sub Example7_16()

' Data from Table 7.1
' Ethylbenzene is 1, Styrene is 2, Hydrogen is 3, Water is 4.
A(1) = 1.124: B(1) = 55.38: C(1) = -18.476: D(1) = 0
A(2) = 2.05: B(2) = 50.192: C(2) = -16.662: D(2) = 0
A(3) = 3.249: B(3) = 0.422: C(3) = 0: D(3) = 0.083
A(4) = 3.47: B(4) = 1.45: C(4) = 0: D(4) = 0.121
'  Calculate delta Cp for C1 reacting to C2 + C3
A(5) = A(2) + A(3) - A(1)
B(5) = B(2) + B(3) - B(1)
C(5) = C(2) + C(3) - C(1)
D(5) = D(2) + D(3) - D(1)
For n = 1 To 5
    A(n) = A(n)
    B(n) = B(n) / 1000#
    C(n) = C(n) / 1000000#
    D(n) = D(n) * 100000#
Next n
Rg = 8.314

' Results from Examples 7.8 and 7.10.
DeltaHR0 = 117440
DeltaGR0 = 83010

'  Starting conditions
y(1) = 0.1
y(2) = 0
y(3) = 0
y(4) = 0.9
Tinit = 973
T = Tinit
T0 = 298.15
P0 = 1
P = 0.1
'  Calculate molar density using bar as the pressure unit
Rgg = 0.00008314
rhoinit = P / Rgg / T
rho = rhoinit
For n = 1 To 4
    yinit(n) = y(n)
    conc(n) = rho * y(n)
Next
' Initial condition used for enthalpy marching
    For n = 1 To 4
       Enthalpy = Enthalpy + y(n) * rho * Rg * (CpInt(n, T) - CpInt(n, T0))
    Next
'  Time step and output control
dtime = 0.00001
ip = 2
Tp = Tinit
```

```
Do  'Main Loop

' Thermodynamic equilibrium constant calculated as in Example 7.15
    K0 = Exp(-DeltaGR0 / Rg / T0)
    K1 = Exp(DeltaHR0 / Rg / T0 * (1 - T0 / T))
    K2 = Exp(-(CpInt(5, T) - CpInt(5, T0)) / T)
    K3 = Exp(DCpRTInt(T) - DCpRTInt(T0))
    Kthermo = K0 * K1 * K2 * K3

'Equilibrium mole fractions are calculated using method of Example 7.13.
'These 'results are calculated for interest only.  They are not needed
'for the main 'calculation.  The code is specific to initial conditions
    G = Kthermo * P0 / P
    eps = (-0.9 * G + Sqr(0.81 * G * G + 0.4 * (1 + G) * G)) / 2 / (1 + G)
    eyEB = (0.1 - eps) / (1 + eps)
    eySty = eps / (1 + eps)

' Kinetic equilibrium constant from Equation 7.36
    KK = Kthermo * P0 / Rgg / T

'Reaction
    kf = 160000 * Exp(-9000 / T)
    RRate = kf * (conc(1) - conc(2) * conc(3) / KK)
    DeltaHR = 117440 + (CpInt(5, T) - CpInt(5, T0)) * Rg

'  Approximate solution based on marching ahead in temperature, Eqn. 7.45
'    T = T - DeltaHR * RRate * dtime / rho / CpMix(T) / Rg

' A more rigorous solution based on marching ahead in enthalpy according
' to Equation 7.42 is given in the next 16 lines of code.
   Enthalpy = Enthalpy - DeltaHR * RRate * dtime

    Thigh = T
    Tlow = T - 1
    Txx = Tlow
    For m = 1 To 20
        Tx = (Thigh + Tlow) / 2#
        DeltaHR = 117440# + (CpInt(5, Tx) - CpInt(5, T0)) * Rg
        DHR = DeltaHR * (rhoinit * 0.1 - rho * y(1)) / rhoinit
        xx = CpInt(1, Tx) - CpInt(1, Tinit)
        DHS = Rg * (0.1 * xx + 0.9 * (CpInt(4, Tx) - CpInt(4, Tinit)))
       If DHR + DHS > Enthalpy Then
            Thigh = Tx
        Else
            Tlow = Tx
        End If
    Next m
    T = Tx
11
    conc(1) = conc(1) - RRate * dtime
    conc(2) = conc(2) + RRate * dtime
    conc(3) = conc(3) + RRate * dtime
    rho = conc(1) + conc(2) + conc(3) + conc(4)
    y(1) = conc(1) / rho
```

```
    y(2) = conc(2) / rho
    y(3) = conc(3) / rho
    y(4) = conc(4) / rho

' Pressure
    P = rho * Rgg * T

' Output trajectory results when temperature has decreased by 1 degree
If T <= Tp Then
    GoSub Output
    Tp = Tp - 2
End If

Rtime = Rtime + dtime
Loop While Abs(y(1) - eyEB) > 0.0000001    'End of main loop

GoSub Output  'Output final values

Exit Sub

Output:
    ip = ip + 1
    Cells(ip, 1) = Rtime
    Cells(ip, 2) = y(2) / (y(1) + y(2))
    Cells(ip, 3) = eySty / (eyEB + eySty)
    Cells(ip, 4) = T
    Cells(ip, 5) = P
    Cells(ip, 6) = y(1)
Return

End Sub
Function Cp(n, T)
    Cp = A(n) + B(n) * T + C(n) * T * T + D(n) / T / T
End Function
Function CpInt(n, T)
    CpInt = A(n) * T + B(n) * T * T / 2 + C(n) * T * T * T / 3 - D(n) / T
End Function
Function DCpRTInt(T)
   DCpRTInt = A(5)* Log(T) + B(5)* T + C(5)* T * T / 2 - D(5) / 2 / T ^ 2
End Function
Function CpMix(T)
   CpMix = y(1)* Cp(1, T)+ y(2)*Cp(2, T)+y(3)* Cp(3, T) + y(4) * Cp(4, T)
End Function
```

enthalpy ahead by one step. The form of the energy balance in Chapter 5 used a mass basis for heat capacities and enthalpies. A molar basis is more suitable for the current problem. The molar counterpart of Equation 5.18 is

$$\frac{d(V\rho_{\text{molar}}H)}{dt} = -V\Delta H_R\mathscr{R} - UA_{\text{ext}}(T - T_{\text{ext}}) \tag{7.42}$$

where $U = 0$ in the current example and H is the enthalpy per mole of the reaction mixture:

$$H = \int_{T_0}^{T} (C_p)_{\text{mix}}\, dT' \tag{7.43}$$

Note that C_P is now in mole units rather than mass units. The quantity $V\rho_{\text{molar}}$ is a not constant since there is a change in moles upon reaction, $\nu = 1$. Expanding the derivative

$$\frac{d(V\rho_{\text{molar}}H)}{dt} = V\rho_{\text{molar}}\frac{dH}{dt} + H\frac{d(V\rho_{\text{molar}})}{dt} = \left[V\rho_{\text{molar}}\frac{dH}{dT} + H\frac{d(V\rho_{\text{molar}})}{dT}\right]\frac{dT}{dt}$$

The dH/dT term is evaluated by differentiating Equation 7.43 with respect to the upper limit of the integral. This gives

$$\left[\rho_{\text{molar}}(C_P)_{\text{mix}} + H\frac{d\rho_{\text{molar}}}{dT}\right]\frac{dT}{dt} = -\Delta H_R\,\mathscr{R} - \frac{U\,A_{\text{ext}}(T - T_{\text{ext}})}{V} \tag{7.44}$$

This result is perfectly general for a constant-volume reactor. It continues to apply when ρ, C_P, and H are expressed in mass units, as is normally the case for liquid systems. The current example has a high level of inerts so that the molar density shows little variation. The approximate heat balance

$$\frac{dT}{dt} = \frac{-\Delta H_R\,\mathscr{R}}{\rho_{\text{molar}}(C_P)_{\text{mix}}} - \frac{UA_{\text{ext}}(T - T_{\text{ext}})}{V\rho_{\text{molar}}(C_P)_{\text{mix}}} \tag{7.45}$$

gives a result that is essentially identical to using Equation 7.42 to match the composite variable $V\rho_{\text{molar}}H$.

Equilibrium Compositions for Multiple Reactions

When there are two or more independent reactions, Equation 7.29 is written for each reaction:

$$\begin{aligned}(K_{\text{thermo}})_{\text{I}} &= \exp\left[\frac{(\Delta G_R^o)_{\text{I}}}{R_g T}\right]\\ (K_{\text{thermo}})_{\text{II}} &= \exp\left[\frac{(\Delta G_R^o)_{\text{II}}}{R_g T}\right]\\ &\vdots\end{aligned} \tag{7.46}$$

so that there are M thermodynamic equilibrium constants associated with M reactions involving N chemical components. The various equilibrium constants can be expressed in terms of the component mole fractions for suitable ideal cases using Equation 7.31 or 7.33. There will be N such mole fractions, but these can be expressed in terms of M reaction coordinates using the reaction coordinate method. For multiple reactions there is a separate reaction coordinate for each reaction, and Equation 7.40 generalizes to

$$y_A = \frac{(N_A)_0 + \sum\limits_{\text{reactions}} \nu_{\text{A,I}}\varepsilon_I}{N_0 + \sum\limits_{\text{reactions}} \nu_{\text{I}}\varepsilon_I} \tag{7.47}$$

EXAMPLE 7.19

At high temperatures, atmospheric nitrogen can be converted to various oxides. Consider only two, NO and NO_2. What is their equilibrium in air at 1500 K and 1 bar pressure?

SOLUTION: Two independent reactions are needed that involve all four components. A systematic way of doing this begins with the formation reactions; but, for the present, fairly simple case, Figure 7.5 includes two reactions that can be used directly:

$$\tfrac{1}{2}N_2 + \tfrac{1}{2}O_2 \rightarrow NO \qquad \text{(I)}$$

$$NO + \tfrac{1}{2}O_2 \rightarrow NO_2 \qquad \text{(II)}$$

The plots in Figure 7.5 give $(K_{\text{thermo}})_I = 0.0033$ and $(K_{\text{thermo}})_{\text{II}} = 0.011$. The ideal gas law is an excellent approximation at the reaction conditions so that Equation 7.31 applies. Since $P = P_0$, there is no correction for pressure. Thus

$$0.0033 = \frac{y_{NO}}{y_{N_2}^{1/2} y_{O_2}^{1/2}} \qquad 0.011 = \frac{y_{NO_2}}{y_{NO} y_{O_2}^{1/2}}$$

A solution using the reaction coordinate method will be illustrated. Equation 2.48 is applied to a starting mixture of 0.21 mol of oxygen and 0.79 mol of nitrogen. Nitrogen is not an inert in these reactions, so the lumping of argon with nitrogen is not strictly justified, but the error will be small. Equation 2.48 gives

$$\begin{bmatrix} N_{N_2} \\ N_{O_2} \\ N_{NO} \\ N_{NO_2} \end{bmatrix} = \begin{bmatrix} 0.79 \\ 0.21 \\ 0 \\ 0 \end{bmatrix} + \begin{bmatrix} -0.5 & 0 \\ -0.5 & -0.5 \\ 1 & -1 \\ 0 & 1 \end{bmatrix} \begin{bmatrix} \varepsilon_{\text{I}} \\ \varepsilon_{\text{II}} \end{bmatrix}$$

or

$$N_{N_2} = 0.79 - 0.5\varepsilon_{\text{I}} \qquad N_{O_2} = 0.21 - 0.5\varepsilon_{\text{I}} - 0.5\varepsilon_{\text{II}}$$

$$N_{NO} = \varepsilon_{\text{I}} - \varepsilon_{\text{II}} \qquad N_{NO_2} = -\varepsilon_{\text{I}} - \varepsilon_{\text{II}}$$

$$N_{\text{total}} = 1 - 0.5\varepsilon_{\text{II}}$$

where the last row was obtained by summing the other four. The various mole fractions are

$$y_{N_2} = \frac{0.79 - 0.5\varepsilon_{\text{I}}}{1 - 0.5\varepsilon_{\text{II}}}$$

$$y_{O_2} = \frac{0.21 - 0.5\varepsilon_{\text{I}} - 0.5\varepsilon_{\text{II}}}{1 - 0.5\varepsilon_{\text{II}}}$$

$$y_{NO} = \frac{\varepsilon_{\text{I}} - \varepsilon_{\text{II}}}{1 - 0.5\varepsilon_{\text{II}}}$$

$$y_{NO_2} = \frac{\varepsilon_{\text{II}}}{1 - 0.5\varepsilon_{\text{II}}}$$

Substitution into the equilibrium conditions gives

$$0.0033 = \frac{\varepsilon_{\text{I}} - \varepsilon_{\text{II}}}{(0.79 - 0.5\varepsilon_I)^{1/2}(0.21 - 0.5\varepsilon_{\text{I}} - 0.5\varepsilon_{\text{II}})^{1/2}}$$

$$0.011 = \frac{\varepsilon_{\text{II}}(1 - 0.5\varepsilon_{\text{II}})^{1/2}}{(\varepsilon_{\text{I}} - \varepsilon_{\text{II}})(0.21 - 0.5\varepsilon_{\text{I}} - 0.5\varepsilon_{\text{II}})^{1/2}}$$

This pair of equations can be solved simultaneously to give $\varepsilon_{\text{I}} = 0.0135$ and $\varepsilon_{\text{II}} = 6.7 \times 10^{-6}$. The mole fractions are $y_{N_2} = 0.7893$, $y_{O_2} = 0.2093$, $y_{NO} = 0.00135$, and $y_{NO_2} = 7 \times 10^{-6}$.

Example 7.19 illustrates the utility of the reaction coordinate method for solving equilibrium problems. There are no more equations than there are independent

chemical reactions. However, in practical problems such as atmospheric chemistry and combustion, the number of reactions is very large. A relatively complete description of high-temperature equilibria between oxygen and nitrogen might consider the concentrations of N_2, O_2, N_2O, N_2O_4, NO, NO_2, N, O, N_2O_2, N_2O_3, N_2O_5, NO_3, O_3, and possibly others. The various reaction coordinates will differ by many orders of magnitude, and the numerical solution would be quite difficult even assuming the various equilibrium constants could be found. The method of false transients would ease the numerical solution but would not help with the problem of estimating the equilibrium constants.

Independent Reactions

In this section we consider the number of independent reactions that are necessary to develop equilibrium relationships between N chemical species. A systematic approach is the following:

1. List all chemical species, both elements and compounds that are believed to exist at equilibrium. By "element" we mean the predominant species at standard state conditions, for example, O_2 for oxygen at 1 bar and 298.15 K.
2. Write the formation reactions from the elements for each compound. The term "compound" includes elemental forms other than the standard one, for example, we would consider monatomic oxygen a compound and write $^1/_2\ O_2 \rightarrow O$ as one of the reactions.
3. The stoichiometric equations are combined to eliminate any elements that are not believed present in significant amounts at equilibrium.

The result of the above procedures is M equations where $M < N$.

EXAMPLE 7.20

Find a set of independent reactions to represent the equilibrium of CO, CO_2, H_2, and H_2O.

SOLUTION: Assume that only the stated species are present at equilibrium. Then there are three formation reactions:

$$\begin{aligned} H_2 + \tfrac{1}{2}O_2 &\rightarrow H_2O \\ C + \tfrac{1}{2}O_2 &\rightarrow CO \\ C + O_2 &\rightarrow CO_2 \end{aligned}$$

The third reaction is subtracted from the second to eliminate carbon, giving the following set:

$$\begin{aligned} H_2 + \tfrac{1}{2}O_2 &\rightarrow H_2O \\ -\tfrac{1}{2}O_2 &\rightarrow CO - CO_2 \end{aligned}$$

These are now added to eliminate oxygen. The result can be rearranged to give

$$H_2 + CO_2 \rightarrow H_2O + CO$$

Thus $N = 4$ and $M = 1$. The final reaction is the water–gas shift reaction.

EXAMPLE 7.21

Find a set of independent reactions to represent the equilibrium products for a reaction between 1 mol of methane and 0.5 mol of oxygen

SOLUTION: It is difficult to decide a priori what species will be present in significant concentrations. Experimental observations are the best guide to constructing an equilibrium model. Lacking this, exhaustive calculations or chemical insight must be used. Except at very high temperatures, free-radical concentrations will be quite low, but free radicals could provide the reaction mechanisms by which equilibrium is approached. Reactions such as $2CH_3\bullet \rightarrow C_2H_6$ will yield higher hydrocarbons so that the number of theoretically possible species is unbounded. In a low-temperature oxidation, such reactions may be impossible. However, the impossibility is based on kinetic considerations, not thermodynamics.

Assume that oxygen and hydrogen will not be present as elements but that carbon may be. Nonelemental compounds to be considered are CH_4, CO_2, CO, H_2O, CH_3OH, and CH_2O, each of which has a formation reaction:

$$\begin{aligned} C + 2H_2 &\rightarrow CH_4 \\ C + O_2 &\rightarrow CO_2 \\ C + \tfrac{1}{2}O_2 &\rightarrow CO \\ H_2 + \tfrac{1}{2}O_2 &\rightarrow H_2O \\ C + 2H_2 + \tfrac{1}{2}O_2 &\rightarrow CH_3OH \\ C + H_2 + \tfrac{1}{2}O_2 &\rightarrow CH_2O \end{aligned}$$

If carbon, hydrogen, and oxygen were all present as elements, none of the formation reactions could be eliminated. We would then have $N = 9$ and $M = 6$. With elemental hydrogen and oxygen assumed absent, two species and two equations can be eliminated, giving $N = 7$ and $M = 4$. Pick any equation containing oxygen—there are five choices—and use it to eliminate oxygen from the other equations. Discard the equation used for the elimination. This reduces M to 5. Now pick any equation containing hydrogen and use it to eliminate hydrogen from the other equations. Discard the equation used for the elimination. This gives $M = 4$. One of the many possible results is

$$\begin{aligned} 3C + 2H_2O &\rightarrow CH_4 + 2CO \\ 2CO &\rightarrow C + CO_2 \\ 2C + 2H_2O &\rightarrow CH_3OH + CO \\ C + H_2O &\rightarrow CH_2O \end{aligned}$$

These four equations are perfectly adequate for equilibrium calculations although they are nonsense with respect to mechanism. Table 7.2 has the data needed to calculate the four equilibrium constants at the standard state of 298.15 K and 1 bar. Table 7.1 has the necessary data to correct for temperature. The composition at equilibrium can be found using the reaction coordinate method or the method of false transients. The four chemical equations are not unique since various members of the set can be combined algebraically without reducing the dimensionality, $M = 4$. Various equivalent sets can be derived, but none can even approximate a plausible mechanism since one of the starting materials, oxygen, has been assumed absent at equilibrium. Thermodynamics provides the destination but not the route.

We have considered thermodynamic equilibrium in homogeneous systems. When two or more phases exist, it is necessary that the requirements for reaction equilibria (i.e., Equations 7.46) be satisfied simultaneously with the requirements for phase equilibria (i.e., that the chemical potentials be equal in each phase). We leave the treatment of chemical equilibria in multiphase systems to the specialized literature, but note that the method of false transients normally works quite well for multiphase systems. The simulation includes reaction—typically confined to one phase—and mass transfer between the phases. The governing equations are given in Chapter 11.

SUGGESTED FURTHER READINGS

A massive but readable classic on chemical kinetics and the extraction of rate data from batch experiments is:

K. J. Laidler, *Reactor Kinetics*, Pergamon, London, 1963 (2 vols.).

This book and many standard texts were written before computers became widely available. They emphasize graphical techniques for fitting data. These methods give valuable qualitative insights that may be missed with too much reliance on least-squares analysis. However, for quantification, the computer wins.

There is an extensive literature, particularly the Russian literature, on material balance closures. The procedures can be quite complicated. The following paper includes a review of the literature.

C. Aldrich and van J. S. J. Deventer Identification of gross errors in material balance measurements by means of neural nets, *Chem. Eng. Sci.*, **49**, 1357–1368 (1994).

The classic text on chemical engineering thermodynamics is now in its seventh edition:

J. M. Smith, H. C. Van Ness, and M. M. Abbott, *Introduction to Chemical Engineering Thermodynamics,* 7th ed., McGraw-Hill, New York, 2004.

Chapters 4 and 13 of that book treat chemical reaction thermodynamics in much greater detail than given here.

The Internet has become the best source for thermodynamic data. Run a search on something like "chemical thermodynamic data" on any serious search engine, and you will find multiple sources, most of which allow free downloads. The data in the standard handbooks (e.g., *Perry's Handbook, 1997*) are still correct but rather capricious in scope and likely to be expressed in archaic units like those sprinkled here and there in this book.

PROBLEMS

7.1 Suppose the following data on the iodination of ethane have been obtained at 603 K using a recirculating gas phase reactor that closely approximates a CSTR. The indicated concentrations are partial pressures in atmospheres and the mean residence time is in seconds.

$[I_2]_{in}$	$[C_2H_6]_{in}$	$\bar{t}$	$[I_2]_{out}$	$[C_2H_6]_{out}$	$[HI]_{out}$	$[C_2H_5I]_{out}$
0.1	0.9	260	0.0830	0.884	0.0176	0.0162
0.1	0.9	1300	0.0420	0.841	0.0615	0.0594
0.1	0.9	2300	0.0221	0.824	0.0797	0.0770

Use nonlinear regression to fit these data to a plausible functional form for $\mathscr{R}$. See Example 7.22 for linear regression results that can provide good initial guesses.

7.2 The disproportionation of *p*-toluenesulfonic acid has the following stoichiometry:

$$3(CH_3C_6H_4SO_2H) \rightarrow CH_3C_6H_4SO_2SC_6H_4CH_3 + CH_3C_6H_4SO_3H + H_2O$$

Kice and Bowers (1962) obtained the following batch data at 70°C in a reaction medium consisting of acetic acid plus 0.56 M H_2O plus 1.0 M H_2SO_4

Time, h	$[CH_3C_6H_4SO_2H]^{-1}$
0	5
0.5	8
1.0	12
1.5	16
4.0	36
5.0	44
6.0	53

The units on $[CH_3C_6H_4SO_2H]^{-1}$ are inverse molarity. Reciprocal concentrations are often cited in the chemical kinetics literature for second-order reactions. Confirm that second-order kinetics provide a good fit and determine the rate constant.

7.3 The decolorization of crystal violet dye by reaction with sodium hydroxide is a convenient means for studying mixing effects in continuous flow reactors. The reaction is

$$(C_6H_4N(CH_3)_2)_3CCl + NaOH \rightarrow (C_6H_4N(CH_3)_2)_3COH + NaCl$$

The first step is to obtain a good kinetic model for the reaction. To this end, the following batch experiments were conducted in laboratory glassware:

Run no.	B1	B2	B3	B4
$[NaOH]_0$	0.02 *N*	0.04 *N*	0.04 *N*	0.04 *N*
Temperature	30	30	38	45

T	*d*(*t*)	*t*	*d*(*t*)	*t*	*d*(*t*)	*t*	*d*(*t*)
0	13.55	0	13.55	0	13.55	0	13.55
2.0	7.87	3.0	2.62	0.5	9.52	0.5	8.72
4.0	4.62	3.6	1.85	1.0	6.68	1.0	5.61
5.0	3.48	4.5	1.08	2.0	3.3	2.0	2.33
6.0	2.65	6.0	0.46	3.0	1.62	3.0	0.95

The time t is in minutes and the dye concentration $d(t)$ is in milliliters of stock dye solution per 100 mL of reactant mixture. The stock dye solution was $7.72 \times 10^{-5} M$. Use these data to fit a rate expression of the form

$$R = k_0 \left[\exp\left(\frac{-T_{\text{act}}}{T} \right) \right] [\text{dye}]^n [\text{NaOH}]^m$$

The unknown parameters are k_0, T_{act}, n, and m. There are several ways they could be found. Use at least two methods and compare the results. Note that the NaOH is present in great excess.

7.4 Use stoichiometry to calculate $c(t)$ for the data of Example 7.6. Then fit k_{I} and k_{II} by minimizing S_C^2.

7.5 The following data were collected in an isothermal, constant-volume batch reactor. The stoichiometry is known and the material balance has been closed. The reactions are A → B and A → C. Assume they are elementary. Determine the rate constants k_{I} and k_{II}.

Time, h	$a(t)$	$b(t)$	$c(t)$
0.1	0.738	0.173	0.089
0.2	0.549	0.299	0.152
0.3	0.408	0.394	0.198
0.4	0.299	0.462	0.239
0.5	0.222	0.516	0.262
0.6	0.167	0.557	0.276
0.7	0.120	0.582	0.298
0.8	0.088	0.603	0.309
0.9	0.069	0.622	0.309
1.0	0.047	0.633	0.320

7.6 The data on the iodination of ethane given in Problem 7.1 have been supplemented by three additional runs done at total pressures of 2 atm:

$[I_2]_{\text{in}}$	$[C_2H_6]_{\text{in}}$	$\bar{t}$	$[I_2]_{\text{out}}$	$[C_2H_6]_{\text{out}}$	$[HI]_{\text{out}}$	$[C_2H_5I]_{\text{out}}$
0.1	0.9	260	0.0830	0.884	0.0176	0.0162
0.1	0.9	1300	0.0420	0.841	0.0615	0.0594
0.1	0.9	2300	0.0221	0.824	0.0797	0.0770
0.1	1.9	150	0.0783	1.878	0.0222	0.0220
0.1	1.9	650	0.0358	1.839	0.0641	0.0609
0.1	1.9	1150	0.0200	1.821	0.0820	0.0803

Repeat Problem 7.1 using the entire set. First do a preliminary analysis using linear regression and then make a final determination of the model parameters using nonlinear regression.

7.7 The following mechanism has been reported for ethane iodination:

$$I_2 + M \rightleftarrows 2I\cdot + M$$
$$I\cdot + C_2H_6 \longrightarrow C_2H_5\cdot + HI$$
$$C_2H_5\cdot + I_2 \longrightarrow C_2H_5I + I\cdot$$

Apply the pseudo-steady hypothesis to the free-radical concentrations to determine a functional form for the reaction rate. Note that M represents any molecule. Use the combined data in Problem 7.6 to fit this mechanism.

7.8 Hinshelwood and Green (1926) studied the homogeneous, gas phase reaction

$$2NO + 2H_2 \rightarrow N_2 + 2H_2O$$

at 1099 K in a constant-volume batch reactor. The reactor was charged with known partial pressures of NO and H_2, and the course of the reaction was monitored by the total pressure. Following are the data from one of their runs. Pressures are in millimeters of mercury. The initial partial pressures were $(P_{NO})_0 = 406$ mm and $(P_{H_2})_0 = 289$. Suppose $\mathscr{R} = k[NO]^m\,[H_2]^n$. Determine the constants in the rate expression.

T (s)	$\Delta P = P - P_0$
8	10
13	20
19	30
26	40
33	50
43	60
54	70
69	80
87	90
110	100
140	110
204	120
310	127
∞	144.5

7.9 The kinetic study by Hinshelwood and Green cited in Problem 7.8 also included initial rate measurements over a range of partial pressures.

$(P_{NO})_0$	$(P_{H_2})_0$	$\mathscr{R}_0$, mm/s
359	400	1.50
300	400	1.03
152	400	0.25
400	300	1.74
310	300	0.92
232	300	0.45
400	289	1.60
400	205	1.10
400	147	0.79

Use these initial rate data to estimate the constants in the rate expression $\mathscr{R} = k[\mathrm{NO}]^m [\mathrm{H_2}]^n$.

7.10 The ordinary burning of sulfur produces SO_2. This is the first step in the manufacture of sulfuric acid. The second step oxidizes SO_2 to SO_3 in a gas–solid catalytic reactor. The catalyst increases the reaction rate but does not change the equilibrium compositions in the gas phase.

(a) Determine the heat of reaction for SO_2 oxidation at 600 K and 1 atm.

(b) Determine the mole fractions at equilibrium of N_2, O_2, SO_2, and SO_3 at 600 K and 1 atm given an initial composition of 79 mol % N_2, 15 mol % O_2, and 6 mol % SO_2. Assume that the nitrogen is inert.

7.11 Critique the enthalpy calculation in the alternative solution of Example 7.18 that is based on Equation 7.45.

7.12 Rework Example 7.18 without inerts. Specifically, determine whether this case shows any discernable difference between solutions based on Equations 7.42 and 7.45.

7.13 Determine the equilibrium distribution of the three pentane isomers given the following data on free energies of formation at 600 K. Assume ideal gas behavior.

$$\Delta G_F^{\mathrm{o}} = 40,000 \text{ J mol}^{-1} \text{ of n-pentane}$$
$$\Delta G_F^{\mathrm{o}} = 34,000 \text{ J mol}^{-1} \text{ of isopentane}$$
$$\Delta G_F^{\mathrm{o}} = 37,000 \text{ J mol}^{-1} \text{ of neopentane}$$

Assume ideal gas behavior.

7.14 Consider molecules A, B, and C reacting in the gas phase. The observed reaction is $A + B \rightleftarrows C$. A postulated mechanism for the observed reaction is

$$\mathrm{A} + \mathrm{B} \xrightarrow{k_1} \mathrm{C}$$
$$\mathrm{A} + \mathrm{C} \xrightarrow{k_2} 2\mathrm{A} + \mathrm{B}$$
$$\mathrm{B} + \mathrm{C} \xrightarrow{k_3} \mathrm{A} + 2\mathrm{B}$$
$$2\mathrm{C} \xrightarrow{k_4} \mathrm{C} + \mathrm{A} + \mathrm{B}$$

Determine the equilibrium composition given $a_0 = b_0$ and $c_0 = 0$. *Hint*: Use stoichiometry to eliminate all but one concentration. Then set $\mathscr{R}_A = \mathscr{R}_B = \mathscr{R}_C = 0$,

7.15 Example 7.19 treated the high-temperature equilibrium of four chemical species: N_2, O_2, NO, and NO_2. Extend the analysis to include N_2O and N_2O_4.

7.16 The following reaction has been used to eliminate NO_x from the stack gases of stationary power plants:

$$\mathrm{NO}_x + \mathrm{NH_3} + 0.5(1.5 - \mathrm{x})\mathrm{O_2} \Leftrightarrow \mathrm{N_2} + 1.5\mathrm{H_2O}$$

A zeolite catalyst operated at 1 atm and 325–500 K is so active that the reaction approaches equilibrium. Suppose that stack gas having the equilibrium composition calculated in Example 7.19 is cooled to 500 K. Ignore any reactions involving CO and CO_2. Assume the power plant burns methane to produce electric power with an overall efficiency of 70%. How much ammonia is required per kilowatt hour in order to reduce

NO_x emissions by a factor of 10, and how much will the purchased ammonia add to the cost of electricity. Obtain the cost of tank car quantities of anhydrous ammonia from the *Chemical Marketing Reporter* or from the Web.

APPENDIX 7.1 LINEAR REGRESSION ANALYSIS

Determination of the model parameters in Equation 7.7 usually requires numerical minimization of the sum of squares, but an analytical solution is possible when the model is a linear function of the independent variables. Take the logarithm of Equation 7.4 to obtain

$$\ln \mathscr{R} = \ln k + m \ln [A] + n \ln [B] + r \ln [R] + s \ln [S] + \cdots \tag{7.48}$$

Define $Y = \ln \mathscr{R}$, $C = \ln k$, $X_1 = \ln[A]$, $X_2 = \ln[B]$, and so on. Then,

$$Y = C + mX_1 + nX_2 + rX_3 \cdots \tag{7.49}$$

Thus Y is a linear function of the new independent variables X_1, X_2, ... Linear regression analysis is used to fit linear models to experimental data. The case of three independent variables will be used for illustrative purposes, although there can be any number of independent variables provided the model remains linear. The dependent variable Y can be directly measured or it can be a mathematical transformation of a directly measured variable. If transformed variables are used, the fitting procedure minimizes the sum of squares for the differences between the transformed data and the transformed model. Nonlinear regression minimizes the sum of squares between the data as actually measured and the model in untransformed form. The results may be substantially different. In particular, a logarithmic transformation will weight small numbers more heavily than large numbers.

The various independent variables can be the actual experimental variables or transformations of them. Different transformations can be used for different variables. The "independent" variables need not be actually independent. For example, linear regression analysis can be used to fit a cubic equation by setting X, X^2, and X^3 as the independent variables.

The sum of squares to be minimized is

$$S^2 = \sum_{\text{data}} (Y - C - mX_1 - nX_2 - rX_3)^2 \tag{7.50}$$

We now regard the experimental data as fixed and treat the model parameters as the variables. The goal is to choose C, m, n, and r such that $S^2 > 0$ achieves its minimum possible value. A necessary condition for S^2 to be a minimum is that

$$\frac{\partial S^2}{\partial C} = \frac{\partial S^2}{\partial m} = \frac{\partial S^2}{\partial n} = \frac{\partial S^2}{\partial r} = 0$$

For the assumed linear form of Equation 7.50,

$$\frac{\partial S^2}{\partial C} = -2\sum_{\text{data}}(Y - C - mX_1 - nX_2 - rX_3)(-1) = 0$$
$$\frac{\partial S^2}{\partial m} = -2\sum_{\text{data}}(Y - C - mX_1 - nX_2 - rX_3)(-X_1) = 0$$
$$\frac{\partial S^2}{\partial n} = -2\sum_{\text{data}}(Y - C - mX_1 - nX_2 - rX_3)(-X_2) = 0$$
$$\frac{\partial S^2}{\partial r} = -2\sum_{\text{data}}(Y - C - mX_1 - nX_2 - rX_3)(-X_3) = 0$$

Rearrangement gives

$$\begin{aligned} JC + m\sum X_1 + n\sum X_2 + r\sum X_3 &= \sum Y \\ C\sum X_1 + m\sum X_1^2 + n\sum X_1X_2 + r\sum X_1X_3 &= \sum X_1Y \\ C\sum X_2 + m\sum X_1X_2 + n\sum X_2^2 + r\sum X_2X_3 &= \sum X_2Y \\ C\sum X_3 + m\sum X_1X_3 + n\sum X_2X_3 + r\sum X_3^2 &= \sum X_3Y \end{aligned} \tag{7.51}$$

where J is the number of data and the summations extend over the data. The various sums can be calculated from the data, and Equations 7.51 can be solved for C, m, n, and r. Equations 7.51 are linear in the unknown parameters and can be solved by matrix inversion. See any text on linear algebra. No solution will exist if there are fewer observations than model parameters, and the model will fit the data exactly if there are as many parameters as observations.

EXAMPLE 7.22

Use linear regression analysis to determine k, m, and n for the data taken at 1 atm total pressure for the ethane iodination reaction in Problem 7.1.

SOLUTION: The assumed linear form is

$$\ln\ \mathscr{R} = \ln\ k + m\ \ln\,[I_2] + n \ln\,[C_2H_5]$$

The data are as follows:

$\bar{t}$(s)	$\mathscr{R}$(atm s^{-1})	$Y = \ln \mathscr{R}$	$X_1 = \ln[I_2]$	$X_2 = \ln[C_2H_6]$
240	7.08×10^{-5}	−9.56	−2.49	−0.123
1300	4.60×10^{-5}	−9.99	−3.21	−0.173
2300	3.39×10^{-5}	−10.29	−3.81	−0.194

Suppose we attempt to evaluate all three constants k, m, and n. Then the first three components of Equations 7.51 are needed. Evaluating the various sums gives

$$\begin{aligned} 3 \ln k - 9.51m - 0.49n &= -29.84 \\ -9.51 \ln k + 31.0203m + 1.60074n &= 95.07720 \\ -0.49 \ln k + 1.60074m + 0.082694n &= 4.90041 \end{aligned}$$

The solution is $\ln k = -8.214$, $m = 0.401$, $n = 2.82$. This model uses as many parameters as there are observations and thus fits the data exactly, giving $S^2 = 0$. One can certainly doubt the significance of such a fit. It is clear that the data are not perfect, since the material balance is not perfect. Additional data could cause large changes in the parameter values. Problem 7.6 addresses this issue. Certainly, the value for n seems high and is likely an artifact of the limited range over which $[C_2H_6]$ was varied. Suppose we pick $n = 1$ on semitheoretical grounds. Then regression analysis can be used to find best values for the remaining parameters. The dependent variable is now $Y = \ln \mathscr{R} - \ln[C_2H_6]$. There is now only one independent variable, $X_1 = \ln[I_2]$. The data are as follows:

$Y = \ln \mathscr{R} - \ln[C_2H_6]$	$X_1 = \ln[I_2]$.
−9.44	−2.49
−9.82	−3.21
−10.10	−3.81

Now only the first two components of Equations 7.51 are used. Evaluating the various sums gives

$$\begin{aligned} 3 \ln k - 9.51m &= -29.36 \\ -9.51 \ln k + 31.0203m &= 93.5088 \end{aligned}$$

Solution gives $\ln k = -9.1988$ and $m = 0.5009$. Since there are now only two fitted parameters, the model does not fit the data exactly, $S^2 > 0$, but the fit is quite good:

$(\ln \mathscr{R})_{\text{observed}}$	$(\ln \mathscr{R})_{\text{predicted}}$
−9.56	−9.57
−9.99	−9.98
−10.29	−10.30

The predictions with $n = 1$ are essentially as good as those with $n = 2.82$. An excellent fit is also obtained with $n = 2$. Thus the data do not allow n to be determined with any confidence. However, a kineticist would probably pick $m = 0.5$ and $n = 1$ based on the simple logic that these values replicate the experimental measurements and are physically plausible.

Regression analysis is a powerful tool for fitting models but can obviously be misused. In the above example, physical reasoning avoids a spurious result. Statistical reasoning is also helpful. Confidence intervals and other statistical measures of goodness of fit can be used to judge whether or not a given parameter is ***statistically significant*** and if it should be retained in the model. Also, statistical analysis can help in the planning of experiments so that the new data will remove a maximum amount of uncertainty in the model. See any standard text on the ***statistical design of experiments***.

Chapter 8

Real Tubular Reactors in Laminar Flow

Piston flow is a **convenient** approximation of a real tubular reactor. The design equations for piston flow are relatively simple and are identical in mathematical form to the design equations for well-mixed batch reactors. The key to their mathematical simplicity is the assumed absence of any radial or tangential variations within the reactor. The dependent variables a, b, $\ldots T$, P change in the axial, down-tube direction but are completely uniform across the tube. This allows the reactor design problem to be formulated as a set of ODEs in a single independent variable z. As shown in previous chapters, such problems are readily solvable given the initial values $a_{\text{in}}, b_{\text{in}}, \ldots, T_{\text{in}}, P_{\text{in}}$.

Piston flow is an **accurate** approximation for some practical situations. It is usually possible to avoid tangential (θ-direction) dependence in practical reactor designs, at least for the case of premixed reactants, which we are considering throughout most of this book. It is harder but sometimes possible to avoid radial variations. A long, highly turbulent reactor is a typical case where piston flow will be a good approximation for most purposes. Piston flow will usually be a bad approximation for laminar flow reactors since radial variations in composition and temperature can be large.

This chapter begins a discussion of design techniques for "real" tubular reactors. By real, we mean reactors for which the convenient approximation of piston flow is so inaccurate that more realistic models must be developed. The chapter is restricted to the classical case of flow in a constant-diameter, circular tube (i.e., a pipe). However, the design techniques and numerical methods presented are also applicable to flows in ducts (i.e., "tubes" with a rectangular cross section) and flat-plate designs (i.e., slit flow). Noncircular cross sections are sometimes used for conventional, macroscale reactors and are the normal case in the microreactors discussed in Chapter 16. Conversely, the numerical methods given in that chapter can be used for conventional tubes. This chapter solves PDEs by the method of lines. Chapter 16 solves them by the method of false transients. Read about both methods before beginning a significant design effort on laminar flow reactors.

Chemical Reactor Design, Optimization, and Scaleup, Second Edition. By E. B. Nauman
Copyright © 2008 John Wiley & Sons, Inc.

This chapter and Chapters 9 and 16 describe a hierarchy of mathematical models suitable for both isothermal and nonisothermal reactions in tubes. The hierarchy is the following:

1. The reactor is in laminar flow. The velocity profile gives a distribution of residence times and thus different extents of reaction for various portions of the fluid. Molecular diffusion is negligible, and thermal diffusion must also be negligible if the reaction is nonisothermal. The performance of the reactor is generally worse than that of piston flow with the same value of $\bar{t}$ but better than that of a CSTR.
2. The effects of the velocity profile are mitigated by molecular diffusion in the radial direction (i.e., the cross-sectional direction). Diffusion in the axial direction is negligible. Reactor performance is better than in a laminar flow reactor with no diffusion. If the radial diffusion is high enough, concentration gradients in the reactor cross section are eliminated, and reactor performance approaches that of piston flow.
3. There is a velocity profile in the reactor and radial diffusion. There is also significant diffusion in the axial direction. The radial diffusion eliminates radial concentration gradients, but axial diffusion complicates matters and lowers reactor performance. In the limit of very high axial diffusion, the reactor becomes perfectly mixed with the performance of a CSTR. This situation is important only for micron-scale reactors and is discussed in Chapter 16.
4. The tube is packed with catalyst pellets. Flow may be either laminar or turbulent. The velocity profile is assumed to be flat. Transfer of heat and mass in the radial direction is modeled using empirical diffusion coefficients that combine the effects of convection and true diffusion in the radial direction. There is no axial diffusion. Details are given in Chapter 9. This model is important only for nonisothermal reactors. It reduces to piston flow if the reaction is isothermal.
5. The reactor is turbulent, the velocity profile is flat, radial mixing is complete, and there is some transfer of heat and mass in the axial direction. The tube can be either packed (e.g., with a catalyst) or open. This model provides an estimate of reaction yields in highly turbulent reactors that is more conservative than assuming piston flow.

In the above hierarchy, this chapter discusses models 1 and 2, Chapter 9 discusses models 4 and 5, and Chapter 16 discusses model 3.

8.1 FLOW IN TUBES WITH NEGLIGIBLE DIFFUSION

Consider isothermal, laminar flow of a Newtonian fluid in a circular tube of radius R, length L, and average fluid velocity $\overline{u}$. When the viscosity is constant, the axial velocity profile is

$$V_z(r) = 2\overline{u}\left[1 - \frac{r^2}{R^2}\right] \tag{8.1}$$

Most industrial reactors in laminar flow have pronounced temperature and composition variations that change the viscosity and alter the velocity profile from the simple parabolic profile of Equation 8.1. These complications are addressed in Section 8.4. However, even the profile of Equation 8.1 presents a serious complication compared to piston flow. There is a velocity gradient across the tube with zero velocity at the wall and high velocities near the centerline. Molecules near the center will follow high-velocity streamlines and will undergo relatively little reaction. Those near the tube wall will be on low-velocity streamlines, will remain in the reactor for long times, and will react to near completion. Thus a gradient in composition develops across the radius of the tube. Molecular diffusion acts to alleviate this gradient but will not completely eliminate it, particularly in liquid phase systems with typical diffusivities of 1.0×10^{-9}–$1.0 \times 10^{-10}\,\mathrm{m^2\ s^{-1}}$ for small molecules and much lower diffusivities for polymers.

When diffusion is negligible, the material moving along a streamline is isolated from material moving along other streamlines. The streamline can be treated as if it were a PFR, and the system as a whole can be regarded as a large number of PFRs in parallel. For the case of straight streamlines and a velocity profile that depends on radial position alone, concentrations along the streamlines at position r are given by

$$V_z(r)\frac{\partial a}{\partial z} = \mathscr{R}_A \tag{8.2}$$

This result is reminiscent of Equation 1.36. We have replaced the average velocity $\overline{u}$ with the velocity corresponding to a particular streamline $V_z(r)$. Equation 8.2 is written as a PDE to emphasize the fact that the concentration $a = a(r, z)$ depends on two independent variables, r and z. However, for a given value of r, Equation 8.2 can be integrated with respect to z as though it were an ODE. The inlet boundary condition associated with the streamline at position r is $a(r,0) = a_{\mathrm{in}}(r)$. Usually, a_{in} will be the same for all values of r, but the case where the entering fluid has a concentration profile can also be treated. The outlet concentration for a particular streamline is found by solving Equation 8.2 and setting $z = L$. The result is the same as for a PFR of length L and velocity $V_z(r)$. The outlet concentrations for the various streamlines are averaged to get the outlet concentration from the reactor as a whole.

8.1.1 Criterion for Neglecting Radial Diffusion

The importance of diffusion in a tubular reactor is determined by a dimensionless parameter $\mathscr{D}_A\bar{t}/R^2 = \mathscr{D}_A L/(\overline{u}R^2)$, which is the molecular diffusivity of component A scaled by the tube size and flow rate. If $\mathscr{D}_A\bar{t}/R^2$ is small, then the effects of diffusion will be small, although the definition of small will depend on the specific reaction mechanism. Merrill and Hamrin (1970) studied the effects of diffusion on first-order reactions and concluded that molecular diffusion can be ignored in reactor design calculations if

$$\frac{\mathscr{D}_A\bar{t}}{R^2} < 0.003 \tag{8.3}$$

Equation 8.3 gives a criterion for neglecting molecular diffusion. It is satisfied in many industrial-scale laminar flow reactors but may not be satisfied in laboratory-scale reactors since they operate with the same values for $\mathscr{D}_A$ and $\bar{t}$ but generally use smaller diameter tubes. Molecular diffusion becomes progressively more important as the size of the reactor is decreased. The effects of molecular diffusion are generally beneficial so that a small reactor will give better results than a large one, a fact that has proved distressing to engineers attempting a scaleup. For purposes of scaleup, it may be better to avoid diffusion and accept the composition gradients on the small scale so that the decrease in diffusion does not cause an unpleasant surprise upon scaleup. Diffusion can be avoided in the small reactor by using a short, fat tube. If diffusion is negligible in the small reactor, it will remain negligible upon scaleup. The alternative is to scale up at constant tube diameter, either in parallel or in series, as discussed in Chapter 3. This will maintain a constant value for the dimensionless diffusivity $\mathscr{D}_A\bar{t}/R^2$.

The Merrill and Hamrin criterion was derived for a first-order reaction. It should apply reasonably well to other simple reactions, but reactions exist that are quite sensitive to diffusion. Examples include the decomposition of free-radical initiators where a few initial events can cause a large number of propagation reactions and coupling or crosslinking reactions where a few events can have a large effect on product properties.

A temperature counterpart of 8.2 is

$$V_z(r)\frac{dT}{dz} = \frac{-\Delta\mathbf{H_R}\mathscr{R}}{\rho C_P} \tag{8.4}$$

where the reader is reminded that $\Delta\mathbf{H_R}\mathscr{R}$ is a sum over all reactions according to Equation 5.16. Equation 8.4 treats each streamline as an adiabatic piston flow reactor. This assumption is rarely useful. The thermal diffusivity $\alpha = \rho C_P/\kappa$ is several orders of magnitude larger than molecular diffusivities in a liquid system. Thus radial diffusion of heat can rarely be neglected, and the practical use of Equation 8.2 is limited to systems where the adiabatic temperature rise, Equation 5.19, is small.

8.1.2 Mixing-Cup Averages

Suppose Equation 8.2 is solved either analytically or numerically to give $a(r, z)$. It remains to find the average outlet concentration when the flows from all the streamlines are combined into a single stream. This average concentration is the ***convected-mean*** or ***mixing-cup average concentration***. It is the average concentration $a_{\text{mix}}(L)$ of material leaving the reactor. This material could be collected in a bucket (a mixing cup) and is what a company is able to sell. It is not the spatial average concentration inside the reactor, even at the reactor outlet. See Problem 8.5 for an explanation of this distinction.

The convected mean at position z is denoted by $a_{\text{mix}}(z)$ and is found by multiplying the concentration on a streamline, $a(r, z)$, by the volumetric flow rate associated with that streamline, $dQ(r) = V_z(r)\ dA_c$, and by summing over all the streamlines. The

result is the molar flow rate of component A. Dividing by the total volumetric flow $Q = \overline{u}A_c$ gives the convected-mean concentration

$$a_{\text{mix}}(z) = \frac{\displaystyle\iint_{A_c} aV_z \, dA_c}{\displaystyle\iint_{A_c} V_z \, dA_c} = \frac{1}{\overline{u}A_c} \iint_{A_c} aV_z \, dA_c \tag{8.5}$$

The double integral in Equation 8.5 is a fairly general definition of the mixing-cup average. It is applicable to arbitrary velocity profiles and noncircular cross sections, but it does assume that the reactor outlet is in a plane perpendicular to the z axis. For the usual case of a circular tube with a velocity profile that is a function of r and not of θ,

$$a_{\text{mix}}(z) = \frac{1}{\overline{u}R^2} \int_0^R a(r, z)V_z(r, z)2r \, dr \tag{8.6}$$

The combination of Equations 8.2 and 8.6 is the simplest, nontrivial example of design equations for a pipe reactor in laminar flow. Solve Equation 8.2 for $a(\mathfrak{r}, L)$; substitute into Equation 8.6, and integrate. The result, the mixing-cup average outlet concentration $a_{\text{mix}}(L)$, is usually denoted just as a_{out}. Calculation of mixing-cup averages is necessary whenever there is a radial variation in concentration or temperature. Equation 8.5 and its obvious generalizations to the concentration of other components and to the mixing-cup average temperature are needed throughout this chapter and much of Chapter 9. If in doubt, calculate the mixing-cup averages. The next example shows that numerical methods are usually needed for this calculation.

EXAMPLE 8.1

Find the mixing-cup average outlet concentration for an isothermal, first-order reaction with rate constant k that is occurring in a laminar flow reactor with a parabolic velocity profile as given by Equation 8.1.

SOLUTION: This is the simplest, nontrivial example of a laminar flow reactor. The solution begins by integrating Equation 8.2 for a specific streamline that corresponds to radial position r. The result is

$$a(r, z) = a_{\text{in}} \exp\left[\frac{-kz}{V_z(r)}\right] \tag{8.7}$$

where k is the first-order rate constant. The mixing-cup average outlet concentration is found using Equation 8.6 with $z = L$:

$$a_{\text{out}} = a_{\text{mix}}(L) = \frac{1}{\overline{u}R^2} \int_0^R \exp\left[\frac{-kL}{V_z(\mathfrak{r})}\right] V_z(r, z)2r \, dr \tag{8.8}$$

This integral can be solved analytically. Its solution is a good test for symbolic manipulators such as Mathematica or Maple. We illustrate its solution using classical methods. Differentiate

Equation 8.1 to obtain a relationship between r and $V_z(r)$:

$$r\,dr = -\frac{dV_z\,R^2}{4\overline{u}} \tag{8.9}$$

Substitute into Equation 8.8 to obtain the integral as a function of V_z:

$$a_{\text{out}} = \frac{a_{\text{in}}}{2\overline{u}^2}\int_0^{2\overline{u}} \exp\left[-\frac{kL}{V_z}\right] V_z\,dV_z \tag{8.10}$$

Now substitute $t = L/V_z$ to obtain an integral with respect to t. Note that $t$ranges from $\overline{t}/2$ to ∞ as V_Z ranges from $2\overline{u}$ to 0 and as r ranges from 0 to 1. Some algebra gives the final result:

$$\frac{a_{\text{out}}}{a_{\text{in}}} = \int_{\overline{t}/2}^{\infty} \exp(-kt)\frac{\overline{t}^2}{2t^3}dt \tag{8.11}$$

This integral is a special function related to the incomplete gamma function. The solution can be considered analytical even though the function may be unfamiliar. In practice, numerical integration is preferred.

Equation 8.11 is the simplest, nontrivial solution to Equation 8.6, which in turn is the simplest design equation for a laminar pipe reactor. It is clear that analytical solutions are rarely possible.

8.1.3 Trapezoidal Rule

The numerical methods used in this chapter are designed to converge $O(\Delta r^2)$ in the radial direction. The trapezoidal rule is recommended for calculating mixing-cup averages because it too converges $O(\Delta r^2)$. Use of the rectangular rule (see Figure 2.1) is not recommended because it converges $O(\Delta r)$ and would negate the accuracy of other calculations. The convergence order for a complex calculation is determined by the most slowly converging of the computational components. Simpson's rule converges $O(\Delta r^3)$ and will calculate $\overline{u}$ exactly when the velocity profile is parabolic but ceases to be exact for the more complex velocity profiles encountered in real laminar flow reactors, nor is it exact for numerical integration of Equation 8.8 except for the trivial case of $a(r, z) = \text{const}$. The use of Simpson's rule does no harm but offers no real advantage.

Consider a tube with a circular cross section and suppose the radius has been divided into I equally sized increments in the radial direction. The general form for the trapezoidal rule is

$$\int_0^R F(r)\,dr \approx \Delta r\left[\frac{F(0)}{2} + \frac{F(I)}{2} + \sum_{i=1}^{I-1} F(i)\right] \tag{8.12}$$

For the case of Equation 8.6,

$$F(r) = 2\pi r a(r) V_z(r) = 2\pi i\,\Delta r\,a(i)V_z(i) \tag{8.13}$$

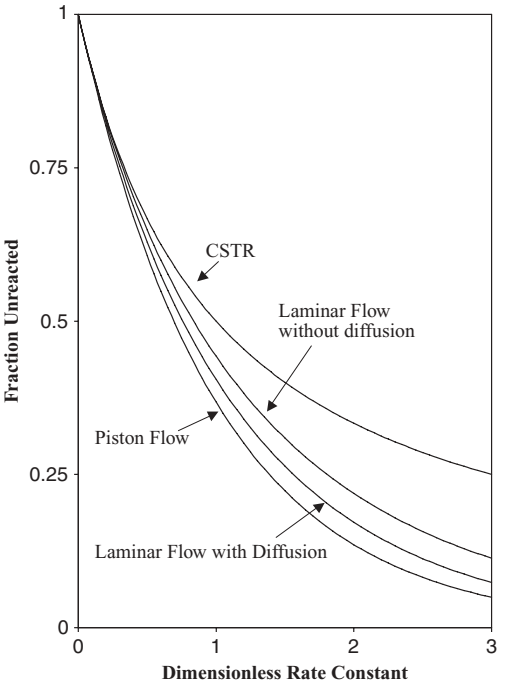

Figure 8.1 Fraction unreacted versus dimensionless rate constant for a first-order reaction in various isothermal reactors. The case illustrated with diffusion is for $\mathscr{D}_A \bar{t}/R^2 = 0.1$.

In this example, $F(0) = 0$ because $r = 0$ and $F(R) = 0$ because $V_z(R) = 0$. The mixing-cup average is determined when the integral of $F(r)$ is normalized by $Q = \pi R^2 \overline{u}$. There is merit in using the trapezoidal rule to calculate $Q = A_c \overline{u}$ by integrating $dQ = 2\pi r V_z \, dr$. Numerical errors of integration tend to cancel when the ratio is taken.

EXAMPLE 8.2

An isothermal pipe reactor with $L = 2$ m, $R = 0.01$ m is being used for a first-order reaction. The rate constant is 0.005 s^{-1}, and $\overline{u} = 0.01 \text{m s}^{-1}$. Equation 8.1 gives the velocity profile. Molecular diffusion is negligible. Determine the outlet concentration from the reactor.

SOLUTION: Example 8.1 laid the groundwork for this case of laminar flow without diffusion. The mixing-cup average is

$$\frac{a_{\text{out}}}{a_{\text{in}}} = \frac{\int_0^R 2\pi r V_z(r) \, \exp[-kL/V_Z(r)] \, dr}{\int_0^R 2\pi r V_z(r) \, dr} \tag{8.14}$$

Code for Example 8.2 illustrates the use of the trapezoidal rule for evaluating both the numerator and denominator in this equation. The results are as follows:

Code for Example 8.2

```
Sub Example8_2()

L = 2               'tube length
Rend = 0.01         'tube radius
ubar = 0.01         'mean velocity
k = 0.005           'first order rate constant
Itotal = 2          'Initial size of radial grid

For jj = 1 To 8   'This outer loop varies the radial grid size to test for convergence

    Itotal = 2*Itotal   'number of radial increments
    dr = Rend/Itotal    'size of radial increment
    Cells (jj,1) = Itotal

    Fsum = 0    'Set to F(0)/2+F(R)/2 for the general trapezoidal rule
    Qsum = 0    'Set to Q(0)/2+ Q(R)/2 for the general trapezoidal rule
    For i = 1 To Itotal-1
        r = i*dr
        Vz = 2*ubar*(1-r^2/Rend^2) ' Parabolic
        Q = r*Vz              'The factor of 2*Pi cancels in the ratio
        F = Q*Exp(-k*L/Vz)
        Fsum = Fsum+F*dr
        Qsum = Qsum+Q*dr
    Next i

    aout = Fsum/Qsum
    Cells(jj,2)=aout
Next jj
End Sub
```

I	a_{out}/a_{in}	Δ
4	0.463646	
8	0.447372	0.016273
16	0.444130	0.003242
32	0.443445	0.000685
64	0.443268	0.000177
128	0.443223	0.000044
256	0.443212	0.000011
512	0.443210	0.000003

The Δ column in this table shows that the change in the value for a_{out}/a_{in} decreases by a factor of about 4 each time I is doubled, as expected for convergence $O(\Delta r^2)$. The change yet to come for complete convergence would be $\frac{1}{4} + \frac{1}{16} + \frac{1}{64} + \cdots = \frac{1}{3}$ of the last Δ. Thus, to six places, the integral is 0.443209. This accuracy can in fact be obtained by extrapolation from the calculation at $I = 64$.

For any given value for $k\bar{t}$($k\bar{t} = 1.0$ in this example), the performance of a laminar flow reactor without diffusion is appreciably worse that that of a PRF (for which $a_{out}/a_{in} = 0.368$ when $k\bar{t} = 1$) and is better than that for a CSTR (for which a_{out}/a_{in}= 0.5 when $k\bar{t} = 1$).

8.1.4 Preview of Residence Time Theory

Example 8.1 derived a specific example of a powerful result of residence time theory. The ***residence time*** associated with a streamline is $t = L/V_z$. The outlet concentration for this streamline is $a_{batch}(t)$. This is a general result applicable to arbitrary kinetics. Example 8.1 treated the case of a first-order reaction where $a_{batch}(t) = a_{in}\ \exp(-kt)$. Assuming no diffusion, the mixing-cup average for the general case is

$$a_{out} = \int_{\bar{t}/2}^{\infty} a_{batch}(t)\frac{\bar{t}^2}{2t^3}dt \tag{8.15}$$

Equation 8.15 can be used for any reaction, even a complex reaction where $a_{batch}(t)$ must be determined by the simultaneous solution of many ODEs. The restrictions on Equation 8.15 are isothermal, laminar flow in a circular tube with a parabolic velocity profile and negligible diffusion.

The condition of negligible diffusion means that the reactor is ***completely segregated***. A further generalization of Equation 8.11 applies to any completely segregated reactor:

$$a_{out} = \int_0^{\infty} a_{batch}(t)f(t)\,dt \tag{8.16}$$

where $f(t)$ is the ***differential distribution function of residence times***. In principle, $f(t)$ is a characteristic of the reactor, not of the reaction. It can be used to predict conversions for any type of isothermal reaction in the same reactor. Chapter 15 discusses experimental ways for measuring $f(t)$. For a parabolic velocity profile in a

diffusion-free, circular tube

$$f(t) = \begin{cases} 0 & t \le \frac{1}{2}\bar{t} \\ \dfrac{\bar{t}^2}{2t^3} & t > \frac{1}{2}\bar{t} \end{cases} \tag{8.17}$$

8.2 TUBE FLOWS WITH DIFFUSION

Figure 8.1 gives conversion curves for an isothermal, first-order reaction in various types of reactor. The curves for a PFR and CSTR are from Equations 1.38 and 1.49. The curve for laminar flow without diffusion is obtained from Equation 8.14 and the software of Example 8.2. Without diffusion, the laminar flow reactor performs better than a CSTR but worse that a PFR. Add radial diffusion and the performance improves. This is illustrated by the curve in Figure 8.1 that is between those for laminar flow without diffusion and piston flow. The intermediate curve is one member of a family of such curves that depends on the parameter $\mathscr{D}_A\bar{t}/R^2$. If $\mathscr{D}_A\bar{t}/R^2$ is small, say $\mathscr{D}_A\bar{t}/R^2 < 3 \times 10^{-3}$ according to Equation 8.3, then radial diffusion is unimportant and reactor performance is similar to that for laminar flow without diffusion. If $\mathscr{D}_A\bar{t}/R^2$ is large, say $\mathscr{D}_A\bar{t}/R^2 > 1$, then the reactor closely approaches the behavior of a PFR even with a parabolic velocity profile. The purpose of Chapter 8 is to quantitatively model the effects of radial diffusion of mass and heat on the yield of possibly complex chemical reactions in tubular reactors, specifically tubes with circular cross sections.

If $\mathscr{D}_A\bar{t}/R^2$ is very large and if the reactor is not too long, then axial diffusion can become significant. Radial diffusion lowers concentration gradients in the radial direction and makes the reactor approach piston flow, generally improving performance. Axial diffusion lowers concentration gradients in the axial direction, makes the reactor approach perfect mixing, and generally hurts performance. This phenomenon is important in micrometer-scale reactors and is discussed in Chapter 16. Chapter 16 also treats tubular reactors with cross sections other than circular.

8.2.1 Convective Diffusion of Mass

A derivation of the convective diffusion equation for axisymmetric flow in a pipe is given in Appendix 8.1. A reasonably general version of the equation is

$$\frac{\partial a}{\partial t} + V_z(r, z)\frac{\partial a}{\partial z} + V_r(r, z)\frac{\partial a}{\partial r} = \mathscr{D}_A\left[\frac{1}{r}\frac{\partial a}{\partial r} + \frac{\partial^2 a}{\partial r^2} + \frac{\partial^2 a}{\partial z^2}\right] + \mathscr{R}_A \tag{8.18}$$

The $\partial a/\partial t$ term in Equation 8.18 corresponds to unsteady operation. It will be used in Chapter 16 where the method of false transients is introduced as a solution technique for PDEs. It is also used to study unsteady reactors in Chapter 14. There are two convection terms:

$$V_z(r, z)\frac{\partial a}{\partial z} + V_r(r, z)\frac{\partial a}{\partial r}$$

Radial convection, $V_r(r, z)\partial a/\partial r$, arises only when $V_z(r, z)$ changes in the axial direction. A change in viscosity due to changes in concentration or temperature can excite

this term, as will be discussed in Section 8.4. For the moment, the radial convection term will be ignored and the axial velocity is assumed to be a function of r alone, $V_z(r, z) = V_z(r)$, as in Equation 8.2. The design equation becomes

$$V_z(r)\frac{\partial a}{\partial z} = \mathscr{D}_A\left[\frac{1}{r}\frac{\partial a}{\partial r} + \frac{\partial^2 a}{\partial r^2} + \frac{\partial^2 a}{\partial z^2}\right] + \mathscr{R}_A \tag{8.19}$$

The axial diffusion terms can be dropped for macroscale reactors for the reasons given in Section 8.2.4. Thus the equation to be solved in most of this chapter is

$$V_z(r)\frac{\partial a}{\partial z} = \mathscr{D}_A\left[\frac{1}{r}\frac{\partial a}{\partial r} + \frac{\partial^2 a}{\partial r^2}\right] + \mathscr{R}_A \tag{8.20}$$

Compare Equation 8.20 to Equation 8.2. The only new phenomenon is radial diffusion that now allows transfer of mass between streamlines. Equation 8.20 assumes that the diffusivity $\mathscr{D}_A$ is constant. A more rigorous design equation is

$$V_z\frac{\partial a}{\partial z} = \frac{1}{r}\frac{\partial}{\partial r}\left[r\mathscr{D}_A\frac{\partial a}{\partial r}\right] + \mathscr{R}_A \tag{8.21}$$

but diffusion data for a specific component are rarely accurate enough or vary enough over the course of a reaction to justify this complication.

If the reaction is complex, a version of Equation 8.20 can be written for each component. This approach is generally satisfactory if the components have similar diffusivities or if there is some dominant component (e.g., a solvent) that is fast diffusing. Major complications occur if the components have significantly different diffusivities and there is no dominant component. See Nauman and Savoca (2001) for a reasonable approach to this situation. The proportional flux model described in that paper is recommended.

Although appreciably simplified, Equation 8.20 remains a full-blown PDE since there are derivatives for both of the independent variables, z and r. The equation assumes radial symmetry with no variation in the θ direction. The boundary conditions associated with Equation 8.20 are

$$\begin{array}{lll} \text{Known inlet concentrations:} & a = a_{\text{in}}(r) & \text{at } z = 0 \\ \text{Impervious walls:} & \dfrac{\partial a}{\partial r} = 0 & \text{at } r = R \\ \text{Radial symmetry:} & \dfrac{\partial a}{\partial r} = 0 & \text{at } r = 0 \end{array} \tag{8.22}$$

A complication arises at $r = 0$ due to the $1/r$ term in Equation 8.20. However, since $\partial a/\partial r$ is also zero at the origin, L'Hospital's rule can be applied to give

$$V_z(r)\frac{\partial a}{\partial z} = \mathscr{D}_A\left[2\frac{\partial^2 a}{\partial r^2}\right] + \mathscr{R}_A \quad \text{at } r = 0 \tag{8.23}$$

8.2.2 Convective Diffusion of Heat

Analogous to Equation 8.20 for mass, following is a convective diffusion equation for heat.

$$\rho C_P V_z(r)\frac{\partial T}{\partial z} = \kappa\left[\frac{1}{r}\frac{\partial T}{\partial r} + \frac{\partial^2 T}{\partial r^2}\right] - \Delta\mathbf{H_R}\mathscr{R} \tag{8.24}$$

More complicated forms can obviously be written, but Equation 8.24 is a good starting point. The boundary conditions associated with Equation 8.24 are

$$\begin{array}{lll} \text{Known inlet temperatures:} & T = T_{\text{in}}(r) & \text{at } z = 0 \\ \text{Known wall temperatures:} & T = T_{\text{wall}}(z) & \text{at } r = R \\ \text{Radial symmetry:} & \dfrac{\partial T}{\partial r} = 0 & \text{at } r = 0 \end{array} \tag{8.25}$$

As written above, the wall boundary condition suggests that $T_{\text{wall}}(z)$ can be specified directly. This is a reasonable assumption for the common case of a metal wall in contact with an organic solution. A more complex situation arises when there is a significant thermal resistance in the wall (e.g., a plastic tube) or when the outside heat transfer coefficient is small. See Appendix 8.2 for the appropriate equations.

The situation at $r = 0$ is directly analogous to Equation 8.23. In the absence of θ dependence, the system must have radial symmetry, and the governing PDE takes a special form:

$$\rho C_P V_z(r)\frac{\partial T}{\partial z} = 2\kappa\left[\frac{\partial^2 T}{\partial r^2}\right] - \Delta\mathbf{H_R}\,\mathscr{R} \quad \text{at } r = 0$$

The equations for heat and mass transfer must be solved simultaneously. They are coupled by the dependence of the reaction rate and heat of reaction on concentration and temperature.

8.2.3 Use of Dimensionless Variables

Simultaneous solution of the convective diffusion equations for mass and heat must be done numerically in all but trivial cases. The solutions can be based on dimensioned variables like z and T, and this has the advantage of keeping the physics of the problem close at hand. However, the solutions are then quite specific and must be repeated whenever a design or operating variable is changed. Somewhat more general solutions, while still numerical, can be obtained through the judicious use of dimensionless variables, dimensionless parameters, and dimensionless functions. Table 8.1 defines a number of such variables.

The dimensionless equations for the convective diffusion of mass and heat are

$$\frac{\partial a^*}{\partial \tau} + \mathscr{V}_z\frac{\partial a^*}{\partial \mathscr{Z}} = \left(\frac{\mathscr{D}_A \bar{t}}{R^2}\right)\left[\frac{1}{\mathscr{r}}\frac{\partial a^*}{\partial \mathscr{r}} + \frac{\partial^2 a^*}{\partial \mathscr{r}^2}\right] + \left(\frac{\mathscr{D}_A \bar{t}}{L^2}\right)\frac{\partial^2 a^*}{\partial \mathscr{Z}^2} + \frac{\bar{t}\,\mathscr{R}_A}{a_{\text{in}}} \tag{8.26}$$

Table 8.1 Summary of Dimensionless Variables

Dimensioned Variable	Dimensionless Variable	Type of Variable
Length coordinate	$\mathcal{z} = z/L$	Independent
Radial coordinate	$\mathcal{r} = r/R$	Independent
Concentration	$a^* = a/a_{\text{in}}$	Dependent
Temperature	$\mathcal{T} = T/T_{\text{ref}}$ or $\mathcal{T} = (T - T_{\text{in}})/(T_{\text{wall}} - T_{\text{in}})$	Dependent
Time	$\tau = t/\bar{t}$	Independent
Velocity	$\mathcal{V}_z(\mathcal{r}) = V_z/\bar{u}$	Function
Radial mass diffusivity	$\mathcal{D}\,\bar{t}/R^2$	Parameter
Axial mass diffusivity	$\mathcal{D}\,\bar{t}/L^2$	Parameter
Radial thermal diffusivity	$\alpha\bar{t}/R^2$	Parameter
Axial thermal diffusivity	$\alpha\bar{t}/L^2$	Parameter
Reaction rate	$\bar{t}\mathcal{R}_A/a_{\text{in}}$	Function
Heat of reaction	$\dfrac{\Delta H_R \mathcal{R}\,\bar{t}}{\rho C_P T_{\text{ref}}}$	Function

and

$$\frac{\partial \mathcal{T}}{\partial \tau} + \mathcal{V}_z \frac{\partial \mathcal{T}}{\partial \mathcal{z}} = \left(\frac{\alpha \bar{t}}{R^2}\right)\left[\frac{1}{\mathcal{r}}\frac{\partial \mathcal{T}}{\partial \mathcal{r}} + \frac{\partial^2 \mathcal{T}}{\partial \mathcal{r}^2}\right] + \left(\frac{\alpha \bar{t}}{L^2}\right)\frac{\partial^2 \mathcal{T}}{\partial \mathcal{z}^2} - \frac{\mathbf{\Delta H_R}\mathcal{R}\,\bar{t}}{\rho C_p T_{\text{ref}}} \tag{8.27}$$

The usual way of defining a dimensionless variable is to divide the dimensioned variable by a quantity with the same dimensions that characterize the system. There are sometimes several possibilities. Reasonable choices for T_{ref} include T_{in}, T_{wall}, and $T_{\text{in}} + T_{\text{adiabatic}}$. A useful variable for heat transfer calculations when the heat of reaction is small is $\mathcal{T} = (T - T_{\text{in}})/(T_{\text{wall}} - T_{\text{in}})$. The dimensionless heat of reaction for this case becomes $\left[\mathbf{\Delta H_R}\mathcal{R}\bar{t}\right] / \left[\rho C_p (T_{\text{wall}} - T_{\text{in}})\right]$.

8.2.4 Criterion for Neglecting Axial Diffusion

Equation 8.26 includes two dimensionless parameters that govern the importance of molecular diffusion relative to convection. The parameters are $\mathcal{D}\,\bar{t}/R^2$ for diffusion in the radial direction and $\mathcal{D}\,\bar{t}/L^2$ for diffusion in the axial direction. They differ in magnitude by a factor of $(L/R)^2$. Expressed in terms of the dimensionless variables a^*, $\mathcal{r}$, and $\mathcal{z}$, all concentration gradients are the same order of magnitude. This means that radial diffusion is more important than axial diffusion by a factor of $(L/R)^2$. Most tubular reactors have $L/R \gg 1$ so that axial diffusion can usually be ignored. An approximate criterion for ignoring axial diffusion of mass is

$$\frac{\mathcal{D}\,\bar{t}}{L^2} < 10^{-3}\left(\frac{R}{L}\right)^2 \tag{8.28}$$

The corresponding criterion for ignoring the axial diffusion of heat is less certain. Replacing the molecular diffusivity $\mathcal{D}_A$ in Equation 8.28 with the thermal diffusivity

α and applying the same criterion are a reasonable approach. Because thermal diffusivities tend to be several orders of magnitude higher than molecular diffusivities, axial diffusion of heat can be important even though the axial diffusion of mass is rarely if ever important in macroscale reactors. Most design studies have ignored the effects of axial diffusion of heat. For laminar flow reactors, the solution techniques of Chapter 16 can be applied. For packed beds and turbulent reactors, Section 9.3 explores the influence of axial diffusion on exothermic reactions. Ignoring the axial diffusion of heat in a macroscale reactor is conservative with respect to predicting and avoiding thermal runaways because axial diffusion mitigates the runways.

8.3 METHOD OF LINES

Appendix 8.3 describes how finite differences can be used to approximate derivatives. Divide the radius of the tube into I increments, $\Delta r = R/I$. For the radial direction we use second-order, central differences:

$$\frac{da}{dr} \approx \frac{a(r+\Delta r) - a(r-\Delta r)}{2\,\Delta r} \qquad \frac{d^2a}{dr^2} \approx \frac{a(r+\Delta r) - 2a(r) + a(r-\Delta r)}{\Delta r^2} \tag{8.29}$$

Substituting these into Equation 8.20 gives

$$\frac{da}{dz} = \frac{\mathscr{D}_A}{V_z}\left[\frac{a(r+\Delta r) - a(r-\Delta r)}{2r\,\Delta r} + \frac{a(r+\Delta r) - 2a(r) + a(r-\Delta r)}{\Delta r^2}\right] + \frac{\mathscr{R}_A}{V_z} \tag{8.30}$$

The PDE has been converted to a set of ODEs. Each version of Equation 8.30 governs the behavior of a as it evolves along a "line" of constant r. The independent variable is z. The main dependent variable is $a(r)$ at location r. Equation 8.30 contains other dependent variables, $a(r+\Delta r)$ and $a(r-\Delta r)$, which are the main dependent variables along their own 'lines.' These side variables couple the set of equations so that they must be solved simultaneously.

The method of lines is one of a myriad possible schemes for solving PDEs. It has the merits of being ***fully explicit*** and easy to implement. Its major weakness is a stability requirement that forces an overly small axial step size, Δz. Some implicit differencing schemes avoid this limitation at the cost of solving sometimes large sets of linear algebraic equations. Chapter 16 describes the method of false transients as applied to PDEs that also allows more freedom in choosing Δz.

8.3.1 Governing Equations for Cylindrical Coordinates

This section applies the method of lines to the equations for convective diffusion of mass and heat. It is convenient to replace r by $r = i\,\Delta r$, $i = 0, \ldots, I$, for coding

Table 8.2 Method-of-Lines Coefficients for Concentration in Cylindrical Coordinates

i	$C_+(i)$	$C_0(i)$	$C_-(i)$
$1 \le i \le I-1$	$\frac{\mathscr{D}_A}{\Delta r^2}\left[\frac{1+2i}{2i}\right]$	$\frac{-2\mathscr{D}_A}{\Delta r^2}$	$\frac{\mathscr{D}_A}{\Delta r^2}\left[\frac{-1+2i}{2i}\right]$
$i = 0$	$\frac{2\mathscr{D}_A}{\Delta r^2}$	$\frac{-4\mathscr{D}_A}{\Delta r^2}$	$\frac{2\mathscr{D}_A}{\Delta r^2}$

purposes. Equation 8.30 becomes

$$V_z(i)\frac{da_i}{dz} = C_+(i)a_{i+1} + C_0(i)a_i + C_-(i)a_{i-1} + (\mathscr{R}_A)_i \tag{8.31}$$

Table 8.2 shows the values for C_+, C, and C_- as a function of i. The coefficients for the centerline, $i = 0$, are derived from Equation 8.23 rather that 8.20. It is specified that $a_{-1} = a_1$.

Values at the wall, $i = I$, are determined from the wall boundary condition. For concentrations in any reactor with solid walls and for temperature in an adiabatic reactor, there is zero slope at the wall. It would be sufficient to set $a_I = a_{I-1}$, but this is only a first-order approximation. Fitting a cubic to the points a_I, a_{I-1}, a_{I-2}, and a_{I-3} and then forcing the slope to be zero at $i = I$ give a smoother estimate that sometimes improves convergence:

$$a_I = \frac{18a_{I-1} - 9a_{I-2} + 2a_{I-3}}{11} \tag{8.32}$$

The condition of radial symmetry is satisfied by setting $a(-1, z) = a(1, z)$ at each axial step in the calculations.

Equation 8.33 gives the method-of-lines equation for the diffusion of heat:

$$\rho C_P V_z(i)\frac{dT_i}{dz} = E_+(i)a_{i+1} + E_0(i)a_i + E_-(i)a_{i-1} + \Delta H_R \mathscr{R} \tag{8.33}$$

Table 8.3 provides the coefficients for cylindrical coordinates.

The simple boundary condition for temperature is $T_I = T_{\text{wall}}(z)$, where $T_{\text{wall}}(z)$ is the external temperature, but see Appendix 8.2 for the case where there is external resistance to heat transfer. The simple boundary condition for adiabatic reactors is

Table 8.3 Method-of-Lines Coefficients for Temperature in Cylindrical Coordinates

i	$E_+(i)$	$E_0(i)$	$E_-(i)$
$1 \le i \le I-1$	$\frac{\kappa}{\Delta r^2}\left[\frac{1+2i}{2i}\right]$	$\frac{-2\kappa}{\Delta r^2}$	$\frac{\kappa}{\Delta r^2}\left[\frac{-1+2i}{2i}\right]$
$i = 0$	$\frac{2\kappa}{\Delta r^2}$	$\frac{-4\kappa}{\Delta r^2}$	$\frac{2\kappa}{\Delta r^2}$

$T_I = T_{I-1}$, but the temperature analog of Equation 8.32 provides a smoother estimate of the zero-slope condition.

8.3.2 Solution by Euler's Method

The set of ODEs represented by Equations 8.30 can be solved by various means. They are first-order, initial-value problems of the type introduced in Chapter 2 for multiple reactions. We use Euler's method. Appling it to Equations 8.31 and 8.33 gives

$$(a_i)_{\text{new}} = (a_i)_{\text{old}} + \frac{\Delta z}{V_z(i)}\left[C_+(i)a_{i+1} + C_0(i)a_i + C_-(i)a_{i-1} + (\mathscr{R}_A)_i\right]_{\text{old}} \tag{8.34}$$

$$(T_i)_{\text{new}} = (T_i)_{\text{old}} + \frac{\Delta z}{\rho C_P V_z(i)}\left[E_+(i)T_{i+1} + E_0(i)T_i + E_-(i)T_{i-1} + (\Delta H_R \mathscr{R})_i\right]_{\text{old}} \tag{8.35}$$

The sets of ODEs represented by Equations 8.34 and 8.35 have $I - 1$ members for each chemical component and another $I - 1$ members for temperature. Three points at the old z location plus source terms evaluated at the old, central location are used to calculate the central point at the new, $z + \Delta z$, location. Figure 8.2 shows a template that illustrates the calculation. The template is initially centered at the point $i = 0$ and is moved to higher values of i until the point $I - 1$ is reached. The value at the wall is obtained from the wall boundary condition, (e.g., Equation 8.32). The template is then returned to $i = 0$ and moved one step in the axial direction, $j_{\text{new}} = j + 1$, until the

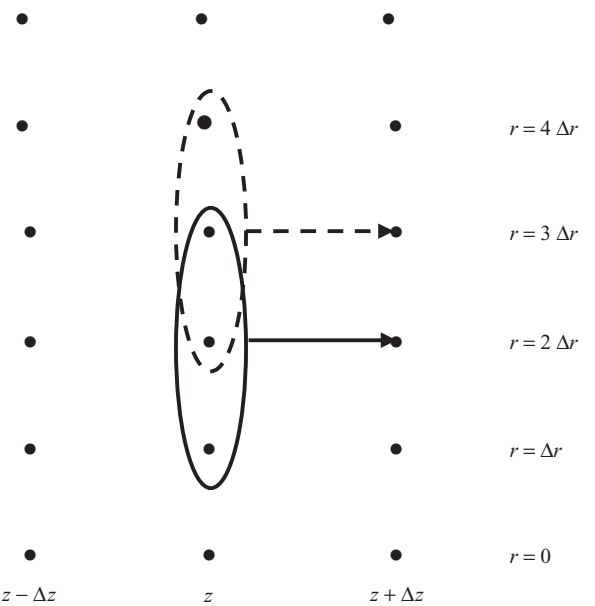

Figure 8.2 Computational template for marching ahead with a sideways shuffle

end of the reactor at $j = J$ is reached. The procedure is colloquially called marching ahead with a sideways shuffle.

8.3.3 Accuracy and Stability

Numerical solutions to PDEs must be tested for convergence as Δr and Δz both approach zero. The finite-difference approximations for radial derivatives converge $O(\Delta r^2)$ and those for the axial derivative used in Euler's method converge $O(\Delta z)$. In principle, just keep decreasing Δr and Δz until results with the desired accuracy are achieved, but it turns out that Δr and Δz cannot be chosen independently when using the method of lines. Instead, values for Δr and Δz are linked through a stability requirement that the overall coefficient on the central dependent variable cannot be negative:

$$1 + \frac{\Delta z}{V_z(i)} C_0(i) \geq 0 \quad \text{for each } 0 \leq i < I \tag{8.36}$$

As shown in Table 8.2, the value of Δz depends on Δr, i, and $V_z(i)$. Pick a value for Δr. Then apply Equation 8.36 to each of the $C_0(i)$ to calculate an acceptable value for Δz for each value of i. Then, choose the smallest value among these. The smallest value usually occurs at $i = I - 1$, and the corresponding, most restrictive value for Δz is usually given by

$$\Delta z_{\max} = \frac{V_z(I-1)\,\Delta r^2}{2\mathscr{D}_A} \tag{8.37}$$

The packed-bed models in Section 9.1 assume a flat velocity profile and are an exception. For them, the smallest value for Δz occurs at the centerline.

For the parabolic profile of Equation 8.1,

$$\Delta z_{\max} = \frac{\overline{u}}{\mathscr{D}_A R^2}(2R\,\Delta r^3 - \Delta r^4) \tag{8.38}$$

This can be put in dimensionless form as

$$\Delta \mathcal{Z}_{\max} = \frac{R^2}{\mathscr{D}_A \bar{t}}(2\,\Delta \mathcal{r}^3 - \Delta \mathcal{r}^4) \tag{8.39}$$

Equations 8.37 and 8.38 impose a very severe restriction on the axial increment. If Δr is halved, Δz must be decreased by a factor of more than 8. The net effect on convergence is that Δz will be far smaller than necessary for convergence in the z direction while Δr is still too large for accurate results. The situation becomes worse when the radial diffusion rate, $\mathscr{D}_A \bar{t}/R^2$, is large. The method of false transients discussed in Chapter 16 can be used, but there is no perfect method for solving PDEs. All methods are computationally intensive.

The stability requirement for the temperature equation is identical to Equations 8.37 and 8.38 once α is substituted for $\mathscr{D}_A$. When the equations for concentration and

temperature are solved together, the stability requirement for temperature will dictate $\Delta z_{\max}$ because $\alpha > \mathscr{D}_A$.

8.3.4 Example Solutions

Examples 8.3 and 8.4 illustrate numerical solutions to simple reaction and heat transfer problems. The code for Example 8.3 can be used to determine the fraction unreacted for a first-order reaction with intermediate values of $\mathscr{D}_A \bar{t}/R^2$ as illustrated in Figure 8.1. Example 8.4 uses the method of lines to solve a classic heat transfer problem.

When the heat of reaction is omitted, Equation 8.24 governs laminar heat transfer in a tube. The case when T_{in} and T_{wall} are both constant and when the velocity profile is parabolic is known as the Graetz problem. An analytical solution to the Graetz problem dates from the nineteenth century but is hard to evaluate. The numerical solution is easier to evaluate and can be extended to more realistic situations. The assumption of a parabolic velocity profile is a major cause of inaccuracy. Heating at the wall flattens the velocity profile and improves heat transfer while cooling elongates the velocity profile and lessens heat transfer. Empirical heat transfer correlations include a viscosity correction factor, for example, the $(\mu_{\text{bulk}}/\mu_{\text{wall}})^{0.14}$ term in Equation 5.36. Section 8.4 takes a more fundamental approach by calculating $V_z(r)$ as it changes down the tube.

EXAMPLE 8.3

Refer to the isothermal tubular reactor in Example 8.2 but suppose now that $\mathscr{D}_A = 5 \times 10^{-9}$ m^2 s^{-1}. Use the method of lines combined with Euler's method to determine the mixing-cup average outlet concentration.

SOLUTION: We set $a_{\text{in}} = 1$ so that the results will be the fraction unreacted. The computation follows that outlined in Section 8.3. Here, I and thus Δr are systematically varied. Values for Δz and the number of axial steps, $J = L/\Delta z$, are calculated using the stability criterion. The trapezoidal rule is used to calculate the mixing-cup average at the end of the reactor. The results are as follows:

I	J	$a_{\text{out}}/a_{\text{in}}$	Δ
8	3	0.381132	
16	22	0.426248	0.045116
32	167	0.431135	0.004887
64	1,322	0.431653	0.000518
128	16,384	0.431694	0.000042
256	84,051	0.431687	−0.000007
512	671,745	0.431685	−0.000002

The code used to produce these results is given in Code for Example 8.3.

Code for Example 8.3

```
Sub Example8_3()
Dim aold(-1 To 512), anew(512), Vz(512)
Dim Cplus(512), C(512), Cminus(512), D(512)

ain = 1
da = 0.000000005
L = 2
r = 0.01
u = 0.01
k = 0.005
Itotal = 4 'Starting value for number of radial increments

For jj = 2 To 8 'This outer loop varies Itotal tocheck convergence
    ttt = Timer

    Itotal = 2 * Itotal
    dr = r / Itotal
    dzmax = u / da / r / r * (2 * r * dr ^ 3 - dr ^ 4)
    Jtotal = Int(L / dzmax) + 1 'convert to integer and round up
    dz = L / Jtotal

'Set constants in Table 8.3 for i = 0
    Vz(0) = 2 * u
    Cplus(0) = 2 * da / dr ^ 2 / Vz(0)
    C(0) = -4 * da / dr ^ 2 / Vz(0)
    Cminus(0) = 2 * da / dr ^ 2 / Vz(0)
    D(0) = -k / Vz(0)

'Set constants in Table 8.3 for i = 1 to Itotal - 1
    For i = 1 To Itotal - 1
        Vz(i) = 2 * u * (1 - (i * dr) ^ 2 / r ^ 2)
        Cplus(i) = da / Vz(i) / dr ^ 2 * (1 + 2 * i) / 2 / i
        C(i) = -2 * da / Vz(i) / dr ^ 2
        Cminus(i) = da / Vz(i) / dr ^ 2 * (-1 + 2 * i) / 2 / i
        D(i) = -k / Vz(i)
    Next

'Set the initial conditions
    For i = 0 To Itotal
        aold(i) = ain
    Next

'March down the tube
    For j = 1 To Jtotal

'This is the sideways shuffle
        aold(-1) = aold(1)
        For i = 0 To Itotal - 1
            dela = dz * (Cplus(i) * aold(i + 1) + (C(i) + D(i)) * aold(i)
                  + Cminus(i) * aold(i - 1))
            anew(i) = aold(i) + dela
        Next i

'Apply the wall boundary condition
        anew(Itotal) = (18 * anew(Itotal - 1) - 9 * anew(Itotal - 2) + 2
* anew(Itotal - 3))/11
```

```
'March a step forward
        For i = 0 To Itotal
            aold(i) = anew(i)
        Next i

    Next j

 'Calculate the mixing cup average

    Sum = 0
    Q = 0
    For i = 1 To Itotal - 1
        Sum = Sum + 2 * dr * i * Vz(i) * anew(i)
        Q = Q + 2 * dr * i * Vz(i)
    Next i
    abar = Sum / Q

'Output results for this mesh size
    Cells(jj, 1) = Itotal
    Cells(jj, 2) = Jtotal
    Cells(jj, 3) = abar
    Cells(jj, 4) = Timer - ttt

Next jj

End Sub
```

EXAMPLE 8.4

Solve the Graetz problem for $\alpha_T \bar{t}/R^2 = 0.4$ and report your results in terms of the dimensionless temperature

$$\tau = \frac{T - T_{\text{in}}}{T_{\text{wall}} - T_{\text{in}}}$$

SOLUTION: The time-dependent and heat-of-reaction terms are omitted from Equation 8.27 to give the governing PDE for the Graetz problem:

$$2(1 - \tau^2)\frac{\partial \mathscr{T}}{\partial \mathscr{Z}} = \left(\frac{\alpha \bar{t}}{R^2}\right)\left[\frac{1}{\tau}\frac{\partial \mathscr{T}}{\partial \tau} + \frac{\partial^2 \mathscr{T}}{\partial \tau^2}\right]$$

where a parabolic velocity profile has been assumed. The inlet boundary condition is $\mathscr{T} = 0$ for all τ. The wall boundary condition is $\mathscr{T} = 1$ for all $\mathscr{Z}$, and the problem is symmetrical about the centerline of the tube.

The coefficients for the marching-ahead equations are obtained from Table 8.3 noting that $\kappa = \alpha/\rho C_P$. The coefficients on temperature sum to 1.0 in each equation. This is necessary because the asymptotic solution, $\mathscr{Z} \gg 1$, must give $\mathscr{T} = 1$ for all τ. Had there been a heat of reaction, the coefficients would be unchanged but a generation term would be added to each equation.

The stability criterion is obtained from Equation 8.38 with α replacing $\mathscr{D}_A$. Code for the solution is shown in **Code for Example 8.4**.

Code for Example 8.4

```
DefLng I-O
Sub Exp_8_4()
' Method of Lines Solution to the Graetz Problem
Dim Told(-1 To 512), Tnew(512), Vz(512)
Dim Cplus(512), C(512), Cminus(512)

Tin = 0
alpha = 0.4
Itotal = 2 'Starting value for number of radial increments

For jj = 2 To 7 'This outer loop varies Itotal to check convergence

    Itotal = 2 * Itotal
    dr = 1 / Itotal
    dzmax = (2 * dr ^ 3 - dr ^ 4) / alpha  'Stability criterion
    Jtotal = Int(1 / dzmax) + 2
    dz = 1 / Jtotal

'Set constants in Table 8.3
    Vz(0) = 2
    Cplus(0) = 2 * alpha / dr ^ 2 / Vz(0)
    C(0) = -4 * alpha / dr ^ 2 / Vz(0)
    Cminus(0) = 2 * alpha / dr ^ 2 / Vz(0)
    For i = 1 To Itotal - 1
        Vz(i) = 2 * (1 - (i * dr) ^ 2)
        Cplus(i) = alpha / Vz(i) / dr ^ 2 * (1 + 2 * i) / 2 / i
        C(i) = -2 * alpha / Vz(i) / dr ^ 2
        Cminus(i) = alpha / Vz(i) / dr ^ 2 * (-1 + 2 * i) / 2 / i
    Next

' Set the initial condition
    For i = 0 To Itotal
        Told(i) = Tin
    Next

'Start the march down the tube
    For j = 1 To Jtotal + 1
        Told(-1) = Told(1)  'Apply symmetry condition
        For i = 0 To Itotal - 1
        'This is the sideways shuffle
           delT = dz * (Cplus(i) * Told(i + 1) + C(i) * Told(i)
                  + Cminus(i) * Told(i - 1))
           Tnew(i) = Told(i) + delT
        Next i
   'Apply the wall boundary condition
        Tnew(Itotal) = 1

   'Update to prepare for another step forward
        If Itotal = 4 Then Cells(j, 1) = (j - 1)/Jtotal 'Output only for Itotal = 4
        For i = 0 To Itotal
           Told(i) = Tnew(i)
           If Itotal = 4 Then Cells(j, i + 2) = Tnew(i) 'Output only for Itotal = 4
        Next i
     Next j
```

```
'End of tube reached.  Calculate the mixing cup average

   Sum = 0
   Q = 0
   For i = 1 To Itotal - 1
       Sum = Sum + 2 * dr * i * Vz(i) * Tnew(i)
       Q = Q + 2 * dr * i * Vz(i)
   Next i
   Tbar = Sum / Q

' Output results for this mesh size
   Cells(jj, 8) = Itotal
   Cells(jj, 9) = Jtotal
   Cells(jj, 10) = Tbar

Next jj

End Sub
```

The method-of-lines solution for a coarse grid with $I = 4$ and $J = 16$ gives the following results for $\mathscr{T}$:

$\mathscr{z}$	$\tau = 0$	$\tau = 0.25$	$\tau = 0.50$	$\tau = 0.75$	$\tau = 1.0$
0	0	0	0	0	1
0.0625	0	0	0	0.5333	1
0.1250	0	0	0.1778	0.5790	1
0.1875	0	0.0569	0.2760	0.6507	1
0.2500	0.0455	0.1209	0.3571	0.6942	1
0.3125	0.1058	0.1884	0.4222	0.7289	1
0.3750	0.1719	0.2544	0.4777	0.7567	1
0.4375	0.2379	0.3171	0.5260	0.7802	1
0.5000	0.3013	0.3755	0.5690	0.8006	1
0.5625	0.3607	0.4295	0.6075	0.8187	1
0.6250	0.4157	0.4791	0.6423	0.8349	1
0.6875	0.4664	0.5246	0.6739	0.8496	1
0.7500	0.5129	0.5661	0.7026	0.8629	1
0.8125	0.5555	0.6041	0.7287	0.8749	1
0.8750	0.5944	0.6388	0.7525	0.8859	1
0.9375	0.6299	0.6705	0.7743	0.8960	1
1.0000	0.6624	0.6994	0.7941	0.9051	1

Figure 8.3 shows these results for $\mathscr{T}$ at the outlet, $\mathscr{z} = 1$. The agreement with fully converged results and equivalently with the analytical solution is quite good. This is the exception rather than the rule. Convergence should always be tested using a finer grid size.

There is no reason that the calculations must be stopped at $\mathscr{z} = 1$. Continuing to $\mathscr{z} = 2$ solves the Graetz problem for $\alpha\bar{t}/R^2 = 0.8$ since $\bar{t}$ will double while α and R are unchanged. Similarly, the results at $\mathscr{z} = 0.5$ give the outlet temperature distribution for a shorter heat exchanger with $\alpha\bar{t}/R^2 = 0.2$.

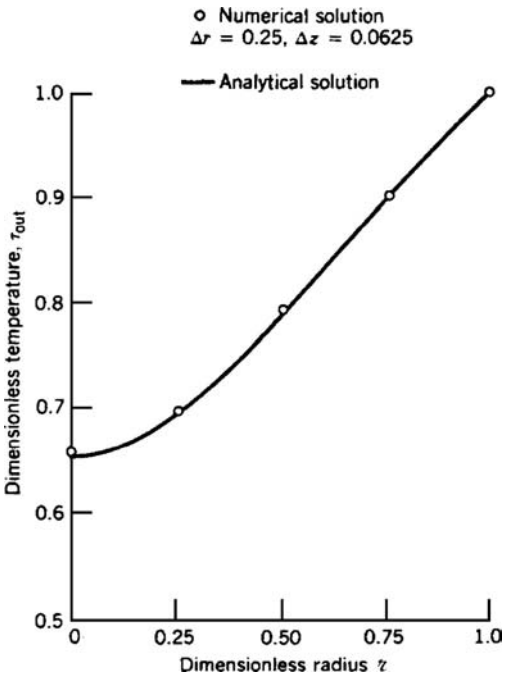

Figure 8.3 Numerical versus analytical solutions to Graetz problem with $\alpha\bar{t}/R^2 = 0.4$.

8.4 EFFECTS OF VARIABLE VISCOSITY

The methodology to this point has assumed the parabolic velocity profile of Equation 8.1. Real fluids have viscosities that are functions of temperature and composition. This means that the viscosity will vary across the radius of a tubular reactor and that the velocity profile will be something other than parabolic. If the viscosity is lower near the wall, as in heating, the velocity profile will be flattened compared to the parabolic distribution. If the viscosity is higher near the wall, as in cooling, the velocity profile will be elongated. These phenomena can be important in laminar flow reactors, affecting performance and even operability. Generally speaking, a flattened velocity profile will improve performance by more closely approaching piston flow. Conversely, an elongated profile will usually hurt performance. This section gives a method for including the effects of variable viscosity in a reactor design problem. It is restricted to low Reynolds numbers, **Re** < 100, and is used mainly for reactions involving compounds with high molecular weights such as greases, waxes, heavy oils, and synthetic polymers. It is usually possible to achieve turbulence with lower molecular weight compounds, and turbulence eliminates most of the problems associated with viscosity changes.

Variable viscosity in laminar tube flows is an example of the coupling of mass, energy, and momentum transport in a reactor design problem of practical significance.

Elaborate computer codes that recognize this coupling in complex flow geometries have been devised and verified. The present examples are representative of a general class of single-phase, variable-viscosity, variable-density problems yet avoid undue complications in mathematical or numerical analysis.

Consider axisymmetric flow in a circular tube so that $V_\theta = 0$. Two additional assumptions are needed to treat the variable-viscosity problem in its simplest form:

(i) The momentum of the fluid is negligible compared to viscous forces, **Re** $<$ 100.

(ii) The radial velocity component V_r is negligible compared to the axial component V_z.

The first of these assumptions drops the momentum terms from the equations of motion, giving a situation known as ***creeping flow***. This leaves V_r and V_z coupled through a pair of simultaneous PDEs. The pair can be solved when circumstances warrant, but the second assumption allows much greater simplification. It allows an uncoupling of the two equations so that V_z is given by a single ODE:

$$0 = -\frac{dP}{dz} + \frac{1}{r}\frac{d}{dr}\left[\mu r \frac{dV_z}{dr}\right] \tag{8.40}$$

Note that pressure is treated as a function of z alone. This is consistent with the assumption of negligible V_r. Equation 8.40 is subject to the boundary conditions of radial symmetry, $dV_z/dr = 0$ at $r = 0$, and zero slip at the wall, $V_z = 0$ at $r = R$.

The key physical requirements for Equation 8.40 to hold are that the fluid be quite viscous, giving a low Reynolds number, and that the viscosity must change slowly in the axial direction, although it may change rapidly in the radial direction. In essence, Equation 8.40 postulates that the velocity profile $V_z(r)$ is in dynamic equilibrium with the radial viscosity profile $\mu(r)$. If $\mu(r)$ changes as a function of z, then $V_z(r)$ will change accordingly, always satisfying Equation 8.40. Any change in V_z will cause a change in V_r; but if the changes in $\mu(r)$ are slow enough, the radial velocity components will be small, and Equation 8.40 will remain a good approximation.

Solving Equation 8.40 for the case of constant viscosity gives the parabolic velocity profile, Equation 8.1 and Poiseuille's equation for pressure drop, Equation 3.18. In the more general case of $\mu = \mu(r)$, the velocity profile and pressure drop are determined numerically.

8.4.1 Governing Equations for Axial Velocity

The first step in developing the numerical method is to find a "formal" solution to Equation 8.40. Observe that Equation 8.40 is variable separable,

$$r\left(\frac{dP}{dz}\right)dr = d\left[\mu r\left(\frac{dV_Z}{dr}\right)\right]$$

This equation can be integrated twice. Note that dP/dz is a constant when integrating with respect to r. The constants of integration are found using the boundary conditions.

The result is

$$V_z(r) = \frac{1}{2}\left[\frac{-dP}{dz}\right]\int_r^R \frac{r_1}{\mu} dr_1 \tag{8.41}$$

where r_1 is a dummy variable of integration. Dummy variables are used to avoid confusion between the variable being integrated and the limits of the integration. In Equation 8.41 V_z is a function of the variable r, the lower limit of the integral, but it is not a function of r_1. The dummy variable is "integrated out" and the value of the integral would be the same if r_1 were replaced by any other symbol.

Equation 8.41 allows the shape of the velocity profile to be calculated (e.g., substitute $\mu =$ constant and see what happens), but the magnitude of the velocity depends on the yet unknown value for *dP/dz*. As is often the case in hydrodynamic calculations, pressure drops are determined through the use of a continuity equation. Here, the continuity equation takes the form of a constant mass flow rate down the tube:

$$W = \pi R^2 \overline{u}_{\text{in}} \overline{\rho}_{\text{in}} = \pi R^2 \bar{u}\bar{\rho} = \int_0^R 2\pi r \rho V_z \, dr \tag{8.42}$$

Substituting Equation 8.41 into 8.42 allows $-dP/dz$ to be determined:

$$-\frac{dP}{dz} = \frac{W}{\pi \int_0^R \rho r \int_r^R r_1/\mu \, dr_1} = \frac{R^2 \overline{u}_{\text{in}} \overline{\rho}_{\text{in}}}{\int_0^R \rho r \int_r^R r_1/\mu \, dr_1} \tag{8.43}$$

This is the local pressure gradient. It is assumed to vary slowly in the z direction. The pressure at position z is

$$P = P_{\text{in}} + \int_0^z \left[\frac{dP}{dz}\right] dz \tag{8.44}$$

Substituting Equation 8.43 into Equation 8.41 gives

$$V_z(r) = \frac{R^2 \overline{u}_{\text{in}}}{2} \frac{\displaystyle\int_r^R r_1/\mu \, dr_1}{\displaystyle\int_0^R \rho/\overline{\rho}_{\text{in}} \, r \int_r^R r_1/\mu \, dr_1 \, dr} = \frac{R^2 \overline{u}_{\text{in}}}{2} \frac{G_1(r)}{G_2} \tag{8.45}$$

where $G_1(r)$ and G_2 are the indicated integrals. If viscosity is constant, analytical integration gives a parabolic profile. Variable viscosity changes the shape of the profile. Variable density changes the mean velocity but does not change the shape of the velocity profile. That is, a density gradient changes V_z but not $\mathcal{V}_z(\tau)$.

8.4.2 Calculation of Axial Velocities

The method of lines can be used to estimate composition and temperature at position $z + \Delta z$ based on a starting point at location z. Physical property correlations can be used to estimate viscosity and density at the new location. These data will be in tabular form, $\mu(i)$ and $\rho(i)$, $i = 0, \ldots, I$. We now show a method for calculating $V_z(i)$ at the

new location. These new values are substituted into the coefficients in Table 8.2 so that the next calculation using the method of lines will reflect the new velocity profile.

The numerical integration techniques require some care. Define

$$G_1(r) = \int_r^1 \left(\frac{r_1}{\mu}\right) dr_1 \approx G_1(i) = \Delta r^2 \sum_i^I \frac{i}{\mu_i} \quad \text{for } i = 0, \ldots, I \tag{8.46}$$

Data for $G_1(i)$ can be stored in tabular form and then used to calculate the second integral:

$$G_2 = \frac{1}{\overline{\rho}_{\text{in}}} \int_0^1 \rho\, r G_1(r)\, dr \approx \frac{\Delta r^2}{\overline{\rho}_{\text{in}}} \sum_0^I i\rho_i G_1(i) \tag{8.47}$$

The inlet to the reactor is usually assumed to have a flat viscosity profile, and we would like the numerical integration to reproduce the parabolic distribution when μ is constant. The G_1 integrand is linear in r and can be integrated exactly using the trapezoidal rule. The result of the G_1 integration is quadratic in r, and this is increased to cubic in r in the G_2 integrand. Thus G_2 cannot be integrated exactly with the trapezoidal rule or even Simpson's rule, and the parabolic velocity profile cannot be exactly reproduced. One possible remedy to this problem is to just live with the error in G_2 since it will decrease $O(\Delta r^2)$. In the Basic program given in Code for Example 8.5, a correction of $\Delta r^3/8$ is added to G_2, so that the parabolic profile is reproduced exactly when μ is constant.

An alternative method for calculating velocity profiles is the method of false transients described in Chapter 16.

EXAMPLE 8.5

Write a program to calculate $V_z(r)$ when μ and ρ vary in the axial direction.

SOLUTION: See Code for Example 8.5. Figure 8.4 compares the results for constant viscosity with those for an elongated velocity profile that is characteristic of high viscosity at the walls. The viscosity for this case varies by a factor of about 55 between the wall and the centerline while the density is constant. Comments in the code suggest examples of variable density and constant viscosity.

8.4.3 Calculation of Radial Velocities

The previous section gave a methodology for calculating $V_z(r)$ given $\mu(r)$ and $\rho(r)$. There will also be a variation of μ and ρ in the z direction. The formulation of Equation 8.43 gives the fully developed velocity profile $V_z(r)$, which corresponds to the local values of $\mu(r)$ and $\rho(r)$ without regard to upstream or downstream conditions. Changes in $V_z(r)$ must be gradual enough that the adjustment from one axial velocity profile to another requires only small velocities in the radial direction. We have assumed V_r to be small enough that it does not affect the equation of motion for

Code for Example 8.5

```
Sub Example8_5()
Dim Vz(512), visc(512), rho(512), G1(512)

Itotal = 10
ubarin = 1            'Mean velocity at reactor inlet
rhoin = 1             'Average density at reactor inlet
R2 = 1                'Square of tube radius
For i = 0 To Itotal   'Replace this code for other examples
    rho(i) = 1        'rhoin + 0.2 * I / Itotal is a variable density case
    visc(i) = Exp(4 * i / Itotal)    'visc(i) = 1 is the constant viscosity case
Next
dr = 1 / Itotal

'Use the trapizodal rule to evaluate G1
G1(Itotal) = 0
For i = 1 To Itotal
    m = Itotal - i
    G1(m) = G1(m + 1) + dr ^ 2 / 2 * ((m + 1) /
                visc(m + 1) + m / visc(m)) * dr
Next

'Now use it to evaluate G2
G2 = 0
For i = 1 To Itotal - 1
    G2 = G2 + i * dr * rho(i) / rhoin * G1(i) * dr
Next
G2 = G2 + rho(Itotal) / rhoin * G1(Itotal) * dr / 2

G2 = G2 + dr ^ 3 / 8  'Correction term

'Calculate the velocity profile
For i = 0 To Itotal
    Vz(i) = R2 * ubarin * rhoin * G1(i) / G2 / 2
Next i

For i = 0 To Itotal
      Vz(i) = G1(i) / G2 / 2
      Cells(i + 1, 1) = i / Itotal
      Cells(i + 1, 2) = rho(i)
      Cells(i + 1, 3) = visc(i)
      Cells(i + 1, 4) = Vz(i)
      Cells(i + 1, 5) = 2 * (1 - i * i / Itotal / Itotal)
Next i

End Sub
```

V_z. This does not mean that V_r is zero. Instead, it can be calculated from the fluid continuity equation

$$\frac{\partial(\rho V_z)}{\partial z} + \frac{(1/r)\partial(r\rho V_r)}{\partial r} = 0 \tag{8.48}$$

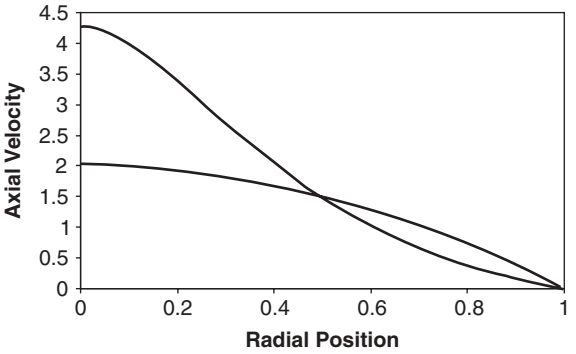

Figure 8.4 Elongation of Velocity Profile due to High Wall Viscosity.

which is subject to the symmetry boundary condition that $V_r(0) = 0$. Equation 8.48 can be integrated to give

$$V_r = \frac{-1}{\rho r}\int_0^r r_1 \frac{\partial(\rho V_z)}{\partial z} dr_1 \tag{8.49}$$

Radial motion of fluid can have a significant, cumulative effect on the convective diffusion equations even when V_r has a negligible effect on the equation of motion for V_z. Thus Equation 8.45 can give an accurate approximation for V_z even though Equations 8.20 and 8.24 need to be modified to account for radial convection. The extended versions of these equations are

$$V_z \frac{\partial a}{\partial z} + V_r \frac{\partial a}{\partial r} = \mathscr{D}_A \left[\frac{1}{r}\frac{\partial a}{\partial r} + \frac{\partial^2 a}{\partial r^2}\right] + \mathscr{R}_A \tag{8.50}$$

$$V_z \frac{\partial T}{\partial z} + V_r \frac{\partial T}{\partial r} = \alpha \left[\frac{1}{r}\frac{\partial T}{\partial r} + \frac{\partial^2 T}{\partial r^2}\right] - \frac{\mathbf{\Delta H_R}\mathscr{R}}{\rho \boldsymbol{C}_P} \tag{8.51}$$

The boundary conditions are unchanged. The method-of-lines solution continues to use a second-order approximation for $\partial a/\partial r$ and merely adds a V_r term to the coefficients for the points at $r \pm \Delta r$.

It is sometimes interesting to calculate the paths followed by nondiffusive fluid elements as they flow through the reactor. These paths are called ***streamlines*** and are straight lines when the V_z profile does not change in the axial direction. The streamlines curve inward toward the center of the tube when the velocity profile elongates, as in cooling or polymerization. They curve outward when the velocity profile flattens, as in heating or depolymerization. Example 13.10 treats a case where they initially curve inward as the viscosity increases due to polymerization but later curve outward as the reaction goes to completion and diffusion mitigates the radial gradient in polymer concentration.

If desired, the streamlines can be calculated from

$$\int_0^{r_{\text{in}}} \rho r_1 V_z(r_1, 0)\, dr_1 = \int_0^r \rho r_1 V_z(r_1, z)\, dr_1 \tag{8.52}$$

This mass balance equation shows that material that is initially at radial position r_{in} will move to radial position r for some downstream location, $z > 0$. A worked example of radial velocities and curved streamlines is given in Example 13.10.

8.5 COMPREHENSIVE MODELS

A systematic method for combining the velocity and pressure calculations with the previous solution techniques for composition and temperature starts with known values for all variables and proceeds as follows:

0. Pick an initial value for Δr.

1. Use the stability criterion, Equation 8.37, to determine an acceptable value for Δz. Note that a parabolic velocity profile cannot be assumed so Equation 8.38 should not be used.

2. Take one axial step and compute new values for $a, b, \ldots, T$. See the code of Examples 8.3 and 8.4 for examples. See Example 13.10 for coding in which the radial velocities are included.

3. Use physical property correlations to estimate new values for μ and ρ.

4. Update $V_z(r)$. See Example 8.5 for sample coding.

5. Calculate $V_r(z)$ using Equation 8.49.

6. Calculate P at the new position using Equations 8.43 and 8.44.

7. Repeat steps 1–6 until $z = L$.

8. Calculate mixing-cup averages for $a, b, \ldots, T$.

9. Halve Δr and repeat steps 1–8 until acceptable convergence is achieved.

An additional complication arises in the rigorous treatment of gas phase reactors with appreciable pressure drop. Section 9.1.2 outlines the methodology in the context of packed-bed reactors. For empty tubes, diffusivities are high in gas phase reactors, and it may be adequate to treat the reactor as a variable-density PFR. See Section 3.3.1.

Development of a comprehensive model for a real tubular reactor is a significant undertaking. Refer to the advice on debugging in Section 5.2.1. Begin with simple cases such as isothermal and adiabatic PFRs. Add and test complications one at a time. Verify continuously. Examples of reasonably comprehensive models are discussed in Chapter 13 in the industrially relevant context of polymer reaction engineering.

8.6 PERFORMANCE OPTIMIZATION

The reaction environment in a macroscale tubular reactor is nonuniform due to the distribution of residence times and diffusion-limited transfer of heat and mass in the radial direction. This section describes two approaches to improving reactor performance.

8.6.1 Optimal Wall Temperatures

The method-of-lines formulation for solving Equations 8.50 and 8.51 does not require that T_{wall} be constant but allows $T_{wall}(z)$ to be an arbitrary function of axial position. A new value of T_{wall} may be used at each step in the calculations, just as a new Δz may be assigned at each step (subject to the stability criterion). The design engineer is thus free to pick a $T_{wall}(z)$ that optimizes reactor performance.

Reactor performance is an issue of selectivity, not of conversion. Otherwise, just push T_{wall} to its maximum possible value. Good selectivity results from an optimal trajectory of time versus temperature for all portions of the reacting fluid, but uniform treatment is difficult in laminar flow due to the large difference in residence time between the wall and centerline. No strategy for controlling the wall temperature can completely eliminate the resultant nonuniformity, but a good strategy for $T_{wall}(z)$ can mitigate the problem. With preheated feed, initial cooling at the wall can help compensate for the long residence times near the wall. With cold feed, initial heating at the wall is needed to start the reaction, but a switch to cooling can be made at some downstream point. A good general approach to determining the optimal $T_{wall}(z)$ is to first find the best single wall temperature, then find the best two-zone strategy, the best three-zone strategy, and so on. The objective function for the optimization can be as simple as the mixing-cup outlet concentration of a desired product. It can also be based on the concept of ***thermal time distributions*** introduced in Section 15.5.3.

Optimization requires that $\alpha\bar{t}/R^2$ have some reasonably high value so that the wall temperature has a significant influence on reactor performance. There is no requirement that $\mathscr{D}_A\bar{t}/R^2$ be large. Thus the method can be used for polymer systems that have thermal diffusivities typical of organic liquids but low molecular diffusivities. The calculations needed to optimize distributed-parameter systems (i.e., sets of PDEs) are much longer than needed to optimize the lumped-parameter systems (i.e., sets of ODEs) studied in Chapter 6, but the numerical approach is the same and is still feasible using small computers.

8.6.2 Static Mixers

Static mixers, also called motionless mixers, consist of tubes or ducts in which stationary vanes (elements) have been installed to promote radial flow. There are many commercial types, some of which are shown in Figure 8.5. A comprehensive review is available. See Thakur et al. (2003). They all function by inducing secondary flows perpendicular to the main, axial flow. A helically coiled tube without inserts also exhibits such flows and gives a limited improvement in performance. A series of helically coiled tubes where the axis of each successive coil is at a 90° angle to the previous coil axis can actually approach piston flow (see Nigam and Saxena, 1984).

The flow geometry in static mixers is complex and difficult to model. Velocity profiles, streamlines, and pressure drops can be computed using programs for

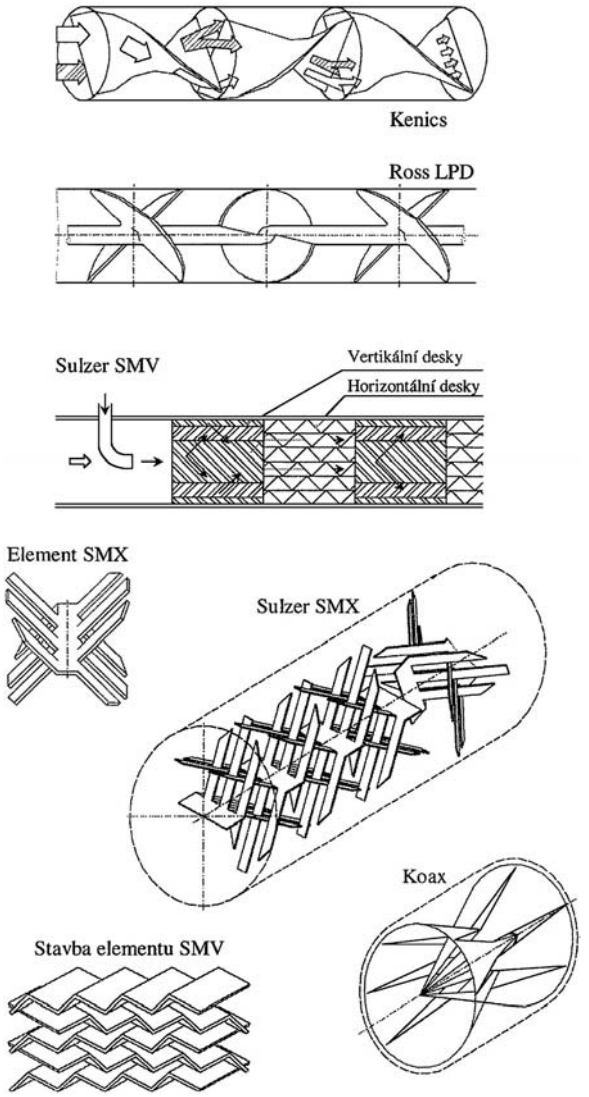

Figure 8.5 Commercial motionless mixers (Drawing Courtesy Professor Pavel Ditl, Czech Technical University)

computational fluid dynamics (CFD) such as Fluent. These programs are computationally intensive and have not been fully verified when applied to exothermic chemical reactions. Experimental verification is generally needed. Older and simpler approaches to modeling static mixers include the axial dispersion model discussed in Chapter 9. Another approach is to use Equation 8.20 for segments of the reactor but to periodically reinitialize the concentration profile. An empirical study (Nigam and

Nauman, 1985) on Kenics-type static mixers found that four of the Kenics elements correspond to one zone of complete radial mixing. The computation is as follows:

1. Start with a uniform concentration profile, $a(z) = a_{\text{in}}$ at $z = 0$.
2. Solve Equation 8.20 using the methods of this chapter and ignoring the presence of the mixing elements.
3. When an axial position corresponding to four mixing elements is reached, calculate the mixing-cup average composition.
4. Restart the solution of Equation 8.20 using a uniform concentration profile equal to the mixing-cup average from the previous set of four elements.
5. Repeat steps 2–4 until the end of the reactor is reached.

This technique should give reasonable results for isothermal first-order reactions. It and other modeling approaches are largely untested for complex and nonisothermal reactions.

8.6.3 Small Effective Diameters

The simplest way of improving radial uniformity in a tubular reactor is to reduce the tube diameter since this will increase $\mathscr{D}_A\bar{t}/R^2$ and $\alpha\bar{t}/R^2$. A practical lower limit for the tube diameter in a conventional shell-and-tube reactor is about $\frac{3}{8}$ in., and even this size may cause concerns about fouling, ease of cleaning, and ease of replacing a leaking tube. Commercial devices such as spiral-wound heat exchangers are common in the food and pharmaceutical industries where the usual aim is to transfer heat to temperature-sensitive materials while minimizing residence times and wall temperatures. Such devices can be used as reactors if the reactions are fast or the desired output is low. Flow is through rectangular ducts or slits rather than tubes and is generally laminar—even for water like fluids—due to the small channel heights and consequently low Reynolds numbers. The velocity profiles are similar to those in a tube in that they have a more or less parabolic shape with zero velocity at the walls and a maximum at the center of the channel. For constant-viscosity flow through a narrow slit,

$$V_z(y) = 1.5\overline{u}\left[1 - \frac{y^2}{H^2}\right] \tag{8.53}$$

Here, y is a distance coordinate analogous to r that is zero at the center of the slit; H is analogous to R and is the slit half-height. Equation 8.53 assumes that the walls at the sides of the slit are so distant that they have no effect on the flow over most of the slit width.

Equation 8.53 predicts that the fastest moving fluid will experience two-thirds of the mean residence time, $0.67\bar{t}$. This is a worthwhile improvement in uniformity compared to a tube where the fastest fluid has only half the mean residence time. However, the major advantage of duct and slit devices is that they can be fabricated

with much smaller effective diameters (e.g., $2H$) while maintaining greater capacity (e,g., multiple slits or very long slits widths) than is feasible with small tubes.

The method of lines is suited for solving the convective diffusion equations for heat and mass in ducts and slits, but rectangular rather than cylindrical coordinates should be used. The governing equations, analogous to Equations 8.20 and 8.24, are given in Chapter 16. The method of false transients as applied to PDEs is given in Chapter 16 and provides an alternative approach to solving these equations. The method of false transients is also used to determine velocity profiles for rectangular ducts for which an analytical solution is not useful.

8.7 SCALEUP OF LAMINAR FLOW REACTORS

Chapter 3 introduced the basic concepts of scaleup for tubular reactors. The theory developed in this chapter allows scaleup of laminar flow reactors on a more substantive basis. ***Model-based scaleup*** supposes that the reactor is reasonably well understood at the pilot scale and that a model of the proposed plant-scale reactor predicts performance that is in reasonably good agreement with the pilot plant data. Then the model is used to estimate performance in the full-scale reactor. The alternative is ***blind scaleup*** where the pilot reactor produces good product and where the scaleup is based on general principles and high hopes. There are business situations where blind scaleup is the best choice, but given your druthers, go for model-based scaleup.

Consider the scaleup of a small, tubular reactor in which diffusion of both mass and heat is important. As a practical matter, the same fluid, the same inlet temperature, and the same mean residence time will be used in the small and large reactors. Substitute fluids and ***cold-flow models*** are sometimes used to study the fluid mechanics of a reactor, but not the kinetics of the reaction.

The goal of a scaleup is to achieve similar product quality at a higher rate. The throughput scaleup factor is S. This determines the flow rate to the large system; and the requirement of constant $\bar{t}$ fixes the volume of the large system. For scaleup of flow in an open tube, the design engineer has two basic variables, R and T_{wall}. An exact scaleup requires that $\mathscr{D}_A\bar{t}/R^2$ and $\alpha\bar{t}/R^2$ be held constant, and the only way to do this is to keep the same tube diameter. Scaling in parallel is exact. Scaling in series is inexact but generally conservative for incompressible fluids. See Section 3.2. Other forms of scaleup will be satisfactory only under special circumstances. One of these circumstances is isothermal laminar flow when $\mathscr{D}_A\bar{t}/R^2$ is small in the pilot reactor.

8.7.1 Isothermal Laminar Flow

Reactors in isothermal laminar flow are exactly scaleable using geometric similarity if diffusion is negligible in the pilot reactor. Converting Equation 8.2 to dimensionless form gives

$$\mathscr{V}_z(\tau)\frac{\partial a}{\partial \mathscr{Z}} = \mathscr{R}_A\bar{t} \tag{8.54}$$

The absolute reactor size as measured by R and L does not appear. Using the same feed composition and the same $\bar{t}$ in a geometrically similar reactor will give a geometrically similar composition distribution; that is, the concentration at the point $(\tau, \mathcal{Z})$ will be the same in the large and small reactors. Similarly, the viscosity profile will be the same when position is expressed in dimensionless form, and this leads to the same velocity profile, pressure drop, and mixing-cup average composition. These statements assume that diffusion really was negligible on the small scale and that the Reynolds number remains low in the large reactor. Blind scaleup will then give the same product from the large reactor as from the small. If diffusion was beneficial at the small scale, reactor performance will worsen upon scaleup. The Reynolds number may become too high upon scaleup for the creeping-flow assumption of Section 8.4 to remain reasonable, but the probable consequence of a higher Reynolds number is improved performance at the cost of a somewhat higher pressure drop.

It may not be feasible to have an adequately low value for $\mathscr{D}_A\bar{t}/R^2$ and still scale using geometric similarity. Recall that reactor scaleups are done at constant $\bar{t}$. The problem is that the pilot reactor would require too high a flow rate and consume too much material when $\mathscr{D}_A\bar{t}/R^2$ is small enough (i.e., R is large enough) and L/R is large enough for reasonable scaleup. The choice is to devise a model-based scaleup. Model the pilot reactor using the actual value for $\mathscr{D}_A\bar{t}/R^2$. Confirm (and adjust) the model based on experimental measurements. Then model the large reactor using the appropriately reduced value for $\mathscr{D}_A\bar{t}/R^2$. If the predicted results are satisfactory, go for it. If the predictions are unsatisfactory, consider using static mixers in the large reactor. These devices lower the effective value for $\mathscr{D}_A\bar{t}/R^2$ by promoting radial mixing. The usual approach to scaling reactors that contain static mixers is to start with geometric similarity but to increase the number of mixing elements to compensate for the larger tube diameter. For mixers of the Kenics-type, an extra element is needed each time the tube diameter is doubled.

8.7.2 Nonisothermal Laminar Flow

The temperature counterpart of $\mathscr{D}_A\bar{t}/R^2$ is $\alpha\bar{t}/R^2$, and if $\alpha\bar{t}/R^2$ is low enough, then the reactor will be adiabatic. Since $\alpha \gg \mathscr{D}_A$, the situation of an adiabatic laminar flow reactor is rare. Should it occur, then $T(\tau, \mathcal{Z})$ will be the same in the small and large reactors, and blind scaleup is possible. More commonly, $\alpha\bar{t}/R^2$ will be so large that radial diffusion of heat will be significant in the small reactor. The extent of radial diffusion will lessen upon scaleup, leading to the possibility of thermal runaway. If model-based scaleup predicts a reasonable outcome, go for it. Otherwise, consider scaling in series or parallel.

SUGGESTED FURTHER READINGS

More detail on solutions of the convective diffusion equation by the method of lines is given in Chapter 8 of the earlier version of this book:

E. B. Nauman, *Chemical Reactor Design, Optimization and Scaleup*, McGraw-Hill, New York, 2002.

The convective diffusion equations for mass and energy are given detailed treatments in most texts on transport phenomena. The classic reference is:

R. B. Bird, W. E. Stewart, and E. N. Lightfoot, *Transport Phenomena*, 2nd Ed., Wiley, New York, 2002.

Practical applications to laminar flow reactors are still mainly in the research literature. The first good treatment of a reactor with variable viscosity is:

S. Lynn and J. E. Huff, Polymerization in a tubular reactor, *AIChE* J., **17**, 475 (1971).

A detailed model of an industrially important reaction, styrene polymerization, is given in:

C. E. Wyman and L. F. Carter, A numerical model for tubular polymerization reactors, *AIChE Symp. Ser.,***72**, 1 (1976).

See also Chapter 13.

The appropriateness of neglecting radial flow in the axial momentum equation yet retaining it in the convective diffusion equation is discussed in:

H. S. McLaughlin, R. Mallikarjun, and E. B. Nauman, The effect of radial velocities on laminar flow, tubular reactor models, *AIChE J.,* **32**, 419 (1986).

PROBLEMS

8.1 Polymerizations often give such high viscosities that laminar flow is inevitable. A typical monomer diffusivity in a polymerizing mixture is 1.0×10^{-10} m^2 s^{-1} (the diffusivity of the polymer will be much lower). A pilot-scale reactor might have a radius of 1 cm. What is the maximum value for the mean residence time before molecular diffusion becomes important? What about a production-scale reactor with $R = 10$ cm?

8.2 The velocity profile for isothermal, laminar, non-Newtonian flow in a pipe can sometimes be approximated as

$$V_z = V_0 \left[1 - \left(\frac{r}{R} \right)^{(\eta+1)/\eta} \right]$$

where η is called the flow index or power law constant. The case $\eta = 1$ corresponds to a Newtonian fluid and gives a parabolic velocity profile. Find $a_{\text{out}}/a_{\text{in}}$ for a first-order reaction given $k\bar{t} = 1.0$ and $\eta = 0.5$. Assume negligible diffusion.

8.3 Repeat Example 8.1 and obtain an analytical solution for the case of first-order reaction and pressure-driven flow between flat plates. The velocity profile is given by Equation 8.53. Feel free to use software for the symbolic manipulations, but do substantiate your results.

8.4 Equations 8.57 and 8.58 in Appendix 8.2 use a third-order approximation to estimate a backward first derivative. Use the methodology of Example 8.6 to estimate the order of convergence for this derivative.

8.5 Equation 8.4 defines the average concentration a_{out} of material flowing from the reactor. Omit the $V_z(r)$ term inside the integral and normalize by the cross-sectional area $A_c = \pi R^2$ rather than the volumetric flow rate Q. The result is the spatial average concentration, a_{spatial} and is what you would measure if the contents of the tube were frozen and a thin

disk of the material cut out and analyzed. In-line devices for measuring concentration may measure a_{spatial} rather than a_{out}. Is the difference important?

(a) Calculate both averages for the case of a parabolic velocity profile and first-order reaction with $k\bar{t} = 1$.

(b) Find the value of $k\bar{t}$ which maximizes the difference between these averages.

8.6 What criterion did Merrill and Hamrin (1970) use for determining that the yield of a first-order reaction was unaffected by diffusion? Specifically, if $\mathscr{D}_A\bar{t}/R^2 = 3 \times 10^{-3}$, what is the maximum difference between $a_{\text{out}}/a_{\text{in}}$ with and without diffusion? At what value for $k\bar{t}$ does this maximum difference occur?

8.7 If a maximum difference of 1% is accepted, when can diffusion be neglected in a laminar flow reactor if the reaction is second order of the form $2A \xrightarrow{k} P$?

8.8 Determine the opposite of the Merrill and Hamlin criterion. That is, find the value of $\mathscr{D}_A\bar{t}/R^2$ above which a laminar flow reactor closely approximates a PFR for a first-order reaction. Make the comparison at $k\bar{t} = 1$. (The interested reader should see if this conclusion holds in light of the axial diffusion results in Chapter 16.)

8.9 Free-radical polymerizations tend to be highly exothermic. The following data are representative of the thermal (i.e., spontaneous) polymerization of styrene:

$$\begin{aligned}
\kappa &= 0.13 \text{ J m}^{-1}\text{s}^{-1}\text{K}^{-1} \\
\mathscr{D}_A &= 1.0 \times 10^{-9}\text{m}^2/\text{s}^{-1} \\
\Delta H &= -8 \times 10^4 \text{ J g-mol}^{-1} \\
C_P &= 1.9 \times 10^3 \text{J kg}^{-1}\text{K}^{-1} \\
\rho &= 950 \text{ kg m}^{-3} \\
a_{\text{in}} &= 9200 \text{ g-moles m}^{-3} \\
L &= 7 \text{ m} \\
\bar{t} &= 1 \text{ h} \\
k &= 1.0 \times 10^{10} \exp(-10{,}000/T) \text{ h}^{-1} \\
T_{\text{in}} &= 120^\circ\text{C} \\
T_{\text{wall}} &= 120^\circ\text{C}
\end{aligned}$$

Assume laminar flow and a parabolic velocity distribution. Calculate the temperature and composition profiles in the reactor. Start with I = 4 and double until your computer cries for mercy. Consider two cases: (a) $R = 0.01$ m and (b) $R = 0.20$ m.

8.10 Suppose the consecutive reactions

$$A \xrightarrow{k_1} B \xrightarrow{k_2} C$$

are elementary with rate constants $k_1 = 4.5 \times 10^{11} \exp(-10{,}000/T)$ h^{-1} and $k_2 = 1.8 \times 10^{12} \exp(-12{,}000/T)$ h^{-1}. The reactions are occurring in a tube in laminar flow with $a_{\text{in}} = 1$, $b_{\text{in}} = c_{\text{in}} = 0$. Both reactions are exothermic with $-\Delta H_1 a_{\text{in}}/(\rho C_P) = -\Delta H_2 a_{\text{in}}/(\rho C_P) = 50$ K. The reactor is operated with $\bar{t} = 1$ h, $T_{\text{in}} = 400$ K, $T_{\text{wall}} = 400$ K. Assume $\alpha\bar{t}/R^2 = 0.1$. Determine a_{out}, b_{out}, and c_{out} given that $\mathscr{D}_A\bar{t}/R^2 = 0.01$ is the same for all components.

8.11 Suppose $A + B \xrightarrow{k} C$ with $ka_{in}\bar{t} = 2$ in a laminar flow tubular reactor with unmixed feed. Component A with initial concentration $a_{in} = 1$ is injected at the center of the tube and component B with initial concentration $b_{in} = 1$ in injected in an annular ring between component A and the wall. The molar flow rates of A and B are equal so that the overall stoichiometry is perfect. Ignore hydrodynamic entrance effects and assume that the velocity profile is parabolic immediately after injection at location $z = 0$.

(a) What is the radial position that initially divides A and B?

(b) Determine $a_{out} = b_{out}$ at the reactor outlet assuming $\mathscr{D}_A\bar{t}/R^2 = \mathscr{D}_B\bar{t}/R^2 = 0.01$.

8.12 Suppose you are marching down the infamous tube and at step j have determined the temperature and composition at each radial point. A correlation is available to calculate viscosity, and it gives the results tabulated below. Assume constant density and **Re** $= 0.1$. Determine the axial velocity profile. Plot your results and compare them to the parabolic distribution.

r/R	Isothermal μ	Cooling μ	Heating μ
1.000	1.0	54.6	0.018
0.875	1.0	33.1	0.030
0.750	1.0	20.1	0.050
0.625	1.0	12.2	0.082
0.500	1.0	7.4	0.135
0.375	1.0	4.5	0.223
0.250	1.0	2.7	0.368
0.125	1.0	1.6	0.607
0	1.0	1.0	1.000

8.13 Derive the equations necessary to calculate $V_z(y)$ given $\mu(y)$ for pressure-driven flow between flat plates.

8.14 What are the boundary conditions associated with V_r? Prove that Equation 8.47 satisfies them.

8.15 Stepwise condensation polymerizations can be modeled as a second-order reaction of the functional groups. Let a be the concentration of functional groups so that $\mathscr{R}_A = -ka^2$. The viscosity relationship

$$\frac{\mu}{\mu_0} = 1 + 100\left[1 - \left(\frac{a}{a_{in}}\right)^3\right]$$

is reasonable for a condensation polymer in a solvent. Determine a_{out}/a_{in} for an isothermal, laminar flow reactor with $k\bar{t} = 2$ and with negligible diffusion. Neglect the radial velocity component V_r.

8.16 Rework Problem 8.15 including V_r; that is, solve Equation 8.50. Also plot the streamlines. See Example 13.10 for guidance.

8.17 Suppose that the viscosity changes in Problem 8.12 are accompanied by density changes according to the following table:

r/R	μ	ρ
1.000	54.6	1.054
0.875	33.1	1.032
0.750	20.1	1.019
0.625	12.2	1.011
0.500	7.4	1.064
0.375	4.5	1.035
0.250	2.7	1.017
0.125	1.6	1.006
0	1	1.000

Calculate the velocity profile and compare it with that calculated for the cooling, constant-density case in Problem 8.12.

APPENDIX 8.1 CONVECTIVE DIFFUSION EQUATION

This appendix presents a simple derivation of the convective diffusion equation applicable to tubular reactors with radial symmetry. The starting point is Equation 1.4 applied to the differential volume element shown in Figure 8.6. The volume element

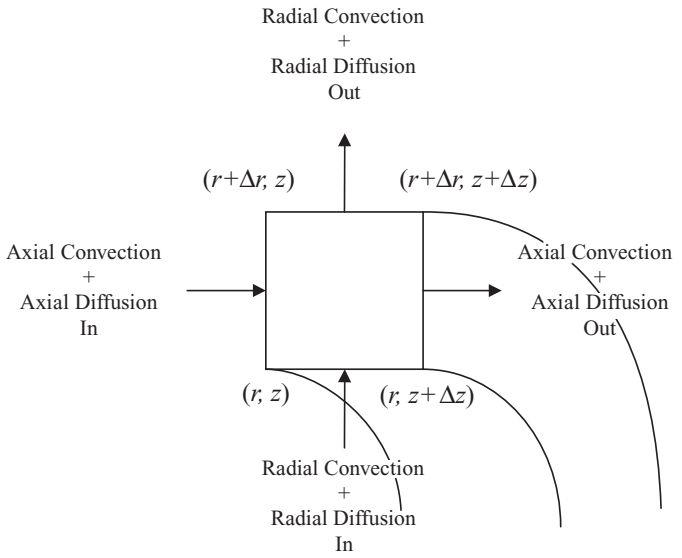

Figure 8.6 Differential volume element in cylindrical coordinates.

is located at point (r, z) and is in the shape of a ring. Note that θ dependence is ignored so that the results will not be applicable to systems with significant natural convection. Component A is transported by radial and axial diffusion and convection. The diffusive flux is governed by Fick's law.

The various terms needed for Equation 1.4 are

$$\text{Radial diffusion in} = -\mathscr{D}_A \left[\frac{\partial a}{\partial r}\right]_r [2\pi r\ \Delta z]$$

$$\text{Axial diffusion in} = -\mathscr{D}_A \left[\frac{\partial a}{\partial z}\right]_z [2\pi r\ \Delta r]$$

$$\text{Radial convection in} = V_r(r)a(r)[2\pi r\ \Delta z]$$

$$\text{Axial convection in} = V_z(z)a(z)[2\pi r\ \Delta r]$$

$$\text{Radial diffusion out} = -\mathscr{D}_A \left[\frac{\partial a}{\partial r}\right]_{r+\Delta r} [2\pi (r+\Delta r)\ \Delta z]$$

$$\text{Axial diffusion out} = -\mathscr{D}_A \left[\frac{\partial a}{\partial z}\right]_{z+\Delta z} [2\pi r\ \Delta r]$$

$$\text{Radial convection out} = V_r(r+\Delta r)a(r+\Delta r)[2\pi r\ \Delta r]$$

$$\text{Axial convection out} = V_z(z)a(z+\Delta z)[2\pi r\ \Delta r]$$

$$\text{Formation of A by reaction} = \mathscr{R}_A[2\pi r \Delta r\ \Delta z]$$

$$\text{Accumulation} = \frac{\partial a}{\partial t}[2\pi r \Delta r\ \Delta z]$$

Applying Equation 1.4, dividing everything by $2\pi r\ \Delta r\ \Delta z$, and rearranging give

$$\frac{\partial a}{\partial t} + \frac{V_z(z+\Delta z)a(z+\Delta z) - V_z(z)a(z)}{\Delta z} + \frac{V_r(r+\Delta r)a(r+\Delta r) - V_r(z)a(z)}{\Delta r}$$
$$= +\frac{\mathscr{D}_A\,[\partial a/\partial r]_{r+\Delta r} - \mathscr{D}_A\,[\partial a/\partial r]_r}{\Delta r} + \mathscr{D}_A \left[\frac{\partial a}{\partial r}\right]_{r+\Delta r}$$
$$\frac{1}{r} + \frac{\mathscr{D}_A\,[\partial a/\partial z]_{z+\Delta z} - \mathscr{D}_A\,[\partial a/\partial z]_z}{\Delta z} + \mathscr{R}_A$$

The limit is now taken as $\Delta z \to 0$ and $\Delta r \to 0$. The result is

$$\frac{\partial a}{\partial t} + \frac{\partial (V_z a)}{\partial z} + \frac{\partial (V_r a)}{\partial r} = \frac{\partial \left[\mathscr{D}_A(\partial a/\partial z)\right]}{\partial z} + \frac{\partial \left[\mathscr{D}_A(\partial a/\partial r)\right]}{\partial r} + \frac{\mathscr{D}_A}{r}\frac{\partial a}{\partial r} + \mathscr{R}_A \tag{8.55}$$

which is a more general version of Equation 8.18.

APPENDIX 8.2
EXTERNAL RESISTANCE TO HEAT TRANSFER

This appendix considers the appropriate wall boundary condition for temperature when the external resistances to heat transfer are significant. We suppose the tube is jacketed with a fluid at temperature T_{ext} that transfers heat to the outer wall of the

tube that is at temperature T_{outer}. The outside heat transfer coefficient is h_0. This heat is conducted across the tube wall to the inner wall, which is at temperature T_{wall}. A steady-state heat balance gives

$$q = h_0(T_{\text{ext}} - T_{\text{outer}}) = \kappa_{\text{wall}}(T_{\text{outer}} - T_{\text{wall}})/\Delta_{\text{wall}}$$

where κ_{wall} is the thermal conductivity of the wall and Δ_{wall} is its thickness.

This same amount of heat must be transferred into the reacting fluid by conduction:

$$q = \kappa \left.\frac{dT}{dr}\right|_R$$

where κ is the thermal conductivity of the reacting fluid. Algebra gives

$$T_{\text{ext}} - T_{\text{wall}} = \beta\kappa \left.\frac{dt}{dr}\right|_R \qquad \text{where } \beta = \frac{\kappa_{\text{wall}} + \Delta_{\text{wall}} h_0}{h_0 \kappa_{\text{wall}}} \tag{8.56}$$

The interested reader should explore the values of β as either or both h_0 and κ_{wall} approach infinity.

Equation 8.56 is the appropriate wall boundary condition associated with Equation 8.24 when there is external resistance to heat transfer. To implement it as part of the method of lines, an estimate for dT/dr at the wall is needed. A first-order approximation is just

$$\left.\frac{dT}{dr}\right|_R \approx \frac{T(R) - T(R - \Delta r)}{\Delta r}$$

Combining this with Equation 8.56 gives

$$T_{\text{wall}} = \frac{\Delta r T_{\text{ext}} + \beta\kappa T(R - \Delta r)}{\Delta r + \beta\kappa}$$

where we have used the fact that $T(R) = T_{\text{wall}}$. [In Chapter 9, $T(R)$ and T_{wall} may be different.]

A more accurate estimate of the first derivative is obtained from a third-order approximation. Fit a cubic through the points $T(R)$, $T(R - \Delta r)$, $T(R - 2\,\Delta r)$, and $T(R - 3\,\Delta r)$ and differentiate to estimate the slope at point R. The derivative approximation is

$$\left.\frac{dT}{dr}\right|_R \approx \frac{-22T(r) + 36T(R - \Delta r) - 18T(R - 2\,\Delta r) + 4T(R - 3\,\Delta r)}{12\,\Delta r} \tag{8.57}$$

and the wall boundary condition becomes

$$T_{\text{wall}} = \frac{6\,\Delta r T_{\text{ext}} - 18\beta\kappa T(R - \Delta r) + 9\beta\kappa T(R - 2\,\Delta r) - 2\beta\kappa T(R - 3\,\Delta r)}{6\,\Delta r - 11\beta\kappa} \tag{8.58}$$

Equation 8.58 reduces to $T_{\text{wall}} = T_{\text{ext}}$ if both h_0 and κ_{wall} are large and reduces to a smooth, zero-slope condition when either h_0 or κ_{wall} are zero (compare Equation 8.32).

APPENDIX 8.3
FINITE-DIFFERENCE APPROXIMATIONS

This appendix describes a number of finite-difference approximations useful for solving second-order PDEs, that is, equations containing terms such as $\partial^2 f/\partial x^2$. The basic idea is to approximate f as a polynomial in x and then to differentiate the polynomial to obtain estimates for derivatives such as $\partial f/\partial x$ and $\partial^2 f/\partial x^2$. The polynomial approximation is a local one that applies to some region of space centered about point $x = 0$. When the point changes, the polynomial approximation will change as well. We begin by fitting a quadratic to the three points shown below.

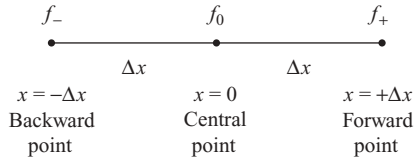

The quadratic has the form

$$f = A + Bx + Cx^2$$

Writing it for the three points gives

$$\begin{aligned} f_- &= A - B\,\Delta x + C\,\Delta x^2 \\ f_0 &= A \\ f_+ &= A + B\,\Delta x + C\,\Delta x^2 \end{aligned}$$

These equations are solved for A, B, and C to give

$$f = f_0 + \left(\frac{f_+ - f_-}{2\,\Delta x}\right) x + \left(\frac{f_+ - 2f_0 + f_-}{2\,\Delta x^2}\right) x^2$$

This is ***a second-order approximation*** and can be used to obtain derivatives up to the second. Differentiate once to obtain

$$\frac{df}{dx} = \left(\frac{f_+ - f_-}{2\,\Delta x}\right) + \left(\frac{f_+ - 2f_0 + f_-}{\Delta x^2}\right) x$$

Differentiating again gives

$$\frac{d^2 f}{dx^2} = \frac{f_+ - 2f_0 + f_-}{\Delta x^2}$$

The value of the first derivative depends on the position at which it is evaluated:

Setting $x = +\Delta x$ gives a ***second-order, forward difference:***

$$\left[\frac{df}{dx}\right]_+ \approx \frac{3f_+ - 4f_0 + f_-}{2\,\Delta x}$$

Setting $x = 0$ gives a ***second-order, central difference:***

$$\left[\frac{df}{dx}\right]_0 \approx \frac{f_+ - f_-}{2\,\Delta x}$$

Setting $x = Ax$ gives a ***second-order, backward difference:***

$$\left[\frac{df}{dx}\right]_- \approx \frac{-f_+ + 4f_0 - 3f_-}{2\,\Delta x}$$

The second derivative is constant (independent of x) for this second-order approximation. We consider it to be a ***central difference***:

$$\left[\frac{d^2f}{dx^2}\right]_0 \approx \frac{f_+ - 2f_0 + f_-}{\Delta x^2}$$

All higher derivatives are zero. Obviously, to obtain a nontrivial approximation to an *n*th derivative requires at least an *n*th-order polynomial. The various nontrivial derivatives obtained from an *n*th-order polynomial will converge $O(\Delta x^n)$.

EXAMPLE 8.6

Apply the various second-order approximations to evaluate derivatives of the function $f = x\,\exp(x)$ at or about the point $x = 0$.

SOLUTION: $f_+ = \Delta x\,\exp(\Delta x)$, $f_0 = 0$, $f_- = -\Delta x\,\exp(-\Delta x)$. The various derivative approximations are

$$\left[\frac{df}{dx}\right]_+ = \frac{3\exp(\Delta x) - \exp(-\Delta x)}{\Delta x}$$

$$\left[\frac{df}{dx}\right]_0 = \frac{\exp(\Delta x) - \exp(-\Delta x)}{2\,\Delta x}$$

$$\left[\frac{df}{dx}\right]_- = \frac{-\exp(\Delta x) + 3\,\exp(-\Delta x)}{2}$$

$$\left[\frac{d^2f}{dx^2}\right]_0 = \frac{\exp(\Delta x) - \exp(-\Delta x)}{\Delta x}$$

Evaluating them as a function of Δx gives the following:

Δx	$\left[\frac{df}{dx}\right]_+$	Δ	$\left[\frac{df}{dx}\right]_0$	Δ	$\left[\frac{df}{dx}\right]_-$	Δ	$\left[\frac{d^2f}{dx^2}\right]$	Δ
1	3.893	—	1.543	—	−0.807	—	2.350	—
$\frac{1}{2}$	2.170	1.723	1.128	0.415	0.805	−0.892	2.084	0.266
$\frac{1}{4}$	1.537	0.633	1.031	0.096	0.526	−0.441	2.021	0.063
$\frac{1}{8}$	1.258	0.279	1.008	0.024	0.757	−0.231	2.005	0.016
$\frac{1}{16}$	1.127	0.131	1.002	0.006	0.877	−0.120	2.001	0.004
$\frac{1}{32}$	1.063	0.0064	1.000	0.002	0.938	0.0061	2.000	0.002
0	1	—	1	—	1	—	2	—

It is apparent that the central-difference approximations for both the first and second derivatives converge $O(\Delta x^2)$. The forward and backward approximations to the first derivative converge $O(\Delta x)$ even though a second-order approximation was used in their derivation. This is because they are really approximating the derivatives at the points $x = \pm\Delta x$ rather than at $x = 0$.

For a **first-*order approximation,*** a straight line is fit between the points $x = 0$ and Δx to get the ***first-order, forward-difference approximation***

$$\left[\frac{df}{dx}\right]_{+\Delta x/2} \approx \frac{f_+ - f_0}{\Delta x}$$

and between the points $x = -\Delta x$ and $x = 0$ to get the ***first-order, backward-difference*** approximation

$$\left[\frac{df}{dx}\right]_{-\Delta x/2} \approx \frac{f_0 - f_-}{\Delta x}$$

These both converge $O(\Delta x)$.

Chapter 9

Packed Beds and Turbulent Tubes

The essence of reactor design is the combination of chemical kinetics with transport phenomena. The chemical kineticist, who can be a chemical engineer but by tradition is a physical chemist, is concerned with the interactions between molecules (and sometimes within molecules) in well-defined systems. By well defined, we mean that all variables that affect the reaction can be controlled at uniform and measurable values. Chemical kinetic studies are usually conducted in small equipment where mixing and heat transfer are excellent and where the goal of having well-defined variables is realistic. Occasionally, the ideal conditions can be retained upon scaleup. Slow reactions in batch reactors or CSTRs are examples. More likely, scaleup to industrial conditions will involve fast reactions in large equipment where mixing and heat transfer limitations may emerge. Transport equations must be combined with the kinetic equations, and this is the realm of the chemical engineer.

Chapter 8 combined transport with kinetics in the purest and most fundamental way. The flow fields were deterministic, time invariant, and calculable. The reactor design equations were applied to simple geometries such as circular tubes and were based on intrinsic properties of the fluid such as molecular diffusivity and viscosity. Such reactors do exist, particularly in polymerizations, as discussed in Chapter 13, but they are less typical of industrial practice than the more complex reactors considered in this chapter.

The models of Chapter 9 contain at least one empirical parameter. This parameter is used to account for complex flow fields that are not deterministic, time invariant, and calculable. We are specifically concerned with packed-bed reactors and turbulent flow reactors. We begin with packed-bed reactors because they are ubiquitous within the petrochemical industry and because their mathematical treatment closely parallels that of the laminar flow reactors in Chapter 8.

Chemical Reactor Design, Optimization, and Scaleup, Second Edition. By E. B. Nauman
Copyright © 2008 John Wiley & Sons, Inc.

9.1 PACKED-BED REACTORS

Packed-bed reactors are very widely used, particularly for solid-catalyzed heterogeneous reactions in which the packing serves as the catalyst. The velocity profile is quite complex. When measured at a small distance from the surface of the packing, velocities are found to be approximately uniform except near the tube wall. Random packing gives more void space and thus higher velocities near the wall. The velocity profile is almost invariably modeled as being flat. This does not mean that the packed bed is modeled as a PFR with negligible radial gradients in composition and temperature. Instead, radial mixing is limited in packed-bed reactors to the point that quite large differences in temperature and composition can develop across the tube. Radial concentration and temperature profiles are modeled using an effective radial diffusivity.

9.1.1 Incompressible Fluids

This section supposes the working fluid is a liquid or that the pressure drop is low enough that the change gas density can be ignored. The governing equation for mass transfer is

$$\bar{u}_s \frac{\partial a}{\partial z} = D_r \left[\frac{1}{r} \frac{\partial a}{\partial r} + \frac{\partial^2 a}{\partial r^2} \right] + \varepsilon \mathscr{R}_A \tag{9.1}$$

Here, D_r is an empirical, radial dispersion coefficient and ε is the void fraction. The units of diffusivity D_r are square meters per second. The major differences between this model and the convective diffusion equation used in Chapter 8 is that the velocity profile is now assumed to be flat and D_r is an empirically determined parameter instead of a molecular diffusivity. The value of D_r depends on factors such as the ratio of tube to packing diameters, the Reynolds number, and (at least at low Reynolds numbers) the physical properties of the fluid. Ordinarily, the same value for D_r is used for all reactants, finessing the problems of multicomponent diffusion and allowing the use of stoichiometry to eliminate Equation 9.1 for some of the components. Note that $\bar{u}_s$ in Equation 9.1 is the superficial velocity, this being the average velocity that would exist if the tube had no packing,

$$\bar{u}_s = \frac{Q}{A_c} = \frac{Q}{\pi R^2} \tag{9.2}$$

Note also that $\mathscr{R}_A$ is the reaction rate per fluid-phase volume and that $\varepsilon \mathscr{R}_A$ is the rate per total volume consisting of fluid plus packing. Except for the appearance of the void fraction ε, there is no overt sign that the reactor is a packed bed. The reaction model is ***pseudohomogeneous*** and ignores the details of interactions between the packing and the fluid. These interactions are lumped into D_r and $\mathscr{R}_A$. The concentration a is the fluid-phase concentration, and the rate expression $\mathscr{R}_A(a, b)$ is based on fluid-phase concentrations. This approach is satisfactory when the reaction is truly homogeneous and the packing merely occupies space without participating in the reaction. For

heterogeneous, solid-catalyzed reactions, the rate is presumably governed by surface concentrations, but the use of pseudohomogeneous kinetic expressions rather than surface concentration is nearly universal for the simple reason that the bulk concentrations can be measured while surface concentrations are not readily measurable. See Chapter 10 to understand the relationship between surface and bulk concentrations. We use Equation 9.1 for both homogeneous and heterogeneous reactions in packed beds. The boundary conditions associated with Equation 9.1 are the same as those for Equation 8.20: a prescribed inlet concentration profile $a_{\text{in}}(r)$ and zero gradients in concentration at the wall and centerline.

The temperature counterpart to Equation 9.1 is

$$\bar{u}_s \frac{\partial T}{\partial z} = E_r \left[\frac{1}{r} \frac{\partial T}{\partial r} + \frac{\partial^2 T}{\partial r^2} \right] - \frac{\varepsilon \, \mathbf{\Delta H_R} \, \mathscr{R}}{\rho C_P} \tag{9.3}$$

where E_r is an empirical radial dispersion coefficient for heat and where $\Delta H_R \mathscr{R}$ has the usual interpretation as a sum. Two of the three boundary conditions associated with Equation 9.3 are the ordinary ones of a prescribed inlet profile and a zero gradient at the centerline. The third boundary condition assumes that there is a film resistance on the inside of the tube so that the wall temperature and the fluid temperature at point R are different:

$$h_r[T_{\text{wall}} - T(R)] = \kappa_r \frac{dt}{dr} \quad \text{at } r = R \tag{9.4}$$

This boundary condition accounts for the especially high resistance to heat transfer that is observed near the wall in packed-bed reactors. Most of the heat transfer within a packed bed is by fluid convection in the axial direction and by conduction through the solid packing in the radial direction. The high void fraction near the wall lowers the effective conductivity in that region. As in Chapter 8, T_{wall} is the inside temperature of the tube, but this may now be significantly different than the fluid temperature $T(R)$ just a short distance in from the wall. The left-hand side of Equation 9.4 gives the rate of heat transfer across the thermal boundary layer. The right-hand side represents heat transfer into the bed by conduction, and κ_r is an effective thermal conductivity.

Equation 9.4 neglects thermal resistance in the wall or in the external heat transfer media. See Appendix 8.2 but note that there is an extra resistance term.

Packed-bed reactors can be adiabatic, and Equation 9.3 takes a particularly simple form with no radial gradients in temperature or composition arising when the feed is premixed. If the fluid is uniform in the radial direction when it enters the reactor, it remains uniform. Thus adiabatic packed beds are normally modeled as PFRs. This assumption may be overly optimistic in terms of yields and selectivities. The axial dispersion model in Section 9.2 adds a correction term to avoid undue optimism. Unmixed feed streams can also be treated provided the reactants enter the reactor in a manner that preserves radial symmetry.

It appears that the complete model for both mass and heat transfer contains four adjustable constants, D_r, E_r, h_r, and κ_r, but E_r and κ_r are constrained by the usual

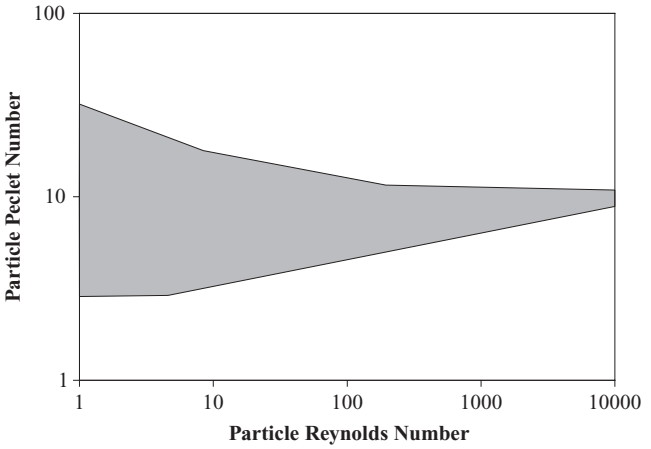

Figure 9.1 Existing data for the radial Peclet number in large-diameter packed beds, $(\mathbf{Pe})_\infty = (\bar{u}_s d_p / D_r)_\infty$ versus $\rho d_p \bar{u}_s / \mu$.

relationship between thermal diffusivity and thermal conductivity:

$$E_r = \frac{\kappa_r}{\rho C_P} \tag{9.5}$$

Thus there are only three independent parameters. We take these to be D_r, h_r, and κ_r. Imperfect but generally useful correlations for these parameters are available. For a summary of published correlations and references to the original literature see Froment and Bischoff (1990) and Dixon and Cresswell (1979).

Figure 9.1 shows a correlation for D_r. The correlating variable is the particle Reynolds number, $\rho d_p \bar{u}_s / \mu$, where d_p is the diameter of the packing. The correlated variable is a dimensionless group known as the ***Peclet number***, $(\mathbf{Pe})_\infty = (\bar{u}_s d_p / D_r)_\infty$, where the ∞ subscript denotes a tube with a large ratio of tube diameter to packing diameter, $d_t / d_p \gg 10$. Peclet numbers are commonly used in reactor design, and this chapter contains several varieties. All are dimensionless numbers formed by multiplying a velocity by a characteristic length and dividing by a diffusivity. The Peclet number used to correlate data for packed beds here in Section 9.1 uses the particle diameter d_p as the characteristic length and D_r as the diffusivity. The axial dispersion model discussed in Section 9.3 can also be applied to packed beds, but the diffusivity is an axial diffusivity.

Many practical designs use packing with a diameter that is an appreciable fraction of the tube diameter. The following relationship is used to correct D_r for large packing:

$$\frac{\bar{u}_s d_p}{D_r} = \frac{(\bar{u}_s d_p / D_r)_\infty}{1 + 19.4(d_p / d_t)^2} \tag{9.6}$$

Shell-and-tube reactors may have $d_t / d_p = 3$ or even smaller. A value of 3 is seen to decrease $\bar{u}_s d_p / D_r$ by a factor of about 3. Reducing the tube diameter from $10 d_p$

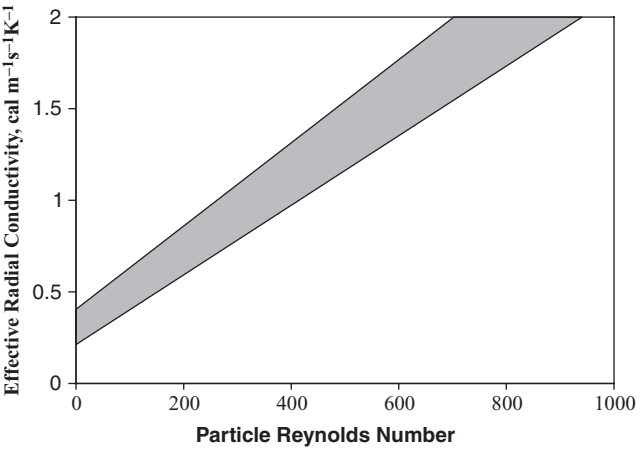

Figure 9.2 Existing data for the effective radial conductivity λ_r.

to $3d_p$ will increase D_r by a factor of about 10. Small tubes can thus have much better radial mixing than large tubes for two reasons: R is lower and D_r is higher.

The experimental results for $(\bar{u}d_p/D_r)_\infty$ in Figure 9.1 show a wide range of values at low Reynolds numbers. The physical properties of the fluid, and specifically its Schmidt number, $\mathbf{Sc} = \mu/(\rho\mathscr{D}_A)$, are important when the Reynolds number is low. Liquids will lie near the top of the range for $(\bar{u}_s d_p/D_r)_\infty$ and gases near the bottom. At high Reynolds numbers, hydrodynamics dominate, and the fluid properties become unimportant aside from their effect on the Reynolds number. This is a fairly general phenomenon and is discussed further in Section 9.2.

Figure 9.2 shows existing data for the effective thermal conductivity of packed beds. These data include both ceramic and metallic packings. More accurate results can be obtained from the semitheoretical predictions of Dixon and Cresswell (1979). Once κ_r is known, the wall heat transfer coefficient can be calculated from

$$\frac{h_r d_p}{\kappa_r} = \frac{3}{(\rho\bar{u}_s d_p/\mu)^{0.25}} \tag{9.7}$$

and E_r can be calculated from Equation 9.5. Thus all model parameters can be estimated. The estimates require knowledge of only two system variables: the packing Reynolds number and the ratio of packing to tube diameters.

We now turn to the numerical solution of Equations 9.1 and 9.3. The solutions are necessarily simultaneous. The numerical techniques of Chapter 8 can be used for the simultaneous solution of Equation 9.3 with as many versions of Equation 9.1 as are necessitated by the number of components. The method of lines is unchanged except for the wall boundary condition and a new stability criterion. The marching-ahead equations (e.g., Eq. 8.31) are unchanged, but the coefficients in Tables 8.2 and 8.3 now use $V(i) = \bar{u}_s$. When the velocity profile is flat, the stability criterion of Equation 8.36

still applies when D_r replaces $\mathscr{D}_A$ but is most demanding at the centerline,

$$\Delta z_{\max} = \frac{\Delta r^2 \bar{u}_s}{4E_r} \tag{9.8}$$

or, in dimensionless form,

$$\Delta \mathcal{Z}_{\max} = \Delta \tau^2 \frac{R^2}{4E_r t_s} \tag{9.9}$$

where $t_s = L/\bar{u}_s$. We have used E_r rather than D_r in the stability criterion because E_r will be larger. Note that t_s is not the residence time. Instead, $\bar{t} < t_s$ because the packing occupies volume that is inaccessible to (nonabsorbed) molecules. The fluid-phase residence time is $\bar{t} = \varepsilon t_s$.

Using a first-order approximation for the derivative in Equation 9.4, the wall boundary condition becomes

$$T(R, z) = \frac{h_r \, \Delta r \, T_{\text{wall}} + \kappa_r T(R - \Delta r, z)}{h_r \, \Delta r + \lambda_r}$$

A smoother approximation for the wall boundary condition is

$$T(R) = \frac{6 \, \Delta r \, h_r \, T_{\text{wall}} + 18\kappa_r T(R - \Delta r) - 9\kappa_r T(R - 2 \, \Delta r) + 2\kappa_r T(R - 3 \, \Delta r)}{6 \, \Delta r \, h_r + 11\kappa_r} \tag{9.10}$$

See Equation 8.58 for the case where there is external resistance to heat transfer. The computational templates for solving Equations 9.1 and 9.3 are similar to those used in Chapter 8. See Figure 8.2.

EXAMPLE 9.1

The catalytic oxidation of *ortho*-xylene to phthalic anhydride is conducted in a multitubular reactor using air at approximately atmospheric pressure as the oxidant. Side reactions including complete oxidation are important but will be ignored in this example. The *ortho*-xylene concentration is low, $a_{\text{in}} = 44$ g m^{-3} at standard temperature and pressure (STP) (0°C, 1 atm), to stay under the explosive limit. Due to the large excess of oxygen, the reaction is pseudo–first order in *ortho*-xylene concentration with $\ln(k) = 20.348 - 13{,}636/T$, where k is in s^{-1}. The tube is packed with 3-mm pellets consisting of V_2O_5 on potassium-promoted silica giving $\varepsilon = 0.6$. The tube has an ID of 50 mm, is 5 m long, and is operated with a superficial velocity of 1.0 m s^{-1}. The inlet conditions are 2.2 atm at 600 K. Ignore pressure drop down the tube. Use $\mu = 3 \times 10^{-5}$ Pa s, $C_P = 0.237$ cal g^{-1}K^{-1}, and $\Delta H = -307$ kcal mol^{-1}. Develop a model for the reactor that calculates radial and axial temperature and concentration profiles. Use the packed-tube model of Section 9.1 to estimate a combination of inlet and wall temperatures that will maximize conversion while keeping the centerline temperature below 700 K.

SOLUTION: It is first necessary to estimate the parameters D_r, E_r, h_r, and κ_r. The particle Reynolds number $\rho d_p \bar{u}_s / \mu$ is 130, and Figure 9.1 gives $(\bar{u}_s d_p / D_r)_\infty \approx 10$. A small correction for d_p/d_t using Equation 9.6 gives $\bar{u}_s d_p / D_r = 8$ so that $D_r = 3.8 \times 10^{-4}$m^2 s^{-1}. The ideal gas

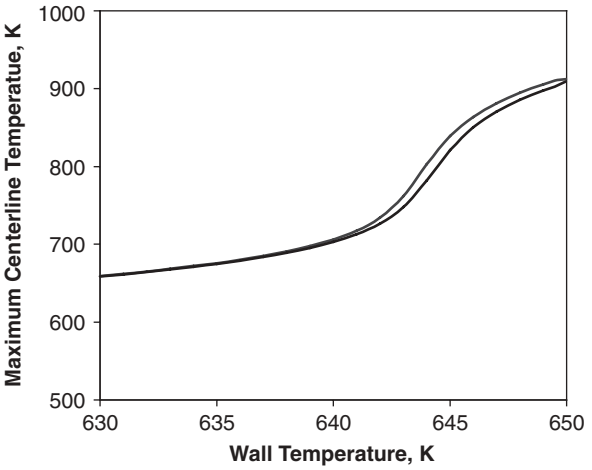

Figure 9.3 Maximum centerline temperature for a phthalic anhydride reactor for $T_{\text{wall}} = 640$ K and inlet temperatures of 500 and 600 K.

law gives $\rho = 1.29$ kg m^{-3} at the inlet conditions, Figure 9.2 gives $\kappa_r = 0.4$ cal m^{-1}s^{-1}K^{-1}, so that $E_r = \kappa_r /(\rho C_P) = 1.3\times\ 10^{-3}$ m^2 s^{-1}. Equation 9.7 gives $h_r d_p/\kappa_r = 0.89$ so that $h_r = 120$ cal m^{-2}s^{-1}.

Code for Example 9.1 calculates radial and axial temperature and concentration profiles. Results are shown in Figures 9.3 and 9.4. The illustrated program produces the curve for $T_{\text{in}} = 600$ K in Figure 9.4.

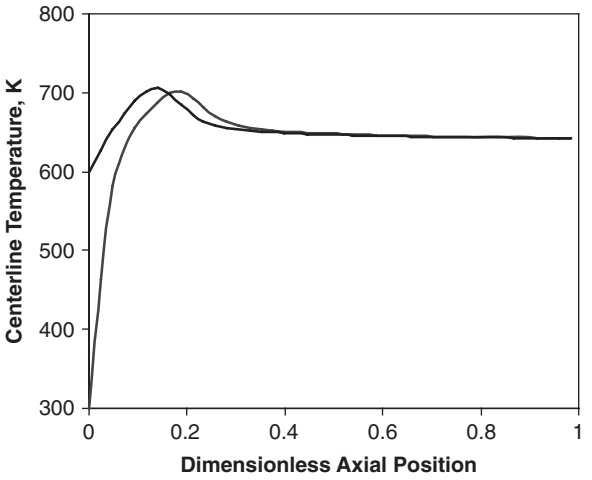

Figure 9.4 Centerline temperatures for a phthalic anhydride reactor for $T_{\text{wall}} = 640$ K and inlet temperatures of 300 and 600 K.

Code for Example 9.1

```
Sub Example9_1()

Dim a(32), T(32)
Dim anew(32), Tnew(32)

D = 0.00038          'Mass dispersion coefficient
E = 0.0013           'Temperature dispersion coefficient
R = 0.025            'Tube radius
ts = 5               'Gas phase residence time
heat = 307000 / 106 'Converts heat of reaction to mass units
hr = 120             'Heat transfer coefficient at the wall
rho = 1240           'Gas density at inlet conditions
Cp = 0.237           'Heat capacity of the gas
kappa = 0.4          'Thermal conductivity
delH = heat / rho / Cp  'Adiabatic temperature rise per gram reacted
Twall = 640
ain = 44
Tin = 600
II = 32              'Number of radial increments
dr = 1 / II
dzmax = R ^ 2 / 4 / E / ts * dr ^ 2
JJmin = 1 / dzmax
jj = JJmin + 1
dz = 1 / jj
ip = 999

GA = D * ts / R / R * dz / dr / dr
GT = E * ts / R / R * dz / dr / dr
C1 = 2 * hr * R * dr * Twall
C2 = 2 * hr * R * dr + 3 * kappa
For i = 0 To II
   a(i) = ain
   T(i) = Tin
Next i
```

```
For j = 1 To jj

k = EXP(20.348 - 13636 / T(0))  'Special equations at the centerline
anew(0) = (1 - 4 * GA) * a(0) + 4 * GA * a(1) - k * ts * dz * a(0)
Tnew(0) = (1 - 4 * GT) * T(0) + 4 * GT * T(1) + delH * k * ts * dz * a(0)
If Tnew(0) > Tmax Then Tmax = Tnew(0) 'Picks maximum centerline temperature

ip = ip + 1   'This code prints centerline temperatures at selected axial locations
If ip = 1000 Then
   ip = 1
   np = np + 1
   Cells(np, 1) = j / jj
   Cells(np, 3) = Tnew(0)
End If

For i = 1 To II - 1   'This code calculates non-centerline temperatures
   k = EXP(20.348 - 13636 / T(i))
   anew(i)=(1-2*GA)*a(i)+GA*(1+0.5/i)*a(i+1)+GA*(1-0.5/i)*a(i-1)-k*ts*dz*a(i)
   Tnew(i)=(1-2*GT)*T(i)+GT*(1+0.5/i)*T(i+1)+GT*(1-0.5/i)*T(i-1)+delH*k*ts*dz*a(i)
Next i

anew(II) = (4 * a(II - 1) - a(II - 2)) / 3
Tnew(II) = (C1 + 4 * kappa * T(II - 1) - kappa * T(II - 2)) / C2

For i = 0 To II
   a(i) = anew(i)
   T(i) = Tnew(i)
Next i

Next j

Cells(1, 4) = Tmax  'Maximum centerline temperature
Cells(2, 4) = a(0)  'Outlet concentration at the centerline
Cells(3, 4) = a(II) 'Outlet concentration at the wall

End Sub
```

The hot spot in a packed-bed reactor normally occurs at the centerline. Figure 9.3 shows the maximum centerline temperature as a function of wall temperature. The results are remarkably insensitive to the inlet temperature, and it is clear that T_{wall} rather than T_{in} must be used for control. Figure 9.4 shows the centerline temperature as a function of axial position. The maximum centerline temperature is insensitive to the inlet temperature, varying by about 3 K for inlet temperatures that vary by 200 K. The conversions for the two cases,$1 - a_{\text{out}}/a_{\text{in}}$, are essentially identical as well, 92.0 and 92.5%, respectively.

The reactor is sensitive to wall temperature. Figure 9.3 shows that a 10 K change from 640 K to 650 K causes the hot spot temperature to increase by about 200 K. This is a classic example of ***parametric sensitivity***, a phenomenon frequently observed with exothermic reactions in tubular reactors. The plant engineer should be very careful in making even modest changes in operating conditions else there be a thermal runaway. The equipment must be designed to contain or safely vent such a runaway, but a costly shutdown and ruined catalyst could still occur. From a modeling viewpoint, accurate calculations of thermal runaway, where $d^2T/d^2z > 0$, will require finer grids in the radial direction because of the large radial temperature gradients. There will also be large axial gradients, and physical stability of the computation may force the use of axial grids smaller than predicted by the stability criterion.

We also note that the simplified reaction in Example 9.1 has the form A $\rightarrow$ B but the real reaction is A $\rightarrow$ B $\rightarrow$ C, and the runaway would almost certainly provoke the undesired reaction B $\rightarrow$ C. To maximize output of product B, it is typically desired to operate just below the value of T_{wall} that would cause a runaway. As a practical matter, models using published parameter estimates are rarely accurate enough to allow a priori prediction of the best operating temperature. Instead, the models are used to guide experimentation and are tuned based on the experimental results.

Whenever there is an appreciable exotherm, scaleup of heterogeneous reactions is normally done in parallel using a shell-and-tube reactor. The pilot reactor may consist of a single tube with the same packing, the same tube diameter, and the same tube length as intended for the full-scale reactor. The scaled-up reactor consists of hundreds or even thousands of these tubes in parallel. Such scaleup appears trivial, but there are occasional problems. See Cybulski et al. (1997). One reason for the problems is that the packing is randomly dumped into the tubes, and random variations can lead to substantial differences in performance. This is a particular problem when d_t/d_p is small. One approach to minimizing the problem has been to use pilot reactors with at least three tubes in parallel. Thus the scaleup is based on an average of three tubes instead of the possibly atypical performance of a single tube.

There is a general trend toward ***structured packing*** and ***monoliths***, particularly in demanding applications such as automotive catalytic converters. In principle, the steady-state performance of such reactors can be modeled using Equations 9.1 and 9.3. However, the parameter estimates in Figures 9.1 and 9.2 and Equations 9.6 and 9.7 were developed for random packing, and even the boundary condition of Equation 9.4 may be inappropriate for monoliths or structured packing. Also, at least for automotive catalytic converters, the pressure drop and the transient behavior of the reactor during startup is of paramount importance. Transient terms $\partial a/\partial t$ and $\partial T/\partial t$ are easily added to Equations 9.1 and 9.3, but the results will mislead. These

terms account for inventory changes in the gas phase but not changes in the amount of material absorbed on the solid surface. The surface inventory may be substantially larger than the gas phase inventory, and a model that explicitly considers both phases and a mass transfer step between them is necessary for time-dependent calculations. This topic is briefly discussed in Section 10.6 and in Chapter 11.

9.1.2 Compressible Fluids in Packed Beds

A problem arises with the models of Section 9.1.1 when the density of the fluid changes appreciably with temperature or pressure. To understand the difficulty, refer to Section 3.1, where variable-density PFRs are treated. We consider only the case where the tube cross section is constant. A more general version of Equation 9.1 is

$$\frac{d\Phi_A}{dz} = \frac{d(u_s a)}{dz} = D_r \left[\frac{1}{r}\frac{\partial a}{\partial r} + \frac{\partial^2 a}{\partial r^2} \right] + \varepsilon \mathscr{R}_A \tag{9.11}$$

where $\Phi_A = u_s a$ is the molar flux. In Chapter 3, an equation of state was used to find u_s at the new axial location. For example, Equation 3.13 can be used:

$$\bar{u}_s = \frac{R_g T}{P} [\Phi_A + \Phi_B + \Phi_C + \cdots + \Phi_I] = \frac{R_g T}{P} \sum \Phi \tag{9.12}$$

The fact that T varies with radial position causes a dilemma. If T varies in the radial direction, so must u_s, and the assumption of a uniform velocity profile is violated. However, the radial variation in density depends on the ratio of wall and centerline temperatures, $T_{\text{wall}}(z)/T(0, z)$, and will typically be reasonably small. A suggested approximation is to use the mixing-cup average temperature in Equation 9.12. Similarly, mixing-cup averages are used to calculate the molar fluxes. This allows calculation of changes in $\bar{u}_s$ that result from pressure drop through the bed, axial changes in temperature, and changes in the number of moles due to reaction. These effects will typically cause much larger changes in u_s than the radial variations.

Corresponding to Equation 9.11 is a modified equation for temperature that is based on the enthalpy flux:

$$\frac{\partial \Phi_H}{\partial z} = \frac{\partial (u_s \rho C_P T)}{\partial z} = \rho C_P E_r \left[\frac{1}{r}\frac{\partial T}{\partial r} + \frac{\partial^2 T}{\partial r^2} \right] - \varepsilon \, \mathbf{\Delta H_R} \, \mathscr{R} \tag{9.13}$$

where $\Phi_H = u_s \rho C_P T$ is the enthalpy flux. Equations 9.11 and 9.13 are solved simultaneously. The methodology for gas phase PFRs is outlined in Section 3.11. Instead of Equation 3.24 we have

$$[\Phi_A(i)]_{\text{new}} = [\Phi_A(i)]_{\text{old}} + \Delta z \big[C_+(i) a_{i+1} + C_0(i) a_i + C_-(i) a_{i-1} + \varepsilon \mathscr{R}_A \big]_{\text{old}} \tag{9.14}$$

and for enthalpy

$$[\Phi_H(i)]_{\text{new}} = [\Phi_T(i)]_{\text{old}} + \Delta z \big[E_+(i) T_{i+1} + E_0(i) T_i + E_-(i) T_{i-1} + \varepsilon \, \mathbf{\Delta H_R} \, \mathscr{R} \big]_{\text{old}} \tag{9.15}$$

Here, the coefficients are the same as those in Tables 8.2 and 8.3 except that D_r replaces $\mathscr{D}_A$ and κ_r replaces κ. Note that $\bar{u}_s$has been incorporated into the molar enthalpy fluxes. The Ergun equation 3.21 for pressure drop in a packed bed is used to calculate P in Equation 9.12. The marching-ahead technique follows the computational scheme for gas phase PFRs in Section 3.1.1, but component concentrations and temperature depend on radial position, mixing-cup averages being used only in connection with Equation 9.12 and possibly with some correlation parameters if they vary significantly down the length of the reactor.

An important embellishment to the foregoing treatment of packed-bed reactors is to allow for temperature and concentration gradients within the catalyst pellets. Intrapellet diffusion of heat and mass is governed by differential equations that are about as complex as those governing the bulk properties of the bed. See Section 10.4.3. A set of simultaneous PDEs (ODEs if the pellets are spherical) must be solved to estimate the extent of reaction and conversion occurring within a single pellet. These local values are then substituted into Equations 9.1 and 9.3 so that we need to solve a set of PDEs that are embedded within a set of PDEs. The resulting system truly reflects the complexity of heterogeneous reactors, but practical solutions rarely go to this complexity. Most industrial reactors are designed on the basis of pseudohomogeneous models as in Equations 9.1 and 9.3, and the local catalyst behavior is described by the effectiveness factor defined in Chapter 10.

9.2 TURBULENCE

Turbulent flow reactors are modeled quite differently from laminar flow reactors. In a turbulent flow field, nonzero velocity components exist in all three coordinate directions, and they fluctuate with time. Statistical methods must be used to obtain time-average values for the various components and to characterize the instantaneous fluctuations about these averages. We divide the velocity into time-average and fluctuating parts:

$$\mathbf{v} = \mathbf{V} + \psi \tag{9.16}$$

where ψ represents the fluctuating velocity and $\mathbf{V}$ is the time-average value:

$$\mathbf{V} = \lim_{t\to\infty} \left(\frac{1}{t}\right) \int_0^t \mathbf{v}\ dt \tag{9.17}$$

The pressure at a point in the system behaves similarly with fluctuating and time-average parts.

Design of a turbulent reactor requires consideration of $\mathbf{V}$ and ψ since both will affect reaction yields. For turbulent flow in long, empty pipes, the time-average velocities in the radial and tangential directions are zero since there is no net flow in these directions. The axial velocity component will have a nonzero time-average profile $V_z(r)$. This profile is considerably flatter than the parabolic profile of laminar flow, but a profile nevertheless exists. The zero-slip boundary condition still applies and forces $V_z(R) = 0$. The time average-velocity changes very rapidly near the tube wall.

The region over which the change occurs is known as the ***hydrodynamic boundary layer.*** Sufficiently near the wall, flow in the boundary layer will be laminar, with attendant limitations on heat and mass transfer. Outside the boundary layer—meaning closer to the center of the tube—the time-average velocity profile is approximately flat. Flow in this region is known as ***core turbulence.*** Here, the fluctuating velocity components are high and give rapid rates of heat and mass transfer in the radial direction. Thus turbulent flow reactors are often modeled as having no composition or temperature gradients in the radial direction. This is not quite the same as assuming piston flow.

9.2.1 Turbulence Models

Axial Dispersion

The first and still most used model of a turbulent tubular reactor is the 100-year old axial dispersion model that is discussed at length in Section 9.3. The model assumes a uniform composition in the radial direction. It also assume $\mathbf{V} = \bar{u}$ and accounts for the fluctuating velocity components by an effective and empirical axial diffusivity.

Direct Numerical Simulation

The equations of motions (Navier–Stokes equations) are deterministic. This means that solutions with *exactly* the same boundary and initial conditions will produce the same results. In very small and simple geometries, it is possible to solve the equations of motions in a turbulent regime using a method similar to the false-transient method discussed in Chapter 16. Practical engineering problems require far too much computer storage and time for this to be feasible.

Reynolds Averaged Equations of Motion

The equations of motions can be time averaged by applying Equations like 9.17 to the various terms in the equations. This gives a set of equations in terms of the time-averaged components of $\mathbf{V}$ that could be solved were it not for the appearance of a term that retains the fluctuating components. Estimating this term, which has six components, is known as the ***Reynolds closure problem*** and is studied in graduate courses in fluid mechanics. The necessary models are complicated, semiempirical, and beyond the scope of this book. They provide the basis for CFD, and the semiempirical nature of the closure explains why CFD remains something of an art. One common model, the $k - \varepsilon$ model, obtains closure by adding two parameters to the calculations. One of the parameter, ε_P, is the power dissipation per unit volume and is often taken as a measure of the intensity of mixing.

9.2.2 Computational Fluid Dynamics

This book has emphasized simple solution techniques that are easy to understand and implement. Simple solutions are a luxury for the engineer, saving personal time at the expense of computer time and memory, which are comparatively cheap. They also allow direct and first-hand knowledge of exactly what the computer is doing. Unfortunately, some problems are too big for simple and easily understood methods to work. Most detailed modeling of turbulence falls into this category and is the domain of CFD.

Computational fluid mechanics has had some notable successes in duplicating experimental results for turbulent reactors, both tubes and tanks. As one example, one simulation closely agreed with experiments for the yield of a Bourne reaction in a fed-batch laboratory reactor that was stirred by a half-moon agitator:

$$\begin{aligned} \mathrm{A} + \mathrm{B} &\xrightarrow{k_\mathrm{I}} \mathrm{R} \\ \mathrm{B} + \mathrm{R} &\xrightarrow{k_\mathrm{II}} \mathrm{S} \qquad k_I \gg k_\mathrm{II} \end{aligned}$$

However, the computation required many days, its details have not been published, and there was no test for convergence. It seems that most CFD studies use the finest grid that they can afford in terms of memory and computing time and then hope for the best. Starting with a coarser grid and then going to the fine grid would allow more faith in the results. This is rarely done, perhaps because the results would be significantly different for the two grid sizes. Note that "convergence" means convergence with respect to grid size. At a given grid size, the CFD programs typically use an iterative solution technique that must also converge.

The CFD experts recognize the need to verify and validate the codes. In this context, ***verification*** refers to proof that the code is actually solving the mathematical equations that constitute the model. Have the computations converged with respect to solution technique and grid size? ***Validation*** asks whether the properly solved equations reflect physical reality. It is fair to say that CFD has not yet emerged as a reliable means for a priori design. Its use to help understand and possibly optimize existing designs can be justified, although its cost in terms of engineering time and even computer time is high. The user must be extensively trained and even then will not know the details of the computation. Indeed, commercial packages have become so large that it is doubtful that any single person understands everything that is inside them.

Large computer models becoming de facto black boxes is an emerging problem that is not confined to CFD. Within chemical reaction engineering, mistakes can be minimized by always comparing the results to those of simple models and by remembering that experiments are the final proof.

9.3 AXIAL DISPERSION MODEL

Suppose a small, sharp pulse of an ideal, nonreactive tracer is injected into a tube at the centerline. An ***ideal tracer*** is identical to the bulk fluid in terms of flow properties but is distinguishable in some nonflow aspect that is detectable with suitable

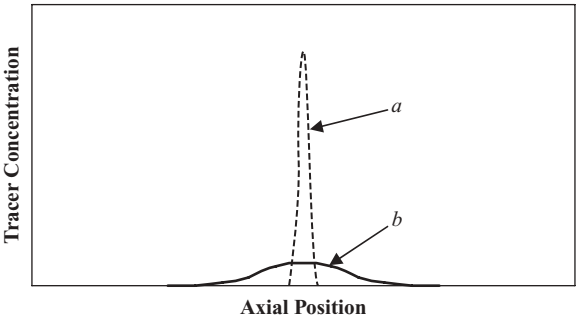

Figure 9.5 Spread of tracer concentration in a highly turbulent reactor: (*a*) immediately after injection; (*b*) at a downstream location.

instrumentation. Typical tracers are dyes, radioisotopes, and salt solutions. Figure 9.5*a* illustrates the pulse shortly after injection. Call this time $t = 0$. The first and most obvious thing is that the pulse moves downstream at a rate equal to the time-average axial velocity $\bar{u}$. In a stationary coordinate system (called an ***Eulerian*** coordinate system), the injected pulse just disappears downstream. Shift to a moving (***Lagrangian***) coordinate system that translates down the tube with the same velocity as the fluid. In this coordinate system, the center of the injected pulse remains stationary, but individual tracer particles spread out due to the combined effects of molecular diffusion and the fluctuating velocity components. If the time-average velocity profile were truly flat, the tracer concentration would soon become uniform in the radial and tangential directions. Figure 9.5*b* illustrates the pulse at location z and time $t = z/\bar{u}$. (Figure 9.5 actually shows mixing-cup average concentrations so that the total area under the injected pulse remains constant even though the tracer has spread in the radial direction as well as in the axial direction.) The spread of tracer is due to ***axial mixing***. Axial mixing is disallowed in the piston flow model and is usually neglected in laminar flow models. The models of Chapter 8 neglected molecular diffusion in the axial direction because axial concentration and temperature gradients are so much smaller than radial gradients. In turbulent flow, eddy diffusion due to the fluctuating velocity components dominates molecular diffusion, and the effective diffusivity is enhanced to the point of virtually eliminating radial gradients and of causing possibly significant amounts of mixing in the axial direction. We seek a simple correction to piston flow that will account for axial mixing and other small departures from ideality. A major use of the model is for isothermal reactions in turbulent, pipeline flows. However, the model that emerges is surprisingly versatile. It can be used for isothermal reactions in open tubes, packed beds whether laminar or turbulent, and motionless mixers. It can also be extended to nonisothermal reactions.

A simple correction to piston flow is to add an axial diffusion term. The resulting equation remains an ODE and is known as the axial dispersion model

$$\bar{u}\frac{da}{dz} = D\frac{d^2a}{dz^2} + \mathscr{R}_A \tag{9.18}$$

or, in dimensionless form,

$$\frac{da}{d\mathcal{z}} = \frac{1}{\mathbf{Pe}}\frac{d^2a}{d\mathcal{z}^2} + \mathcal{R}_A\bar{t} \tag{9.19}$$

The parameter D is known as the ***axial dispersion coefficient***, and the dimensionless number $\mathbf{Pe} = \bar{u}L/D$ is the axial Peclet number. Caution is needed at this point. The **Pe** is different than the Peclet number $\bar{u}_s d_p/D_r$ used in Section 9.1. It is also different than the Peclet numbers $\bar{u}d_t/D$ and $\bar{u}_s d_p/D$ used for the correlations in Figures 9.7 and 9.8 (see below).

At high Reynolds numbers, D depends solely on fluctuating velocities in the axial direction. These fluctuating axial velocities cause mixing by a semirandom process that is conceptually similar to molecular diffusion except that the fluid elements being mixed are much larger than molecules. The same value for D is used for each component in a multicomponent system.

At lower Reynolds numbers, the axial velocity profile will not be flat, and it might seem that another correction must be added to Equation 9.18. It turns out, however, that Equation 9.18 remains a good model for real turbulent reactors (and even some laminar ones) given suitable values for D and sufficiently long reactors. The model lumps the combined effects of fluctuating velocity components, nonflat velocity profiles, and molecular diffusion into the single parameter D.

At a close level of scrutiny, real systems behave differently than predicted by the axial dispersion model, but the model is useful for many purposes. Values for **Pe** can be determined experimentally using transient experiments with nonreactive tracers. Specifically, the spread in concentration of an injected pulse is used to determine **Pe.** See Figure 9.5 and the discussion on the axial dispersion model in Section 15.2.2. A correlation for D that combines experimental and theoretical results is shown in Figure 9.6. The dimensionless number $\bar{u}d_t/D$ depends on the Reynolds number and

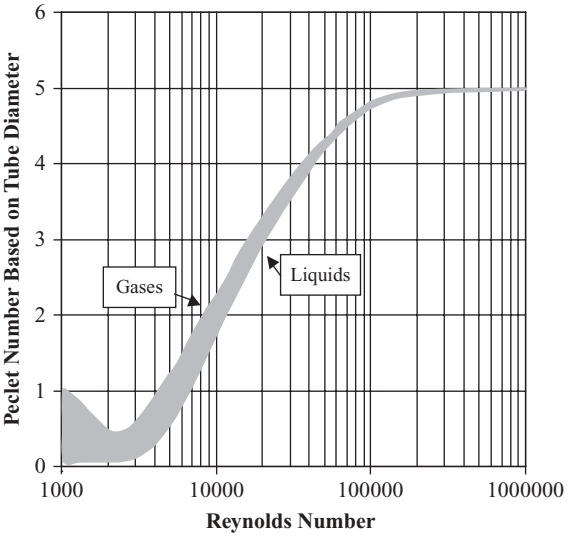

Figure 9.6 Peclet number $\mathbf{Pe} = \bar{u}d_t/D$ versus Reynolds number $\mathbf{Re} = \rho d_t \bar{u}/\mu$ for flow in open tube.

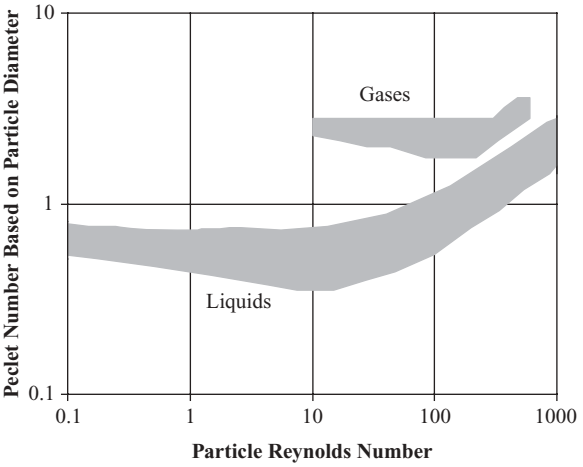

Figure 9.7 Peclet number $\mathbf{Pe} = \bar{u}_s d_p / D$ versus Reynolds number $\mathbf{Re} = \rho d_p \bar{u}_s / \mu$ for packed beds.

on molecular diffusivity as measured by the Schmidt number $\mathbf{Sc} = \mu/(\rho \mathscr{D}_A)$, but the dependence on **Sc** is weak for $\mathbf{Re} > 5000$. As indicated in Figure 9.6, data for gases will lie near the top of the range and data for liquids will lie near the bottom. For high **Re**, $\bar{u} d_t / D = 5$ is a reasonable choice.

The model can also be applied to packed beds. Figure 9.7 illustrates the range of existing data.

9.3.1 Danckwerts Boundary Conditions

The axial dispersion model has a long and honored history within chemical engineering. It was first used by Langmuir (1908), who also used the correct boundary conditions. These boundary conditions are subtle. Langmuir's work was forgotten, and it was many years before the correct boundary conditions were rediscovered by Danckwerts (1953).

The boundary conditions normally associated with Equation 9.18 are known as the Danckwerts, or ***closed***, boundary conditions. They are obtained from mass balances across the inlet and outlet of the reactor. We suppose that the piping to and from the reactor is small and has a high **Re**. Thus, if we were to apply the axial dispersion model to the inlet and outlet streams, we would find $D_{\text{in}} = D_{\text{out}} = 0$, which is the definition of a closed system. See Figure 9.8. The flow in the inlet

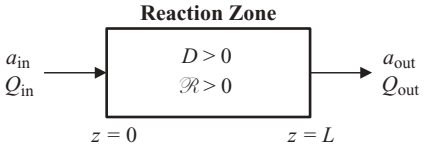

Figure 9.8 Axial dispersion model applied to closed system.

pipe is due solely to convection and has magnitude $Q_{\text{in}}a_{\text{in}}$. The flow just inside the reactor at location $z = 0+$ has two components. One component, $Q_{\text{in}}a(0+)$, is due to convection. The other component, $-DA_c[da/dz]_{0+}$, is due to (eddy) diffusion from the relatively high concentrations at the inlet toward the lower concentrations within the reactor. The inflow to the plane at $z = 0$ must be matched by material leaving the plane at $z = 0+$ since no reaction occurs in a region that has no volume. Thus, at steady state,

$$Q_{\text{in}}\, a_{\text{in}} = Q_{\text{in}}\, a(0+) - DA_c \left[\frac{da}{dz}\right]_{0+} \quad a_{\text{in}} = a(0+) - \frac{1}{\mathbf{Pe}} \left[\frac{da}{d\not{z}}\right]_{0+} \tag{9.20}$$

is the inlet boundary condition for a closed system. This inlet boundary condition is really quite marvelous. Equation 9.20 predicts a discontinuity in concentration at the inlet to the reactor so that $a_{\text{in}} \neq a(0+)$ if $D > 0$. This may seem counterintuitive until the behavior of a CSTR is recalled. At the inlet to a CSTR, the concentration goes immediately from a_{in} to a_{out}. The axial dispersion model behaves as a CSTR in the limit as $D \to \infty$. It behaves as a PFR, which has no inlet discontinuity, when $D = 0$. For intermediate values of D, an inlet discontinuity in concentration exists but is intermediate in size. The concentration $a(0+)$ results from backmixing between entering material and material downstream in the reactor. For a reactant, $a(0+) < a_{\text{in}}$.

The outlet boundary condition is just

$$\left[\frac{da}{dz}\right]_L = 0 \qquad \text{or} \qquad \left[\frac{da}{d\not{z}}\right]_1 = 0 \tag{9.21}$$

This result assumes concentration to be continuous at $z = L$, a fact that is obvious. Obvious? Langmuir was a Nobel laureate and Danckwerts is regarded by many as the father of chemical engineering science.

The zero-slope condition may seem counterintuitive. CSTRs behave in this way, but PFRs do not. The reasonableness of the assumption can be verified by a limiting process on a system with an open outlet as discussed in Example 9.2. The Danckwerts boundary conditions are further explored in Example 9.2, which treats ***open*** systems. The end result is that the boundary conditions are somewhat unimportant in the sense that closed and open systems behave identically as reactors.

9.3.2 First-Order Reactions

Equation 9.18 is a linear, second-order ODE with constant coefficients. An analytical solution is possible when the reaction is first order. The general solution to Equation 9.18 with $\mathscr{R}_A = -ka$ is

$$a(z) = C_1 \exp\left[(1+p)\frac{\mathbf{Pe}}{2}\frac{z}{L}\right] + C_2 \exp\left[(1-p)\frac{\mathbf{Pe}}{2}\frac{z}{L}\right] \tag{9.22}$$

where $\mathbf{Pe} = \bar{u}L/D$ and

$$p = \sqrt{1 + \frac{4k\bar{t}}{\mathbf{Pe}}} \tag{9.23}$$

The constants C_1 and C_2 are evaluated using the boundary conditions, Equations 9.20 and 9.21. The outlet concentration is found by setting $z = L$**.** Algebra gives

$$\frac{a_{\text{out}}}{a_{\text{in}}} = \frac{4p \exp(\mathbf{Pe}/2)}{(1+p)^2 \exp[(p\,\mathbf{Pe})/2] - (1-p)^2 \exp[-(p\,\mathbf{Pe})/2]} \tag{9.24}$$

Conversions predicted from Equation 9.24 depend only on the values of $k\bar{t}$ and **Pe**. The predicted conversions are smaller than those for piston flow but larger than those for perfect mixing. In fact,

$$\lim_{\mathbf{Pe}\to\infty} \frac{a_{\text{out}}}{a_{\text{in}}} = e^{-k\bar{t}} \tag{9.25}$$

so that the model approaches piston flow in the limit of high Peclet number (low D). Also,

$$\lim_{\mathbf{Pe}\to 0} \frac{a_{\text{out}}}{a_{\text{in}}} = \frac{1}{1+k\bar{t}} \tag{9.26}$$

so that the axial dispersion model approaches perfect mixing in the limit of low Peclet number (high D)**.** The model is thus universal in the sense that it spans the expected range of performance for well-designed real reactors. However, it should not be used or be used with caution for **Pe** below about 8. At low **Pe**, the physics of the model becomes unrealistic except for the short, micron-scale reactors studied in Chapter 16.

EXAMPLE 9.2

Equation 9.24 was derived for a closed system. Repeat the derivation for the **open** system with $D_{\text{in}} > 0$ and $D_{\text{out}} > 0$ shown in Figure 9.9.

SOLUTION: An open system extends from $-\infty$ to $+\infty$ as shown in Figure 9.9. The key to solving this problem is to note that the general solution, Equation 9.22, applies to each of the above regions, inlet, reaction zone, and outlet. If $k = 0$, then $p = 0$. Each of the equations contains two constants of integration. Thus a total of six boundary conditions are required:

1. The far inlet boundary condition: $a = a_{\text{in}}$ at $z = -\infty$
2. Continuity of concentration at $z = 0$: $a(0-) = a(0+)$

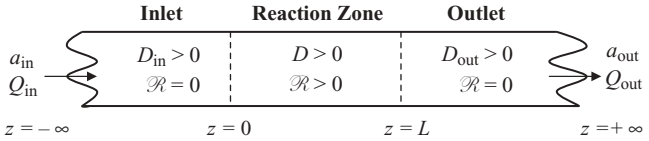

Figure 9.9 Axial dispersion model applied to open system.

3. Continuity of flux at $z = 0$: $Q_{\text{in}}\, a(0-) - A_c\, [da/dz]_{0-} = Q_{\text{in}}\, a(0+) - A_c\, [da/dz]_{0+}$
4. Continuity of concentration at $z = L$: $a(L-) = a(L+)$
5. Continuity of flux at $z = L$: $Q_{\text{in}}\, a(L-) - A_c [da/dz]_{L-} = Q_{\text{in}}\, a(L+) - A_c [da/dz]_{L+}$
6. The far outlet boundary condition: $a = a_{\text{out}}$ at $z = +\infty$

A substantial investment in algebra is needed to evaluate the six constants, but the result is remarkable. The exit concentration from an reactor is identical to that from a closed reactor provided they have the same values for D and $k\bar{t}$. Equation 9.24 works for both cases and is independent of D_{in} and D_{out}! The physical basis for this result depends on the concentration profile $a(z)$ for $z < 0$. When $D_{\text{in}} = 0$, as for a closed inlet, the concentration is constant at a_{in} until $z = 0+$, when it suddenly plunges to $a(0+)$. When $D_{\text{in}} > 0$, as for an open inlet, the concentration begins with a_{in} at $z = -\infty$ and gradually declines until it reaches exactly the same concentration, $a(0+)$, at exactly the same location, $z = 0+$. Within the reactor and at the outlet, the open and closed systems have the same concentration profile. The open and closed systems satisfy the outlet boundary condition, Equation 9.21.

9.3.3 Utility of the Axial Dispersion Model

Chapters 8 and Section 9.1 gave preferred models for laminar flow and packed-bed reactors. The axial dispersion model can also be used for these reactors but is generally not the preferred model. Proper roles for the axial dispersion model are the following.

Isothermal, Turbulent Pipeline Flows

Turbulent pipeline flow is the original application of the axial dispersion model. For most kinetic schemes, piston flow predicts the highest possible conversion and selectivity. The axial dispersion model provides a less optimistic estimate, but the difference between the piston flow and axial dispersion models is usually small. For an open tube in well-developed turbulent flow, the assumption of piston flow is normally quite accurate unless the reaction is driven to near completion.

Isothermal Packed Beds

A packed reactor has a velocity profile that is nearly flat, and for the usual case of uniform a_{in}, no concentration gradients will arise unless there is a radial temperature gradient. If there is no reaction exotherm (and if $T_{\text{in}} = T_{\text{wall}}$), the model of Section 9.1 degenerates to piston flow. This is overly optimistic for a real packed bed, and the axial dispersion model provides a correction. The correction will usually be small. Note that $\bar{u}$ should be replaced by $\bar{u}_s$ and that the void fraction ε should be inserted before the reaction term (e.g., $k\bar{t}$ becomes $\varepsilon k\bar{t}$ for reactions in a packed bed). Figure 9.7 gives $D\varepsilon/(\bar{u}_s d_p) \approx 2$ for moderate values of the particle Reynolds number. This gives $\mathbf{Pe} = \varepsilon L/(2d_p)$ or $\mathbf{Pe} \approx 300$ for the packed tube of Example 9.1. Again, the assumption of piston flow is quite reasonable unless the reaction goes to near completion. It should be emphasized that the assumption of an isothermal reaction should be based on a small heat of reaction, for example, as in transesterifcation, where the energy of a

bond broken is approximately equal to that of a bond made, or when inerts are present in large quantities. Calculate the adiabatic temperature rise. Sooner or later it will emerge on scaleup.

Adiabatic Reactors

Like isothermal reactors, adiabatic reactors with a flat velocity profile will have no radial gradients in temperature or composition. There are axial gradients, and the axial dispersion model, including its extension to temperature in Section 9.4, can account for axial mixing. As a practical matter, it is difficult to build a small adiabatic reactor. Wall temperatures must be controlled to simulate the adiabatic temperature profile in the reactor, and guard heaters may be needed at the inlet and outlet to avoid losses by radiation. Even so, it is likely that uncertainties in the temperature profile will mask the relative small effects of axial dispersion.

Laminar Pipeline Flows

The axial dispersion model can be used for laminar flow reactors if the reactor is so long that $\mathscr{D}_A\bar{t}/R^2 > 0.125$. With this high value for $\mathscr{D}_A\bar{t}/R^2$, the initial radial position of a molecule becomes unimportant. It diffuses across the tube and samples many streamlines, some with high velocity and some with low velocity, during its stay in the reactor. It will travel with an average velocity near $\bar{u}$ and will emerge from the long reactor with a residence time close to $\bar{t}$. The axial dispersion model is a reasonable approximation for overall dispersion in a long laminar flow reactor. The appropriate value for D in the laminar region is known from theory,

$$D = \mathscr{D}_A + \frac{\bar{u}^2 R^2}{48\mathscr{D}_A} \tag{9.27}$$

As seen in Chapter 8, the stability criterion becomes quite demanding when $\mathscr{D}_A\bar{t}/R^2$ is large. The axial dispersion model may then be a useful alternative to solving Equation 8.20.

Motionless Mixers

These interesting devices consist of a tube or duct within which static elements are installed to promote cross-channel flow. See Figure 8.5 and Section 8.7.2. Static mixers are quite effective in promoting radial mixing in laminar flow, but their geometry is too complex to allow solution of the convective diffusion equation on a routine basis. A review article by Thakur et al. (2003) provides some empirical correlations. The lack of published data prevents a priori designs that utilize static mixers, but the axial dispersion model is a reasonable way to correlate pilot plant data. Chapter 15 shows how **Pe** can be measured using inert tracers.

Static mixers are typically less effective in turbulent flow than an open tube when the comparison is made on the basis of constant pressure drop or capital cost.

Whether laminar or turbulent, design correlations are generally lacking or else are vendor proprietary and have rarely been subject to peer review

9.3.4 Nonisothermal Axial Dispersion

The axial dispersion model is readily extended to nonisothermal reactors. The turbulent mixing that leads to flat concentration profiles will also give flat temperature profiles. An expression for the axial dispersion of heat can be written in direct analogy to Equation 9.18:

$$\bar{u}\frac{dT}{dz} = E\frac{d^2T}{dz^2} - \frac{2U}{\rho C_P}\frac{(T - T_{extl})}{R} - \frac{\Delta \mathbf{H_R}\,\mathscr{R}}{\rho C_P} \tag{9.28}$$

where E is the axial dispersion coefficient for heat and where the usual summation conventions applies to $\Delta H_R \mathscr{R}$. For well-developed turbulence, the thermal Peclet number $(\mathbf{Pe})_{\text{thermal}} = \bar{u}L/E$ should be smaller than the mass Peclet number $\mathbf{Pe} = \bar{u}L/D$ but similar in magnitude**.** At lower Reynolds numbers, one would expect $\bar{u}L/E$ to depend on a thermal Schmidt number $(\mathbf{Sc})_{\text{thermal}} = \mu/\rho\alpha_T = \mu C_P/\kappa$, which is more commonly called the Prandtl number. The inside heat transfer coefficient h can be estimated from standard correlations such as Equation 5.38.

The boundary conditions associated with Equation 9.28 are of the Danckwerts type:

$$Q_{in}T_{in} = Q_{in}T(0+) - EA_c\left[\frac{dT}{dz}\right]_{0+} \tag{9.29}$$

$$\left[\frac{dT}{dz}\right]_L = 0 \tag{9.30}$$

Correlations for E are not widely available. The more accurate model given in Section 9.1 is preferred for nonisothermal reactions in packed beds. However, as discussed previously, this model degenerates to piston flow for an adiabatic reaction. The nonisothermal axial dispersion model is an alternative design methodology available for adiabatic reactions in packed beds and for nonisothermal reactions in turbulent pipeline flows. The fact that $E > D$ provides some basis for estimating E. Recognize that the axial dispersion model is a correction to what would otherwise be treated as piston flow. Thus, even setting $E = D$ should improve the accuracy of the predictions.

Only numerical solutions are possible when Equation 9.28 is solved simultaneously with Equation 9.18. This is true even for first-order reactions because of the intractable nonlinearity of the Arrhenius temperature dependence.

9.3.5 Shooting Solutions to Two-Point Boundary Value Problems

The numerical solution of Equations 9.18 and 9.28 is more complicated than the solution of the first-order ODEs that govern piston flow or of the first-order ODEs

that result from applying the method of lines to PDEs. The reason for the complication is the second derivative in the axial direction, d^2a/dz^2.

Apply finite-difference approximations to Equation 9.19 using a backward difference for $da/d\mathcal{z}$ and a central difference for $d^2a/d\mathcal{z}^2$. The result is

$$a_{j+1} = (2 + \mathbf{Pe}\ \Delta\mathcal{z})\,a_j - (1 + \mathbf{Pe}\ \Delta\mathcal{z})a_{j-1} - \mathbf{Pe}\ \mathscr{R}_A\bar{t}\,\Delta\mathcal{z}^2 \tag{9.31}$$

Thus the value for the next, $j + 1$, point requires knowledge of two previous points, j and $j - 1$. To calculate a_2 we need to know both a_1 and a_0. The boundary conditions, Equations 9.20 and 9.21, give neither of these directly. In finite-difference form, the inlet boundary condition is

$$a_1 = (1 + \mathbf{Pe}\ \Delta\mathcal{z})a_0 - \mathbf{Pe}\ \Delta\mathcal{z}\,a_{\text{in}} \tag{9.32}$$

where a_{in} is known. Thus if we guess a_0, we can calculate a_1 using Equation 9.32 and can then use Equation 9.31 to march down the tube. The outlet boundary condition is

$$a_{J+1} = a_J \tag{9.33}$$

where J is the number of steps in the axial direction. If Equation 9.33 is satisfied, the correct value for a_0 was guessed. Otherwise, guess a new a_0. This approach is known as forward shooting.

The forward-shooting method seems straightforward but is troublesome to use. What we have done is to convert a two-point boundary value problem into an easier-to-solve initial-value problem. Unfortunately, the conversion gives a numerical computation that is ***ill conditioned***. Extreme precision is needed at the inlet of the tube to get reasonable accuracy at the outlet. The phenomenon is akin to problems that arise in the numerical inversion of matrices and Laplace transforms.

EXAMPLE 9.3

Use forward shooting to solve Equation 9.19 for a first-order reaction with $\mathbf{Pe} = 16$ and $k\bar{t} = 2$. Compare the result to the analytical solution, Equation 9.24.

SOLUTION: Set $\Delta\mathcal{z} = \frac{1}{32}$ so that $\mathbf{Pe}\ \Delta\mathcal{z} = 0.5$ and $\mathbf{Pe}\ k\bar{t}\,\Delta\mathcal{z}^2 = 0.03125$. Set $a_{\text{in}} = 1$ so that dimensionless or normalized concentrations are determined. Equation 9.31 becomes

$$a_{j+1} = 2.53125a_j - 1.5a_{j-1}$$

The computation is started using Equation 9.32,

$$a_1 = 1.5a_0 - 0.5$$

Results for a succession of guesses for a_0 are as follows:

a_0	a_{32}	a_{33}
0.90342	−20.8	−33.0
0.90343	0.93	1.37
0.903429	−1.24	−2.06
0.9034296	0.0630	0.0004
0.90342965	0.1715	0.1723
0.903429649	0.1693	0.1689
0.9034296493	0.1699	0.1699

The answer by the shooting method is $a_{\text{out}} = 0.17$. The analytical result is $a_{\text{out}} = 0.1640$. Note that the shooting method requires extreme precision on guesses for a_0 to obtain an answer of limited accuracy for a_{out}. Better accuracy with the numerical approach can be achieved with a smaller step size or a more sophisticated integration routine, but better integration gives a more accurate value only after the right guess for a_0 is made. Smaller step sizes do not eliminate the ill conditioning inherent in forward shooting.

The best solution to such numerical difficulties is to change methods. Integration in the reverse direction eliminates most of the difficulty. Go back to Equation 9.19. Continue to use a second-order central-difference approximation for $d^2a/d\mathcal{z}^2$ but now use a first-order forward-difference approximation for $da/d\mathcal{z}$. Solve the resulting finite-difference equation for a_{j-1}:

$$a_{j-1} = (2 - \mathbf{Pe}\,\Delta\mathcal{z})a_j - (1 - \mathbf{Pe}\,\Delta\mathcal{z})a_{j+1} - \mathbf{Pe}\,\mathcal{R}_A\bar{t}\,\Delta\mathcal{z}^2 \tag{9.34}$$

The marching-ahead equation becomes a marching-backward equation. The method is called ***reverse shooting***. The procedure is to guess $a_J = a_{\text{out}}$ and then to set $a_{J-1} = a_J$ in order to satisfy the zero-slope boundary condition at the outlet. The index j in Equation 9.34 begins at $J-2$ and is decremented by 1 until $j = 0$ is reached. The reaction rate continues to be evaluated at the central, jth point. The test condition is whether a_{in} is correct when calculated using the inlet boundary condition

$$a_{\text{in}} = a_0 + \frac{a_0 - a_1}{\mathbf{Pe}\Delta\mathcal{z}} \tag{9.35}$$

EXAMPLE 9.4 ***Repeat Example 9.3 using reverse shooting.***

SOLUTION: With $J = 32$, $\mathbf{Pe} = 16$, and $k\bar{t} = 2$, Equation 9.34 gives

$$a_{j-1} = 1.53125a_j - 0.5a_{j+1}$$

Guess $a_{32} = a_{\text{out}}$ and then set $a_{31} = a_{32}$. Calculate a_j down to $j = 0$. Then compare a_{in} to the value calculated using Equation 9.35, which for this example is just $a_{\text{in}} = 3a_0 - 2a_1$. Some results are as follows:

a_{32}	a_{in}
0.16	1.0073
0.15	0.9444
0.159	1.0010
0.158	0.9947

Thus we obtain $a_{\text{out}} = 0.159$ for a step size of $\Delta z = 0.03125$. The ill-conditioning problem has been solved, but the solution remains inaccurate due to the simple integration scheme and large step size.

The next example illustrates the use of reverse shooting in solving a problem in nonisothermal axial dispersion and shows how Runge–Kutta integration can be applied to second-order ODEs.

EXAMPLE 9.5

Assume a first-order reaction and compare the nonisothermal axial dispersion model to piston flow. The reactor is turbulent with **Re** = 10,000. Pick the reaction parameters so that the reactor is near a region of thermal runaway.

SOLUTION: The axial dispersion model requires the simultaneous solution of Equations 9.18 and 9.28. Piston flow is governed by the same equations except that $D = E = 0$. The following parameter values give rise to a near runaway:

$$
\begin{aligned}
k_0\bar{t} &= 2.0 \times 10^{11} \quad \text{(dimensionless)} \\
T_{\text{act}} &= 10,000\,\text{K} \\
\frac{2h\bar{t}}{\rho C_P R} &= 10 \quad \text{(dimensionless)} \\
-\frac{\Delta H_R a_{\text{in}}}{\rho C_P} &= 200\,\text{K} \\
T_{\text{in}} &= T_{\text{wall}} = 374,\,\text{K}
\end{aligned}
$$

These parameters are enough to run the piston flow case. The axial dispersion model needs dispersion coefficients. Plausible values at **Re** = 10,000 are

$$
\frac{D}{\bar{u}d_t} = 0.45 \qquad \frac{D}{\bar{u}L} = 4.5
$$

$$
\frac{E}{\bar{u}d_t} = 0.60 \qquad \frac{E}{\bar{u}L} = 6.0
$$

where we have assumed a low aspect ratio, $L/d_t = 10$, to magnify the effects of axial dispersion.

When the axial dispersion terms are present, $D > 0$ and $E > 0$, Equations 9.18 and 9.28 are second order. We will use reverse shooting and Runge–Kutta integration. The Runge–Kutta scheme (Appendix 2.1) applies only to first-order ODEs. To use it here, Equations 9.18 and 9.28 must be converted to an equivalent set of first-order ODEs. This can be done by defining

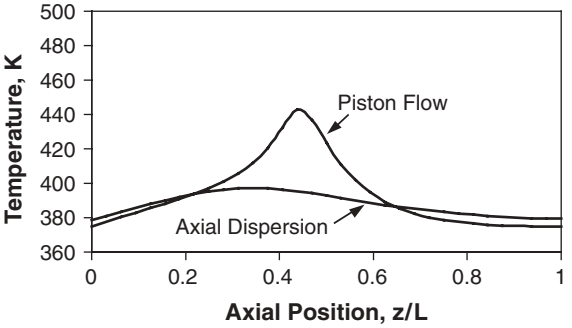

Figure 9.10 Comparison of piston flow and axial dispersion models at near runaway condition.

two auxiliary variables:

$$a' = \frac{da}{d\mathcal{Z}} \qquad T' = \frac{dT}{d\mathcal{Z}}$$

Then Equations 9.18 and 9.28 can be written as a set of four first-order ODEs with boundary conditions as indicated below:

$$\frac{da}{d\mathcal{Z}} = a' \qquad a = a_{\text{out}} \quad \text{at } \mathcal{Z} = 1$$

$$\frac{da'}{d\mathcal{Z}} = \frac{a' + k_0\bar{t}\,\exp\left(-T_{\text{act}}/T\right)a}{(D/\bar{u}L)} \qquad a' = 0 \quad \text{at } \mathcal{Z} = 1$$

$$\frac{da}{d\mathcal{Z}} = T' \qquad T = T_{\text{out}} \quad \text{at } \mathcal{Z} = 1$$

$$\frac{dT'}{d\mathcal{Z}} = \frac{T' + \dfrac{(2h\bar{t})}{(\rho C_P R)}(T - T_{\text{wall}}) - \left[\dfrac{-(\Delta \mathrm{H}_R a_{\text{in}})}{(\rho C_P)}\right] k_0\bar{t}\,\exp\left(\dfrac{T_{\text{act}}}{T}\right) a/a_{\text{in}}}{E/\bar{u}L} \qquad T' = 0 \quad \text{at } \mathcal{Z} = 1$$

There are four equations in four dependent variables, a, a', T, and T'. They can be integrated using the Runge–Kutta method as outlined in Appendix 2.1. Note that they are integrated in the reverse direction, for example, $a_1 = a_0 - \mathscr{R}_A\,\Delta\mathcal{Z}/2$.

A double trial-and-error procedure is used to determine a_0 and T_0. This is done by a random search in a sample program, Code for Example 9.5. Simultaneous satisfaction of the boundary conditions for concentration and temperature was aided by using an output response that combined the two errors. Results are shown in Figure 9.10.

The axial dispersion model provides a lower and thus ***more*** conservative estimate of conversion than does the piston flow model given the same values for the input parameters. There is a more subtle possibility. The model may show that it is possible to operate with ***less*** conservative values for some parameters, for example, higher values for T_{in} and T_{wall}, without provoking adverse side reactions.

Code for Example 9.5

```
Private k0, Tact, h, heat, Tin, Twall, D, E
```

```
Sub Example9_5()

Dim a(128), T(128)

k0 = 200000000000#
Tact = 10000
h = 10
heat = 200
Tin = 374
Twall = 374
ain = 1
jj = 32
dz = 1 / jj
a0 = ain
T0 = Tin
D = 0.045
E = 0.06

'Start with the piston flow case
For j = 1 To jj
   R0 = RxRate(a0, T0)
   S0 = Source(a0, T0)
   a1 = a0 + R0 * dz / 2
   T1 = T0 + S0 * dz / 2
   R1 = RxRate(a1, T1)
   S1 = Source(a1, T1)
   a2 = a0 + R1 * dz / 2
   T2 = T0 + S1 * dz / 2
   R2 = RxRate(a2, T2)
   S2 = Source(a2, T2)
   a3 = a0 + R2 * dz
   T3 = T0 + S2 * dz
   R3 = RxRate(a3, T3)
   S3 = Source(a3, T3)
   a0 = a0 + (R0 + 2 * R1 + 2 * R2 + R3) / 6 * dz
   T0 = T0 + (S0 + 2 * S1 + 2 * S2 + S3) / 6 * dz
   a(j) = a0
   T(j) = T0
Next

For j = 0 To jj
   Cells(j + 2, 3) = j / jj
   Cells(j + 2, 6) = j / jj
   Cells(j + 2, 4) = a(j)
   Cells(j + 2, 7) = T(j)
Next
```

```
' Axial dispersion case

aout = Cells(2, 2)   'Put a starting guess for aout in cell B2
Tout = Cells(3, 2)   'Put a starting guess Tout in cell B3
Test = 100          'Arbitrarily high value
a(0) = aout
T(0) = Tout

Do

a0 = a(o)
T0 = T(0)
ap0 = 0
Tp0 = 0
TMa = 0

For j = 1 To jj
   Rp0 = RxRateP(a0, ap0, T0, Tp0)
   Sp0 = SourceP(a0, ap0, T0, Tp0)
   R0 = ap0
   S0 = Tp0
   a1 = a0 - R0 * dz / 2
   T1 = T0 - S0 * dz / 2
   ap1 = ap0 - Rp0 * dz / 2
   Tp1 = Tp0 - Sp0 * dz / 2
   Rp1 = RxRateP(a1, ap1, T1, Tp1)
   Sp1 = SourceP(a1, ap1, T1, Tp1)
   R1 = ap1
   S1 = Tp1
   a2 = a0 - R1 * dz / 2
   T2 = T0 - S1 * dz / 2
   ap2 = ap0 - Rp1 * dz / 2
   Tp2 = Tp0 - Sp1 * dz / 2
   Rp2 = RxRateP(a2, ap2, T2, Tp2)
   Sp2 = SourceP(a2, ap2, T2, Tp2)
   R2 = ap2
   S2 = Tp2
   a3 = a0 - R2 * dz
   T3 = T0 - S2 * dz
   ap3 = ap0 - Rp2 * dz
   Tp3 = Tp0 - Sp2 * dz
   Rp3 = RxRateP(a3, ap3, T3, Tp3)
   Sp3 = SourceP(a3, ap3, T3, Tp3)
   R3 = ap3
   S3 = Tp3
   a0 = a0 - (R0 + 2 * R1 + 2 * R2 + R3) / 6 * dz
   T0 = T0 - (S0 + 2 * S1 + 2 * S2 + S3) / 6 * dz
   ap0 = ap0 - (Rp0 + 2 * Rp1 + 2 * Rp2 + Rp3) / 6 * dz
   Tp0 = Tp0 - (Sp0 + 2 * Sp1 + 2 * Sp2 + Sp3) / 6 * dz
   If TMa < T0 Then
      TMa = T0
      zma = 1 - j * dz
   End If
```

```
   a(j) = a0
   T(j) = T0
Next

Atest = a0 - D * ap0 - ain
TTest = T0 - E * Tp0 - Tin
Ctest = Abs(Atest) + Abs(TTest)

If Ctest < Test Then
   Test = Ctest
   aout = a(0)
   Tout = T(0)
   Cells(2, 2) = aout
   Cells(3, 2) = Tout
      For j = 0 To jj
      Cells(j + 2, 5) = a(jj - j)
      Cells(j + 2, 8) = T(jj - j)
      Cells(15, 2) = Test
   Next
End If

   a(0) = aout + 0.001 * (0.5 - Rnd)
   T(0) = Tout + 0.1 * (0.5 - Rnd)

Loop
End Sub
```

```
Function RxRate(a, T)
RxRate = -k0 * Exp(-Tact / T) * a
End Function
```

```
Function Source(a, T)
Source = h * (Twall - T) - heat * RxRate(a, T)
End Function
```

```
Function RxRateP(a, ap, T, Tp)
RxRateP = (ap + k0 * Exp(-Tact / T) * a) / D
End Function
```

```
Function SourceP(a, ap, T, Tp)
SourceP = (Tp + h * (T - Twall) + heat * RxRate(a, T)) / E
End Function
```

9.3.6 Axial Dispersion with Variable Density

The axial dispersion equation for the variable-density case is written in terms of the component flux:

$$\frac{d\Phi_A}{dz} = \frac{d(\bar{u}a)}{dz} = D\frac{d^2a}{dz^2} + \mathscr{R}_A \tag{9.36}$$

Similar equations can be written for the other components and for the enthalpy flux. An equation for the pressure drop is also required. The boundary conditions are of the Danckwerts type if the system is closed and are those of Example 9.2 for an open system. The shooting method of solution can be used for the closed system. The open system is more easily solved using the method of false transients described in Chapter 16.

9.4 SCALEUP AND MODELING CONSIDERATIONS

Previous chapters have discussed how isothermal or adiabatic reactors can be scaled up. Nonisothermal reactors are more difficult. They can be scaled by maintaining the same tube diameter or by a modeling approach. The challenge is to increase tube diameter upon scaleup. This is rarely possible; when possible, it should be based on good models. If the model predictions for the scaled reactor are good and if you have confidence in the model, proceed with scaleup.

What models should be used either for scaleup or to correlate pilot plant data? Section 9.1 gives the preferred models for nonisothermal reactions in packed beds. These models have a reasonable experimental basis even though they use empirical parameters D_r, h_r, and κ_r to account for the packing and the complexity of the flow field. For laminar flow in open tubes, use the methods in Chapter 8. For highly turbulent flows in open tubes (with reasonably large L/d_t ratios) use the axial dispersion model in both the isothermal and nonisothermal cases. The assumption $D = E$ will usually be safe, but do calculate how a PFR would perform. If there is a substantial difference between the PFR model and the axial dispersion model, understand the reason. For transitional flows, it is usually conservative to use the methods of Chapter 8 to calculate yields and selectivities but to assume turbulence for pressure drop calculations.

SUGGESTED FURTHER READINGS

The heat and mass transfer phenomena associated with packed-bed reactors are described in:

G. F. Froment and K. B. Bischoff, *Chemical Reaction Analysis and De*sign, 2nd Ed., Wiley, New York, 1990.

Correlations for heat transfer in packed beds are still being developed. Enthusiasts of CFD anticipate using it to model nonisothermal packed beds, but the predictions still need to be tweaked. The more classic and time-tested work is:

A. G. Dixon and D. L. Cresswell, Theoretical prediction of effective heat transfer parameters in packed deds, *AIChE J*., **25**, 663–676 (1979).

A review article describing the occasionally pathological behavior of packed bed reactors is:

A.Cybulski, G. Eigenberger, and A. Stankiewicz, Operational and structural nonidealities in modeling and design of multitubular catalytic reactors, *Ind. Eng. Chem. Res*., **36**, 3140–3148 (1997).

Chapter 15 provides additional discussion of the axial dispersion model and of methods for measuring dispersion coefficients. A more advanced account is given in:

E. B. Nauman and B. A. Buffliam, *Mixing in Continuous Flow Systems,* Wiley, New York, 1983.

Chapter 16 applies the axial dispersion model to micrometer-scale reactors.

Run an Internet search on static and motionless mixers to learn more about the utility of these devices, but be leery of the hype.

PROBLEMS

9.1 Use the packed tube model of Example 9.1 to estimate a combination of inlet and wall temperatures that will maximize conversion while keeping the centerline temperature below 690 K.

9.2 Example 9.1 on the partial oxidation of *ortho*-xylene uses a pseudo-first-order kinetic scheme. For this to be justified, the oxygen concentration must be approximately constant, which in turn requires low oxygen consumption and a low pressure drop. Are these assumptions reasonable for the reactor in Example 9.1? Specifically, estimate the pressure drop and the ratio of the residual oxygen concentration to the residual *ortho*-xylene concentration at the reactor outlet for the case of $T_{\text{in}} = 600$ K.

9.3 Phthalic anhydride will, in the presence of the V_2O_5catalyst of Example 9.1, undergo complete oxidation with $\Delta H_R = -760$ kcal mol^{-1}. Suppose the complete oxidation is pseudo–first order in phthalic anhydride concentration and that $\ln(k_{\text{II}}) = 11.8 - l0000/T$.

(a) To establish an upper limit on the yield of phthalic anhydride, pretend the reaction can be run isothermally. Determine yield as a function of temperature when both reactions are considered.

(b) To gain insight into the potential for a thermal runaway, calculate the adiabatic temperature rise if only the first oxidation goes to completion (i.e., A $\rightarrow$ B) and if both the oxidations steps go to completion (i.e., A $\rightarrow$ B$\rightarrow$ C).

(c) Determine the value for T_{wall} will just cause a thermal runaway. This gives an upper limit on T_{wall} for practical operation of the nonisothermal reactor. Take extra care to control error in your calculations.

(d) Based on the constraint found in (c), determine the maximum value for the phthalic anhydride yield in the packed tube.

9.4 An alternative route to phthalic anhydride is the partial oxidation of naphthalene. The heat of reaction is -430 kcal mol^{-1}. This reaction can be performed using a promoted V_2O_5 catalyst on silica, much like that considered in Example 9.1. Suppose $\ln(k) = 31.17 - 19100/T$ for the naphthalene oxidation reaction and that the subsequent, complete oxidation of phthalic anhydride follows the kinetics of Problem 9.3. Suppose it is desired to use the same reactor as in Example 9.1 but with $a_{\text{in}} = 53$ g m^{-3}.

Determine values for T_{in} and T_{wall} that maximize the output of phthalic anhydride from naphthalene.

9.5 A gas phase reaction, A + B $\xrightarrow{k}$ C + D, is performed in a packed-bed reactor at essentially constant temperature and pressure. The following data are available: $d_t = 0.3$ m, $L = 8$ m, $\varepsilon = 0.5$, $D_r = 0.0005$ m^2 s^{-1}, $\bar{u}_s = 0.25$ m s^{-1}, $a_{in} = b_{in}$. The current operation using premixed feed gives $Y = a_{out}/a_{in} = 0.02$. There is a safety concern about the premixing step. One proposal is to feed A and B separately. Component A would be fed into the base of the bed using a central tube with diameter 0.212 m and component B would be fed to the annulus between the central tube and the reactor wall. The two streams would mix and react only after they entered the bed. The concentrations of the entering components would be increased by a factor of 2, but the bed-average concentrations and $\bar{u}_s$ would be unchanged. Determine the fraction unreacted that would result from the proposed modification.

9.6 Nerve gas is to be thermally decomposed by oxidation using a large excess of air in a 5-cm-ID tubular reactor that is approximately isothermal at 620°C. The entering concentration of nerve gas is 1% by volume. The outlet concentration must be less than 1 part in 10^{12} by volume. The observed half-life for the reaction is 0.2 s. Use $\rho = 0.39$ kg m^{-3} and $\mu = 4 \times 10^{-5}$ Pa s. How long should the tube be for an inlet velocity of 20 m s^{-1}? What will be the pressure drop given an atmospheric discharge?

9.7 Example 9.1 used a distributed-parameter-system of simultaneous PDEs for the phthalic anhydride reaction in a packed bed. Axial dispersion is a lumped-parameter system of simultaneous ODEs that can also be used for a packed bed. Apply the axial dispersion model to the phthalic reaction using D as determined from Figure 9.7 and $E = 1.33\ D$. Compare your results to those obtained in Example 9.1.

9.8 Determine the yield of a second order reaction, A + B $\xrightarrow{k}$ product with $a_{in} = b_{in}$ in an isothermal tubular reactor governed by the axial dispersion model. Specifically, plot fraction unreacted versus $a_{in}k\bar{t}$ for a variety of **Pe**. Be sure to show the limiting cases that correspond to a PFR and a CSTR.

9.9 Water at room temperature is flowing through a 20-cm-ID pipe at **Re** = 1000. What is the minimum tube length needed for the axial dispersion model to provide a reasonable estimate of reactor performance?

9.10 The marching equation for reverse shooting, Equation 9.24, was developed using a first-order backward-difference approximation for *da/dz* even though a second-order approximation was necessary for d^2a/dz^2. Since the locations $j-1$, j, $j+1$ are involved anyway, would it not be better to use a second-order central-difference approximation for *da/dz*?

(a) Would this allow convergence ($O\Delta z^2$) for the reverse-shooting method?

(b) Notwithstanding the theory, run a few values of J, differing by factors of 2, to experimentally confirm the orders of convergence for the two methods.

9.11 The piston flow model in Example 9.5 shows a thermal runaway (defined as $d^2T/dz^2 > 0$) when $T_{in} = T_{wall} = 374$. Will the axial dispersion model show a runaway? If so, at what value of $T_{in} = T_{wall}$?

Chapter 10

Heterogeneous Catalysis

The first eight chapters of this book treated homogeneous reactions. Chapter 9 provided models for packed-bed reactors, but the reaction kinetics are pseudohomogeneous so that the rate expressions are based on fluid-phase concentrations. There is a good reason for this. Fluid-phase concentrations are what can be measured. The fluid-phase concentrations at the outlet are what can be sold.

Chapter 10 begins a more detailed treatment of heterogeneous reactors. The discussion assumes the fluid phase is a gas since this is the predominant case. This chapter continues the use of pseudohomogeneous models for steady-state, packed-bed reactors but derives expressions for the reaction rate that reflect the underlying kinetics of surface-catalyzed reactions. The kinetic models are ***site competition models*** that apply to a variety of catalytic systems including the enzymatic reactions treated in Chapter 12. Here in Chapter 10, the example system is a ***solid-catalyzed gas reaction*** that is typical of the traditional chemical industry. A few important examples are as follows:

- Ethylene is selectively oxidized to ethylene oxide using a silver-based catalyst in a fixed-bed reactor. Ethylene and oxygen are supplied from the gas phase and ethylene oxide is removed by it. The catalyst is stationary. Undesired, kinetically determined byproducts include carbon monoxide and water. The goal is to produce ethylene oxide and no byproducts.
- Ethylbenzene is dehydrogenated in a fixed-bed reactor to give styrene. Hydrogen is produced as a stoichiometrically determined byproduct. Undesired byproducts including toluene, benzene, light hydrocarbons, coke, and additional hydrogen are kinetically determined. The goal is to produce only styrene and the stoichiometrically inevitable hydrogen.
- The final step in the methanol-to-gasoline process can be done in an adiabatic, fixed-bed reactor using a zeolite catalyst. A product mixture similar to ordinary gasoline is obtained. As typical of polymerizations, a pure reactant is converted to a complex mixture of products.
- Catalytic reformers take linear alkanes (e.g., *n*-pentane) and produce branched alkanes (e.g., *i*-pentane). The catalyst is finely divided platinum on Si_2O_3.

Chemical Reactor Design, Optimization, and Scaleup, Second Edition. By E. B. Nauman
Copyright © 2008 John Wiley & Sons, Inc.

Reforming is a common refinery reaction that begins with a complex mixture of reactants and produces a complex mixture of products.

- The catalytic converter on a car uses a precious metal-based, solid catalyst, usually in the form of a monolith, to convert unburned hydrocarbons and carbon monoxide to carbon dioxide. Many different reactants are converted to two products, CO_2 and water.

Many more examples could be given. They all involve ***interphase mass transfer*** combined with chemical reaction. Gas phase reactants are adsorbed onto a solid surface, react, and the products are desorbed. Most solid catalysts are supplied as cylindrical pellets with lengths and diameters in the range of 2–10 mm. More complex shapes and monoliths can be used when it is important to minimize pressure drop. The catalyst is ***microporous*** with pores ranging in diameter from a few angstroms to a few micrometers. See Figure 10.1. The internal surface area, accessible through the pores, is enormous, up to 2000 m^2 per gram of catalyst. The internal surface area dwarfs the nominal, external area and accounts for most of the catalytic activity. The catalytic sites are atoms or molecules on the internal surface. The structural material of the catalyst particle is often an oxide such as alumina (Al_2O_3) or silica (SiO_2). The structural material may provide the catalytic sites directly or may ***support*** a more expensive substance such as finely divided platinum. When heat transfer is important, the catalyst pellets are randomly packed in small-diameter (10–50-mm) tubes that are often quite long (2–10 m). A fluidized bed of small (50-μm) catalyst particles can also be used. If the adiabatic temperature change is small, the pellets are packed in large-diameter vessels. Annular flow reactors (see Figure 3.2) are used when it is important to minimize the outlet pressure. Another approach is to flow the gas through

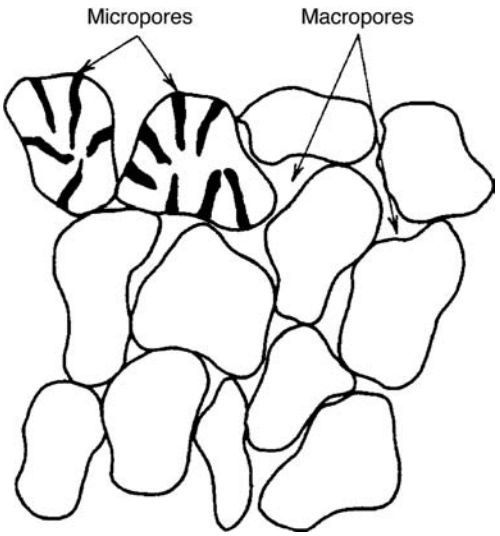

Figure 10.1 Cartoon of bimodal catalyst pore structure.

the labyrinth of a monolithic catalyst, as in automobile exhaust systems. Regardless of the specific geometry used to contact the gas and the solid, all these schemes require a complex set of mass transfer and reaction steps, usually accompanied by heat transfer.

10.1 OVERVIEW OF TRANSPORT AND REACTION STEPS

Molecules enter the reactor with uniform concentrations a_{in} and leave with mixing-cup concentrations a_{out}. In between, they undergo the following steps:

1. Bulk transport of the reactants to the vicinity of a catalyst particle
2. Mass transfer across a film resistance from the bulk gas phase to the external surface of the porous catalyst
3. Transport of the reactants into the catalyst particle by diffusion through the pores
4. Adsorption of reactant molecules onto the internal surface of the catalyst
5. Reaction between adsorbed components on the internal surface
6. Desorption of product molecules from the surface to the pores
7. Diffusion of product molecules out of the pores to the external surface of the pellet
8. Mass transfer of the products across a film resistance into the bulk gas phase
9. Bulk transport of products to the reactor outlet.

All these steps can influence the overall reaction rate. The reactor models of Chapter 9 are used to predict the bulk, gas phase concentrations of reactants and products at point (r, z) in the reactor. They directly model only steps 1 and 9, and the effects of steps 2–8 are lumped into the pseudohomogeneous rate expression $\mathscr{R}(a, b, \ldots)$, where $a, b, \ldots$ are the bulk, gas phase concentrations. The overall reaction mechanism is complex, and the rate expression is necessarily empirical. Heterogeneous catalysis remains an experimental science. The techniques of this chapter are useful to interpret experimental results. Their predictive value is limited.

The goal at this point is to examine steps 2–8 in more detail so that the pseudohomogeneous reaction rate can reflect the mechanisms occurring within or on the catalyst. We seek a quantitative understanding of steps 2–8 with a view toward improving the design of the catalyst and the catalytic reactor. The approach is to model the steps individually and then to couple them together. The modeling assumes that the system is at steady state. The coupling is based on the fact that each of steps 2–8 must proceed at the same rate in a steady-state system and that this rate, when expressed as moles per volume of gas phase per time, must equal the reaction rates in steps 1 and 9.

10.2 GOVERNING EQUATIONS FOR TRANSPORT AND REACTION

Consider an observed reaction of the form A + B → P + Q occurring in a packed-bed reactor:

Step 1. The entering gas is transported to point (r, z) in the reactor and reacts with rate $\varepsilon \mathscr{R}$. Equation 9.1 governs the combination of bulk transport and pseudohomogeneous reaction. We repeat it here:

$$\bar{u}_s \frac{\partial a}{\partial z} = D_r \left[\frac{1}{r} \frac{\partial a}{\partial r} + \frac{\partial^2 a}{\partial r^2} \right] + \varepsilon \mathscr{R}_A \tag{10.1}$$

The initial and boundary conditions are given in Chapter 9. The present treatment does not change the results of Chapter 9 but instead provides a rational basis for using pseudohomogeneous kinetics for a solid-catalyzed reaction. The axial dispersion model in Chapter 9, again with pseudohomogeneous kinetics, is an alternative to Equation 10.1 that can be used when the radial temperature and concentration gradients are small.

Step 2. Refer to Figure 10.2 reactant A in the gas phase at position (r, z) has concentration $a(r, z)$. It is transported across a film resistance and has concentration $a_s(r, z)$ at the external surface of the catalyst pellet that is located at point (r, z). The detailed geometry of the gas and solid phases is ignored, so that both phases can exist at the same spatial location. The bulk and surface concentrations at location (r, z) are related through a mass transfer coefficient.

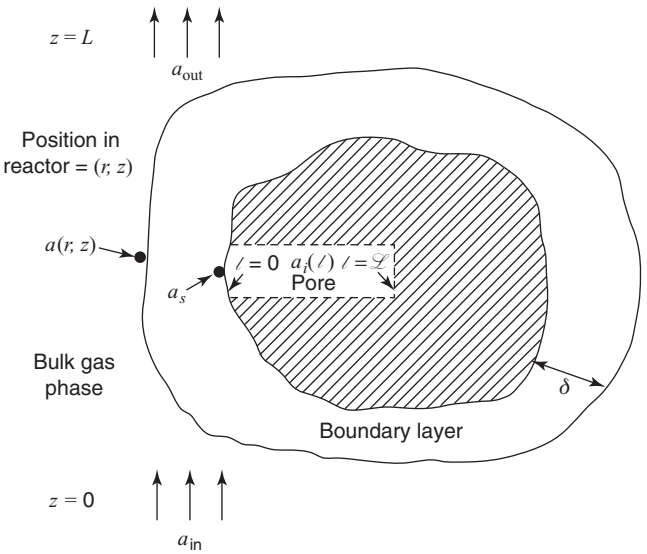

Figure 10.2 Pore and film resistances in catalyst particle.

The steady-state flux across the interface must be equal to the reaction rate. Thus, for component A,

$$\mathscr{R}_A = k_s A_s (a_s - a) \tag{10.2}$$

where k_s is a mass transfer coefficient and A_s is the external surface area of catalyst per unit volume of the gas phase. The units of k_s are moles per time per area per concentration driving force. These units simplify to length per time. The units on A_s are area per volume so that the product $k_s A_s$ has dimensions of reciprocal time.

Step 3. Transport within a catalyst pore is usually modeled as a one-dimensional diffusion process. The coordinate system is indicated in Figure 10.2. The pore is assumed to be straight and to have length $\mathscr{L}$. The concentration inside the pore is $a_l(\ell, r, z)$, where ℓ is the position inside the pore measured from the external surface of the catalyst particle. There is no convection inside the pore, and the diameter of the pore is assumed to be so small that there are no concentration gradients in the radial direction. The governing equation is an ODE:

$$0 = \mathscr{D}_A \frac{d^2 a_\ell}{d\ell^2} + \mathscr{R}_A \tag{10.3}$$

The solution to this equation, which is detailed in Section 10.4.1, gives the concentration at position ℓ down a pore that has its mouth located at position (r, z) in the reactor. The reaction rate in Equation 10.3 remains based on the gas phase concentrations.

Step 4. A reactant molecule is adsorbed onto the internal surface of the catalyst. The adsorption step is modeled as an elementary reaction, the simplest version of which is

$$\mathrm{A(gas)} + \mathrm{S(solid)} \xrightarrow{k_a} \mathrm{AS(solid)} \qquad \mathscr{R} = k_a a(l, r, z)[\mathrm{S}] \tag{10.4}$$

This kinetic relationship provides the necessary link between the gas phase concentration a and the concentration of A in its adsorbed form, which is denoted as [AS]. The units for ***surface concentration*** are moles per unit area of catalyst surface. Here, S denotes a catalytically active site on the surface, also with units of moles per unit area of catalyst surface. The absorbed A occupies one of the sites, the concentration of these occupied sites being denoted as [AS].

Step 5. A surface reaction occurs between adsorbed species. The prototypical reaction is

$$\mathrm{AS} + \mathrm{BS} \xrightarrow{k_R} \mathrm{PS} + \mathrm{QS} \qquad \mathscr{R} = k_R[\mathrm{AS}][\mathrm{BS}] \tag{10.5}$$

where the product molecules P and Q are formed as adsorbed species and also occupy catalytic sites. The surface reaction provides the link between reactant concentrations and product concentrations.

Step 6. The products are desorbed to give the gas phase concentrations p and q. The simplest desorption mechanism is written as

$$\text{PS(solid)} \xrightarrow{k_d} \text{P(gas)} + \text{S(solid)} \quad \mathscr{R} = k_d[\text{PS}] \tag{10.6}$$

The catalytic sites S consumed in step 4 are released in step 6.

Step 7. Product species, now in the gas phase, diffuse outward through the pores, the governing equations being similar to those used for the inward diffusion of reactants:

$$0 = \mathscr{D}_P \frac{d^2 p_\ell}{d\ell^2} + \mathscr{R}_P \tag{10.7}$$

The product molecules emerge from the interior of the catalyst at the same location, (r, z), that the reactants entered.

Step 8. Product species diffuse across the fluid boundary layer at the external surface of the catalyst:

$$\mathscr{R}_P = k_s A_s (p_s - p) \tag{10.8}$$

Nominally, the value of $k_s A_s$ might be different for the different species. In practice, the difference is ignored.

Step 9. Product species generated at location (r, z) are transported to the reactor outlet. The governing equation is

$$\bar{u}_s \frac{\partial p}{\partial z} = D_r \left[\frac{1}{r} \frac{\partial p}{\partial r} + \frac{\partial^2 p}{\partial r^2} \right] + \varepsilon \mathscr{R}_P \tag{10.9}$$

Steps 1–9 constitute a model for heterogeneous catalysis in a fixed bed reactor. There are many variations, particularly for steps 4–6. For example, the Eley – Rideal mechanism described in Problem 10.4 envisions an adsorbed molecule reacting directly with a molecule in the gas phase. Other models contemplate a mixture of surface sites that can have different catalytic activity. For example, the platinum and the alumina used for hydrocarbon reforming may catalyze different reactions. Alternative models lead to rate expressions that differ in the details, but the functional forms for the rate expressions are usually similar.

10.3 INTRINSIC KINETICS

It is possible to eliminate the mass transfer resistances in steps 2, 3, 7, and 8 by grinding the catalyst to a fine powder and exposing it to a high-velocity gas stream. The concentrations of reactants immediately adjacent to what would normally be internal catalytic surface become equal to the bulk gas concentrations. The resulting kinetics are known as ***intrinsic kinetics*** since they are intrinsic to the catalyst surface and not to the geometry of the pores or the pellets or the reactor. Most research

in heterogeneous catalysis is concerned with the measurement, understanding, and modification of intrinsic kinetics.

When the mass transfer resistances are eliminated, the various gas phase concentrations become equal: $a_l(\ell, r, z) = a_s(r, z) = a(r, z)$. The very small particle size means that heat transfer resistances are minimized so that the catalyst particles are isothermal. The recycle reactor of Figure 4.2 is an excellent means for measuring the intrinsic kinetics of a finely ground catalyst. At high recycle rates, the system behaves as a CSTR. It is sometimes called a ***gradientless reactor*** since there are no composition and temperature gradients in the catalyst bed or in a catalyst particle.

10.3.1 Intrinsic Rate Expressions from Equality of Rates

Suppose a gradientless reactor is used to obtain intrinsic rate data for a catalytic reaction. Gas phase concentrations are measured, and the data are fit to a rate expression using the methods of Chapter 7. The rate expression can be arbitrary:

$$R = ka^m b^n p^r q^s \tag{10.10}$$

As discussed in Chapter 7, this form can provide a good fit of the data if the reaction is not too close to equilibrium. However, most reaction engineers prefer a mechanistically based rate expression. This section describes how to obtain plausible functional forms for $\mathscr{R}$ based on simple models of the surface reactions and on the observation that all the rates in steps 2–8 must be equal at steady state. Thus the rate of transfer across the film resistance equals the rate of diffusion into a pore equals the rate of adsorption equals the rate of reaction equals the rate of desorption and so on. This rate is the pseudohomogeneous rate used in steps 1 and 9.

EXAMPLE 10.1

Consider the heterogeneously catalyzed reaction A → P. Derive a plausible form for the intrinsic kinetics. The goal is to determine a form for the reaction rate $\mathscr{R}$ that depends only on gas phase concentrations.

SOLUTION: Under the assumption of intrinsic kinetics, all mass transfer steps are eliminated, and steps 4–6, determine the reaction rate. The simplest possible version of steps 4–6 treats them all as elementary, irreversible reactions:

$$\begin{aligned}
\text{A(gas)} + \text{S(solid)} &\xrightarrow{k_a} \text{AS(solid)} & \mathscr{R} &= k_a a_\ell [\text{S}] \\
\text{AS(solid)} &\xrightarrow{k_R} \text{PS(solid)} & \mathscr{R} &= k_R [\text{AS}] \\
\text{PS(solid)} &\xrightarrow{k_a} \text{P(gas)} + \text{S(solid)} & \mathscr{R} &= k_d [PS]
\end{aligned}$$

The reaction rates must be equal at steady state. Thus,

$$\mathscr{R} = k_a a_\ell [\text{S}] = k_R [\text{AS}] = k_d [\text{PS}]$$

A site balance ties these equations together:

$$S_0 = [\text{S}] + [\text{AS}] + [\text{PS}]$$

The site balance specifies that the number of empty plus occupied sites is a constant, S_0. Equality of the reaction rates plus the site balance gives four independent equations. Combining them allows a solution for $\mathscr{R}$ while eliminating the surface concentrations [S], [AS], and [PS]. Substitute the various reaction rates into the site balance to obtain

$$S_0 = \frac{\mathscr{R}}{k_a a_\ell} + \frac{\mathscr{R}}{k_R} + \frac{\mathscr{R}}{k_d}$$

But $a_\ell = a$ for intrinsic kinetics. Making this substitution and solving for $\mathscr{R}$ gives

$$\mathscr{R} = \frac{S_0 a}{1/k_a + (1/k_R + 1/k_d)\,a} = \frac{S_0 k_a a}{1 + (k_a/k_R + k_a/k_d)\,a} \tag{10.11}$$

Redefining constants gives

$$\mathscr{R} = \frac{ka}{1 + k_A a} \tag{10.12}$$

Equation 10.12 is the simplest—and most generally useful—model that reflects heterogeneous catalysis. The active sites S are fixed in number, and the gas–phase molecules of component A compete for them. When the gas–phase concentration of component A is low, most of the sites are empty and the $k_A a$ term in the denominator of Equation 10.12 is small so that the reaction is first order in a. When a is large, all the active sites are occupied, and the reaction rate reaches a saturation value of k/k_A.

The form of Equation 10.12 is widely used for multiphase reactions. The same model, with slightly different physical interpretations, is used for enzyme catalysis and cell growth. See Chapter 12.

EXAMPLE 10.2

Repeat Example 10.1 but now assume that each of steps 4–6 is reversible.

SOLUTION: The elementary reaction steps of adsorption, reaction, and desorption are now reversible. From this point on, we will set $a_\ell = a$, $p_\ell = p$, and so on since the intrinsic kinetics are desired. The relationships between a_ℓ, a_s, and a are addressed in Section 10.4 using an effectiveness factor. The various reaction steps are

$$\text{A(gas)} + \text{S(solid)} \underset{k_a^-}{\overset{k_a^+}{\rightleftarrows}} \text{AS(solid)} \qquad \mathscr{R} = k_a^+ a[\text{S}] - k_a^-[\text{AS}]$$

$$\text{AS(solid)} \underset{k_R^-}{\overset{k_R^+}{\rightleftarrows}} \text{PS(solid)} \qquad \mathscr{R} = k_R^+[\text{AS}] - k_R^-[\text{PS}]$$

$$\text{PS(solid)} \underset{k_d^-}{\overset{k_d^+}{\rightleftarrows}} \text{P(gas)} + \text{S(solid)} \qquad \mathscr{R} = k_d^+[\text{PS}] - k_d^- p[\text{S}]$$

As in Example 10.1, the rates must all be equal at steady state:

$$\mathscr{R} = k_a^+ a[\mathrm{S}] - k_a^-[\mathrm{AS}] = k_R^+[\mathrm{AS}] - k_R^-[\mathrm{PS}] = k_d^+[\mathrm{PS}] - k_d^- p[\mathrm{S}]$$

The site balance is the same as in Example 10.1:

$$\mathrm{S}_0 = [\mathrm{S}] + [\mathrm{AS}] + [\mathrm{PS}]$$

As in Example 10.1, equality of the reaction rates plus the site balance gives four independent equations. Combining them allows a solution for $\mathscr{R}$ while eliminating the surface concentrations [S], [AS], and [PS]. After much algebra and a redefinition of constants,

$$\mathscr{R} = \frac{k_f a - k_r p}{1 + k_A a + k_P p} \tag{10.13}$$

The rather messy result for $\mathscr{R}$ before the redefinition of constants is given in Problem 10.1.

The numerator of Equation 10.13 is the expected form for a reversible, first-order reaction. The denominator shows that the reaction rate is retarded by all species that are adsorbed. This reflects competition for sites. Inerts can also compete for sites. Thus, the version of Equation 10.13 that applies when adsorbable inerts are present is

$$\mathscr{R} = \frac{k_f a - k_r p}{1 + k_A a + k_P p + k_I i} \tag{10.14}$$

where i is the gas phase concentration of inerts. The inerts may be intentionally added or they may be undesired contaminates. When they are contaminates, their effect on the reaction rate represents a form of deactivation, in this case ***reversible deactivation,*** that ceases when the contaminate is removed from the feed.

Examples 10.1 and 10.2 used the fact that steps 4, 5, and 6 must all proceed at the same rate. This matching of rates must always be true in a steady-state system, and, as illustrated in the foregoing examples, can be used to derive expressions for the intrinsic reaction kinetics. There is another concept with a time-honored tradition in chemical engineering that should be recognized. It is the concept of the ***rate-determining step*** or the ***rate-controlling step***.

10.3.2 Models Based on Rate-Controlling Step

The idea is that a single step of steps 2–8 may be so much slower than the other steps that it determines the overall reaction rate. Suppose that step 4, adsorption, is very slow. Then the mass transfer steps prior to adsorption (film transfer and pore diffusion) will proceed at the same slow rate but will in effect go to completion. The pores will be filled will gas at the bulk concentration: $a_\ell = a_s = a$. The reactant molecules in the gas phase are queued awaiting adsorption. Most of the catalytic sites will be empty because, with slow adsorption, the reaction and desorption steps can match the adsorption rate at low concentration.

The concept of the rate-determining step has been widely employed in the literature starting with Hougen and Watson (1947). The advantage of this approach is that it generates kinetic models with somewhat less algebra than the equal-rate approach. It has the disadvantage of giving less general models that may also mislead the unwary experimentalist into thinking that surface mechanisms can be unambiguously determined from steady-state experiments. This is rarely possible.

Irreversible Unimolecular Reactions

Consider the irreversible catalytic reaction A $\rightarrow$ P of Example 10.1. There are three kinetic steps: adsorption of A, the surface reaction, and desorption of P. All three steps must occur at exactly the same rate, but the relative magnitudes of the three rate constants, k_a, k_R, k_d, determine the concentration of surface species. Suppose that k_a is much smaller that the other two rate constants. Then the surface sites will be mostly unoccupied so that [S] $\approx S_0$. Adsorption is the rate-controlling step. As soon as a molecule of A is absorbed, it reacts to P, which is then quickly desorbed. If, on the other hand, the reaction step is slow, the entire surface will be saturated with A waiting to react, [AS] $\approx S_0$, and the surface reaction is rate controlling. Finally, it may be that k_d is small. Then the surface will be saturated with P waiting to desorb, [PS] $\approx S_0$, and desorption is rate controlling. The corresponding forms for the overall rate are

Adsorption is rate controlling:	$\mathscr{R} = k_a S_0 a$	(first order in A)
Surface reaction is rate controlling:	$\mathscr{R} = k_R S_0$	(zero order in A)
Desorption is rate controlling:	$\mathscr{R} = k_d S_0$	(zero order in A)

These results can be confirmed by taking the appropriate limits on the rate constants in Equation 10.11.

Reversible Unimolecular Reactions

The intrinsic reaction steps in heterogeneously catalyzed reactions are often reversible. The various limiting cases can be found by taking limits before redefining constants, for example, taking limits on Equation 10.11, not Equation 10.12. However, a more direct route is to assume that the fast steps achieve equilibrium before deriving the counterpart to Equation 10.11.

EXAMPLE 10.3

Suppose that adsorption is much slower than surface reaction or desorption for the heterogeneously catalyzed reaction A $\overrightarrow{\longleftarrow}$ P. Deduce the functional form of the pseudohomogeneous, intrinsic kinetics.

SOLUTION: The adsorption step is slow, reversible, and rate-controlling. Its equation remains

$$\text{A(gas)} + \text{S(solid)} \underset{k_a^-}{\overset{k_a^+}{\rightleftarrows}} \text{AS(solid)} \qquad \mathscr{R} = k_a^+ a[\text{S}] - k_a^-[\text{AS}]$$

The reaction and desorption steps are assumed to be so fast compared with adsorption that they achieve equilibrium:

$$\frac{[\text{PS}]}{[\text{AS}]} = \frac{k_R^+}{k_R^-} = K_R \qquad \frac{p[\text{S}]}{[\text{PS}]} = \frac{k_d^+}{k_d^-} = K_d$$

The site balance is unchanged from Examples 10.1 and 10.2:

$$S_0 = [\text{S}] + [\text{AS}] + [\text{PS}]$$

There are enough equations to eliminate the surface equations from the reaction rate. After redefinition of constants,

$$\mathscr{R} = \frac{k_f a - k_r p}{1 + k_P p} \tag{10.15}$$

When the adsorption step determines the rate, component A no longer retards the reaction. Any A that is adsorbed will quickly react, and the concentration of [AS] sites will be low. Note that the desorption step is now treated as being reversible. Thus any P in the gas phase will retard the reaction even if the surface reaction is irreversible, $k_r = 0$.

EXAMPLE 10.4

Repeat Example 10.3 assuming now that the surface reaction controls the rate.

SOLUTION: Appropriate equations for the adsorption, reaction, and desorption steps are

$$\frac{[\text{AS}]}{a[\text{S}]} = \frac{k_a^+}{k_a^-} = K_a$$

$$\mathscr{R} = k_R^+[\text{AS}] - k_R^-[\text{PS}]$$

$$\frac{p[\text{S}]}{[\text{PS}]} = \frac{k_d^+}{k_d^-} = K_d$$

The site balance is unchanged. Elimination of [S], [AS], and [PS] gives

$$\mathscr{R} = \frac{S_0[k_R^+ K_a K_d a - k_R^- p]}{K_d + K_a K_d a + p} = \frac{k_f a - k_r p}{1 + k_A a + k_P p} \tag{10.16}$$

This result is experimentally indistinguishable from the general form, Equation 10.12, derived in Example 10.1 using the equality-of-rates method. Thus, assuming a particular step to be rate controlling may not lead to any simplification of the intrinsic rate expression. Furthermore, when a simplified form such as Equation 10.15 is experimentally determined, it does not necessarily justify the assumptions used to derive the simplified form. Other models may lead to the same form.

Bimolecular Reactions

Models of surface-catalyzed reactions involving two gas phase reactants can be derived using either the equal-rates method or the method of rate-controlling steps. The latter technique is algebraically simpler and is used in the next example.

EXAMPLE 10.5

Derive a Hougen and Watson-type model for the overall reaction $2A \rightarrow P$ assuming that the surface reaction is the rate-determining step.

SOLUTION: A plausible mechanism for the observed reaction is

$$\begin{aligned} A + S &\rightleftarrows AS \\ 2AS &\longrightarrow PS \\ PS &\rightleftarrows P + S \end{aligned}$$

The adsorption and desorption steps are identical to those in Example 10.4.

$$\frac{[AS]}{a[S]} = \frac{k_a^+}{k_a^-} = K_a \qquad \frac{p[S]}{[PS]} = \frac{k_d^+}{k_d^-} = K_d$$

The rate for the reaction step is

$$\mathscr{R} = k_R[AS]^2$$

The site balance is identical to those in previous examples:

$$S_0 = [S] + [AS] + [PS]$$

Elimination of the surface concentrations gives

$$\mathscr{R} = \frac{S_0^2 K_a^2 k_R a^2}{(1 + K_A a + p/K_d)^2} = \frac{k a^2}{(1 + k_A a + k_P p)^2} \tag{10.17}$$

The retardation due to adsorption appears as a square because two catalytic sites are involved. It is likely that the reaction, a dimerization, requires that the reacting [AS] groups must be physically adjacent for reaction to occur. The square in the denominator is intended to account for this.

Examples of Hougen and Watson kinetic models, which are sometimes called Langmuir–Hinshelwood models, can be derived for a great variety of assumed surface mechanisms. See Butt (1980) and *Perry's Handbook* (1997) for collections of the many possible models. The models usually have numerators that are the same as would be expected for a homogeneous reaction. The denominators reveal the heterogeneous nature of the reactions. They come in almost endless varieties, but all reflect competition for the catalytic sites by the adsorbable species.

10.3.3 Recommended Models

Enthusiastic theoreticians have created far too many models of solid-catalyzed gas reactions. As suggested earlier, it is difficult to distinguish between them given any reasonable experimental program and essentially impossible to distinguish between them if the experimental program is confined to steady-state measurements. Recall the rampaging elephants of Section 7.1. Recall also that Equation 10.10 provides a reasonable fit with no more than $N + 1$ adjustable constants, where N is the number of components including adsorbable inerts. For a solid-catalyzed reaction, the following form is recommended:

$$\mathscr{R} = \frac{\text{rate expression for homogeneous reaction}}{(\text{site competition terms})^n} \tag{10.18}$$

where $n = 1$ if the reaction is unimolecular and $n = 2$ if it is bimolecular. The numerator should contain only one rate constant plus an equilibrium constant if the reaction is reversible. See Section 7.2.2.

For reactions of the form A $\rightleftarrows$ P, the recommended rate expression is

$$\mathscr{R} = \frac{k(a - p/K_{\text{kinetic}})}{1 + k_A a + k_P p + k_I i} \tag{10.19}$$

For reactions of the form A $\rightleftarrows$ P + Q, the recommended rate expression is

$$\mathscr{R} = \frac{k(a - pq/K_{\text{kinetic}})}{1 + k_A a + k_P p + k_Q q + k_I i} \tag{10.20}$$

For reactions of the form $A + B \rightleftarrows$ P, the recommended rate expression is

$$\mathscr{R} = \frac{k(ab - p/K_{\text{kinetic}})}{(1 + k_A a + k_B b + k_P p + k_I i)^2} \tag{10.21}$$

For reactions of the form A + B $\rightleftarrows$ P + Q, the recommended rate expression is

$$\mathscr{R} = \frac{k(ab - pq/K_{\text{kinetic}})}{(1 + k_A a + k_B b + k_P p + k_Q q + k_I i)^2} \tag{10.22}$$

Each of these expressions has a primary rate constant, k,and an equilibrium constant than can be ignored if the reaction is essentially irreversible. The primary rate constant is usually fit to an Arrhenius temperature dependence while the temperature dependence of the equilibrium constant is determined using the methods of Section 7.2. The recommended kinetic expressions also contain an adsorption constant for each reactive component plus a lumped constant for adsorbable inerts. These denominator constants can be fit to an Arrhenius temperature dependence as well, but the activation energies are usually small since the denominator constants are ratios of rate constants and the individual activation energies will tend to cancel. The usual range of temperature measurements is small enough that the denominator constants can be regarded as independent of temperature. The power of 2 in the denominator when the forward reaction is bimolecular is somewhat arbitrary. The same quality fit can usually be achieved using n =1 with different values for the adsorption constants. Proper fitting

of the adsorption constants demands an extensive experimental program where the gas phase concentrations of reactants and products are varied over a wide range.

10.4 EFFECTIVENESS FACTORS

Few fixed-bed reactors operate in a region where the intrinsic kinetics are applicable. The particles are usually large to minimize pressure drop, and this means that diffusion within the pores, steps 3 and 7, can limit the reaction rate. Also, the superficial fluid velocity may be low enough that the external film resistances of steps 2 and 8 become important. A method is needed to estimate actual reaction rates given the intrinsic kinetics and operating conditions within the reactor. The usual approach is to define the ***effectiveness factor*** as

$$\eta = \frac{\text{actual reaction rate}}{\text{rate predicted from intrinsic kinetics}} \tag{10.23}$$

and then to correlate η with the operating conditions in the reactor.

The global design equation used for steps 1 and 9 is modified to include the effectiveness factor:

$$\bar{u}_s \frac{\partial a}{\partial z} = D_r \left[\frac{1}{r} \frac{\partial a}{\partial r} + \frac{\partial^2 a}{\partial r^2} \right] + \varepsilon \eta \mathscr{R}_A \tag{10.24}$$

where $\mathscr{R}_A$ now represents the intrinsic but still pseudohomogeneous kinetics. Suppose the intrinsic kinetics are known and that η has been determined as a function of local operating conditions in the reactor. Then steps 2–8 can be ignored. Their effects are built into the effectiveness factor and the intrinsic kinetics, and the reactor design methods of Chapter 9 can be applied with no changes other than using $\varepsilon \eta \mathscr{R}_A$ as the rate expression.

What is needed at this point is a correlation or other means for estimating η at every point in the reactor. This may be done empirically, for example, by running a single tube of what ultimately will be a multitubular reactor. However, some progress has been made in determining η from first principles. We outline the salient results achieved to date.

10.4.1 Pore Diffusion

The most important mass transfer limitation is diffusion in the micropores of the catalyst. A simplified model of pore diffusion treats the pores as long, narrow cylinders of length $\mathscr{L}$. The narrowness allows radial gradients to be neglected so that concentrations depend only on the distance ℓ from the mouth of the pore. Equation 10.3 governs diffusion within the pore. The boundary condition at the mouth of the pore is

$$a_\ell = a_s \quad \text{at } \ell = 0$$

The other boundary condition is

$$\frac{da_\ell}{d\ell} = 0 \quad \text{at } \ell = \mathscr{L}$$

An analytical solution is possible when the reaction is first order, for example, a reaction of the form A → P with adsorption as the rate-controlling step. Then Equation 10.3 becomes

$$0 = \mathscr{D}_A \frac{d^2 a_\ell}{d\ell^2} - k a_\ell$$

Solution subject to the boundary conditions gives

$$\frac{a_\ell}{a_s} = \frac{\exp(-2\mathscr{L}\sqrt{k/\mathscr{D}_A})\exp(\ell\sqrt{k/\mathscr{D}_A}) + \exp(-\ell\sqrt{k/\mathscr{D}_A})}{1 + \exp(-2\mathscr{L}\sqrt{k/\mathscr{D}_A})}$$

This gives the concentration profile inside the pore, $a_\ell(\ell)$. The total rate of reaction within a pore can be found using the principle of equal rates. The reaction rate within a pore must equal the rate at which reactant molecules enter the pore. Molecules enter by diffusion. The flux of reactants molecules diffusing into a pore of diameter d_{pore} equals the reaction rate. Thus,

$$\begin{aligned}\text{Actual rate} = \mathscr{R}_A &= \left(\tfrac{1}{4}\pi d_{\text{pore}}^2\right)\left[-\mathscr{D}_A \frac{da_\ell}{d\ell}\right]_{\ell=0} \\ &= \left(\tfrac{1}{4}\pi d_{\text{pore}}^2\right) a_s \mathscr{D}_A \sqrt{\frac{k}{\mathscr{D}_A}}\left[\frac{1 - \exp(-2\mathscr{L}\sqrt{k/\mathscr{D}_A})}{1 + \exp(-2\mathscr{L}\sqrt{k/\mathscr{D}_A})}\right]\end{aligned}$$

is the actual rate as affected by pore diffusion. If there were no diffusion limitation inside the pore, the entire volume of the pore would have concentration a_s and the intrinsic rate would apply:

$$\text{Intrinsic rate} = \left(\tfrac{1}{4}\pi d_{\text{pore}}^2\right)\mathscr{L} k a_s$$

The ratio of actual rate to intrinsic rate is the effectiveness factor

$$\eta = \frac{\mathscr{D}_A}{k\mathscr{L}}\sqrt{\frac{k}{\mathscr{D}_A}}\left[\frac{1 - \exp(-2\mathscr{L}\sqrt{k/\mathscr{D}_A})}{1 + \exp(-2\mathscr{L}\sqrt{k/\mathscr{D}_A})}\right] = \frac{\tanh(\mathscr{L}\sqrt{k/\mathscr{D}_A})}{\mathscr{L}\sqrt{k/\mathscr{D}_A}} \tag{10.25}$$

It depends only on $\mathscr{L}\sqrt{k/\mathscr{D}_A}$ which is a dimensionless group known as the ***Thiele modulus***. The Thiele modulus can be measured experimentally by comparing actual rates to intrinsic rates. It can also be predicted from first principles given an estimate of the pore length $\mathscr{L}$. Note that the pore radius does not enter the calculations (although the effective diffusivity will be affected by the pore radius when d_{pore} is less than about 100 nm).

EXAMPLE 10.6

A commercial process for the dehydrogenation of ethylbenzene uses 3-mm spherical catalyst particles. The rate constant is 15 s^{-1}, and the diffusivity of ethylbenzene in steam is $4 \times 10^{-5} m^2$ s^{-1} under reaction conditions. Assume that the pore diameter is large enough that this bulk diffusivity applies. Determine a likely lower bound for the isothermal effectiveness factor.

SOLUTION: The lowest η corresponds to the largest value for $\mathscr{L}$. Suppose $\mathscr{L} = R_p =$ 1.5 mm. Then

$$\mathscr{L}\sqrt{\frac{k}{\mathscr{D}_A}} = 0.92$$

and

$$\eta_{\min} = \frac{\tanh(0.92)}{0.92} = 0.79$$

Many theoretical embellishments have been made to the basic model of pore diffusion as presented here. Effectiveness factors have been derived for reaction orders other than first and for Hougen and Watson kinetics. These require a numerical solution of Equation 10.3. Shape and tortuosity factors have been introduced to treat pores having geometries other than the idealized cylinders considered here. The ***Knudsen diffusivity*** or a combination of Knudsen and bulk diffusivities has been used for very small pores. While these studies have theoretical importance and may help explain some observations, they are not yet developed well enough for predictive use. Our ability to characterize the internal structure of a porous catalyst is still rather rudimentary, and this imposes a basic limitation on theoretical predictions. We give a brief account of Knudsen diffusion.

In bulk diffusion, the predominant interaction of molecules is with other molecules in the fluid phase. This is the ordinary kind of diffusion, and the corresponding diffusivity is denoted as $\mathscr{D}_A$. At low gas densities in small-diameter pores, the mean free path of molecules may become comparable to the pore diameter. Then, the predominant interaction is with the walls of the pore, and diffusion within a pore is governed by the Knudsen diffusivity $\mathscr{D}_K$. This diffusivity is predicted by the kinetic theory of gases to be

$$\mathscr{D}_K = \frac{d_{\text{pore}}}{3}\sqrt{\frac{8R_gT}{\pi M_A}} \tag{10.26}$$

where M_A is the molecular weight of the diffusing species.

EXAMPLE 10.7

Repeat Example 10.6 assuming a pore diameter of 20 nm $= 2 \times 10^{-8}$ m. The reaction temperature is 625°C.

SOLUTION:

$$\mathscr{D}_K = \frac{2 \times 10^{-8}}{3}\sqrt{\frac{8}{\pi}\frac{8.314\,\text{J}}{\text{mol K}}\frac{898\,\text{K}}{0.106\,\text{kg mol}^{-1}}} = 3 \times 10^{-6}\ \text{m}^2\ \text{s}^{-1}$$

This is an order of magnitude less than the bulk diffusivity, and

$$\mathscr{L}\sqrt{\frac{k}{\mathscr{D}_K}} = 3.5 \qquad \eta_{\min} = \frac{\tanh(3.5)}{3.5} = 0.29$$

EXAMPLE 10.8

How fine would you have to grind the ethylbenzene catalyst for laboratory kinetic studies to give the intrinsic kinetics? Assume the pore diameter of Example 10.7.

SOLUTION: Take $\eta = 0.98$ as an adequate approach to the intrinsic kinetics. Setting this value for η and solving Equation 10.25 for $\mathscr{L}\sqrt{k/\mathscr{D}_K}$ gives $\mathscr{L}\sqrt{k/\mathscr{D}_K} = 0.248$. Suppose $k = 15\,\mathrm{s}^{-1}$ and $\mathscr{D}_K = 3 \times 10^{-6}\,\mathrm{m}^2\,\mathrm{s}^{-1}$.

Then $\mathscr{L} = 1.1 \times 10^{-4}\mathrm{m} = 110\ \mu\mathrm{m}$.

The value for $\mathscr{L}$ is conservatively interpreted as the particle diameter. This is a perfectly feasible size for use in a laboratory reactor. Due to pressure drop limitations, it is too small for a full-scale packed bed. However, even smaller catalyst particles, ≈50 μm, are used in fluidized-bed reactors. For such small particles we can assume $\eta = 1$ even for the 3 nm pore diameters found in some cracking catalysts.

When the Knudsen and bulk diffusivities are significantly different, η is determined by the smaller of the two. The pore diameters for most commercial catalysts are in the range 1 to 100 nm. At a typical operating temperature of about 700 K, this gives Knudsen diffusivities in the range of 10^{-6}–$10^{-8}\ \mathrm{m}^2\,\mathrm{s}^{-1}$. Bulk diffusivities at atmospheric pressure will usually be in the range of 10^{-4}–$10^{-6}\ \mathrm{m}^2\ \mathrm{s}^{-1}$. The Knudsen diffusivity is independent of pressure, but the bulk diffusivity varies approximately as P^{-1}. Thus Knudsen diffusion will determine η at low to moderate pressures, but the bulk diffusivity can be limiting at high pressures. When the two diffusivities are commensurate, the combined effect is actually worse than either acting alone. The following equation is adequate for most purposes:

$$\frac{1}{\mathscr{D}_{\mathrm{eff}}} = \frac{1}{\mathscr{D}_K} + \frac{1}{\mathscr{D}_A} \tag{10.27}$$

A more rigorous result together with theoretical justification has been given by Rothfield (1963).

10.4.2 Film Mass Transfer

The concentration of gas over the active catalyst surface at location l in a pore is $a_l(l)$. The pore diffusion model of Section 10.4.1 linked concentrations within the pore to the concentration at the pore mouth, a_s. The film resistance between the external surface of the catalyst (i.e., at the mouth of the pore) and the concentration in the bulk gas phase is frequently small. Thus, $a_s \approx a$ is typical, and the effectiveness factor depends only on diffusion within the particle. However, situations exist where the film resistance also makes a contribution to η so that steps 2 and 8 must be considered. This contribution can be determined using the principle of equal rates; that is, the overall reaction rate equals the rate of mass transfer across the stagnant film at the external surface of the particle. Assume A is consumed by a first-order reaction. The results of the previous section give the overall reaction rate as a function

of the concentration at the external surface, a_s:

$$\mathscr{R}_A = \text{actual rate} = -\left[\frac{\tanh(\mathscr{L}\sqrt{k/\mathscr{D}_A})}{\mathscr{L}\sqrt{k/\mathscr{D}_A}}\right] k a_s \tag{10.28}$$

The overall effectiveness factor for the first-order reaction is defined using the bulk gas concentration a:

$$\mathscr{R}_A = -\eta k a \tag{10.29}$$

The concentrations a_s and a are coupled by the rate of mass transfer across the film:

$$\mathscr{R}_A = k_s A_s (a_s - a) \tag{10.30}$$

Equations 10.28, 10.29, and 10.30 are combined to eliminate a_s and to obtain an expression for $\mathscr{R}_A$ based on the bulk gas phase concentration a. The reaction rate has the form of Equation 10.29 with

$$\eta = \frac{k_s A_s \tanh(\mathscr{L}\sqrt{k/\mathscr{D}_A})}{k_s A_s \mathscr{L}\sqrt{k/\mathscr{D}_A} + k \tanh(\mathscr{L}\sqrt{k/\mathscr{D}_A})} = \frac{k_s A_s \eta_0}{k_s A_s + k\eta_0} \tag{10.31}$$

where η_0 is the effectiveness factor ignoring film resistance; that is, η_0 is given by Equation 10.25.

When multiplied by the void fraction ε, Equation 10.29 is the appropriate reaction rate to use in global models such as Equation 10.1. The reaction rate would be $-\varepsilon k a$ if there were no mass transfer resistance. The effectiveness factor η accounts for pore diffusion and film resistance so that the effective rate is $-\eta\varepsilon k a$.

Typically, the film resistance is important only when the internal pore resistance is also important. If the Thiele modulus is small, the film resistance will usually be negligible. This idea is explored in Problems 10.11 and 10.12.

Reactions other than first order can be treated numerically, but a priori predictions of effectiveness factors are rarely possible even for the simple cases considered here. The approach of Examples 10.6–10.8 can sometimes be used to estimate whether mass transfer resistances are important. When mass transfer is important, effectiveness factors are determined experimentally.

10.4.3 Nonisothermal Effectiveness

Catalyst supports such as silica and alumina have low thermal conductivities so that temperature gradients within catalyst particles are likely in all but the finely ground powders used for intrinsic kinetic studies. There may also be a film resistance to heat transfer at the external surface of the catalyst. Thus the internal temperatures in a catalyst pellet may be substantially different than the bulk gas temperature. The definition of the effectiveness factor, Equation 10.23, is unchanged, but an exothermic reaction can have reaction rates inside the pellet that are higher than would be predicted using the bulk gas temperature. In the absence of a diffusion limitation, $\eta > 1$ would be expected for an exothermic reaction. (The case $\eta > 1$ is also possible for some isothermal reactions with weird kinetics.) Mass transfer limitations may have a larger

effect on the rate than the increased temperature. Thus $\eta < 1$ is also possible for an exothermic reaction. For an endothermic reaction, both the temperature gradient and mass transfer limitation act to lower η so that $\eta < 1$ is expected. In either case, however, an accurate model for η should reflect the temperature gradient within the catalyst particles.

The theory of nonisothermal effectiveness is sufficiently well advanced to allow estimates for η. The analysis requires simultaneous solutions for the concentration and temperature profiles within a pellet. The solutions are necessarily numerical. Solutions are feasible for actual pellet shapes (such as cylinders) but are significantly easier for spherical pellets since this allows a one-dimensional form for the energy equation:

$$\lambda_{\text{eff}} \left(\frac{d^2T}{dr_p^2} + \frac{2}{r_p} \frac{dT}{dr_p} \right) - \mathbf{\Delta H_R}\ \mathscr{R} = 0 \tag{10.32}$$

where r_p is the radial coordinate within a pellet and λ_{eff} is the effective thermal conductivity for the pellet. The boundary conditions associated with Equation 10.32 are $T = T_s$ at the external surface and $dT/dr_p = 0$ at the center of the pellet. Equation 10.32 must be solved simultaneously with component balance equations. The pore diffusion model of Section 10.4.1 is inappropriate for this purpose. Instead, we use a model for mass transfer that is directly compatible with the heat transfer model. This model is

$$\mathscr{D}_{\text{eff}} \left(\frac{d^2a}{dr_p^2} + \frac{2}{r_p} \frac{da}{dr_p} \right) + \mathscr{R}_A = 0 \tag{10.33}$$

subject to the boundary conditions that $a = a_s$ at the external surface and that $da/dr_p = 0$ at the center. Equation 10.33 is obviously consistent with Equation 10.32. Numerical solutions to these simultaneous equations have been given by Weisz and Hicks (1962) for the case of a first-order, irreversible reaction. The solution for η depends on three dimensionless groups: an Arrhenius number $\Delta E \big/ (R_g T_s)$ which is the ratio of the activation temperature to the temperature at the external surface of the particle, a heat generation number

$$\beta = \frac{-\Delta H_R\ \mathscr{D}_{\text{eff}} a_s}{\lambda_{\text{eff}} T_s}$$

and a modified Thiele modulus

$$\frac{d_p}{2} \sqrt{\frac{k}{\mathscr{D}_{\text{eff}}}}$$

Figure 10.3 shows results for an Arrhenius number of 20. With plausible estimates for λ_{eff} and $\mathscr{D}_{\text{eff}}$, the magnitude of η can be calculated. For the special case of $\Delta H_R = 0$ (i.e., $\beta = 0$), Equation 10.33 is an alternate to the pore diffusion model for isothermal effectiveness. It predicts rather different results. For example, suppose $(d_p/2)\sqrt{k/\mathscr{D}_{\text{eff}}} = \mathscr{L}\sqrt{k/\mathscr{D}_A} = 1$. Then Equation 10.25 gives $\eta = 0.76$ while the solution of Equation 10.33 (see Figure 10.3 with $\beta = 0$) gives $\eta = 0.99$. The lesson

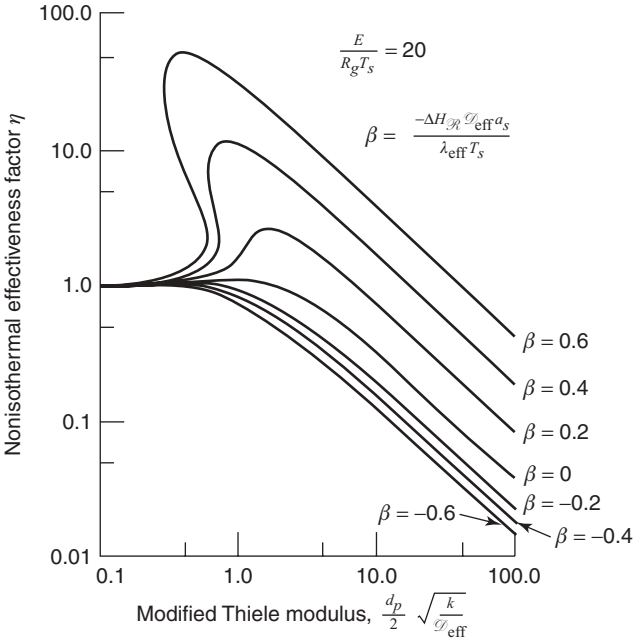

Figure 10.3 Nonisothermal effectiveness factors for first-order reactions in spherical pellets. [Adapted from P. B. Weisz and J. S. Hicks, *Chem. Eng. Sci.,* 17, 265 (1962)].

from this is that $\mathscr{D}_{\text{eff}}$ and $\mathscr{D}_A$ are fundamentally different quantities and have different values for the same physical system.

10.4.4 Deactivation

The definition of effectiveness factor, Equation 10.23, can be expanded to account for deactivation processes that decrease the activity of a catalyst as a function of time. In this context, the intrinsic kinetics in Equation 10.23 should be determined using a new, freshly prepared catalytic surface. The activity of the surface and thus the actual rate of reaction will change with time so that $\eta = \eta(\theta)$ where θ is the time the catalyst has been ***on stream***. It is necessary to consider deactivation processes in reactor designs since they can have a marked effect on process economics and even operability. Deactivation is usually classified as being either physical or chemical in nature, but this classification is somewhat arbitrary. ***Physical deactivation*** includes blocking of pores by entrained solids, loss of active sites due to agglomeration (***site sintering***), closure of pores by internal collapse (***support sintering***), and the reversible loss of active sites by physical adsorption of impurities. ***Chemical deactivation*** includes the irreversible loss of active sites through chemisorption of impurities, loss of sites due to coking, and pore blockage due to coking.

Some deactivation processes are reversible. Deactivation by physical adsorption occurs whenever there is a gas phase impurity that is below its critical point. It can be reversed by eliminating the impurity from the feed stream. This form of deactivation is better modeled using a site competition model that includes the impurities, for example, any of Equations 10.19–10.22, rather than using the effectiveness factor. Water may be included in the reaction mixture so that the water–gas shift reaction will minimize the formation of coke. Off-line decoking can be done by high-temperature oxidation. Deactivation by chemisorption can be modeled using a time-dependent effective factor and requires a chemical treatment to remove the chemically bonded poison from the catalytic surface. Except for physical adsorption, catalytic activity can never be restored completely. Even with continuous reactivation, the catalyst will gradually decline in activity and have a finite life that must be considered in the overall process economics. A change of catalyst for a large reactor can cost millions of dollars.

The catalyst used in fluidized-bed catalytic crackers is deactivated by the coking that occurs during one pass through the reactor, a matter of seconds. Other catalysts can last for years, with the gradual decline in activity being accommodated by a gradual increase in reaction temperature. The effectiveness factor may decrease by a factor of 5 before the catalyst is changed. The selectivity of the reaction will usually drop during the course of the run. The decision to change the catalyst is usually based on this loss of selectivity but can be based on a temperature limitation imposed by materials of construction.

Some deactivation processes lower the number of active sites S_0. Others add mass transfer resistances. In either case, they cause a reduction in the reaction rate that is reflected by a time-dependent effectiveness factor:

$$[\text{Actual rate}] = \eta(\theta)\ [\text{intrinsic rate of fresh catalyst}] \tag{10.34}$$

Some progress has been made in developing theoretical expressions for $\eta(\theta)$ for deactivation processes such as coking. Deactivation by loss of active sites can be modeled as a chemical reaction proceeding in parallel with the main reaction. It may be substantially independent of the main reaction. Site sintering, for example, will depend mainly on the reaction temperature. It is normally modeled as a second-order reaction:

$$\frac{dS_0}{d\theta} = -k_S S_0^2$$

The number of active sites is a multiplicative factor in the rate of the main reaction. See, for example, Equations 10.11 and 10.16. Thus, the decline in reaction rate can be modeled using a time-dependent effectiveness factor. A reasonable functional form is

$$\eta(\theta) = \frac{\eta_0}{1 + k_D\theta} \tag{10.35}$$

which results from the second-order model of site sintering. An alternative to Equation 10.35 is a first-order model:

$$\eta(\theta) = \eta_0 \exp(-k_D\theta) \tag{10.36}$$

It is necessary to determine $\eta(\theta)$ under reaction conditions, and a life test should be included in any catalyst development effort. The data from this test will allow η to be fitted as a function of time on stream, θ. Equations 10.35 and 10.36 can obviously be used to model deactivation processes other than site sintering, and k_D can be regarded as an empirical constant with units of reciprocal time.

Typically, $(k_D)^{-1} \gg \bar{t}$, and the global design equation (e.g., Equation 10.1) can be solved independently of the deactivation process. The packed-bed reactor will operate at an approximate steady state that will track the slowly changing catalyst activity. The rate at which this slow change occurs dictates the process design. If the catalyst deactivates in seconds, continuous regeneration is necessary, and fixed-bed reactors are infeasible. Fluidized-bed and other moving-solids reactors are used to continuously circulate the catalyst between reaction and regeneration zones. If the catalyst degenerates in days, fixed-bed reactors are usually regenerated in situ. Typically, several packed beds in parallel are operated in a swing cycle between reaction and regeneration modes. If the catalyst degenerates in years, the new catalyst is charged and the spent catalyst is returned to the vendor for regeneration or recovery of valuable components such as precious metals.

Do not infer from the above discussion that all the catalyst in a fixed bed ages at the same rate. This is not usually true. Instead, the time-dependent effectiveness factor will vary from point to point in the reactor. The deactivation rate constant k_D will be a function of temperature. It is usually fit to an Arrhenius temperature dependence. For chemical deactivation by chemisorption or coking, deactivation will normally be much higher at the inlet to the bed. In extreme cases, a sharp deactivation front will travel slowly down the bed. Behind the front, the catalyst is deactivated so that there is little or no conversion. At the front, the conversion rises sharply and becomes nearly complete over a short distance. The catalyst ahead of the front does nothing, but it remains active until the front advances to it. When the front reaches the end of the bed, the entire catalyst charge is regenerated or replaced.

10.5 EXPERIMENTAL DETERMINATION OF INTRINSIC KINETICS

A CSTR is the preferred method for measuring intrinsic kinetics. The finely ground catalyst is packed into a short, fixed bed within a recycle reactor such as that shown in Figure 4.2. Alternatively, the catalyst is put in a mesh cage and rotated at high speed so that the catalyst and cage act as the agitator of a CSTR. The reaction rate for component A is calculated as if the reaction were homogeneous:

$$\mathscr{R}_A = \frac{a_{\text{out}} - a_{\text{in}}}{\bar{t}} = \frac{a_{\text{out}} - a_{\text{in}}}{(\varepsilon V / Q_{\text{out}})} \tag{10.37}$$

The mass of the catalyst does not appear. However, physical intuition or the S_0 terms in Equations 10.11 and 10.16 suggest that doubling the amount of catalyst should double the reaction rate. How are rate data taken on a CSTR translated to a packed-bed reactor or even to another CSTR operating with a different catalyst density?

Homogeneous reactions occur in the fluid phase, and the volume available for reaction is εV. Solid-catalyzed reactions occur on the catalyst surface, and the area available for the reaction is $V\rho_c a_c$, where V is the total reactor volume (i.e., gas plus catalyst), ρ_c is the average density of catalyst in the reactor (i.e., mass of catalyst per total reactor volume), and a_c is the surface area per mass of catalyst. The pseudohomogeneous reaction rate calculated using Equation 10.37 is multiplied by εV to get the rate of formation of component A in moles per time. The equivalent heterogeneous rate is based on the catalyst surface area and is multiplied by $V\rho_c a_c$ to obtain the rate of formation of component A in moles per time. Setting the two rates equal gives

$$\varepsilon V \mathscr{R}_{\text{homogeneous}} = V\rho_c a_c \mathscr{R}_{\text{heterogeneous}}$$

The void fraction used in this equation and in Equation 9.1 should be the ***total void fraction*** that includes pore volume. We now distinguish it from the ***superficial void fraction*** used in the Ergun equation and in the packed-bed correlations of Chapter 9. The pore volume is accessible to gas molecules and can constitute a substantial fraction of the gas phase volume. Pore volume is included in reaction rate calculations through the use of the total void fraction. The superficial void fraction ignores the pore volume. It is the appropriate parameter for the hydrodynamic calculations because fluid velocities go to zero at the external surface of the catalyst particles. The pore volume is accessible by diffusion, not bulk flow.

The homogeneous and heterogeneous rates are related by

$$\mathscr{R}_{\text{homogeneous}} = \frac{\rho_c a_c}{\varepsilon_{\text{total}}} \mathscr{R}_{\text{heterogeneous}} \tag{10.38}$$

and Equation 10.1 should be written as

$$\bar{u}_s \frac{\partial a}{\partial z} = D_r \left[\frac{1}{r} \frac{\partial a}{\partial r} + \frac{\partial^2 a}{\partial r^2} \right] + \varepsilon_{\text{total}}\, \eta(\theta) [\mathscr{R}_A]_{\text{intrinsic pseudohomogeneous}} \tag{10.39}$$

However, the intrinsic pseudohomogeneous rate used in Equation 10.39 is not identical to the rate determined from the CSTR measurements since the catalyst density will be different. The correction procedure is as follows:

1. Calculate $\mathscr{R}_A$ from the CSTR data using Equation 10.37.
2. Divide by the stoichiometric coefficient for component A, ν_A, to obtain $\mathscr{R}_{\text{homogeneous}}$ for the CSTR.
3. Use Equation 10.38 to calculate $\mathscr{R}_{\text{heterogeneous}}$ using the CSTR values for ρ_c, a_c, and $\varepsilon_{\text{total}}$.
4. Determine ρ_c, a_c, and $\varepsilon_{\text{total}}$ for the packed bed.
5. Use Equation 10.38 again, now determining $\mathscr{R}_{\text{homogeneous}}$ for the packed bed.

Alternatively, write the global design equation as

$$\bar{u}_s \frac{\partial a}{\partial z} = D_r \left[\frac{1}{r} \frac{\partial a}{\partial r} + \frac{\partial^2 a}{\partial r^2} \right] + \eta(\theta) \rho_c a_c \left[\mathscr{R}_A \right]_{\text{heterogeneous}} \tag{10.40}$$

Note that $[\mathscr{R}_A]_{\text{heterogeneous}}$ has units of moles per square meter per second but remains a function of gas phase concentrations.

EXAMPLE 10.9

A recycle reactor containing 101 g of catalyst is used in an experimental study. The catalyst is packed into a segment of the reactor having a volume of 125 cm^3. The recycle lines and pump have an additional volume of 150 cm^3. The particle density of the catalyst is 1.12 g cm^{-3}, its internal void fraction is 0.505, and its surface area is 400 $\text{m}^2\ \text{g}^{-1}$. A gas mixture is fed to the system at 150 $\text{cm}^3\ \text{s}^{-1}$. The inlet concentration of reactant A is 1.6 mol m^{-3}. The outlet concentration of reactant A is 0.4 mol m^{-3}. Determine the intrinsic pseudohomogeneous reaction rate, the rate per unit mass of catalyst, and the rate per unit surface area of catalyst. The reaction is A $\rightarrow$ P so $\nu_A = -1$.

SOLUTION: The gas phase volume $\varepsilon_{\text{total}} V$ is the entire reactor except for the volume taken up by mechanical parts and by the skeleton of the catalyst particle:

$$\varepsilon_{\text{total}} V = 125 + 150 - \frac{101}{1.12}(1 - 0.505) = 230\,\text{cm}^3$$

$$\varepsilon_{\text{total}} = \frac{230}{275} = 0.836$$

$$\bar{t} = \frac{230\,\text{cm}^3}{150\,\text{cm}^3\ \text{s}^{-1}} = 1.53\,\text{s}$$

The intrinsic pseudohomogeneous rate as determined using the CSTR is

$$[\mathscr{R}_A]_{\text{homogeneous}} = \mathscr{R}_A = \frac{0.4 - 1.6}{1.53} = -0.783\,\text{mol}\ \text{m}^{-3}\ \text{s}^{-1}$$

The average density of the catalyst is

$$\rho_c = \frac{101}{275} = 0.367\text{g}\ \text{cm}^{-3} = 367\,\text{kg}\ \text{m}^{-3}$$

and

$$[\mathscr{R}_A]_{\text{catalyst mass}} = \frac{\varepsilon_{\text{total}} \mathscr{R}_A}{\rho_c} = -1.78 \times 10^{-3}\,\text{mol}\ \text{kg}^{-1}\ \text{s}^{-1}$$

$$[\mathscr{R}_A]_{\text{heterogeneous}} = [\mathscr{R}_A]_{\text{surface area}} = \frac{\varepsilon_{\text{total}} \mathscr{R}_A}{\rho_c a_c} = -4.45 \times 10^{-9}\,\text{mol}\ \text{m}^{-2}\ \text{s}^{-1}$$

Example 10.9 used two different definitions of the catalyst density and at least two more definitions are in common usage. The value $\rho_c = 367$ refers to the ***reactor average density***. It is quite low in the example because so much of the reactor volume is empty. Normally, the reactor would be packed almost completely, and the reactor average density would approach the ***bulk density***. The bulk density is what would be

measured if the catalyst were dumped into a large container and gently shaken. The bulk density is not stated in the example, but it would be about 800 kg m^{-3} for the catalyst pellets prior to grinding. The catalyst will pack to something less that the bulk density in a small-diameter tube. The ***pellet density*** in the example is 1120 kg m^{-3}. It is the mass of a catalyst pellet divided by the external volume of the pellet. The final density is the ***skeletal density*** of the pellet. It is the density of the solid support and equals $1120/(1-0.505) = 2260$ kg m^{-3} for the example catalyst. The various densities fall in the order

$$\rho_c < \rho_{\text{bulk}} < \rho_{\text{pellet}} < \rho_{\text{skeletal}}.$$

EXAMPLE 10.10

Suppose the reaction in Example 10.9 is first order. Determine the pseudohomogeneous rate constant, the rate constant based on catalyst mass, and the rate constant based on catalyst surface area.

SOLUTION: Since $\mathscr{R}_A = -ka_{\text{out}}$ for a CSTR, the rates in the previous example are just divided by the appropriate exit concentrations to obtain k**.** The ordinary gas phase concentration is used for the pseudohomogeneous rate:

$$k_{\text{homogeneous}} = \frac{0.783}{0.4} = 1.96 \text{ s}^{-1}$$

The reactant concentration per unit mass is used for the rate based on catalyst mass:

$$[a_{\text{out}}]_{\text{catalyst mass}} = \frac{\varepsilon_{\text{total}} a_{\text{out}}}{\rho_c} = 9.11 \times 10^{-4} \text{mol kg}^{-1}$$

$$k_{\text{catalyst mass}} = \frac{[\mathscr{R}_A]_{\text{catalyst mass}}}{[a_{\text{out}}]_{\text{catalyst mass}}} = 1.96 \text{ s}^{-1}$$

Similarly,

$$k_{\text{surface areas}} = \frac{[\mathscr{R}_A]_{\text{surface area}}}{[a_{\text{out}}]_{\text{surface area}}} = \frac{[\mathscr{R}_A]_{\text{surface area}}}{\frac{\varepsilon_{\text{total}}\ a_{\text{out}}}{\rho_c a_c}} = \frac{4.45 \times 10^{-9}}{2.28 \times 10^{-9}} = 1.96 \text{ s}^{-1}$$

EXAMPLE 10.11

The piping in the recycle reactor of Example 10.9 has been revised to lower the recycle line and pump volume to 100 cm^3. What effect will this have on the exit concentration of component A if all other conditions are held constant?

SOLUTION: The catalyst charge is unchanged. If the reaction is truly heterogeneous and there are no mass transfer resistances, the rate of reaction of the component should be unchanged. More specifically, the pseudohomogeneous rate for the CSTR will change since the

gas phase volume and residence time change, but the heterogeneous rate should be the same:

$$\varepsilon_{\text{total}} V = 125 + 100 - \frac{101}{1.12}(1 - 0.505) = 180\,\text{cm}^3$$

$$\varepsilon_{\text{total}} = \frac{180}{225} = 0.800$$

$$\rho_c = \frac{101}{225} = 0.449\,\text{g cm}^{-3} = 449\,\text{kg m}^{-3}$$

$$\bar{t} = \frac{180\,\text{cm}^3}{150\,\text{cm}^3\,\text{s}^{-1}} = 1.20\,\text{s}$$

Assume $[\mathscr{R}_A]_{\text{catalyst mass}} = \varepsilon_{\text{total}} \mathscr{R}_A / \rho_c = -1.78 \times 10^{-3}\,\text{mol kg}^{-1}\text{s}^{-1}$ as in Example 10.9, and convert to a pseudohomogeneous rate for the CSTR:

$$[\mathscr{R}_A]_{\text{homogeneous}} = \frac{\rho_c [\mathscr{R}_A]_{\text{catalyst mass}}}{\varepsilon_{\text{total}}} = -0.999\,\text{mol m}^{-3}\,\text{s}^{-1}$$

Now assume $a_{\text{in}} = 1.6\,\text{mol m}^{-3}$ and use Equation 10.38 to find a_{out}. The result is

$$a_{\text{out}} = a_{\text{in}} + \bar{t}[\mathscr{R}_A]_{\text{homogeneous}} = 0.401\,\text{mol m}^{-3}$$

This is identical within rounding error to the exit concentration in Example 10.9.

It is a good idea to run the laboratory reactor without catalyst to check for homogeneous reactions. However, this method does not work when the homogeneous reaction involves reactants that do not occur in the feed but are created by a heterogeneous reaction. It then becomes important to maintain the same ratio of free volume to catalyst volume in the laboratory reactor used for intrinsic kinetic studies as in the pilot or production reactors.

10.6 UNSTEADY OPERATION AND SURFACE INVENTORIES

The global design equations for packed beds, (e.g., Equations 10.1, 10.9, 10.39, and 10.40) all have the same limitation as does the axial dispersion model treated in Chapter 9. They all assume steady-state operation. Adding an accumulation term $\partial a / \partial t$ accounts for the change in the gas phase inventory of component A but not for the surface inventory of A in the adsorbed form. The adsorbed inventory can be a large multiple of the gas phase inventory.

EXAMPLE 10.12

Estimate the surface inventory of component A for the catalytic CSTR in Example 10.9. Assume that the surface reaction is rate-controlling and that A is the only adsorbed species. Suppose A is a moderately large molecule that occupies a site that is 1 nm × 1 nm.

SOLUTION: If the surface reaction controls the overall rate, all the active sites will be occupied. Assume that the entire surface is active so that it will be covered with a monolayer of A molecules. The surface area is $101(400) = 40400\ \text{m}^2$ (4 ha or 10 U.S. acres!).

$$\text{Adsorbed A} = \frac{40400}{10^{-18}} = 4 \times 10^{22}\ \text{molecules} = 0.067\ \text{mol}$$

$$\text{Gas phase A} = (0.4\ \text{mol m}^{-3})(230 \times 10^{-6}\ \text{m}^3) = 9.2 \times 10^{-5}\ \text{mol}$$

Thus the surface contains 700 times more A than the gas phase.

EXAMPLE 10.13

How long will it take the reactor in Example 10.9 to achieve steady state?

SOLUTION: The surface is estimated to contain 0.067 mol of A in adsorbed form. The inlet gas contains 1.6 mol A m^{-3} and is flowing at 150 $\text{cm}^3\ \text{s}^{-1}$ so that A is entering the reactor at a rate of 0.00024 mol s^{-1}. Five minutes is needed to supply the surface if all the incoming gas were adsorbed. Fifteen to 30 min would be a reasonable startup time. Recall that the reactor has a gas phase residence time V/Q_{out} of only 1.5 s! The mean residence time of the adsorbed species is 700 times larger than that for a nonadsorbed molecule.

Anyone wishing to model the startup transient of a packed-bed reactor or to explore the possible benefits of periodic operation on selectivity should consider whether surface inventories are significant. The above examples show that they certainly can be. The unsteady versions of equations like 10.1 should be supplemented with separate component balances for the adsorbed species. It may also be necessary to write separate energy balances for the gas and solid phases. Chapter 11 gives the general methodology for treating the component and energy balances in multiphase reactors, but implementation requires considerable sophistication.

The presence of surface inventories does not prevent solution of the steady-state design equations (e.g., Equations 10.1, 10.9, 10.39, and 10.40) by the method of false transients. Just add an accumulation term $\partial a/\partial t$ to the equation and use the method outlined in Chapter 16. However, the transient approach to the steady state will be faster than it would be in real time.

SUGGESTED FURTHER READINGS

A chemical engineering classic is:

J. M. Smith, *Chemical Engineering Kinetics,* 3rd ed., McGraw-Hill, New York, 1981.

Another standard text that emphasizes gas-solid reactions is:

J. B. Butt, *Reaction Kinetics and Reactor Design*, 2nd ed., Marcel Dekker, New York, 2000.

For an extensive but qualitative review of catalyst deactivation see:

C. Bartholomew, Catalyst deactivation and regeneration, in *Kirk-Othmer Encyclopedia of Chemical Technology*, Wiley, Hoboken, NJ, 2003.

PROBLEMS

10.1 The precursor result from which Equation 10.13 was obtained is

$$\mathscr{R} = \frac{S_0[(k_a^+ k_R^+ k_d^+)a - (k_a^- k_R^- k_d^-)p}{(k_a^- k_R^- + k_a^- k_d^+ + k_R^+ k_d^+) + k_a^+(k_R^+ + k_R^- + k_d^+)a + k_d^-(k_a^- + k_R^+ + k_R^-)p}$$

Take the limit as k_a^+ and k_a^- both approach zero with a fixed ratio between them, $k_a^+ / k_a^- = K_a$. The magnitude of $\mathscr{R}$ decreases and the functional form changes. Explain the physical basis for these changes.

10.2 What happens to $\mathscr{R}$ in Problem 10.1 when desorption is rate controlling?

10.3 Repeat Examples 10.3 and 10.4 for the case where desorption is rate controlling.

10.4 The Eley–Rideal mechanism for gas–solid heterogeneous catalysis envisions reaction between a molecule adsorbed on the solid surface and one that is still in the gas phase. Consider a reaction of the form

$$\mathrm{A} + \mathrm{B} \rightarrow \mathrm{P}$$

There are two logical possibilities for the reaction mechanism:

(a) A(gas) + BS(solid) → PS(solid)

(b) A(gas) + BS(solid) → P(gas) + S(solid)

Determine the form of the pseudohomogeneous, intrinsic kinetics for each of these cases. Assume that the surface reaction step, as shown above, is rate limiting.

10.5 The ethylbenzene dehydrogenation catalyst of Example 3.1 has a first-order rate constant of 3.752 s^{-1} at 700°C. How does this compare to the catalyst used by Wenner and Dybdal (1948)? They reported

$$k = 12{,}600 \exp \frac{-19{,}800}{T}$$

where $\mathscr{R} = k P_{\mathrm{EB}}$ with k in pound moles per hour per atmosphere per pound of catalyst and T in degrees Rankine and P_{EB} is the partial pressure of ethylbenzene in atmospheres. The bulk density of the catalyst is 90 lb ft^{-3} and the void fraction is 0.4.

10.6 An observed, gas solid-catalyzed reaction is A + B → P. Suppose the surface mechanism is

$$\begin{aligned}
\mathrm{A} + \mathrm{S} &\rightleftarrows \mathrm{AS} & \frac{[\mathrm{AS}]}{a[\mathrm{S}]} &= K_{\mathrm{I}} \\
\mathrm{B} + \mathrm{S} &\rightleftarrows \mathrm{BS} & \frac{[\mathrm{BS}]}{b[S]} &= K_{\mathrm{II}} \\
\mathrm{AS} + \mathrm{BS} &\xrightarrow{k} \mathrm{PS} + \mathrm{S} & \mathscr{R} &= k[\mathrm{AS}][\mathrm{BS}] \\
\mathrm{PS} &\rightleftarrows \mathrm{P} + \mathrm{S} & \frac{p[\mathrm{S}]}{[\mathrm{PS}]} &= K_{\mathrm{IV}}
\end{aligned}$$

Determine the functional form of the rate equation.

10.7 The following surface mechanism has been evoked to explain an observed reaction:

$$A_2 + 2S \rightleftarrows 2AS \quad \text{(I)}$$

$$B + S \rightleftarrows BS \quad \text{(II)}$$

$$AS + BS \rightleftarrows CS + DS \quad \text{(III)}$$

$$CS \rightleftarrows C + S \quad \text{(IV)}$$

$$DS \rightleftarrows D + S \quad \text{(V)}$$

(a) What is the observed reaction?

(b) Develop a Hougen and Watson kinetic model assuming reaction III is rate controlling.

10.8 Repeat Problem 10.7 assuming that reaction I is rate controlling.

10.9 The catalytic hydrogenation of butyraldehyde to butanol,

$$H_2 + C_3H_7CH(=O) \rightleftarrows C_3H_7CH_2OH$$

has a reported (Cropley *et al*. (1984) rate equation of the form

$$\mathscr{R} = \frac{k(P_{H_2}P_{Bal} - P_{BOH}/K_{eq})}{(1 + K_1P_{H_2} + K_2P_{BAL} + K_3P_{BOH})^2}$$

where P_{H_2}, P_{BAL} and P_{BOH} are the partial pressures of hydrogen, butyraldehyde, and butanol, respectively.

(a) Develop a surface reaction model to rationalize the observed form of the kinetics.

(b) Is K_{eq} the thermodynamic or kinetic equilibrium constant? Is it a function of pressure?

10.10 Bimolecular reactions are sometimes catalyzed using two different metals dispersed on a common support. A mechanism might be

$$A + S_1 \rightleftarrows AS_1$$

$$B + S_2 \rightleftarrows BS_2$$

$$AS_1 + BS_2 \rightleftarrows PS_1 + QS_2$$

$$PS_2 \rightleftarrows P + S_2$$

$$QS_2 \rightleftarrows Q + S_2$$

Derive a Hougen and Watson kinetic model assuming that the surface reaction is rate controlling.

10.11 Consider a nonporous catalyst particle where the active surface is all external. There is obviously no pore resistance, but a film resistance to mass transfer can still exist. Determine the isothermal effectiveness factor for first-order kinetics. *Hint:* The actual reaction rate is $\mathscr{R}_A = -ka_s$.

10.12 Refer to Equation 10.31 and consider a catalyst pellet (not finely ground) for which $\eta_0 \approx 1$. What will be the value of η when film resistance is included? The obvious answer to this question is also the solution to Problem 10.11, but go one step beyond the obvious and ask what is likely to be the magnitude of k when $\eta_0 \approx 1$. What does this imply for η?

10.13 A platinum catalyst supported on Al_2O_3 is used for the oxidation of sulfur dioxide:

$$SO_2 + {}^1\!/_2\, O_2 \rightarrow SO_3 \qquad \Delta H_R = -95 \text{ kJ mol}^{-1}$$

The catalyst consists of 3-mm pellets that pack to a bulk density of 1350 kg m^{-3} and $\varepsilon = 0.5$. Mercury porosimetry has found $R_{\text{pore}} = 5$ nm. The feed mixture to a differential reactor consisted of 5 mol % SO_2 and 95 mol % air. The following initial rate data were obtained at atmospheric pressure:

T, K	$\mathscr{R}$, mol h^{-1}(g catalyst)$^{-1}$
653	0.031
673	0.053
693	0.078
713	0.107

Do an order-of-magnitude calculation for the nonisothermal effectiveness factor. ***Hint:*** Use the pore model to estimate an isothermal effectiveness factor and obtain $\mathscr{D}_{\text{eff}}$ from that. Assume $\lambda_{\text{eff}} = 0.15$ J m^{-1} s^{-1} K.

10.14 Suppose that catalyst pellets in the shape of right-circular cylinders have a measured effectiveness factor η when used in a packed-bed reactor for a first-order reaction. In an effort to increase catalyst activity, it is proposed to use a pellet with a central hole of radius $R_h < R_p$. Determine the best value for R_h/R_p based on an effective diffusivity model similar to Equation 10.33. Assume isothermal operation; ignore any diffusion limitations in the central hole, and assume that the ends of the cylinder are sealed to diffusion. You may assume that k, R_p, and $\mathscr{D}_{\text{eff}}$ are known.

Hints: First convince yourself that there is an optimal solution by considering the limiting cases of η near zero where a large hole can almost double the catalyst activity and of η near unity where any hole hurts because it removes catalyst mass. Then convert Equation 10.33 to the form appropriate to an infinitely long cylinder. Brush up on your Bessel functions or trust your symbolic manipulator if you go for an analytical solution. Figuring out how to best display the results is part of the problem.

10.15 Work Problem 10.14 using the pore diffusion model rather than the effective diffusivity model.

10.16 Charge the reactor with the optimized pellets from Problem 10.14 or 10.15. What does it do to the value for $\eta(\theta)\rho_c a_c[\mathscr{R}_A]_{\text{heterogeneous}} = \eta(\theta)\varepsilon_{\text{total}}[\mathscr{R}_A]_{\text{homogeneous}}$ used to model the reactor? If you have not worked Problem 10.14 or 10.15, assume the new pellet increases the reaction rate per pellet by a factor of 1.5 when $R_h/R_p = 0.5$.

Chapter 11

Multiphase Reactors

The packed-bed reactors discussed in Chapters 9 and 10 are multiphase reactors, but the solid phase is stationary, and convective flow occurs only through the fluid phase. The reaction kinetics are pseudohomogeneous, and component balances are written only for the fluid phase.

Chapter 11 treats reactors where mass and component balances are needed for at least two phases and where there is interphase mass transfer. Most examples have two fluid phases, typically gas–liquid. Reaction is usually confined to one phase, although the general formulation allows reaction in any phase. A third phase, when present, is usually solid and usually catalytic. The solid phase may be either mobile or stationary. Some example systems are given in Table 11.1.

When two or more phases are present, it is rarely possible to design a reactor on a strictly first-principles basis. Rather than starting with the mass, energy, and momentum transport equations as was done for the laminar flow systems in Chapter 8, we tend to use simplified flow models with empirical correlations for mass transfer coefficients and interfacial areas. The approach is conceptually similar to that used for friction factors and heat transfer coefficients in turbulent flow systems. It usually provides an adequate basis for design and scaleup, although extra care must be taken to confirm that the correlations are appropriate.

Multiphase reactors can be batch, fed batch, or continuous. Most of the design equations derived in this chapter are general and apply to any of these operating modes. They will be derived for unsteady operation. The unsteady material balances include the inventories in both phases and mass transfer between the phases so that steady-state solutions found by the method of false transients will be true transients if the initial conditions are correct. Compare Section 10.6.

11.1 GAS–LIQUID AND LIQUID–LIQUID REACTORS

After specifying the phases involved in the reaction, it is necessary to specify the contacting regimes. The ideal contacting regimes for reactors with two fluid phases are as follows:

1. Both phases are perfectly mixed.
2. One phase is perfectly mixed and the other phase is in piston flow.

Chemical Reactor Design, Optimization, and Scaleup, Second Edition. By E. B. Nauman
Copyright © 2008 John Wiley & Sons, Inc.

Table 11.1 Examples of Multiphase Reactors

Reaction	First Phase	Second Phase	Third Phase
Phenol alkylation	Phenol	Gaseous alkenes	None
Refinery alkylation	Liquid alkanes (e.g., isobutane)	Gaseous alkenes (e.g., 1-butene)	HF or H_2SO_4
Aerobic fermentation	Water + organic carbon source	Air	Bacteria
Anaerobic fermentation	Water + sugar	Carbon dioxide	Yeast
Fluidized catalytic cracking (FCC)	Heavy oils, C_{18}+	Fluidized catalyst particles	None
Trickle bed hydrocracking	Refinery residues, C_{30}+	Hydrogen	Stationary catalyst particles

3. The phases are in countercurrent piston flow.
4. The phases are in cocurrent piston flow.

These simple situations can be embellished. For example, the axial dispersion model can be applied to the piston flow elements. However, uncertainties in reaction rates and mass transfer coefficients may mask secondary effects such as axial dispersion.

There is a realistic fifth possibility in stirred tank reactors:

5. The continuous phase is well mixed but there is a dispersed phase. The particles in the dispersed phase behave as PFRs. They are in contact with the continuous phase but are isolated from each other and have an exponential distribution of residence times. This case is treated in Examples 11.17 and 15.12.

11.1.1 Two-Phase Stirred Tank Reactors

Stirred tanks are often used for gas–liquid reactions. The usual geometry is for the liquid to enter at the top of the reactor and to leave at the bottom. The gas enters through a sparge ring underneath the impeller and leaves through the vapor space at the top of the reactor. A simple but effective way of modeling this and many similar situations is to assume perfect mixing within each phase.

Figure 11.1 gives a conceptual view of a ***two-phase, continuous flow, stirred tank reactor,*** that is, a two-phase CSTR. For convenience we refer to one phase as being liquid and to the other as being gas, but the mixing and contacting scheme shown in Figure 11.1 can also apply to liquid–liquid systems. It can even apply to two gas phases separated by a membrane. Both phases are assumed to be internally homogeneous. They contact each other through an interface that has area A_i, with units of area per unit volume. The total interfacial area is $A_i V$, where $V = V_l + V_g$ is the ***working volume*** in the reactor as measured under operating conditions. The working volume ends at the top of the liquid level and is measured while gas is being

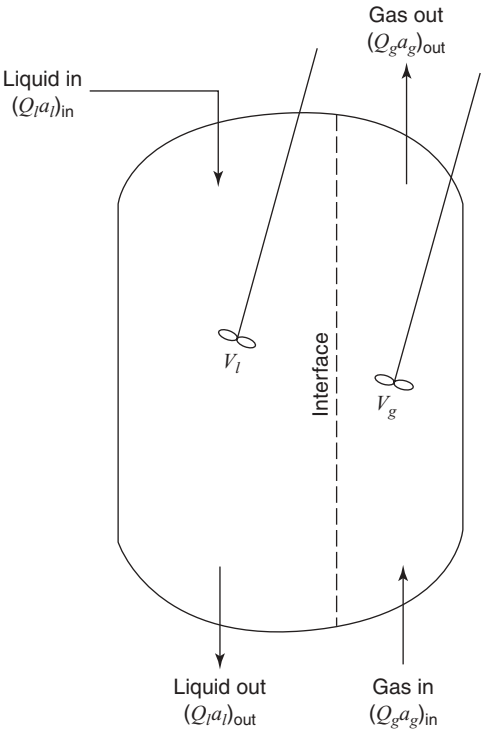

Figure 11.1 Two-phase, continuous flow stirred tank reactor.

added (i.e., the ***gassed*** condition). The working volume excludes the vapor space at the top of the reactor. The ***gas phase holdup*** is the ratio V_g/V and the ***liquid phase holdup*** is V_l/V. The interfacial area $A_i V$ usually excludes the contact area between the vapor space and the liquid at the top of the reactor. The justification for this is that most gas–liquid reactors have gas bubbles as a dispersed phase. This gives a much larger interfacial area than the nominal contact area at the top of the reactor. There are exceptions, for example, polyester reactors where byproduct water is removed only through the nominal interface at the top of the reactor, but these are old and inefficient designs. This nominal area scales as $S^{2/3}$ while the contact area with a dispersed phase can scale as S.

Mass Transfer Rates

Mass transfer occurs across the interface. The rate of mass transfer is proportional to the interfacial area and the concentration driving force. Suppose component A is being transferred from the gas to the liquid. The concentration of A in the gas phase is a_g and the concentration of A in the liquid phase is a_l. Both concentrations have units of moles per cubic meter, but they are not directly comparable because they are in different phases. This fact makes mass transfer calculations more complicated than

heat transfer calculations since the temperature is the temperature regardless of what phase it is measured in, and the driving force for heat transfer across an interface is just the temperature difference $T_g - T_l$. For mass transfer, the driving force is not $a_g - a_l$. Instead, one of the concentrations must be converted to its equivalent value in the other phase.

The conversion is done using the equilibrium relationship between the gas- and liquid phase concentrations, typically Henry's law. Thus the gas phase concentration that is equivalent to a_l is $K_H a_l$, where K_H is ***Henry's law constant***:

$$a_g^* = K_H a_l^* \tag{11.1}$$

Henry's law constant is dimensionless when a_g and a_l have units of moles per cubic meter, but published values for K_H sometimes have units of atmospheres or torr per mole fraction. Thus the gas phase concentration is often expressed in terms of its partial pressure and the liquid phase concentration is expressed as a mole fraction. The asterisks in Equation 11.1 remind us that Henry's law is an equilibrium relationship. Equation 11.1 is not satisfied merely because gas and liquid phases are brought in brief contact. Instead, the difference between a_g and its liquid phase equivalent, $K_H a_l$, provides the driving force for mass transfer that could ultimately lead to equilibrium and the satisfaction of Equation 11.1:

$$\text{Mass transfer rate} = K_g A_i V (a_g - K_H a_l) \tag{11.2}$$

where K_g is the overall mass transfer coefficient based on the equivalent gas phase driving force, $a_g - K_H a_l$, and A_i is the ***interfacial area per unit volume*** of the reactor. As written, the mass transfer rate is positive when mass is transferred from the gas phase to the liquid phase, but this is arbitrary.

Equation 11.2 replaces the liquid phase concentration with an equivalent gas phase concentration. It is obviously possible to do it the other way, replacing the gas phase concentration with an equivalent liquid concentration. Then

$$\text{Mass transfer rate} = K_l A_i V \left(\frac{a_g}{K_H} - a_l \right) \tag{11.3}$$

where K_l is the overall mass transfer coefficient based on the equivalent liquid phase driving force, $a_g/K_H - a_l$.

Equations 11.2 and 11.3 base the driving force on concentrations that have normal SI units of moles per cubic meter. Experimental measurements and literature correlations usually give the composite quantity $K_g A_i$ rather than the individual variables. Units for the composite quantities $K_g A_i$ and $K_l A_i$ are reciprocal seconds. By themselves K_g and K_l have units of velocity, meters per second. Concentrations units are appropriate when the focus is on reactor design since reaction rates also depend on concentration. However, the mass transfer literature frequently bases the liquid phase driving force on mole fractions and the gas phase driving force on mole fractions or partial pressures. This leads to units for $K_g A_i$ such as moles per cubic meter per second per gas phase mole fraction or moles per cubic meter per second per pascal. Example 11.9 includes a conversion of such units into SI units. The SI units are

meters per second for K_g, reciprocal meters for A_i, and seconds for $K_g A_i$. The units of $K_g A_i V(a_g - K_H a_l))$ should be moles per second regardless of the units used for concentration. The quantity $K_g(a_g - K_H a_l)$ has units of flux, moles per square meter per second.

Equations 11.2 and 11.3 must predict the same rate, but it is not necessarily true that K_H has the same value in these equations. If Henry's law holds rigorously, then K_H is constant, and

$$K_l = K_H K_g \tag{11.4}$$

The mass transfer coefficients K_g and K_l are overall coefficients analogous to an overall heat transfer coefficient in a shell-and-tube heat exchanger. The overall coefficient in a heat exchanger has three components, an inside coefficient, a wall resistance, and an outside coefficient. Analogs exist in mass transfer. For the inside coefficient, we consider the driving force between the bulk liquid concentration and liquid concentration at the interface:

$$\text{Mass transfer rate} = k_l A_i V(a_l^* - a_l) \tag{11.5}$$

The analog of the outside coefficient is

$$\text{Mass transfer rate} = k_g A_i V(a_g - a_g^*) \tag{11.6}$$

In these equations, a_l^* is analogous to the inside wall temperature and a_g^* is analogous to the outside wall temperature. In the absence of a wall resistance, the liquid and gas temperatures at the interface are equal. For mass transfer, the concentrations at the interface are not numerically equal but are assumed to be in equilibrium and governed by Equation 11.1. The proportionality constant K_H in Equation 11.1 can be Henry's law constant, but there is no guarantee that Henry's law will apply over the necessary concentration range. More generally, K_H is a function of composition and temperature that serves as a (local) proportionality constant between the gas- and liquid phase concentrations at equilibrium.

Equations 11.4 and 11.5 can be combined to find the interfacial concentrations:

$$a_l^* = \frac{a_g^*}{K_H^*} = \frac{k_g a_g + k_l a_l}{k_g K_H^* + k_l}$$

where K_H^* denotes the local value for the Henry's law constant at the interface. The usual case for a gas–liquid system is $k_g K_H^* \gg k_l$ so that the liquid-side resistance is controlling. Then $a_g^* \approx a_g$ and

$$a_l^* \approx \frac{a_g}{K_H^*} \tag{11.7}$$

If Henry's law holds throughout the composition range, then K_H will have the same value in all of these equations. Furthermore, all the mass transfer rates in these equations are equal. Algebra gives

$$K_l = K_H K_g = \frac{1}{1/k_l + 1/(K_H k_g)} \tag{11.8}$$

which is reminiscent of the equation for the overall heat transfer coefficient between a tube and a jacket except that there is no wall resistance. A ***membrane reactor*** has the mass transfer equivalent of a wall resistance.

EXAMPLE 11.1

Suppose an aerobic fermentation is being conducted in an agitated vessel at 38°C and that $k_l A_i = 0.1\ s^{-1}$ and $k_g A_i = 20\ s^{-1}$ have been measured for the mass transfer of oxygen from air at atmospheric pressure. Determine $K_l A_i$ and $K_g A_i$.

SOLUTION: A standard reference gives $K_H = 4.04 \times 10^7$ mm of Hg per mole fraction for oxygen in water at 38°C (standard references are notoriously reluctant to change units). Thus an oxygen partial pressure of 160 Torr will be in equilibrium with water containing 3.95×10^{-6} mole fraction oxygen. The corresponding oxygen concentrations work out to be 10.7 mol m^{-3} for the gas phase and 0.219 mol m^{-3} for the liquid phase. Thus the dimensionless value for Henry's law constant is 48.9. Substitute this and the given values for $k_l A_i$ and $k_g A_i$ into Equation 11.8 to obtain $K_l A_i = 0.1\ s^{-1}$ and $K_g A_i = 0.002\ s^{-1}$. The calculation also shows that the gas-side resistance is negligible compared to the liquid-side resistance. This is typical except when the gas being transferred reacts very rapidly in the liquid. See the discussion of enhancement factors in Section 11.1.5.

EXAMPLE 11.2

What happens if the air in Example 11.1 is replaced with pure oxygen?

SOLUTION: With pure oxygen, the composition is uniform in the gas phase so that $a_g^* = a_g$. There is no resistance to mass transfer in a phase consisting of a pure component. However, the gas-side resistance is already negligible in Example 11.1. Thus the conversion to pure oxygen has no effect on $K_l A_i$ and $K_g A_i$ as calculated in that example. Going to pure oxygen will increase a_g^* and a_l^* by factors of about 5. What this does to the mass transfer rate depends on the response of the organism to the increased oxygen supply. If the organism's growth was strictly limited by oxygen—as it is in some wastewater treatment processes—the oxygen transfer rate could increase by a factor of 5, and the dissolved oxygen concentration a_l would remain low. If the fermentation was limited by something else, there might be no effect except that the dissolved oxygen content would increase by a factor of 5.

Membrane Reactors

Consider the two-phase stirred tank shown in Figure 11.1 but suppose there is a membrane separating the phases. The equilibrium relationship of Equation 11.1 no longer holds. Instead, the mass transfer rate across the interface is given by

$$\text{Mass transfer rate} = D_A \frac{a_g^*/K_H - a_l^*}{\Delta x} \tag{11.9}$$

where a_g^*/K_H is the liquid-equivalent concentration on the gas side of the membrane, a_l^* is the concentration on the liquid side, and D_A is the effective diffusivity in the membrane based on the liquid phase driving force. With these revised definitions for a_g^* and a_l^* , Equations 11.5 and 11.6 continue to hold and are equal to the mass transfer rate in Equation 11.9. Equation 11.9 does not require K_H to be constant throughout the range of compositions in the reactor; but if it is constant, the overall mass transfer coefficient is

$$K_l = \frac{1}{1/k_l + \Delta x/D_A + 1/(K_H k_g)} \tag{11.10}$$

The middle term, $\Delta x/D_A$, corresponds to the wall resistance in a shell-and-tube heat exchanger. It is now the membrane resistance to mass transfer. The parameter D_A is very dependent on the species since membranes can be quite selective. Recall that the designations "liquid" and "gas" are arbitrary. The same equations can be used for liquid–liquid and gas–gas membrane reactors. Values for the effective diffusivity D_A, depend on which driving force is used in the calculations. Equation 11.9 uses the liquid phase driving force. Multiply by K_H to find the equivalent value for D_A based on a gas phase driving force. Experimental values for D_A depend strongly on the species being transported and on which phase is present inside the membrane. Many membranes are strongly asymmetric so that the phase inside the membrane is the phase in contact with the side of the membrane having larger pores.

Phase Balances for Components

Unsteady-state material balances can be written for each phase. For the general case of unsteady operation and variable physical properties, the liquid phase balance is

$$\frac{d(V_l a_l)}{dt} = (Q_l a_l)_{\text{in}} + k_l A_i V(a_l^* - a_l) + V_l(\mathscr{R}_A)_l - (Q_l a_l)_{\text{out}} \tag{11.11}$$

Note that the accumulation and reaction terms are based on the volume of the liquid phase but that the mass transfer term is based on the working volume $V = V_l + V_g$. The gas phase balance is

$$\frac{d(V_g a_g)}{dt} = (Q_g a_g)_{\text{in}} - k_g A_i V(a_g^* - a_g) + V_g(\mathscr{R}_A)_g - (Q_g a_g)_{\text{out}} \tag{11.12}$$

The individual component balances are conceptually identical to component balances written for a homogeneous system, Equation 1.6, but there is now a source term due to mass transfer across the interface. There are two equations (ODEs) and two primary unknowns, a_g and a_l. The concentrations at the interface, a_l^* and a_g^*, are also unknown but can be found using the equilibrium relationship, Equation 11.1, and the equality of transfer rates, Equations 11.5 and 11.6. For membrane reactors, Equation 11.9 supplements Equation 11.1. Solution is possible whether or not K_H is constant, but

the case where it is constant allows a_l^* and a_g^* to be eliminated directly:

$$\frac{d(V_l a_l)}{dt} = (Q_l a_l)_{\text{in}} + K_l A_i V \left(\frac{a_g}{K_H} - a_l \right) + V_l (\mathscr{R}_A)_l - (Q_l a_l)_{\text{out}} \quad (11.13)$$

$$\frac{d(V_g a_g)}{dt} = (Q_g a_g)_{\text{in}} - K_l A_i V \left(\frac{a_g}{K_H} - a_l \right) + V_g (\mathscr{R}_A)_g - (Q_g a_g)_{\text{out}} \quad (11.14)$$

We have elected to use the overall mass transfer coefficient K_l, which is based on the equivalent liquid phase driving force, $a_g/K_H - a_l$, but this choice was arbitrary so that K_g and $a_g - K_H a_l$ could have been used instead. Equations 11.13 and 11.14 can be used for membrane reactors when K_l is given by Equation 11.10.

Operating Modes

The component and mass balances are quite general and apply to any operating mode, for example, batch, semibatch, or steady state. Table 11.2 gives examples for the various modes.

The flow terms are dropped for batch reactors, but mass transfer between the phases can still occur. The long-time solutions to Equations 11.11 and 11.12 give the equilibrium concentrations and volumes for the two phases. This can be considered an application of the method of false transients wherein an equilibrium problem is solved using simultaneous ODEs rather than simultaneous algebraic equations. In this case, however, the transient should be a true transient since inventories in both phases are accounted for. Long-time solutions should be computed even for batch reactions that do not go to completion since this provides a test of the reactor model. Does the equilibrium solution make sense? The general design problem for a batch reactor allows V, V_g, V_l, and A_i to vary during the course of the reaction. Like the variable-volume batch reactions considered in Section 2.6, solutions can be quite complex. In two-phase systems, an equation of state is needed for each phase.

Fed-batch operation with the liquid charged initially followed by continuous gas sparging is quite common for gas–liquid reactions. Set $(Q_{\text{in}})_l = (Q_{\text{out}})_l = 0$ and

Table 11.2 Two-Phase Reactions in Stirred Tank Reactors

Mode	Example
Batch	Condensation reaction where the condensation product forms second phase
Semibatch, reactant addition	Batch alkylation where gaseous alkene is continuously charged
Semibatch, product removal	Aerobic fermentation where byproduct CO_2 is allowed to escape
Continuous	Bleaching of paper pulp with Cl_2 or ClO_2

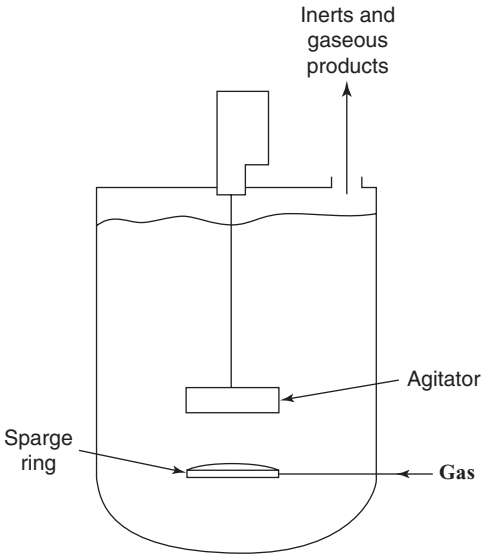

Figure 11.2 Mechanically agitated vessel with gas sparging.

$d(V_g a_g)/dt = 0$. Typically, $(\mathscr{R}_A)_g = 0$ as well. Do not set $(Q_{\text{out}})_g = 0$ as it is usually necessary to remove inerts (e.g., nitrogen in an aerobic fermentation or saturates for an alkylation). This form of semibatch reaction is useful when the gas has a low solubility in the liquid. The equipment can be a conventional stirred tank with a sparge ring as shown in Figure 11.2. When heat transfer is important, much of the reactor volume can be provided by a heat exchanger in a recycle loop. Figure 11.3 illustrates a semibatch reactor used for phenol alkylation. The tank in that process acts as a collection vessel and has no agitator. Gas–liquid mixing is provided by a proprietary mixing nozzle, and the pump provides general circulation.

Semibatch or fully continuous operation with continuous removal of a byproduct gas is also common. Continuous removal of the byproduct gas can avoid an equilibrium limitation, for example, by removing byproduct water in an esterification. The pressure in the vapor space can be reduced or a dry, inert gas can be sparged to increase A_i and lower a_g^*, thereby increasing mass transfer and lowering a_l so that the forward reaction can proceed.

The time derivatives in Equations 11.11 and 11.12 are dropped for steady-state continuous flow, although the method of false transients may still be convenient for solving these equations. The general case is somewhat less complicated than for two-phase batch reactions since system parameters such as V, V_g, V_l, and A_i will have steady-state values. Still, a realistic solution can be quite complicated.

In the relatively simple examples that follow, the system parameters are assumed known. Finding them for a real problem may require a sophisticated effort in modeling and measurement. Measurement techniques are discussed in Section 11.1.2.

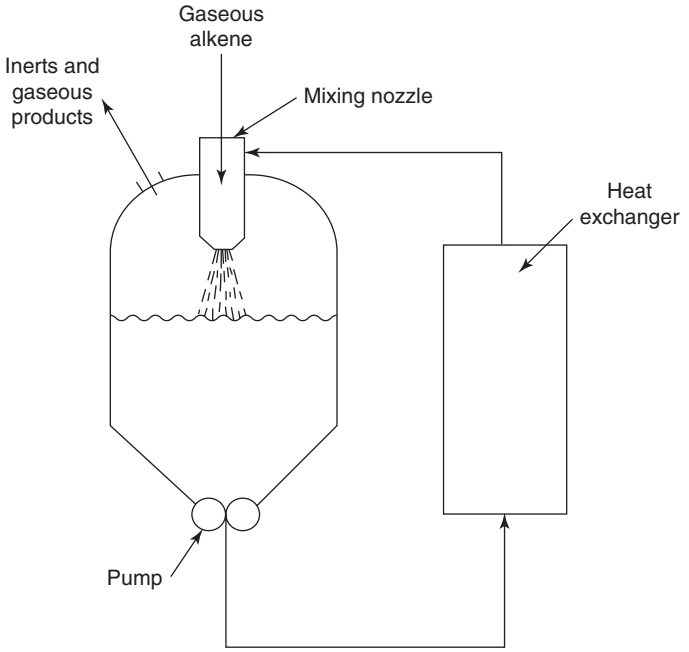

Figure 11.3 Semibatch alkylation reactor.

EXAMPLE 11.3

The gas supply for the stirred tank in Examples 11.1 and 11.2 is suddenly changed from air to pure oxygen. How long does it take for the dissolved oxygen concentration to reach its new value? Assume the tank is operated in a batch mode with respect to water. Ignore any evaporation of water and any reaction involving oxygen. Ignore any changes in volumetric flow rate of the gas and assume that V_l and V_g remain constant

SOLUTION: The initial liquid phase concentration of oxygen is 0.219 mol m^{-3} as in Example 11.1. The final oxygen concentration will be 1.05 mol m^{-3}. The phase balances, Equations 11.11 and 11.12, govern the dynamic response. The flow and reaction terms are dropped from the liquid phase balance to give

$$\frac{da_l}{dt} = \frac{k_l A_i}{[V_l/V]}(a_l^* - a_l)$$

As a first approximation, suppose that the concentration of oxygen in the gas phase changes instantly from 20.9% oxygen to 100% oxygen. Then a_l^* will change instantly from 0.219 to 1.05 mol m^{-3}, and the gas phase balance is not required. In Example 11.1 $k_l A_i = 0.1$ s^{-1} was specified, so the only unknown parameter is the liquid holdup, V_l/V. A typical value for a mechanically agitated tank is 0.9. The liquid phase balance becomes

$$\frac{da_l}{dt} = \frac{0.1}{[0.9]}(a_l^* - a_l)$$

subject to the initial condition that $a_l = 0.219$ at $t = 0$. Solution gives

$$a_l = 1.05 - 0.83\exp(-0.111t)$$

The 95% response time is 27 s.

EXAMPLE 11.4

The assumption in Example 11.3 that the gas composition changes instantly is suspicious. Remedy this defect in the analysis.

SOLUTION: The liquid phase balance is unchanged except that a_l^* now varies with time, $a_l = a_l(t)$. The gas phase balance comes from Equation 11.12. When simplified for the present case it becomes

$$\frac{da_g}{dt} = \frac{Q_g}{V_g}(a_g)_{\text{in}} - \frac{k_g A_i}{[V_g/V]}(a_g^* - a_g) - \frac{Q_g}{V_g}a_g$$

This introduces the gas phase residence time, V_g/Q_g, as a new parameter. It also introduces an ambiguity regarding the term $k_g A_i(a_g^* - a_g)$. There is no resistance to mass transfer within a pure component so $k_g A_i \to \infty$ and $a_g^* - a_g \to 0$. Thus $k_g A_i(a_g^* - a_g)$ is an indeterminate form of the $\infty \times 0$ variety. Its value must continue to equal the rate at which oxygen is transferred into the liquid phase. Equation 11.5 remains true and the pair of simultaneous ODEs become

$$\frac{da_l}{dt} = \frac{k_l A_i}{[V_l/V]}(a_l^* - a_l) = \frac{k_l A_i}{[V_l/V]}\left(\frac{a_g}{K_H} - a_l\right)$$

$$\frac{da_g}{dt} = \frac{Q_g}{V_g}(a_g)_{\text{in}} - \frac{k_l A_i}{[V_g/V]}\left(\frac{a_g}{K_H} - a_l\right) - \frac{Q_g}{V_g}a_g$$

The initial conditions are $a_l = 0.219$ and $a_g = 10.7$ mol m^{-3} at $t = 0$. An analytical solution is possible but messy. The solution depends on the values of $k_l A_i$ and V_l/V as in Example 11.3 and additionally the value of V_g/Q_g. In essence, Example 11.3 assumed $V_g/Q_g \approx 0$ so that the gas phase concentration quickly responded to the change in inlet concentration.

EXAMPLE 11.5

Suppose that the liquid phase in a gas–liquid CSTR contains a catalyst for the first-order reaction of a compound supplied from the gas phase. The reaction is

$$\text{A} \to \text{products} \qquad \mathscr{R} = ka_l$$

The reactor is operated in the semibatch mode with component A being sparged into the stirred tank. Unreacted A and the reaction products leave through the gas phase so that the mass of liquid remains constant. To the extent that these assumptions are true and the catalyst does not deactivate, a pseudo–steady state can be achieved. Find $(a_g)_{\text{out}}$. Assume that Henry's law is valid throughout the composition range and ignore any changes in the gas density.

SOLUTION: Both phases are assumed to be perfectly mixed so that $(a_g)_{\text{out}}$ is just a_g. Equation 11.13 provides the material balance for component A in the liquid phase:

$$0 = K_l A_i V \left(\frac{a_g}{K_H} - a_l \right) - V_l k a_l$$

$$0 = (Q_g a_g)_{\text{in}} - K_l A_i V \left(\frac{a_g}{K_H} - a_l \right) - (Q_g a_g)_{\text{out}}$$

There are two equations and two unknowns. Eliminating a_l gives

$$(a_g)_{\text{out}} = a_g = \frac{(a_g)_{\text{in}}}{1 + V_l k (K_l A_i V)/[Q K_H (K_l A_i V + V_l k)]}$$

where Q denotes the inlet and outlet gas flow rates since the gas density is constant.

Complete conversion of component A requires a high mass transfer rate, $U_l A_i \to \infty$, combined with a high reaction rate, $k \to \infty$. If $k \to \infty$ while $U_l A_i$ remains finite, the reaction is ***mass transfer limited.*** Some of the entering gas will not be absorbed and thus will not react. This situation is sometimes called ***bypassing***.

EXAMPLE 11.6

Suppose the liquid phase reaction is

$$\text{A} + \text{B} \to \text{products} \qquad \mathscr{R} = k a_l b_l$$

where A is a sparingly soluble gas that is sparged continuously and where a minor component, B, is charged to the vessel initially. Assume that component B is nonvolatile and that the gas-side film resistance is negligible. Determine $a_l(t)$ and $b_l(t)$.

SOLUTION: Example 11.5 treats a system that could operate indefinitely since the liquid phase serves only as a catalyst. The present example is more realistic since the liquid phase is depleted and the reaction eventually ends. The assumption that the gas-side resistance is negligible is equivalent to assuming that $a_g^* = a_g$ throughout the course of the reaction. Equilibrium at the interface then fixes $a_l^* = a_g/K_H$ at all times. Dropping the flow and accumulation terms in the balance for the liquid phase, that is, Equation 11.11, gives

$$0 = k_l A_i V \left(\frac{a_g}{K_H} - a_l \right) - V_l k a_l b_l$$

Solving for a_l yields

$$a_l = \frac{k_l A_i V a_g / K_H}{k_l A_i V + V_l k b}$$

Note that a_l will gradually increase during the course of the reaction and will reach its saturation value, a_g/K_H, when B is depleted. Dropping the accumulation term for $a_l(t)$ represents a form of the pseudo-steady-state hypothesis.

Since component B is not transferred between phases, its material balance has the usual form for a batch reactor:

$$\frac{db_l}{dt} = -k a_l b_l = -k \left[\frac{k_l A_i V a_g / K_H}{k_l A_i V + V_l k b} \right] b_l = \frac{-k' b_l}{1 + k_B b_l}$$

The appearance of this "heterogeneous" form for the rate expression reflects the presence of a mass transfer step in series with the reaction step. If the parameter values are known, this ODE for $b_l(t)$ can be integrated subject to the initial condition that $b_l = (b_l)_0$ at $t = 0$. The result can then be used to find $a_l(t)$.

The question arises as to how V, V_g, V_l, and A_i might vary during the course of the reaction. The problem statement does not give the necessary information to determine this. The reader is encouraged to create and solve some plausible scenarios, one of which allows V, V_g, V_l, and A_i to remain approximately constant.

EXAMPLE 11.7

Carbon dioxide is sometimes removed from natural gas by reactive absorption in a tray column. The absorbent, typically an amine, is fed to the top of the column and gas is fed at the bottom. Liquid and gas flow patterns are similar to those in a distillation column with gas rising, liquid falling, and gas–liquid contacting occurring on the trays. Develop a model for a multitray CO_2 scrubber assuming that individual trays behave as two-phase stirred tank reactors.

SOLUTION: The liquid phase reaction has the form C + A → P which we assume to be elementary with rate constant k. Suppose there are J trays in the column and that they are numbered starting from the bottom. Figure 11.4 shows a typical tray and indicates the notation. Since the column has many trays (typically 20 or more), composition changes on each tray are

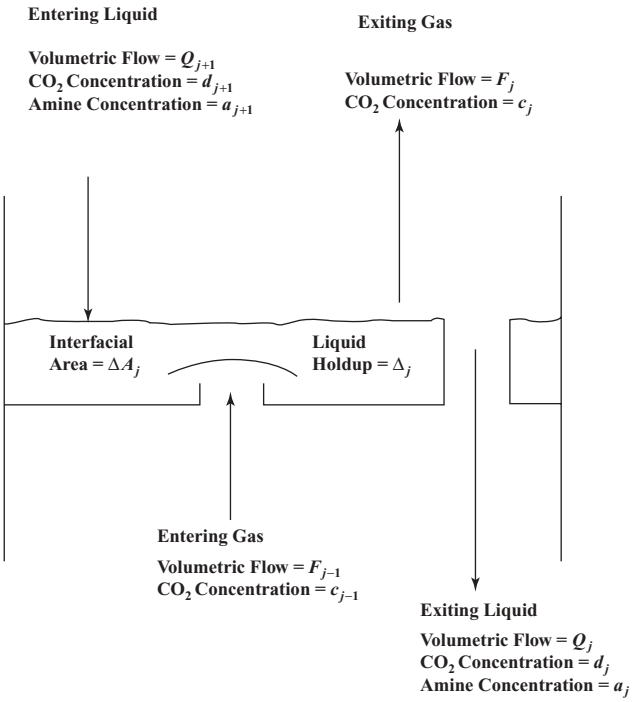

Figure 11.4 Typical tray in tray column reactor used for acid gas scrubbing.

small, and it is reasonable to assume perfect mixing within each phase on an individual tray. The system is at steady state, and there is no reaction in the gas phase. The gas phase balance for CO_2 is given by Equation 11.12, which simplifies to

$$0 = F_{j-1}c_{j-1} - k_g\ \Delta A_i \left(c_j - c_j^*\right) - F_j c_j$$

where ΔA_i is the interfacial area per tray. For the dissolved but unreacted CO_2 in the liquid phase, Equation 11.11 becomes

$$0 = Q_{j+1}d_{j+1} + k_l\ \Delta A_i \left(d_j^* - d_j\right) - \Delta V\ ka_j d_j - Q_j d_j$$

The liquid phase balance for the amine is

$$0 = Q_{j+1}a_{j+1} - \Delta V\ ka_j d_j - Q_j a_j$$

In the current notation, Equations 11.6 and 11.7 give

$$d_j^* = \frac{k_g c_j + k_l d_j}{k_g K_H^* + k_l} \qquad c_j^* = \frac{k_g c_j + k_l d_j}{k_g + k_l/K_H^*}$$

so that the interfacial concentrations can be calculated (although by an interative process when K_H is not constant). The inputs to the jth tray are c_{j-1}, d_{j+1}, a_{j+1}, F_{j-1}, and Q_{j+1}. Suppose these are known. Then there are three equations and three compositional unknowns: c_j, d_j, and a_j. There are also two unknown flow rates, F_j and Q_j, which may change significantly from the top to the bottom of the column. Stagewise values for these can be calculated from equations of state and overall mass balances for the two phases. Most gas-scrubbing systems are designed to remove acid gases such as H_2S and SO_2 in addition to CO_2. Additionally, the heats of absorption can be significant so that energy balances may be needed as well. The overall computation can be quite complex, involving upward of three nonlinear equations per tray so that hundreds of simultaneous algebraic equations must be solved simultaneously. This can be done using the multidimensional Newton method described in Appendix 4.1. Another possibility is to use the method of false transients to convert the algebraic equations to first-order ODEs subject to some assumed initial concentration profile in the column. Still another approach is to guess the composition of, say, the exiting liquid stream at the bottom of the column. With this initial guess, a sequential, tray-by-tray calculation is possible that involves simultaneous solution of only the basic set of 5–10 equations per tray. This approach is conceptually similar to the shooting method described in Section 9.5. It presents similar difficulties due to numerical ill-conditioning for which there is no easy remedy.

Example 11.7 hints at the complications that are possible in reactive gas absorption. Gas absorption is an important unit operation that has been the subject of extensive research and development. Large, proprietary computer codes are available for purchase, and process simulation tools such as Aspen can do the job. However, as shown in Example 11.8, simple but useful approximations are sometimes possible.

EXAMPLE 11.8

With highly reactive absorbents, the mass transfer resistance in the gas phase can be controlling. Determine the number of trays needed to reduce the CO_2 concentration in a methane stream from 5% to 100 ppm (by volume) assuming the liquid mass transfer and reaction steps are fast. A 0.9-m-diameter column is to be operated at 8 atm and 50°C with a gas feed rate of 0.2 $m^3\ s^{-1}$. The trays are bubble caps operated with a 0.1-m liquid level. Literature correlations suggest $k_g = 0.002$ m s^{-1} and $\Delta A_i = 20$ m^2 per square meter of tray area.

SOLUTION: Ideal gas behavior is a reasonable approximation for the feed stream. The inlet concentrations are 287 mol m^{-3} of methane and 15 mol m^{-3} of carbon dioxide. The column pressure drop is mainly due to the liquid head on the trays and will be negligible compared to 8 atm unless there is an enormous number of trays. Thus the gas flow rate F will be approximately constant for the column as a whole. With fast reaction and a controlling gas-side resistance, $c_j^* = 0$. The liquid phase balance gives everything that is necessary to solve the problem:

$$0 = Fc_{j+1} - Fc_j - k_g\,\Delta A_i c_j$$

and

$$\frac{c_{j+1}}{c_j} = 1 + \frac{k_g\,\Delta A_i}{F} = 1.13$$

For the column as a whole,

$$\frac{c_0}{c_J} = (1.13)^J = \frac{0.05}{0.0001}$$

Solution gives $J = 51$ trays. The indicated separation appears feasible in a bubble cap column although the design engineer should not be content with the glib assumption of negligible liquid-side resistance. The design engineer should also question the use of trays rather than structured packing.

Overall and Phase Balances for Mass

The examples so far in this chapter were designed to be simple yet show some essential features of gas–liquid reactors. Only component balances for the phases, Equations 11.11 and 11.12, have been used. They are reasonably rigorous, but they do not provide guidance regarding how the various operating parameters can be determined. This is done in Section 11.1.2. Also, total mass balances must supplement the component balances in order to handle the general case of semibatch operation where parameters such as V, V_g, V_l, and A_i can all vary with time.

An overall mass balance is written for the system as a whole. Interphase mass transfer does not appear in the system mass balance since gains in one phase exactly equal losses in the other. The net result is conceptually identical to Equation 1.3, but there are now two inlets and two outlets and the total inventory is summed over both

phases. The result is

$$\frac{d(V_g\rho_g + V_l\rho_l)}{dt} = (Q_{\text{in}}\rho_{\text{in}})_l + (Q_{\text{in}}\rho_{\text{in}})_g - (Q_{\text{out}}\rho_{\text{out}})_l - (Q_{\text{out}}\rho_{\text{out}})_g \tag{11.15}$$

The phase mass balances are more complicated since the mass in a phase can grow or wane due to interphase mass transfer. The phase balances are

$$\frac{d(V_l\rho_l)}{dt} = (Q_{\text{in}}\rho_{\text{in}})_l - (Q_{\text{out}}\rho_{\text{out}})_l + \sum_{\text{components}} M_A k_l A_i V(a_l^* - a_l) \tag{11.16}$$

$$\frac{d(V_g\rho_g)}{dt} = (Q_{\text{in}}\rho_{\text{in}})_g - (Q_{\text{out}}\rho_{\text{out}})_g - \sum_{\text{components}} M_A k_g A_i V(a_g - a_g^*) \tag{11.17}$$

where M_A is the mass per mole (kilograms per mole) for component A. Equation 11.5 holds for each component so that Equations 11.16 and 11.17 sum to Equation 11.15. The film coefficients should depend on eddy diffusion more than molecular diffusion and, like the axial dispersion coefficient in Chapter 9, should be approximately the same for all chemical species. An exception to this statement occurs when a component is rapidly consumed by chemical reaction. Another exception is a membrane reactor where the membrane may be quite selective, that is, D_A can vary greatly between species.

Energy Balances

When the reaction temperatures are unknown, two heat balances are also needed:

$$\begin{aligned}\frac{d(V_l\rho_l H_l)}{dt} &= (Q_l\rho_l H_l)_{\text{in}} + U A_{\text{ext}}(T_{\text{ext}} - T_l) \\ &\quad + h_i A_i V(T_g - T_l) - V_l(\Delta H_R \mathscr{R})_l - (Q_l\rho_l H_l)_{\text{out}}\end{aligned} \tag{11.18}$$

$$\begin{aligned}\frac{d(V_g\rho_g H_g)}{dt} &= (Q_g\rho_g H_g)_{\text{in}} - h_i A_i V(T_g - T_l) \\ &\quad - V_g(\Delta H_R \mathscr{R})_g - (Q_g\rho_g H_g)_{\text{out}}\end{aligned} \tag{11.19}$$

These equations allow for interphase heat transfer with h_i as the heat transfer coefficient. As written, they envision heat transfer to the environment to occur only through the liquid phase since it is normally the continuous phase.

The mass and energy balances for the various components constitute the complete design equations for a two-phase reactor with perfect mixing in each phase, although these equations must be supplemented by physical property relationships and parameter correlations. Solutions for the single-phase versions of these equations occupied most of Chapters 2, 4, and 5. The reader will appreciate that these equations are rarely used in their full form even for single-phase systems. A full solution for the two-phase case may require an extensive modeling effort, but an approximate solution can provide substantial insight and can motivate a more substantial study.

11.1.2 Measurement of Mass Transfer Coefficients

Fundamental theory is insufficient to predict mass transfer coefficients and liquid phase holdup. This section describes experimental methods for determining them and gives typical values. A great many correlations are available in the literature, but stirred tanks have many design variations. Liquid phase properties can have a large effect on the results. Rheology (e.g., non-Newtonian behavior) is important for fermentations and polymerizations. Correlations may be based on small-scale experiments using well-defined conditions, but clean and dirty fluids behave differently due to the effects of interfacial agents on bubble coalescence. Most industrial processes and fermentations in particular are dirty almost by definition. Suspended solids retard mass transfer. An additive intended to solve one problem can cause another; for example, antifoaming agents can reduce mass transfer. Because of this complexity, great care must be taken in using any literature correlation. To understand the complexity, browse through the appropriate sections of the *Handbook of Industrial Mixing* (Paul et al., 2003), but rejoice that measurement techniques for $k_l A_i$ and phase holdup are relatively simple if the liquid phase reaction is not too fast. See also the typical values in Table 11.3.

Transient Techniques for Nonreactive Systems

The transient technique discribed in this section is commonly used to measure gas-to-liquid transfer rates in a stirred tank that is batch with respect to the liquid phase. The results can usually be used for CSTRs since a moderate liquid throughput will have little effect on $k_l A_i$ or holdup. The composition of the liquid phase should approximate that intended for actual operation, but for the purposes of the experiment gas should not react in either phase. Holdup is determined from the height of the liquid with and without gas flow. The mass transfer coefficient is determined by a sudden step change in gas composition similar to that in Example 11.3. A typical measurement sparges air into the vessel until the liquid phase saturates with respect to oxygen. The air supply is suddenly replaced with nitrogen at the same volumetric flow rate, and a dissolved oxygen meter is used to monitor the oxygen content in the liquid phase. The analysis is similar to that in Example 11.4 but slightly simpler because $(a_g)_{\text{in}} = 0$

Table 11.3 Typical Operating Ranges for Gas–Liquid Contacting Devices

Device	Liquid Holdup, V_l/V	$k_l A_i$, s^{-1}
Mechanically agitated tanks	0.9	0.02–0.2
Tray columns	0.15	0.01–0.05
Packed columns	0.05	0.005–0.02
Bubble columns	0.95	0.005–0.0

Source: Data from Harnby *et al*. (1985).

for $t > 0$. The phase balances are

$$\frac{da_l}{dt} = \frac{k_l A_i}{[V_l/V]}\left(\frac{a_g}{K_H} - a_l\right) \tag{11.20}$$

$$\frac{da_g}{dt} = -\frac{k_l A_i}{[V_g/V]}\left(\frac{a_g}{K_H} - a_l\right) - \frac{Q_g}{V_g}a_g \tag{11.21}$$

These equations contain only one unknown parameter, $k_l A_i$. Assume values for it and solve Equations 11.20 and 11.21 simultaneously. Compare the calculated results to the experimental measurements using nonlinear least-squares analysis as in Equation 7.8. This is the preferred modern approach, but the precomputer literature relied on computationally simpler methods for fitting $k_l A_i$.

Equations 11.20 and 11.21 are linear, first-order ODEs with coefficients that are assumed constant. The equations can be combined to give a second-order ODE in a_l:

$$\frac{d^2a_l}{dt^2} + \left(\frac{k_l A_i V}{V_l} + \frac{k_l A_i K_H}{V_g} + \frac{Q_g}{V_g}\right)\frac{da_l}{dt} + \frac{k_l A_i V Q_g a_l}{V_l V_g} = 0 \tag{11.22}$$

This equation can be used to estimate $k_l A_i$ from an experimental $a_l(t)$ curve in at least three ways:

1. ***Initial second-derivative method:*** At $t = 0$, $da_l/dt = 0$. Therefore,

$$\left[\frac{1}{a_l}\frac{d^2a}{dt^2}\right]_0 = -\frac{k_l A_i V Q}{V_l V_g} \tag{11.23}$$

   so that $k_l A_i$ can be calculated assuming the other parameters are known. This method suffers the obvious difficulty of measuring a second derivative.

2. ***Inflection point method:*** At the inflection point, $d^2a_l/dt^2 = 0$ and

$$\left[\frac{1}{a_l}\frac{da_l}{dt}\right]_{\text{inflet}} = \left[\frac{d\ln a_l}{dt}\right]_{\text{inflet}} = \frac{-k_l A_i V}{k_l A_i V V_g/Q_l + k_l A_i V V_H K_H/Q + V_l} \tag{11.24}$$

   This method is reasonable in terms of accuracy and allows brief experiments.

3. ***Asymptotic method:*** For most systems, $V_l/(k_l A_i) \gg V_g/Q$. Then at long times,

$$a_l(t) = \exp\left[\frac{-k_l A_i V t}{V_l}\right] \tag{11.25}$$

   When applicable, this method is the least demanding in terms of experimental accuracy. It is merely necessary to estimate the slope of what should be a straight line when $\ln a_l$ is plotted versus t. By comparison, the inflection point method requires estimating the slope at an earlier time before it is constant.

Measurements using Liquid Phase Reactions

Liquid phase-reactions, and the oxidation of sodium sulfite to sodium sulfate in particular, are sometimes used to determine $k_l A_i$. As for the transient method, the system is batch with respect to the liquid phase. Pure oxygen is sparged into the vessel. A pseudo–steady state results. There is no gas outlet, and the inlet flow rate is adjusted so that the vessel pressure remains constant. Under these circumstances, the inlet flow rate equals the mass transfer rate. Equations 11.5 and 11.12 are combined to give a particularly simple result:

$$Q_g a_g = k_l A_i V (a_l^* - 0) = k_l A_i V a_l^* = \frac{k_l A_i V a_g}{K_H}$$

or

$$k_l A_i = \frac{Q_g K_H}{V} \tag{11.26}$$

EXAMPLE 11.9

An article in the literature reports the absorption rate of pure oxygen into a sodium sulfite solution at 20°C using an agitated vessel having a liquid depth of 3 ft. A large excess of oxygen was continuously injected into the tank through a sparge ring located just under the agitator. The liquid reaction (sulfite oxidation) was semibatch, but there was sufficient sodium sulfite present so that the dissolved oxygen concentration was approximately zero throughout the experiment. The oxygen consumption was measured using gas flow rates. For a particular set of operating conditions, the result was reported as $K_g A_i = 0.04$ lb-mol h^{-1} ft^{-3} atm^{-1}. What was actually measured and what is its value in SI units?

SOLUTION: The experimental conditions are consistent with Equation 11.26 so that $k_l A_i$ was measured. The experimental result was reported as $K_g A_i$ because the overall mass transfer coefficient was based on the equivalent gas phase driving expressed in partial pressure units rather than concentration units. Because a pure gas was sparged, $k_g \to \infty$, and $K_l = k_l$. Equation 11.4 relates K_g and K_l through Henry's law constant.

The overall driving force for mass transfer is $\Delta P_i = P_{gO_2} - P_{lO_2}$ where $(P_{O_2})_l$ is the concentration of oxygen in the liquid phase expressed as an equivalent partial pressure. For the experimental conditions, $(P_{O_2})_l \approx 0$ due to the fast liquid phase reaction. The oxygen pressure on the gas side varies due to the liquid head. Assume that the pressure at the top of the tank was 1 atm. Then $(P_{O_2})_g = 0.975$ atm since the vapor pressure of water at 20°C should be subtracted. At the bottom of the tank, $(P_{O_2})_g = 1.0635$ atm. The logarithmic mean is appropriate: $\Delta P_i = 1.018$ atm. Thus the transfer rate was

$$K_g A_i \, \Delta P_i = 0.04 \times 1.018 = 0.0407 \text{ lb-mol ft}^{-3} \text{ h}^{-1} = 0.181 \text{ mol m}^{-3} \text{ s}^{-1}$$

The same rate must be found when the rate is expressed as $k_l A_i a_l^*$, where a_l^* is the solubility of oxygen in water at 20°C and 1.018 atm. Henry's law gives $a_l^* = 1.46$ mol m^{-3}. Thus,

$$k_l A_i = \frac{0.181}{1.46} = 0.124 \text{ s}^{-1}$$

Typical Values

Table 11.3 shows typical parameter values for mechanically agitated tanks and other gas–liquid contacting devices. Not shown are values for $k_g A_i$ since these are usually so large that they have no influence on the mass transfer rate.

Actual Flow Patterns

The assumption of a well-mixed liquid phase is reasonable by the criteria used for single-phase stirred tanks. The same assumption is normally made for the gas phase, but with less justification. Since the gas phase is dispersed and coalescence is retarded in dirty systems, one might prefer a ***segregated flow*** model in which gas bubbles circulate as discrete entities. This is possibility 5 in Section 11.1. If the gas is pure, the bubbles decrease in size as they age, but there is no change in composition. If the gas contains inerts, as when air is used as an oxygen source, the oxygen content will be depleted in bubbles that have remained in the system a long time. This has no practical effect in steady-state operation as long as the liquid phase is well mixed and reaction is confined to the liquid phase. The liquid will be continually contacting the entire population of bubbles, and the measured mass transfer coefficients reflect the average contents of the bubbles with respect to size and gas concentration. Similarly, the fact that pressure varies as a function of position in the reactor makes no real difference provided that the mass transfer measurements are made on the full-scale vessel. The subtleties of bubble circulation and coalescence would be important if, for example, a second-order reaction occurred in the gas phase. ***Population balance methods*** must be used when the fate of individual bubbles is important. These methods are applied to the distribution of residence times in Chapter 15 and are briefly discussed in Example 11.17.

11.1.3 Fluid–Fluid Contacting in Piston Flow

Table 11.4 lists reactors used for systems with two fluid phases. The gas–liquid case is typical, but most of these reactors can be used for liquid–liquid systems as well. Stirred tanks and packed columns are also used for three-phase systems where the third phase is a catalytic solid. The equipment listed in Table 11.4 is sometimes used for separations, but our interest is on reactions in steady-state systems. The contact regimes in this table are discussed at the introduction to Section 1.1.

Stirred tanks are usually modeled assuming both phases are well mixed. See Section 1.5 for conditions under which this assumption is reasonable. Tray columns are usually modeled as well mixed on each tray so that the overall column is modeled as a series of two-phase stirred tanks. (Distillation trays with tray efficiencies greater than 100% have some progressive flow within a tray.) When reaction is confined to a single well-mixed phase, the flow regime for the other phase makes little difference; but when the reacting phase approximates piston flow, the flow regime in the other phase becomes important. The important cases are where both phases approximate piston flow, either countercurrent or cocurrent.

Table 11.4 Typical Flow and Mixing Regimes for Gas–Liquid Reactors

Type of Reactor	Liquid Phase	Gas Phase	Contacting Regime
Stirred tank with sparged gas	Continuous, well mixed	Discontinuous, but usually assumed well mixed	1
Stirred tank with discrete paricles	Continuous, well mixed	Discontinuous and segregated	5
Rotating disc columns and pulsed columns	Continuous, piston flow	Dispersed, piston flow	3
Bubble columns	Continuous, piston flow	Dispersed, piston flow	3 or 4
Packed columns	Continuous or trickle, piston flow	Continuous, trickle, or dispersed; piston flow	3
Tray columns	Continuous and well mixed on individual tray	Discontinuous but often assumed well mixed on individual tray	1
Spray towers	Discontinuous, piston flow	Continuous, typically well mixed	3

For simplicity of discussion and notation, we will refer to one phase as being liquid and the other phase as being gas. The gas phase flows upward in the $+z$ direction. The liquid phase may flow upward (cocurrent) or downward. A steady-state but otherwise general component balance gives

$$\pm\frac{d(A_l\bar{u}_l a_l)}{dz} = A_l(\mathscr{R}_A)_l + k_l A_i'(a_l^* - a_l) \tag{11.27}$$

where A_l is the cross-sectional area of the liquid phase, $\bar{u}_l$ is its velocity, and A_i' is the interfacial area per unit height of the column. The plus sign on the derivative in Equation 11.27 is used for cocurrent flow; the minus sign is used for countercurrent flow. Most gas–liquid contactors operate in countercurrent flow. An example is the rotating disk column shown in Figure 11.5. The deep-shaft fermentor shown in Figure 11.6 is an exception, as is the trickle-bed reactor discussed in Section 11.2. Both operate cocurrently.

The gas phase material balance is

$$\frac{d(A_g\bar{u}_g a_g)}{dz} = A_g(\mathscr{R}_A)_g - k_g A_i'(a_g^* - a_g) \tag{11.28}$$

Equations 11.27 and 11.28 contain one independent variable, z, and two dependent variables, a_l and a_g. There are also two auxiliary variables, the interfacial compositions a_l^* and a_g^*. They can be determined using Equations 11.5 and 11.6 (with A_i'

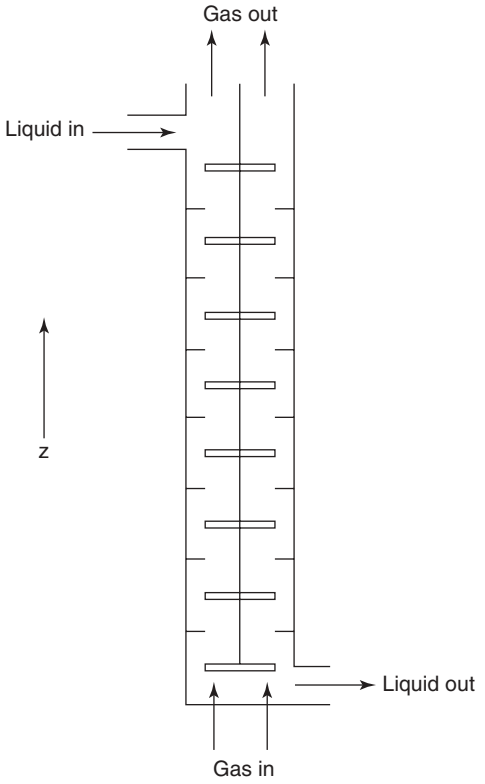

Figure 11.5 Rotating disc contactor with countercurrent downward flow of liquid and upward flow of gas or lower density liquid.

replacing A_i). The general case regards K_H in Equation 11.1 as a function of composition. When Henry's law applies throughout the composition range, overall coefficients can be used instead of the individual film coefficients. This allows immediate elimination of the interface compositions:

$$\pm\frac{d(A_l\bar{u}_l a_l)}{dz} = A_l(\mathscr{R}_A)_l + K_l A_i'\left(\frac{a_g}{K_H} - a_l\right) \tag{11.29}$$

$$\frac{d(A_g\bar{u}_g a_g)}{dz} = A_g(\mathscr{R}_A)_g - K_l A_i'\left(\frac{a_g}{K_H} - a_l\right) \tag{11.30}$$

All the parameters in these equations will be functions of z. Bubbles will grow as they rise in the column due to the lower hydrostatic head, and a_g will decrease even for a pure gas. Bubble coalescence and breakup may be important. Depletion or enrichment

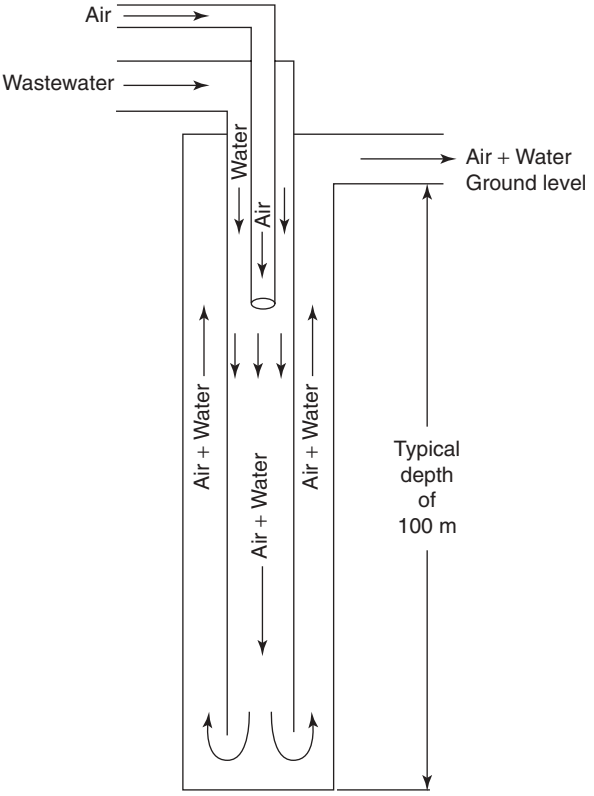

Figure 11.6 Deep-shaft fermentor for wastewater treatment.

of the gas phase due to reaction and mass transfer may be important. The ***air lift*** provided by the upward flow of gas may augment or even replace a conventional pump for the liquid phase. These effects are important in a device such as a deep-shaft fermentor. Bubbles breaking the surface will be large due to the pressure change and may be depleted in oxygen so that little or no mass transfer occurs in the upper part of the column. In the lower part of the fermentor, oxygen partial pressures of 2 atm (total pressure of 10 atm) will give a very high driving force for mass transfer. A rigorous analysis of a deep-shaft fermentor or of any two-phase tubular reactor is a difficult problem in fluid mechanics. Most literature studies have made simplifying assumptions such as constant A_l and A_i. Table 11.5 lists a number of possible simplifications. To some extent, this table should be read in the negative, as many of the assumptions will not be satisfied in real gas–liquid systems. They are more likely to be satisfied in a liquid–liquid system.

Examples 11.10 and 11.11 avoid complications by assuming that all operating parameters are independent of position.

Table 11.5 Possible Simplifying Assumptions for Gas–Liquid Reactors

Assumption	Possible Rationale
P constant	Short column or column operated at high pressure or with a discontinuous liquid phase
a_g and a_g^* constant	P constant and reactant gas pure or fed at high rate
$A_l\bar{u}_l\rho_l$ and $A_g\bar{u}_g\rho_g$ constant	Constant mass flow in each phase, i.e., negligible net mass transfer
A_l and A_g constant	Consistent with constant pressure and negligible net mass transfer
k_lA_i constant	Redispersion of gas compensates for coalescence and pressure effects; negligible depletion of reactive component or else high level of inerts present in gas phase
$\lvert dP/dz\rvert = \rho_l g$	Gas lift negligible so that liquid exerts normal static bead

EXAMPLE 11.10

Determine phase concentrations for a liquid–liquid reaction in a packed-bed reactor. The reactive component is dilute in both phases. It enters the reactor in one phase but undergoes a pseudo-first-order reaction in the other phase. All parameters are constant.

SOLUTION: The phase in which reaction occurs will be denoted by the subscript l, and the other phase will be denoted by the subscript g. Henry's law constant will be replaced by a ***liquid–liquid partition coefficient*** but will still be denoted by K_H. Then the system is governed by Equations 11.29 and 11.30 with $(\mathscr{R}_A)_l = -ka_l$ and $(\mathscr{R}_A)_g = 0$. The governing equations are

$$\pm\frac{da_l}{dz} = \frac{-ka_l}{\bar{u}_l} + \frac{K_lA_i'}{A_l\bar{u}_l}\left(\frac{a_g}{K_H} - a_l\right)$$

$$\frac{da_g}{dz} = -\frac{K_lA_i'}{A_g\bar{u}_g}\left(\frac{a_g}{K_H} - a_l\right)$$

The initial conditions are $a_g = a_{\text{in}}$ at $z = 0$, $a_l = 0$ at $z = 0$ for cocurrent flow and $a_l = 0$ at $z = L$ for countercurrent flow.

The ODEs are linear with constant coefficients. They can be converted to a single second-order ODE, much like Equation 11.22, if an analytical solution is desired. A numerical solution is easier and better illustrates what is necessary for anything but the simplest problem. Convert the independent variable to dimensionless form, $\mathscr{z} = z/L$. Then

$$\pm\frac{da_l}{d\mathscr{z}} = -\frac{kLa_l}{\bar{u}_l} + \frac{K_lA'L_i}{A_l\bar{u}_l}\left(\frac{a_g}{K_H} - a_l\right)$$

$$\frac{da_g}{d\mathscr{z}} = -\frac{K_lA_i'L}{A_g\bar{u}_g}\left(\frac{a_g}{K_H} - a_l\right)$$

Solutions for the cocurrent and countercurrent cases are displayed in Figure 11.7. The countercurrent case requires calculations of the shooting type where values for $(a_l)_{\text{out}} = a_l(z = 0)$ are guessed until the initial condition that $(a_l)_{\text{in}} = 0$ is satisfied. Normalized concentrations with $a_{\text{in}} = 1$ can be used. The solution is governed by four dimensionless constants. The values used

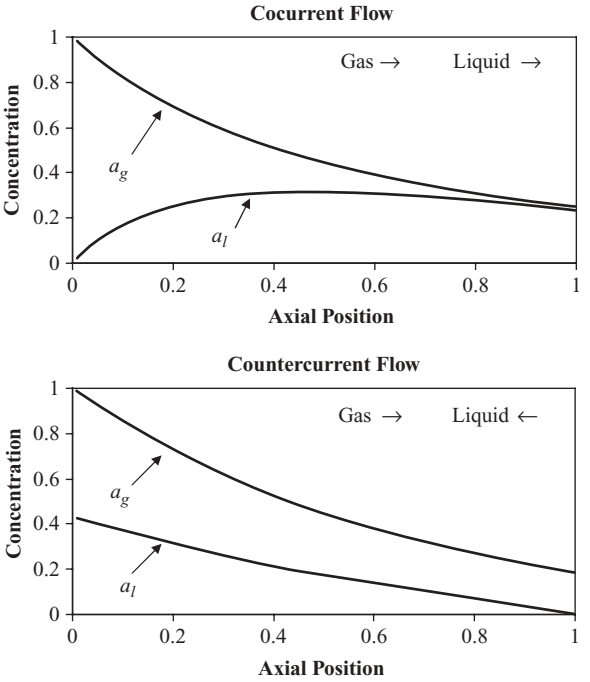

Figure 11.7 Pseudo-first-order reaction in one phase with reactant supplied from the other phase. See Example 11.10.

for Figure 11.7 are

$$\frac{kL}{\bar{u}_l} = 2 \qquad \frac{K_l A_i' L}{A_l \bar{u}_l} = 1 \qquad \frac{K_l A_i' L}{A_g \bar{u}_g} = 1 \qquad K_H = 0.5$$

EXAMPLE 11.11

Assume the pseudo-first-order reaction in Example 11.10 was A + B → C with component B present in great excess. Now suppose that B is confined to the l phase and is present in limited supply, $(b_l)_{\text{in}} = b_{\text{in}}$. Determine the phase concentrations in the reactor of Example 11.11.

SOLUTION: There are now three ODEs to be solved. They are

$$\pm\frac{da_l}{d\cancel{z}} = -\frac{kLa_l b_l}{\bar{u}_l} + \frac{K_l A' L_i}{A_l \bar{u}_l}\left(\frac{a_g}{K_H} - a_l\right)$$

$$\frac{da_g}{d\cancel{z}} = -\frac{K_l A_i' L}{A_g \bar{u}_g}\left(\frac{a_g}{K_H} - a_l\right)$$

$$\pm\frac{db_l}{d\cancel{z}} = -\frac{kLa_l b_l}{\bar{u}_l}$$

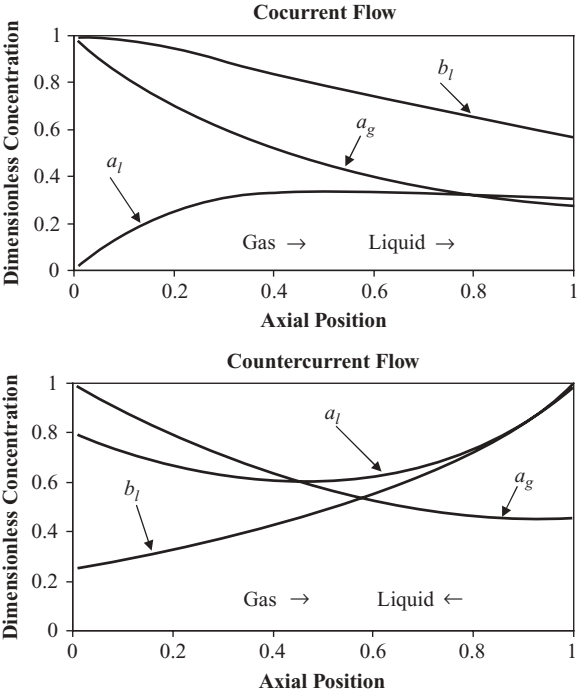

Figure 11.8 Reaction A + B → C in two-phase reactor with a fed from nonreaction phase and B from reacting phase. See Example 11.11.

Numerical solutions using the parameter values of Example 11.10 but with $b_{\text{in}} = 1$ are shown in Figure 11.8. The countercurrent case now requires guesses for both $(a_l)_{\text{out}} = a_l(z = 0)$ and $(b_l)_{\text{out}} = b_l(z = 0)$ to satisfy the initial conditions that $(a_l)_{\text{in}} = 0$ and $(b_l)_{\text{in}} = b_{\text{in}}$ are satisfied.

11.1.4 Other Mixing Combinations

Piston Flow in Contact with a CSTR

A liquid phase reaction in a spray tower is conceptually similar to the transpired wall reactors in Section 3.3. The liquid drops are in piston flow but absorb components from a well-mixed gas phase. The rate of absorption is a function of z as it can be in a transpired wall reactor. The component balance for the piston flow phase is

$$\frac{d(A_l \bar{u}_l a_l)}{dz} = A_l(\mathscr{R}_A)_l + k_l A_i'(a_l^* - a_l) \tag{11.31}$$

The component balance for the CSTR phase is

$$0 = (Q_g a_g)_{\text{in}} - \int_0^L k_g A_i'(a_g^* - a_g)\, dz + V_g(\mathscr{R}_A)_g - (Q_g)_{\text{out}}\, a_g \tag{11.32}$$

There are four unknowns: $a_g = (a_g)_{\text{out}}$, which is independent of z, and a_g^*, a_l^*, and a_l, which will generally vary in the z direction. Equations 11.5 and 11.6 can be used to calculate the interfacial concentrations a_g^* and a_l^* if a_g and a_l are known. A numerical solution for the general case begins with a guess for a_g. This allows Equation 11.31 to be integrated so that a_g^*, a_l^*, and a_l are all calculated as functions of z. The results for a_g^* are substituted into Equation 11.32 to check the assumed value for a_g. Analytical solutions are possible for a few special cases.

EXAMPLE 11.12

Solve Equations 11.31 and 11.32 for the simple case of constant parameters and a pseudo-first-order reaction occurring in the liquid phase of a component supplied from the gas phase. The liquid phase is in piston flow, and the gas phase is well mixed. The gas phase film resistance is negligible. The inlet concentration of the reactive component is a_{in}.

SOLUTION: Note that $K_l = k_l$ when the gas-side resistance is negligible. Then Equations 11.31 simplifies to

$$\frac{da_l}{dz} = -\frac{ka_l}{\bar{u}_l} + \frac{k_l A_i'}{A_l \bar{u}_l}\left(\frac{a_g}{K_H} - a_l\right) = \left[\frac{k_l A_i'}{A_l \bar{u}_l K_H}\right] a_g - \left[\frac{k}{\bar{u}_l} + \frac{k_l A_i'}{A_l \bar{u}_l}\right] a_l$$

Integrate this ODE subject to the initial condition that $a_l = 0$ at $z = 0$. The result is

$$a_l = \frac{a_g k_l A_i'}{K_H[kA_l + k_l A_i']}\left[1 - \exp\left(-\frac{[kA_l + k_l A_i']}{A_l \bar{u}_l} z\right)\right] = a_g C_1[1 - \exp(-C_2 z)]$$

where C_1 and C_2 are constants. This result gives the concentration profile in the liquid phase, but the gas phase concentration is still unknown, and the component balance for the gas phase is necessary. Equation 11.32 simplifies to

$$0 = Q_g a_{\text{in}} - \int_0^L k_g A_i'(a_g^* - a_g)\, dz - Q_g a_g$$

The mass transfer term in this equation is indeterminate since $k_l \to \infty$ and $a_g^* - a_g \to 0$. The indeterminacy is overcome by equating Equations 11.5 and 11.6. Thus,

$$0 = Q_g a_{\text{in}} - \int_0^L k_l A_i'\left(\frac{a_g}{K_H} - a_l\right) dz - Q_g a_g$$

or

$$a_g = a_{\text{in}} - \int_0^L \frac{k_l A_i'}{Q_g}\left(\frac{a_g}{K_H} - a_l\right) dz = a_g = a_{\text{in}} - a_g \frac{k_l A_i'}{\bar{u}_g A_g} \int_0^L \left\{\frac{1}{K_H} - C_1[1 - \exp(-C_2 z)]\right\} dz$$

Integrating and solving for a_g give

$$a_g = \frac{a_{\text{in}}}{1 + [k_l A_i'/(\bar{u}_g A_g)]\,\{L/K_H - C_1 L + (C_1/C_2)[1 - \exp(-C_2 L)]\}}$$

$$= \frac{a_{\text{in}}}{1 + \dfrac{k_l A_i' L}{\bar{u}_g A_g}\left\{1/K_H - \dfrac{k_l A_i'}{K_H[kA_l + k_l A_i']} + \dfrac{A_l \bar{u} k_l A_i'}{K_H[kA_l + k_l A_i']^2 L}\left[1 - \exp\left(-\dfrac{[kA_l + k_l A_i']}{A_l \bar{u}_l} L\right)\right]\right\}}$$

With some algebra, the parameters used in this expression can all be related to four dimensionless groups used in Example 11.10: $kL/\bar{u}_l$, $K_l A_i' L/(A_l \bar{u}_l)$, $K_l A_i' L/(A_g \bar{u}_g)$, K_H.

Using the same numerical values as in Example 11.10 gives $C_1 = \frac{2}{3}$, $C_2 L = 3$, $a_g = 0.393 a_{\text{in}}$ and $a_l = 0.262[1 - \exp(-3z/L]$.

Axial Dispersion

Enthusiastic modelers sometimes add axial dispersion terms to their two-phase piston flow models. The component balances are

$$\pm \frac{d(A_l \bar{u}_l a_l)}{dz} = A_l D_l \frac{d^2 a_l}{dz^2} + A_l(\mathscr{R}_A)_l + k_l A_i'(a_l^* - a_l) \tag{11.33}$$

$$\frac{d(A_g \bar{u}_g a_g)}{dz} = A_g D_g \frac{d^2 a_g}{dz^2} + A_g(\mathscr{R}_A)_g - k_g A_i'(a_g^* - a_g) \tag{11.34}$$

where D_l and D_g are the axial dispersion coefficients for the two phases. In principle, Equations 11.33 and 11.34 can include the entire range of flow in a phase, from perfect mixing (e.g., $D_l \to \infty$) to piston flow (e.g., $D_l \to 0$). In practice, the axial dispersion model is best suited to model small deviations from piston flow. Values for the dispersion coefficients can be measured using the tracer techniques described in Chapter 15. It is usually possible to find tracers that remain in one phase (e.g., nonvolatile liquids or sparingly soluble gases).

11.1.5 Prediction of Mass Transfer Coefficients

As mentioned in Section 11.1.2, fundamental theory is insufficient to predict mass transfer coefficients from first principles. However, existing results do provide a framework for interpreting and sometimes extrapolating experimental results.

Surface Renewal Theory

The ***film model*** for interphase mass transfer envisions a stagnant film of liquid adjacent to the interface. A similar film may also exist on the gas side. These hypothetical films act like membranes and cause diffusional resistances to mass transfer. The concentration on the gas side of the liquid film is a_l^*; that on the bulk liquid side is a_l; and concentrations within the film are governed by the one-dimensional, steady-state

diffusion equation:

$$\mathscr{D}_A \frac{d^2a}{dx^2} = 0$$

This ODE is subject to the boundary conditions that $a_l = a_l^*$ at $x = 0$ and $a = a_l$ at $x = \delta$. The solution is

$$a(x) = a_i^* + (a_l - a_l^*)\frac{x}{\delta}$$

The flux through the film is given by

$$\text{Flux (mol m}^{-2}\text{ s}^{-1}) = -\mathscr{D}_A \frac{da}{dx} = \frac{\mathscr{D}_A}{\delta}(a_l^* - a_l) = k_l(a_l^* - a_l) \tag{11.35}$$

or

$$k_l = \frac{\mathscr{D}_A}{\delta} \tag{11.36}$$

Equation 11.36 gives the central result of film theory; and, as is discussed in any good text on mass transfer, it happens to be wrong. Experimental measurements show k proportional to $\sqrt{\mathscr{D}_A}$ rather than to $\mathscr{D}_A$, at least when the liquid phase is turbulent.

Two rather similar models have been devised to remedy the problems of simple film theory. Both the ***penetration theory*** of Higbie and the ***surface renewal theory*** of Danckwerts replace the idea of steady-state diffusion across a film with transient diffusion into a semi-infinite medium. We give here a brief account of surface renewal theory.

Surface renewal theory envisions a continuous exchange of material between the bulk fluid and the interface. Eddy diffusion brings material of uniform composition a_l to the interface and exposes it to the gas phase for a period of time t. The exposed fluid is then replaced with fresh fluid. Diffusion during the exposure period is governed by

$$\frac{\partial a}{\partial t} = \mathscr{D}_A \frac{\partial^2 a}{\partial x^2} \tag{11.37}$$

This PDE is subject to the initial condition that $a = a_l$ at $t = 0$ and boundary conditions that $a = a_l^*$ at $x = 0$ and $a = a_l$ at $x = \infty$. The solution is differentiated to calculate the flux as in Equation 11.35. Unlike that result, however, the flux into the surface varies with the exposure time t, being high at first but gradually declining as the concentration gradient at $x = 0$ decreases. For short exposure times,

$$\text{Flux} = -\mathscr{D}_A \left[\frac{\partial a}{\partial x}\right]_{x=0} = (a_i^* - a_l)\sqrt{\frac{\mathscr{D}_A}{\pi t}}$$

This result gives the flux for a small portion of the surface that has been exposed for exactly t seconds. Other portions of the surface will have been exposed for different times and thus will have different instantaneous fluxes. To find the average flux, we need the differential distribution of exposure times, $f(t)$. Danckwerts assumed an

exponential distribution:

$$f(t) = \frac{1}{\tau} \exp\left(-\frac{t}{\tau}\right)$$

where $f(t)\,dt$ is the fraction of the interfacial area that has been exposed from t to $t + dt$ seconds and τ is the mean exposure time. Distribution functions are further explained in Chapter 15. The average flux is

$$\int_0^\infty \left[\frac{1}{\tau} \exp\left(-\frac{t}{\tau}\right)\right] (a_l^* - a_l)\sqrt{\frac{\mathscr{D}_A}{\tau}}\,dt = (a_i^* - a_l)\sqrt{\frac{\mathscr{D}_A}{\tau}} \tag{11.38}$$

so that

$$k_l = \sqrt{\frac{\mathscr{D}_A}{\tau}} \tag{11.39}$$

in agreement with experimental observations for turbulent systems.

Enhancement Factors

This section considers gas absorption with fast liquid phase reaction of the component being absorbed. Even a slow reaction in the bulk liquid can give $a_l \to 0$ since the volume of the bulk liquid can be quite large. Thus the existence of any reaction will increase mass transfer by increasing the overall driving force, but a slow reaction does not change k_l as predicted by Equation 11.39. With a much faster reaction, however, component A will be significantly consumed as it diffuses into the turbulent eddy. The concentration gradient at the interface remains high, increasing the flux and increasing the value of k_l. The magnitude of the effect can be predicted by adding a reaction term to Equation 11.37:

$$\frac{\partial a}{\partial t} = \mathscr{D}_A \frac{\partial^2 a}{\partial x^2} + \mathscr{R}_A \tag{11.40}$$

The initial and boundary conditions are identical to those for Equation 11.37: $a = a_l^*$ at $x = 0$ and $a = a_l$ at $x = \infty$. For a first-order reaction, $\mathscr{R}_A = -ka$, and Equation 11.40 has an analytical solution. Using this solution to find the average flux gives

$$k_l = \sqrt{\frac{[1 + (k\tau)^2]\mathscr{D}_A}{\tau}} = (k_l)_0\sqrt{[1 + (k\tau)^2]} = (k_l)_0\,\mathscr{E} \tag{11.41}$$

where $\mathscr{E}$ is the ***enhancement factor*** and $(k_l)_0$ denotes what the mass transfer coefficient would be if there were no reaction, that is, as given by Equation 11.39. Paired measurements of k_l and $(k_l)_0$ have been used to estimate τ. It is typically on the order of 10^{-2} or 10^{-3} s so that a very fast reaction with rate constant $k > 10\ \text{s}^{-1}$ is needed to measurably enhance the mass transfer coefficient.

Any fast reaction can enhance mass transfer. Consider a very fast second-order reaction between the gas phase component A and a liquid component B. The concentration of B will quickly fall to zero in the vicinity of the freshly exposed

surface; and a reaction plane where $b = 0$ will gradually move away from the interface. If components A and B have similar liquid phase diffusivities, the enhancement factor is

$$\mathscr{E} = 1 + \frac{b_l}{a_l^*}$$

Since a_l^* is small for sparingly soluble gases, the enhancement factor can be quite large.

11.2 THREE-PHASE REACTORS

Some reactors involve three or even more phases. The current section discusses the fairly specific situation of a gas phase, a liquid phase, and a solid phase.

Trickle-Bed Reactors

The solid is stationary, catalytic, and usually microporous. The liquid flows in a trickling regime where it wets the external surface of the catalyst but leaves substantial voidage available for the flow of gas. The usual industrial design is for cocurrent, downward flow of both liquid and gas. Such reactors find wide use in the hydrogenation and hydrodesulfurization of heavy petroleum fractions. The goal is to simultaneously contact gas (e.g., hydrogen) and liquid (e.g., a heavy hydrocarbon) on a catalytic surface. The liquid phase supplies one of the reactants and also acts as a transfer medium between the gas phase and the solid phase. The design intent is for the liquid to wet the solid completely since any direct exposure of the solid to the gas phase would not contribute to the reaction.

Piston flow is a reasonable approximation for the liquid and gas phases. The design equations of Section 11.1.3 can be applied by adding an effective pseudohomogeneous reaction rate for the liquid phase:

$$\pm\frac{d(A_l \bar{u}_l a_l)}{dz} = A_l[(\mathscr{R}_A)_l + \varepsilon\eta(\mathscr{R}_A)_s] + k_l A_i'(a_l^* - a_l) \tag{11.42}$$

$$\frac{d(A_g \bar{u}_g a_g)}{dz} = A_g(\mathscr{R}_A)_g - k_g A_i'(a_g^* - a_g) \tag{11.43}$$

Compare Equation 11.42 to the Equation 9.1. The standard model for a two-phase packed-bed reactor is a PDE that allows for radial dispersion. Most trickle-bed reactors have large diameters and operate adiabatically so that radial gradients do not arise. They are thus governed by ODEs. If a mixing term is required, the axial dispersion model can be used for one or both of the phases. See Equations 11.33 and 11.34.

The pseudohomogeneous reaction term in Equation 11.42 is analogous to that in Equation 9.1. We have explicitly included the effectiveness factor η to emphasize the heterogeneous nature of the catalytic reaction. The discussion in Section 10.5 on the measurement of intrinsic kinetics remains applicable, but it is now necessary to ensure that the liquid phase is saturated with the gas when the measurements are made. The void fraction ε is based on relative areas occupied by the liquid and solid

phases. Thus

$$\varepsilon = \frac{A_l}{A_l + A_s} \qquad \text{where } A_g + A_l + A_s = A_c \tag{11.44}$$

The effectiveness factor accounts for the diffusional resistances in the liquid-filled catalyst pores. It does not account for the mass transfer resistance between the liquid and gas phases. This is the job of the k_l and k_g terms.

Homogeneous, liquid phase reactions may also be important in trickle beds, and a strictly homogeneous term has been included in Equation 11.42 to note this fact. There is usually no reaction in the gas phase. Normally, the gas phase merely supplies or removes the gaseous reactants (e.g., H_2 in and H_2S out in hydrodesulfurization).

The central difficulty in applying Equations 11.42 and 11.43 is the usual one of estimating parameters. Order-of-magnitude values for the liquid holdup and $k_l A_i'$ are given for packed beds in Table 11.3. Empirical correlations are unusually difficult for trickle beds. Vaporization of the liquid phase is common. From a formal viewpoint, this effect can be accounted for through the mass transfer term in Equations 11.42 and 11.43. In practice, results are specific to a particular chemical system and operating mode. Proprietary models are the rule.

Gas-Fed Slurry Reactors

These reactors contain suspended solid particles. A discontinuous gas phase is sparged into the reactor. Coal liquefaction is an example where the solid is consumed by the reaction. The three phases are hydrogen, a hydrocarbon solvent–product mixture, and solid coal. Microbial cells immobilized on a particulate substrate are an example of a three-phase system where the suspended, solid phase is catalytic. The liquid phase is water that contains the organic substrate. The gas phase supplies oxygen and removes carbon dioxide. The solid phase consists of microbial cells grown on the surface of a nonconsumable solid such as activated carbon.

A general model for a gas–liquid–solid reactor would have to consider homogeneous reactions occurring within the various phases and up to three sets of heterogeneous reactions: gas–liquid, gas–solid, and liquid–solid. Such a general treatment adds notational complexity without providing additional insight. When the solid acts only as a catalyst, pseudohomogeneous models can usually be used an in the trickle-bed case. Biochemical reactions are often treated in this manner using rate expressions similar in form to those for gas–solid heterogeneous catalysis. Noncatalytic fluid–solid reactions are more difficult since the ***age*** of individual particles may be important. This may require the use of ***population balance models.*** See Example 11.17 and Chapter 15. A slurry reactor with consumable solids can be self-classifying. Particles will stay in the reactor when they are large but will be entrained in the liquid stream as they decrease in size. Careful hydrodynamic design can lead to complete conversion of the solid phase.

11.3 MOVING-SOLIDS REACTORS

Fixed-bed reactors are ideal for many solid-catalyzed gas reactions. The contacting of the solid by the gas tends to be quite uniform. Long contact times are possible; small-diameter tubes provide good heat transfer, but the large particle sizes needed to minimize pressure drop lead to diffusional resistances within the catalyst particles. Scaleup is usually done using many small-diameter tubes in parallel rather than a single large-diameter bed. If catalyst deactivation is rapid, the fixed-bed geometry may cause problems in regeneration. For gas–solid noncatalytic reactions, the solid particles may shrink or grow as the reaction proceeds. This too is not easily accommodated in a fixed bed.

Many types of gas–solid reactors have been designed to allow motion of the solid relative to the fixed walls of the reactors. This motion is desired for one of the following reasons:

1. To enhance heat transfer between the particle and the environment
2. To enable the use of small particles
3. To enable continuous regeneration of catalyst particles
4. To facilitate continuous removal of ash and slag
5. To accommodate size changes of the particles accompanying the reaction

The particle motion can be accomplished by purely mechanical means—perhaps aided by gravity—as in rotary cement kilns and fireplace grates. Chemical engineers usually prefer designs where the particle motion is brought about through hydrodynamic forces that are generated by a fluid phase that also participates in the reaction. Such designs tend to be more controllable and scalable, although scalability can be a problem. Sophisticated pilot plant and modeling efforts are usually necessary for any form of ***fluidized-bed reactor.***

Small particles can be fluidized with liquid or gas. The gas case is the more common, and beds fluidized with a gas have received attention from researchers that is disproportionate to their use in industry. The hydrodynamics of fluidization are interesting, and many aspects of fluidization can be studied in small equipment at room temperature and atmospheric pressure. This makes it well suited to academic research. A large number of fluidization regimes have been elucidated, and Figure 11.9 illustrates the more common regimes applicable to the catalyst particles typically of a bed fluidized by a gas. The particles are spherical with an average diameter of about 50 μm. The size distribution is fairly broad with 95 wt % in the range of 30–100 μm. The particles are microporous with a particle density just over 1 g cm^{-3} but with a skeletal density of about 2.5. They rest on a microporous distributor plate and, at low flow rates, form a packed bed. The pressure drop across the bed increases with increasing flow rate, and the drag on the particles becomes significant. When the pressure drop just equals the weight of the bed, the particles become suspended and mobile enough to be stirred mechanically, but relatively little solids motion is caused just by the gas flow. This is the state of ***incipient fluidization*** illustrated in Figure 11.9*b*. The gas velocity at this point is called the ***minimum fluidization velocity*** $u_{\min}$.

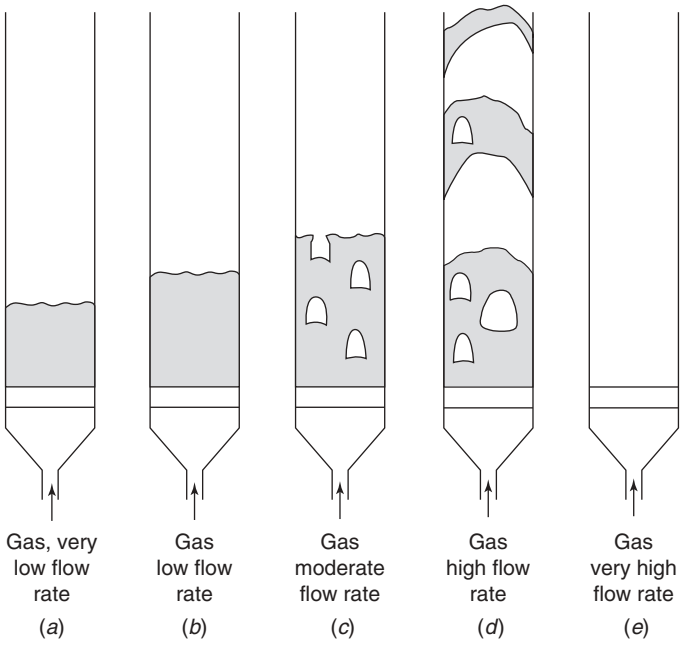

Figure 11.9 Fluidization regimes in batch fluidized bed at low multiples of minimum fluidization velocity: (*a*) packed bed; (*b*) incipient fluidization; (*c*) bubbling fluidization; (*d*) slugging fluidization; (*e*) pneumatic transport.

As the gas flow is increased beyond $u_{\min}$, the behavior of the bed depends on the density difference between the particles and the suspending fluid. If the density difference is small, as in a liquid-fluidized bed, the bed continues to expand and enters a region known as ***particulate fluidization***. Similar behavior is less commonly observed in gas-fluidized beds where it is known as ***delayed bubbling***. More common is a sharp transition to the ***bubbling regime*** where pockets of gas form at the distributor plate and move upward through the bed. These voids are essentially free of solid particles and behave much like bubbles in a gas–liquid system. The voids grow as they rise in the bed due to pressure reduction; they can coalesce; and they provide a stirring mechanism for the suspended particles. Figure 11.9*c* illustrates the bubbling regime of fluidization that lasts until the superficial gas velocity is many times higher than $u_{\min}$. At this point, the bubbles are so large that they span the reactor and cause slugging. Solids at the center of the bed are conveyed upward but rain down near the walls. Figure 11.9*d* depicts the ***slugging*** regime. Still higher gas velocities are used in industrial reactors, and the bed behaves in a smoother fashion. A regime called ***turbulent fluidization*** applies when the upper boundary of the bed is still reasonably well defined. Beyond this are ***fast fluidization*** and finally the ***pneumatic transport*** regime where the gas velocity exceeds the terminal velocity for even the larger particles. A batch fluidized bed operating even in the bubbling or faster regimes will elute some of the smaller particles, and it is normal practice to use a cyclone to

return these particles to the bed. Internal baffles are sometimes used to promote more uniform contacting of the gas and solid.

11.3.1 Bubbling Fluidization

The dynamics of bubble formation and growth and of solids movement within the bubbling fluidized beds have been analyzed in great detail, and elaborate computer simulations have been developed for all regimes of fluidization. The reader is referred to the specialized literature for details on such models. Here we describe a fairly simple model that is applicable to the bubbling regime and that treats a catalytic fluidized bed much like a gas–liquid reactor.

The bubbles play the role of the gas phase. The role of the liquid is played by an ***emulsion phase*** that consists of solid particles and suspending gas in a configuration similar to that at incipient fluidization. The quasi-phases are in cocurrent flow with mass transfer between the phases and with a solid-catalyzed reaction occurring only in the emulsion phase. The downward flow of solids that occurs near the walls is not explicitly considered in this simplified model.

For the emulsion phase,

$$A_e u_e \frac{da_e}{dz} = A_e D_e \frac{d^2 a_e}{dz^2} + A_e \mathscr{R}_A + K_m A_i' (a_b - a_e) \tag{11.45}$$

where D_e is an axial dispersion coefficient, the kinetics are pseudohomogeneous with rate equal to that at incipient fluidization, and K_m is an overall mass transfer coefficient. Henry's law constant does not appear since, at equilibrium, the concentrations would be the same in each phase. Axial dispersion in the bubble phase is ignored. Thus,

$$A_b u_b \frac{da_b}{dz} = -K_m A_i' (a_b - a_e) \tag{11.46}$$

These equations are seen to be special cases of Equations 11.33 and 11.34. The exit concentration is averaged over both phases:

$$a_{\text{out}} = \frac{A_e u_e (a_e)_{\text{out}} + A_b u_b (a_b)_{\text{out}}}{A_e u_e + A_b u_b} \tag{11.47}$$

Values for the various parameters in these equations can be estimated from published correlations. See Suggested Further Readings. It turns out, however, that bubbling fluidized beds do not perform particularly well as chemical reactors. At or near incipient fluidization, the reactor approximates piston flow. The small catalyst particles give effectiveness factors near 1, and the pressure drop—equal to the weight of the catalyst—is moderate. However, the catalyst particles are essentially quiescent so that heat transfer to the vessel walls is poor. At higher flow rates, the bubbles promote mixing in the emulsion phase and enhance heat transfer, but at the cost of increased axial dispersion. The emulsion phase approaches the performance of a CSTR with its inherent lower yield for most reactions. To make matters worse, mass transfer between the emulsion and bubble phases becomes limiting to the point that some of the

entering gas completely bypasses the catalytic emulsion phase. The system behaves like the reactor in Example 11.5.

11.3.2 Fast Fluidization

There are relatively few processes that use a fluidized catalyst. Those that do typically operate with gas velocities high enough to completely entrain the particles. The operating regime is called ***fast fluidization*** or ***transport line fluidization*** and is illustrated in Figure 11.9*e*. Elutriated particles are continuously collected in a cyclone and recycled back to the inlet of the reactor. The fluidized catalytic cracking (FCC) process used in many oil refineries is the most important example of this type of fluidized reactor. The catalyst deactivates so rapidly by coking that it survives just one trip through a riser reactor. It is then collected, regenerated, and recycled back to the inlet to the reactor. The regeneration step uses air to burn off the coke.

A well-defined bed of particles does not exist in the fast-fluidization regime. Instead, the particles are distributed more or less uniformly throughout the reactor. The two-phase model does not apply. Typically, the cracking reactor is described with a pseudohomogeneous, axial dispersion model. The maximum contact time in such a reactor is quite limited because of the low catalyst densities and high gas velocities that prevail in a fast-fluidized or transport line reactor. Thus the reaction must be fast or low conversions must be acceptable. Also, the catalyst must be quite robust to minimize particle attrition.

11.3.3 Spouted Beds

A very different regime of fluidization is called ***spouting.*** Spouting can occur—and is usually undesirable—in a normal fluidized bed if the gas is introduced at localized points rather than being distributed evenly over the reactor cross section. See Figure 11.10*a*. The velocity in the spout is high enough to entrain all particles, but they disengage in the low-velocity regions above the bed. This causes circulation of particles with upward movement in the spout but with motion that is generally downward in the bed. Contact times within the spout are quite short, and little reaction occurs there. Thus the freely spouted bed in Figure 11.10*a* would show relatively low yields for a catalytic reaction. In Figure 11.10*b*, however, the gas is forced to turn around and flow cocurrently with the downward-moving particles. The reaction environment in this region is close to that in a fixed-bed reactor, but the overall reactor is substantially better than a fixed-bed reactor in terms of fluid–particle heat transfer and heat transfer to the reactor walls. To a reasonable approximation, the reactor in Figure 11.10*b* can be modeled as a PFR with recycle. The fluid mechanics of spouting have been examined in detail so that model variables such as pressure drop, gas recycle rate, and solids circulation rate can be estimated. Spouted bed reactors use relatively large particles. One-millimeter (1000-μm) particles are typical, compared to 40–100 μm for most fluidizable catalysts.

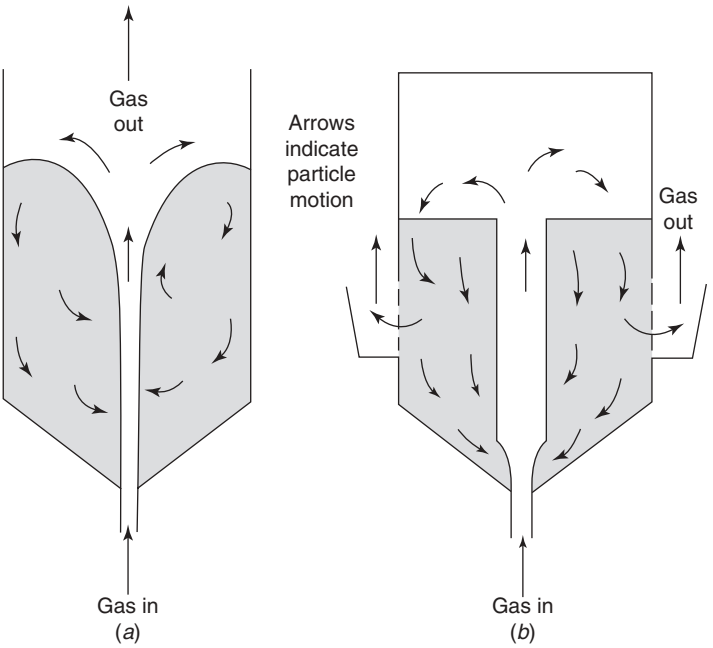

Figure 11.10 Spounted bed reactor with (*a*) normal gas outlet and (*b*) side outlet.

The spouting regime of fluidization is used for the fluid–solid noncatalytic reactions, especially drying and combustion.

11.3.4 Liquid-Fluidized Beds

The solids and the fluid have similar densities in liquid fluidization. The consequence is that most liquidized beds operate in the particulate regime where there is a smooth transition from incipient fluidization to "pneumatic" transport without bubble formation or slugging. They typically operate at near isothermal conditions and have good mass transfer between the liquid and the suspended solids. As a first approximation, the solid phase is well mixed and the liquid phase is in piston flow. There may also be a gas phase. Typical applications are in cell culture, including wastewater treatment. The specialized literature gives details.

11.4 NONCATALYTIC FLUID–SOLID REACTIONS

Cases where a solid directly participates in an overall reaction include the burning of solid fuels, the decoking of cracking catalyst, the reduction of iron ore with hydrogen, and the purification of water in an ion exchange bed. A unifying aspect of all these examples is that the solid participates directly, appears in the reaction stoichiometry, and will ultimately be consumed or exhausted. Often the size and shape of the

Table 11.6 Examples of Fluid–Solid Noncatalytic Reactions

Particle Geometry Largely Unaffected by Reaction	Particle Geometry Strongly Affected by Reaction
Decoking of catalyst pellets	Combustion of coal
Ion exchange reactions	Reduction of ore
Hydrogen storage in metal lattice	Production of acetylene from CaC_2
Semiconductor doping	Semiconductor etching

fluid–solid interface will change as the reaction proceeds. Mass transfer resistances are frequently important, and the magnitude of these resistances may also change with the extent of reaction. The diversity of possible chemistries and physical phenomena is too great to allow comprehensive treatment. We necessarily take a limited view and refer the reader to the research literature on specific processes.

A glib generalization is that the design equations for noncatalytic fluid–solid reactors can be obtained by combining the intrinsic kinetics with the appropriate transport equations. The experienced reader knows that this is not always possible even for the solid-catalyzed reactions considered in Chapter 10 and is much more difficult when the solid participates in the reaction. The solid surface is undergoing change. See Table 11.6. Measurements usually require transient experiments. As a practical matter, the measurements will normally include mass transfer effects and are often made in pilot-scale equipment intended to simulate a full-scale reactor.

Consider a gas–solid reaction of the general form

$$\nu_A \mathrm{A} + \nu_S \mathrm{S} \rightarrow \text{products}$$

Any of the following mass transfer resistances can be important:

Film diffusion. With a fast surface reaction on a nonporous particle, fluid-phase mass transfer limitations can arise.

Pore diffusion. With porous particles, pore diffusion is likely to limit reaction rates at the internal surface.

Product layer diffusion. Many fluid–solid reactions generate ash or oxide layers that impede further reaction.

Sublimation. Some solids sublime and react only after they enter the gas phase. Heat transfer can be the rate-limiting step.

Finally, of course, the surface reaction itself can be rate limiting.

A useful semiempirical approach to noncatalytic surface reactions is to postulate a rate equation of the form

$$\mathscr{R}_A = \nu_A k a^n A_i \tag{11.48}$$

where $n = 1$ and $n = 0$ are typical choices. Equation 11.48 does not address the mechanism of the surface reaction but supposes that the rate will be proportional to

the exposed area and perhaps to the concentration of A in the gas phase. Note that the "concentration" of the solid does not appear in the reaction rate, but the rate is specific to a given solid. The constant k and perhaps even n will change if the composition of the solid changes.

The case of $n = 1$ is a reasonable approximation for a great variety of cases while $n = 0$ covers another common situation where the reaction rate is limited by the disengagement of molecules from the surface. The rate $\mathscr{R}_A$ has its usual interpretation as moles formed per unit volume of reactor per unit time when A_i is the surface area of the fluid–solid interface per unit volume of reactor. For single-particle experiments, A_i will be the surface area and $\mathscr{R}_A$ will be in moles reacted per unit time.

EXAMPLE 11.13

Explore the suitability of Equation 11.48 for modeling various forms of mass transfer and kinetic limitations to the surface reaction.

SOLUTION: We consider in turn each possibility for the rate-limiting step. Most of the cases use $n = 1$. For film diffusion control,

$$\mathscr{R}_A = k_g A_i (a_s - a)$$

where a_s is the gas phase concentration of component A just above the reacting solid. When the film resistance is limiting, $a_s \approx 0$; and, with a redefinition of constants, the reaction rate has the form of Equation 11.48.

If pore diffusion is controlling, we repeat the effectiveness factor calculations in Chapter 10. Equation 10.29 has the form of Equation 11.48, and it includes both film resistance and pore diffusion.

Diffusion through a product layer can be treated like a film resistance. The surface concentration a_s is measured inside the ash layer at the unburned surface of the particle. If the ash thickness is constant and $a_s \approx 0$, then the rate has the form of Equation 11.48. The ash thickness will probably increase with time, and this will cause the rate constant applicable to a single particle to gradually decline with time.

Sublimation, dissolution, and ablative processes in general can be fit using $n = 0$ in Equation 11.48. The actual reaction, if there is one, occurs in the fluid phase with kinetics independent of Equation 11.48. Specifically, Equation 11.48 with $n = 0$ might be used to model dissolution without reaction.

A strict kinetic limitation based on the gas phase reactant can be modeled using a variable value for n although experience shows that a first-order rate expression with $n = 1$ often provides an excellent fit to experimental data regardless of the underlying reaction mechanism. A site competition model such as Equation 10.12 can also be used.

A strict kinetic limitation based on reaction of the solid can be modeled using $n = 0$. In this case, a flat solid surface will erode at a uniform rate. This possibility is explored in Example 11.16.

The analysis of fluid–solid reactions is easier when the particle geometry is independent of the extent of reaction. The left-hand column of Table 11.6 lists some situations where this assumption is reasonable. However, even when the reaction

geometry is fixed, moving boundary problems and sharp reaction fronts are the general rule for fluid–solid reactions. The next few examples explore this point.

EXAMPLE 11.14

Model the movement of the reaction front in an ion exchange column.

SOLUTION: We suppose that the mass transfer and diffusion steps are fast compared to bulk transport by convection. This is the design intent for ion exchange columns. The reaction front moves through the bed at a speed dependent only on the supply of fluid-phase reactants. Assuming piston flow in a constant-diameter column, the location of the reaction front is given by

$$z(t) = \frac{1}{C_A} \int_0^t a_{\text{in}}(t_1)\bar{u}(t_1)\, dt_1 \tag{11.49}$$

Here, C_A is the capacity of the ion exchange resin measured in moles of A per unit volume. The integral in Equation 11.49 measures the amount of material supplied to the reactor since startup. ***Breakthrough*** occurs no later than $z = L$ when all the active sites in the ion exchange resin are occupied. Breakthrough will occur earlier in a real bed due to axial dispersion in the bed or to mass transfer or reaction rate limitations.

EXAMPLE 11.15

Coke formation is a major cause of catalyst deactivation. Decoking is accomplished by periodic oxidations in air. Consider a microporous catalyst that has its internal surface covered with a uniform layer of coke. Suppose that the decoking reaction is stopped short of completion. What is the distribution of residual coke under the following circumstances:

(a) The oxidation is reaction rate limited?

(b) The oxidation is pore diffusion limited?

SOLUTION: For part (a), oxygen has access to the entire internal surface. We expect uniform combustion and a gradual reduction in coke thickness throughout the catalyst pellet. If a completely clean surface is required for catalytic activity, partial decoking will achieve very little.

For part (b), the reaction is fast, and oxygen is consumed as soon as it contacts carbon. Thus there are two zones in the pellet. The outer zone contains oxygen and no carbon. The inner zone contains carbon at its original thickness and no oxygen. The reaction is confined to a narrow front between the zones. The rate at which the front advances is determined by the rate of diffusion of oxygen and the extent of carbon loading in the pores. It can be modeled using an effective diffusivity model such as Equation 10.33. According to this model, the diffusional resistance occurs in the carbon-free spherical shell that starts at the external surface and ends at the reaction front. The size of this shell increases with time so that the diffusional resistance increases and the reaction rate decreases. The interior temperature of the catalyst particle may substantially exceed the bulk temperature, but this does not increase the reaction rate because of the diffusion limitation. The high temperature does increase the risk of catalyst deactivation

through sintering Partial oxidations in the diffusion-controlled regime give partial restoration of catalyst activity since some of the surface is completely cleaned. Decoking has been studied extensively because of its importance to the chemical industry. The two cases considered in this example are known as the ***uniform*** and ***shell progressive*** models, respectively. See Lee (1985) for further details.

EXAMPLE 11.16

Model the consumption of a solid when the gas phase reactant is available at constant concentration and the reaction products are gaseous.

SOLUTION: With a constant, Equation 11.48 written for the solid component becomes

$$\mathscr{R}_S = \nu_S k a^n A_i = \nu_S k' A_i$$

Take the single-particle viewpoint so that A_i is the surface area of the particle and $\mathscr{R}_S$ is in moles per hour. The volumetric consumption rate of the solid is

$$\frac{dV_S}{dt} = \frac{\nu_S k' A_i}{(\rho_{\text{molar}})_S} \tag{11.50}$$

The ratio V_S/A_i is the ***linear burn rate***. We suppose it to be constant. Thus,

$$\frac{dz_S}{dt} = \frac{\nu_S k'}{(\rho_{\text{molar}})_S} = k'' \tag{11.51}$$

The direction of the burn is normal to the surface at every point that is in contact with the gas. Thus, z_S is measured perpendicular to the reaction front. It is best measured using a planar solid so that A_i is constant but can be inferred from short-term experiments on spherical particles or even from careful multiparticle experiments.

The concept of linear burning rate is not confined to the reaction of a gas with a solid. The fuses on fireworks are designed to burn at a constant linear rate. The flame front on solid rocket fuel progresses at a constant linear rate. Both examples have two reactants (fuel and an oxidizer) premixed in the solid. Heat transfer limits the burning rate. These materials are merely fast burning. Unlike explosives, they not do propagate a sonic shock wave that initiates further reaction.

EXAMPLE 11.17

Uniformly sized spheres are fed to a CSTR where they undergo a reaction that consumes the surface at a constant rate of k'' in meters per second. What fraction of the initial population will survive the reactor and what will be the average size upon exiting the reactor?

SOLUTION: The radius of a single particle decreases with time according to the equation

$$R(t) = R_0 - k''t \tag{11.52}$$

provided $t < R_0/k''$. There is no unique answer for the average size and survival probability since the population statistics depend on the distribution of time spent in the reactor by the various particles. We consider two cases: the particles are in piston flow and the particles are well mixed.

The piston flow case assumes that the particles spend the same time in the reactor, $\bar{t}$, even though the fluid phase is well mixed. This case resembles the mass transfer situation of piston flow in contact with a CSTR considered in Section 11.1.4 . The particles leave the reactor with size $R_0 - k''\bar{t}$. None will survive if $\bar{t} > R_0/k''$. Note that $\bar{t}$ is the mean residence time of the solid particles, not of the fluid phase.

The other case assumes that the fluid particles are well mixed. Specifically, assume they have an exponential distribution of residence times so that

$$f(t) = \frac{1}{\bar{t}} \exp\left(-\frac{t}{\bar{t}}\right) \tag{11.53}$$

where $f(t)\,dt$ is the fraction of the particles remaining in the reactor for a time between t and $t + dt$ seconds. The reasonableness of this assumption for a phase within a CSTR will become apparent in Chapter 15. Again, $\bar{t}$ is the mean residence time for the particles. The fraction of particles that survive the reactor is equal to the fraction that has a residence time less than $t_{\text{burn}} = R_0/k''$:

$$\text{Fraction surviving} = \int_0^{t_{\text{burn}}} f(t)\,dt \tag{11.54}$$

The average size of the surviving particles is obtained by weighting $R(t)$ by the differential distribution function and integrating over the range of possible times:

$$\bar{R} = \int_0^{t_{\text{burn}}} R(t) f(t) dt \tag{11.55}$$

Equations 11.54 and 11.55 apply to any distribution of particle residence times provided the linear consumption rate is constant. They do not require that the fluid phase is perfectly mixed, only that the consumption rate is strictly controlled by the surface reaction. For the special case of an exponential distribution of residence times per Equation 11.53, some calculus gives

$$\text{Fraction surviving} = 1 - \exp\left(-\frac{t_{\text{burn}}}{\bar{t}}\right)$$

And the mean size of these surviving particles is

$$\bar{R} = (R_0 - k''\bar{t})\left[1 - \exp\left(-\frac{t_{\text{burn}}}{\bar{t}}\right)\right] + k'' t_{\text{burn}} \exp\left(-\frac{t_{\text{burn}}}{\bar{t}}\right) \tag{11.56}$$

If $t_{\text{burn}} = R_0/k'' = \bar{t}$, then 63% of the particles survive their sojourn through the reactor, compared to none for the piston flow case. The average size of the surviving particles is $0.37R_0$.

11.5 SCALEUP OF MULTIPHASE REACTORS

The design equations presented in this chapter are independent of scale. The various parameters embedded in them are highly scale dependent. The parameter estimates are almost entirely empirical, and this means that the reactor designer must depend on literature correlations if anything approaching a priori design is attempted. With few exceptions, the a priori design of a multiphase system is highly uncertain and rarely attempted. We turn instead to the problem of scaling up a multiphase pilot reactor. How can experiments on a small unit generate confidence in a proposed design?

11.5.1 Gas–Liquid Reactors

Small multiphase reactors are needed to estimate the reaction kinetics. The concept of intrinsic kinetics applies to gas–liquid reactors, but the elimination of all mass transfer resistances may not be possible even at the small scale. Thus, the reaction kinetics may be confounded with mass transfer limitations. These confounded results need to be obtained using a reactor large enough that literature correlations for $k_l A_i$ can be applied. Direct measurement of $k_l A_i$ using one of the methods in Section 11.1.2 is highly desirable as well. There are numerous literature correlations for mass transfer coefficients and gas–phase holdups in gas–liquid reactors. For stirred tanks, there are also correlations for agitator power in both the gassed and ungassed states. Compare the pilot plant results to the values predicted from these correlations. If they agree and if the literature correlations have an experimental base that includes large equipment, a scaleup using the correlations is likely to succeed.

If $k_l A_i$. is known with good accuracy, it may be possible to back out the intrinsic kinetics using the methods of Section 7.1. Knowing the intrinsic kinetics may enable a scaleup where $k_l A_i.(a_l^* - a_l)$ is different in the large and small units. However, it is better to adjust conditions in the pilot reactor so that they are identical to those expected in the larger reactor. Good pilot plants have this versatility. The new conditions may give suboptimal performance in the pilot unit but achievable performance in the full-scale reactor.

Mass transfer is generally improved in deep vessels due to the higher partial pressure of the gaseous component being transferred. The price for the improvement is the greater pumping energy needed to sparge the gas at the greater depth. Experiments run in the pilot unit at various liquid levels can be used to test this concept. The agitator speed should be varied over a wide range. If performance improves with increasing depth, scaleup to a large vessel should be reasonable. Another possible test method is to pressurize the vessel to increase the partial pressure of the component being transferred or to enrich the entering gas (e.g., by using, say, 30% oxygen rather than atmospheric oxygen). If performance improves, scaleup is likely to succeed. Alternatively, the tricks just mentioned may be designed into the larger unit as a means of overcoming any scaleup problems.

Does increased agitator speed improve performance in the pilot plant? If so, there is a potential scaleup problem. Installing a variable-speed drive with a somewhat oversized motor can provide some scaleup insurance, the cost of which is apt to be minor compared to the cost of failure.

EXAMPLE 11.18

Consider a gas-sparged CSTR with reaction occurring only in the liquid phase. Suppose a pilot-scale reactor gives a satisfactory product. Propose a scaleup to larger vessel.

SOLUTION: Ideally, the scaleup will maintain the same inlet concentrations for the two phases, the same relative flow rates and holdups for the two phases, and the same ratio of gas transferred to liquid throughput. It is also necessary to maintain a constant residence time in the liquid phase. It is simple to set the flow rates:

$$S = \left[\frac{Q_2}{Q_1}\right]_l = \left[\frac{Q_2}{Q_1}\right]_g \tag{11.57}$$

We would also like the following to be true, but their achievement is less direct than for the flow rates:

$$S = \left[\frac{V_2}{V_1}\right]_l = \left[\frac{V_2}{V_1}\right]_g = \frac{V_2}{V_1} \tag{11.58}$$

$$\left[\frac{V k_l A_i (a_l^* - a_l)}{Q_l}\right]_2 = \left[\frac{V k_l A_i (a_l^* - a_l)}{Q_l}\right]_1 \tag{11.59}$$

We can operate at the required liquid volume—say by putting the reactor on load cells—but the gas phase volume and thus the total volume may change upon scaleup. Correlations are needed for the gas phase holdup and for $k_l A_i$. A typical correlation for $k_l A_i$ is that by Middleton (1985):

$$k_l A_i = C \left(\frac{P_g}{V_l}\right)^{0.7} (\bar{u}_s)_g^{0.6}$$

where C is a constant, P_g is the agitator power in the gassed condition, and $(\bar{u}_s)_g$ is the superficial gas velocity. It was obtained by experiments using only one agitator in one tank, but it is a place to start. Suppose the pilot-scale vessel is scaled using geometric symmetry. Then A_c scales as $S^{2/3}$ and $(\bar{u}_s)_g = Q_g/A_c$ scales as $S^{2/3}$. This fact imposes a limit on scaleup since scaling by too large a factor could blow the water out of the vessel. Consider $S = 64$ so that $(\bar{u}_s)_g$ increases by a factor of 4 upon scaleup. Can the pilot vessel accept a factor of 4 increase in the sparging rate and what does that do to the holdup? Alternatively, can the gas rate in the small vessel be lowered without too much impact on product quality? Suppose for the moment that experiments at the increased rate indicate no problem and that it causes only a minor increase in holdup. Then a geometrically similar scaleup will satisfy Equation 11.58, and Equation 11.59 will be satisfied if $k_l A_i$ can be held constant upon scaleup. (Actually, a_g^* will increase upon scaleup due to the greater liquid head so $k_l A_i$ can decrease, but this will usually be a small effect.) The Middleton correlation says $k_l A_i$ will be constant if

$$\left[\frac{(P_g/V_l)_2}{(P_g/V_l)_1}\right]^{0.7} \left[\frac{[(\bar{u}_s)_g]_2}{[(\bar{u}_s)_g]_1}\right]^{0.6} = 1$$

The factor of 4 increase in $(\bar{u}_s)_g$ allows $(P_g/V_l)_2$ to decrease to $0.3(P_g/V_l)_1$. This suggests that the installed horsepower for the full-scale plant would be about a third of that calculated for a conservative scaleup with constant power per volume. This will have a major impact on cost and is too large to ignore. The engineer can do any of the following;

1. Search the literature for correlations for $k_l A_i$ and holdup to see if they predict a similar scaleup.
2. Operate the pilot plant over a wide range of agitator speeds and gas rates to confirm operability and to develop correlations for $k_l A_i$ and holdup applicable to the particular geometry of the pilot reactor.
3. Contact mixing equipment vendors for a recommended scaleup. They have proprietary correlations and extensive experience on similar scaleups. They will also guarantee success, although their liability will be limited to the value of the equipment and not for consequential damages.

Probably all three things should be done.

11.5.2 Gas-Moving Solids Reactors

As mentioned in Section 11.3, fluidized-bed reactors are difficult to scale. One approach is to build a ***cold flow model*** of the process. This is a unit in which the solids are fluidized to simulate the proposed plant, but at ambient temperature and with plain air as the fluidizing gas. The objective is to determine the gas and solid flow patterns. Experiments using both adsorbed and nonadsorbed tracers can be used in this determination. The nonadsorbed tracer determines the gas phase residence time using the methods of Chapter 15. The adsorbed tracer also measures time spent on the solid surface, from which the ***contact time distribution*** can be estimated. See Section 15.4.2.

SUGGESTED FURTHER READINGS

Multiphase mass transfer is a vast topic. A general reference for gas–liquid and solid–liquid mass transfer in stirred tank reactors is:

E. L. Paul et al., *Handbook of Industrial Mixing*, Wiley, New York, 2003.

Bubble columns are reviewed in:

H. A. Jakobsen et al., Modeling of bubble column reactors: Progress and limitations, *Ind. Eng. Chem. Res.*, **44**, 5107–5151 (2005).

The following reviews emphasize those forms of fluidization used in industrial reactors:

J. R. Grace et al., Fluidized beds, *Multiphase Flow Handbook*, CRC Press, Boca Raton, FL, 2006.
H. T. Bi et al., A state-of-the-art review of gas-solid turbulent fluidization, *Chem. Eng. Sci.*, **55**, 4789–4825 (2000).

For a comprehensive treatment of spouted bed reactors consult:

Y. Arkun et al., Modeling of spouted bed chemical reactors, in N. P. Cheremisinoff (Ed.), *Encyclopedia of Fluid Mechanics,* Vol. 4, *Solids and Gas-Solids*, Gulf, Houston, TX, 1986, pp. 1089–1025.

The state-of-the-art for understanding the details of liquid-fluidized beds is given in:

S. Limtrakul et al., Solids motion and holdup profiles in liquid fluidized beds, *Chem. Eng. Sci.*, **60**, 1889–1900 (2005).

PROBLEMS

11.1 Henry's law constant K_H for carbon dioxide in water at 30°C is 11.1 10^7 mm of Hg per mole fraction. What is the dimensionless value for K_H so that a_l and a_g have the same units?

11.2 Complete Example 11.4 for the case where $V_g/Q_g = 20$ s. Solve the governing ODEs analytically or numerically as you prefer. How does this more rigorous approach change the 95% response time calculated in Example 11.3?

11.3 The algebra needed for the solution in Example 11.5 is a bit messy. Check the result for plausibility by studying the behavior of the solution in various limits. Specifically, determine a_g when the following variables become, one at a time, either zero or infinity: Q, k, K_l. Explain your results for the cases when one of k andK_l is infinite but the other is finite.

11.4 A reactive gas is slowly bubbled into a column of liquid. The bubbles are small, approximately spherical, and are well separated from each other. Assume Stokes's law and ignore the change in gas density due to elevation. The gas is pure and reacts in the liquid phase with first-order kinetics. Derive an expression for the size of the bubbles as a function of height in the column. Carefully specify any additional assumptions you need to make.

11.5 Example 11.5 treats a reaction that is catalyzed by a stagnant liquid phase. Find the outlet concentration of component A for the limiting case of high catalytic activity, $k \to \infty$. Repeat for the limiting case of high mass transfer, $k_l A_i \to \infty$.

11.6 Example 11.6 ignored the accumulation term for $a_l(t)$ in Equation 11.11. How does the result for a_l change if this term is retained? Consider only the asymptotic result as $t \to \infty$.

11.7 Confirm that the solutions in Examples 11.10 and 11.11 satisfy an overall material balance.

11.8 Find an analytical solution for the pair of ODEs in Example 11.10 for (a) the (easy) the cocurrent case and (b) the countercurrent case.

11.9 The low-pressure chemical vapor deposition of silicon nitride on silicon involves two gaseous reactants, dichlorosilane and ammonia. The following reactions are believed important under typical conditions of $P = 1$ Torr and $T = 1000$–1200 K:

$$\mathrm{SiH_2Cl_2} + \tfrac{4}{3}\mathrm{NH_3} \longrightarrow \tfrac{1}{3}\mathrm{Si_3N_4} + 2\mathrm{HCl} + 2\mathrm{H_2} \qquad \text{(I)}$$

$$\mathrm{SiH_2Cl_2} \rightleftarrows \mathrm{SiCl_2} + \mathrm{H_2} \qquad \text{(II)}$$

$$\mathrm{SiCl_2} + \tfrac{4}{3}\mathrm{NH_3} \longrightarrow \tfrac{1}{3}\mathrm{Si_3N_4} + 2\mathrm{HCI} + \mathrm{H_2} \qquad \text{(III)}$$

$$\mathrm{NH_3} \longrightarrow \tfrac{1}{2}\mathrm{N_2} + \mathrm{H_2} \qquad \text{(IV)}$$

Suppose the reactant gases are supplied continuously in large excess and flow past a single wafer of silicon. By performing multiple experiments, the growth of the nitride layer can be determined as a function of time and reactant concentrations. Develop an experimental program to determine rate expressions for reactions I–IV. Note that reactions I, III, and IV are heterogeneous while reaction II occurs in the gas phase. It is possible to include N_2, H_2, and HCl in the feed if this is useful. Exiting gas phase concentrations cannot be measured.

11.10 The shell progressive model in Example 11.15(b) envisions a mass transfer limitation. Is the limitation more likely to be based on oxygen diffusing in or on the combustion products diffusing out?

11.11 Determine the position of the reaction front in the diffusion-limited decoking of a spherical cracking catalyst. *Hint:* Use a version of Equation 11.49 but correct for the spherical geometry and replace the convective flux with a diffusive flux.

11.12 Example 11.14 assumed piston flow when treating the moving-front phenomenon in an ion exchange column. Expand the solution to include an axial dispersion term. How should breakthrough be defined in this case?

11.13 The transition from Equation 11.50 to Equation 11.51 seems to require the step that $dV_S/A_i = d[V_S/A_i] = dz_S$. This is not correct in general. Is the validity of Equation 11.51 limited to situations where A_i is actually constant?

11.14 An overly simplified model of fluidized-bed combustion treats the solid fuel as spherical particles freely suspended in upward-flowing gas. Suppose the particles react with zero-order kinetics and that there is no ash or oxide formation. It is desired that the particles be completely consumed by position $z = L$. This can be done in a column of constant diameter or in a column where the diameter increases or decreases with increasing height. Which approach is better with respect to minimizing the reactor volume? Develop a model that predicts the position of the particle as a function of time spent in the reactor. Ignore particle-to-particle interactions.

11.15 Suppose the pilot-scale stirred tank of Example 11.18 is at the ragged edge of acceptable operation so that $(\bar{u}_s)_g$ cannot be increased upon scaleup. Neither can Q_g/Q_l be decreased. What can be done to avoid a scaleup limitation? Your proposed solution should utilize the existing pilot reactor for experimental confirmation.

Chapter 12

Biochemical Reaction Engineering

Biochemical engineering is a vibrant branch of chemical engineering with a significant current presence and even greater promise for the future. In terms of development, it can be compared to the petrochemical industry in the 1920s. Despite its major potential, biochemical engineering has not yet been integrated into the standard undergraduate curriculum for chemical engineers. This means that most graduates lack an adequate background in biochemistry and molecular biology. The present brief chapter will not remedy the deficiency. Instead, it introduces those aspects of biochemical reactor design that can be understood without detailed knowledge of the underlying biological sciences. A chemical engineer can make contributions to the field without becoming a biochemist or molecular biologist, just as chemical engineers made contributions to the petrochemical industry with sometimes rudimentary knowledge of organic chemistry.

Proteins are key ingredients to life and to biochemistry. They are linear polymers of amino acids. The general formula for an amino acid is

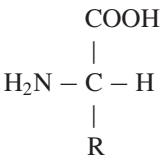

where R represents 1 of about 20 different radicals found in nature. The amino and carboxy groups condense and eliminate water to form proteins. When proteins are formed in a living cell, the sequence of amino acids is dictated by the deoxyribonucleic acid (DNA) within the cell. The term genetic engineering refers to manipulation of DNA to alter the recipe. Despite the name, genetic engineering is not an engineering discipline but a branch of molecular biology similar in spirit to organic synthesis. This chapter is not concerned with genetic engineering as such. Biochemical engineering (or sometimes agricultural engineering) comes later when genetically engineered organisms are to be grown in mass. Many current applications of biochemical

Chemical Reactor Design, Optimization, and Scaleup, Second Edition. By E. B. Nauman
Copyright © 2008 John Wiley & Sons, Inc.

engineering are based on naturally occurring organisms and biocatalysts. The products range from small, simple molecules such as methane and ethanol to moderately complex compounds such as penicillin to therapeutic proteins such as human growth factor to whole cells such as yeast and potentially to multicell aggregates such as skin. Some of these compounds (e.g., ethanol and penicillin) can be produced by traditional organic synthesis. Thus a working distinction between biochemical reaction engineering and "ordinary" chemical reaction engineering is the involvement of biocatalysts, specifically proteins having catalytic activity and known as ***enzymes***.

12.1 ENZYME CATALYSIS

Enzymes are proteins that catalyze reactions. Thousands of enzymes have been classified and there is no clear limit as to the number that exists in nature or can be created artificially. Enzymes have one or more catalytic sites that are similar in principle to the active sites on a solid catalyst that are discussed in Chapter 10, but there are major differences in the nature of the sites and in the nature of the reactions they catalyze. Mass transport to the active site of an enzyme is usually done in the liquid phase. Reaction rates in moles per volume per time are several orders of magnitude lower than rates typical of solid-catalyzed gas reactions. Optimal temperatures for enzymatic reactions span the range typical of living organisms, from about 4°C for cold-water fish to about 40°C for birds and mammals to over 100°C for thermophilic bacteria. Enzymatic reactions require very specific molecular orientations before they can proceed. As compensation for the lower reaction rates, enzymatic reactions are highly selective. They often require specific stereoisomers as the reactant (termed the ***substrate*** in the jargon of biochemistry) and can generate stereospecific products. Enzymes are subject to inhibition and deactivation, like other forms of catalysis.

12.1.1 Michaelis–Menten Kinetics

Suppose the reaction S $\rightarrow$ P occurs using an enzyme as a catalyst. The following reaction mechanism is postulated:

$$\begin{aligned} \mathrm{S} + \mathrm{E} &\rightleftarrows \mathrm{SE} & \frac{[\mathrm{SE}]}{s[\mathrm{E}]} &= K \\ \mathrm{SE} &\longrightarrow \mathrm{P} + \mathrm{E} & \mathscr{R} &= k[\mathrm{SE}] \end{aligned}$$

where s denotes the substrate concentration, E denotes the active site, and SE denotes the adsorbed complex. This mechanism is somewhat different than that used for gas–solid catalysis since there is no explicit desorption step. In essence, product desorption is assumed to be instantaneous. The site balance is

$$[\mathrm{SE}] + [\mathrm{E}] = E_0$$

Substituting for [SE] and [E] gives

$$\frac{\mathscr{R}}{k} + \frac{\mathscr{R}}{ksK} = E_0$$

and

$$\mathscr{R} = \frac{E_0 ks}{1/K + s} = \frac{k's}{1 + k_S s} \tag{12.1}$$

which is the functional form expected when there is competition for active sites. Just as for gas–solid reactions, the reaction rate for a first-order reaction depends linearly on the amount of catalyst but reaches a maximum value as the substrate concentration increases. See Figure 12.1*a*. Biochemists usually express

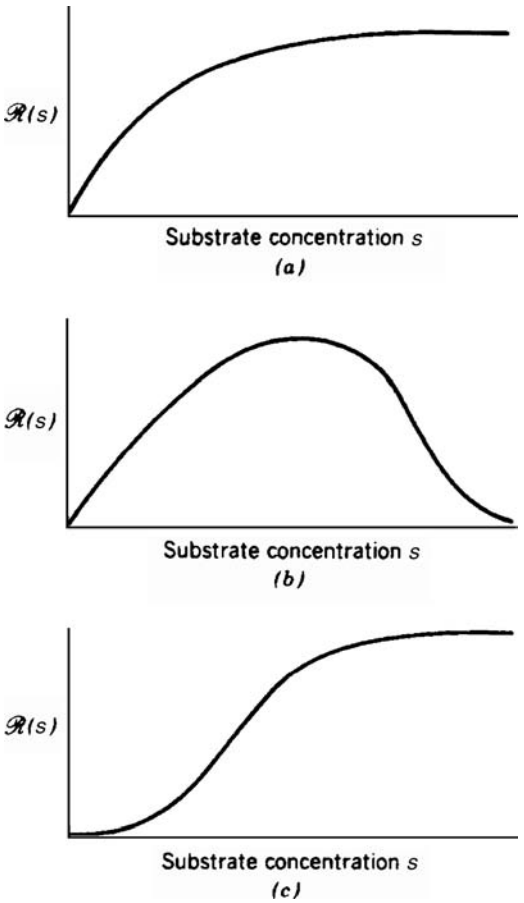

Figure 12.1 Effects of substrate (reactant) concentration on the rate of enzymatic reactions: (*a*) simple Michaelis–Menten kinetics; (*b*) substrate inhibition; (*c*) activation.

Equation 12.1 as

$$\mathscr{R} = \frac{E_0 k s}{K_M + s} = \frac{\mathscr{R}_{\max} s}{K_M + s} \tag{12.2}$$

where K_M is called the Michaelis constant. Either of Equations 12.1 and 12.2 contains two adjustable constants that must be found by fitting experimental data. Their form is equivalent to Hougan and Watson (or Langmuir–Hinshelwood) kinetics for the gas–solid reaction S → P with negligible adsorption, but the Michaelis–Menten equation was derived first.

Simple Michaelis–Menten kinetics exhibit the saturation behavior in Figure 12.1*a*. Enzyme systems can also show the more complex behavior in Figures 12.1*b* and *c*. Figure 12.1*b* illustrates ***substrate inhibition*** where high reactant concentrations lead to a decrease in reaction rate. The sigmoidal rate curve shown in Figure 12.1*c* illustrates ***substrate activation***. These phenomena can be modeled with variants of Michaelis–Menten kinetics involving two or more substrate molecules being adsorbed at a single site or enzyme molecules having two or more interacting sites.

EXAMPLE 12.1

Suppose an enzymatic reaction has the following mechanism:

$$\mathrm{S} + \mathrm{E} \rightleftarrows \mathrm{SE} \qquad \frac{[\mathrm{SE}]}{s[\mathrm{E}]} = K$$

$$\mathrm{S} + \mathrm{SE} \rightleftarrows \mathrm{S^2E} \qquad \frac{[\mathrm{S^2E}]}{s[\mathrm{E}]} = K_2$$

$$\mathrm{SE} \longrightarrow \mathrm{P} + \mathrm{E} \qquad \mathscr{R} = k[\mathrm{SE}]$$

Determine the functional form of the rate equation.

SOLUTION: The total concentration of active sites is

$$[\mathrm{S^2E}] + [\mathrm{SE}] + [\mathrm{E}] = E_0$$

The two equilibrium relations and the rate expression allow the unknown surface concentrations $[\mathrm{S^2E}]$, [SE], and [E] to be eliminated. The result is

$$\mathscr{R} = \frac{E_0 k s}{1/K + s + K_2 s^2} \tag{12.3}$$

This equation gives $\mathscr{R}(0) = 0$, a maximum at $s = \sqrt{K_M / K_2}$, and $\mathscr{R}(\infty) = 0$. The assumed mechanism involves a first-order surface reaction with inhibition of the reaction if a second substrate molecule is adsorbed. A similar functional form for $\mathscr{R}(s)$ can be obtained by assuming a second-order, dual-site model. As in the case of gas–solid heterogeneous catalysis, it is not possible to verify reaction mechanisms simply by steady-state rate measurements.

EXAMPLE 12.2

Suppose the reaction mechanism is

$$\begin{aligned} S + E &\rightleftarrows SE & \frac{[SE]}{s[E]} &= K \\ S + E &\rightleftarrows S^2E & \frac{[S^2E]}{s[E]} &= K_2 \\ SE &\longrightarrow P + E & \mathscr{R}_I &= k[SE] \\ S^2E &\longrightarrow SE + P + E & \mathscr{R}_{II} &= k_2[S^2E] \end{aligned}$$

Determine the functional form for $\mathscr{R}(s)$.

SOLUTION: This case is different than any previously considered site models since product can be formed by two distinct reactions.

The overall rate is

$$\mathscr{R}_P = \mathscr{R}_I + \mathscr{R}_{II} = k[SE] + k_2[S^2E]$$

The site balance is the same as in Example 12.1. Eliminating the unknown surface concentrations gives

$$\mathscr{R}_P = \frac{E_0(ks + k_2K_2s^2)}{1/K + s + K_2s^2} \tag{12.4}$$

As written, this rate equation exhibits neither inhibition nor activation. However, the substrate inhibition of Example 12.1 occurs if $k_2 = 0$, and substrate activation occurs if $k = 0$.

Second-order enzymatic reactions require two adsorption events at the same site. For the reaction A + B → P, there may be a compulsory order of adsorption (e.g., first A, then B) or the two reactants may adsorb in a random order. Different assumptions lead to slightly different kinetic expressions, but a general form with theoretical underpinnings is

$$\mathscr{R} = \frac{k'ab}{1 + k_Aa + k_Bb + k_{AB}ab} \tag{12.5}$$

In summary, the simple Michaelis–Menten form of Equation 12.1 is usually sufficient for first-order reactions. It has two adjustable constants. Equation 12.4 is available for special cases where the reaction rate has an interior maximum or an inflection point. It has three adjustable constants after setting either $k_2 = 0$ (inhibition) or $k = 0$ (activation). These forms are consistent with two adsorptions of the reactant species. They each require three constants. The general form of Equation 12.4 has four constants, which is a bit excessive for a first-order reaction. The general form for a reaction of the A + B → P type, Equation 12.5, also requires four constants, although it is possible that one or two of them will be zero.

The temperature dependence of enzymatic reactions is modeled with an Arrhenius form for the main rate constant, k'. The practical range of operating temperatures is usually small, but the activation energies can be quite large. Temperature dependence of the inhibition constants can usually be ignored.

12.1.2 Inhibition, Activation, and Deactivation

Reactant molecules cause the substrate inhibition and activation discussed in Section 12.1.1. These effects and deactivation can also be caused by other molecules and by changes in environmental conditions.

Reversible inhibition ceases when the inhibiting molecule is removed from the system. The molecules can be eliminated from the feed in a flow system or from a batch reaction by a separation process such as dialysis. Two kinds of reversible inhibition are distinguished. ***Competitive inhibition*** occurs when an inhibitor molecule occupies a site before it is occupied by a substrate molecule. The assumed mechanism is

$$\mathrm{I} + \mathrm{E} \rightleftarrows \mathrm{IE}$$

Noncompetitive inhibition occurs when the inhibiting molecule is adsorbed after the substrate molecule has been absorbed. The assumed mechanism is

$$\mathrm{I} + \mathrm{SE} \rightleftarrows \mathrm{ISE}$$

The two forms of inhibition can occur together. Their combined effects are modeled by changing the denominator of the rate equation. For an irreversible first-order reaction, a suitable rate equation is

$$\mathscr{R} = \frac{k's}{1 + k_S s + k_I i + k_{SI} si} \tag{12.6}$$

where $k_{SI} = 0$ for purely competitive inhibition and $k_I = 0$ for purely noncompetitive inhibition.

Some enzymes require ***cofactors*** to activate catalysis. Typical cofactors are metal atoms, ammonia, and small organic molecules that associate with the enzyme and help structure the catalytic site. To conduct an enzymatic reaction, the necessary cofactors must be supplied along with the substrate and the enzyme. In cell metabolism, a variety of these cofactors act in conjunction with inhibitors to control the metabolic rate.

Deactivation generally refers to a change in the physical structure of the enzyme, often caused by an increase in temperature. Some of the amino acids in a protein chain are hydrophobic. Others are hydrophilic. Proteins in solution ***fold*** into elaborate but characteristic shapes to increase like-to-like interactions within the polymer and between the polymer and the solvent. The folded state is the ***native or natural state*** and is the state in which enzymes have their catalytic activity. At high temperatures, random thermal forces disrupt the folded chain and destroy the catalytic sites. Very high temperatures will cause coagulation or other structural and chemical changes. This leads to ***irreversible deactivation***, and the proteins are ***denatured***. Mammalian

enzymes typically deactivate at temperatures above 45°C, but some enzymes continue to function at 100°C. Lower temperatures can cause unfolding without permanent damage to the enzyme. ***Reversible deactivation*** caused by relatively low temperatures or by short times at high temperatures can be reversed just by lowering the temperature.

Deactivation of both reversible and irreversible varieties can have chemical causes such as pH changes. If the pH change is small, it can sometimes be modeled using an inhibition term in the Michaelis–Menten equation. Larger changes in pH can reversibly alter the configuration of the enzyme, and still larger changes may destroy it. Enzymes can be deactivated by other enzymes or by chemical agents such as ozone and chlorine.

12.1.3 Immobilized Enzymes

Some enzymes are cheap enough to be used in one-time applications such as washing clothes or removing blood stains from leather. Others are so expensive that they must be recycled or otherwise reused. One method to achieve this is to put an ultrafilter, operating in the cross-flow mode, on the discharge stream of a continuous process. See Figure 12.2. Small molecules pass through the filter, but large molecules such

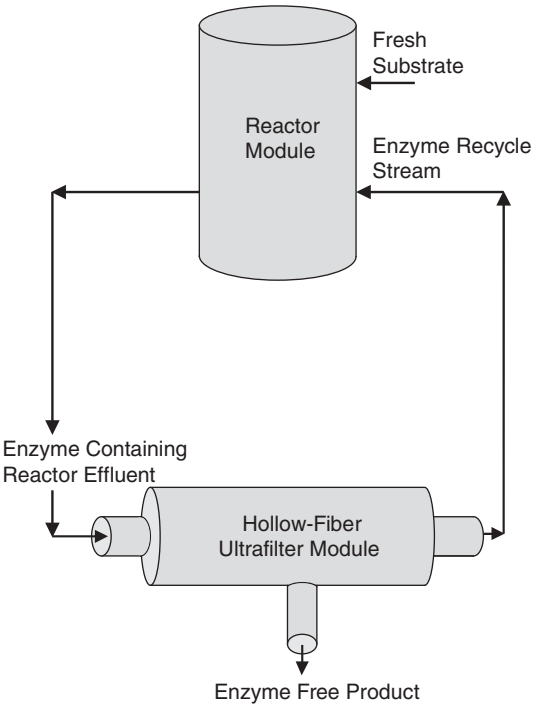

Figure 12.2 Membrane reactor system.

as the enzyme are retained and recycled. The enzymes can also be entrapped within a porous solid, for example, within the large-pore side of an asymmetric membrane. These are examples of ***immobilization by physical entrapment***.

Immobilization by adsorption onto surfaces such as activated carbon or an ion exchange resin gives a reversible and relatively weak bond, but this can be sufficient to increase the retention time in a flow system to acceptable levels. Recall Section 10.6, where it was shown that the residence time of an adsorbed species can be much larger than that of the mobile phase, in essence giving more time for catalysis.

Immobilization by chemical bonding gives strong, irreversible attachments to a solid support. The bonds are normally covalent but can be electrostatic. Typical supports are functionalized glass and ceramic beads and fibers. Enzymes are sometimes crosslinked to form a gel. Occasionally, enzymes can be flocculated while retaining catalytic activity.

All these immobilization techniques run the risk of altering activity compared to the native enzyme. Improved activity is occasionally reported, but this is the exception. The immobilization techniques listed above are in approximate order of loss in activity. Physical entrapment normally causes no change. Adsorption will distort the shape of the molecule compared to the native state. The effect of covalent bonding depends on the location of the bond relative to an active site. If remote from the site, it may have no effect. The chemical nature of the support can affect activity. Crosslinking requires two covalent attachments per enzyme molecule and is thus likely to distort the shape of the enzyme to the point that catalytic activity is lost. Such distortions are even more likely, but not inevitable, for coagulated or flocculated enzymes. On the positive side, immobilization tends to stabilize enzymes against deactivation.

Immobilization can give rise to mass transfer limitations that do not occur for freely suspended enzymes in their native state. As a formality, these limitations can be incorporated into an effectiveness factor:

$$\eta = \frac{\text{observed reaction rate}}{\text{rate when enzyme is in its native state}} \tag{12.7}$$

This definition recognizes that immobilization (e.g., at cellular membranes) is the native state for some enzymes. Although interesting mathematics are possible, effectiveness factors are measured experimentally, as was the case for the solid-catalyzed gas phase reactions discussed in Chapter 10. Effectiveness factors greater than 1 are possible.

12.1.4 Reactor Design for Enzyme Catalysis

When the product from a biochemical reactor is intended for use as a food or drug, the design process is subject to a set of government-mandated checks and balances to assure safe and effective finished products. The process must conform to a methodology known as current good manufacturing practice, or CGMP (usually shortened to ***GMP***). Subject to this requirement for special care and documentation, the

design of a biochemical reactor is conceptually similar to that for ordinary chemical reactors.

Confined Enzymes in Steady-State Flow Reactors

The confinement can be accomplished using the membrane reactor of Figure 12.2 or by a packed-bed reactor in which the enzymes are immobilized within the packing or by using a solid–liquid fluidized bed in which the enzymes are immobilized within the fluidized particles. All these geometries have a common feature that makes the reactor analysis relatively simple: No enzymes enter or leave the system during steady-state operation. Due to the high cost of enzymes, such reactors are a desirable way of performing enzyme catalysis.

The easiest reactor to analyze is a steady-state CSTR. Biochemists call it a ***chemostat*** because the chemistry within a CSTR is maintained in a static condition. Biochemists use the ***dilution rate*** to characterize the flow through a CSTR. The dilution rate is the reciprocal of the mean residence time.

EXAMPLE 12.3

Suppose S $\rightarrow$ P according to first-order Michaelis–Menten kinetics. Find s_{out} for a CSTR.

SOLUTION: Most enzyme reactors use such high concentrations of water that the fluid density is constant. Applying Michaelis–Menten kinetics to the component balance for a steady-state CSTR gives

$$s_{\text{in}} - \frac{\bar{t} E_0 k s_{\text{out}}}{K_M + s_{\text{out}}} = s_{\text{out}}$$

Solving for s_{out} gives

$$s_{\text{out}} = \left[s_{\text{in}} - K_m - E_0 k\bar{t} - \sqrt{(s_{\text{in}} - K_M - E_0 k\bar{t})^2 + 4 s_{\text{in}} K_M} \right] \Big/ 2$$

The reverse solution, finding the value of $\bar{t}$ needed to achieve a desired value for s_{out}, is easier. Equation 1.54 gives the reverse solution for the general case where the reaction rate depends on s_{out} alone and density is constant. Applying Equation 1.54 to the present case gives

$$\bar{t} = \frac{(s_{\text{in}} - s_{\text{out}})(K_M + s_{\text{out}})}{E_0 k s_{\text{out}}}$$

Most biochemical reactors operate with dilute reactants so that they are nearly isothermal. This means that the packed-bed model of Section 9.1 is equivalent to piston flow. The axial dispersion model of Section 9.3 can be applied, but the correction to piston flow is usually small and requires a numerical solution if Michaelis–Menten kinetics are assumed.

EXAMPLE 12.4

Suppose S → P according to first order Michaelis–Menten kinetics. Find s_{out} for a PFR

SOLUTION: The design equation for a PFR gives

$$\bar{u}\frac{ds}{dz} = \frac{-E_0 k s}{K_M + s}$$

subject to the initial condition $s = s_{in}$ at $z = 0$. The solution is implicit in s_{out}:

$$s_{out} \exp\left[\frac{s_{out} - s_{in}}{K_M}\right] = s_{in} \exp\left[\frac{-E_0 k \bar{t}}{K_M}\right]$$

The corresponding solution for $\bar{t}$ is explicit:

$$\bar{t} = \frac{s_{in} - s_{out} - K_M \ln (s_{in}/s_{out})}{E_0 k}$$

Enzyme-Catalyzed Batch Reactions

Michaelis–Menten theory assumes equilibrium between occupied and unoccupied site:

$$\mathrm{S} + \mathrm{E} \underset{kr}{\overset{kf}{\rightleftarrows}} \mathrm{SE} \qquad \frac{[\mathrm{SE}]}{s[\mathrm{E}]} = \frac{k_f}{k_r} = K$$

If the enzyme charged to a batch reactor is pristine, some time will be required before equilibrium is reached. This time is usually short compared to the batch reaction time and can be ignored. Furthermore, $s_0 \gg E_0$ is usually true so that the depletion of substrate to establish the equilibrium is negligible. This means that Michaelis–Menten kinetics can be applied throughout the reaction cycle and the kinetic behavior of a batch reactor will be similar to that of a packed-bed PFR, as illustrated in Example 12.4. Simply replace $\bar{t}$ with t_{batch} to obtain the approximate result for a batch reactor. This approximation is an example of the quasi-steady hypothesis discussed in Section 2.5.3.

EXAMPLE 12.5

Formulate the governing equations for an enzyme-catalyzed batch reaction of the form S → P. The enzyme is pristine when charged to the reactor. Do not invoke the quasi-steady hypothesis.

SOLUTION: The reactions are

$$\mathrm{S} + \mathrm{E} \rightarrow \mathrm{SE} \qquad \mathscr{R}_{\mathrm{I}} = k_f \left[s[\mathrm{E}] - \frac{[\mathrm{SE}]}{K}\right]$$

$$\mathrm{SE} \rightarrow \mathrm{E} + \mathrm{P} \qquad \mathscr{R}_{\mathrm{II}} = k[\mathrm{SE}]$$

The corresponding ODEs for a constant-volume batch reaction are

$$\frac{ds}{dt} = -k_f\left[s[\mathrm{E}] - \frac{[\mathrm{SE}]}{K}\right] \qquad s = s_0 \quad \text{at } t = 0$$

$$\frac{d[\mathrm{E}]}{dt} = -k_f\left[s[\mathrm{E}] - \frac{[\mathrm{SE}]}{\mathrm{K}}\right] + k[\mathrm{SE}] \qquad [\mathrm{E}] = E_0 \quad \text{at } t = 0$$

$$\frac{d[\mathrm{SE}]}{dt} = k_f\left[s[\mathrm{E}] - \frac{[\mathrm{SE}]}{\mathrm{K}}\right] - k[\mathrm{SE}] \qquad [\mathrm{SE}] = 0 \quad \text{at } t = 0$$

$$\frac{dp}{dt} = k[\mathrm{SE}] \qquad p = 0 \quad \text{at } t = 0$$

The initial condition for [SE] assumes that the enzyme was charged to the reactor in pristine condition. It makes no difference whether the enzyme is free or immobilized provided the reaction follows Michaelis–Menten kinetics.

Free Enzymes in Flow Reactors

Substitute $t = z/\bar{u}$ into the ODEs of Example 12.5. They then apply to a steady-state PFR that is fed with freely suspended, pristine enzyme. There is an initial distance down the reactor before the quasi-steady equilibrium is achieved between S in solution and S that is adsorbed on the enzyme. Under normal operating conditions, this distance will be short. Except for the loss of catalyst at the end of the reactor, the PFR will behave identically to the confined enzyme case of Example 12.4. Unusual behavior will occur if k_f is small or if the substrate is very dilute so $s_{\text{in}} \approx E_{\text{in}}$. Then, the full equations in Example 12.5 should be (numerically) integrated.

The case for a CSTR is similar. Under normal operating conditions, the solution in Example 12.3 will apply to free enzymes as well as to confined enzymes. Like the PFR case, unusual behavior will occur if k_f is small or if the substrate is very dilute so $s_{\text{in}} \approx E_{\text{in}}$.

EXAMPLE 12.6

Formulate the governing equations for an enzyme-catalyzed reaction of the form S → P in a CSTR. The enzyme is pristine when it enters the reactor. Do not invoke the quasi-steady hypothesis.

SOLUTION: The reactions are the same as in Example 12.5. The steady-state performance of a CSTR is governed by algebraic equations, but time derivatives can be useful for finding the steady-state solution by the method of false transients. The governing equations are

$$V\frac{ds}{dt} = Qs_{\text{in}} - k_f\left[s[\mathrm{E}] - \frac{[\mathrm{SE}]}{K}\right]V - Qs$$

$$V\frac{d[\mathrm{E}]}{dt} = QE_0 - Vk_f\left[s[\mathrm{E}] - \frac{[\mathrm{SE}]}{\mathrm{K}}\right] + Vk[\mathrm{SE}] - Q[\mathrm{E}]$$

$$V\frac{d[\mathrm{SE}]}{dt} = Vk_f\left[s[\mathrm{E}] - \frac{[\mathrm{SE}]}{K}\right] - Vk[\mathrm{SE}] - Q[\mathrm{SE}]$$

$$V\frac{dp}{dt} = k[\mathrm{SE}] - Qp$$

It was assumed that $[\mathrm{SE}]_{\mathrm{in}} = p_{\mathrm{in}} = 0$.

12.2 CELL CULTURE

Whole cells are grown for a variety of reasons. The cells may perform a desired transformation of the substrate (e.g., waste water treatment); the cells themselves may be the desired product (e.g., yeast production); or the cells may produce a desired product (e.g., penicillin). In the latter case, the desired product may be excreted, as for the penicillin example, and recovered in relatively simple fashion. If the desired product is retained within the cell walls, it is necessary to ***lyse*** (rupture) the cells and recover the product from a complex mixture of cellular proteins. This approach is often needed for therapeutic proteins that are created by recombinant DNA technology. The resulting separation problem is one of more challenging aspects of biochemical engineering. However, culture of the cells can be quite difficult experimentally. A major fraction of ordinary soil bacteria have never been successfully cultured in the laboratory. The easiest cells to grow are microbes that live independently in their natural environment. These include bacteria, yeasts, and molds. Bacteria and yeasts are single celled. Molds are multicelled but have relatively simple structures and nutritional requirements. Harder to grow are cells extracted from higher order plants and animals since they normally rely on complex interactions with other cells in the parent organism.

Microbial culture is also called ***fermentation*** and is most commonly a batch process (although oxygen may be supplied continuously and gaseous byproducts removed continuously). The chemistry of cell growth is extremely complex and, even in the simplest living cells, is only partially understood. The common gut bacterium, *Escherichia coli*, utilizes approximately 1000 enzymes. The nutrient mixture for cell growth must include a carbon source, which is typically a sugar such as glucose, and sources for nitrogen, phosphorus, and potassium and a large variety of trace elements. Oxygen may be required directly (***aerobic*** fermentations) or may be obtained from a carbohydrate, which also serves as the carbon source (***anaerobic*** fermentations). Some bacteria, called ***facultative anaerobes***, utilize molecular oxygen when available but can survive and grow without it. For others, called ***strict anaerobes***, oxygen is a poison. Some microbes can be grown using ***defined media***. This is a nutrient source consisting of simple sugars and salts in which all chemical components are identified as to composition and quantity. ***Complex media*** contain uncharacterized substances, typically proteins from natural sources.

Batch fermentation begins with an initial charge of cells called an ***inoculum***. Growth of the desired cell mass usually occupies a substantial portion of the batch

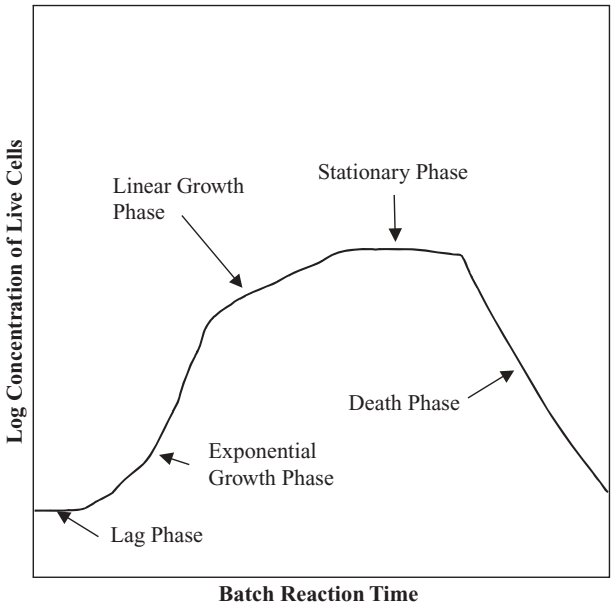

Figure 12.3 Idealized growth phases for a batch fermentation.

cycle and, conceptually at least, follows the curve illustrated in Figure 12.3. During the initial lag phase, cells are adjusting themselves to the new environment. Most microbes, and particularly bacteria, are extremely adaptable and can utilize a variety of carbon sources. For example, some can ferment both five- and six-carbon sugars. However, unique enzymes are generally required for each source. These are called ***induced enzymes*** and are manufactured by the cell in response to the new environment. The induction period is called the ***lag phase*** and will be short if the fermentation medium is similar to that used in culturing the inoculum. If the chemistry is dramatically different, appreciable cell death may occur before the surviving cells have retooled for the new environment.

Exponential growth occurs after cell metabolisms have adjusted and before a key nutrient becomes limiting or toxic products accumulate. In the ***exponential growth phase***, the total cell mass will increase by a fixed percentage during each time interval, typically doubling every few hours. Ultimately, however, the growth rate must slow and stop. A ***linear growth phase*** can occur in semibatch fermentations when some key reactant is supplied at a fixed rate. The oxygen supply may limit cell growth or the carbon source (substrate) may be fed to the system at a fixed rate. Ultimately, cell mass achieves a maximum and the culture enters a ***stationary or maintenance phase***. A stationary population can be sustained using continuous culture techniques as described below, but the stationary phase is typically rather brief in batch fermentations. It is followed by a ***death phase*** where cells die or sporulate. The number of viable cells usually follows an exponential decay curve during this period. The cells

can reduce their nutritional requirements in time of stress, and surviving cells will cannibalize the bodies of cells that lyse.

Models for batch culture can be constructed by assuming mechanisms for each phase of the cycle. These mechanisms must be reasonably complicated to account for a lag phase and for a prolonged stationary phase. ***Unstructured models*** treat the cells as a chemical entity that reacts with its environment. ***Structured models*** include some representation of the internal cell chemistry. ***Metabolic models*** focus on the energy-producing mechanisms within the cells.

12.2.1 Growth Dynamics

This section gives models for the rates of birth, growth, and death of cell populations. We seek models for (1) the rate at which biomass is created, (2) the rates at which substrates are consumed, (3) the rates at which products are generated, (4) the maintenance requirements for a static population, and (5) the death rate of cells. The emphasis is on unstructured models.

Biomass Production

Biomass is usually measured by dry weight of viable cells per unit volume, X. We bypass the sometimes tricky problems associated with this measurement except to say that it is the province of the microbiologist and usually involves plate cultures and filtration followed by drying. Suppose there is one limiting nutrient, S, and that all other nutrients are available in excess. Then the ***Monod model*** for growth is

$$\mathscr{R}_X = \mu X = \mu_{\max}\left[\frac{s}{K_s + s}\right]X \tag{12.8}$$

where μ is the specific growth rate for cell mass. Typical units are grams per liter per hour for $\mathscr{R}_X$, reciprocal hours for μ and $\mu_{\max}$, and grams per liter for s, X, and K_S. A typical value for $\mu_{\max}$ under optimal conditions of temperature and pH is 1 h^{-1}. If the primary substrate is abundant, Equation 12.8 gives exponential growth:

$$X = X_0 e^{\mu_{\max}(t-t_0)} \tag{12.9}$$

where X_0 is the inoculum size and t_0 is the time when the induction phase ends. Equation 12.9 models induction as a pure time delay. The exponential growth phase ends when a substrate concentration becomes limiting.

It is possible for two or more substrates to become simultaneously limiting. Define a growth limitation factor $G_i < 1$ for substrate i such that

$$\mathscr{R}_X = \mu X = \mu_{\max} X G_1$$

when growth is limited only by substrate 1, for example, $G_1 = s/(K_S + s)$ in Equation 12.8. The factor $G_1$is determined by growth experiments that manipulate the single variable s_1. Dual limitations can be modeled using a multiplicative form

$$\mathscr{R}_X = \mu_{\max} X G_1 G_2 \tag{12.10}$$

but this usually underestimates the growth rate. Another possibility is

$$\mathscr{R}_X = \mu_{\max} X \min[G_1, G_2] \tag{12.11}$$

but this usually overestimates the growth rate. Define the substrates so that $G_1 \leq G_2$. A compromise model is

$$\mathscr{R}_X = \mu_{\max} X G_1 G_2^{\alpha_{12}} \tag{12.12}$$

where α_{12} is an empirical interaction parameter that is fit to data having at least one experiment with dual limitations.

Any substance present in great excess can inhibit growth or even cause death. Metabolic products are often toxic to the organism that produces them. Thus a batch fermentation can be limited by accumulation of products as well as by depletion of the substrate. A simple model for growth in the presence of an inhibitor is

$$\mathscr{R}_X = \mu_{\max} X \left[\frac{s}{K_S + s}\right]\left[1 - \frac{p}{p_{\max}}\right]^m = \mu X G_S G_P \tag{12.13}$$

where p is the concentration of the inhibiting material, $p_{\max}$ is the value for p at which growth stops, and m is an empirical constant. Note that Equation 12.13 uses a multiplicative combination of the growth-limiting factors, G_S and G_P. This may be overly pessimistic if G_S is appreciably less than 1. Equation 12.12 can be used if data are available to fit α_{12}.

Cell cultures can be inhibited by an excessive concentration of the substrate. One way to model substrate inhibition is to include an S^2 term in the denominator of the rate equation. See Equation 12.4.

Substrate Consumption

Consumption of substrates and generation of products can be described using empirical yield coefficients. Yields are usually based on the amount of limiting substrate that has been consumed. Thus, $Y_{P/S}$ denotes the mass of product produced per mass of substrate consumed and $Y_{X/S}$ denotes the dry mass of cells produced per mass of substrate consumed. The value for $Y_{P/S}$ is not stoichiometrically determined and will vary within a growth cycle. When glucose is anaerobically fermented by yeast, part of the carbon will appear as ethanol and coproduct CO_2, part will be incorporated into the cell mass, and minor amounts will appear as excreted byproducts. A typical cell composition on a dry-weight basis is about 50% carbon, 7% hydrogen, 12% nitrogen, 30% oxygen, and 1% other. The empirical formula $C_5H_7O_2N$ can be useful for back-of-the-envelope calculations. An upper limit on $Y_{X/S}$ of about 2 g of dry cell mass per gram of carbon in the substrate is predicted using this average composition. The actual value for $Y_{X/S}$ will be about half the upper limit, the balance of the carbon being used to generate energy. This missing half is accounted for by the $Y_{P/S}$ terms summed over all excreted products. An internally consistent model for cell growth

closes the mass balance for carbon and other nutrients. The mass balance has the form

$$Y_{X/S} + \sum_{\text{products}} Y_{P/S} = 1 \tag{12.14}$$

Equation 12.14 applies to all the elements that comprise a cell, but it is normally applied in the form of a carbon balance. The dominant terms in the balance are carbon in the cells, measured through $Y_{X/S}$, and carbon in the ***primary metabolites*** (e.g., ethanol and CO_2), measured through the $Y_{P/S}$ terms for these metabolites.

A convenient way to model the consumption of substrate is to divide it between consumption that is associated with the growth of new cells and consumption that is required to maintain existing cells:

$$\mathscr{R}_S = -\frac{\mathscr{R}_X}{Y_{X/S}} - M_S X \tag{12.15}$$

Here, M_S is the maintenance coefficient for substrate S. Typical units on M_S are grams of substrate per gram of dry cell mass per hour. Table 12.1 gives maintenance coefficients for various organisms and substrates. The maintenance coefficient for oxygen is denoted M_O. It is dependent on both the organism and the carbon source.

Maintenance requirements exist for nitrogen and other elements (e.g., phosphorus). They are relatively small but must be supplied to maintain a stationary cell population.

Excreted Products

Most of the carbon going into a cell is converted to cell mass or to primary metabolic products. An aerobic fermentation may give CO_2 and water as the only products. The anaerobic fermentation of glucose by yeast normally gives 2 moles of ethanol and 1 moles of CO_2 for each mole of glucose. A lactic acid fermentation gives 2 moles of lactic acid per mole of glucose. Some bacteria have several metabolic pathways and can utilize a variety of five- and six-carbon sugars to produce ethanol, formic acid, acetic acid, lactic acid, succinic acid, CO_2, and H_2 depending on the environment. The

Table 12.1 Maintenance Coefficients for Various Organisms and Substrates

Organism	Substrate	M_S,h^{-1}	M_O,h^{-1}
Acetobacterium woodii	Lactate	0.07	Anaerobic
Aerobacter aerogenes	Citrate	0.06	0.05
	Glucose	0.05	0.05
	Glycerol	0.08	0.11
Saccharomyces cerevisiae	Glucose	0.02	0.02
Escherichia coli	Glucose	0.05	0.02
Penicillium chrysogenum	Glucose	0.02	0.02

Note: Data for *A. woodii* from Peters *et al.* (1998). Other data from Roels and Kossen, (1978).

specific mix of products, even for a fixed substrate and organism, depends on factors such as the phase of growth in the batch cycle, the pH of the medium, and whether or not molecular oxygen is available. For example, the fermentation of glucose by *Bacillus polymyxa* gives a mixture of ethanol, acetic acid, lactic acid, and butanediol; but butanediol can be obtained in almost stoichiometric yield:

$$C_6H_6(OH)_6 + \frac{1}{2}O_2 \rightarrow C_4H_8(OH)_2 + 2CO_2 + H_2O$$

late in a batch cycle with an acidic medium and aeration. Occasionally, optimal growing conditions are suggested just by the overall stoichiometry and energetics of the metabolic reactions. For example, ethanol can be produced anaerobically: This reaction has a negative change in free energy so it can support microbial growth. An anaerobic fermentation for butanediol releases free hydrogen and has less favorable energetics. Thus one might expect more alcohol than butanediol under strictly anaerobic conditions. With oxygen available, the butanediol route produces more energy and is favored, although, with enough oxygen, the reaction may go all the way to CO_2 and water. More detailed predictions require kinetic models of the actual metabolic pathways in a cell. The energy-producing pathways are now known to a large extent, and structured, metabolic models are becoming possible.

Assume the product distribution is known and fixed. Then all products can be lumped into a single equivalent product, P, which is stoichiometrically linked to the substrate. On a mass basis, carbon from the substrate must match the carbon appearing as product plus carbon utilized in making biomass. When there is no change in the cell mass,

$$\mathscr{R}_P = -\mathscr{R}_S$$

The experimental quantity $Y_{X/S}$ includes both uses of the substrate. Define $\hat{Y}_{X/S}$ as the theoretical yield of cell mass per mass of substrate if energy requirements are ignored, that is, $\hat{Y}_{X/S} \approx 2$ for carbon. Then product formation can be expressed in terms of cell mass and growth of cell mass:

$$\mathscr{R}_P = -\mathscr{R}_S - \frac{\mathscr{R}_X}{\hat{Y}_{X/S}} = \frac{\mathscr{R}_X}{Y_{X/S}} - \frac{R_X}{\hat{Y}_{X/S}} + M_S X \tag{12.16}$$

The microbiology literature distinguishes between products which are formed during the growth of cell mass (***growth-associated*** products) and those which are made during the stationary phase (***non–growth-associated***). Growth-associated products have a production rate proportional to $\mathscr{R}_X$ while the production rate for non-growth-associated products is proportional to the cell mass X. The primary metabolites are both since they are generated during cell growth and during maintenance. This fact is reflected in Equation 12.16. Excreted enzymes (***extracellular enzymes***) and antibiotics are usually non–growth associated. They are sometimes called ***secondary metabolites***.

Cell Death

Spontaneous death or sporulation of cells is commonly modeled as a first-order process. Equation 12.8 (or 12.12) is modified to include a disappearance term:

$$\mathscr{R}_X = \mu X - k_d X = \mu_{\max} X \left[\frac{s}{K_S + s} \right] - k_d X \tag{12.17}$$

This model does not predict a stationary phase in a batch fermentation if k_d is constant. A nearly stationary phase can be modeled if k_d is made to depend on the accumulation of a toxic product.

If there is insufficient substrate for maintenance, the lysing of some cells to supply the maintenance requirements of others can be modeled as

$$\mathscr{R}_X = -k_d - Y_{X/S} M_X X \quad \text{for s} = 0 \tag{12.18}$$

Here, the factor of $Y_{X/S}$ is merely a rough estimate of the amount of carbon that can be reutilized. The theoretical upper limit is $\widehat{Y}_{X/S}$.

Death kinetics are obviously important in chemical or thermal ***sterilization***. The spores formed by some bacteria are the hardest to kill. Problem 12.3 gives data for a representative case.

12.2.2 Reactors for Freely Suspended Cells

The typical bioreactor is a two-phase stirred tank. It is a three-phase stirred tank if the cells are counted as a separate phase, but they are usually lumped into the aqueous phase that contains the microbes, dissolved nutrients, and soluble products. The gas phase supplies oxygen and removes byproduct CO_2. The most common operating mode is batch with respect to biomass, batch or fed batch with respect to nutrients, and fed batch with respect to oxygen. Reactor aeration and the supply of oxygen are discussed in Chapter 11. There is a rumor that mammalian cells are so fragile that agitation must be laminar. This appears to be wrong. Mammalian cells do rupture (lyse) in agitated vessels, but this seems due more to the breaking of bubbles on the surface rather than to turbulence near the impeller. Surfactants that migrate to the water–gas interface and prevent adherence of cells at the interface can largely eliminate lysing.

Fermentation vessels tend to be large because reaction rates are low. Typical batch reaction times are measured in days. Freely suspended mammalian cells are cultivated in conventionally agitated reactors up to 20,000 L in volume. Ethanol production with freely suspended yeast uses vessels 100 times larger, and wastewater treatment by the activated sludge process or in lagoons can be larger by another factor of 100.

Batch Reactors

The reaction rates presented in Section 12.2.1 can be combined to give a fairly comprehensive model for cell growth, substrate consumption, and product generation in

a batch bioreactor. The model is necessarily of the unstructured variety and contains many empirical constants. Concentrations are measured on a weight basis with typical units of grams per liter or milligrams per liter. Such measures are sometimes denoted as weight per volume (w/v). A dimensionless weight-per-weight measure, denoted as w/w, is also common and is preferred for mathematical modeling.

EXAMPLE 12.7

Develop a model for the anaerobic batch fermentation of glucose to ethanol and coproduct CO_2 using *S. cerevisiae*. The starting mixture contains 10% glucose. The inoculum is 0.0005 w/w. Product inhibition stops cell growth at 14% ethanol. Assume $k_d = 0$ but allow cannibalization of cellular material when the substrate is completely consumed.

SOLUTION: The initial conditions for a batch reactor are $s = s_0$ and $X = X_0$ at $t = 0$. Equation 12.13 gives the cell growth when there is inhibition by the product:

$$\frac{dX}{dt} = \mathscr{R}_X = \mu_{\max} X \left[\frac{s}{K_S + s}\right]\left[1 - \frac{p}{p_{\max}}\right]^m \quad \text{at } t = 0$$

Cannibalization according to Equation 12.18 begins when $s = 0$:

$$\frac{dX}{dt} = \mathscr{R}_X = -Y_{X/S} M_X X$$

Equation 12.15 governs substrate consumption. For a batch reactor with all the substrate charged initially,

$$\frac{ds}{dt} = -\frac{\mathscr{R}_X}{Y_{X/S}} - M_S X$$

Excreted products are governed by Equation 12.16:

$$\frac{dp}{dt} = \frac{\mathscr{R}_X}{Y_{X/S}} - \frac{\mathscr{R}_X}{Y_{X/S}} + M_S X \qquad p = 0 \quad \text{at } t = 0$$

As with most modeling efforts, the mathematical formulation is the easy part. Picking the right parameter values from the literature or experiments is more work. An immediate task is to decide how to characterize the substrate and product concentrations. The balance equations for substrate and product apply to the carbon content. The glucose molecule contains 40% carbon by weight so s will be 0.4 times the glucose concentration, and $s_0 = 0.04$. Similarly, p measures the carbon content of the excreted products. Two-thirds of the excreted carbon appears as ethanol, and ethanol is 52% carbon by weight. Thus p will be $0.52/0.67 = 0.78$ times the ethanol concentration, and the value of $p_{\max}$ that corresponds to 14% ethanol is 0.109.

A typical value for $\mu_{\max}$ is 0.5 h^{-1}. Use $K_S = 0.001$ on a carbon-equivalent, weight-per-weight basis (but see Problem 12.4). Assume $m = 1$.

Turning to the substrate balance, yeast cells contain about 50% carbon. The cell mass is measured as total dry weight, not just carbon. This gives $\widehat{Y}_{X/S} = 2$ when s is measured as the carbon equivalent of glucose. A reasonable value for $Y_{X/S}$ is 1 so that half the carbon goes into biomass and half meets the associated energy requirements. The maintenance coefficient in carbon-equivalent units is 0.008 h^{-1}. Using these parameter estimates, the three simultaneous

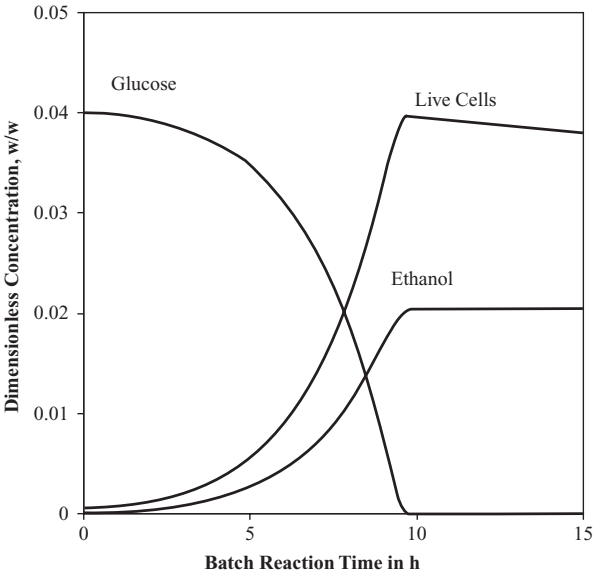

Figure 12.4 Simulation of a batch *S. cerevisiae* fermentation.

ODEs for $s > 0$ become

$$\frac{dX}{dt} = \mathscr{R}_X = 0.5X\left[\frac{s}{0.00001 + s}\right]\left[1 - \frac{p}{0.109}\right] \qquad X = 0.0005 \quad \text{at } t = 0$$

$$\frac{ds}{dt} = -\mathscr{R}_X - 0.008X \qquad s_0 = 0.04 \quad \text{at } t = 0$$

$$\frac{dp}{dt} = \frac{\mathscr{R}_X}{2} + 0.008X \qquad p = 0 \quad \text{at } t = 0$$

For s =0,

$$\frac{dX}{dt} = -0.008X \qquad \frac{ds}{dt} = \frac{dp}{dt} = 0$$

The solution is shown in Figure 12.4.

Most high-value fermentation products are made in batch. Vinification and brewing are examples where the desired products are excreted and cell mass is undesired. High-end nonexcreted products such as inteferon and human insulin are produced in batch fermentations that typically use a genetically altered variety of *E. coli*. The cells are harvested and lysed to obtain the desired product as part of a complex mixture. Mammalian cells used to produce therapeutic proteins are treated in much the same way. Viable whole cells are the desired product in the commercial batch culture of baker's yeast (*S. cerevisiae*) and in the mixed-strain culture (of a yeast, *Saccharomyces exiguous*, with a bacterium, *Lactobacillus sanfrancisco*) used to make

sourdough bread. These are all expensive low-volume products for which batch fermentation is satisfactory. Continuous fermentation is attractive for high-volume bulk chemicals such as fuel-grade ethanol and lactic acid.

Continuous Stirred Tanks Without Biomass Recycle

The chemostat without biomass recycle is a classic CSTR. The reactor is started in the batch mode. Inlet and outlet flows are begun during the exponential growth phase. The input stream contains all necessary nutrients (except oxygen, which is sparged continuously) but no cells. The outlet stream contains cells, unreacted nutrients, and fermentation products. If the flow rate is low enough, a steady state will be reached with the continuous production of cells being matched by their outflow. If the flow rate is too high, ***washout*** occurs and the cell population is lost. This fact leads to a marvelous method for selecting the fastest growing species from a mixed culture. Inoculate a batch reactor using wild microbes from dirt or other natural sources. Convert to continuous operation at a low flow rate but gradually increase the flow rate. The last surviving species is the fastest growing (for the given substrate, pH, temperature, etc.).

Since $X_{\text{in}} = 0$, the steady-state cell balance for a CSTR is

$$\bar{t}\,\mathscr{R}_X = X_{\text{out}}$$

The growth rate in a CSTR has the general form $\mathscr{R}_X = \mu \mathrm{X}_{\text{out}}$. Thus,

$$\bar{t}\mu X_{\text{out}} = X_{\text{out}}$$

This equation can always be satisfied with $X_{\text{out}} = 0$ so that the washout condition is always possible as a steady state. This steady state is achieved when there is no inoculum or when the flow rate is too high. A nontrivial solution with $X_{\text{out}} > 0$ requires that $\bar{t}\mu = 1$ or

$$\mu = \frac{1}{\bar{t}} \tag{12.19}$$

A microbiologist would say that the growth rate equals the dilution rate in a steady-state chemostat.

The substrate balance is

$$s_{\text{in}} - \bar{t}\left(\frac{\mathscr{R}_X}{Y_{X/S}} + M_S X_{\text{out}}\right) = s_{\text{out}}$$

Substituting $\mathscr{R}_X = \mu X_{\text{out}}$ and solving for X_{out} give

$$X_{\text{out}} = \frac{s_{\text{in}} - s_{\text{out}}}{\bar{t}\mu/Y_{X/S} + \bar{t}M_S} = \frac{[s_{\text{in}} - s_{\text{out}}]Y_{X/S}}{1 + \bar{t}Y_{X/S}M_S} \tag{12.20}$$

A mass balance for product gives

$$p_{\text{out}} = p_{\text{in}} + \bar{t}\left[\frac{\mu X_{\text{out}}}{Y_{X/S}} - \frac{\mu X_{\text{out}}}{\widehat{Y}_{X/S}} + M_S X_{\text{out}}\right] = p_{\text{in}} + \frac{X_{\text{out}}}{Y_{X/S}} - \frac{X_{\text{out}}}{\widehat{Y}_{X/S}} + \bar{t} M_S X_{\text{out}} \tag{12.21}$$

Equations 12.20 and 12.21 apply to any functional form for the growth rate μ. There are three unknowns in these equations: X_{out}, s_{out}, and p_{out}. A third equation is needed. It comes from substituting some specific functional form for μ into Equation 12.19. For example, if μ is given by Equation 12.13, the third equation is

$$\mu_{\max}\left[\frac{s_{\text{out}}}{K_S + s_{\text{out}}}\right]\left[1 - \frac{p_{\text{out}}}{p_{\max}}\right]^m = \frac{1}{\bar{t}} \tag{12.22}$$

Equations 12.20, 12.21, and 12.22 are solved simultaneously for X_{out}, S_{out}, and p_{out}.

EXAMPLE 12.8

Suppose the batch reactor in Example 12.7 has been converted to a CSTR. Determine its steady-state performance at a mean residence time of 4 h. Ignore product inhibition.

SOLUTION: Set $m = 0$ to ignore production inhibition. Then Equation 12.22 can be solved for s_{out}:

$$s_{\text{out}} = \frac{K_S}{\bar{t}\mu_{\max} - 1} \tag{12.23}$$

The parameters used in Example 12.7 were $K_S = 0.001$, $\mu_{\max} = 0.5$, and $\bar{t} = 4$. This gives $s_{\text{out}} = 0.001$ and $\mu = \mu_{\max}/2 = 0.25$. These values and M_S are substituted into Equation 12.20 to give $X_{\text{out}} = 0.0378$. Equation 12.21 is then used to calculate $p_{\text{out}} = 0.0201$. A carbon balance confirms the results. Carbon enters as s_{in} and leaves as $s_{\text{out}} + X_{\text{out}}/2 + p_{\text{out}}$: $0.040 = 0.001 + 0.0378/2 + 0.0201 = 0.040$.

It is clear from Equation 12.19 that $\bar{t}\mu_{\max} > 1$ is necessary to avoid washout. However, it is not sufficient. The sufficient condition is found from the requirement that $s_{\text{out}} < s_{\text{in}}$ at steady state. This gives

$$\bar{t}\mu_{\max} > 1 + \frac{K_S}{s_{\text{in}}} \tag{12.24}$$

Operating near the washout point maximizes the production rate of cells. A feedback control system is needed to ensure that the limit is not exceeded. The easiest approach is to measure cell mass, for example, by measuring turbidity and using the signal to control the flow rate. Figure 12.5 shows how cell mass varies as a function of $\bar{t}$ for the system of Examples 12.7 and 12.8. The minimum value for $\bar{t}$ is 2.05 h. Cell production is maximized at $\bar{t} = 2.37$ h.

Microbial kinetics can be quite complex. Multiple steady states are always possible, and oscillatory behavior is common, particularly when there are two or more

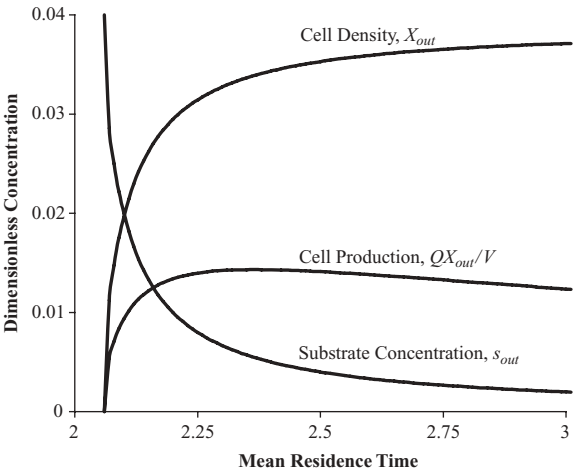

Figure 12.5 Production of *S. cerevisiae* in a CSTR.

microbial species in competition. The term ***chemostat*** can be quite misleading for a system that oscillates in the absence of a control system.

Continuous Stirred Tanks with Biomass Recycle

When the desired product is excreted, closing the system with respect to biomass offers a substantial reduction in the cost of nutrients. The idea is to force the cells into a sustained stationary or maintenance period where there is relatively little substrate used to grow biomass and where production of the desired product is maximized. One approach is to withhold some key nutrient so that cell growth is restricted but to supply a carbon source and other components needed for the desired product. It is sometimes possible to maintain this state for weeks or months and to achieve high volumetric productivities. There will be spontaneous cell loss (i.e., $k_d > 0$), and true steady-state operation requires continuous purging and makeup. The purge can be achieved by incomplete separation and recycle of the cells or by an explicit purge stream as shown in Figure 12.6. Cell makeup can be achieved by allowing some cell growth in the reactor. An alternative that is better in terms of raw material efficiency is to grow the makeup cells in a separate reactor that has nutrient levels chosen for growth rather than maintenance.

The ***activated sludge*** process for wastewater treatment uses recycle of live cells. The flow diagram of Figure 12.6 applies, but the cell filter is just a settling tank. The purge stream consists of excess (nonrecycled) sludge plus entrained water. A goal is to oxidize organics without generating too much sludge since this creates a separate disposal problem. Another goal is to operate the process with minimum amounts of supplemental nutrients that are needed for cell growth but may be missing in the feed stream. This is not a problem for ordinary sewage, which is rich in nutrients, but can

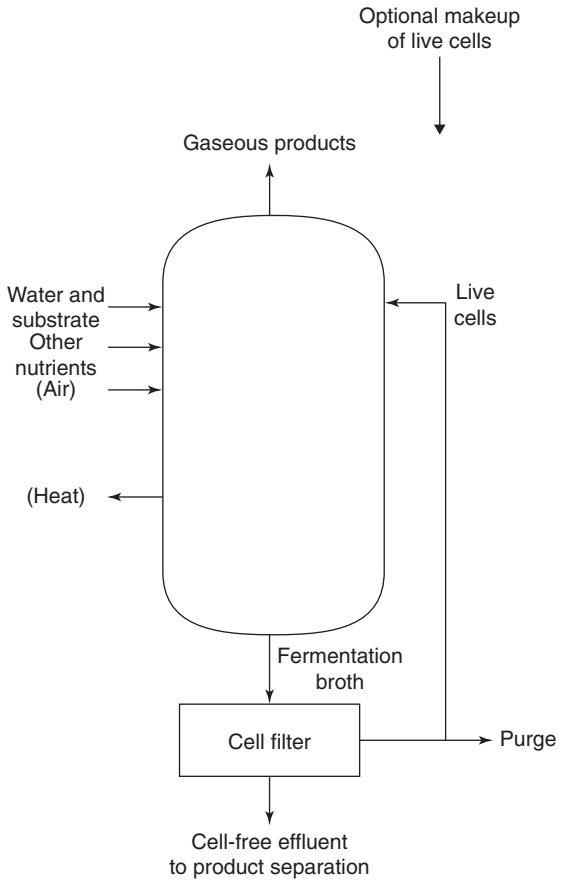

Figure 12.6 Continuous fermentor with recycle of live cells.

arise in the treatment of industrial and agricultural wastewater, for example, there may be a nitrogen deficiency. Recycling live cells lowers the need for supplemental nitrogen.

For a typical wastewater treatment plant, the "reactor" in Figure 12.6 consists of several agitated and aerated tanks in series. This is aerobic ***digestion***. Anaerobic digestion is also used in wastewater treatment, and the sludge from an anaerobic process can also be recycled, albeit in the absence of air. Anaerobic digestion with or without sludge recycle is one possible way of treating the purge stream from an aerobic activated sludge process. Another way of treating this waste stream is to sterilize it so that it can be used as a fertilizer. Fermentation using thermophyllic bacteria at about 60°C destroys human pathogens. A continuous process is necessary for economic operation. The design criterion for this and other continuous sterilization processes is a guaranteed minimum value for the ***first appearance time*** t_{first} (the

smallest residence time, see Chapter 15). The mean residence time $\bar{t}$ is relatively unimportant.

Piston Flow Bioreactors

There are several commercial examples of continuous flow bioreactors that approximate piston flow. The deep-shaft fermentors described in Chapter 11 have been used for wastewater treatment when land is very expensive. Beer has been brewed in an unstirred tower using a flocculating variety of yeast that settles to the bottom of the tower. Most plants for fuel-grade ethanol and lactic acid are continuous, and some designs approximate piston flow. Monod kinetics give low outlet concentrations of substrate even in a single CSTR because K_S is usually small. See Equation 12.24. However, PFR kinetics give still lower values for s_{out}, and this can be important in cases like wastewater treatment. Wastewater treatment lagoons are designed to have progressive flow from inlet to outlet. Sterilization by chlorine or ozone is best done in a PFR. Continuous bioreactors often use a tubular reactor or a flat-plate heat exchanger for ***continuous thermal sterilization*** of the substrate. The need to reduce viable organisms by many orders of magnitude justifies use of the axial dispersion model. See Section 9.3. Note, however, that U.S. Food and Drug Administration (FDA) requirements for the highest grade of biological purity (***water for injection***, or ***WFI***) must be sterilized by distillation or reverse osmosis.

12.2.3 Immobilized Cells

Like enzymes, whole cells are sometimes immobilized by attachment to a surface or by entrapment within a support. One motivation for this is similar to the motivation for using biomass recycle in a continuous process. The cells are grown under optimal conditions for cell growth but are used at conditions optimized for production of a secondary metabolite. A hollow-fiber reactor, similar to those used for cross-flow filtration, can be used to entrap the cells while allowing input of the substrate and removal of products. Attachment of the cells to a nonreactive material such as alumina allows a great variety of reactor types including packed beds, fluidized and spouted beds, and air-lift reactors. Packed beds with a biofilm on the packing are commonly used for wastewater treatment. A semicommercial process for beer used an air-lift reactor to achieve reaction times of one day compared to five to seven days for the normal batch process. Unfortunately, the beer suffered from a "mismatched flavor profile" that was attributed to mass transfer limitations.

The advantages of immobilizing cells that can be grown in free suspensions are limited. Systems that are closed or substantially closed with respect to biomass such as those illustrated in Figures 12.2 and 12.6 allow much the same benefits. However, some cells from multicelled plants and animals can only be grown when anchored to a surface and when interacting with adjacent cells. When the synthetic structure used for growth resembles the naturally occurring structure, the reaction

is called ***tissue culture*** (as opposed to ***cell culture***) and is discussed in the next section.

12.2.4 Tissue Culture

Merriam Webster's Unabridged Dictionary defines "tissue" as "an aggregate of cells usually of a particular kind or kinds together with their intercellular substance that form one of the structural materials out of which the body of a plant or an animal is built up." The easier forms of tissue culture involve plants. The most common form of tissue culture, ***meristem culture***, reproduces whole, genetically identical plants from tiny cuttings of a parent plant. This technique has been widely adopted by the nursery industry to mass produce named varieties of ornamental plants. The multicellular fungus *Aspergillus niger* has long been used to produce citric and other organic acids. It is typically grown on a solid substrate, mimicking its natural growth as a black mold. Growth can be with limited moisture or submerged. *Penicillium chrysogenum* is another common mold that can be immobilized and grown in batch, fed-batch, or continuous processes.

The more challenging forms of tissue culture involve two or more types or animal cells grown simultaneously. Good progress has been made on skin replacements with products approved by the FDA Administration. Martin and Vermette (2005) discuss the reaction engineering aspects of tissue culture and conclude that the womb with its good mass transfer and essentially zero shear is ideal for growing complicated structures.

12.3 COMBINATORIAL CHEMISTRY

The idea behind combinatorial chemistry is based on the monkey theorem of probability theory. Given enough monkeys typing long enough, one of them will almost surely reproduce a Shakespearen play. Combinatorial chemistry envisions synthesizing myriad chemicals or, by recombinant DNA technology, myriad cell lines, and one of them will almost surely satisfy an identified need. This approach to product design is not confined to biochemical engineering but has found it greatest use in the pharmaceutical industry and is thus included in this chapter. Other applications include new catalysts, new superconductors, and new polymers. The ultimate goal would be enough physical understanding to obviate the need for extensive experimentation, but that time has not arrived.

The problems with combinatorial chemistry are twofold: monkeys cost money and their output must be screened for relevancy. Has *Hamlet* been written?

To achieve reasonable cost, both the synthesis and analysis steps must be done at a small scale. The milliliter scale is now the state of the art but still smaller scales will become possible. See Chapter 16. For the moment, small shaker flasks and microtiter plates can be used to screen hundreds of experiments. Once tentatively identified at the small scale, the chosen molecule or cell line must be made in sufficient quantities

for standard test procedures and finally for production. Thus begins a classic exercise in scaleup.

SUGGESTED FURTHER READINGS

Specialized books on biochemical engineering by leaders in the field include:

J. F. Bailey and D. F. Ollis, *Biochemical Engineering Fundamentals*, 2nd ed., McGraw-Hill, New York, 1986.

H. W. Blanch and D. S. Clark, *Biochemical Engineering*, Marcel Dekker, New York, 1996.

M. L. Shuler and F. Kargi, *Bioprocess Engineering: Basic Concepts*, 2nd ed., Prentice-Hall, Upper Saddle River, NJ, 2001.

PROBLEMS

12.1 It has been proposed that some enzymes exist in active and inactive forms that are in equilibrium. The active form binds substrate molecules for subsequent reaction while the inactive form does not. The overall reaction mechanism might be

$$\begin{aligned} \mathrm{E} &\rightleftarrows \mathrm{I} & \frac{[\mathrm{I}]}{[\mathrm{E}]} &= K_I \\ \mathrm{S} + \mathrm{E} &\rightleftarrows \mathrm{SE} & \frac{[\mathrm{SE}]}{s[\mathrm{E}]} &= K \\ \mathrm{SE} &\longrightarrow \mathrm{P} + \mathrm{E} & \mathscr{R} &= k[\mathrm{SE}] \end{aligned}$$

Derive a kinetic model for this situation.

12.2 Set the time derivatives in Example 12.6 to zero to find the steady-state design equations for a CSTR with a Michaelis–Menten reaction. An analytical solution is possible. Find the solution and compare it to the solution in Example 12.3. Under what conditions does the quasi-steady solution in Example 12.3 become identical to the general solution in Example 12.6?

12.3 Wang et. al. (1979) report the death kinetics of *Bacillus stearothermophilus* spores using wet, thermal sterilization. Twenty minutes at 110°C reduces the viable count by a factor of 10^4. The activation temperature, $\Delta E/R_g$, is 34,200 K. How long will it take to deactivate by a factor of 10^7 at 120°C?

12.4 A literature value for the Monod constant for a *S. cerevisiae* fermentation is $K_S = 25$ mg/L (Blanch and Clark, 1996). How does this affect the simulation in Example 12.7?

12.5 A limiting case of Monod kinetics has $K_S = 0$ so that cell growth is zero order with respect to substrate concentration. Rework Example 12.7 for this situation, but do remember to stop cell growth when $s = 0$. Compare your results for X and p with those of Example 12.7. Make the comparison at the end of the exponential phase.

12.6 A simple way to model the lag phase is to suppose that the maximum growth rate $\mu_{\max}$ evolves to its final value by a first-order rate process: $\mu_{\max} = \mu_\infty[1 - \exp(-\alpha t)]$. Repeat Example 12.7 using $\alpha = 1\ \mathrm{h}^{-1}$. Compare your results for X, s, and p with those of Example 12.7. Make the comparison at the end of the exponential phase.

12.7 Equation 12.17 postulates that spontaneous deaths occur throughout the batch cycle. This means that dX/dt is initially negative. Is it possible to lose the inoculum completely if the induction period is too long? Long induction periods correspond to small values of α in the lag-phase model of Problem 12.6. Is there a critical value for α at which the inoculum is lost?

12.8 Consider the CSTR with biomass recycle shown in Figure 12.6.

(a) Determine a criterion for achieving a nontrivial steady state in a reactor that is closed with respect to biomass. Does it have anything to do with the residence time for cells? Does the criterion include the limiting case of no cell makeup, birth, death, or purge.

(b) The purge stream means that the cells have a finite residence time in the reactor although it will be much longer than that for the liquid phase (i.e., water, excreted products, unreacted substrate). What is the mean residence time for cells? Does it depend on whether the makeup cells are fed to the reactor or whether they are born in the reactor?

(c) How long does it take for the reactor to approximate the steady state found in part (a)?

Chapter 13

Polymer Reaction Engineering

Polymer reaction engineering is a specialized but important branch of chemical reaction engineering. The odds strongly favor the involvement of chemical engineers with polymers at some point in their career. The kinetics of polymerization reactions can be treated using the basic concepts of Chapters 1–5, but the chemistry and mathematics are more complicated than in the examples given there. The number of chemical species participating in a polymerization is potentially infinite, and the mathematical description of a batch polymerization requires an infinite set of differential equations. Analytical and numerical solutions are more difficult than for the small sets of equations dealt with thus far. Polymerizations also present some interesting mechanical problems in reactor design. Viscosity increases dramatically with molecular weight, and a polymer solution is typically 10^2–10^6 times more viscous than an ordinary liquid. Molecular diffusivities in polymer solutions are lowered by similar factors. Laminar flow is the rule; pressure drops are high; agitation is difficult; and heat and mass transfer limitations can be very severe. The polymer reaction engineer sometimes confronts these problems head on but most often seeks to avoid them through clever reactor design.

13.1 POLYMERIZATION REACTIONS

Polymerization reactions are classified as being either ***chain growth*** **or** ***step growth.*** In the chain growth variety, a small molecule reacts with a growing polymer chain to form an incrementally longer chain:

$$\mathrm{M} + \mathrm{P}_l \rightarrow \mathrm{P}_{l+1} \qquad l = 1, 2, \ldots \tag{13.1}$$

where M represents the small molecule which is called the ***monomer*** and P_l denotes a polymer chain consisting of l monomer units that are chemically bonded. The chain may also contain a residual fragment of an ***initiator*** molecule that started the growth. A synonym for chain growth polymerization is ***addition*** polymerization, so named become the monomer adds to the chain one unit at a time. The most important chain

Chemical Reactor Design, Optimization, and Scaleup, Second Edition. By E. B. Nauman
Copyright © 2008 John Wiley & Sons, Inc.

growth polymers are ***vinyl addition polymers*** formed by the opening of a double bond. There is no byproduct other than energy, often in copious amounts. Important examples are ethylene polymerizing to form polyethylene and propylene polymerizing to form polypropylene.

A quite different polymerization mechanism has two polymer molecules reacting together to form a larger new molecule:

$$P_l + P_m \rightarrow P_{l+m} \qquad l, m = 1, 2, \ldots \tag{13.2}$$

The length increases in steps of size l and m that can be quite large, particularly near the end of the polymerization. This is called ***step growth*** polymerization because the polymerization can occur in fairly large steps. A synonym is ***condensation*** polymerization because the reactants are condensed together and usually give a condensation byproduct. The condensation reaction involves the breaking and making of covalent bonds of rather similar energy so that the heat of reaction is moderate. Important examples of condensation polymerizations are the reaction of phenol with formaldehyde to form phenolic resins and the reaction of terephthalic acid with ethylene glycol to form polyethylene terephthalate (PET). The condensation byproduct is water in both these examples.

13.1.1 Step Growth Polymerizations

Condensation polymers are often formed from two distinct monomers, each of which is difunctional. The monomers have the forms AMA and BNB, where A and B are functional groups which react to couple the M and N units and form a condensation byproduct, AB, and M and N are the ***mer*** units that form the polymer chain. The first step in the polymerization forms a dimer:

$$\mathrm{AMA} + \mathrm{BNB} \rightarrow \mathrm{AMNB} + \mathrm{AB}$$

Trimers can be formed in two ways giving two different structures:

$$\mathrm{AMNB} + \mathrm{AMA} \rightarrow \mathrm{AMNMA} + \mathrm{AB}$$
$$\mathrm{AMNB} + \mathrm{BNB} \rightarrow \mathrm{BNMNB} + \mathrm{AB}$$

Tetramers can be formed in three ways, but the structures are identical:

$$\mathrm{AMNMA} + \mathrm{BNB} \rightarrow \mathrm{AMNMNB} + \mathrm{AB}$$
$$\mathrm{BNMNB} + \mathrm{AMA} \rightarrow \mathrm{AMNMNB} + \mathrm{AB}$$
$$2\mathrm{AMNB} \rightarrow \mathrm{AMNMNB} + \mathrm{AB}$$

This example of step growth polymerization has two monomers that can react with each other but not with themselves. There is only one dimer. It can react with itself or with either of the monomers. This pattern continues indefinitely with two trimers, one self-reactive tetramer, and so on. Molecules with an odd number of mer units will come in two forms, A–A and B–B. Molecules with an even number have the form A–B.

Stoichiometry

Reactions of the form AMA + BNB → polymer are known as ***binary polycondensations.*** The original concentrations of the A and B end groups must be closely matched for the reaction to generate a polymer having a high molecular weight. Denote the concentrations of (unreacted) end groups as [A] and [B], and suppose that A is the limiting end group. Then the stoichiometric ratio is defined as

$$S_{AB} = \frac{[\mathrm{A}]_0}{[\mathrm{B}]_0} \leq 1 \tag{13.3}$$

If the reaction goes to completion, the polymer molecules will have the form B–B, and the final concentration of B end groups will be $[\mathrm{B}]_0 - [\mathrm{A}]_0$. The ***number-average chain length*** is

$$\bar{l}_N = \frac{\text{monomers present initially}}{\text{molecules present after polymerization}} = \frac{([\mathrm{B}]_0 + [\mathrm{A}]_0)/2}{([\mathrm{B}]_0 - [\mathrm{A}]_0)/2} = \frac{1 + S_{AB}}{1 - S_{AB}} \tag{13.4}$$

The factor of 2 appears in this equation because each polymer molecule has two end groups. A pesky factor of 2 haunts many polymer equations. It factors out in this example, but we are not always so lucky.

EXAMPLE 13.1

Determine the stoichiometric requirements for achieving various degrees of polymerization for a binary polycondensation.

SOLUTION: Table 13.1 shows results calculated using Equation 13.4.
The stoichiometric requirement for a binary polycondensation is very demanding. High-molecular-weight polymer, say $\bar{l}_N > 100$, requires a weighing accuracy that is difficult to achieve in a flow system.

Table 13.1 Number-Average Chain Lengths for Binary Polycondensations Going to Completion

S_{AB}	$\bar{l}_N$
0.2	1.5
0.333	2
0.5	3
0.8	9
0.9	19
0.98	99
0.99	199
0.998	999

Example 13.1 shows one reason why binary polycondensations are usually performed in batch vessels with batch-weighing systems. Another reason is that some polycondensation reactions involve polyfunctional molecules that will crosslink and plug a continuous flow reactor. An example is phenol, which is trifunctional when condensed with formaldehyde. It can react at two ortho locations and one para location to build an infinite, three-dimensional network. This may occur even when the stoichiometry is less than perfect. See Problem 13.3 for a specific example. In a batch polymerization, any crosslinked polymer is removed after each batch, while it can slowly accumulate and eventually plug a flow reactor.

Self-condensing monomers of the form AMB avoid a stoichiometry restriction. The idea is to synthesize the monomer using conditions where the A and B end groups are not reactive but polymerize the monomer under conditions where the end groups do react. An important example is the polymerization of PET. A large excess of ethylene glycol is reacted with terephthalic acid to form a nominal trimer, diglycol terephthalate:

$$2HOCH_2CH_2OH + HO\overset{O}{\overset{||}{C}}\phi\overset{O}{\overset{||}{C}}OH \rightarrow HOCH_2CH_2O\overset{O}{\overset{||}{C}}\phi\overset{O}{\overset{||}{C}}OCH_2CH_2OH$$

This new "monomer" is separated from the excess glycol and polymerized. The monomer has two hydroxy end groups; but with catalysis and temperature, it will self-condense to give ethylene glycol as the byproduct. The overall result is a one-to-one reaction of terephthalic acid with ethylene glycol, but a substantial amount of glycol is internally recycled.

Equilibrium Limitations

Self-condensing monomers have $S_{AB} = 1$ and can therefore react to infinite molecular weight. Unfortunately, free lunches are rare. The cost of this lunch is that most self-condensations are reversible, so the condensation product must be removed for the reaction to proceed. The condensation of diglycol terephthalate gives high-molecular-weight polymer only if byproduct ethylene glycol is removed. The condensation of lactic acid to poly(lactic acid) proceeds only if byproduct water is removed. The normal technique for removal is to raise the temperature and lower the pressure so that the condensation product evaporates. The polymer industry calls this ***devolatilization.*** It can occur spontaneously if the condensation product is a gas like HCl but requires substantial effort for high-boiling byproducts such as water and ethylene glycol. Equilibrium limitations are avoided when the condensation product has negligible solubility in the reaction medium. An example is the formation of salt when the sodium salt of bisphenol A reacts with epichlorohydrin to form epoxy resins with NaCl as the insoluble byproduct.

The reversibility of polycondensation reactions sometimes provides a method for plastics recycling. Reacting the polymer with the condensation product, AB, can quickly reduce the degree of polymerization to a self-condensing trimer. The trimer can be purified by distillation and repolymerized to give the equivalent of virgin polymer that is once again suitable for food contact applications. Reacting PET with ethylene glycol is the glycolysis route to PET recycling. Unfortunately, the overall process is substantially more expensive than the process for making virgin PET.

Other Complications in Condensation Polymerizations

Cyclization occurs naturally in many condensation polymerizations. A polymer molecule of the form A–B reacts with itself to form a cyclic compound. For binary polycondensations, the number of mers in the ring will be even since only the even-numbered chains are self-condensing. High solvent concentrations increase ring formation. Small molecules cannot form rings due to steric hindrance, and the reactive ends on large molecules are unlikely to meet due to statistics. Thus a plot of cyclic oligomer concentration versus mer number will have a sharp lower limit, a maximum, and a gradually declining tail.

Solubility limits may arise when oligomers beyond a certain length precipitate from the reaction medium. Solubility generally decreases with increasing molecular weight so this phenomenon is fairly common. Precipitation generally stops the reaction for condensation polymers, and solubility limits can be used advantageously to prepare oligomers of a fixed molecular weight. Solubility limits can usually be avoided by adding a good solvent to the reaction medium.

Chain stoppers are unifunctional molecules of the form AX or BX where the X moiety is nonreactive. They are used to stop the polymerization at a desired point or to stabilize the polymer chains by endcapping.

Random condensation copolymers can be formed by adding a third monomer to the reaction mix. For example, some 1,4-butanediol might replace some of the ethylene glycol in a PET polymerization. Suppose the three monomers are AMA, BNB, and BZB. The resulting polymer will have a structure such as

MNMNMNMZMNMNMZMNMZMNMNMNMN . . .

The polymer is sometimes called a ***terpolymer*** because three monomers are involved, but the term copolymer is used inclusively for any polymer formed from more than one monomer. In the absence of BZB, AMA and BNB will polymerize to form a ***strictly alternating copolymer***. When BZB is added, the polymer still alternates with respect to the M mers but is random with respect to the N and Z mers. Of course, the enthusiastic chemist might add some AYA or even some AWB to the mix. They will all happily copolymerize, albeit at different rates.

13.1.2 Chain Growth Polymerizations

The most important example of an addition polymerization is the homopolymerization of a vinyl monomer. The general formula for a vinyl monomer is

$$\begin{array}{l} R_1 \quad R_3 \\ | \quad\ \ | \\ C = C \\ | \quad\ \ | \\ R_2 \quad R_4 \end{array} \tag{13.5}$$

The most important vinyl monomers have a simpler form:

$$\begin{array}{l} CH_2{=}CH \\ \qquad\ \ | \\ \qquad\ \ R \end{array} \tag{13.6}$$

This monomer is ethylene when R is hydrogen, propylene when R is a methyl group, styrene when R is a benzene ring, and vinyl chloride when R is chlorine. The polymers formed from these four monomers account for the majority of all commercial plastics. The polymers come in great variety and are made by many different processes. All of the vinyl polymerizations share a characteristic that is extremely important from the viewpoint of reactor design. They are so energetic that control of the reaction exotherm is a key factor in all designs.

Thermal Effects in Addition Polymerizations

Table 13.2 shows the heats of reaction (per mole of monomer reacted) and nominal values of the adiabatic temperature rise for complete polymerization.

The point made by Table 13.2 is clear even though the calculated values for ΔT_{adia} should not be taken literally for the vinyl addition polymers. All of these

Table 13.2 Typical Heats of Polymerization

Polymer	Polymerization Type	ΔH (kJ mol^{-1})	Adiabatic ΔT (°C)
Polyethylene	Vinyl addition	95.0	1610
Polyvinyl chloride	Vinyl addition	95.8	730
Polystyrene	Vinyl addition	69.9	320
Polymethyl methacralate	Vinyl addition	56.5	270
Polycaprolactam	Ring opening	15.9	68
Polysulfone	Condensation	25.1	24
Polycarbonate	Condensation	0	0
Polyethylene terephthalate	Condensation	0	0

polymers have ceiling temperatures where polymerization stops. Some, like polyvinyl chloride, will dramatically decompose, but most will approach equilibrium between monomer and low-molecular-weight polymer. A controlled polymerization yielding high-molecular-weight polymer requires substantial removal of heat or operation at low conversions. Both approaches are used industrially.

The other entries in Table 13.2 show that heat removal is not a problem for most ring-opening and condensation polymerizations. Polycaprolactam, (Nylon 6) is an addition polymer but with rather similar bond energies for the monomer and the polymer. The reaction exotherm is small enough that large parts are made by essentially adiabatic reaction in a mold. An equilibrium between monomer and polymer does exist for polycaprolactam, but it occurs at commercially acceptable molecular weights.

Equilibrium between Monomer and Polymer

A monomer-with-polymer equilibrium is quite different from the polymer-with-condensation product equilibrium discussed in Section 13.1.1. If the condensation product is removed from the reaction mixture, a condensation polymer increases in molecular weight. If the monomer is removed when it is in equilibrium with the polymer, the polymer depolymerizes to re-form the monomer. At temperatures suitable for long-term use, the equilibrium will be shifted toward stable polymer. However, at fabrication temperatures and at the high temperatures common in devolatilization, the production of monomer and low-molecular-weight oligomers can be significant.

Polymer Structure

The simple vinyl monomer of Equation 13.6 can be arranged in several ways along the polymer chain to give distinct materials with markedly different physical properties. The first consideration is whether the polymerization proceeds ***head to head*** or ***head to tail***. The head-to-head arrangement has the pendant R groups on adjacent carbon atoms. It is quite uncommon. Most polymers are of the head-to-tail variety with the pendant groups separated by a carbon atom in the polymer backbone. The next structural distinction is ***tacticity***. It is a stereochemical property that depends on the tetrahedral nature of carbon bonds. If the pendant R groups are all on the same side relative to the carbon–carbon bonds along the backbone, the polymer is ***isotactic***. If they strictly alternate, the polymer is ***syndiotactic***. If they alternate at random, the polymer is ***atactic***. Polyethylene has no tacticity since the pendant group is hydrogen. Ordinary polypropylene is isotactic, but syndiotactic and atactic varieties are available. Ordinary polystyrene is atactic, although a syndiotactic variety has been introduced.

Diene-based polymers such as polybutadiene have other structural distinctions. The linear versions of these polymers have one residual double bond for each mer. When the double bonds are in the polymer chain, the cis and trans stereoisomers

are possible. The double bonds can appear as pendant vinyl groups, which can then exhibit tacticity.

Most commercial polymers are substantially ***linear***. They have a single chain of mers that forms the backbone of the molecule. ***Side chains*** can occur and can have a major effect on physical properties. An elemental analysis of any polyolefin [e.g., polyethylene, polypropylene, poly(1-butene)] gives the same empirical formula, CH_2, and it is only the nature of the side chains that distinguishes between the polyolefins. Polypropylene has methyl side chains on every other carbon atom along the backbone. Side chains at random locations are called ***branches.*** Branching and other polymer structures can be deduced using analytical techniques such as ^{13}C nuclear magnetic resonance (NMR).

Copolymerization (e.g., of 1-butene or 1-hexene with ethylene) gives ***short-chain branching***, for example, the branches contain three or five carbon atoms. The random location of the side chains lowers the crystallinity and density. ***Long-chain branching*** refers to branches that are similar in length to the polymer backbone and occurs in polyethylene manufactured using the high-pressure process. These branches also lower the crystallinity and density. ***Star polymers*** have three or more long chains originating from a common point. They are formed when the polymerization is initiated with a polyfunctional molecule.

The logical extension of branching is ***crosslinking***, where the polymer becomes an immense three-dimensional molecule. Originally distinct polymer chains are connected by chemical bonds or ionic attractions between two or more chains. Lightly crosslinked materials swell in a solvent to form a gel but do not dissolve. Heavily crossedlinked polymers can be as hard as a bowling ball. Intentional crosslinking is done after thermosetting polymers (e.g., phenolic and epoxy resins) and rubbers are molded into their final shapes. Unintentional crosslinking shows up as defects in polymer films (known as gels or fish eyes) or can shut down reactors.

Vinyl copolymers contain mers from two or more vinyl monomers. Most common are ***random copolymers*** that are formed when the monomers polymerize simultaneously. They can be made by most polymerization mechanisms. ***Block copolymers*** are formed by reacting one monomer to completion and then replacing it with a different monomer that continues to add to the same polymer chain. The polymerization of a ***diblock copolymer*** stops at this point. ***Triblock and multiblock polymers*** continue the polymerization with additional monomer depletion and replenishment steps. The polymer chain must retain its ability to grow throughout the process. This is possible for a few polymerization mechanisms that give ***living polymers.***

13.2 MOLECULAR WEIGHT DISTRIBUTIONS

The ***molecular weight distribution*** (***MWD***) is of vital importance for polymers of all types. It determines the ease of manufacture, the ease of fabrication, and the end-use properties of the polymer. A proper kinetic description of a polymerization requires determination of the molecular weight distribution of the polymer in addition to the usual concepts of conversion and selectivity.

13.2.1 Distribution Functions and Moments

Theoretical MWDs are usually based on the chain length rather than the molecular weight. A multiplicative factor, molecular weight per mer, can be applied at the end of any calculation. The subtle differences due to end groups are usually ignored. Let $c_l, l = 1, 2, \ldots$, be the concentration of polymer chains having length l. The discrete-valued function c_l is sometimes called the molecular weight distribution, but it does not obey the rules of a probability distribution since it does not sum to 1. Instead,

$$\sum_{l=1}^{\infty} c_l = c_{\text{polymer}} \tag{13.7}$$

where c_{polymer} is the total polymer concentration. A proper probability function is

$$f(l) = \frac{c_l}{c_{\text{polymer}}} \quad \text{so that} \quad \sum_{l=1}^{\infty} f(l) = 1 \tag{13.8}$$

where $f(l)$ is the fraction of the total number of polymer molecules that has length l. Both c_l and $f(l)$ are defined only for integer values of $l, l = 1, 2, \ldots$, but when c_l is measured experimentally, it is difficult to resolve individual oligomers beyond the first few, and c_l appears to be a continuous function of l. Integrals then replace the sums in Equations 13.7 and 13.8. When $f(l)$ is a continuous function of l, $f(l)\, dl$ gives the fraction of the molecules having lengths in the range from l to $l + dl$. See Chapter 15 for a similar definition of a differential distribution function applicable to residence times. Here in this chapter, summations will be used rather than integrals.

The moments of the MWD, $\mu_n, n = 1, 2, 3, \ldots$, are defined as

$$\mu_n = \sum_{l=1}^{\infty} l^n c_l \quad \text{or} \quad \mu_n = \sum_{l=1}^{\infty} l^n f(l) \quad n = 0,\ 1,\ 2,\ \ldots \tag{13.9}$$

where $\mu_0 = c_{\text{polymer}}$ when c_l is used to define the moments and $\mu_0 = 1$ when $f(l)$ is used. Note that definitions of the zeroth moment differ by a factor of c_{polymer}. Statisticians use the $\mu_0 = 1$ form. The polymer literature uses both. The number-average chain length (which is proportional to the number-average molecular weight) is obtained from the first moment:

$$\bar{l}_N = \frac{\mu_1}{\mu_0} = \frac{\sum_{l=1}^{\infty} l c_l}{c_{\text{polymer}}} = \sum_{l=1}^{\infty} l f(l) \tag{13.10}$$

An experimental determination of the MWD conceptually sorts the polymer molecules into bins, with one bin for each degree of polymerization, $l = 1, 2, \ldots$. The contents of the bin are counted, and $f(l)$ is the fraction (by number) found in bin l. The bins could also be weighed to give a weight fraction in each bin. This defines the function $g(l)$. Since weight is proportional to chain length, the distribution by weight is

$$g(l) = \frac{l f(l)}{\bar{l}_N} \qquad \sum_{l=1}^{\infty} g(l) = 1 \tag{13.11}$$

where the factor of $\bar{l}$ is included so that the probabilities sum to 1. The ***weight-average chain length*** is

$$\bar{l}_W = \sum_{l=1}^{\infty} l g(l) = \frac{1}{\bar{l}} \sum_{l=1}^{\infty} l^2 f(l) = \frac{\mu_2}{\mu_0 \mu_1} \tag{13.12}$$

The ratio of weight- to number-average chain lengths is the **polydispersity**,

$$\text{PD} = \frac{\bar{l}_W}{\bar{l}_N} \geq 1 \tag{13.13}$$

This dimensionless number measures the breadth of the MWD. It is 1 for a ***monodisperse*** population (e.g., for monomers before reaction) and 2 for many polymerization mechanisms.

13.2.2 Addition Rules for Molecular Weight

Suppose w_1 kilograms of a polymer with chain lengths $(\bar{l}_N)_1$ and $(\bar{l}_W)_1$ are mixed with w_2 kilograms of a polymer with chain lengths $(\bar{l}_N)_2$ and $(\bar{l}_W)_2$. Then the mixture has the following properties:

$$(\bar{l}_N)_{\text{mix}} = \frac{w_1 + w_2}{w_1/(\bar{l}_N)_1 + w_2/(\bar{l}_N)_2} \tag{13.14}$$

$$(\bar{l}_W)_{\text{mix}} = \frac{w_1(\bar{l}_W)_1 + w_2(\bar{l}_W)_2}{w_1 + w_2} \tag{13.15}$$

These rules are needed in reactor design calculations when newly formed polymer is added to existing polymer.

13.2.3 Molecular Weight Measurements

When the full distribution is needed, it is measured by size exclusion chromatography (also called gel permeation chromatography). This is a solution technique that requires dissolution of the polymer in a solvent such as tetrahydrofuran or tetrachlorobenzene. For polymers that require exotic solvents or solution temperatures above about 150°C, a simple measurement of solution viscosity can be a useful surrogate for the actual molecular weight. The viscosity of the pure polymer (i.e., a polymer ***melt*** viscosity) can also be used. Such simplified techniques are often satisfactory for routine quality control, particularly for condensation polymers such as PET that vary in average molecular weight but usually have a polydispersity of 2.

Size exclusion chromatography is primarily a research tool. The instrument is calibrated using polystyrene standards, and results are normally reported as ***polystyrene-equivalent molecular weights,*** not the actual molecular weights of the polymer being tested, which may or may not be known. Furthermore, ***a low-molecular-weight cutoff*** of 2000–3000 is usually employed. Thus the measurements are more comparative than absolute. For theoretical calculations involving condensation polymers, everything is

included, even the monomers. For addition polymers, it is normal practice to exclude monomer from the calculations. Low-molecular-weight oligomers are usually excluded as well.

The detector installed on a size exclusion chromatograph determines whether the measured MWD is by number, by weight, or even by viscosity. Modern instruments include software to convert from one distribution to another. They also compute number-average, weight-average, and *Z*-average molecular weights, the last one being related to the third moment of the distribution. All these numbers are relative to the polystyrene standards.

13.3 KINETICS OF CONDENSATION POLYMERIZATIONS

The generic condensation polymerization begins with monomers AMA and BMB and produces molecules of the forms A–A, B–B, and A–B. Each step of the reaction generates a longer polymer by the step growth mechanism of Equation 13.2 and produces 1 mole of condensation product, AB.

13.3.1 Conversion

Suppose that the reactivity of the A and B end groups is independent of the chains to which they are attached. This is a form of the ***equal-reactivity assumption*** that is needed for almost all analytical solutions to polymer kinetic problems. If it is satisfied, we can ignore the details of the polymerization and just concentrate on the disappearance of the end groups. For a batch system,

$$\frac{d[\mathrm{A}]}{dt} = -k[\mathrm{A}][\mathrm{B}] = -k\frac{d[\mathrm{B}]}{dt}$$

The initial condition for this ODE is based on Equation 13.3, $[\mathrm{A}]_0 = S_{AB}[\mathrm{B}]_0$. The solution is

$$X_A = 1 - \frac{1 - S_{AB}}{\exp\left[(1 - S_{AB})[\mathrm{B}]_0 kt\right] - S_{AB}} \tag{13.16}$$

where X_A is the conversion of the limiting end group, A. The conversion depends on S_{AB} and on the dimensionless reaction time, $[\mathrm{B}]_0 kt$. Perfect initial stoichiometry, as for a self-condensing monomer, gives an indeterminant form to which L'Hospital's rule may be applied:

$$X_A = 1 - \frac{1}{1 + [\mathrm{B}]_0 kt} \quad \text{for } S_{AB} = 1 \tag{13.17}$$

We see from Equations 13.16 and 13.17 that the conversion of end groups obeys the kinetics of a simple second-order reaction, the second-order reaction having perfect initial stoichiometry in the case of Equation 13.17.

13.3.2 Number- and Weight-Average Chain Lengths

Solutions for the general case are

$$\bar{l}_N = \frac{1 + S_{AB}}{1 + S_{AB} - 2X_A S_{AB}} \tag{13.18}$$

$$\bar{l}_W = \frac{(1 + S_{AB})\left(1 + X_A^2 S_{AB}\right) + 4X_A S_{AB}}{(1 + S_{AB})\left(1 - X_A^2 S_{AB}\right)} \tag{13.19}$$

For zero conversion, $\bar{l}_N = \bar{l}_W = 1$ since only monomers are present initially. At high conversion, Equation 13.18 approaches Equation 13.4. The PD for the complete conversion case is

$$\text{PD} = \frac{\bar{l}_W}{\bar{l}_N} = \frac{\left(1 + 6S_{AB} + S_{AB}^2\right)}{(1 + S_{AB})^2} \tag{13.20}$$

The PD is 2 for perfect stoichiometry or self-condensing monomers, but Equation 13.4 shows that $\bar{l}_N \to \infty$ for this case. The PD of 2 is an asymptotic value that applies exactly only in the limit of high-molecular-weight. However, the PD closely approaches 2 at quite low chain lengths.

EXAMPLE 13.2

Determine PD as a function of chain length for binary polycondensations that go to completion.

SOLUTION: The final chain length is limited by stoichiometry. Equation 13.4 is used to relate $\bar{l}_N$ and S_{AB} at complete conversion. The PD is then calculated using Equation 13.20.

As shown in Table 13.3, the PD becomes experimentally indistinguishable from 2 at a chain length of about 10.

Table 13.3 Polydispersities for Binary Polycondensations Reacting to Completion

X_A	S_{AB}	$\bar{l}_N$	PD
1	0	1	1
1	0.2	1.5	1.5556
1	0.3333	2	1.7500
1	0.6667	5	1.9600
1	0.8182	10	1.9900
1	0.9048	20	1.9975
1	0.9608	50	1.9996
1	0.9802	100	1.9999

EXAMPLE 13.3

Limited reaction times or incomplete byproduct removal can control the conversion in a self-condensing polymerization. How does the PD of these polymers compare to those in Example 13.2 where the reaction went to completion with imperfect stoichiometry? Make the comparison at the same average chain length.

SOLUTION: The number- and weight-average chain lengths for a self-condensing polymerization are obtained from Equation 13.18 and 13.19 by setting $S_{AB} = 1$:

$$\bar{l}_N = \frac{1}{1 - X_A} \tag{13.21}$$

$$\bar{l}_W = \frac{1 + X_A}{1 - X_A} \tag{13.22}$$

so that

$$\text{PD} = 1 + X_A \tag{13.23}$$

Table 13.4 tabulates results at the same value of $\bar{l}_N$ as in Table 13.3.

Table 13.4 Polydispersities for Self-Condensing Polymerizations

X_A	S_{AB}	$\bar{l}_N$	PD
0	1	1	1
0.33	1	1.5	1.33
0.50	1	2	1.50
0.80	1	5	1.80
0.90	1	10	1.90
0.95	1	20	1.95
0.98	1	50	1.98
0.99	1	100	1.99

The polydispersities are lower than when the same average chain length is prepared by a binary polycondensation going to completion. The stoichiometry-limited, binary polycondensations have a higher PD because the monomer in stoichiometric excess (the B monomer) is included in the calculations. This broadens the MWD.

13.3.3 Molecular Weight Distribution Functions

The probability distribution for chain lengths in a binary polycondensation is

$$f(l) = \begin{cases} \dfrac{2(1 - X_A S_{AB})(1 - X_A)}{1 + S_{AB} - 2X_A S_{AB}} X_A^{l-1} S_{AB}^{l/2} & \text{if } l \text{ is even} \\ \dfrac{(1 - X_A S_{AB})^2 + S_{AB}(1 - X_A)^2}{1 + S_{AB} - 2X_A S_{AB}} X_A^{l-1} S_{AB}^{(l-1)/2} & \text{if } l \text{ is odd} \end{cases} \tag{13.24}$$

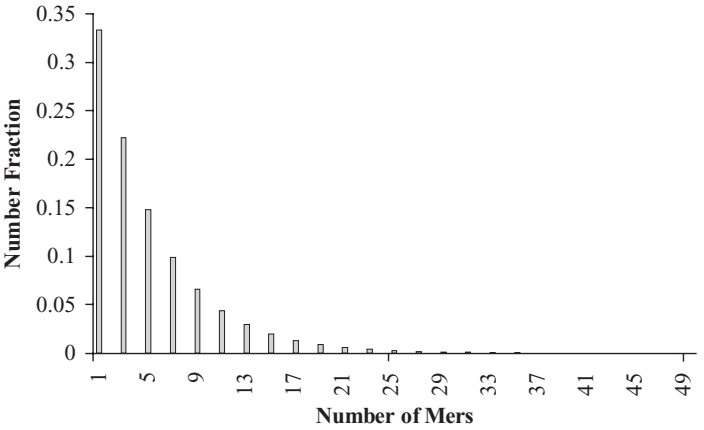

Figure 13.1 Molecular weight distribution by number fraction for binary polycondensation going to completion with $\bar{l}_n = 5$ and $\bar{l}_W = 9.8$.

Figures 13.1 and 13.2 illustrate these distributions by number and weight. The most abundant species by number is always the monomer, even for the case of perfect stoichiometry. The distribution by weight usually shows an interior maximum. Note that the even-numbered mers are missing because the A-type end groups are reacted to completion.

If $S_{AB} = 1$, Equation 13.24 reduces to a simple form:

$$f(l) = (1 - X_A)X_A^{l-1} \quad \text{for all } l \tag{13.25}$$

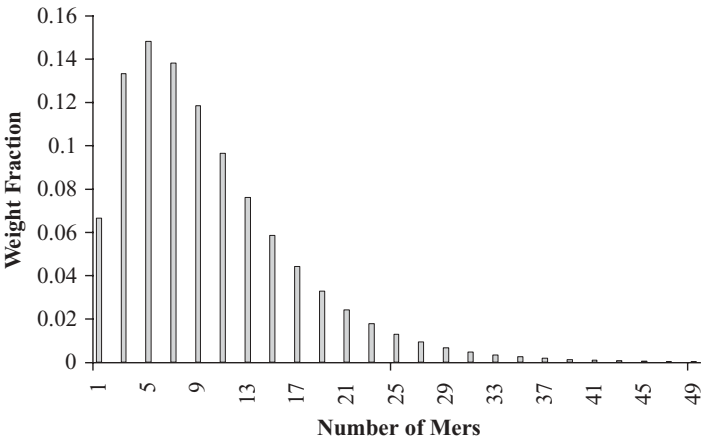

Figure 13.2 Molecular weight distribution by weight fraction for binary polycondensation going to completion with $\bar{l}_N = 5$ and $\bar{l}_W = 9.8$.

This is the famous ***Flory distribution.*** It is also known as the ***most probable distribution***. Equation 13.25 expresses it in terms of the fractional conversion, but Equation 13.21 can be used to replace X_A with $\bar{l}_N$. The result is

$$f(l) = \frac{1}{\bar{l}_N}\left[1 - \frac{1}{\bar{l}_N}\right]^{l-1} \tag{13.26}$$

Note that $\mu_0 = 1$ for this and most other theoretical distribution functions. The mean of the Flory distribution is (obviously) $\bar{l}_N$, and

$$\text{PD} = 1 + X_A = 2 - \frac{1}{\bar{l}_N} \tag{13.27}$$

The equal-reactivity assumption is sometimes wrong. Suppose the reaction in Equation 13.2 is elementary but the rate constant $k_{l,m}$ depends on l and m. The usual case is for the reactions involving the monomers and smaller oligomers to be relatively fast but for the rate dependence to vanish for reasonably long chains. Then calculations based on equal reactivity are usually adequate if the desire is to make polymer of high molecular weight. If a detailed accounting is needed, brute-force numerical calculations can be used. Numerical solutions for $\bar{l}_N$ of a few hundred were feasible in the early 1960s, and any reasonable kinetic scheme is now solvable in detail.

EXAMPLE 13.4

Calculate the MWD for a self-condensing polymerization with $k_{m,n} = k_0/(m + n)$, where m and n are the chain lengths of the reacting molecules. Stop the calculations when $\bar{l}_N = 5$. Compare the results with those of the Flory distribution.

SOLUTION: Polymer of length m is formed by the reaction of any two molecules whose lengths sum to m. It is consumed when it reacts with any molecule. The batch rate equation governing the formation of polymer of length m is

$$\frac{dc_m}{dt} = \frac{k_0}{m}\sum_{n=1}^{m-1} c_n c_{m-n} - c_m \sum_{n=1}^{\infty} \frac{k_0}{m+n} c_n$$

Code for Example 13.4 shows the solution. The time scale is arbitrary. Reaction continues until $\bar{l}_N = 5$ is reached. The code is computationally inefficient but straightforward. Execution times are trivial because $\bar{l}_N$ is small. Results are $\bar{l}_W = 7.04$ and PD $= 1.41$ compared to $\bar{l}_W = 9$ and PD $= 1.8$ for the equal-reactivity case. See Figure 13.3. Convergence requires both an adequately small time step and a sufficiently high value for the maximum chain length that is included in the calculations. The equal-reactivity case is the more demanding with respect to both of these requirements. The results for the equal-reactivity case—as calculated using the program—compare closely to the theoretical distribution, Equations 13.26 and 13.27.

Code for Example 13.4

```
Sub Exp13_4()
Dim c(1000)
c(1) = 1      'Starting concentration of monomer
xk = 1        'Arbitrary value for rate constant
dt = 0.001    'Time step for Euler's method
Ip = 0        'Ip = 0 for equal reactivity.  Ip = 1 for variable reactivity
Lbar = 5      'Desired chain length

MaxL = 10 * Lbar  'Maximul chain length to be included in the calculations

Do            'React until the mean chain length = u1/u0 = Lbar
   u0 = 0
   u1 = 0
   u2 = 0
   For m = 1 To MaxL          'Chains of length m will be from formed
      Sum = 0
      For n = 1 To m - 1     'Chains of lengths n and m-n react to form chains of length m
         Sum = Sum + c(n) * c(m - n)  'Sum is the product of concentrations of all chains
                                      'that will react to produce a chain of length m
      Next n
      If Ip > 0 Then
         Form = xk / m * Sum   'Rate of formation of chains of length m
      Else
         Form = xk * Sum       ' Equal reactivity case
      End If
      Consume = 0
```

```
      For n = 1 To MaxL          'Chains of all lengths will react with chains of length m
         If Ip > 0 Then
            Consume = Consume + xk / (m + n) * c(n)  'Multiply this by c(m) to get the
                                     'the rate at which chains of length m are consumed
         Else
            Consume = Consume + xk * c(n)   'Equal reactivity case
         End If
      Next n
      c(m) = c(m) + (Form - Consume * c(m)) * dt
      u0 = u0 + c(m)             'Moments 0, 1, and 2 are calculated
      u1 = u1 + m * c(m)
      u2 = u2 + m * m * c(m)
   Next m
Loop While u1 / u0 < Lbar

For m = 1 To MaxL
   Cells(m, 1) = m
   Cells(m, 2 + Ip) = c(m)
   Cells(1, 5 + Ip) = u0
   Cells(2, 5 + Ip) = u1 / u0
   Cells(3, 5 + Ip) = u2 / u0 / u1
   Cells(4, 5 + Ip) = u2 / u1 / u1
Next m

End Sub
```

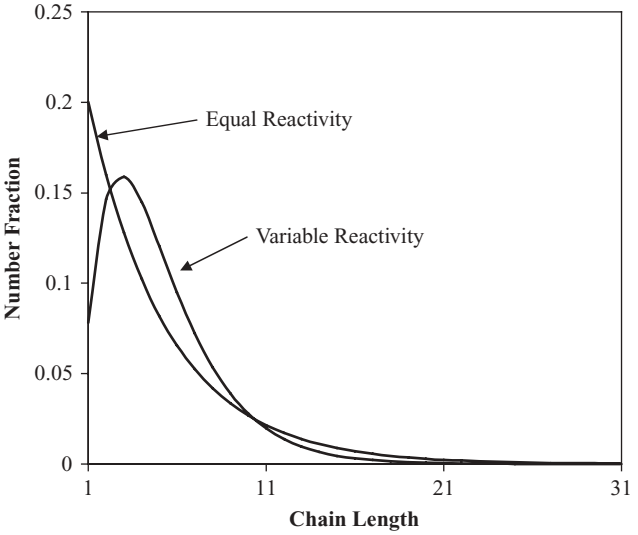

Figure 13.3 Molecular weight distributions by number for the equal-reactivity and variable-reactivity cases of Example 13.4.

13.4 KINETICS OF ADDITION POLYMERIZATIONS

Most addition polymerizations involve vinyl or diene monomers. The opening of a double bond can be catalyzed in several ways. Free-radical polymerization is the most common method for styrenic monomers, whereas coordination metal catalysis (Zigler–Natta and metallocene catalysis) is important for olefin polymerizations. The specific reaction mechanism may generate some catalyst residues, but there are no true coproducts. There are no stoichiometry requirements, and equilibrium limitations are usually unimportant so that quite long chains are formed; $\bar{l}_N > 500$ is typical of addition polymers.

The first step in an addition polymerization is ***initiation*** to form a polymer chain of length 1:

$$\mathrm{M} + \mathrm{I} \rightarrow \mathrm{IP}_1 \tag{13.28}$$

The moiety denoted as I is the initiator group. It can be as simple as a free radical or as complicated as a transition metal atom bonded to organic ligands and located on a catalytic support. The next step in the polymerization is ***propagation***, that is, the repeated insertion of monomer units into the chain to create an incrementally longer chain:

$$\mathrm{M} + \mathrm{IP}_l \rightarrow \mathrm{IP}_{l+1} \qquad l = 1, 2, \ldots \tag{13.29}$$

The propagation reaction is a more mechanistic version of Equation 13.1 and accounts for most of the monomer consumption. The growth of the chain can be stopped by

chain transfer, the simplest form of which is chain transfer to monomer:

$$\mathrm{M} + \mathrm{IP}_l \rightarrow \mathrm{IP}_1 + \mathrm{P}_l \qquad l = 1, 2, \ldots \tag{13.30}$$

Here, P_l is a finished polymer molecule and IP_1 starts a new chain. Growth is also stopped by ***termination***. It deactivates the initiator group and gives a finished polymer molecule.

13.4.1 Living Polymers

A batch, anionic polymerization (e.g., of styrene catalyzed by butyl lithium) is among the simplest addition polymerizations to analyze. Butyl lithium is added to a solution of styrene monomer to form $\mathrm{Li^+Bu^-P_1}$ as the first propagating species. The initiation step is fast and consumes I_0 molecules each of the initiator and of the monomer to give I_0 growing polymer chains. If the reaction is maintained at moderate temperatures, say $<50^\circ$C, and if there are no contaminates such as water, CO_2, or oxygen, then there are no chain transfer or termination reactions. The I_0 chains constitute ***living polymer*** molecules that continue to grow until all the monomer is consumed. The average chain length will be

$$\bar{l}_N(t \rightarrow \infty) = \frac{M_0}{I_0}$$

The chains share the same chemical environment and grow at the same average rate. If the final chain length is large, all the molecules will have more or less the same size and the resulting polymer will be approximately monodisperse. Furthermore, if a second monomer is added to the system after the first has been depleted, a block copolymer can be formed.

The present section analyzes the above concepts in detail. There are many different mathematical methods for analyzing MWDs. The ***method of moments*** is particularly easy when applied to a living polymer polymerization. Equation 13.30 shows the propagation reaction, each step of which consumes one monomer molecule. Assume equal reactivity. Then for a batch polymerization,

$$\frac{dM}{dt} = -k_p M \sum_{l=1}^{\infty} c_l = -k_p M \mu_0 = -k_p M I_0 \tag{13.31}$$

where $\mu_0 = I_0$ is the total concentration of polymer molecules and is constant for living polymer. Equation 13.31 is subject to the initial condition that $M = M_0 - I_0$ at $t = 0$, zero time being just after the fast initiation step that consumes I_0 monomer molecules. The solution to Equation 13.31 is

$$M = M(t) = (M_0 - I_0)\exp(-k_p I_0 t) \tag{13.32}$$

Polymer of length i is formed when polymer of length $i - 1$ reacts with monomer and is consumed when it itself reacts with monomer:

$$\frac{dc_l}{dt} = k_p M c_{l-1} - k_p M c_l = k_p M (c_{l-1} - c_l) \tag{13.33}$$

The time variable is transformed to incorporate M. Set $d\tau = k_p M\, dt$. The *relationship* between transformed time τ and real time t is found by integrating Equation 13.31 with τ as the independent variable. This gives

$$\tau = \frac{M_0 - I_0}{I_0}[1 - \exp(-k_p I_0 t)] = \frac{M_0 - I_0 - M}{I_0} \tag{13.34}$$

The point of the transformation is that Equation 13.33 becomes beautifully simple:

$$\frac{dc_l}{d\tau} = c_{l-1} - c_l \tag{13.35}$$

Equation 13.35 is one member of an infinite set of ODEs, one ODE for each $l = 1, 2, \ldots, \infty$. Add them all up to obtain

$$\sum_{l=1}^{\infty} \frac{dc_l}{d\tau} = \frac{d\sum_{l=1}^{\infty} c_l}{d\tau} = \frac{d\mu_0}{d\tau} = -c_1 + (c_1 - c_2) + (c_2 - c_3) + \cdots = 0$$

which is an ODE for μ_0. To obtain ODEs for μ_1 and μ_2, multiply Equation 13.34 by l and l^2 and then sum:

$$\begin{aligned}\sum_{l=1}^{\infty} l\frac{dc_l}{d\tau} &= \frac{d\sum_{l=1}^{\infty} lc_l}{d\tau} = \frac{d\mu_1}{d\tau} \\ &= -c_1 + 2(c_1 - c_2) + 3(c_2 - c_3) + \cdots = c_1 + c_2 + c_3 + \cdots = \mu_0\end{aligned}$$

$$\begin{aligned}\sum_{l=1}^{\infty} l^2\frac{dc_l}{d\tau} &= \frac{d\sum_{l=1}^{\infty} l^2 c_l}{d\tau} = \frac{d\mu_2}{d\tau} \\ &= -c_1 + 4(c_1 - c_2) + 9(c_2 - c_3) + \cdots \\ &= 3c_1 + 5c_2 + 7c_3 + \cdots = \mu_0 + 2\mu_1\end{aligned}$$

The infinite set of simultaneous ODEs has been transformed to a set of moment equations. They are also infinite in number, but they can be solved sequentially. The first three members of the set are

$$\begin{aligned}\frac{d\mu_0}{d\tau} &= 0 & \mu_0 &= I_0 \quad \text{at } \tau = 0 \\ \frac{d\mu_1}{d\tau} &= \mu_0 & \mu_1 &= I_0 \quad \text{at } \tau = 0 \\ \frac{d\mu_2}{d\tau} &= \mu_0 + 2\mu_1 & \mu_2 &= I_0 \quad \text{at } \tau = 0\end{aligned}$$

As a practical matter, knowing moments 0, 1, and 2 is usually adequate to describe a MWD (academicians are not always practical). The initial condition for all the moments is $\mu_n = I_0$ at $\tau = 0$. Solution for the first three moments for the living polymer case gives

$$\begin{aligned}\mu_0 &= I_0 \\ \mu_1 &= I_0(\tau + 1) \\ \mu_2 &= I_0(\tau^2 + 3\tau + 1)\end{aligned}$$

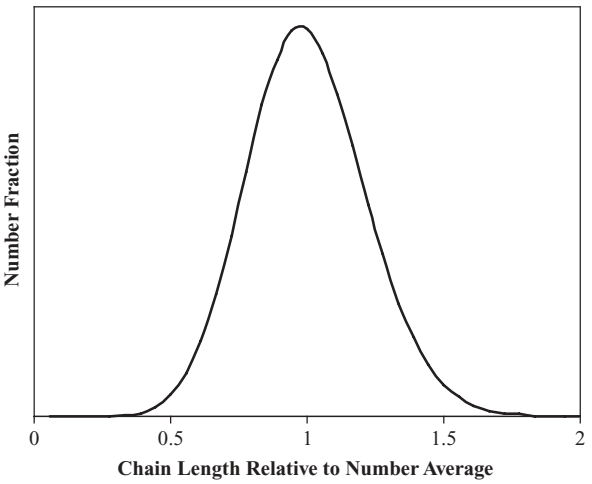

Figure 13.4 Molecular weight distributions for a polymer having a polydispersity of 1.05.

From these we find

$$\bar{l}_N = \frac{\mu_1}{\mu_0} = \tau + 1 \tag{13.36}$$

$$\bar{l}_W = \frac{\mu_2}{\mu_1} = \frac{\tau^2 + 3\tau + 1}{\tau + 1} \tag{13.37}$$

$$\text{PD} = \frac{\bar{l}_W}{\bar{l}_N} = \frac{\mu_0 \mu_2}{\mu_1^2} = \frac{\tau^2 + 3\tau + 1}{(\tau + 1)^2} \tag{13.38}$$

Equation 13.34 allows τ to be calculated from M, M_0, and I_0. Suppose 1000 moles of monomer are reacted with 1 mole of initiator and that the polymerization goes to completion. Equation 13.34 gives $\tau = 999$ so that Equation 13.36 predicts $\bar{l}_N = 1000$ and Equation 13.38 predicts PD = 1.001. The highest PD predicted for a batch, living polymerization is 1.25 at $\bar{l}_N = 2$.

Anionic polymerizations make the molecular weight standards that are used to calibrate size exclusion chromatographs. Actual measurements for the $\bar{l}_N = 1000$ case give a PD of about 1.05. The difference is attributed to impurities in the feed that cause terminations and thus short chains. Also, the chromatograph has internal dispersion so that a truly monodisperse sample would show some spread. Even so, a PD of 1.05 is extremely narrow by polymer standards. This does not mean it is narrow in an absolute sense. Figure 13.4 shows the MWD by number for a polymer having a PD of 1.05. The spread in molecular weights relative to the mean is appreciable.

13.4.2 Free-Radical Polymerizations

A typical free-radical polymerization involves all of the steps in addition polymerization: initiation, propagation, chain transfer, and termination. In contrast to anionic

and cationic polymerization, which can give living polymers, the lifetime of growing polymer chains is short under free-radical catalysis, typically on the order of milliseconds. The quasi-steady hypothesis discussed in Section 2.5.3 is usually applied in theoretical analyses because growing chains are terminated at approximately the same rate at which they are initiated. Although some monomers will initiate spontaneously upon heating (***thermal initiation***), a chemical initiator is usually used as the original source of free radicals. A typical initiator decomposes according to first-order kinetics to yield two free radicals:

$$\mathrm{I}_2 \xrightarrow{k_i} 2f\ \mathrm{I}\cdot \quad \mathscr{R} = k_i[\mathrm{I}_2]$$

The factor of f reflects the fact that some of the free radicals immediately recombine into stable molecules that do not initiate polymerization. A primary radical formed by the chemical initiator reacts with monomer to form a propagating radical that contains one monomer unit:

$$\mathrm{I}\cdot + \mathrm{M} \rightarrow \mathrm{IP}_1\cdot$$

This is the starting chain and is identical to the IP_1 species in Equation 13.28, The $\cdot$ notation explicitly shows the free-radical nature of the polymerization, and the moiety denoted by I represents a fragment from the chemical initiator, for example, a butyl group when t-butyl peroxide is the initiator. The propagation reaction is

$$\mathrm{M} + \mathrm{IP}_l\cdot \rightarrow \mathrm{IP}_{l+1}\cdot \qquad l = 1, 2, \ldots \qquad \mathscr{R}_p = k_p M \sum_{l=1}^{\infty} [\mathrm{IP}_l\cdot] = k_p M[\mathrm{P}\cdot]$$

where $[P\cdot]$ denotes the total concentration of growing chains. The constant value for k_p assumes equal reactivity.

Various forms of chain transfer are common. Chain transfer to monomer stops chain growth but initiates a new chain of length 1. It acts to limit the polymer molecular weight without reducing conversion. Chain transfer to polymer causes long-chain branching. Chain transfer to solvent limits molecular weight and may reduce conversion depending on the fate of the transferred free-radical. Chain transfer to a free-radical scavenger such as t-butylcatechol inhibits polymerization.

In contrast to chain transfer, termination reactions destroy free radicals. Two mechanisms are considered. ***Termination by combination*** produces a single molecule of dead polymer:

$$\mathrm{IP}_l\cdot + \mathrm{IP}_m\cdot \rightarrow \mathrm{IP}_{l+m}\mathrm{I} \qquad \mathscr{R} = k_c[\mathrm{P}\cdot]^2$$

The free radicals combine to form a carbon-to-carbon bond and give a saturated polymer molecule with initiator fragments on both ends. ***Termination by disproportionation*** produces two polymer molecules, one of which will contain a double bond:

$$\mathrm{IP}_l\cdot + \mathrm{IP}_m\cdot \rightarrow \mathrm{IP}_p + \mathrm{IP}_q \qquad \mathscr{R} = k_d[\mathrm{P}\cdot]^2$$

where $l + m = p + q$.

Chain lifetimes are small and the concentration of free radicals is low. To a reasonable approximation, the system consists of unreacted monomer, unreacted initiator, and dead polymer. The quasi-steady hypothesis gives

$$\frac{d[\mathrm{P}\cdot]}{dt} = fk_i[I_2] - (k_c + k_d)[\mathrm{P}\cdot]^2 \approx 0$$

where it was assumed that the termination rate constants k_c and k_d are independent of chain length. Solving for [P·] and substituting into the propagation rate gives

$$\mathscr{R}_p = k_p M[\mathrm{P}\cdot] = k_p M\sqrt{\frac{2fk_i[\mathrm{I}_2]}{k_c + k_d}} \tag{13.39}$$

The propagation reaction accounts for nearly all the consumption of monomer. Thus Equation 13.39 predicts that the polymerization rate will be first order in monomer concentration and half order in initiator concentration. This is confirmed by experiments at low polymer concentrations but can be violated at high polymer concentrations. The termination mechanisms require pairwise interactions between large molecules, and these become increasingly difficult at high polymer concentrations due to chain entanglements. The propagation reaction is less affected, and the net rate of polymerization can actually increase. The phenomenon of the rate increasing as M decreases is a form of autoacceleration known as the ***gel effect***. It is particularly noticeable in the polymerization of methyl methacrylate. See Section 2.5.4 and Figure 2.5.

The ratio of propagation rate to termination rate gives the ***dynamic chain length*** of the growing polymer. Ignoring chain transfer,

$$(\bar{l}_N)_{\text{live}} = \frac{k_p M}{\sqrt{2f(k_c + k_d)k_i[\mathrm{I}_2]}} \tag{13.40}$$

The dynamic chain length is the number-average length of the growing chain before termination. The dead polymer will have the same average length as live polymer if termination is by disproportionation and will have twice this length if termination is by combination.

The growing polymer chains have the most probable distribution defined by Equation 13.26. Typically, $\bar{l}_N$ is large enough that PD ≈ 2 for the growing chains. It remains 2 when termination occurs by disproportionation. Example 13.5 shows that the PD drops to 1.5 for termination by pure combination. The addition rules of Section 13.2.2 can be applied to determine $1.5 <$ PD < 2 for mixed-mode terminations, but disproportionation is the predominate form for commercial polymers.

EXAMPLE 13.5

Determine the instantaneous distributions of chain lengths by number and weight before and after termination by combination. Apply the quasi-steady and equal-reactivity assumptions to a batch polymerization with free-radical kinetics and chemical initiation.

SOLUTION: The equal-reactivity assumption says that k_p and k_c are independent of chain length. The quasi-steady hypothesis gives $d[\mathrm{R}\cdot]/dt = 0$. Applying these to a material balance

for growing chains of length l gives

$$k_p M[\mathrm{P}_{l-1}\cdot] - k_p M[\mathrm{P}_l\cdot] - k_c[\mathrm{P}_l\cdot][\mathrm{P}\cdot] = 0$$

where $[\mathrm{P}\cdot]$ denotes the entire population of growing chains. Solving for $[\mathrm{P}_l\cdot]$ gives

$$[\mathrm{P}_l\cdot] = \frac{k_p M[\mathrm{P}_{l-1}\cdot]}{k_p M + k_c[\mathrm{P}\cdot]} = \omega[\mathrm{P}_{l-1}\cdot]$$

where ω is a proportionality factor that is constant at any instant of time. Thermal initiation creates species $[\mathrm{P}_1\cdot]$, and propagation takes it from there. The relative concentrations of chain lengths are distributed according to the following:

Chain Length, l	Relative Concentration, $[\mathrm{P}_l\cdot]/[\mathrm{P}_1\cdot]$
1	1
2	ω
3	ω^2
$\vdots$	$\vdots$

This is a geometric progression which sums to $1/(1-\omega)$. The fraction of the growing chains with length l is

$$f(l) = (1-\omega)\omega^{l-1}$$

which is identical in form to Equation 13.25. Thus the growing polymer chains have a Flory distribution. The dead polymer may have a different and narrower distribution. It is narrower due to the averaging process that results when termination is by combination. An unusually long chain will usually combine with a shorter chain, giving a sum that is not too different from the average sum.

The ***moment-generating function*** of a probability distribution is defined as an exponentially weighted summation over the range of the distribution. This exponentially weighted sum has the property that

$$\lim_{s\to 0} \frac{d^n}{ds^n} \sum_{l=1}^{\infty} f(l)e^{sl} = \mu_n$$

where $\mu_0 = 1$. For termination by combination, we assume that termination occurs between pairs of growing chains chosen completely at random. A theorem in probability theory for the addition of two independent random variables is

$$\sum_{l=1}^{\infty} f_{\text{dead}}(l)e^{sl} = \left[\sum_{l=1}^{\infty} f_{\text{live}}(l)e^{sl}\right]^2$$

Differentiating both sides once and then twice and taking limits as $s \to 0$ give $(u_1)_{\text{dead}} \to 2(u_1)_{\text{live}}$, $(u_2)_{\text{dead}} \to 2(u_1^2 + u_2)_{\text{live}}$, and $\text{PD}_{\text{dead}} = (1 + \text{PD}_{\text{live}})/2$. Since $\text{PD}_{\text{live}} \approx 2$ for polymer of reasonable high molecular weight, $\text{PD}_{\text{dead}} \approx 1.5$ would be the expected result for termination by combination.

Unlike the convention for condensation polymers, calculations of $\bar{l}_N$ for free-radical polymers exclude unreacted monomer. High-molecular-weight polymer is formed at the beginning of a polymerization, and the molecular weight remains approximately constant as the reaction proceeds. Conversion in a free-radical polymerization means the conversion of monomer to high-molecular-weight polymer. A reaction mixture at 50% conversion may consist of 50% monomer and 50% polymer with a number-average molecular weight of 100,000 ($\bar{l}_N \approx 1000$). The viscosity of the polymerizing mixture at 50% conversion might be 10,000 times higher than that of the pure monomer. In contrast, molecular weight increases gradually in a polycondensation, and really high molecular weights are not achieved until near the end of a batch reaction. Conversion in a polycondensation refers to consumption of the stoichiometrically limiting end group, and 50% conversion with $S_{AB} = 1$ gives dimer. See Table 13.4. The viscosity of the reaction mixture at 50% conversion is perhaps twice that of the pure monomer(s). Figure 13.5 compares viscosity versus conversion curves for the two types of polymerizations. Living polymer systems behave more like condensation polymerizations since the molecular weight builds slowly. Transitional metal catalyses behave like free-radical polymerizations with high-molecular-weight polymer created at the onset.

The above discussion has been based on conventional free-radical catalysis. There has been substantial research on long-lived free radicals that can give a living polymer without the severe cleanliness requirements of anionic polymerizations. Unfortunately, it has not yet had commercial success.

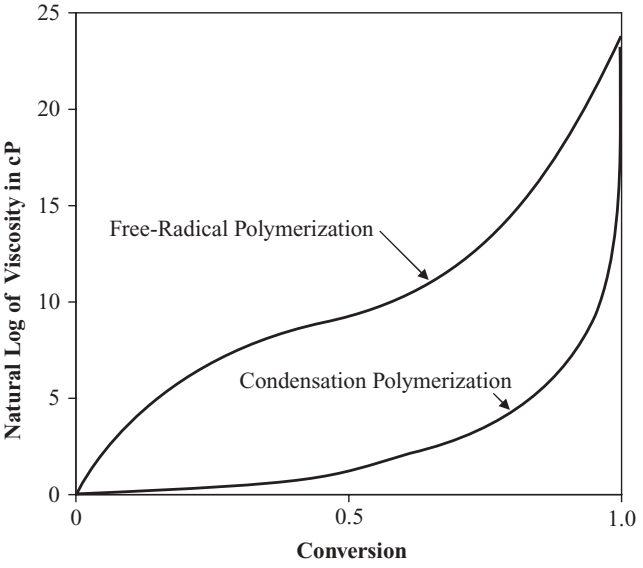

Figure 13.5 Representative profiles of viscosity versus conversion for free-radical and condensation polymerizations. The endpoint is 99.9% conversion with a number-average chain length of 1000.

13.4.3 Transition Metal Catalysis

Ziegler–Natta catalysis enabled the polymerization of propylene and has subsequently come into wide use for the polymerization of olefins and dienes. The classic Ziegler–Natta catalyst is $TiCl_3$ plus $Al(C_2H3)_3$, but there are variants that use other transition metals such as chromium and nickel. Polymerization is believed to occur by the repeated insertion of a double bond from the monomer into a previously formed metal-to-carbon bond. The homogeneous form, where the polymerization occurs in a solvent for the polymer, gives linear polyethylene (HDPE) of low polydispersity, PD ≈ 2. Heterogeneous forms are used for gas phase polymerization in a fluidized-bed reactor. The catalyst is typically supported on $MgCl_2$ and is introduced into the bed as a fine powder. These supported catalysts give high yields, high activities, and high stereospecificity for polypropylene but give polymer of undesirably high polydispersity, PD > 10. It is believed that the catalyst remains active and that chain transfer to monomer or to hydrogen controls the molecular weight. The PD is attributed to large site-to-site variations in activity.

More recent inventions are the metallocene catalysts based on zirconium. They offer more uniform catalyst activity and can give a relatively narrow molecular weight distribution. More importantly, they offer better control over structure and copolymer composition distributions. There has been a fantastic flurry of research of metallocenes with over 20,000 literature publications.

The chemical mechanisms of transition metal catalysis are complex. The dominant kinetic steps are propagation and chain transfer. There is no termination step for the polymer chains, but the catalytic sites can be activated and deactivated. The expected form for the propagation rate is

$$\mathscr{R}_p = k_p IM$$

where I is the concentration of active sites. All the catalytic sites are presumed active for homogeneous catalysis. However, cocatalysts such as $Al(C_2H_3)_3$ or methylaluminoxane (MAO) are required for the reaction to proceed, and their presence or absence will affect the value of I. Mass transfer limitations can arise in supported systems because the catalytic sites become buried under a deposited film of polymer. Monomer solubility and diffusion in the polymer are included in some models of polymerization kinetics. A segregated model that follows the course of individual active sites is needed for gas-to-solid heterogeneous polymerizations.

13.4.4 Vinyl Copolymerizations

Vinyl monomers are often copolymerized with free-radical or coordination metal catalysis but occasionally by other mechanisms. Random copolymers are important items of commerce. The two monomers are present together in the reaction mixture and copolymerize to give more-or-less random arrangements of the monomers along the polymer chain.

Consider the polymerization of two vinyl monomers denoted by X and Y. Each propagation reaction can add either an X or a Y to the growing polymer chain, and

it is unrealistic to assume that the monomers have equal reactivities. Furthermore, reaction probabilities can depend on the composition of the polymer chain already formed. We suppose they depend only on the last member added to the chain. The growing chain to which an X-mer was last added is denoted as IX_n, and I denotes the catalytic site. There are four propagation reactions to consider:

$$\begin{aligned}
IX_n + X &\xrightarrow{k_{XX}} IX_{n+1} \qquad \mathscr{R} = k_{XX}[IX_n]x \\
IX_n + Y &\xrightarrow{k_{XY}} IY_{n+1} \qquad \mathscr{R} = k_{XY}[IX_n]y \\
IY_n + X &\xrightarrow{k_{YX}} IX_{n+1} \qquad \mathscr{R} = k_{YX}[IY_n]x \\
IY_n + Y &\xrightarrow{k_{YY}} IY_{n+1} \qquad \mathscr{R} = k_{YY}[IY_n]y
\end{aligned}$$

The initiation and termination steps may also come in several varieties, but they will have little effect on overall chain composition provided the chains are long. The monomer consumption rates are

$$\begin{aligned}
\mathscr{R}_X &= -k_{XX}[IX_n]x - k_{YX}[IX_n]x \\
\mathscr{R}_Y &= -k_{XY}[IX_n]y - k_{YY}[IY_n]y
\end{aligned}$$

The ratio of these propagation rates is the ratio in which the two monomers are incorporated into the polymer:

$$\frac{x_p}{y_p} = \frac{k_{XX}[IX_n]x + k_{YX}[IY_n]x}{k_{XY}[IX_n]y + k_{YY}[IY_n]y} = \frac{x}{y}\left[\frac{k_{XX}[IX_n] + k_{YX}[IY_n]}{k_{XY}[IX_n] + k_{YY}[IY_n]}\right]$$

This result can be simplified considerably by observing that, except for end effects, the number of transitions from X to Y along the polymer chain (i.e., structures like –XY–) must equal the number of transitions from Y to X (i.e., structures like –YX–). This requires that

$$k_{XY}[IX_n]y = k_{YX}[IY_n]x$$

Substitution gives the promised simplification:

$$\frac{x_p}{y_p} = \frac{x}{y}\left[\frac{r_X x + y}{x + r_Y y}\right] \tag{13.41}$$

where $r_X = k_{XX}/k_{XY}$ and $r_Y = k_{YY}/k_{YX}$ are known as ***copolymer reactivity ratios***. The quantity x_p/y_p is the instantaneous ratio at which the two monomers are being incorporated into the polymer. It is usually different than the ratio of the monomers themselves, x/y. If $r_X > 1$, monomer X tends to homopolymerize so that sequences like –XX– will be favored. If $r_X < 1$, copolymerization is preferred, and sequences like –XY– will be common. Copolymer reactivity ratios are measured by measuring the polymer compositions that result from polymerizations run at low conversion. Extensive compilations are available in the literature. Reactivity ratios are largely independent of temperature since they are ratios of rate constants having similar activation energies. They are heavily dependent on the polymerization mechanism. Finding new catalysts that give desired values for r_X and r_Y is an active area of industrial research.

EXAMPLE 13.6

The following data were obtained using low conversion batch experiments on the bulk (solvent-free), free-radical copolymerization of styrene (X) and acrylonitrile (Y). Determine the copolymer reactivity ratios for this polymerization.

Mole Percent Styrene in Monomer Mixture	x/y	x_p/y_p	Mole Percent Styrene in Instantaneous Polymer
50	1.00	1.36	0.576
60	1.50	1.58	0.613
70	2.33	1.93	0.659
80	4.00	2.61	0.723
90	9.00	4.66	0.823

SOLUTION: The conversion is low so that the polymer composition is given by Equation 13.41 with the monomer concentrations at their initial values. There are five data and only two unknowns, so that nonlinear regression is appropriate. The sum-of-squares to be minimized is

$$\text{SS} = \sum_{i=1}^{5} \left(\frac{(x_p)_i}{(y_p)_i} - \frac{x_i}{y_i} \left[\frac{r_X x_i + y_i}{x_i + r_Y y_i} \right] \right)^2$$

Quantities with the subscript i are experimental data. Values for r_X and r_Y are determined using any convenient minimization technique. See Appendix 6.1.

The results are $r_X = 0.41$ and $r_Y = 0.04$.

In a batch reactor, the relative monomer concentrations will change with time because the two monomers react at different rates. For polymerizations with a short chain life, the change in monomer concentration results in a ***copolymer composition distribution*** where polymer molecules formed early in the batch will have a different composition from molecules formed late in the batch. For living polymers, the drift in monomer composition causes a corresponding change down the growing chain. This phenomenon can be used advantageously to produce ***tapered block copolymers.***

When uniform copolymers are desired, polymerization is best done in a CSTR. A semibatch polymerization with the more reactive monomer being added to the system continuously is also possible. There is also a special, happenstance case where the monomer and polymer compositions are equal:

$$\frac{x_p}{y_p} = \frac{x}{y} \quad \text{if} \quad \left[\frac{r_X x + y}{x + r_Y y} \right] = 1 \tag{13.42}$$

Equation 13.42 gives the condition that a ***copolymer azeotrope*** exists. The azeotropic composition is

$$\left[\frac{x}{y} \right]_{\text{azeotrope}} = \left[\frac{1 - r_Y}{1 - r_X} \right] \tag{13.43}$$

which implies either both $r_X > 1$ and $r_Y > 1$ or both $r_X < 1$ and $r_Y < 1$. The situation with $r_X < 1$ and $r_Y < 1$ is the more common. The styrene/acrylonitrile system with $r_X = 0.41$ and $r_Y = 0.04$ has an azeotrope at 62 mol % (76 w %) styrene. Commercial polymer is manufactured with this composition. The narrow composition distribution gives superior color and clarity.

EXAMPLE 13.7

A 50/50 (molar) mixture of styrene and acrylonitrile is batch polymerized by free-radical kinetics until 80 % molar conversion of the monomers is achieved. Determine the copolymer composition distribution.

SOLUTION: **T**he solution to this problem does not require knowledge of the polymerization rate but only that polymerization somehow occurs to the specified extent. Suppose a small amount, *dx*, of monomer X is polymerized. The corresponding amount, *dy*, of monomer Y that copolymerizes is given by Equation 13.41. For a batch reaction,

$$\frac{dx}{dy} = \frac{x}{y}\left[\frac{r_X x + y}{x + r_Y y}\right] \tag{13.44}$$

This equation can be integrated analytically, but a numerical solution is simpler. Set $x_0 = y_0 = 0.5$. Take small steps, Δy, and calculate the corresponding values for Δx until $x + y = 0.2$. Some results are as follows:

Moles of Monomer Remaining	Mole Fraction of Styrene in Monomer	Instantaneous Mole Fraction of Styrene in Polymer	Cumulative Mole Fraction of Styrene in Polymer
1.0000	0.5000	0.5755	0.5755
0.8	0.4818	0.5698	0.5728
0.6	0.4538	0.5612	0.5693
0.4	0.4033	0.5467	0.5644
0.2	0.2743	0.5109	0.5564

This is a free-radical polymerization with short chain lives. The first molecules formed contain nearly 58 mol % styrene when there is only 50% styrene in the monomer mixture. The relative enrichment of styrene in the polymer depletes the concentration in the monomer, and both the polymer and monomer concentrations drift lower as polymerization proceeds. If the reaction went to completion, the last 5% or so of the polymer would be substantially pure polyacrylonitrile.

The change in polymer composition as a result of monomer drift gives a ***macroscopic composition distribution***. It can be eliminated by polymerizing at the azeotrope, by polymerizing to low conversion, by continuously adding the more reactive monomer in a semibatch reactor, or by polymerizing in a CSTR, the last method

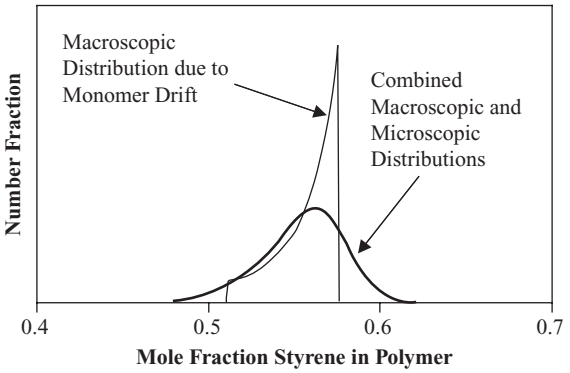

Figure 13.6 Copolymer composition distribution resulting from the batch polymerization of styrene and acrylonitrile.

usually preferred for polymers with short chain lives. There is also a ***microscopic composition distribution*** due to statistical fluctuations at the molecular level. Two molecules formed from the same monomer mixture will not have the same sequence down the chain or exactly the same overall composition. The microscopic distribution follows binomial (coin-tossing) statistics and will exist even if the polymer is manufactured at an azeotrope. Simulations using random numbers can determine the microscopic composition. To simulate a macroscopically uniform sample that contain 60 mol % X and 40 mol % Y on average, flip a coin with a 60/40 bias $\bar{l}_N$ times. Do this for enough molecules that the statistics become clear. Figure 13.6 shows the combined macroscopic and microscopic distributions for the batch polymerization of Example 13.7.

Sequence length distributions are occasionally important. They measure the occurrences of structures like –YXY–, –YXXY–, and –YXXXY– in a random copolymer. They can be calculated from the reactivity ratios and the polymer composition. See, for example, Ham (1964). They can be measured by ^{13}C NMR.

The copolymerization theory presented here assumes that the reactivity of a growing chain depends on the last mer added to the chain. Chemical theorists point out that there can be ***penultimate effects*** where reactivity depends on the next to the last (penultimate) mer as well as the last (ultimate) mer. Thus –XX would behave differently than –YX. This is undoubtedly true, but the extra complexity seldom seems unjustified from a reaction engineering viewpoint.

13.5 POLYMERIZATION REACTORS

The properties of a polymer depend not only on its gross chemical composition but also on its MWD, copolymer composition distribution, branch length distribution, and so on. The same monomer(s) can be converted to widely differing polymers depending on the polymerization mechanism and reactor type. This is an example of ***product by process,*** and no single product is best for all applications. Thus there

Table 13.5 Classification of Polymerization Reactions

Continuous Phase	Dispersed Phase	Type of Polymerization	Example Systems
Polymer dissolved in monomer	None	Homogeneous bulk polymerization	Poly(methyl methacrylate) in methyl methacrylate monomer
Polymer dissolved in solvent	None	Homogeneous solution polymerization	Polymerization of high-density polyethylene in hexane
Polymer in solution	Any (e.g., a condensation product or another polymer phase)	Heterogeneous bulk or solution polymerization	Salt precipitating from condensation reaction Prepolymerized rubber precipitating from styrene solution as polystyrene is formed
Water or other nonsolvent	Polymer or polymer in solution	Suspension, dispersion, or emulsion polymerization	Emulsion polymerization of rubber latex Suspension polymerization of expandable polystyrene
Liquid monomer	Polymer swollen with monomer	Precipitation or slurry polymerization	Polypropylene dispersed in liquid propylene
Gaseous monomer	Polymer	Gas phase polymerization	Fluidized-bed process for high-density polyethylene

are several commercial varieties each of polyethylene, polystyrene, and polyvinyl chloride that are made by distinctly different processes.

Table 13.5 classifies polymerization reactions by the number and type of phases involved in the reaction. The most important consideration is whether the continuous phase contains a significant concentration of high-molecular-weight polymer. When it does, the reactor design must accommodate the high viscosities and low diffusivities typical of concentrated polymer solutions. It is the design of reactors for operation with a continuous polymer phase that most distinguishes polymer reaction engineering from ordinary chemical reaction engineering. When the polymer-rich phase is dispersed, the chemical kinetics and mass transfer steps may be very complex, but the qualitative aspects of the design resemble those of the heterogeneous reactors treated in Chapter 11.

A polymerization reactor will be heterogeneous whenever the polymer is insoluble in the mixture from which it was formed. This is a fairly common situation and gives rise to the precipitation, slurry, and gas phase polymerizations listed in Table 13.5. If the polymer is soluble in its own monomers, a dispersed-phase polymerization requires the addition of a nonsolvent (typically water) together with appropriate interfacial agents. These extraneous materials require additional downstream purification and separation and may compromise product quality. ***Bulk polymerizations*** from pure, undiluted monomer are nominally preferred, although the use of a solvent to ease processing problems is quite common. For high-volume polymers, like high-volume chemicals, continuous operation is generally preferred over batch.

13.5.1 Stirred Tanks with a Continuous Polymer Phase

Continuous flow, stirred tank reactors are widely used for free-radical polymerizations. They have two main advantages: The solvent or monomer can be boiled to remove the heat of polymerization, and fairly narrow molecular weight and copolymer composition distributions can be achieved. Using a cold feed stream is also a suitable way to control temperature. Stirred tanks or functionally equivalent loop reactors are used for the transition metal polymerization of olefins and dienes when the catalyst is homogeneous. The CSTRs are used for the low-molecular-weight portions of condensation polymerizations when the stoichiometry requirements are not severe. The principal disadvantage of CSTRs is that high conversions are difficult to achieve. They suffer from the usual problem of low average reaction rate. A second problem at high conversion is that the viscosity can be several orders of magnitude higher than the design limit for stirred tanks. Some practical designs use stirred tanks up to about 75% conversion with further polymerization in a tubular reactor.

Molecular Weight Distributions

CSTRs produce the narrowest possible MWDs for fast-chain-growth, short-chain lifetime polymerizations like free-radical and coordination metal catalysis. The mean residence time in the CSTR will be minutes to hours, and the chain lifetimes are fractions of a second. Any chain that initiates in the CSTR will finish its growth there. All the polymer molecules are under identical, well-mixed conditions and will have as narrow an MWD (typically PD $\approx$ 2) as is possible for the given kinetic scheme.

Condensation polymers and living addition polymers continue to grow throughout their stay in the reactor. All the chains in a CSTR grow in the same reaction environment and, subject to the equal-reactivity assumption, grow at the same rate. The chain lengths at the reactor outlet will be proportional to the time spent in the reactor since initiation. As discussed in Chapter 15, the reaction times in a CSTR have an exponential distribution. This gives an exponential distribution of chain lengths.

The most probable distribution approximates an exponential distribution whenever $\bar{l}_N$ is reasonably long. The polydispersity of a condensation polymer made in a CSTR will be approximately 2, as it is in a batch reactor. The same argument applies to a living polymer. It will also emerge from a CSTR with a PD of 2, dramatically different from the narrow molecular weight distribution possible for a living polymer in a batch reactor. CSTRs cannot be used to produce block copolymers or homopolymers with narrow molecular weight distributions. They can be used for most other polymers of commercial utility. For heterogeneous polymerizations with a suspended catalyst, they will not eliminate the problem in site-to-site variations in activity but will produce as narrow an MWD as is possible for the catalyst.

EXAMPLE 13.8

Apply the method of moments to an anionic polymerization in a CSTR.

SOLUTION: Assume that initiation occurs instantly as fresh monomer enters the reactor. A monomer balance for the CSTR gives

$$M_0 - I_0 - k\bar{t}MI_0 \sum_{i=1}^{\infty} c_i = M$$

or

$$M = \frac{M_0 - I_0}{1 + k_p \bar{t} I_0} \tag{13.45}$$

A balance on polymer of length l gives an infinite set of algebraic equations:

$$k_p \bar{t} c_{l-1} M - k_p \bar{t} c_l M = c_l$$

Sum these equations from $l = 1$ to $l = \infty$ to obtain

$$\mu_0 = I_0$$

Multiply them by l and l^2 and use the methods of Section 13.3.2 to obtain

$$\bar{l}_N = \nu' + 1 \tag{13.46}$$

$$\bar{l}_W = \frac{2(\nu')^2 + 3\nu' + 1}{\nu' + 1} \tag{13.47}$$

where $\nu' = k_p M \bar{t}$. Divide $\bar{l}_W$ by $\bar{l}_N$ and take the limit as $\nu' \to \infty$ to show that PD $\to 2$ in the limit of high molecular weight.

An isothermal batch reactor produces a fairly narrow MWD except possibly at high conversions. Conditions will vary from the start to the end of a batch reaction, and the MWD will broaden. The dynamic chain length of a free-radical polymer will because of changes in monomer concentration and initiation rate, although usually not by much when measured by the cumulative $\bar{l}_N$ and $\bar{l}_W$ of the finished polymer. When the catalyst is heterogeneous, an isothermal batch reactor will produce

approximately the same result as for a CSTR except possibly at high conversions. Of course, maintaining isothermal operation may not be easy.

Heat Transfer

Heat removal is the major issue for vinyl addition polymerizations, and CSTRs are well suited for this application. The homogeneous nucleation possible with heat transfer by boiling allows easy scaleup at nearly isothermal conditions. In very large vessels, a temperature difference between the top and the bottom will arise due to the static head, but this has not been found to cause operational difficulties. The actual removal of heat occurs in the overhead condenser. There is sometimes a concern about fouling the condenser with polymer, but this problem can usually be overcome by good design and is not a problem when the polymer is soluble in the condensing liquid. Boiling heat transfer is routinely used for addition polymerizations. Temperature control by precooling the feed is occasionally used. A CSTR is obviously suited for precooled feeds while a PFR is not. Sensible heat transfer through the vessel walls or internal coils can be used in small reactors. Loop reactors, where most of the reactor volume is in the heat exchangers, are preferred for large reactors.

Most condensation polymers have negligible heats of reaction. See Table 13.2. Heat must be supplied to evaporate byproducts such as water or ethylene glycol. An external heat exchanger is the best method for heating large reactors. Flashing the recycle stream as it enters the vessel also aids in removing the condensation by-product.

Copolymerizations

The uniform chemical environment of a CSTR makes it ideally suited for the production of copolymers. If the assumption of perfect mixing is justified, there will be no macroscopic composition distribution due to monomer drift, but the mixing time must remain short upon scaleup. See Sections 1.5 and 4.4. A real stirred tank or loop reactor will more closely approach perfect mixing when the circulation rate is high. The narrowing of the macroscopic composition distribution as a function of circulation rate can be modeled. When the macroscopic distribution becomes commensurate in breadth to the microscopic distribution, further inputs of power are unwarranted.

Laminar flow is almost inevitable in a polymer reactor when the polymer phase is continuous. Molecular diffusivities are also low. This combination suggests that segregation is a possibility in a stirred tank reactor. See Chapter 15. A segregated stirred tank gives broader MWDs, higher conversions, and broader copolymer composition distributions than a CSTR that has good internal mixing. Given the appropriate rate expressions, calculations are quite feasible for the limiting cases of complete segregation and perfect mixing. These tend to be alarming since the copolymer composition distribution in a completely segregated CSTR will be even broader that that for a batch reactor. Fortunately, there is little real evidence of segregation in industrial reactors. It seems that segregation is an academic concept with little practical relevance.

13.5.2 Tubular Reactors with a Continuous Polymer Phase

Web-coating polymerizations (e.g., used for photographic film and coated abrasives) achieve a piston flow reaction environment. Mechanically driven screw devices used as finishing reactors for PET closely approximate piston flow. Motionless mixers can as well. However, polymer reactors that closely approximate piston flow are the exception.

Tubular reactors are occasionally used for bulk, continuous polymerizations. A monomer or monomer mixture is introduced at one end of the tube and, if all goes well, a high-molecular-weight polymer emerges at the other. The classic example is the high-pressure polymerization of ethylene in a single tube approximately 1.75 in. in diameter and several miles long. Scaleup is done by adding another mile to the tube length. Some polystyrene plants use single-tube or shell-and-tube reactors as finishing reactors after the bulk of the polymer has been made. These commercial examples skirt three types of instability that can arise in tubular polymerizers:

Velocity profile elongation — Low fluid velocities near the tube wall give rise to high extents of polymerization, high viscosities, and yet lower velocities. The velocity profile elongates, possibly to the point of hydrodynamic instability.

Thermal runaway — Temperature control in a tubular polymerizer depends on convective diffusion of heat. This becomes difficult in a large-diameter tube, and temperatures may rise to a point where a thermal runaway becomes inevitable.

Tube-to-tube interactions — The problems of velocity profile elongation and thermal runaway can be eliminated by using a multitubular reactor with many small-diameter tubes in parallel. Unfortunately, this introduces another form of instability. Tubes may plug with polymer that cannot be displaced using the low-viscosity inlet fluid. Imagine a 1000-tube reactor with 999 plugged tubes!

Reacting to low conversions avoids most problems. The polyethylene example uses a single, small-diameter tube. This avoids thermal runaway and mitigates the velocity elongation problem. The polystyrene reactor avoids the multitubular stability problem by using a substantially polymerized, high-viscosity feed.

Figure 13.7 illustrates stability regimes for the thermally initiated polymerization of styrene for laminar flow in a single tube. Design and operating variables are the physical dimensions of the tube, the operating temperatures and pressures, and the flow rate. The aspect ratio L/R is unimportant provided it is reasonably large, and the operating pressure is unimportant unless it is so high that liquid compressibility becomes significant. Steady-state operation can be described by four variables: T_{in}, T_{wall}, R, and $\bar{t}$. Figure 13.7 shows the influence of two of these with the other two held constant at plausible values. Stable operation is easy to achieve in a capillary tube because mass and thermal diffusion removes gradients in the radial direction. Thus the viscosity is uniform across the tube, and no hot spots develop. As the tube

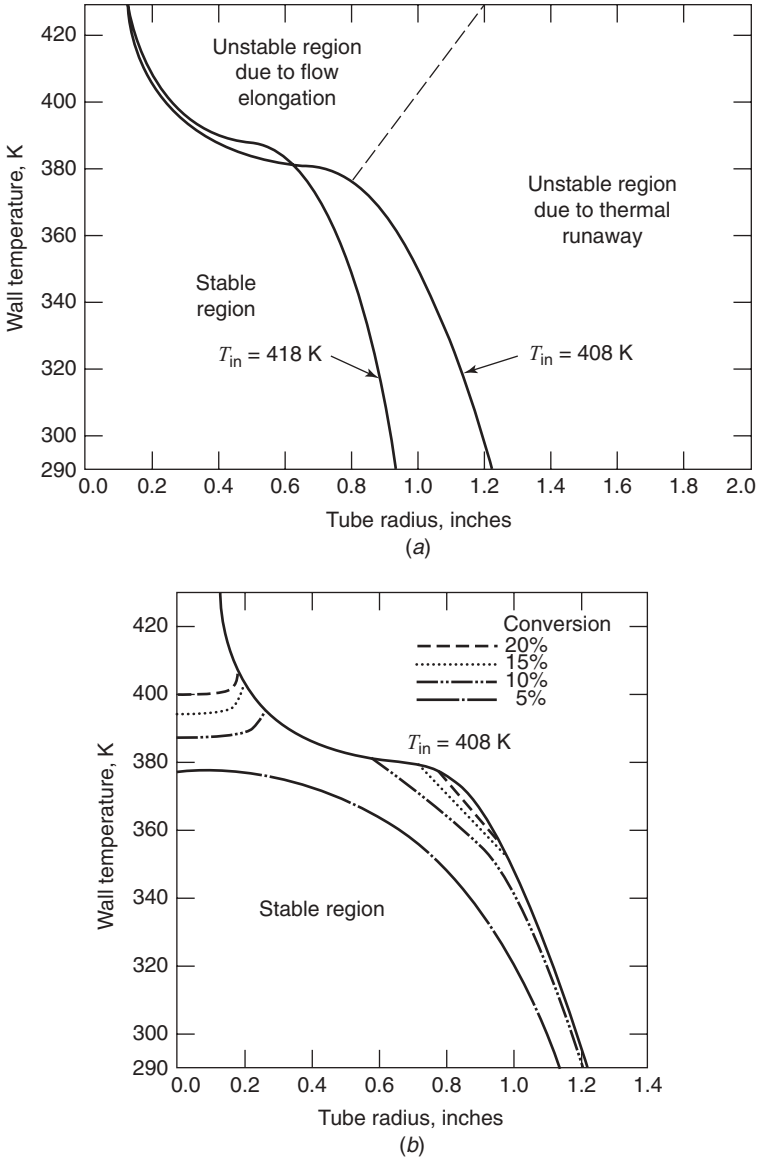

Figure 13.7 Performance of a laminar flow, tubular reactor for the bulk polymerization of styrene with $T_m = 135°$ K and $\bar{t} = 1\ h$: (*a*) stability regions; (*b*) monomer conversion in stable region.

diameter is increased, mass and heat transfer become progressively more difficult. The mass diffusivity is several orders of magnitude lower than the thermal diffusivity; concentration gradients develop before thermal gradients; and velocity profile elongation emerges as the first limit on conversion. In still larger tubes, operation is limited by thermal stability. For the polystyrene example of Figure 13.7, a thermal

runaway is predicted if the tube radius exceeds 1.25 in. This is true even if the tube wall were held at 0 K (pretending the model remains valid).

The polystyrene example in Figure 13.7 incorporates a detailed kinetic model of the polymerization. The model uses a reasonably sophisticated description of viscosity as a function of temperature, polymer concentration, and molecular weight. The convective diffusion equations for mass and heat are solved together with the effects of viscosity on the velocity profile. Assembling such a model requires weeks of effort. The following examples are simpler but illustrate design methodology for tubular polymerizers. We begin with a lumped-parameter model for the polymerization of styrene.

EXAMPLE 13.9

Illustrate temperature and molecular weight changes in a tubular reactor by constructing a lumped-parameter model of styrene polymerization in a tube.

SOLUTION: The model ignores radial gradients and assumes a flat velocity profile in a tube of constant cross section. The $a(d\bar{u}/dz)$ term in Equation 3.5 is ignored even though density varies with the extent of polymerization. Thus,

$$\bar{u}(z)\frac{dm}{dz} = -\mathscr{R}_p$$

The energy balance is

$$\frac{dT}{dz} = \frac{-\Delta H_R \mathscr{R}_p}{\bar{u}\rho C_P} - \frac{2U}{\bar{u}\rho C_P R}(T - T_{\text{ext}})$$

The inside heat transfer coefficient is controlling, as is calculated from

$$\frac{hD}{k_T} = 1.86\,\mathbf{Gz}^{1/3}\left(\frac{\mu_{\text{bulk}}}{\mu_{\text{wall}}}\right)^{0.14}$$

Cumulative values for the chain lengths are calculated as a function of position down the tube using differential forms for Equations 13.14 and 13.15:

$$(\bar{l}_N)_{\text{new}} = \frac{w + dw}{w/(\bar{l}_N)_{\text{old}} + dw/(\bar{l}_N)_{\text{instant}}} \tag{13.48a}$$

$$(\bar{l}_W)_{\text{new}} = \frac{w(\bar{l}_W)_{\text{old}} + dw(\bar{l}_W)_{\text{instant}}}{w + dw} \tag{13.48b}$$

where w is the weight of polymer.

The propagation rate and instantaneous chain lengths are calculated using the model of Hui and Hamielec (1972). The viscosity correlation is due to Kim and Nauman (1992). Despite the simplification to piston flow, predictions of the model are in good agreement with experimental results for the shell-and-tube postreactor used in some polystyrene processes. The effluent from a train of polymerization reactors is a solution of 70% polystyrene ("70% solids" in the jargon of the polymer industry) in a mixture of unreacted styrene and diluent ethyl benzene. A multistage flash is used to remove the solvents. Devolatilization begins by preheating the reactor effluent to 250°C in a shell-and-tube heat exchanger. Table 13.6 shows results for a preheater that was designed in the 1960s but continues to be used today. Physical properties, design parameters, and the kinetic model are included in Code for Example 13.9.

Table 13.6 Model Predictions for Polystyrene Preheater

z	Styrene	Polymer	$\bar{l}_N$	$\bar{l}_W$	PD	°C
0.00	0.240	0.700	960	2016	2.10	170.0
0.30	0.229	0.711	954	2006	2.10	186.9
0.60	0.211	0.729	933	1981	2.12	202.2
0.90	0.186	0.754	888	1941	2.19	216.5
1.20	0.158	0.782	821	1891	2.30	229.5
1.50	0.131	0.809	750	1841	2.46	240.0
1.80	0.108	0.832	689	1800	2.61	247.6
2.10	0.090	0.850	643	1769	2.75	252.4
2.40	0.077	0.863	611	1746	2.86	255.0
2.70	0.067	0.873	589	1729	2.94	256.2
3.00	0.059	0.881	573	1717	3.00	256.4
3.30	0.053	0.887	562	1707	3.04	256.1
3.60	0.049	0.891	553	1700	3.07	255.3

The results in Table 13.6 represent a design error. It appears that the original designers ignored the heat of polymerization. The tubes are twice as long as necessary for the original production rate. This leads to polymerization at relatively high temperatures, a significant loss in molecular weight, and an increase in polydispersity. Modern plants can still use this design because production rates are much higher, but smaller diameter tubes are desirable.

Code for Example 13.9

```
Sub Example13_9()

'Physical Properties of Entering Fluid in SI Units
MWSty = 104.15
Cp = 1880#
HeatReact = 670000#
ThermCond = 0.126
CummLn = 960              'Inlet number average chain length
PD = 2.1                  'Inlet polydispersity
CummLw = PD * CummLn
WPoly = 0.7               'Inlet polystyrene content
Wdil = 0.06               'Inlet ethylbenzene content
WSty = 1 - WPoly - Wdil   'Inlet styrene content

'Design and Operating Variables in SI Units but Temperature in C
TubeDia = 0.027
TubeLength = 3.6
PrintInterval = 0.3    'Output results at these length increments
Qmass = 5 / 3600
TcIn = 170
TcWall = 240
Twall = TcWall + 273.15
T = TcIn + 273.15
```

```
' Initialization
ip = 1                      'Output counter
dtime = 0.25                'Time step
z = 0
GoSub Caption      'Prints Excel Column Headers

'  Main Loop
Do

   RhoSty = 924 - 0.918 * Tc      'Density of styrene (same for ethylbenzene)
   RhoPoly = 1084 - 0.605 * Tc    'Density of polystyrene
   RhoMix = WPoly * RhoPoly + (1 - WPoly) * RhoSty
   Sty = RhoMix * WSty
   GoSub Kinetics

   dWSty = (-RP - RD - RT + RU) * dtime / RhoMix
   dWPoly = RP * dtime / RhoMix
   NumMoles = WPoly / CummLn + dWPoly / Ln
   CummLn = (WPoly + dWPoly) / NumMoles
   CummLw = (WPoly * CummLw + dWPoly * Lw) / (WPoly + dWPoly)

   WPoly = WPoly + dWPoly
   WSty = WSty + dWSty
   Tv = Twall
   GoSub Viscosity
   ViscWall = Visc
   Tv = T
   GoSub Viscosity
   Velocity = Qmass / RhoMix / (3.14159 * TubeDia * TubeDia / 4)
   Re = RhoMix * TubeDia * Velocity / Visc
   Pr = Cp * Visc / ThermCond
   U = (Re * Pr * TubeDia / TubeLength) ^ (1 / 3) * (Visc / ViscWall) ^ 0.14
   U = U * ThermCond / TubeDia * 1.86
   dT = (HeatReact * RP + 4 / TubeDia * (Twall - T) * U) / RhoMix / Cp * dtime
   T = T + dT
   Tc = T - 273.16
   Time = Time + dtime
   z = z + Velocity * dtime

   If Int(z / PrintInterval) >= ip Then  'Controls output interval
      ip = ip + 1
      GoSub Output
      If z >= TubeLength Then Exit Sub
   End If

Loop While z < TubeLength
ip = ip + 1
GoSub Output

Exit Sub
```

(*continued*)

Code for Example 13.9 (*continued*)

```
Kinetics:  'Kinetics subroutine, all variables shared with main
   Kp = 100900# * Exp(-3557 / T)
   A1 = 2.57 - 0.00505 * T
   A2 = 9.56 - 0.0176 * T
   A3 = -3.03 + 0.00785 * T
   Ft = Exp(-2 * (A1 * WPoly + A2 * WPoly ^ 2 + A3 * WPoly ^ 3))
   Kt = 12050000# * Exp(-844 / T) * Ft
   KFM = 22180# * Exp(-6377 / T)
   KI = 20.19 * Exp(-13810 / T)
   B1 = -0.0985 + 0.000777 * T - 0.00000204 * T * T + 0.00000000179 * T ^ 3
   CM = KFM / Kp + B1 * WPoly
   RP = Kp * (2 * KI * Sty ^ 3 / Kt) ^ 0.5 * Sty
   Beta = Kt * RP / Kp / Kp / Sty ^ 2
   Ln = (CM + Beta + 1) / (CM + Beta / 2)
   Lw = (2 * CM + 3 * Beta) / (CM + Beta) ^ 2
Return

Viscosity:  'Viscosity Subroutine.  All variables are shared with main.
   V = (3.915 * WPolyt - 5.437 * WPoly * 2 + (0.623 + 1387 / Tv) * WPoly ^ 3)
   V = (CummLw * MWSty) ^ 0.18 * V
   Visc = Exp(-13.04 + 2013 / Tv + V)
Return

Output:  'Outputs Results to Excel Cells
   Cells(ip, 2) = z
   Cells(ip, 3) = WSty
   Cells(ip, 4) = WPoly
   Cells(ip, 5) = CummLn
   Cells(ip, 6) = CummLw
   Cells(ip, 7) = CummLw / CummLn
   Cells(ip, 8) = Tc
Return

Caption:  'Prints Column Headers
   Cells(1, 2) = "Length"
   Cells(1, 3) = "WSty"
   Cells(1, 4) = "WPoly"
   Cells(1, 5) = "CummLn"
   Cells(1, 6) = "CummLw"
   Cells(1, 7) = "PD"
   Cells(1, 8) = "Temp"
Return

End Sub
```

The piston flow model of Example 13.9 happens to give good predictions for the thermal runaway of a polymerization starting with pure styrene. Results are shown in Figure 13.8 and are in surprisingly good agreement with those of the more rigorous distributed-parameter model used for Figure 13.7. The predicted runaway at a tube diameter of 0.061 m is similar to that shown in Figure 13.7. The lumped-parameter

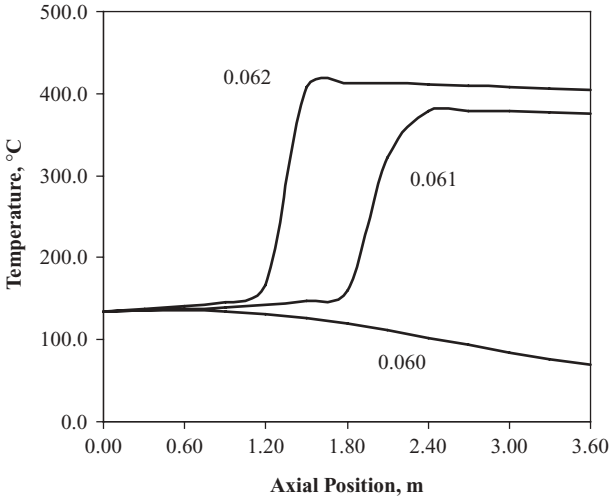

Figure 13.8 Temperature profiles using a simplified model of a tubular reactor with pure styrene feed, $T_{\text{in}} = 135°\text{C}$ and $T_{\text{wall}} = 20°\text{C}$. The parameter is the tube diameter in meters.

model of Example 13.9 takes no account of hydrodynamics and predicts stable operation in regions where the velocity profile is elongated to the point of instability. It also overestimates conversion in the stable regions. The next example illustrates the computations that are needed to include hydrodynamics in a tubular reactor calculation. The methodology follows that in Section 8.4.

EXAMPLE 13.10

Model the performance of a laminar flow, tubular reactor for the polymerization of a self-condensing monomer. Assume second-order kinetics based on end-group concentrations with $a_{\text{in}}k\bar{t} = 1$ and a negligible heat of reaction. Ignore any condensation product. Assume density is constant and viscosity varies with conversion as $\mu = \mu_0(100 - 99a/a_{\text{in}})$, where a is the concentration of remaining end groups. Assume that an average value for the diffusion group, $\mathscr{D}_A\bar{t}/R^2 = 0.1$, applies to all end groups. Include the radial velocity term in the convective diffusion equation and plot streamlines in the reactor.

SOLUTION: The problem requires solution of the convective diffusion equation for mass but not for energy. Rewriting Equation 8.50 in dimensionless form gives

$$\mathscr{V}_z\frac{\partial a}{\partial \mathscr{Z}} + \left(\frac{L}{R}\right)\mathscr{V}_r\frac{\partial a}{\partial \mathscr{r}} = \frac{\mathscr{D}_A\bar{t}}{R^2}\left[\frac{1}{\mathscr{r}}\frac{\partial a}{\partial \mathscr{r}} + \frac{\partial^2 a}{\partial \mathscr{r}^2}\right] + \bar{t}\mathscr{R}_p \tag{13.49}$$

The polymerization rate is assumed to be second order with respect to the end-group concentration, $\mathscr{R}_p = ka^2$. The boundary conditions are a specified inlet concentration, zero flux at the wall, and symmetry at the centerline.

The dimensionless velocity component in the axial direction, $\mathscr{V}_z = V_z/\bar{u}$, is calculated using Equation 8.45. Note that $\bar{u} = \bar{u}_{\text{in}}$ when density and cross section are constant. The component in the radial direction, $(L/R)\mathscr{V}_r$, is calculated using a dimensionless

version of Equation 8.49:

$$\left(\frac{L}{R}\right)\mathcal{V}_r^{\circ} = \frac{-1}{\rho\tau}\int_0^{\tau} \tau_1 \frac{\partial(\rho\mathcal{V}_z^{\circ})}{\partial\mathcal{Z}} d\tau_1 \tag{13.50}$$

A first-order difference approximation for the axial derivative, $\partial(\rho\mathcal{V}_z^{\circ})/\partial\mathcal{Z}$, is consistent with the first-order convergence of Euler's method. The convected-mean concentration is calculated from the dimensionless version of Equation 8.5:

$$a_{\text{mix}}(\mathcal{Z}) = 2\int_0^1 a(\tau,\mathcal{Z})\mathcal{V}_z^{\circ}(\tau,\mathcal{Z})\tau d\tau \tag{13.51}$$

The streamlines are calculated using a dimensionless version of Equation 8.52 in which the density has been assumed constant:

$$\int_0^{\tau_{\text{in}}} \tau_1 \mathcal{V}_z^{\circ}(\tau_1, 0)\, d\tau_1 = \int_0^{\tau} \tau_1 \mathcal{V}_z^{\circ}(\tau_1, z)\, d\tau_1 \tag{13.52}$$

Values for τ_{in} are selected and the integral on the left-hand side of Equation 13.52 is evaluated. Evaluation of the right-hand side proceeds from $\tau = 0$ up to some value $\tau_1 = \tau$, where the value of the integral exactly matches the original value on the left-hand side. The streamline has moved from τ_{in} to τ .

The overall solution is based on the method of lines discussed in Chapter 8. The resulting ODEs can then be solved by any convenient method. Code for Example 13.10 uses Euler's method. Figure 13.9 shows the behavior of the streamlines. There is a rapid elongation at the reactor inlet followed by a slow return to the initial parabolic velocity profile as diffusion and continued reaction gradually reduce radial concentration gradients.

Systematic verification is needed for a program as complex as this. The following tests were made using Itotal = 64.

1. Turn off the reaction by setting RateConst = 0. The resulting final value for the mixing-cup average, AvgC, is 1, confirming the material balance.
2. Set the initial $Vz(i) = 1$ and turn off the updating. This gives piston flow. The calculated result for AvgC for a second-order reaction is 0.4998 versus 0.5 in theory.
3. Set the viscosity to a constant. Then the downstream velocity profile keeps the initial parabolic form and the streamlines are straight.
4. Set the viscosity to a constant, set DA = 0.00001 so that diffusion is negligible, and set Order = 1. Then the final value for AvgC is 0.4430 versus 0.4432 calculated in Example 8.2.
5. Delete the radial convection term but otherwise run the full simulation. This gives AvgC = 0.5284. Now add the radial term to get 0.5403.
6. Run the full simulation at various values for Itotal. Convergence is rapid, giving $a_{\text{out}}/a_{\text{in}} = 0.5403$.

A verification sequence like this helps in debugging and lends confidence to the final results. These tests verify that the model is working as expected. However, the streamline calculations are imprecise and need a smaller grid than is necessary for conversion calculations.

Code for Example 13.10

```
Public aold(256)
Sub Example13_10()
Dim Vz(256)
Dim Vr(256)
Dim FlowInt(256)   'Right-Hand side of Equation 13.52
Dim FlowInt0(256)  'Left-Hand side of Equation 13.52
Dim Stream(256)    'Radial position of streamline with initial position i*dr
Dim G1(256)        'Used to calculate Vz per Example 8.5
Dim anew(256)

Itotal = 64
dr = 1 / Itotal
DA = 0.1
RateConst = 1
Order = 2    'Reaction order
Ip = 1       'Used for output control

For I = 0 To Itotal  'Initial conditions
   aold(I) = 1
   Vz(I) = 2 * (1 - (I * dr) ^ 2)
Next

'Calculate the the left-hand side of Equation 13.52
Sum = 0
For I = 1 To Itotal
    Sum = Sum + I * dr * Vz(I) * dr
    FlowInt0(I) = Sum
Next
Do   'Start of main loop

    dz = dr * dr * Vz(Itotal - 1) / DA   'Stability criterion, refer to Equation 8.29
    If dz >0.001 Then dz = 0.001 'Set maximum dz to ensure accuracy or reaction stability
    If z + dz > 1 Then dz = 1 - z   'The last step goes exactly to the end of the reactor

    'Centerline concentration, refer to Equation 8.26
    a = DA * 4 / dr / dr / Vz(0)
    B = -a
    anew(0) = a * dz * aold(1) + (1 + B * dz) * aold(0)
    anew(0) = anew(0) - RateConst * aold(0) ^ Order * dz / Vz(0)

    'Interior concentrations, refer to Equation 8.25
    For I = 1 To Itotal - 1
        C1 = DA * 0.5 / I / dr / dr / Vz(I)
        C2 = DA / dr / dr / Vz(I)
        a = C1 + C2
        C = -C1 + C2
        B = -a - C
        anew(I) = a * dz * aold(I + 1) + (1 + B * dz) * aold(I) + C * dz * aold(I - 1)
        anew(I) = anew(I) - RateConst * aold(I) ^ Order * dz / Vz(I)
        ' Radial convection terms, refer to Equation 13.49
        anew(I) = anew(I) - Vr(I) / Vz(I) * (aold(I + 1) - aold(I - 1)) / 2 / dr * dz
    Next
```

(*continued*)

Code for Example 13.10 (*continued*)

```
    'Wall concentration, refer to Equation 8.24
    anew(Itotal) = (4 * anew(Itotal - 1) - anew(Itotal - 2)) / 3

    For I = 0 To Itotal
        aold(I) = anew(I)
    Next

    ' Calculate axial velocity component using the code of Example 8.8
    G1(Itotal) = 0
    For ii = 1 To Itotal
        I = Itotal - ii
        G1(I) = G1(I + 1) + dr ^ 2 * I / visc(I)
    Next
    G2 = 0

    For I = 1 To Itotal - 1
        G2 = G2 + I * dr * G1(I) * dr
    Next
   G2 = G2 + Itotal * dr * G1(Itotal) * dr / 2

    ' The new value for Vz is G1(i) / G2 /2 but calculate the
    ' radial component prior to updating Vz

    G3 = 0
    For I = 1 To Itotal
        G3 = G3 + I * dr * (G1(I) / G2 / 2 - Vz(I)) / dz * dr
        '  G3 is the integral in Equation 13.50
        Vr(I) = -G3 / I / dr
    Next I

    ' Update Vz
    Vz(0) = G1(0) / G2 / 2
    For I = 1 To Itotal
        Vz(I) = G1(I) / G2 / 2
    Next I  'The velocity calculations are complete for the current value of z

    'dz will be so small that outputing all values would be inconvenient
    'The code from here to the end of the main Do loop is skipped most of the time

    Ifprint = Ifprint + 1
    If Ifprint = 200 Then
       GoSub Output
       Ifprint = 1
    End If

    z = z + dz

Loop While z < 1

GoSub Output

Exit Sub

Output:
```

```
 Ip = Ip + 1       'Output will be to this row of cells

'  Calculate mixing cup average
AvgC = 0
avgV = 0
For I = 0 To Itotal
    AvgC = AvgC + anew(I) * Vz(I) * I * dr * dr  'Factor of 2Pi will cancel
    avgV = avgV + Vz(I) * I * dr * dr            'Factor of 2Pi will cancel
Next
AvgC = AvgC / avgV

'Begin streamline calculations by determining the right-hand side of Equation 13.52
   Sum = 0
   For I = 1 To Itotal
      Sum = Sum + I * dr * Vz(I) * dr
      FlowInt(I) = Sum
   Next

  ' Locate radial position of streamlines.  Use linear interpolation
  ' to smooth the results for display.
   For iii = 1 To 3
      ii = iii * Itotal / 4     'Will calculate streamlines initially at r = .25,
        0.5, 0.75
      For I = 1 To Itotal - 2
         If FlowInt0(ii) > FlowInt(I) Then
            del = (FlowInt(I + 1) - FlowInt(I))
            del = (FlowInt0(ii) - FlowInt(I)) / del
            Stream(ii) = (I + del) * dr
          End If
       Next
       Cells(Ip, 1) = z
       Cells(Ip, iii + 1) = Stream(ii)  'Position of streamline at axial location z
       Cells(Ip, 5) = AvgC              'Average concentration at axial location z
    Next iii
      Cells(1, 1) = 0      'Initial value of z
      Cells(1, 2) = 0.25   'Initial positions of the streamlines
      Cells(1, 3) = 0.5
      Cells(1, 4) = 0.75
      Cells(1, 5) = 1      'Initial average concentration
Return

End Sub
Function visc(ii)
     visc = 100 - 99 * aold(ii)
End Function
```

Example 13.10 treats an isothermal polymerization, but adding Equation 8.51 to include temperature dependence causes no special problems. Modern computers can easily solve small sets of simultaneous PDEs. Very large sets, say the 10,000 or so that are needed to describe individual species in a polymerization going to high molecular weight, are still expensive to solve. A key to easy computability in polymer

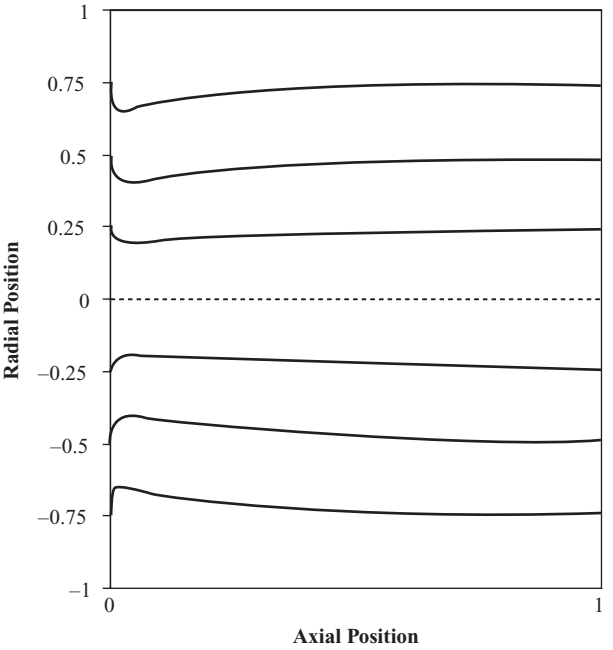

Figure 13.9 Curved streamlines resulting from polycondensation in the laminar flow reactor of Example 13.10.

reactor design is ***lumping,*** where various molecular species are combined and treated as a single entity. Example 13.10 uses the end-group concentration to form a single-lump containing all the molecules. Some models of polycondensations treat the first 20 or so oligomers exactly and then use one or more lumps to characterize the rest of the population. Models for chain growth polymers are mainly of the single-lump variety. A more sophisticated treatment is needed to account for the dependence of molecular diffusivity on chain length, but a satisfactory design methodology has not yet emerged. Lumping is not confined to polymerizations. Comprehensive models of oil refineries use lumping to reduce the number of tracked species from about 5000 to about 1000.

Extruders

Extruders are mechanical devices used to melt and pump polymers. We discuss them here in the context of tubular reactors because extruders resemble them in many ways and may indeed more closely approximate a PFR than an open tube. Chapter 16 in Paul et al. (2003) discusses extruders and other devices intended for mixing viscous liquids. Extruders are extremely expensive, provide very little volume for a chemical reaction, and are thus generally unsuited for polymerizations. They can be economically used for polymer modification reactions such as grafting. Although they

give a broad distribution of residence times, those fluid elements that move through the extruder the fastest also are the hottest. This is largely due to a phenomenon known as viscous dissipation where heat is generated by the shear imparted to the polymer. The coupling of short residence times with high temperatures provides a form of compensation and a relative uniform reaction environment. See the discussion of thermal time distributions in Section 15.4.3.

13.5.3 Suspending-Phase Polymerizations

Many polymerizations use a low-viscosity nonsolvent to suspend the polymer phase. Water is the most common suspending phase. Table 13.7 characterizes a variety of reaction mechanisms in which water is the continuous phase.

The reaction engineering aspects of these polymerizations are similar. Good heat transfer to a comparatively inviscid phase makes them suitable for vinyl addition polymerizations. Free-radical catalysis is mostly used, but cationic catalysis is used for nonaqueous dispersion polymerization (e.g., of isobutene). High conversions are generally possible, and the resulting polymer, either as a latex or as beads is directly suitable for some applications (e.g., paints, gel permeation chromatography beads, expanded polystyrene). Suspension polymerizations are run in the batch model. Continuous emulsion polymerization is common.

Emulsion Polymerization

Emulsion polymerization uses soaps and anionic surfactants to create two-phase systems having long-term stability. The key steps in a batch emulsion polymerization are the following:

- Water and emulsifier are charged to the reactor, and the emulsifier forms aggregates known as ***micelles***.
- One or more sparingly soluble monomers are charged to the reactor to form suspended drops. The monomer quickly saturates the aqueous phase.

Table 13.7 Classification of Polymerization Mechanisms that Use Water as the Continuous, Suspending Phase

Process Parameter	Polymerization Type Emulsion → Dispersion → Suspension
Stabilizer type	Soaps → inorganic salts
Agitation requirements	Low → high
Stability of dispersion	High → low
Particle size	0.2–200 μm
Purity of Polymer	Low → high

- A water-soluble, free-radical initiator is charged to the reactor and initiates polymerization in the water phase.
- A chain growing in water soon becomes insoluble. It separates from the aqueous phase and penetrates a micelle, forming a ***seed***. It may also add to an existing polymer particle.
- Mass transfer of monomer from the suspended drops through the aqueous phase to the seeded particles continues throughout the polymerization.
- The suspended drops of monomer are eventually depleted and polymerization stops.

There are many variations on this theme. Fed-batch and continuous emulsion polymerizations are common. Continuous polymerization in a CSTR is dynamically unstable when free emulsifier is present. Oscillations with periods of several hours will result but can be avoided by feeding the CSTR with seed particles made in a batch or tubular reactor.

Dispersion Polymerization

The suspending phase plays a more passive role in this form of polymerization. Dispersion polymerizations are typically batch processes with little or no mass transfer through the suspending phase. The monomer and initiator are charged to the reactor and react in a batch mode. Nonaqueous solvents are frequently used as the suspending phase. A great variety of surfactants are used, including polymers and block copolymers. The particle size of the polymer beads is generally a few micrometers, intermediate between those of emulsion and suspension polymerization. Agitation requirements are also intermediate. Through control of the surfactant type and concentration, monodispersed particles and core–shell structures can be made.

Suspension Polymerization

Water is the suspending phase. Inorganic salts and vigor agitation prevent coalescence and agglomeration. The reaction mode is batch. The largest use of suspension polymerization is for the manufacture of expandable polystyrene beads.

Gas Phase Polymerization

The fluidized-bed processes for polyolefins use gaseous monomers as the suspending phase. Finely ground catalyst particles containing a transition metal catalyst on a support such as $MgCl_2$ are fed continuously to the reactor. Polymerization occurs on the surface of the catalyst particle and the polymer ultimately encapsulates the particle. A cyclone separates the solid particles from unreacted monomer. The monomer is cooled and recycled. Temperature control is achieved by using cold monomer feed, by cooling the recycled monomer, and by heat transfer to the vessel walls. Fluidized-bed reactors are often modeled as being well mixed with respect to both phases. A typical residence time for the gas phase will be 20 s. That for the polymer will be a few hours.

Precipitation and Slurry Polymerization

Many polymers are insoluble in the reaction mixture from which they are formed. Upon significant polymerization, they precipitate to form a separate phase. The chemistry and reaction cycle must be managed to avoid agglomeration. Assuming this is possible, heat transfer is the major issue. Boiling of the suspending phase is used (e.g., when liquid propylene suspends polypropylene) and so is sensible heat transfer. Loop reactors may have most of their volume in the form of shell-and-tube heat exchangers. Reactor models normally assume CSTR behavior, although more detailed models are possible for loop reactors.

13.6 SCALEUP CONSIDERATIONS

The basic issues of scaleup are the same for polymer reactors as for ordinary chemical reactors. The primary problem is that the capacity for heat and mass transfer increases less rapidly than the reactor volume and throughput. The remedies are also similar, but the high viscosities characteristic of polymers cause special problems. These problems are most acute when the polymer phase is continuous.

13.6.1 Binary Polycondensations

End-point control is needed for binary polycondensations going to high molecular weight. The reaction must be stopped at the desired point and the polymer chains can be end-capped to prevent further polymerization. An example is the use of methyl chloride to endcap sodium-terminated chains. Classic mixing time problems arise in large tanks. Similar problems of stopping the reaction exist for batch vinyl polymerizations. Using multiple injection points for the chain stopper is a possibility. Stopping the polymerization with a quench and dilution with cold solvent is another.

Tubular reactors are used for some polycondensations. Para-blocked phenols can be reacted with formalin to form linear oligomers. When the same reactor is used with ordinary phenol, plugging will occur if the tube diameter is above a critical size even though the reaction stoichiometry is outside the region that causes gelation in a batch reactor. Polymer chains at the wall continue to receive formaldehyde by diffusion from the center of the tube and can crosslink. ***Local stoichiometry*** is not preserved when the reactants have different diffusion coefficients. See Section 2.8.

13.6.2 Self-Condensing Polycondensations

The removal of condensation byproducts becomes increasingly difficult upon scaleup. Some commercial PET processes use CSTRs for the early stages of the reaction where most of the byproduct ethylene glycol is removed. They use only the top, visible surface of the liquid for mass transfer and rely on jacket heating to supply the latent heat of vaporization. The surface area scales as $S^{2/3}$ and limits the production rate in some processes because the previous limit, a downstream finishing reactor, has been

improved. A pump-around loop containing a heat exchanger with a flash into the top of the CSTR is one possibility for increasing capacity.

The finishing reactors used for PET and other equilibrium-limited polymerizations pose a classic scaleup problem. Small amounts of the condensation product are removed using devolatilizers (rotating-disk reactors) that create surface area mechanically. They scale as $S^{2/3}$.

13.6.3 Living Addition Polymerizations

The main problem with a living polymer is maintaining the strict cleanliness that is demanded by the chemistry. This is a particularly severe problem for large-scale batch polymerizations, but it is a problem more of economics than technology. Living polymerizations are usually run to near completion, so that end-point control is not a problem. Most living polymerizations operate at low temperatures, -40 to $+40^{\circ}$C, to avoid chain transfer reactions. Thus temperature control is a significant scaleup problem. The usual approach is to use 85–95 w % solvent and to rely on sensible heat transfer to the vessel walls.

The sanitation requirements are easier to meet in continuous operation, but polymerizations in a tubular geometry raise a stability issue. Living polymer formed near the wall will continue to grow due to the outward diffusion of monomer. The fear is that this very high molecular weight polymer will eventually plug the reactor or at least cause a severe form of velocity profile elongation. Possibly, there is a maximum tube diameter for stable operation. Tubular reactors have apparently not been used for living polymerizations even though the low polydispersities would be an advantage in some applications. CSTRs have been used, but the polydispersity advantage of a living polymerization is lost. The exit polydispersity will be 2.

13.6.4 Vinyl Addition Polymerizations

Heat removal is the key problem in scaling up a vinyl polymerization. Section 5.3 discusses the general problem and ways of avoiding it. Processes where the polymer phase is suspended in a nonsolvent are relatively easy to scale up. If the pilot plant reactor is sensitive to modest changes in agitator speed or reactant addition rates, there are likely to be mixing time or dispersion quality problems upon scaleup. In batch processes, end-point control can also be a problem, but it is usually managed by reacting to near completion and controlling the temperature and initiator concentrations to give the desired molecular weight. Tubular geometries often have a diameter limit beyond which scaleup must proceed in parallel or series. The mechanically stirred, tube-cooled reactors (also called ***stirred tube reactors***) that are commonly used for polystyrene have such a limit as well. Modern designs use three or more reactors in series to increase single-train capacity. This is analogous to adding extra length to a high-pressure polyethylene reactor and is a form of scaling in series.

SUGGESTED FURTHER READINGS

A recent, general reference on polymerization reaction engineering is:

T. Meyer and J. Keurentjes (Ed.), *Handbook of Polymer Reaction Engineering*, Wiley, Hoboken, NJ, 2005.

A comprehensive treatment of molecular weight distributions is given in:

L. H. Peebles, Jr., *Molecular Weight Distributions in Polymers,* Interscience, New York, 1971.

A briefer survey of suitable mathematical techniques for determining molecular weight distributions is given in:

D. C. Chappelear and R. H. Simon, Polymerization reaction engineering, *Adv. Chem.,* **91,** 1 (1969).

There are a large number of proprietary process models for the industrially important polymerizations. Public domain descriptions of these commercial models are seldom complete enough to allow independent evaluation. Given below are a few general references and models published in the referred literature.

A sophisticated model of the high-pressure process for polyethylene is described in:

S. K. Gupta, A. Kumar, and M. V. E. Krisltnamurthy, Simulation of tubular low-density polyethylene, *Polym. Eng. Sci.,* **25**, 37 (1985).

An example of a design and optimization study using a fairly sophisticated model for styrene polymerization is given in:

R. Mallikarjun and E. B. Nauman, A staged multitubular process for crystal polystyrene, Polym. *Process Eng.,* **4**, 31 (1986).

A modern polystyrene process consists of a CSTR followed by several stirred tube reactors in series. A description of this typical process is given in:

C.-C. Chen, Continuous production of solid polystyrene in back-mixed and linear-flow reactors, *Polym. Eng. Sci*., **40**, 441 (2000).

An overview of the various dispersed-phase polymerizations is:

R. Arshady, Suspension, emulsion, and dispersion polymerization: A methodological survey, *Colloid Polym. Sci*., **270**, 717 (1992).

PROBLEMS

13.1 A binary polycondensation of AMA and BNB is to be performed in a batch reactor. A number-average chain length of at least 100 is required. What minimum accuracy is required for weighing the two components?

13.2 Find some real chemistry where a binary polycondensation will give a homopolymer, that is, AMA reacts with BMB to form poly-M.

13.3 The phenol–formaldehyde polycondensation readily forms gels. The generally accepted limits for avoiding them are $[\text{Phenol}]_0 < 0.75[\text{Formaldehyde}]_0$ when the catalyst is a strong acid or $[\text{Formaldehyde}]_0 > 1.5[\text{Phenol}]_0$ when the catalyst is a strong base. Are these limits universal for a trifunctional monomer condensing with a difunctional monomer or are they specific to the phenol–formaldehyde reaction? Assume the three sites are equally reactive. (Practical experience shows the gelation point to be at $S_{AB} >$

0.8. This is presumably due to lower reactivity of the para position compared with the ortho positions.) A good answer to this question may require recourse to the literature. Becoming acquainted with percolation theory might be helpful in understanding the phenomenon.

13.4 Refer to Equations 13.24 governing the MWD for a binary poly condensation. Derive and explain each of the limiting cases: $S_{AB} = 0$, $S_{AB} = 1$, $X_A = 0$, and $X_A = 1$.

13.5 Use Equation 13.26 to find the moments μ_0 through μ_2 for the Flory distribution. Use your results to validate Equation 13.27.

13.6 Find the standard deviation of the Flory distribution as given by Equation 13.26 and relate it to the polydispersity. Extend the calculations in Problem 13.5 to μ_3. Find the kurtosis of the distribution in the limit of high conversion.

13.7 The Flory distribution gives a polydispersity of 2 in the limit of high conversion. Yet, a thought experiment suggests that a small batch of self-condensing molecules would eventually condense to form a single cyclic molecule. Reconcile this apparent inconsistency.

13.8 Determine the copolymer composition for a styrene–acrylonitrile copolymer made at the azeotrope (62 mol % styrene). Assume $\bar{l}_N = 1000$. One approach is to use the Gaussian approximation to the binomial distribution. Another is to "synthesize" 100,000 or so molecules using a random-number generator and to sort them by composition.

13.9 Find the analytical integral of Equation 13.44.

13.10 A continuous polymerization train consisting of two stirred tanks in series is used to copolymerize styrene, $r_X = 0.41$, and acrylonitrile, $r_Y = 0.04$. The flow rate to the first reactor is 3000 kg h^{-1} and a conversion of 40% is expected. Makeup styrene is fed to the second reactor and a conversion of 30% (based on the 3000 kg h^{-1} initial feed) is expected there. What should be the feed composition and how much styrene should be fed to the second reactor if a copolymer containing 58 wt % styrene is desired?

13.11 Derive the equivalent of Equation 13.41 when penultimate effects are considered.

13.12 Consider a laminar flow tubular polymerizer with cooling at the tube wall. At what radial position will a hot spot develop: at the tube wall, at the centerline, or at an intermediate radius? Justify your answer. Will the situation change with heating at the wall?

13.13 Use Code for Example 13.9 to explore thermal runaway. Feed pure styrene at 135°C and maintain a wall temperature of 300 K. At what tube diameter does the reactor run away? Repeat varying T_{wall}. Is the case of $T_{\text{wall}} = 400$ K with a tube radius of 0.4 in. predicted to be stable? Compare your results to those for the detailed model shown in Figure 13.7. Rationalize any differences.

13.14 Use the kinetic model in Code for Example 13.9 to design a CSTR for the production of polystyrene. The entering feed is pure styrene. It is desired to produce 50% by weight of polystyrene with a number-average molecular weight of 85,000. The feed flow rate is 25,000 kg h^{-1} Determine the required operating temperature and reactor capacity (in mass units).

13.15 The reactor in Problem 13.14 is to be cooled by autorefrigeration. Determine the boil-up rate in the reactor assuming that the condensate is returned to the reactor without subcooling.

13.16 Suppose the reactor sized in Problem 13.14 is converted to manufacture a styrene–acrylonitrile copolymer containing 36% acrylonitrile by weight. Assume 50% conversion as before. What is the required feed composition to the reactor and what is the composition of the unreacted monomer mixture?

Chapter 14

Unsteady Reactors

The general material balance of Section 1.1 contains an accumulation term that enables its use for unsteady-state reactors. This term is used to solve steady-state design problems by the method of false transients. We turn now to solving real transients. The great majority of chemical reactors are designed for steady-state operation. However, even steady-state reactors must occasionally start up and shut down. Also, an understanding of process dynamics is necessary to design the control systems needed to handle upsets and to enable operation at steady states that would otherwise be unstable.

Unsteady mass and energy balances consider three kinds of accumulation:

Total mass: $d(\hat{\rho}V)/dt$.

Component moles: $d(\hat{a}V)/dt$.

Enthalpy: $d(\hat{H}\hat{\rho}V)/dt$.

These accumulation terms are added to the appropriate steady-state balances to convert them to unsteady balances. The carets indicated averages over the volume of the system, for example,

$$\hat{\rho} = \iiint_V \rho \, dV$$

The three accumulation terms represent the change in the total mass inventory, the molar inventory of component A, and the heat content of the system. The carets can be dropped for a stirred tank, and this is the most useful application of the theory.

14.1 UNSTEADY STIRRED TANKS

The steady-state balance for total mass is

$$0 = Q_{\text{in}}\,\rho_{\text{in}} - Q_{\text{out}}\,\rho_{\text{out}}$$

A well-mixed stirred tank (which we will continue to call a CSTR despite possibly discontinuous flow) has $\hat{\rho} = \rho_{\text{out}}$. The unsteady-state balance for total mass is obtained

Chemical Reactor Design, Optimization, and Scaleup, Second Edition. By E. B. Nauman
Copyright © 2008 John Wiley & Sons, Inc.

just by including the accumulation term:

$$\frac{d(\rho_{\text{out}} V)}{dt} = Q_{\text{in}}\,\rho_{\text{in}} - Q_{\text{out}}\,\rho_{\text{out}} \tag{14.1}$$

Liquid phase systems with approximately constant density are common. Thus the usual simplification of Equation 14.1 is

$$\frac{dV}{dt} = Q_{\text{in}} - Q_{\text{out}}$$

The component balance for the general case is

$$\frac{d(a_{\text{out}} V)}{dt} = Q_{\text{in}}\,a_{\text{in}} - Q_{\text{out}}\,a_{\text{out}} + V\mathscr{R}_A \tag{14.2}$$

The general case treats time-dependent volumes, flow rates, and inlet concentrations. The general case must be used for most startup and shutdown transients, but some dynamic behavior can be effectively analyzed with the constant-volume, constant-flow rate version of Equation 14.2:

$$\bar{t}\frac{da_{\text{out}}}{dt} = a_{\text{in}} - a_{\text{out}} + \bar{t}\mathscr{R}_A$$

The case of $a_{\text{in}} = a_{\text{in}}(t)$ will force unsteady output, as will sufficiently complex kinetics.

The enthalpy balance for a reasonably general situation is

$$\frac{d(V\rho_{\text{out}}H_{\text{out}})}{dt} = Q_{\text{in}}\rho_{\text{in}}H_{\text{in}} - Q_{\text{out}}\rho_{\text{out}}H_{\text{out}} - V\,\Delta H_R\,\mathscr{R} + P_I + U A_{\text{ext}}(T_{\text{ext}} - T_{\text{out}}) \tag{14.3}$$

which is identical to Equation 5.24. A more general case is discussed in Problem 14.15. Typical simplifications are constant volume and flow rate, constant density, and replacement of enthalpy with$C_P(T - T_{\text{ref}})$. This gives Equation 5.28:

$$\bar{t}\frac{dT_{\text{out}}}{dt} = T_{\text{in}} - T_{\text{out}} - \frac{\bar{t}\,\Delta H_R\mathscr{R}_A}{\rho C_P} + \frac{P_I}{V\rho C_P} + \frac{U A_{\text{ext}}}{V\rho C_P}(T_{\text{ext}} - T_{\text{out}})$$

Equations 14.1–14.3 are a set of simultaneous ODEs that govern the performance of an unsteady CSTR. The minimum set is just Equation 14.2, which governs the reaction of a single component with time-varying inlet concentration. The maximum set has separate ODEs for each of the variables V, H_{out}, a_{out}, $b_{\text{out}}\ldots$. These are the ***state variables***. The ODEs must be supplemented by a set of initial conditions and by any thermodynamic relations needed to determine dependent properties such as density and temperature. The maximum set will consist of Equations 14.1, 14.3 and N versions of Equation 14.2, where N is the number of components in the system. The maximum dimensionality is thus $2 + N$. It can always be reduced to 2 plus the number of independent reactions using the reaction coordinate method of Section 2.14. However, such reductions are unnecessary from a computational viewpoint and disguise the physics of the problem.

14.1.1 Transients in Isothermal CSTRs

If the system is isothermal with $T_{out} = T_{in}$, Equation 14.3 is unnecessary. Unsteady behavior in an isothermal perfect mixer is governed by a maximum of $N + 1$ ODEs. Except for highly complicated reactions such as polymerizations (where N is theoretically infinite), solutions are usually straightforward. Numerical methods for unsteady CSTRs are similar to those used for steady-state PFRs, and analytical solutions are usually possible when the reaction is first order.

Stability

The first consideration is stability. Is there a stable steady state? The answer is usually yes for isothermal systems.

EXAMPLE 14.1

Consider a first-order reaction occurring in a CSTR where the inlet concentration of reactant has been held constant at a_0 for $t < 0$. At time $t = 0$, the inlet concentration is changed to a_1. Find the outlet response for $t > 0$ assuming isothermal, constant-volume, constant-density operation.

SOLUTION: The solution uses a simplified version of Equation 14.2:

$$\bar{t}\frac{da_{out}}{dt} = a_1 - a_{out} + \bar{t}\mathscr{R}_A \quad \text{for } t > 0$$

A general solution for constant a_1 and $\mathscr{R}_A = -ka_{out}$ is

$$a_{out} = \frac{a_1}{1 + k\bar{t}} + C \exp\left[-\frac{(1 + k\bar{t})t}{\bar{t}}\right]$$

as may be verified by differentiation. The constant C is found from the value of a_{out} at $t = 0$. For the current problem, this initial condition is the steady-state output from the reactor given an input of a_0:

$$a_{out} = \frac{a_0}{1 + k\bar{t}} \quad \text{at } t = 0$$

Applying the initial condition gives

$$a_{out} = \frac{a_1 + (a_0 - a_1)\exp[-(1 + k\bar{t})t/\bar{t}]}{1 + k\bar{t}}$$

as the desired solution. Figure 14.1 illustrates the solution and also shows the effect of restoring a_{in} to its original value at some time $t > 0$.

Example 14.1 shows how an isothermal CSTR with first-order reaction responds to an abrupt change in inlet concentration. The outlet concentration moves from an initial steady state to a final steady state in a gradual fashion. If the inlet concentration is returned to its original value, the outlet concentration returns to its original value. If the time period for an input disturbance is small, the outlet response is small. The magnitude of the outlet disturbance will never be larger than the magnitude of the inlet

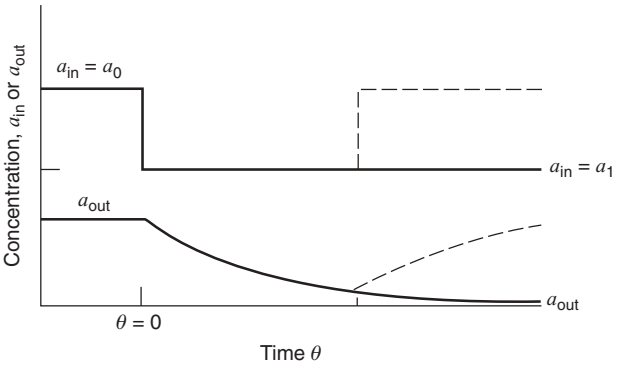

Figure 14.1 Dynamic response of a CSTR to changes in inlet concentration of a component reacting with first-order kinetics.

disturbance. The system is stable. Indeed, it is ***open-loop stable***, which means that steady-state operation can be achieved without resort to a feedback control system. This is the usual but not inevitable case for isothermal reactors.

The steady-state design equations (i.e., Equations 14.1–14.3 with the accumulation terms zero) can be solved to find one or more steady states. However, the solution provides no direct information about stability. On the other hand, if a transient solution reaches a steady state, then that steady state is stable and physically achievable from the initial conditions used in the calculations. If the same steady state is found for all possible initial conditions, then that steady state is unique and globally stable. This is the usual case for isothermal reactions in a CSTR. Example 14.2 and Problem 14.6 show that isothermal systems can have multiple steady states or may never achieve a steady state, but the chemistry of these examples is contrived. Multiple steady states are more common in nonisothermal reactors, although at least one steady state is usually stable. Systems with stable steady states may oscillate or be chaotic for some initial conditions. Example 14.9 gives an experimentally verified example.

EXAMPLE 14.2

Suppose the rabbits and lynx of Section 2.5.4 become migratory. Model their behavior given a steady stream of rabbits and lynx entering a grassy plain. Ignore the depletion of grass.

SOLUTION: The ODEs governing the population of rabbits and lynx are

$$\bar{t}\frac{dr_{out}}{dt} = r_{in} - r_{out} + \bar{t}(k_I g r_{out} - k_{II} l_{out} r_{out})$$

$$\bar{t}\frac{dl_{out}}{dt} = l_{in} - l_{out} + \bar{t}(k_{II} l_{out} r_{out} - k_{III} l_{out})$$

Figure 14.2 shows the numerical solution. Except for a continuous input of 10 rabbits and 1 lynx per unit time, the parameter values and initial conditions are the same as used for Figure 2.6. The batch reactor has been converted to a CSTR. The oscillations in the CSTR are smaller and have a higher frequency than those in the batch reactor, but a steady state is not achieved.

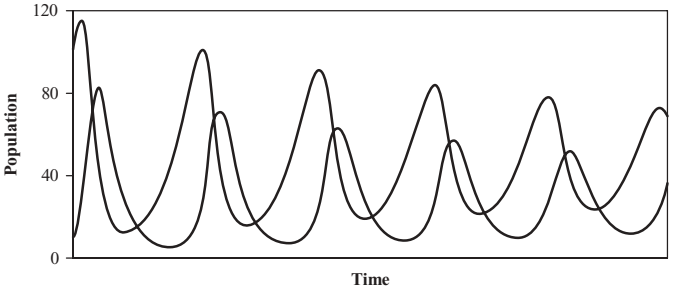

Figure 14.2 Population dynamics on a well-mixed grassy plain with constant migration of rabbits and lynx. Compare this to the nonmigratory case in Figure 2.6.

Example 14.2 demonstrates that sustained oscillations are possible even in an isothermal flow system. This is hardly surprising since they are possible in a batch system provided there is an energy supply.

The rabbit and lynx problem does have stable steady states. A ***stable steady state*** is insensitive to small perturbations in the system parameters. Specifically, small changes in the initial conditions, inlet concentrations, flow rates, and rate constants lead to small changes in the observed response. It is usually possible to stabilize a reactor by using a control system. Controlling the input rate of lynx can stabilize the rabbit population. Section 14.1.2 considers the more realistic control problem of stabilizing a nonisothermal CSTR at an unstable steady state.

Startup and Shutdown Strategies

In addition to safe operation, the usual goal of a reactor startup is to minimize production of off-specification material. This can sometimes be accomplished perfectly.

EXAMPLE 14.3

The initial portion of a reactor startup is usually fed batch. Determine the fed-batch startup transient for an isothermal, constant-density stirred tank reactor. Suppose the tank is initially empty and is filled at a constant rate Q_0 with fluid having concentration a_{in}. A first-order reaction begins immediately. Find the concentration within the tank, a, as a function of time $t < t_{\text{full}}$.

SOLUTION: Equation 14.1 simplifies to

$$\frac{dV}{dt} = Q_{\text{in}}$$

so that $V = Q_{\text{in}}t$ throughout the filling period. Equation 14.2 becomes

$$V\frac{da}{dt} + a\frac{dV}{dt} = Q_{\text{in}}a_{\text{in}} - Vka$$

Note that $Q_{\text{out}} = 0$ during the filling period. Substituting $V = Q_{\text{in}}t$ and some algebra gives

$$t\frac{da}{dt} + (1 + kt)a = a_{\text{in}}$$

The initial condition is $a = a_{in}$ at $t = 0$. The solution is

$$a = \frac{a_{in}[1 - \exp(-kt)]}{kt} \tag{14.4}$$

This result applies until the tank is full at time $t_{full} = V_{full}/Q_{in}$. If the tank fills rapidly, $t_{full} \rightarrow 0$ and $a_{full} \rightarrow a_{in}$. If the tank fills slowly, $t_{full} \rightarrow \infty$ and $a_{full} \rightarrow 0$. By regulating Q_{in}, we regulate t_{full} and can achieve any desired concentration in the range from zero to a_{in}.

The fed-batch scheme of Example 14.3 is one of many possible ways to start a CSTR. It is generally desired to begin continuous operation only when the vessel is full and when the concentration within the vessel has reached its steady-state value. This gives a ***bumpless*** startup. The results of Example 14.3 show that a bumpless startup is possible for an isothermal, first-order reaction. Some reasoning will convince you that it is possible for any single, isothermal reaction. It is not generally possible for multiple reactions.

A simpler (and faster) way to achieve a bumpless startup is to ***fast fill and hold***. In the limiting case, the fill is instantaneous, and the reactor acts in a batch mode until the desired steady-state concentration is reached.

EXAMPLE 14.4

Compare the fed-batch and fast-fill-and-hold methods for achieving a bumpless startup.

SOLUTION: Steady-state operation will use the values V_{full} and Q_{full} and will give a steady-state outlet concentration of

$$a_{out} = \frac{a_{in}}{1 + k\bar{t}} = \frac{a_{in} Q_{full}}{Q_{full} + k V_{full}} \tag{14.5}$$

We want this concentration to be achieved at the end of the fed-batch interval when $t = t_{full} = V_{full}/Q_{in}$. Equate the concentrations in Equations 14.4 and 14.5 and solve for Q_{in}. The solution is numerical. Suppose $V_{full} = 5\ m^3$, $Q_{full} = 2\ m^3\ h^{-1}$, $k = 3.5\ h^{-1}$, and $a_{in} = 15\ mol\ m^{-3}$. Then $a_{out} = 1.54\ mol\ m^{-3}$. Now assume values for Q_{in}, calculate t_{full}, and substitute into Equation 14.4 until this concentration is obtained. The result is $Q_{in} = 1.8\ m^3\ h^{-1}$ and $t_{full} = 2.78$ h.

The fast-fill-and-hold method instantaneously achieves a full reactor, in which the concentration follows batch, first-order kinetics until the desired a_{out} is reached. Equation 14.5 is equated to $a_{in} \exp(-kt_{hold})$. An analytical solution is possible for this case:

$$t_{hold} = \frac{\ln(1 + k\bar{t})}{k} \tag{14.6}$$

The steady-state conversion is achieved at 0.65 h compared to 2.78 h for the fed-batch startup.

Obviously, the fast-fill-and-hold method is preferred from the viewpoint of elapsed time. More importantly, the fed-batch method requires an accurate process model that may not be available. The fast-fill-and-hold method can use a process model or it can use a real-time measurement of concentration.

Neither method will achieve a bumpless startup for complex kinetic schemes such as fermentations. There is a general method, known as ***constant RTD control***, that can minimize the amount of off-specification material produced during the startup of a complex reaction (e.g., a fermentation or polymerization) in a CSTR. It does not require a process model or even a real-time analyzer. We first analyze shutdown strategies, to which it is also applicable.

EXAMPLE 14.5

A CSTR is operating at steady state with a first-order reaction. It is desired to shut it down. Suppose this is done by setting $Q_{\text{in}} = 0$ while maintaining $Q_{\text{out}} = Q$ until the reactor is empty. Assume isothermal, constant-density operation with first-order reaction.

SOLUTION: Stopping the input flow will cause the system to behave as a batch reactor even though the outlet flow continues. The initial concentration of the batch is the steady-state value $a_{\text{in}}/(1 + k\bar{t})$, and the concentration decreases exponentially as the vessel discharges:

$$a_{\text{out}} = \frac{a_{\text{in}} \exp(-kt)}{1 + k\bar{t}} \tag{14.7}$$

where we have assumed the shutdown transient to start at time $t = 0$. The transient lasts until the vessel is empty, $t_{\text{empty}} = \bar{t}$, assuming the discharge rate is held constant at its initial value.

Turning off the feed and passively letting the reactor empty itself is a common way of shutting down a CSTR. The conversion increases during the discharge period, but this may not be a problem. Perhaps the reactor was already operating at such high conversion that the increase is of no consequence. For complex reactions, however, the increase in conversion may mean that the product is off-specification. So, we consider the following problem: The reactor is operating and full of good material. It is desired to shut it down while producing no material that is off-specification.

One approach is to quickly dump the entire contents, but this is likely to exceed the capacity of downstream equipment. Another approach allows a gradual discharge while maintaining constant product quality.

EXAMPLE 14.6

Explore the consequences of the following shutdown strategy for an isothermal, constant-density CSTR that has been operating at steady state: At time zero, the discharge flow rate is increased by a factor $1 + \delta$. Simultaneously, the inlet flow rate is made proportional to the fluid volume in the vessel. When does the vessel empty and what happens to the composition of the discharge stream during the shutdown interval?

SOLUTION: The control strategy is to set the inlet flow rate proportional to the active volume in the vessel:

$$Q_{\text{in}} = \frac{V(t)}{\bar{t}} \tag{14.8}$$

where $1/\bar{t}$ is the proportionality constant. This is the same proportionality constant that related flow rate to volume during the initial period of steady-state operation. During the shutdown transient, the inlet flow rate gradually declines from its steady-state value of Q_0. Equation 14.1 becomes

$$\frac{dV}{dt} = \frac{V}{\bar{t}} - (1+\delta)Q_0 \tag{14.9}$$

The initial condition is $V = V_0$ at $t = 0$. Solving this ODE and setting $V = 0$ give

$$t_{\text{empty}} = \bar{t}\ \ln\left[\frac{1+\delta}{\delta}\right] \tag{14.10}$$

These shutdown times are moderate: $2.4\bar{t}$ for $\delta = 0.1$ and $3\bar{t}$ for $\delta = 0.05$. Equation 14.2 governs the outlet concentration during the shutdown interval. For this shutdown strategy, it becomes

$$a_{\text{out}}\frac{dV}{dt} + V\frac{da_{\text{out}}}{dt} = \frac{a_{\text{in}}V}{\bar{t}} - (1+\delta)a_{\text{out}}Q_0 + V\mathscr{R}_A$$

Substituting Equation 14.9 and simplifying give

$$\bar{t}\frac{da_{\text{out}}}{dt} = a_{\text{in}} - a_{\text{out}} + \bar{t}\mathscr{R}_A$$

This equation applies for $t \geq 0$, and when t is exactly zero, a_{out} has its steady-state value, which is determined from the steady-state design equation:

$$0 = a_{\text{in}} - a_{\text{out}} + \bar{t}\mathscr{R}_A$$

Compare these results to see that $da_{\text{out}}/dt = 0$ so that the outlet concentration does not change during the shutdown transient.

Example 14.6 derives a rather remarkable result. Here is a way of gradually shutting down a CSTR while keeping a constant outlet composition. The derivation applies to an arbitrary $\mathscr{R}_A$ and can be extended to include multiple reactions and adiabatic reactions. It has been experimentally verified for a polymerization (Nauman and Carter, 1974). It can be generalized to shut down a train of CSTRs in series. The reason it works is that the material in the tank always experiences the same mean residence time and residence time distribution (RTD) as existed during the original steady state. Hence it is called constant RTD control. It will cease to work in a real vessel when the liquid level drops below the agitator.

Constant RTD control can be applied in reverse to start up a vessel while minimizing off-specification materials. For this form of startup, a near steady state is first achieved with a minimum level of material and thus with minimum throughput. When the product is satisfactory, the operating level is gradually increased by lowering the discharge flow while applying Equation 14.8 to the inlet flow. The vessel fills, the flow rate increases, but the RTD is constant.

Product Transitions

A common practice in the manufacture of polymers and specialty chemicals is to use the same basic process for multiple products. Batch reactions obviously lend themselves to this practice, but continuous production lines are also switched from one product to another as dictated by market demand. This is routinely done at production rates of 50 tons h^{-1}. There is strong economic incentive to minimize downtime and to minimize the production of off-specification product. A complete shutdown and restart might minimize the amount of off-specification product but will cause appreciable downtime. A running transition will maintain productivity but may generate a large amount of off-specification material. Combination strategies such as partially empting a reactor before making a chemical change are sometimes used. When the reactor can be modeled as one or more CSTRs in series, Equations 14.1–14.3 provide the general framework for studying product transitions.

EXAMPLE 14.7

A plastics company has two products in a CSTR. Product I, a homopolymer, is made by the reaction

$$\mathrm{A} \rightarrow \mathrm{P} \qquad \mathscr{R} = k_{\mathrm{I}} a$$

Product II is a C-modified version of the homopolymer made by a second reaction:

$$\mathrm{P} + \mathrm{C} \xrightarrow{k_{\mathrm{II}}} \mathrm{Q} \qquad \mathscr{R} = k_{\mathrm{II}} pc$$

The reactor operates at constant volume, constant density, constant flow rate and isothermally. The only difference between the two products is the addition of component C to the feed when product 2 is made.

Explore methods for making a running transition from product I to product II. There is no P or Q in the reactor feed.

SOLUTION: One version of Equation 14.2 is written for each reactant,

$$\begin{aligned}
\bar{t}\frac{da_{\mathrm{out}}}{dt} &= a_{\mathrm{in}} - a_{\mathrm{out}} - \bar{t}k a_{\mathrm{out}} \\
\bar{t}\frac{dp_{\mathrm{out}}}{dt} &= -p_{\mathrm{out}} + \bar{t}(k_I a_{\mathrm{out}} - k_{\mathrm{II}} p_{\mathrm{out}} c_{\mathrm{out}}) \\
\bar{t}\frac{dq_{\mathrm{out}}}{dt} &= -q_{\mathrm{out}} + \bar{t}_{\mathrm{I}} k_{\mathrm{II}} p_{\mathrm{out}} c_{\mathrm{out}} \\
\bar{t}\frac{dc_{\mathrm{out}}}{dt} &= c_{\mathrm{in}} - c_{\mathrm{out}} - \bar{t}k_{\mathrm{II}} p_{\mathrm{out}} c_{\mathrm{out}}
\end{aligned}$$

The analysis from this point will be numerical. Suppose $a_{\mathrm{in}} = 20$ mol m^{-3} for both products, $c_{\mathrm{in}} = 9$ mol m^{-3} when product 2 is being made at steady state, $\bar{t} = 1$ h, $k_{\mathrm{I}} = 4\ h^{-1}$, and $k_{\mathrm{II}} = 1\ h^{-1}\ m^3\ mol^{-1}$. This kinetic system allows only one steady state. It is stable and can be found by solving the governing ODEs starting from any initial condition. The steady-state response when making product I is $a_{\mathrm{out}} = 4$ mol m^{-3} and $p_{\mathrm{out}} = 16$ mol m^{-3}. When product II is made, $a_{\mathrm{out}} = 4$ mol m^{-3}, $p_{\mathrm{out}} = 8$ mol m^{-3}, $q_{\mathrm{out}} = 8$ mol m^{-3}, and $c_{\mathrm{out}} = 1$ mol m^{-3}.

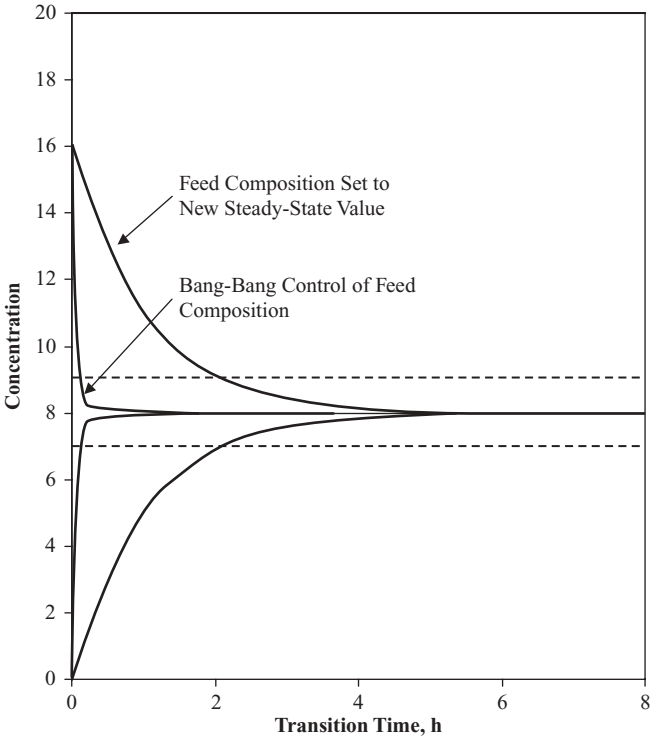

Figure 14.3 Transitions from product I to product II in Example 14.7.

Consider a transition from product I to product II. The simplest case is just to add component C to the feed at the required steady-state concentration of $c_{in} = 9$ mol m^{-3}. The governing ODEs are solved subject to the initial condition that the reactor initially contains the steady-state composition corresponding to product I. Figure 14.3 shows the leisurely response toward the new steady state. The dotted lines represent the specification limits for product II. They allow any Q concentration between 7 and 9 mol m^{-3}. The outlet composition enters the limits after 2.3 h. The specification for product I allows 1 mol m^{-3} of Q to be present, but the rapid initial increase in the concentration of Q means that the limit is quickly exceeded. The total transition time is about 2 h, and some 100 tons of off-specification material would be produced.

A far better control strategy is available. Figure 14.3 shows the response to a form of ***bang-bang control*** where C is charged as rapidly as possible to quickly change the reactor concentration to 11 mol m^{-3}. This is the first bang and is assumed to be instantaneous. The second bang completely stops the feed of C for 12 min. This prevents the outlet concentration of Q from overshooting its steady-state value. After the 12-min duration of the second bang, the inlet concentration of Q is set to its steady-state value. The transition time is reduced to about 7 min and the amount of off-specification material to about 6 tons. This is not yet the optimal response, which probably shows some overshoot in the outlet concentration of Q, but it is a reasonable start. Problems 14.9 and 14.10 pursue this problem.

Chapter 6 introduced the concept of functional optimization. Several examples in that chapter addressed the problem of finding the optimum temperature profile, $T_{wall}(z)$, for a steady-state tubular reactor. Product transition strategies are also problems in functional optimization, but the functions to be determined are now functions of time such as $a_{in}(t)$ and $Q_{in}(t)$. As suggested by the bang-bang strategy in Example 14.7, the optimal functions are typically discontinuous. A typical bang-bang strategy is to set $a_{in}(t)$ to a high value, hold it there for a period of time, then shift $a_{in}(t)$ to a low value, hold it there for a period of time, and then shift $a_{in}(t)$ to the appropriate value for the new steady state. This problem immediately translates to parameter optimization: the high value, the low value, and two time periods. Optimal control theory shows that this form of discontinuous input is frequently the best possible control strategy.

14.1.2 Nonisothermal Stirred Tank Reactors

Nonisothermal stirred tanks are governed by an enthalpy balance that contains the heat of reaction as a significant term. If the heat of reaction is unimportant so that a desired T_{out} can be imposed on the system regardless of the extent of reaction, then the reactor dynamics can be analyzed by the methods of the previous section. This section focuses on situations where Equation 14.3 must be considered as part of the design. Even for these situations, it is usually possible to control a steady-state CSTR at a desired temperature. If temperature control can be achieved rapidly, then isothermal design techniques again become applicable. Rapid means on a time scale that is fast compared to reaction times and composition changes.

EXAMPLE 14.8

The styrene polymerization example 5.7 shows three steady states. The middle steady state with $a_{out} = 0.738$ and $T_{out} = 403$ K is unstable. Devise a control system that stabilizes operation near it.

SOLUTION: There are several theoretical ways of stabilizing the reactor, but temperature control is the normal choice. The reactor in Example 5.7 was adiabatic. Some form of heat exchange must be added. Possibilities are to control the inlet temperature, to control the pressure in the vapor space thereby allowing reflux of styrene monomer at the desired temperature, or to control the jacket or external heat exchanger temperature. The following example regulates the jacket temperature. Refer to Example 5.7. The component balance on styrene is unchanged from Equation 5.29:

$$\frac{da_{out}}{d\tau} = a_{in} - a_{out} - 2 \times 10^{10} \exp\left(-\frac{10{,}000}{T_{out}}\right) a_{out}$$

A heat exchange term is added to the energy balance, Equation 5.30, to give

$$\frac{dT_{out}}{d\tau} = T_{in} - T_{out} + \frac{8 \times 10^{12} \exp(-10{,}000/T_{out}) a_{out}}{a_{in}} + \frac{UA_{ext}\bar{t}}{V\rho C_p}(T_{ext} - T)$$

The heat transfer group $\frac{UA_{ext}\bar{t}}{(V\rho C_p)}$ is dimensionless. Assume its value is 0.02.

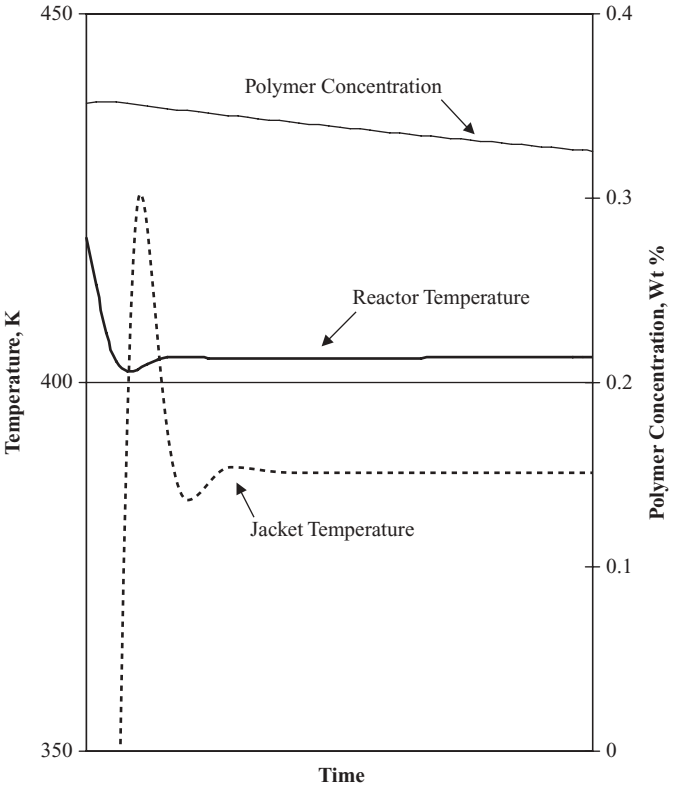

Figure 14.4 Stabilization of a nonisothermal CSTR near a metastable steady state.

A controller is needed to regulate T_{ext}. The industrial choice would be a two-term controller, proportional plus reset. We skirt the formal control issues and use a simple controller of the form

$$T_{ext} = 375 + 20(T_{set} - T)$$

Suppose the reactor has been started using the fast-fill-and-hold method and has reached $a = 0.65$ at $T = 420$ K. Continuous flow is started with $a_{in} = 1$, $T_{in} = 375$ K, and $T_{set} = 404$ K. Figure 14.4 shows the response. The temperature response is very rapid, but the conversion increases slightly during the first seconds of operation. Absent temperature control, the reaction would have run away. The concentration is slowly evolving to its eventual steady-state value of about 0.26. There is a small offset in the temperature because the controller has no reset term.

EXAMPLE 14.9

This example cites a real study of a laboratory CSTR that exhibits complex dynamics and limit cycles in the absence of a feedback controller. We cite the work of Vermeulen and Fortuin

(1986), who studied the acid-catalyzed hydration of 2,3-epoxy-1-propanol to glycerol:

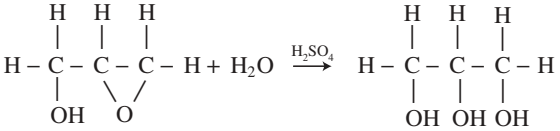

The reactor has separate feed streams for an aqueous solution of the epoxy and for an aqueous solution of the acid. Startup begins with the vessel initially full of acid.

SOLUTION: The chemistry seems fairly simple. The water concentration is high and approximately constant so that the reaction is pseudo–first order with respect to the epoxy. The rate is also proportional to the hydrogen ion concentration h. Thus

$$\mathscr{R} = k_0 \exp\left[\frac{-\Delta E}{R_g T}\right] eh$$

where e is the epoxy concentration. Sulfuric acid dissociates in two equilibrium steps:

$$H_2SO_4 \rightleftarrows H^+ + HSO_4^- \qquad K_1 = \frac{[H^+][HSO_4^-]}{[H_2SO_4]}$$

$$HSO_4^- \rightleftarrows H^+ + SO_4^{2-} \qquad K_2 = \frac{[H^+][SO_4^{2-}]}{[HSO_4^-]}$$

The hydrogen ion concentration can be found from

$$\frac{h_{\text{out}}^3}{K_1} + h_{\text{out}}^{2+} + (K_2 - s_{\text{out}})h_{\text{out}} - 2K_2 s_{\text{out}} = 0$$

where s is the total sulfate concentration.

There are three ODEs that govern the system. For sulfate, which is not consumed,

$$\bar{t}\frac{ds_{\text{out}}}{dt} = s_{\text{in}} - s_{\text{out}} \quad s_{\text{out}} = s_0 \quad \text{at } t = 0$$

For the epoxy,

$$\bar{t}\frac{de_{\text{out}}}{dt} = e_{\text{in}} - e_{\text{out}} - k_0\bar{t}\exp\left[\frac{-\Delta E}{R_g T}\right] e_{\text{out}} h_{\text{out}} \qquad e_{\text{out}} = 0 \quad \text{at } t = 0$$

For temperature,

$$(\rho V C_P + m_I C_I)\frac{dT_{\text{out}}}{dt} = \rho Q (C_P)_{\text{in}} T_{\text{in}} - \rho Q C_P T_{\text{out}} + U A_{\text{ext}}(T_{\text{ext}} - T_{\text{out}}) + P_I - \Delta H_R \rho V k_0 \exp\left[\frac{-\Delta E}{R_g T}\right] e_{\text{out}} h_{\text{out}} \qquad T_{\text{out}} = T_0 \quad \text{at } t = 0$$

This heat balance contains a term not seen before: $m_I C_I$ is the mass times specific heat of the agitator and vessel walls. Although the model is nominally for constant physical properties, Vermeulen and Fortuin found a better fit to the experimental data when they used a slightly different specific heat for the inlet stream, $(C_P)_{\text{in}}$.

Figure 14.5 shows a comparison between experimental results and the model. The startup transient has an initial overshoot followed by an apparent approach to steady state. Oscillations begin after a phenomenally long delay, $t > 10\bar{t}$, and the system

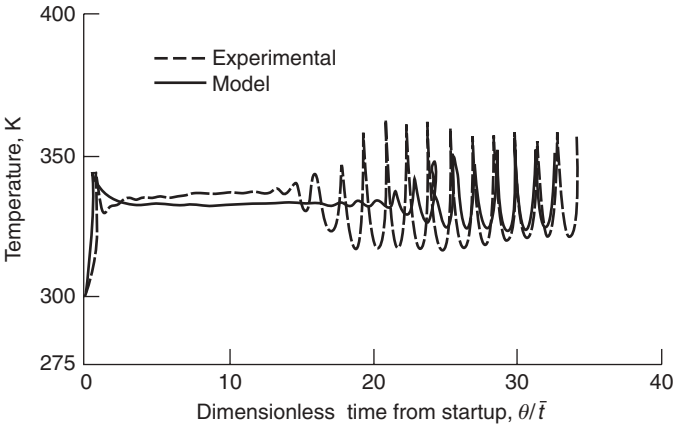

Figure 14.5 Experimental and model results for the acid-catalyzed hydration of 2.3-epoxy-propanol to glycerol.

goes into a limit cycle. The long delay before the occurrence of the oscillations is remarkable. So is the good agreement between model and experiment. Two facts are apparent: Quite complex behavior is possible with a simple model, and one should wait a long time before reaching firm conclusions regarding stability. The conventional wisdom is that steady state is closely approached after three to five mean residence times.

14.2 UNSTEADY PISTON FLOW

Dynamic analysis of PFRs is fairly straightforward and rather unexciting for incompressible fluids. Piston flow causes the dynamic response of the system to be especially simple. The form of response is a limiting case of that found in real systems. We have seen that piston flow is usually a desirable regime from the viewpoint of reaction yields and selectivities. It turns out to be somewhat undesirable from a control viewpoint since there is no natural dampening of disturbances.

Unlike stirred tanks, PFRs are distributed systems with one-dimensional gradients in composition and physical properties. Steady-state performance is governed by ODEs and dynamic performance is governed by PDEs, albeit simple, first-order PDEs. Figure 14.6 illustrates a component balance for a differential volume element:

$$\text{Formation} + \text{input} - \text{output} = \text{Accumulation}$$

$$\mathscr{R}_A \Delta V + aQ - \left[aQ + \frac{\partial (aQ)}{\partial z} \Delta z \right] = \frac{\partial a}{\partial t} \Delta V$$

or

$$\frac{\partial a}{dt} + \frac{1}{A_c} \frac{\partial (aQ)}{\partial z} = \frac{\partial a}{dt} + \frac{1}{A_c} \frac{\partial (A_c \bar{u} a)}{\partial z} = \mathscr{R}_A \tag{14.11}$$

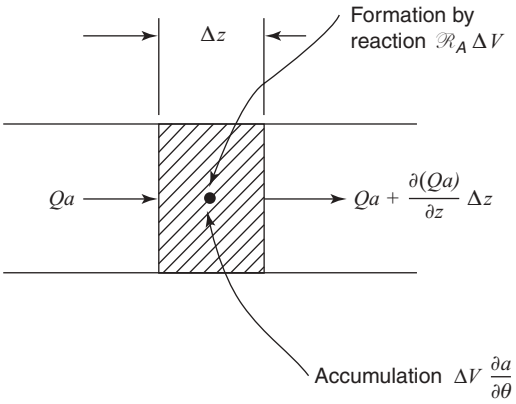

Figure 14.6 Differential volume element in unsteady PFR.

where $A_c = \Delta V / \Delta z$ is the cross-sectional area of the tube. The tube has rigid walls and a fixed length so $\partial V \big/ \partial t = 0$. Compare Equation 14.11 to Equations 3.4 and 3.5. All we have done is add an accumulation term. An overall mass balance gives

$$\frac{\partial \rho}{dt} + \frac{1}{A_c} \frac{\partial(\rho Q)}{\partial z} = 0 \tag{14.12}$$

If ρ is constant, Equation 14.12 shows Q to be constant everywhere within the tube at any instant of time. If Q_{in}varies with time, then $Q(z)$ will immediately adjust to this new value because the fluid is incompressible. Then Equation 14.11, the component balance, simplifies to

$$\frac{\partial a}{dt} + \bar{u} \frac{\partial a}{\partial z} = \mathscr{R}_A \tag{14.13}$$

This result is valid for variable A_c but not for variable ρ. It governs a PFR with a time-dependent inlet concentration but with other properties constant. The final simplification supposes that A_c is constant so that $\bar{u}$ is constant everywhere in the tube. Then Equation 14.13 has a simple analytical solution:

$$\frac{z}{\bar{u}} = \int_{a_{\text{in}}(t - z/\bar{u})}^{a(t,z)} \frac{da_1}{\mathscr{R}_A} \tag{14.14}$$

Formal verification that this result actually satisfies Equation 14.13 is an exercise in partial differentiation, but a physical interpretation will confirm its validity. Consider a small group of molecules that are in the reactor at position z at time t. They have been in the reactor for $z/\bar{u}$ seconds and entered at clock time $t - (z/\bar{u})$ when the inlet concentration was $a_{\text{in}}(t - z/\bar{u})$. Their composition has subsequently evolved according to batch reaction kinetics. Equation 1.33 gives the time needed to go from an initial concentration to a current concentration when there is a single reaction in an ideal batch reactor. Equation 14.14 is just Equation 1.33 with different notation.

Molecules leaving the reactor at time t entered it at time $t - \bar{t}$. Thus,

$$\frac{L}{\bar{u}} = \bar{t} = \int_{a_{\text{in}}(t-\bar{t})}^{a_{\text{out}}(t)} \frac{da_1}{\mathscr{R}_A} \tag{14.15}$$

When a_{in} is constant, Equation 14.14 is a solution of Equation 3.1 evaluated at position z, and Equation 14.15 is a solution evaluated at the reactor outlet.

The temperature counterpart of Equation 14.11 is

$$\frac{\partial(\rho H)}{\partial t} + \rho Q \frac{\partial H}{\partial z} = \frac{\partial(\rho H)}{\partial t} + \rho \bar{u} A_c \frac{\partial H}{\partial z} = -\Delta H_R \mathscr{R} A_c + U A'_{\text{ext}}(T_{\text{ext}} - T) \tag{14.16}$$

With constant physical properties and A_c this becomes

$$\frac{\partial T}{\partial t} + \bar{u}\frac{\partial T}{\partial z} = \frac{-\Delta H \mathscr{R}}{\rho C_p} + \frac{2U}{R\rho C_P}(T_{\text{ext}} - T) \tag{14.17}$$

If the reactor is adiabatic, $U = 0$ and Equation 14.17 has the following formal solution:

$$\frac{z}{\bar{u}} = \int_{T_{\text{in}}(t-z/\bar{u})}^{T(t,z)} \frac{\rho C_P}{-\Delta H_R \mathscr{R}} dT' \tag{14.18}$$

This formal solution is not useful for finding $T(t, z)$ since the reaction rate will depend on composition. It does, however, show that the temperature at time t and position z is determined by inlet conditions at time $t - z/\bar{u}$. Temperature, like composition, progresses in a batchlike trajectory from its entering value to its exit value without regard for what is happening elsewhere in the tube. Heat exchange to the environment, $U > 0$, does not change this fact provided T_{ext} is uncoupled to T. A solution for $a_{\text{out}}(t)$ and $T_{\text{out}}(t)$ can be found by solving the ODEs that govern steady-state piston flow:

$$\bar{u}\frac{da}{dz} = \mathscr{R}_A$$
$$\bar{u}\frac{dT}{dz} = \frac{-\Delta H \mathscr{R}}{\rho C_p} + \frac{2U}{R\rho C_P}(T_{\text{ext}} - T)$$

Solve these ODEs subject to the initial conditions that $a = a_{\text{in}}(t - \bar{t})$ and $T = T_{\text{in}}(t - \bar{t})$ at $z = 0$. Evaluate the solution at $z = L$ to obtain $a_{\text{out}}(t)$ and $T_{\text{out}}(t)$.

The most important fact about piston flow is that disturbances at the inlet are propagated down the tube with no dissipation due to mixing. They arrive at the outlet $\bar{t}$ seconds later. This pure time delay is known as ***dead time***. Systems with substantial amounts of dead time oscillate when feedback control is attempted. This is caused by the controller responding to an output caused by an input $\bar{t}$ seconds ago. The current input may be completely different. ***Feedforward*** control represents a theoretically sound approach to controlling systems with appreciable dead time. Sensors are installed at the inlet to the reactor to measure fluctuating inputs. The

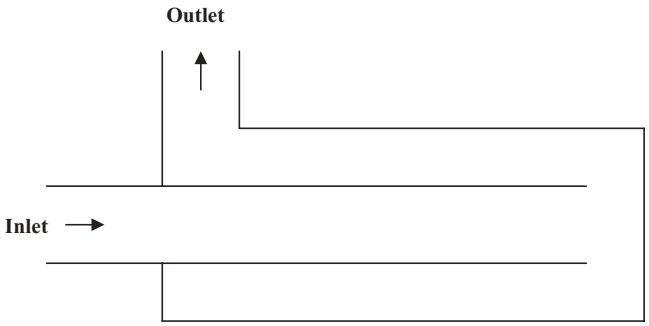

Figure 14.7 A PFR with feedback of heat.

appropriate responses to these inputs are calculated using a model. The model used for the calculations may be imperfect but can be improved using feedback of actual responses. In ***adaptive*** control, this feedback of results is done automatically using a special error signal to correct the model.

Piston flow reactors lack any internal mechanisms for memory. There is no axial dispersion of heat or mass. What has happened previously has no effect on what is happening now. Given a set of inlet conditions (a_{in}, T_{in}, T_{ext}), only one output (a_{out}, T_{out})is possible. A PFR cannot exhibit steady-state multiplicity unless there is some form of external feedback. External recycle of mass or heat can provide this feedback and may destabilize the system. Figure 14.7 shows an example of external feedback of heat that can lead to the same multiple steady states possible with a CSTR. Another example is when the vessel walls or packing has significant thermal capacity. In such cases, a second heat balance must be added to supplement Equation 14.16. See Section 10.6 for a comparable result.

14.3 UNSTEADY CONVECTIVE DIFFUSION

The unsteady version of the convective diffusion equation is obtained just by adding a time derivative to the steady version. Equation 8.32 for the convective diffusion of mass becomes

$$\frac{\partial a}{\partial t} + V_z(r)\frac{\partial a}{\partial z} = \mathscr{D}_A\left[\frac{\partial^2 a}{\partial z^2} + \frac{1}{r}\frac{\partial a}{\partial r} + \frac{\partial^2 a}{\partial r^2}\right] + \mathscr{R}_A \tag{14.19}$$

The analogous equation for the convective flow of heat is

$$\frac{\partial T}{\partial t} + V_z(r)\frac{\partial T}{\partial z} = \alpha_T\left[\frac{1}{r}\frac{\partial T}{\partial r} + \frac{\partial^2 T}{\partial r^2} + \frac{\partial^2 T}{\partial z^2}\right] - \frac{\Delta H_R \mathscr{R}}{\rho C_P} \tag{14.20}$$

These equations assume that the reactor is single phase and that the surroundings have negligible heat capacity. In principle, Equations 14.19 and 14.20 can be solved numerically using the simple methods of Chapters 8 and 9. The two-dimensional problem in r and z is solved for a fixed value of t. A step forward in t is taken, the

two-dimensional problem is resolved at the new t, and so on. A better approach is to use the method of false transients discussed in Chapter 16.

The axial dispersion model discussed in Section 9.3 is a simplified version of Equation 14.19. Analytical solutions for unsteady axial dispersion are given in Chapter 15.

SUGGESTED FURTHER READINGS

This chapter has presented time-domain solutions of unsteady material and energy balances. The more usual undergraduate treatment of dynamic systems is given in a course on control and relies heavily on Laplace transform techniques. One suitable reference is:

G. Stephanopoulos, *Chemical Process Control: An Introduction to Theory and Practice,* Prentice-Hall, Englewood Cliffs, NJ, 1984.

A more recent book that stresses numerical solutions using Matlab is:

B. W. Bequette, *Process Dynamics: Modeling, Analysis and Simulation*, Prentice-Hall, Englewood Cliffs, NJ, 1998.

Unsteady reaction data are often an excellent means for estimating physical parameters that would be difficult or impossible to elucidate from steady-state measurements. However, the associated problems in nonlinear optimization can be formidable. A review and comparison of methods is given by:

L. T. Biegler, J. J. Damiano, and G. E. Blau, Nonlinear parameter estimation: A case study comparison, *AIChE J*., 32, 29–45 (1986).

PROBLEMS

14.1 Determine the fractional filling rate Q_{fill}/Q that will fill an isothermal, constant-density stirred tank reactor while simultaneously achieving the steady-state conversion corresponding to flow rate Q. Assume a second-order reaction with $a_{\text{in}}k\bar{t} = 1$ and $\bar{t} = 5$ h at the intended steady state.

14.2 Devise a fast-fill-and-hold startup strategy for the reaction of Problem 14.1.

14.3 Suppose the consecutive elementary reactions

$$2\text{A} \xrightarrow{k_{\text{I}}} \text{B} \xrightarrow{k_{\text{II}}} \text{C}$$

occur in an isothermal CSTR. Suppose $a_{\text{in}}k_{\text{I}}\bar{t} = 2$, and $k_{\text{II}} = 1$ with $b_{\text{in}} = c_{\text{in}} = 0$. Determine the steady-state outlet composition and explore system stability by using a variety of initial conditions, a_{in} and b_{in}.

14.4 Find a nontrivial (meaning $r_{\text{out}} > 0$ and $l_{\text{out}} > 0$) steady state for the rabbit and lynx problem in Example 14.2. Test its stability by making small changes in the system parameters.

14.5 Suppose the following reactions are occurring in an isothermal perfect mixer:

$$\text{A} + \text{B} \rightarrow 2\text{B} \qquad \mathscr{R}_{\text{I}} = k_{\text{I}}ab$$

Suppose there is no B in the feed but that some B is charged to the reactor at startup. Can this form of startup lead to stable operation with $b_{in} = 0$ but $b_{out} > 0$?

14.6 Suppose the following reactions are occurring in an isothermal CSTR:

$$\begin{aligned} A + 2B &\rightarrow 3B \quad \mathscr{R}_I = k_I a b^2 \\ B &\rightarrow C \quad \mathscr{R}_{II} = k_{II} b \end{aligned}$$

Since the autocatalytic reaction is third order, a steady-state material balance gives a cubic in b_{out}. This means there are one or three steady-states. Suppose $b_{in}/a_{in} = \frac{1}{15}$ and explore the stability of the single or middle steady-state for each of the following cases:

(a) $a_{in}^2 k_I \bar{t} = 190$, $k_{II}\bar{t} = 4.750$ (a small disturbance from the steady-state gives damped oscillations)

(b) $a_{in}^2 k_I \bar{t} = 225$, $k_{II}\bar{t} = 5.625$ (a small disturbance from the steady-state gives sustained oscillations)

(c) $a_{in}^2 k_I \bar{t} = 315$, $k_{II}\bar{t} = 7.875$ (a small disturbance from the steady-state gives undamped oscillations and divergence to a new steady-state)

See Gray and Scott (1984) for a detailed analysis of this (hypothetical) reaction system.

14.7 Determine t_{full} for the fed-batch method of Examples 14.3 and 14.4 in the limiting cases as $k \rightarrow \infty$ and $k \rightarrow 0$. *Hint:* The range is $\bar{t} < t_{full} < 2\bar{t}$. Determining one of these limits is an easy exercise using L'Hospital's rule.

14.8 Suppose there are two parallel, first-order reactions in a steady-state CSTR. Refer to Example 14.4 and show that neither method can achieve a bumpless startup if the reactions have different rate constants. Is it possible to use a combination of the fed-batch and fast-fill-and-hold strategies to achieve a bumpless startup? A numerical example will be sufficient.

14.9 Improve the control strategy for the product transition in Example 14.7. Ignore mixing time constraints, flow rate limitations on the addition of component C, and any constraints on the allowable value for c_{out}. The concentration of Q can exceed its steady-state value of 8 mol m^{-3} but must not be allowed to go outside the upper specification limit of 9 mol m^{-3}.

14.10 The transition control strategy in Example 14.7 quickly increases the concentration of C in the vessel from 0 to 11 mol m^{-3}. This means that c_{out} = 11 mol m^{-3}, at least temporarily. Suppose the downstream recovery system is unable to handle more than 2 mol m^{-3} of unreacted C. The obvious start to the transition is to quickly charge enough C to the reactor to get $c_{out} = 2$ mol m^{-3}, but then what?

14.11 Use the inlet temperature rather than the jacket temperature to control the reactor in Example 14.8.

14.12 Suppose the reactor in Example 14.8 remains in batch mode after the fast-fill-and-hold startup. Will the temperature control system still work? A preliminary answer based on the approximate kinetics of Example 14.8 is sufficient, but see the next problem.

14.13 Use the more rigorous kinetic model in Code for Example 13.9 to repeat the previous problem. Also consider how the viscosity increase might affect the heat transfer group. Use the viscosity correlation in Code for Example 13.9.

14.14 Control systems can fail in many ways, and highly energetic reactions like the styrene polymerization in Example 14.8 raise major safety concerns. The contents of the vessel

are similar to napalm. Discuss ways of preventing accidents or of mitigating the effects of accidents. Is there one best method for avoiding a disastrous runaway?

14.15 Standard thermodynamic texts give a more general version of Equation 14.3. See Smith et al. (2001). This more general version is

$$\frac{d}{dt}[\rho(H - PV)V] = [H_{\text{in}} + \tfrac{1}{2}\bar{u}_{\text{in}}^2 + Z_{\text{in}}g_{\text{in}}]Q_{\text{in}}\rho_{\text{in}} - [H_{\text{out}} + \tfrac{1}{2}\bar{u}_{\text{out}}^2 + Z_{\text{out}}g_{\text{out}}]Q_{\text{out}}\rho_{\text{out}} - V\Delta H_R\mathscr{R} + UA_{\text{ext}}(T_{\text{ext}} - T_{\text{out}})$$

Identify the added terms. When could they be important? When might other terms be important? Remember, this is a CSTR, not a spaceship, but note the extra terms included in Example 14.9.

14.16 Referring to Example 14.9, Vermeulen and Fortuin (1986) estimated all the parameters in their model from physical data. They then compared model predictions to experimental results and from this they made improved estimates using nonlinear regression. Their results were as follows:

Parameter	Estimate from Physical Data	Estimate from Regression Analysis	Units
ρQ	0.0019	0.001881615	kg s^{-1}
ρV	0.30	0.2998885	kg
$m_I C_I$	392	405.5976	J K^{-1}
e_{in}	8.55	8.532488	mol kg^{-1}
$(C_P)_{\text{in}}$	2,650	2785.279	J $kg^{-1}K^{-1}$
C_P	2,650	2,517,017	J $kg^{-1}K^{-1}$
s_{in}	0.15	0.1530875	mol kg^{-1}
k_0	8.5×10^{10}	8.534612×10^{10}	kg $mol^{-1}s^{-1}$
UA_{ext}	30	32.93344	J $s^{-1}K^{-1}$
$-\Delta H_R$	88,200	87927.31	J mol^{-1}
q	30	32.62476	J s^{-1}
T_{in}	273.91	273.9100	K
T_{ext}	298.34	298.3410	K
E/R_g	8827	8815.440	K
K_1	1000	1,000	mol kg^{-1}
K_2	0.012023	0.012023	mol kg^{-1}
T_0	300.605	300.605	K
e_0	0	0	mol kg^{-1}
s_0	0.894	0.894	mol kg^{-1}

(a) Show that, to a good approximation,

$$h_{\text{out}} = 0.5\left[s_{\text{out}} - K_2 + \sqrt{s_{\text{out}}^2 + 6s_{\text{out}}K_2 + K_2^2}\right]$$

(b) Using the parameter estimates obtained by regression analysis, confirm the qualitative behavior shown in Figure 14.5. A sophisticated integration routine may be necessary, but it is not necessary to match Vermeulen and Fortuin exactly.

(c) The parameter-fitting procedure used experimental data from a single run. Determine the sensitivity of the model by replacing the regression estimates with the physical estimates. What does this suggest about the reproducibility of the experiment?

(d) Devise a means for achieving steady operation at high conversion to glycerol. Undesirable side reactions may become significant at 423 K. At atmospheric pressure and complete conversion, the mixture boils at 378 K.

14.17 Entering engineering freshmen tend to choose their curriculum based on job demand for the current graduating class. It is easy to change curricula in the freshman year but it becomes difficult in subsequent years. Thus we might model the engineering education process as a stirred tank with $\bar{t}_s = 1$ year followed by a PFR with $\bar{t}_p = 3$ years. Does this model predict a good balance of supply and demand? What strategy would you suggest to a freshman whose sole concern is being in high demand upon graduation?

14.18 Blood vessels have elastic walls that expand or contract due to changes in pressure or the passage of corpuscles. How should Equations 14.11 and 14.12 be modified to reflect this behavior?

Chapter 15

Residence Time Distributions

Reactor ***design*** usually begins in the laboratory with a kinetic study. Data are taken in small-scale, specially designed equipment that hopefully (but not inevitably) approximates an ideal, isothermal reactor: batch, perfectly mixed stirred tank, or piston flow. The laboratory data are fit to a kinetic model using the methods of Chapter 7. The kinetic model is then combined with a transport model to give the overall design.

Suppose now that a pilot plant or full-scale reactor has been built and operated. How can its performance be used to confirm the kinetic and transport models and to improve future designs? Reactor ***analysis*** begins with an operating reactor and seeks to understand several interrelated aspects of actual performance: kinetics, flow patterns, mixing, mass transfer, and heat transfer. The present chapter is concerned with the analysis of flow and mixing processes and their interactions with kinetics. It uses ***residence time theory*** as the major tool for the analysis.

In a batch reactor, all molecules enter and leave together. If the system is isothermal, reaction yields depend only on the elapsed time and on the initial composition. The situation in flow systems is more complicated but not impossibly so. The counterpart of the batch reaction time is the age of a molecule. Aging begins when a molecule enters the reactor and ceases when it leaves. The total time spent within the boundaries of the reactor is known as the exit age, or ***residence time***, t. Except in batch and piston flow reactors, molecules leaving the system will have a variety of residence times. The distribution of residence times provides considerable information about homogeneous, isothermal reactions. For single first-order reactions, knowledge of the ***residence time distribution*** (RTD) allows the yield to be calculated exactly, even in flow systems of arbitrary complexity. For other reaction orders, it is usually possible to calculate tight limits within which the yield must lie. Even if the system is nonisothermal and heterogeneous, knowledge of the RTD provides substantial insight regarding the flow processes occurring within it.

15.1 RESIDENCE TIME THEORY

The time that a molecule spends in a reactive system will affect its probability of reacting; and the measurement, interpretation, and modeling of RTDs are important

Chemical Reactor Design, Optimization, and Scaleup, Second Edition. By E. B. Nauman
Copyright © 2008 John Wiley & Sons, Inc.

aspects of chemical reaction engineering. Part of the inspiration for residence time theory came from the ***black-box*** analysis techniques used by electrical engineers to study circuits. These are ***stimulus–response*** or ***input–output*** methods where a system is disturbed and its response to the disturbance is measured. The measured response, when properly interpreted, is used to predict the response of the system to other inputs. For residence time measurements, an inert tracer is injected at the inlet to the reactor, and the tracer concentration is measured at the outlet. The injection is done in a standardized way to allow easy interpretation of the results, which can then be used to make predictions. Predictions include the dynamic response of the system to arbitrary tracer inputs. More important, however, are the predictions of the steady-state yield of reactions in continuous flow systems. All this can be done without opening the black box.

15.1.1 Inert Tracer Experiments

Transient experiments with inert tracers are used to determine RTDs. In real systems, they will be actual experiments. In theoretical studies, the experiments are mathematical and are applied to a dynamic model of the system.

Negative Step Changes and the Washout Function

Suppose that an inert tracer has been fed to a CSTR for an extended period of time, giving $C_{\text{in}} = C_{\text{out}} = C_0$ for $t < 0$. At time $t = 0$, the tracer supply is suddenly stopped so that $C_{\text{in}} = 0$ for $t > 0$. Equation 14.2 governs the transient response of the system. For $t > 0$,

$$V\frac{dC_{\text{out}}}{dt} = -Q_{\text{out}}C_{\text{out}}$$

where constant-volume operation with $\mathscr{R}_C = 0$ has been assumed. The solution is

$$\frac{C_{\text{out}}(t)}{C_0} = \exp\left[-\frac{Q_{\text{out}}t}{V}\right] = \exp\left[-\frac{t}{\bar{t}}\right] \tag{15.1}$$

Tracer molecules originally in the system at time $t = 0$ gradually wash out. The exponential form of Equation 15.1 is specific to a CSTR, but the concept of ***washout*** applies to any flow system. Consider some time $t > 0$ when the fraction of molecules remaining in the system is $W(t) = C(t)/C_0$. These molecules must necessarily have entered the reactor before time $t = 0$ since no tracer was fed after that time. Thus these molecules have residence times of t or longer. The residence time ***washout function*** is defined as

$$W(t) = \begin{array}{l}\text{fraction of molecules leaving the system that} \\ \text{experienced a residence time greater than } t\end{array} \tag{15.2}$$

It is apparent that $W(0) = 1$ since all molecules must have a residence time of zero or longer and that $W(\infty) = 0$ since all molecules will eventually leave the system. Also, the function $W(t)$ will be nonincreasing.

Washout experiments can be used to measure the RTD in continuous flow systems. A good step change must be made at the reactor inlet. The concentration of tracer molecules leaving the system must be accurately measured at the outlet. If the tracer has a background concentration, it is subtracted from the experimental measurements. The flow properties of the tracer molecules must be similar to those of the reactant molecules. It is usually possible to meet these requirements in practice. The major theoretical requirement is that the inlet and outlet streams have unidirectional flows so that molecules that once entered the system stay in until they exit, never to return. Systems with unidirectional inlet and outlet streams are ***closed*** in the sense of the axial dispersion model, that is, $D_{\text{in}} = D_{\text{out}} = 0$. See Sections 9.3.1 and 15.5.2. Most systems of chemical engineering importance are closed to a reasonable approximation.

The use of inert tracer experiments to measure RTDs can be extended to systems with multiple inlets and outlets, multiple phases within the reactor, and species-dependent residence times. The present discussion ignores these complications, but see Suggested Further Readings.

Positive Step Changes and the Cumulative Distribution Function

Residence time distributions can also be measured by applying a positive step change to the inlet of the reactor: $C_{\text{in}} = C_{\text{out}} = 0$ for $t < 0$ and $C_{\text{in}} = C_0$ for $t > 0$. Then the outlet response, $F(t) = C_{\text{out}}(t)/C_0$, gives the ***cumulative distribution function***:

$$F(t) = \begin{array}{l}\text{fraction of molecules leaving the system that} \\ \text{experienced a residence time less than } t\end{array} \tag{15.3}$$

Properties of the cumulative distribution function are $F(0) = 0$, $F(\infty) = 1$, and $F(t)$ is nondecreasing. It is related to the washout function by

$$F(t) = 1 - W(t) \tag{15.4}$$

Thus measurement of one readily gives the other. The washout experiment is generally preferred since $W(\infty) = 0$ will be known a priori but $F(\infty) = C_0$ must usually be measured. The positive step change will also be subject to possible changes in C_0 during the course of the experiment. However, the positive step change experiment requires a smaller amount of tracer since the experiment will be terminated before the outlet concentration fully reaches C_0.

Impulse Response and the Differential Distribution Function

Suppose a small amount of tracer is instantaneously injected at time $t = 0$ into the inlet of a reactor. All the tracer molecules enter together but leave at varying times. The tracer concentration at the outlet is measured and integrated with respect to time. The integral will be finite and proportional to the total quantity of tracer that was injected. The concentration measurement at the reactor outlet is normalized by this

integral to obtain the ***impulse response function***:

$$f(t) = \frac{C_{\text{out}}(t)}{\int_0^\infty C_{\text{out}}(t)\,dt} \tag{15.5}$$

This function has the physical interpretation as

$$f(t)\,dt = \text{ fraction of molecules leaving the system that experienced a residence time between } t \text{ and } t + dt \tag{15.6}$$

It is normally called the ***differential distribution function*** (of residence times). It is also known as the density function or frequency function. It is the analog for a continuous variable (e.g., residence time t) of the probability distribution for a discrete variable (e.g., chain length l). The "fraction" that appears in Equations 15.2, 15.3, and 15.6 can be interpreted as a probability, but now it is the probability that t will fall within a specified range rather than the probability that t will have some specific value. Compare Equations 13.8 and 15.5.

The differential distribution is related to the cumulative distribution and to the washout function by

$$\begin{aligned} f(t) &= \frac{dF}{dt} = -\frac{dW}{dt} \\ F(t) &= \int_0^t f(t')\,dt' \\ W(t) &= \int_t^\infty f(t')\,dt' \end{aligned} \tag{15.7}$$

Its properties are that $f(t) \geq 0$ and that

$$\int_0^\infty f(t)\,dt = 1 \tag{15.8}$$

Experimental determination of the density function requires rapid injection of tracer molecules at the inlet to the system. Ideally, a finite number of molecules will be injected in an infinitesimal period of time. Think of quick injection using a syringe.

Mathematically, $f(t)$ can be determined from $F(t)$ or $W(t)$ by differentiation according to Equation 15.7. This is the easiest method when working in the time domain. It can also be determined as the response of a dynamic model to a unit impulse or Dirac ***delta function***. The delta function is a convenient mathematical artifact that is usually defined as

$$\begin{aligned} &\delta(t) = 0 \qquad t \neq 0 \\ &\int_{-\infty}^{\infty} \delta(t)\,dt = 1 \end{aligned} \tag{15.9}$$

The delta function is everywhere zero except at the origin, where it has an infinite discontinuity, a discontinuity so large that the integral under it is unity. The limits of integration need only include the origin itself; Equation 15.9 can equally well be written as

$$\int_{0-}^{0+} \delta(t)\,dt = 1$$

The delta function has another integral of substantial use:

$$\int_{-\infty}^{\infty} \phi(t)\,\delta(t - t_0)\,dt = \phi(t_0) \tag{15.10}$$

where $\phi(t)$ is any "ordinary" function. This suggests that $\delta(t)$ itself is not an ordinary function. Instead, it can be considered as the limit of an ordinary function. This is illustrated in Example 15.1 while Example 15.2 shows how delta functions are used in connection with Laplace transforms.

15.1.2 Means and Moments

Residence time distributions can be described by any of the functions $W(t)$,$F(t)$, or $f(t)$. They can also be described using an infinite set of parameters known as ***moments:***

$$\mu_n = \int_0^{\infty} t^n f(t)\,dt \tag{15.11}$$

where $n = 0, 1, 2, \ldots$. Compare Equation 13.9. These moments are also called ***moments about the origin.*** The zeroth moment is 1. A useful result for $n > 0$ is

$$\mu_n = n \int_0^{\infty} t^{n-1} W(t)\,dt \tag{15.12}$$

Equation 15.12 is preferred for the experimental determination of moments.

The first moment is the mean of the distribution or the mean residence time:

$$\bar{t} = \int_0^{\infty} t f(t)\,dt = \int_0^{\infty} W(t)\,dt \tag{15.13}$$

Thus $\bar{t}$ can be found from inert tracer experiments. It can also be found from measurements of the system inventory and throughput since

$$\bar{t} = \frac{\hat{\rho} V}{\rho_{\text{out}} Q_{\text{out}}}$$

Agreement of the $\bar{t}$'s calculated by these two methods provides a good check on experimental accuracy. Occasionally, Equation 15.13 is used to determine an unknown volume or an unknown density from inert tracer data.

Roughly speaking, the first moment, $\bar{t}$, measures the size of a RTD, while higher moments measure its shape. The ability to characterize shape is enhanced by using ***moments about the mean***:

$$\mu_n' = \int_0^{\infty} (t - \bar{t})^n f(t)\,dt \tag{15.14}$$

Of these, the second is the most interesting and has a special name, the ***variance***:

$$\sigma_t^2 = \mu_2' = \int_0^{\infty} (t - \bar{t})^2 f(t)\,dt \tag{15.15}$$

Expanding the parenthetical term and integrating term by term give

$$\sigma_t^2 = \mu_2' = \int_0^\infty (t - \bar{t})^2 f(t)\,dt = \int_0^\infty (t^2 - 2t\bar{t} + \bar{t}^2)^2 f(t)\,dt$$
$$= \mu_2 - 2\bar{t}\mu_1 - \bar{t}^2\mu_0 = \mu_2 - \bar{t}^2 \tag{15.16}$$

This equation is normally used to calculate the variance from experimental data, μ^2 being calculated from Equation 15.11 or 15.12 using $n = 2$ and $\mu_1 = \bar{t}$ being calculated using $n = 1$. Note that either $W(t)$ or $f(t)$ can be used to calculate the moments. Use the one that was obtained directly from an experiment. If moments of the highest possible accuracy are desired, the experiment should be a negative step change to get $W(t)$ directly. Even so, accurate moments beyond the second are difficult to obtain under the best of circumstances. The weightings of t^n or t^{n-1} in Equation 15.11 or 15.12 place too much emphasis on the tail of the RTD to allow accurate numerical results.

The subscript t on σ_t^2 denotes that this variance has units of time squared. The ***dimensionless variance*** measures the breadth of a distribution in a way that is independent of the magnitude of $\bar{t}$:

$$\sigma^2 = \frac{\sigma_t^2}{\bar{t}^2} = \frac{\mu_2}{\bar{t}^2} - 1 \tag{15.17}$$

The dimensionless variance has been used extensively, perhaps excessively, to characterize mixing. For piston flow, $\sigma^2 = 0$; for a CSTR, $\sigma^2 = 1$. Most turbulent flow systems have dimensionless variances that lie between zero and 1, and σ^2 can then be used to fit a variety of residence time models, as will be discussed in Section 15.2. The dimensionless variance is generally unsatisfactory for characterizing laminar flows where $\sigma^2 > 1$ is normal in liquid systems.

The entire RTD can be made dimensionless. A ***normalized distribution*** has the residence time replaced by the ***dimensionless residence time***, $\tau = t/\bar{t}$. The first moment of a normalized distribution is 1, and all the moments are dimensionless. Normalized distributions allow flow systems to be compared in a manner that is independent of their volume and throughput. For example, all CSTRs have the same normalized RTD, $W(\tau) = \exp(-\tau)$. Similarly, all PFRs have $f(\tau) = \delta(\tau - 1)$.

15.2 RESIDENCE TIME MODELS

This section opens the black box in order to derive residence time models for common flow systems. The box is closed again in Section 15.3 where the predictions can be based on either models or measurements.

15.2.1 Ideal Reactors and Reactor Combinations

The ideal flow reactors are the CSTR and the PFR. (This chapter later introduces a third kind of ideal reactor, the segregated CSTR, but it has the same distribution

of residence times as the regular, perfectly mixed CSTR.) Real reactors sometimes resemble these ideal types or they can be assembled from combinations of the ideal types.

Single CSTR

The washout function for a CSTR is found from its response to a negative step change in tracer concentration, Equation 15.1:

$$W(t) = e^{-t/\bar{t}} \tag{15.18}$$

A CSTR has an ***exponential distribution*** of residence times. The corresponding differential distribution can be found from Equation 15.7:

$$f(t) = (1/\bar{t})e^{-t/\bar{t}} \tag{15.19}$$

Example 15.1 shows how it can be determined in the time domain as the response to a delta function input.

EXAMPLE 15.1

Apply a delta function input to a CSTR to determine $f(t)$.

SOLUTION: This solution illustrates a possible definition of the delta function as the limit of an ordinary function. Disturb the reactor with a rectangular tracer pulse of duration Δt and height $A/\Delta t$ so that A units of tracer are injected. The input signal is $C_{\text{in}} = 0,\ t < 0; C_{\text{in}} = A/\Delta t,\ 0 < t < \Delta t$; and $C_{\text{in}} = 0,\ t > \Delta t$. The outlet response is found from the dynamic model of a CSTR, Equation 14.2. The result is

$$C_{\text{out}} = \begin{cases} 0 & t < 0 \\ \left(\dfrac{A}{\Delta t}\right)[1 - e^{-t/\bar{t}}] & 0 < t < \Delta t \\ \left(\dfrac{A}{\Delta t}\right)[1 - e^{-\Delta t/\bar{t}}]\, e^{-t/\bar{t}} & t > \Delta t \end{cases}$$

Now consider the limit as Δt approaches zero. L'Hospital's rule shows that

$$\lim_{\Delta t \to 0} \frac{A}{\Delta t[1 - e^{-\Delta t/\bar{t}}]} = \frac{A}{\bar{t}}$$

The transient response to a pulse of infinitesimal duration is

$$C_{\text{out}} = \begin{cases} 0 & t < 0 \\ \dfrac{A}{\bar{t}} & t = 0 \\ \left(\dfrac{A}{\bar{t}}\right) e^{-t/\bar{t}} & t > 0 \end{cases}$$

The differential distribution is the response to a ***unit impulse***. Setting $A = 1$ gives the expected result, Equation 15.19.

Pulse shapes other than rectangular can be used to obtain the same result. Triangular or Gaussian pulses could be used, for example. The limit must be taken as the pulse duration becomes infinitesimally short while the amount of injected tracer remains finite. Any of these limits will correspond to a delta function input.

The above example shows why it is mathematically more convenient to apply step changes rather than delta functions to a system model. This remark applies when working with dynamic models in their normal form, that is, in the ***time domain***. Transformation to the ***Laplace domain*** allows easy use of delta functions as system inputs.

EXAMPLE 15.2

Use Laplace transform techniques to apply a delta function input to a CSTR to determine $f(t)$.

SOLUTION: Define the Laplace transform of $C_{\text{out}}(t)$ with respect to the transform parameter s as

$$\mathcal{L}_s[C_{\text{out}}(t)] = \int_0^\infty C_{\text{out}}(t)e^{-st}\,dt$$

The governing ODE,

$$V\frac{dC_{\text{out}}}{dt} = QC_{\text{in}} - QC_{\text{out}}$$

transforms to

$$V s\mathcal{L}_s[C_{\text{out}}(t)] - VC_{\text{out}}(0) = Q\mathcal{L}_s[C_{\text{in}}(t)] - Q\mathcal{L}_s[C_{\text{out}}(t)]$$

The $C_{\text{out}}(0)$ term is the initial condition for the concentration within the tank. It is zero when the input is a delta function. Such a system is said to be ***initially relaxed***. The term $\mathcal{L}_s[C_{\text{in}}(t)]$ is the Laplace transform of the input signal, a delta function in this case. The Laplace transform of $\delta(t)$ is 1. Substituting and solving for $a_{\text{out}}(k)$ gives

$$\mathcal{L}_s[C_{\text{out}}(t)] = \frac{\mathcal{L}_s[C_{\text{in}}(t)]}{1+\bar{t}s} = \frac{1}{1+\bar{t}s} = \frac{(1/\bar{t})}{(1/\bar{t})+s}$$

This equation is inverted to give the time-domain concentration $f(t) = C_{\text{out}}(t)$. The result is Equation 15.19.

EXAMPLE 15.3

Determine the first three moments about the origin and about the mean for the RTD of a CSTR.

SOLUTION: Use Equation 15.12 and $W(t) = e^{-t/\bar{t}}$ to obtain the moments about the origin:

$$\mu_n = \int_0^\infty t^n f(t)\,dt = \left(\frac{1}{\bar{t}}\right)\int_0^\infty t^n e^{-t/\bar{t}}\,dt$$
$$= \bar{t}^n\int_0^\infty x^n e^{-x}\,dx = \bar{t}^n\Gamma(n+1) = n!\bar{t}^n$$

where $\Gamma(n+1) = n!$ is the gamma function. Thus, for a CSTR, $\mu_1 = \bar{t}$, $\mu_2 = 2\bar{t}^2$, and $\mu_3 = 6\bar{t}^3$. To find the moments about the mean, the parenthetical term in Equation 15.14 is expanded and the resulting terms are evaluated as moments about the origin. Equation 15.16 gave the result for $n = 2$. Proceeding in the same way for $n = 3$ gives

$$\mu_3' = \int_0^\infty (t - \bar{t})^3 f(t)\, dt = = \mu_3 - 3\bar{t}\mu_2 + 2\bar{t}^3 \tag{15.20}$$

Equations 15.16 and 15.20 apply to any RTD. For the exponential distribution of a CSTR, $\mu_2' = \sigma_t^2 = \bar{t}^2$ (so that $\sigma^2 = 1$) and $\mu_3' = 2\bar{t}^3$. The general result for a CSTR is $\mu_n' = (n-1)\bar{t}^n$.

Piston Flow Reactor

Any input signal of an inert tracer is transmitted through a PFR without distortion but with a time delay of $\bar{t}$ seconds. When the input is a negative step change, the output will be a delayed negative step change. Thus for a PFR,

$$W(t) = \begin{cases} 1 & t < \bar{t} \\ 0 & t > \bar{t} \end{cases} \tag{15.21}$$

The same logic can be used for a delta function input.

EXAMPLE 15.4

The differential distribution can be defined as the outlet response of a system to a delta function input.

SOLUTION: The dynamic model governing the flow of an inert tracer through an unsteady PFR is Equation 14.13 with $\mathscr{R}_C = 0$:

$$\frac{\partial C}{dt} + \bar{u}\frac{\partial C}{\partial z} = 0 \tag{15.22}$$

The solution has any input signal being transmitted without distortion:

$$C(t, z) = C_{\text{in}}\left(t - \frac{z}{\bar{u}}\right)$$

Evaluating this solution at the reactor outlet gives

$$C_{\text{out}}(t) = C(t, L) = C_{\text{in}}(t - \bar{t})$$

The input to the reactor is the delta function $\delta(t)$ so the output is as well, $\delta(t - \bar{t})$. Thus,

$$f(t) = \delta(t - \bar{t}) \tag{15.23}$$

for a PFR. In light of this result, the RTD for piston flow is called a ***delta distribution***.

EXAMPLE 15.5

Determine the moments about the origin and about the mean for a PFR.

SOLUTION: Equation 5.11 becomes

$$\mu_n = \int_0^\infty t^n f(t)\,dt = \int_0^\infty t^n \delta(t - \bar{t})\,dt$$

Applying the integral property of the delta function, Equation 15.10, gives $\mu_n = \bar{t}^n$. The moments about the mean are all zero.

Fractional Tubularity Model

Piston flow has $\sigma^2 = 0$. A CSTR has $\sigma^2 = 1$. Real reactors can have $0 < \sigma^2 < 1$. A model that reflects this possibility consists of a stirred tank in series with a PFR, as indicated in Figure 15.1*a*. Other than the mean residence time itself, the model contains only one adjustable parameter. This parameter is called the ***fractional tubularity***, τ_p, and is the fraction of the system volume that is occupied by the piston flow element. Figure 15.1*b* shows the washout function for the fractional tubularity model.

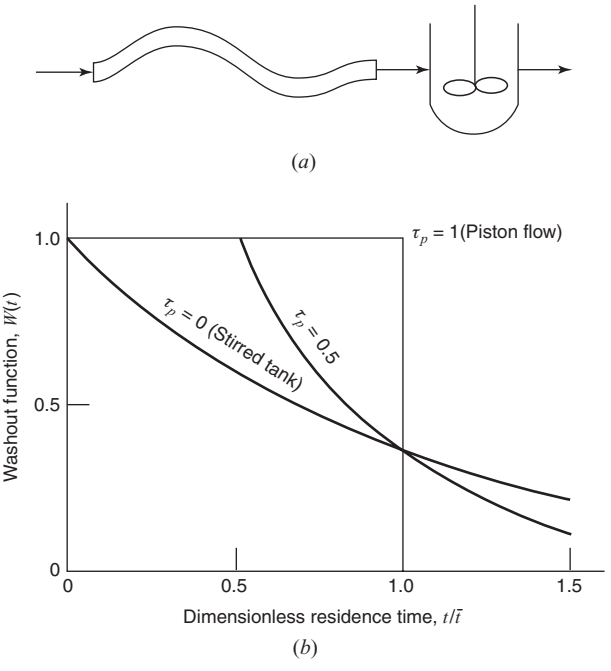

Figure 15.1 Fractional tubularity model: (*a*) physical representation; (*b*) washout function.

Its equation is

$$W(t) = \begin{cases} 1 & t < \tau_p \bar{t} \\ \exp\left[-\dfrac{(t - \tau_p \bar{t})}{\bar{t}(1 - \tau_p)}\right] & t > \tau_p \bar{t} \end{cases} \tag{15.24}$$

This equation can be fit to experimental data in several ways. The model exhibits a sharp first ***appearance time,*** $t_{\text{first}} = \tau_p \bar{t}$, which corresponds to the fastest material moving through the system. The mean residence time is found using Equation 15.13, and $\tau_p = t_{\text{first}}/\bar{t}$ is found by observing the time when the experimental washout function first drops below 1.0. It can also be fit from the slope of a plot of $\ln W$ versus t. This should give a straight line (for $t > t_{\text{first}}$) with slope $1/(\bar{t} - t_{\text{first}})$. Another approach is to calculate the dimensionless variance and then to obtain τ_p from

$$\tau_p = 1 - \sigma \tag{15.25}$$

All these approaches have been used. However, the best method for the great majority of circumstances is nonlinear least squares, as described in Section 7.1.1.

The fractional tubularity model has been used to fit residence time data in fluidized-bed reactors. It is also appropriate for modeling real stirred tank reactors that have small amounts of dead time, as would perhaps be caused by the inlet and outlet piping. It is not well suited to modeling systems that are nearly in piston flow since such systems rarely have sharp first appearance times.

Tanks-in-Series Model

A simple model having fuzzy first appearance times is the tanks-in-series model illustrated in Figure 15.2. The washout function is

$$W(t) = e^{-Nt/\bar{t}} \sum_{i=0}^{N-1} \frac{N^i t^i}{i! \bar{t}^i} \tag{15.26}$$

The corresponding differential distribution is

$$f(t) = \frac{N^N t^{N-1} e^{-Nt/\bar{t}}}{(N-1)! \bar{t}^{N-1}} \tag{15.27}$$

where N (an integer) is the number of tanks in series. Each tank, individually, has volume V/N and mean residence time $\bar{t}/N$. The model reduces to the exponential distribution of a single stirred tank for $N = 1$. It approaches the delta distribution of piston flow as $N \to \infty$. The model is well suited to modeling small deviations from piston flow. Physical systems that consist of N tanks (or compartments or cells) in series are fairly common, and the model has obvious utility for these situations. The model is poorly suited for characterizing small deviations from the exponential distribution of a single stirred tank because N takes only integer values. However, extensions to the basic tanks-in-series model allow N to take noninteger values and even $N < 1$. The ***fractional tank extension*** has a physical interpretation as N equal-sized tanks followed by one smaller tank. See Stokes and Nauman (1970) or the

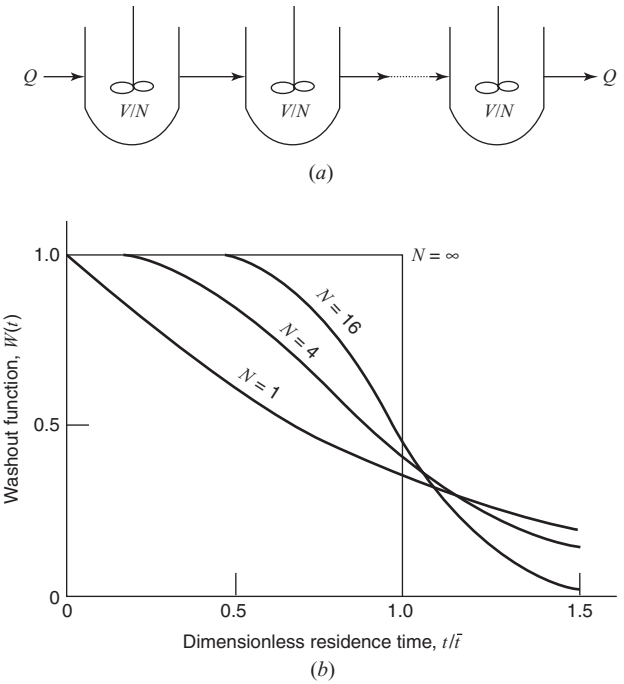

Figure 15.2 Tanks-in-series model: (*a*) physical representation; (*b*) washout function.

Suggested Further Readings. Another extension to the basic model extends the fact that

$$\sigma^2 = \frac{1}{N} \tag{15.28}$$

when N is an integer. Using Equation 15.28 for noninteger N is possible but destroys the physical basis for the model. The factorial in the denominator of Equation 15.27 must be interpreted as a gamma function. Thus the model is called the ***gamma function extension*** to the tanks-in-series model.

Recycle Reactors

High rates of external recycle have the same effect on the RTD as high rates of internal recycle in a stirred tank. The recycle reactor in Figure 4.2 can represent a physical design or it can be a model for a stirred tank. The model requires the once-through RTD. In principle, this distribution can be measured by applying a step change or delta function at the reactor inlet, measuring the outlet response, and then destroying the tracer before it has a chance to recycle. In practice, theoretical models for the once-through distribution are used. The easiest way of generating the composite distribution is by simulation.

EXAMPLE 15.6

Determine the washout function if a diffusion-free, laminar flow reactor is put in a recycle loop. Assume that 75% of the reactor effluent is recycled per pass.

SOLUTION: Refer to Figure 4.2 and set $Q = Q_{in} = Q_{out} = 0.25\ m^3\ s^{-1}$, $q = 0.75\ m^3\ s^{-1}$, and $V = 1\ m^3$. Then $\bar{t}$ is 4 s for the overall system and 1 s for the once-through distribution. The differential distribution corresponding to laminar flow in a tube was found in Section 8.1.3. The corresponding washout function can be found using Equation 15.7. See also Section 15.2.2. The once–through washout function is

$$W(t) = \frac{1}{4t^2} \qquad t > \frac{1}{2}$$

Now select a few hundred thousand molecules. Twenty-five percent will leave after one pass through the reactor. For each of them, pick a random number, $0 < \text{Rnd} < 1$, and use the washout function to find a corresponding value for their residence time in the system, t. This requires a numerical solution when $W(t)$is a complicated function, but for the case at hand

$$t = t_1 = \sqrt{\frac{1}{4W_1}} \qquad \text{where } W_1 = \text{Rnd}$$

Of the 75% that survive the first pass, 25% will leave after the second pass. Their residence time will be

$$t = t_1 + t_2 = \sqrt{\frac{1}{4W_1}} + \sqrt{\frac{1}{4W_2}}$$

where W_1 and W_2 are determined from independently selected random numbers. This procedure is repeated until nearly all the molecules have left. The various residence times are then sorted by duration, starting from the lowest value for t. The sorted results are counted as a function of t and the counts are divided by the original number of molecules. The result is the washout function for the system with recycle. Equation 15.13 provides a test for whether the original number of molecules was large enough. The integral of the tabulated washout function should exceed $0.999\bar{t}$ for reasonable accuracy. Results are shown in Figure 15.3.

The methodology of Example 15.6 works for any once-through RTD. The calculations will require a very large number of original molecules if the recycle ratio is large. The data in Figure 15.3 came from a starting population of $2^{18} = 262{,}144$ molecules, and the recycle ratio Q/q was only 3 : 1. This first appearance time for a reactor in a recycle loop is the first appearance time for the once-through distribution divided by $Q/q + 1$. It is thus 0.125 in Figure 15.3 and declines rather slowly as the recycle ratio is increased. However, even at $Q/q = 3$, the washout function is remarkably close to that for the exponential distribution.

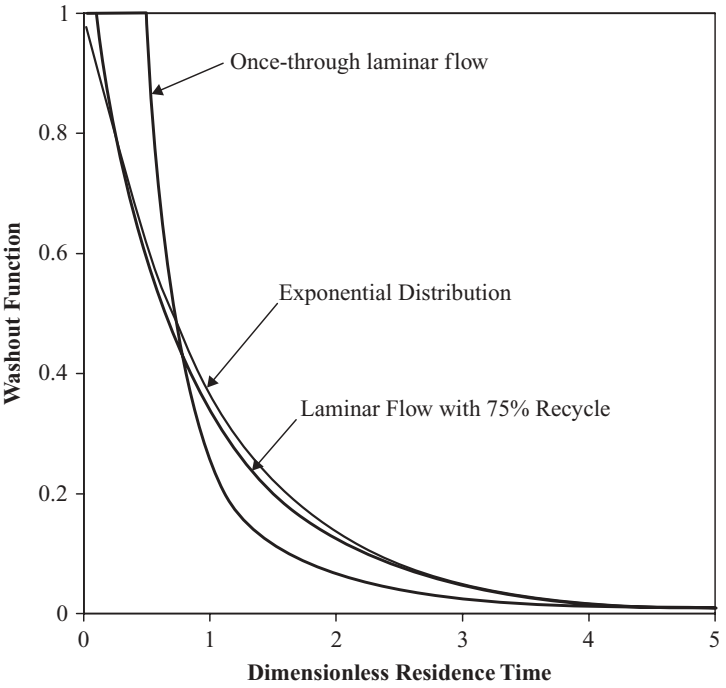

Figure 15.3 Effect of recycle on laminar flow reactor.

Pathological Behavior

An important use of residence time measurements is to diagnose flow problems. As indicated previously, the first test is whether or not $\bar{t}$ has its expected value. A low value suggests fouling or stagnancy. A high value is more likely caused by experimental error.

The second test supposes that $\bar{t}$ is reasonable and compares the experimental washout curve to what would be expected for the physical design. The comparison is made to an ideal washout curve with the same value for $\bar{t}$. Suppose that the experimental curve is initially lower than the ideal curve. Then the system exhibits ***bypassing***. On the other hand, suppose the tail of the distribution is higher than expected. Then the system exhibits ***stagnancy***. Bypassing and stagnancy are easy to distinguish when the reactor is close to piston flow so that the experimental data can be compared to a step change. See Figure 15.4. They are harder to distinguish in stirred tanks because the comparison is made to an exponential curve. Figure 15.5*a* shows a design with poorly placed inlet and outlet connections that would cause bypassing. Figure 15.5*b* shows the two washout functions. Bypassing causes the washout curve to initially decline faster than the exponential distribution. However, the integral under the two curves must be the same since they have the same $\bar{t}$. See Equation 15.13. If the experimental washout function initially declines faster than expected, it must later decline more slowly.

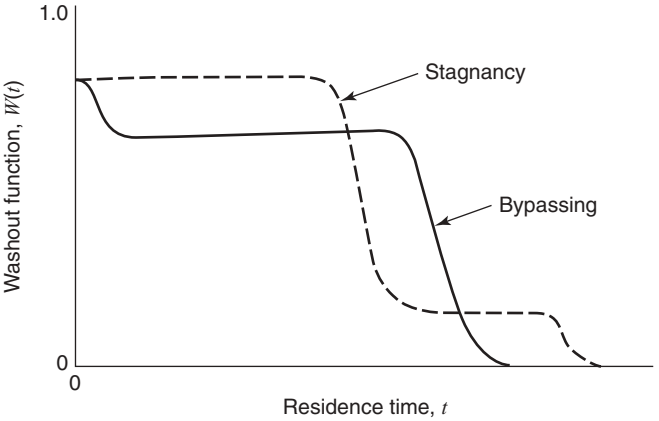

Figure 15.4 Bypassing and stagnancy in a system near piston flow.

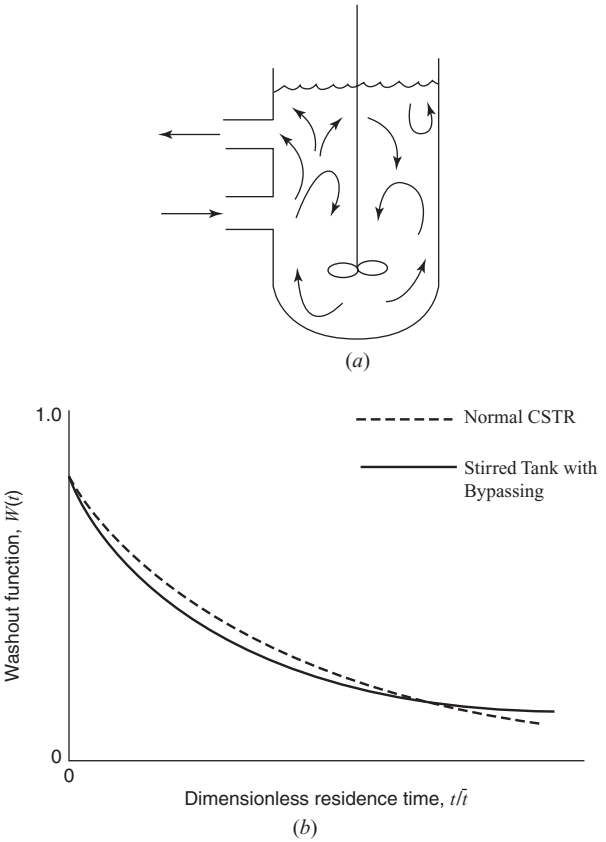

Figure 15.5 Pathological residence time behavior in a poorly designed stirrred tank: (*a*) physical representation; (*b*) washout function.

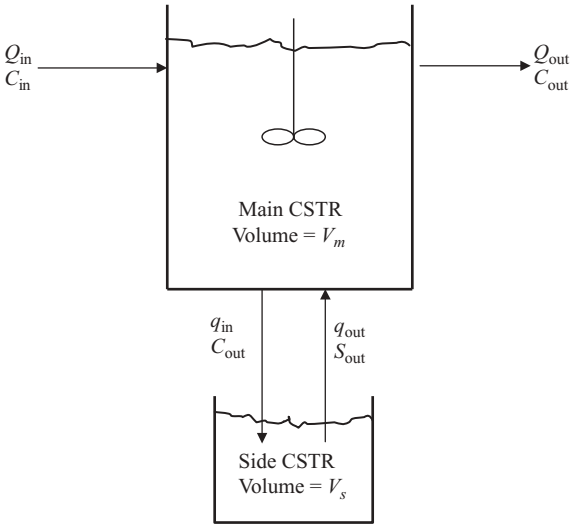

Figure 15.6 Side capacity model of stagnancy in a CSTR.

When a stirred tank exhibits either bypassing or stagnancy, $\sigma^2 > 1$ so that the tanks-in-series model predicts $N < 1$. It is more common to model bypassing or stagnancy using vessels in parallel. A stirred tank might be modeled using large and small tanks in parallel. To model bypassing, the small tank would have a residence time lower that that of the large tank. To model stagnancy, the small tank would have the longer residence time. The ***side capacity model*** shown in Figure 15.6 can also be used and is physically more realistic than a parallel connection of two isolated tanks.

EXAMPLE 15.7

Determine the washout function for the side capacity model given $Q = 8$ m^3 h^{-1}, $q = 0.125$ m^3 h^{-1}, $V_m = 7$ m^3, and $V_s = 1$.

SOLUTION: Material balances for the two tanks are

$$V_m \frac{dC_{out}}{dt} = QC_{in} + qS_{out} - QC_{out} - qC_{out}$$

$$V_s \frac{dS_{out}}{dt} = qC_{out} - qS_{out}$$

These can be solved by classical methods (i.e., eliminate S_{out} to obtain a second-order ODE in C_{out}), by Laplace transformation techniques, or by numerical integration. The initial conditions for the washout experiment are that the entire system is full of tracer at unit concentration, $C_{out} = S_{out} = 1$. Figure 15.7 shows the result of a numerical simulation. The difference between the model curve and that for a normal CSTR is subtle and would not normally be detected by

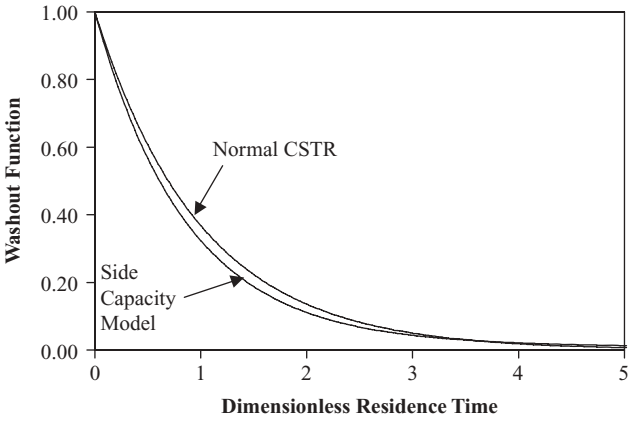

Figure 15.7 Effect of stagnant zone in stirred tank reactor according to side capacity model.

a washout experiment. The semilog plot in Figure 15.8 clearly shows the two time constants for the system, but the second one emerges as such low values of $W(t)$ that it would be missed using experiments of ordinary accuracy.

The stagnant region can be detected if the mean residence time is known independently, that is, from Equation 1.41 Suppose we know that $\bar{t} = 1$ h for this reactor and that we truncate the integration of Equation 15.13 after 5 h. If the tank were well mixed [i.e., if $W(t)$ had an exponential distribution], the integration of Equation 15.13 out to $5\bar{t}$ would give an observed $\bar{t}$ of 0.993 h. Integration of the stagnancy model out to $5\bar{t}$ gives only 0.913 h. This difference is large enough to be detected and to initiate a search for the missing reactor volume.

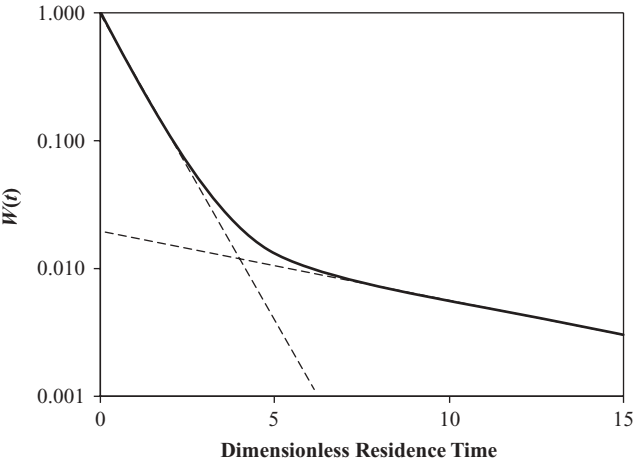

Figure 15.8 Semilog plot of washout function showing two time constants in side capacity model.

15.2.2 Hydrodynamic Models

This section describes residence time models that are based on a hydrodynamic description of the process. The theory is simplified, but the resulting models still have substantial utility as conceptual tools and for describing some real flow systems.

Laminar Flow Without Diffusion

Section 8.1.3 anticipated the use of RTDs to predict the yield of isothermal, homogeneous reactions, and Equation 8.11 gave the differential distribution function that corresponds to a parabolic velocity profile in a tube. This specific result is now derived in a more general way.

The velocity profile in a tube of length L is $V_z(r)$. The normal case is for $V_z(r)$ to have its maximum value at the centerline and to monotonically decline toward $V_z(r) = 0$ at $r = R$. The volumetric flow rate is Q. The fraction of that flow rate associated with the region from the centerline to radial position r is found from the following integral:

$$F(r) = \frac{1}{Q} \int_0^r 2\pi r' V_Z(r')\, dr' \tag{15.29}$$

Perform this integration to obtain a function of r that goes from 0 to 1 as r ranges from 0 to R. Here, $F(r)$ gives the fraction of material leaving the reactor that flowed through it at a location of r or less. The residence time of material traveling along the streamlines at position r is

$$t = \frac{L}{V_z(r)} \tag{15.30}$$

Material flowing at a position less than r has a residence time less than t because the velocity will be higher closer to the centerline. Thus $F(r) = F(t)$ gives the fraction of material leaving the reactor with a residence time less than t where Equation 15.30 relates r to t. The fraction $F(t)$ satisfies the definition, Equation 15.3, of a cumulative distribution function. Integrate Equation 15.29 to get $F(r)$. Then solve Equation 15.30 for r and substitute the result to replace r with t. When the velocity profile is parabolic, the equations become

$$F(t) = F(r) = \frac{2r^2R^2 - r^4}{R^4} \qquad t = \frac{\bar{t}}{2[1 - r^2/R^2]}$$

Elimination of r gives

$$F(t) = 1 - \frac{\bar{t}^2}{4t^2} \qquad t > \frac{\bar{t}}{2} \tag{15.31}$$

Differentiating this result gives the differential distribution found in Equation 8.11. The washout function is

$$W(t) = \begin{cases} 1 & t < \dfrac{\bar{t}}{2} \\ \dfrac{\bar{t}^2}{4t^2} & t > \dfrac{\bar{t}}{2} \end{cases} \tag{15.32}$$

This function is shown in Figure 15.9. It has a sharp first appearance time at $t_{\text{first}} = \bar{t}/2$ and a slowly decreasing tail. When $t > 4.3\bar{t}$, the washout function for parabolic flow decreases more slowly than that for an exponential distribution. Long residence times are associated with material near the tube wall; $r/R = 0.94$ for $t = 4.3\bar{t}$. This material is relatively stagnant and causes a very broad distribution of residence times. In fact, the second moment and thus the variance of the RTD would be infinite in the complete absence of diffusion.

The above derivation assumes straight streamlines and a monotonic velocity profile that depends on only one spatial variable, r. These assumptions substantially ease the derivation but are not necessary. Analytical expressions for the RTDs have been derived for noncircular ducts, non-Newtonian fluids, and helically coiled tubes. Computational fluid dynamics has been used for really complicated geometries such as motionless mixers.

In the absence of diffusion, all hydrodynamic models show infinite variances. This is a consequence of the ***zero-slip*** condition of hydrodynamics that forces $V_z = 0$ at the walls of a vessel. In real systems, molecular diffusion will ultimately remove

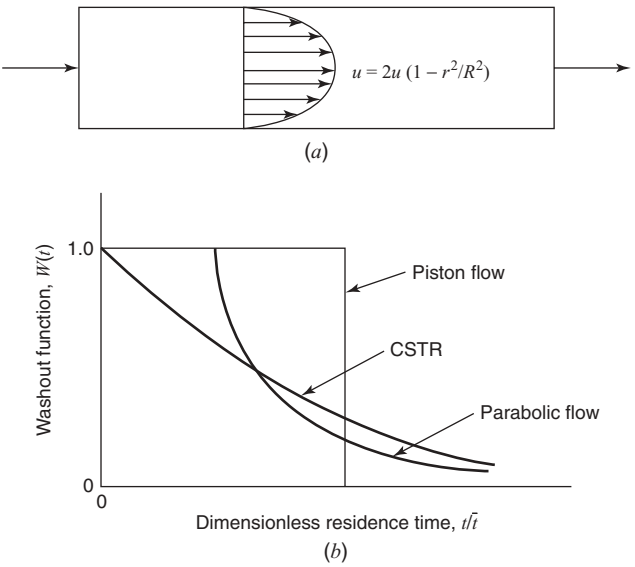

Figure 15.9 Residence time distribution for laminar flow in a circular tube: (*a*) physical representation; (*b*) washout function.

molecules from the stagnant regions near walls. For real systems, $W(t)$ will asymptotically approach an exponential distribution and will have finite moments of all orders. However, molecular diffusivities are low for liquids, and σ^2 may be large indeed. This fact suggests the general inappropriateness of using σ^2 to characterize the RTD in a laminar flow system. Turbulent flow is less of a problem due to eddy diffusion, which typically results in an exponentially decreasing tail at fairly low multiples of the mean residence time.

Axial Dispersion

Rigorous models for RTDs require use of the convective diffusion equation, Equation 14.19. Such solutions, either analytical or numerical, are rather difficult. Example 15.4 solved the simplest possible version of the convective diffusion equation to determine the RTD of a PFR. The derivation of $W(t)$ for parabolic flow was actually equivalent to solving

$$\frac{\partial C}{\partial t} + 2\bar{u}\left[\frac{1-r^2}{R^2}\right]\frac{\partial C}{\partial z} = 0$$

subject to a negative step change of inert tracer. We go now to the simplest version of the convective diffusion equation that actually involves diffusion or a diffusion-like term. It is the axial dispersion model, written here in time-dependent form,

$$\frac{\partial C}{\partial t} + \bar{u}\frac{\partial C}{\partial z} = D\frac{\partial^2 C}{\partial z^2} \tag{15.33}$$

The appropriate boundary conditions are the closed variety discussed in Section 9.3.1. The initial condition is a negative step change at the inlet. A full analytical solution is available but complex. For $\mathbf{Pe} = \bar{u}L/D > 16$, the following result is an excellent approximation:

$$W(\tau) = 1 - \int_0^{\tau} \frac{\mathbf{Pe}}{4\pi\theta^3}\exp\left[\frac{-\mathbf{Pe}(1-\theta)^2}{4\theta}\right]d\theta \tag{15.34}$$

where $\tau = t/\bar{t}$ is the dimensionless residence time. The model is defined for $0 < \mathbf{Pe} < \infty$, and the extreme values correspond to perfect mixing and piston flow, respectively. The axial dispersion model shows a fuzzy first appearance time. It is competitive with and generally preferable to the tanks-in-series model for modeling small deviations from piston flow. It should be used with caution for large deviations. As discussed in Chapter 9, predictions of the model at small **Pe** are likely to fail under close scrutiny.

EXAMPLE 15.8

Find the relationship between **Pe** and σ^2.

SOLUTION: The first step in the solution is to find a residence time function for the axial dispersion model. Either $W(t)$ or $f(t)$ would do. The function has **Pe** as a parameter. The methods of Section 15.1.2 could then be used to determine σ^2 which will give the desired relationship between **Pe** and σ^2.

We will begin by attempting to determine $f(t)$ for a closed system governed by the axial dispersion model.

Equation 15.33 is the system model. It is a linear PDE with constant coefficients and can be converted to an ODE by Laplace transformation. Define

$$\mathcal{L}_k[C(t,z)] = \int_0^\infty C(t,z)e^{-kt}\,dt$$

Note that the transform parameter is now being denoted as k. Equation 15.33 can be transformed term by term much like the transformation of an ODE. The result is

$$k\mathcal{L}_k[C(t,z)] - C(0,z) + \bar{u}\frac{d\mathcal{L}_k[C(t,z)]}{dz} = D\frac{d^2\mathcal{L}_k[C(t,z)]}{dz^2} \tag{15.35}$$

This is a second-order ODE with independent variable z and dependent variable $\mathcal{L}_k[C(t,z)]$, which is a function of z and of the transform parameter k. The term $C(t,0)$ is the initial condition and is zero for an initially relaxed system. There are two spatial boundary conditions. These are the Danckwerts conditions of Section 9.3.1. The form appropriate to the inlet of an unsteady system is a generalization of Equation 9.16 to include time dependency:

$$\bar{u}C_{\text{in}}(t) = \bar{u}C(t,0+) - D\left[\frac{\partial C(t,z)}{\partial z}\right]_{z=0+}$$

The outlet boundary condition for this unsteady but closed system is a generalization of Equation 9.17:

$$\left[\frac{\partial C(t,z)}{\partial z}\right]_{z=L} = 0$$

To use these boundary conditions with Equation 15.35, they must be transformed. The result for the inlet is

$$\bar{u}\mathcal{L}_k[C_{\text{in}}(t)] = \bar{u}\mathcal{L}_k[C(t,0+)] - D\left[\frac{d\mathcal{L}_k[C(t,z)]}{dz}\right]_{z=0+}$$

The inlet disturbance is applied through the inlet boundary condition with $C_{\text{in}}(t) = \delta(t)$ so that $\mathcal{L}_k[C_{\text{in}}(t)] = 1$. The outlet boundary condition is just $[d\mathcal{L}_k[C_{\text{in}}(t)]/dz]_{z=L} = 0$.

The cumbersome notation of the Laplace transform can be simplified. Assume $\mathcal{L}_s[C(t,z)]$ is a function of k and z. Denote it as $a = a(k,z)$ and set $C(0,z) = 0$. Also shift to a dimensionless length coordinate $\mathcal{Z} = z/L$. Then Equation 15.35 and its associated (transformed)

boundary conditions become

$$\begin{aligned} \frac{da}{d\mathcal{Z}} &= \frac{1}{\mathbf{Pe}}\frac{d^{2a}}{d\mathcal{Z}^2} - k\bar{t}a \\ a_{\text{in}} &= a(0+) - \frac{1}{\mathbf{Pe}}\left[\frac{da}{d\mathcal{Z}}\right]_{0+} \\ \left[\frac{da}{d\mathcal{Z}}\right]_1 &= 0 \end{aligned} \tag{15.36}$$

These equations are identical to Equations 9.15, 9.16, and 9.17 when we set $\mathscr{R}_A$ equal to $-ka$. The solution is necessarily identical as well. We evaluate that solution at $\mathcal{Z} = 1$ to obtain

$$a_{\text{out}}(k) = \frac{4p\ \exp(\mathbf{Pe}/2)}{(1+p)^2\ \exp(p\,\mathbf{Pe}/2) - (1-p)^2\ \exp(-p\,\mathbf{Pe}/2)} \tag{15.37}$$

where $p = \sqrt{1 + 4k\bar{t}/\mathbf{Pe}}$. Equation 15.37 gives the Laplace transform of the outlet response to an inlet delta function; that is, $a_{\text{out}}(k) = \mathcal{L}_k[f(t)]$. In principle, Equation 15.37 could be inverted to obtain $f(t)$ in the time domain. This daunting task is avoided by using properties of the Laplace transform to obtain

$$\mu_n = (-1)^n \lim_{k\to 0} \frac{d^n a(k)}{dk^n} \tag{15.38}$$

Equation 15.38 allows moments of a distribution to be calculated from the Laplace transform of the differential distribution function without need for finding $f(t)$. It works for any $f(t)$. The necessary algebra for the present case is formidable but finally gives the desired relationship:

$$\sigma^2 = \frac{2}{\mathbf{Pe}} - \frac{2}{\mathbf{Pe}^2}\left[1 - \exp(-\mathbf{Pe})\right] \tag{15.39}$$

To find **Pe** for a real system, perform a residence time experiment; calculate σ^2, and then use Equation 15.39 to calculate **Pe**.

The use of Equation 15.39 is limited to closed systems like that illustrated in Figure 15.10*a*. Measurement problems arise whenever $D_{\text{in}} > 0$ or $D_{\text{out}} > 0$. See Figure 15.10*b* and suppose an impulse is injected into the system at $z = 0$. If $D_{\text{in}} > 0$, some of the tracer may enter the reactor, then diffuse backward up the inlet stream, and ultimately reenter. If $D_{\text{out}} > 0$, some material leaving the reactor will diffuse back into the reactor to exit a second time. These molecules will be counted more than once by the tracer detection probes. The measured response function is not $f(t)$ but another function, $g(t)$, which has a larger mean:

$$\mu_1 = \left[1 + \frac{D_{\text{in}} + D_{\text{out}}}{\bar{u}L}\right]\bar{t} = \left[1 + \frac{1}{\mathbf{Pe}_{\text{in}}} + \frac{1}{\mathbf{Pe}_{\text{out}}}\right]\bar{t} \tag{15.40}$$

If μ_1 is erroneously interpreted as $\bar{t}$, results from an open system give significant errors when the inlet and outlet Peclet numbers are less than about 100. If the openness of the system cannot be avoided, the recommended approach is to rescale $g(t)$ so that

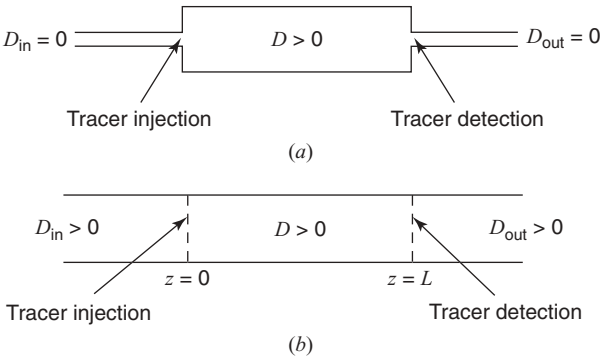

Figure 15.10 Transient response measurements for systems governed by the axial dispersion model: (*a*) closed system; (*b*) open system.

it has the correct mean:

$$[g(t)]_{\text{rescaled}} = \frac{\bar{t}\,g(t)}{\int_0^\infty t\,g(t)\,dt} = \frac{\bar{t}\,g(t)}{\mu_1} \tag{15.41}$$

The rescaled function is still not $f(t)$ but should be a reasonable approximation to it.

15.3 REACTION YIELDS

The black box is closed again. This section assumes that the system is isothermal and homogeneous and that its RTD is known. Reaction yields can be predicted exactly for first-order reactions. For other reactions, an exact prediction requires additional information about the state of mixing in the system, but knowledge of just the RTD is usually sufficient to calculate close bounds on the reaction yield.

15.3.1 First-Order Reactions

For an isothermal, first-order reaction, the probability that a particular molecule reacts depends only on the time it has spent in the system:

$$P_R = 1 - e^{-kt}$$

To find the conversion for the reactor, we need the average reaction probability for a great many molecules that have flowed through the system. The averaging is done with respect to residence time since residence time is what determines the individual reaction probabilities:

$$X_A = \bar{P}_R = \int_0^\infty (1 - e^{-kt}) f(t)\,dt = 1 - \int_0^\infty e^{-kt} f(t)\,dt$$

Expressing this result in terms of the fraction unreacted gives a simpler form:

$$Y_A = \frac{a_{\text{out}}}{a_{\text{in}}} = \int_0^\infty e^{-kt} f(t)\, dt = 1 - k \int_0^\infty e^{-kt} W(t)\, dt \tag{15.42}$$

For numerical integration, use whichever of $f(t)$ or $W(t)$ was determined experimentally. If a positive step change was used to determine $F(t)$, convert to $W(t)$ using Equation 15.4.

EXAMPLE 15.9

Use residence time theory to predict the fraction unreacted for an isothermal, homogeneous, first-order reaction occurring in a CSTR and a PFR.

SOLUTION: For the stirred tank, $W(t) = \exp(-t/\bar{t})$. Substitution into Equation 15.42 gives

$$\frac{a_{\text{out}}}{a_{\text{in}}} = 1 - k \int_0^\infty e^{-kt} e^{-t/\bar{t}} dt = \frac{1}{1 + k\bar{t}}$$

For the PFR use $f(t) = \delta(t)$ and recall Equation 15.10 to obtain

$$\frac{a_{\text{out}}}{a_{\text{in}}} = \int_0^\infty e^{-kt} \delta(t - \bar{t})\, dt = e^{-k\bar{t}}$$

EXAMPLE 15.10

Use residence time theory to predict the fraction unreacted for a closed reactor governed by the axial dispersion model.

SOLUTION: Equation 15.42 gives

$$\frac{a_{\text{out}}}{a_{\text{in}}} = \int_0^\infty e^{-kt} f(t)\, dt = \pounds_k[f(t)] \tag{15.43}$$

Thus the fraction unreacted is the Laplace transform with respect to the transform parameter k of the differential distribution function.

Example 15.8 used a delta function input in the Laplace domain to find $\pounds_k[f(t)]$. The result was Equation 15.37. Comparison with Equation 15.43 shows that $a_{\text{out}}(k)$ has already been normalized by a_{in} and is thus the fraction unreacted, Y_A.

Given $\pounds_k[f(t)]$ for any reactor, you automatically have an expression for the fraction unreacted for a first-order reaction with rate constant k. Alternatively, given $a_{\text{out}}(k)$, you also know the Laplace transform of the differential distribution of residence time (e.g., $\pounds_k[f(t)] = \exp(-k\bar{t})$ for a PFR). This fact resolves what was long a mystery in chemical engineering science. What is $f(t)$ for an open system governed by the axial dispersion model? Chapter 9 shows that the conversion in an open system is identical to that of a closed system. Thus the RTDs must be the same. It

cannot be directly measured in an open system because time spent outside the system boundaries does not count as residence but does affect the tracer measurements.

Equation 15.43 can be generalized to include operation with unsteady inlet concentrations where $a_{in} = a_{in}(t)$. The result is an unsteady output given by

$$a_{out}(t) = \int_0^\infty a_{in}(t - t')e^{-kt'} f(t')\,dt' = \int_{-\infty}^{t} a_{in}(t)e^{-k(t-t')} f(t - t')\,dt' \qquad (15.44)$$

This result allows the unsteady output to be calculated when component A reacts with first-order kinetics. The case $k = 0$, corresponding to an inert tracer, is also of interest:

$$C_{out}(t) = \int_0^\infty C_{in}(t - t')f(t')\,dt' = \int_{-\infty}^{t} C_{in}(t')f(t - t')\,dt' \qquad (15.45)$$

Equation 15.45 is applicable to nonisothermal systems since there is no chemical reaction.

EXAMPLE 15.11

Suppose the input of an inert tracer to a CSTR varies sinusoidally:

$$C_{in}(t) = C_0(1 + \beta \sin \omega t) \qquad \beta \le 1$$

Find the outlet response. What is the maximum deviation in C_{out} from its midpoint C_0?

SOLUTION: For a stirred tank, $f(t) = (1/\bar{t}) \exp(-t/\bar{t})$. The second integral in Equation 15.45 can be used to calculate the outlet response:

$$\begin{aligned} C_{out}(t) &= \int_{-\infty}^{t} C_{in}(t')f(t - t')\,dt' = \int_{-\infty}^{t} C_0(1 + \beta \sin \omega t')\,(1/\bar{t}) \exp\left[-\frac{(t - t')}{\bar{t}}\right] dt' \\ &= C_0 \frac{1 + \beta(\sin \omega t - \omega \bar{t} \cos \omega t)}{1 + \omega^2 \bar{t}^2} \end{aligned}$$

The output tracer signal is attenuated and shows a phase shift, but there is no change in frequency. All solutions to Equations 15.44 and 15.45 have these characteristics. Differentiate $\sin \omega t - \omega \bar{t} \cos \omega t$ to show that the maximum deviation occurs when $\cot \omega t = -\omega \bar{t}$. Some trigonometry then shows that the maximum deviation is

$$|C_{out} - C_0|_{max} = \frac{\beta}{\sqrt{1 + \omega^2 \bar{t}^2}} \qquad (15.46)$$

This result is useful in designing stirred tanks to damp out concentration fluctuations (e.g., as caused by a piston pump feeding the catalyst to a reactor). High-frequency noise is most easily dampened, and a single stirred tank is an efficient means for such dampening. A PFR gives no dampening. Of course, if the reactor is a stirred tank, a preliminary dampening step may not be necessary.

Chapter 14 and Section 15.2 used an unsteady-state model of a system to calculate the output response to an inlet disturbance. Equations 15.44 and 15.45 show that a dynamic model is unnecessary if the entering compound is inert or disappears according to first-order kinetics. The only needed information is the RTD, and it can be determined experimentally.

15.3.2 Other Reactions

For reaction other than first order, the reaction probability depends on the time that a molecule has been in the reactor and on the concentration of other molecules encountered during that time. The RTD does not allow a unique estimate of the extent of reaction, but some limits can be found.

Complete Segregation

A perfect mixer has an exponential distribution of residence times: $W(t) = \exp(-t/\bar{t})$. Can any other continuous flow system have this distribution? Perhaps, surprisingly, the answer to this question is a definite yes. To construct an example, suppose the feed to a reactor is encapsulated. The size of the capsules is not critical. They must be large enough to contain many molecules but must remain small compared to the dimensions of the reactor. Imagine them as small ping-pong balls as in Figure 15.11*a*.

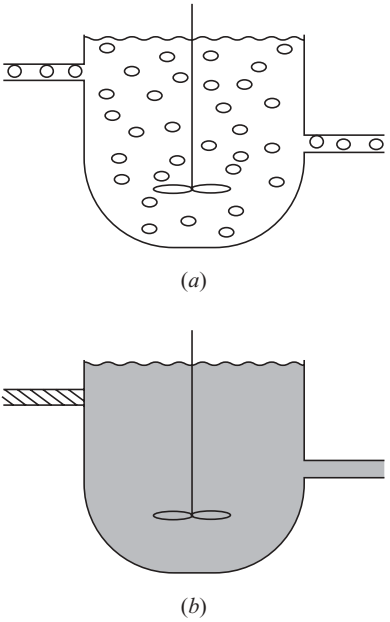

Figure 15.11 Extremes of micromixing in a stirred tank reactor: (*a*) ping-pong balls circulating in a agitated vessel, the completely segregated stirred tank reactor; (*b*) molecular homogeneity, the perfectly mixed CSTR.

The balls are agitated gently enough not to break them but well enough to randomize them within the vessel. In the limit of high agitation, the vessel can approach perfect mixing with respect to the ping-pong balls. A sample of balls collected from the outlet stream will have an exponential distribution of residence times:

$$W(t_b) = e^{-t_b/\bar{t}}$$

The molecules in the system are carried along by the balls and will also have an exponential distribution of residence time, but they are far from perfectly mixed. Molecules that entered together stay together, and the only time they mix with other molecules is at the reactor outlet. The composition within each ball evolves with time spent in the system as though the ball was a small batch reactor. The exit concentration within a ball is the same as that in a batch reactor after reaction time t_b.

We have just described a ***completely segregated stirred tank reactor.*** It is one of the ideal flow reactors discussed in Section 1.4. It has an exponential distribution of residence times but a reaction environment that is very different from that within a perfectly mixed stirred tank.

The completely segregated stirred tank can be modeled as a set of PFRs in parallel, with the lengths of the individual piston flow elements being distributed exponentially. Any RTD can be modeled as piston flow elements in parallel. Simply divide the flow evenly between the elements and then cut the tubes so that they match the shape of the washout function. See Figure 15.12. A reactor modeled in this way is said to be ***completely segregated.*** Its outlet concentration is found by averaging the concentrations of the individual PFRs:

$$a_{\text{out}} = \int_0^\infty a_{\text{batch}}(t) f(t)\, dt \tag{15.47}$$

where $a_{\text{batch}}(t)$ is the concentration of a batch or piston flow reactor after reaction time t. The inlet concentration is the same for each batch and provides the initial condition for finding $a_{\text{batch}}(t)$.

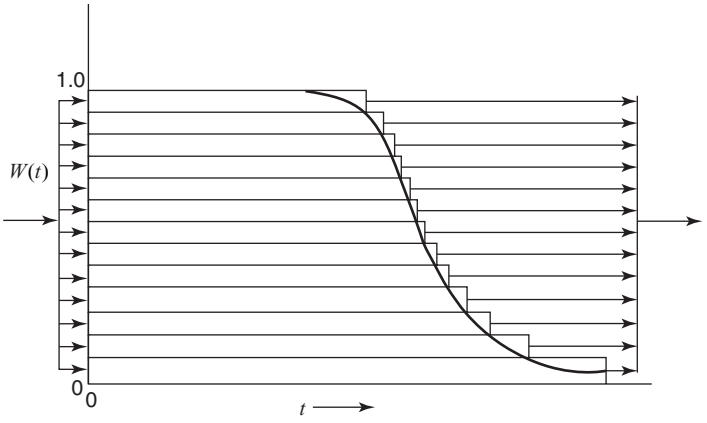

Figure 15.12 Arbitrary RTD modeled as PFRs in parallel.

EXAMPLE 15.12

Find the outlet concentration from a completely segregated stirred tank for a first-order reaction. Repeat for a second-order reaction with $\mathscr{R}_A = -ka^2$.

SOLUTION: The RTD is exponential, $f(t) = (1/\bar{t})\exp(-t/\bar{t})$. For first-order kinetics, $a_{\text{batch}}(t) = \exp(-kt)$, and Equation 15.47 gives

$$a_{\text{out}} = \left(\frac{1}{\bar{t}}\right)\int_0^\infty a_{\text{in}} e^{-kt} e^{-t/\bar{t}}\, dt = \frac{1}{1+k\bar{t}}$$

which is the same as the outlet concentration of a normal CSTR. ***The conversion of a first-order reaction is uniquely determined by the RTD.***

For a second-order reaction, $a_{\text{batch}}(t) = a_{\text{in}}/(1 + a_{\text{in}}kt)$, and Equation 15.47 gives

$$\frac{a_{\text{out}}}{a_{\text{in}}} = \int_0^\infty \frac{e^{-t/\bar{t}}\, dt}{(1+a_{\text{in}}kt)\bar{t}} = \frac{\exp[(a_{\text{in}}k\bar{t})^{-1}]}{a_{\text{in}}k\bar{t}} \int_{(a_{\text{in}}k\bar{t})^{-1}}^\infty \frac{e^{-x}}{x} dx$$

The integral can be evaluated using a tabulated function known as the exponential integral function, but numerical integration is easier. Figure 15.13 shows the performance of a segregated stirred tank and compares it to that of a normal, perfectly mixed CSTR (see Equation 1.51). Segregation gives better performance, but a PFR will be still better. The cross-hatched region in Figure 15.13 represents the conversion limits in normally designed reactors for a second-order reaction of the 2A → P type with dimensionless rate constant $a_{\text{in}}k\bar{t}$ and for reactions of the type A + B → P with perfect initial stoichiometry. The region marked "prohibited" has better performance than a PFR and is impossible. The region marked "bypassing" has worse performance than a CSTR. It is possible to operate in this region, but it can be avoided through good engineering.

The largest difference in conversion between complete segregation and perfect mixing in a stirred tank reactor is 0.07, which occurs at $a_{\text{in}}k\bar{t} = 16$, complete segregation giving the higher

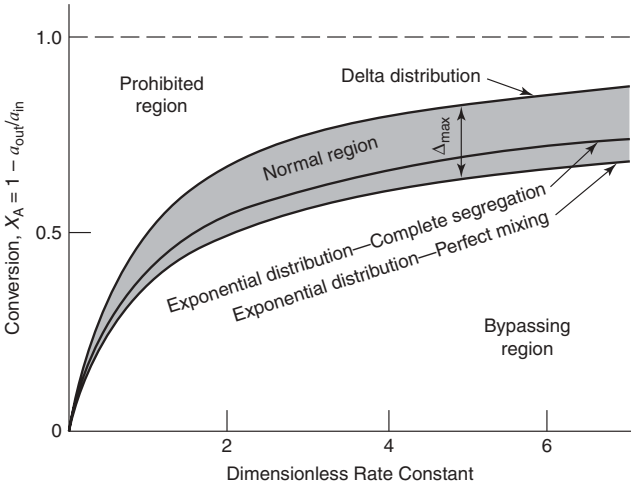

Figure 15.13 Conversion of second-order reaction in three ideal flow reactors.

conversions. The largest difference between piston flow and a normal CSTRs is 0.192, which occurs at $a_{in}k\bar{t} = 4.9$. The differences shown in Figure 15.13 are not very large in absolute terms but can have a profound effect on the reactor volume needed to achieve high conversion. In practice, single-phase CSTRs are similar to normal CSTRs with perfect internal mixing. In suspended-phase systems such as a continuous-suspension polymerization, the system is physically segregated and Equation 15.47 applies.

Maximum Mixedness

For reactions other than first order, the conversion depends not only on the residence time distribution but also on mixing between molecules having different ages. The age of a molecule is the time it has been in the reactor, and mixing between molecules with different ages is called ***micromixing.*** Completely segregated reactors have no mixing between molecules of different ages, and this zero level of micromixing is possible with any RTD. At the opposite extreme, normal CSTRs have perfect mixing between molecules, but perfect mixing in a flow system implies an exponential distribution of residence times. Perfect micromixing is impossible except with the exponential distribution. Other RTDs have some maximum possible level of micromixing, which is known as ***maximum mixedness.*** Less micromixing than this is always possible. More would force a change in the RTD.

A qualitative picture of micromixing is given in Figure 15.14. The x axis, labeled "macromixing," measures the breadth of the RTD. It is zero for piston flow, fairly broad for the exponential distribution of a stirred tank, and broader yet for situations involving bypassing or stagnancy. The y axis is micromixing, which varies from none to complete. The y axis also measures how important micromixing effects can be. They are unimportant for piston flow and have maximum importance for stirred tank reactors. Well-designed reactors will usually fall in the ***normal region*** bounded by the three apexes, which correspond to piston flow, a perfectly mixed CSTR, and a completely segregated CSTR. The line connecting the normal and segregated stirred tanks is vertical since these reactors have the same RTD. Without even measuring the RTD, we can determine limits on the performance of most real reactors just by

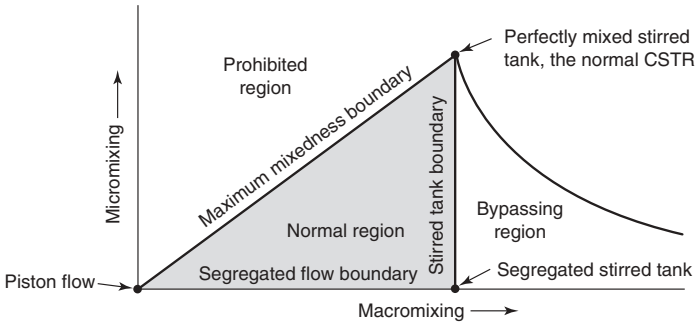

Figure 15.14 Macromixing versus micromixing; schematic representation of mixing space.

calculating the performance at the three apexes of the normal region. The calculations require knowledge only of the rate constants and the mean residence time.

When the RTD is known, the uncertainty about reactor performance is greatly reduced. A real system must lie somewhere along a vertical line in Figure 15.14. The upper point on this line corresponds to maximum mixedness and usually provides one bound on reactor performance. Whether it is an upper or lower bound depends on the reaction mechanism. The lower point on the line corresponds to complete segregation and provides the opposite bound on reactor performance. The complete segregation limit can be calculated from Equation 15.47. The maximum mixedness limit is found by solving ***Zwietering's differential equation:***

$$\frac{da}{d\lambda} + \frac{f(\lambda)}{W(\lambda)}[a_{\text{in}} - a(\lambda)] + \mathscr{R}_A = 0 \tag{15.48}$$

The solution does not use an initial value of a as a boundary condition. Instead, the usual boundary condition associated with Equation 15.48 is

$$\lim_{\lambda \to \infty} \frac{da}{d\lambda} = 0 \tag{15.49}$$

which is another way of saying that a must have a finite value in the limit of large λ. The outlet concentration from a maximum mixedness reactor is found by evaluating the solution to Equation 15.48 at $\lambda = 0$ since $a_{\text{out}} = a(0)$.

EXAMPLE 15.13

Solve Zwietering's differential equation for arbitrary reaction kinetics and an exponential RTD.

SOLUTION: The exponential distribution has $f(\lambda)/W(\lambda) = 1/\bar{t}$ so Equation 15.48 becomes

$$\frac{da}{d\lambda} + \frac{[a_{\text{in}} - a(\lambda)]}{\bar{t}} + \mathscr{R}_A = 0$$

Observe that the boundary condition will be satisfied if

$$\frac{[a_{\text{in}} - a(\lambda)]}{\bar{t}} + \mathscr{R}_A = 0$$

for all λ since this gives $da/d\lambda = 0$ for all λ. Set $\lambda = 0$ to obtain

$$a_{\text{out}} = a(0) = a_{\text{in}} + \bar{t}\ \mathscr{R}_A$$

Although this is an unusual solution to an ODE, it is the expected result since a stirred tank at maximum mixedness is a normal CSTR.

An analytical solution to Equation 15.48 can also be obtained for a first-order reaction. The solution is Equation 15.43. Beyond these cases, analytical solutions are difficult since the $\mathscr{R}_A$ is usually nonlinear. For numerical solutions, Equation 15.48 can be treated as though it were an initial-value problem. Guess a value for $a_{\text{out}} = a(0)$. Integrate Equation 15.48. If $a(\lambda)$ remains finite at large λ, the correct $a(0)$ has been

guessed. For any other $a(0)$, $a(\lambda)$ will tend toward $\pm\infty$ as $\lambda \to \infty$. This numerical approach is similar to the shooting methods of Chapter 9.5 even though the current ODE is only first order. The computed results are very sensitive to the guessed values for $a(0)$, and small changes will cause $a(\lambda)$ to range from $-\infty$ to $+\infty$. This sensitivity is beneficial since it allows $a(0)$ to be calculated with high precision.

EXAMPLE 15.14

Solve Zwietering's differential equation for the RTD corresponding to two stirred tanks in series. Use second-order kinetics with $a_{in}k\bar{t} = 5$.

SOLUTION: Equations 15.26 and 15.27 give the RTDs for the tanks-in-series model. For $N = 2$,

$$\frac{f(\lambda)}{W(\lambda)} = \frac{4\lambda}{\bar{t} + \lambda}$$

Set $a_{in} = 1$ so that a_{out} is the fraction unreacted. Then Zwietering's differential equation becomes

$$\frac{da}{d\tau} + \frac{4\tau}{1 + 2\tau}(1 - a) - 5a^2 = 0$$

where $\tau = \lambda/\bar{t}$. Solution by Euler's method with $\Delta\tau = 0.0625$ gives the following results:

$a(0)$	$a(\infty)$
0	$-\infty$
0.1	$-\infty$
0.2	$-\infty$
0.3	$+\infty$
0.25	$-\infty$
⋮	⋮
0.276	$-\infty$
0.277	$+\infty$

Obviously, $a_{out} = a(0)$ can be calculated with high precision. It happens that the precise estimate is not very accurate because of the large step size, but this can be overcome using a smaller $\Delta\tau$ or a more sophisticated integration technique. An accurate value is $a_{out} = 0.287$.

EXAMPLE 15.15

Calculate limits on the fraction unreacted for a second-order reaction with $a_{in}k\bar{t} = 5$. Consider the following states of knowledge:

(a) You know the batch kinetics, the reactor volume and throughput, and the reactor operating temperature. It is from these values that you calculated $a_{in}k\bar{t} = 5$.

(b) You have measured the RTD and know that it closely matches that for two stirred tanks in series.

(c) You know that the reactor physically consists of two stirred tanks in series.

SOLUTION: The limits you can calculate under part (a) correspond to the three apexes in Figure 15.14. The limits are 0.167 for a PFR (Equation 1.46), 0.358 for a CSTR (Equation 1.51), and 0.299 for a completely segregated stirred tank. The last limit was obtained by integrating Equation 15.47 in the form

$$\frac{a_{\text{out}}}{a_{\text{in}}} = \int_0^\infty \frac{e^{-\tau}}{1+5\tau} d\tau$$

Thus from part (a) we know that the fraction unreacted lies somewhere between 0.167 and 0.358.

The limits for part (b) are at the endpoints of a vertical line in Figure 15.14 that corresponds to the RTD for two tanks in series. The maximum mixedness point on this line is 0.287 as calculated in Example 15.14. The complete segregation limit is 0.233 as calculated from Equation 15.47 using $f(t)$ for the tanks-in-series model with $N = 2$:

$$\frac{a_{\text{out}}}{a_{\text{in}}} = \int_0^\infty \frac{4\tau e^{-2\tau}}{1+5\tau} d\tau$$

Thus knowledge of the RTD has narrowed the possible range of the fraction unreacted. It is now known to be between 0.233 and 0.287.

Part (c) considers the mixing extremes possible with the physical arrangement of two tanks in series. The two reactors could be completely segregated so one limit remains 0.233 as calculated in part (b). The other limit corresponds to two CSTRs in series. The first reactor has half the total volume so that $a_{\text{in}} k\bar{t}_1 = 2.5$. Its output is 0.463. The second reactor has $(a_{\text{in}})_2 k\bar{t}_2 = 1.16$, and its output is 0.275. This is a tighter bound than calculated in part (b). The fraction unreacted must lie between 0.233 and 0.275.

Part (c) in Example 15.15 illustrates an interesting point. It may not be possible to achieve maximum mixedness in a particular physical system. Two tanks in series—even though they are perfectly mixed individually—cannot achieve the maximum mixedness limit that is possible with the RTD of two tanks in series. There exists a reactor (albeit semi-hypothetical) that has the same RTD but that gives lower conversion for a second-order reaction than two perfectly mixed CSTRs in series. The next section describes such a reactor. When the physical configuration is known, as in part (c) above, it may provide a closer bound on conversion than provided by the maximum mixed reactor described in the next section.

Bounding Theorem

The states of complete segregation and maximum mixedness represent limits on the extent of micromixing that is possible with a given RTD. In complete segregation, molecules that enter together stay together. They are surrounded by molecules having

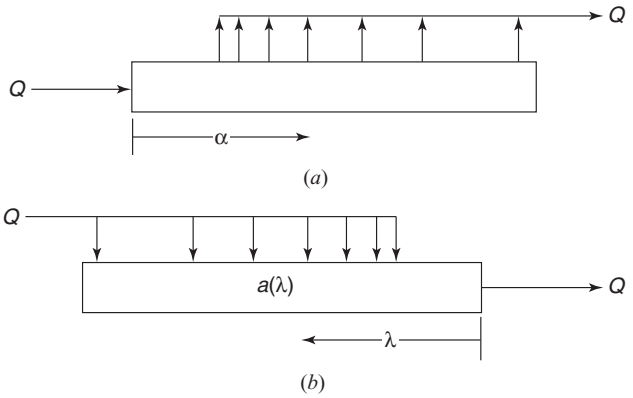

Figure 15.15 Extreme mixing models for an arbitrary RTD: (*a*) complete segregation; (*b*) maximum mixedness.

the same age and mix with molecules having different ages only when they leave the reactor. This mixing situation can be represented by a parallel collection of piston flow elements, as shown in Figure 15.12. It can also be represented as a single PFR with a large number of side exits. See Figure 15.15*a*. The size and spacing of the side exits can be varied to duplicate any RTD. Thus piston flow with side exits is capable of modeling any RTD. It is a completely segregated model since molecules in the reactor mix only with other molecules having exactly the same age.

Another way of modeling an arbitrary RTD is to use a single PFR with a large number of side entrances. See Figure 15.15*b*. The size and spacing of the entrances can be adjusted to achieve a given RTD. Thus Figure 15.15 shows two ways of representing the same RTD. The second way is quite different than the first. Molecules flow in through the side entrances and immediately mix with molecules that are already in the system. This is a maximum mixedness reactor, and there is substantial mixing between molecules having different ages. Since there is only one exit, molecules that are mixed together will leave together, but they may have entered at different times. By way of contrast, there is only one entrance to the completely segregated reactor. Molecules that are mixed together in a completely segregated reactor must necessarily have entered together but they may leave separately.

Equation 15.47 governs the performance of the completely segregated reactor, and Equation 15.48 governs the maximum mixedness reactor. These reactors represent extremes in the kind of mixing that can occur between molecules having different ages. Do they also represent extremes of performance as measured by conversion or selectivity? The ***bounding theorem*** provides a partial answer:

> Suppose $\mathscr{R}_A$ is a function of a alone and that both $d\mathscr{R}_A/da$ and $d^2\mathscr{R}_A/da^2$ do not change sign over the range of concentrations encountered in the reactor. Then, for a system having a fixed RTD, Equations 15.47 and 15.48 provide absolute bounds on the conversion of component A, the conversion in a real system necessarily falling within the bounds. If $d^2\mathscr{R}_A/da^2 > 0$, conversion is

maximized by maximum mixedness and minimized by complete segregation. If $d^2\mathscr{R}_A/da^2 < 0$, the converse is true. If $d^2\mathscr{R}_A/da^2 = 0$, micromixing has no effect on conversion.

EXAMPLE 15.16

Apply the bounding theory to an nth-order reaction, $\mathscr{R} = -ka^n$.

SOLUTION:

$$\frac{d\mathscr{R}_A}{da} = -nka^{n-1} \qquad \frac{d^2\mathscr{R}_A}{da^2} = -n(n-1)ka^{n-2}$$

The first derivative is always negative. The second derivative is negative if $n > 1$, is zero if $n = 1$, and is positive if $n < 1$. Since it does not change sign for a fixed n, the bounding theorem applies. For $n > 1$ (e.g., second-order reactions), $d^2\mathscr{R}_A/da^2 < 0$ and conversion is highest in a completely segregated reactor. For $n = 1$, the reaction is first order, and micromixing does not affect conversion. For $n < 1$ (e.g., half-order), $d^2\mathscr{R}_A/da^2 > 0$, and maximum mixedness gives the highest possible conversion.

The bounding theory gives ***sufficient*** conditions for reactor performance to be bounded by complete segregation and maximum mixedness. These conditions are not ***necessary***. In particular, the requirement that $d^2\mathscr{R}_A/da^2$ keep the same sign for $0 < a < a_{\text{in}}$ is not necessary. Some reactions show maximum rates so that the first derivative changes yet the bounding theory still applies provided $d^2\mathscr{R}_A/da^2$ does not change sign. If the second derivative does change sign, examples have been found which give a maximum conversion at an intermediate level of micromixing.

Micromixing Models

Process models based on the convective diffusion equation have an inherent level of micromixing. Examples of such models include laminar flow with or without radial diffusion and the axial dispersion model. The models can be used to predict a RTD. With that distribution comes a specific extent of micromixing, and the model contains no adjustable parameter to vary the extent of micromixing that does not also vary the RTD. Predictions from such models are used directly without explicit concern for micromixing. The RTD corresponding to the models could be associated with a range of micromixing, but this would be inconsistent with the physical model.

Empirical models like fractional tubularity and tanks in series have a range of micromixing corresponding to their RTDs and sometimes a smaller range consistent with their physical configuration. For such models it would seem desirable to have a micromixing model that, by varying some parameter, spans the possible range from maximum mixedness to complete segregation. It happens, however, that segregation is rarely observed in single-phase reactors.

The difference between complete segregation and maximum mixedness is largest when the reactor is a stirred tank and is zero when the reactor is a PFR. Even for the

stirred tank case, it has been difficult to find experimental evidence of segregation for single-phase reactions. Real CSTRs approximate perfect mixing when observed on the time and distance scales appropriate to industrial reactions provided that the feed is premixed. Even with unmixed feed, the experimental observation of segregation requires very fast reactions. The standard assumption of perfect mixing in a CSTR is usually justified. Worry when a highly reactive component is separately fed and when the reaction is sensitive to mixing time. See Section 4.6.

It is common to refer to the gross flow patterns in the reactor as ***macromixing*** and to molecular-level mixing as micromixing. In this simplified view, the RTD is determined by the macromixing, and micromixing is then imposed without substantially altering the RTD. Some thought about laminar flow with diffusion will convince you that this idea is not rigorous in general, but it does work for the exponential distribution of a stirred tank. The ***packet diffusion model*** supposes that the entering fluid is rapidly dispersed in small packets that are approximately the same size as the ***Kolmogorov scale of turbulence***:

$$\eta = \left(\frac{\mu^3}{\rho^3 \varepsilon_P} \right)^{1/4} \tag{15.50}$$

where ε_P is the power dissipation per unit mass of fluid. The ***Kolmogorov*** (also spelled Kolmogoroff) scale ranges from 10 to 100 μm in most flow fields, although sizes as low as 1 μm can be reached in the confined impingement jet mixers discussed in Section 16.1.3

Following a rapid initial dispersion to the Kolmogorov scale, the packets continue to evolve in size and shape but at a relatively slow rate. Molecular-level mixing occurs by diffusion between packets, and the rates of diffusion and of the consequent chemical reaction can be calculated. Early versions of the model assumed spherical packets of constant and uniform size. Variants now exist that allow the packet size and shape to evolve with time. Regardless of the details, these packets are so small that they typically equilibrate with their environment in much less than a second. This is so fast compared to the usual reaction half-lives and to the mean residence time in the reactor that the vessel behaves as if it were perfectly mixed.

In laminar flow stirred tanks, the packet diffusion model is replaced by a ***slab diffusion model***. The diffusion and reaction calculations are similar to those for the turbulent flow case. Again, the conclusion is that perfect mixing is almost always a good approximation for all but the fastest reactions.

15.4 EXTENSIONS OF RESIDENCE TIME THEORY

The results in this chapter are restricted in large part to steady-state, homogeneous, isothermal systems. More general theories have been developed. The next few sections briefly outline some extensions of residence time theory.

15.4.1 Unsteady Flow Systems

The RTD is normally considered a steady-state property of a flow system, but material leaving a reactor at some time θ will have a distribution of residence times regardless of whether the reactor is at steady state. The washout function for an unsteady reactor is defined as

$W(\theta, t) =$ fraction of material leaving reactor at time θ that remained in the system for a duration greater than t, i.e., that entered before time $\theta - t$

A simple equation applies to a variable-volume CSTR:

$$W(\theta, t) = \exp\left[-\int_{\theta-t}^{\theta} \frac{Q_{\text{in}}}{V} d\theta'\right] \tag{15.51}$$

where $dV/d\theta = Q_{\text{in}} - Q_{\text{out}}$. The washout function can be used in the usual way to compute instantaneous values for the moments and reaction yields, including limits of complete segregation and maximum mixedness. The unsteady stirred tank is a maximum mixedness reactor when the tank is perfectly mixed. This is the usual case, and the reaction yield is more easily calculated using Equation 14.2 than by applying Zwietering's differential equation to the unsteady RTD. Equation 15.47 applies to the complete segregation case appropriate to dispersed-phase reaction systems.

15.4.2 Contact Times

The yield of a gas–solid heterogeneous reaction depends not on the total time molecules spend in the reactor but on the time they spend on the catalyst surface. The ***contact time distribution*** provides a standardized measure of time spent in the absorbed state. A functional definition is provided by the following equation applicable to a first-order, heterogeneous reaction in an isothermal reactor:

$$\frac{a_{\text{out}}}{a_{\text{in}}} = \int_0^{\infty} e^{-kt_c} f_c(t_c)\, dt_c \tag{15.52}$$

where $f_c(t_c)$ is the differential distribution function for contact time. Equation 15.52 is directly analogous to Equation 15.43 and even provides a way of measuring $f_c(t_c)$. Vary the reaction temperature, and thus the rate constant k, over a wide range to measure $a_{\text{out}}(k)$ and then obtain $f_c(t_c)$ by inverse Laplace transformation. This approach has been used for a gas-fluidized bed, for which the assumption of isothermal operation is reasonable. The experiments detected bypassing as discussed in Section 11.3.1. Contact time distributions can also be measured using a combination of absorbable tracers. See Pustelnik and Nauman (1991).

15.4.3 Thermal Times

The analog of the residence time for a nonisothermal reaction is the thermal time:

$$t_T = \int_0^t \exp\left(\frac{-T_{\text{act}}}{T}\right) dt' \tag{15.53}$$

This is an integral along a molecule's path that weights time and temperature in the manner appropriate to homogeneous but nonisothermal reactions. For a first-order reaction,

$$\frac{a_{\text{out}}}{a_{\text{in}}} = \int_0^\infty e^{-k_0} f_T(t_T)\, dt_T \tag{15.54}$$

where $f_T(t_T)$is the differential distribution of thermal times and k_0 is the preexponential factor, the Arrhenius temperature dependence of the reaction having been incorporated in t_T. No measurement of $f_T(t_T)$ has been reported, but model-based calculations have been made for moving wall devices such as extruders. The results show that a surprisingly uniform reaction environment is possible despite diffusion-free laminar flow and large point-to-point variations in temperatures. What happens is that the hot regions are associated with high velocities and low residence times. The integral in Equation 15.53 gives a similar value for t_T in the hot regions as in the cold regions that have long residence times.

For a more complete discussion of the analogy between thermal times and residence times, see Nauman (1977).

15.5 SCALEUP CONSIDERATIONS

There are three situations where a RTD can be scaled up with confidence:

1. The pilot reactor is turbulent and approximates piston flow. The larger reactor will have the same value of $\bar{t}$ and an aspect ratio L/R at least as great as that of the pilot reactor. These possibilities include the normal ways of scaling up a tubular reactor: in parallel, in series, by geometric similarity, and by constant pressure drop. The aspect ratio increases upon scaleup except when scaling in parallel or with geometric similarity, and the Reynolds number increases except when scaling in parallel. See Section 3.2 for the details. When scaling in parallel, the larger reactor will have the same RTD as the small one. For the other forms of scaleup, the RTD will more closely approach the delta distribution.
2. The pilot reactor is a tube in isothermal or adiabatic laminar flow, and molecular diffusion is negligible. The larger reactor will have the same value for $\bar{t}$ and will remain in laminar flow. The RTD will be unchanged by the scaleup. If diffusion in the small reactor did have an influence, it will lessen upon scaleup, and the RTD will approach that for the diffusion-free case. This will hurt yield and selectivity.

3. The pilot reactor is a CSTR. The large reactor will be geometrically similar to the small one, and the scaleup will be done at constant power per unit volume. This form of scaleup exploits the fact that small vessels typically use impeller speeds that are faster than necessary to achieve a close approach to the exponential distribution. Scaleup will eventually cause problems because the ratio of circulation to throughput scales with the impeller speed, and this will decrease when scaling at constant power per unit volume. Correlations exist for the pumping capacity of common impellers, so that the ratio of circulation to throughput can be calculated. If it is maintained at a reasonable value, say 8 : 1, the RTD will remain close to exponential. Better, the impeller speed can be decreased in the small unit to anticipate what will be feasible in the large unit. Decrease it by a factor of $S^{2/9}$, where S is the intended scaleup factor for throughput. See Table 4.1. Scaling with constant power per unit volume will maintain the same Kolmogorov eddy size, so that micromixing should not become a problem.

SUGGESTED FURTHER READINGS

The ideas explored in this chapter are discussed at length in:

E. B. Nauman, and B. A. Buflham, *Mixing in Continuous Flow System,* Wiley, New York, 1983.

Much of the material is also available in:

E. B. Nauman, Invited review: Residence time distributions, *I&EC Research*, 2008.

PROBLEMS

15.1 A step change experiment of the turnoff variety gave the following results:

t	$C_{out}(t)/C_{out}(0)$
0	1.00
5	1.00
10	0.98
15	0.94
20	0.80
30	0.59
45	0.39
60	0.23
90	0.08
120	0.04

where t is in seconds. Estimate $\bar{t}$.

15.2 Determine the dimensionless variance of the RTD in Problem 15.11. Then use Equation 15.39 to fit the axial dispersion model to this system. Is axial dispersion a reasonable model for this situation?

15.3 What if anything can be said about the RTD in a nonisothermal (i.e., $T_{in} \neq T_{out}$) CSTR with variable density (i.e., $\rho_{in} \neq \rho_{out}$ and $Q_{in} \neq Q_{out}$)?

15.4 A washout experiment is performed on a CSTR to measure its mean residence time. What is the effect of starting the experiment before the outlet concentration has fully reached C_0? Assume that the normalized output response is based on the outlet concentration measured at $t = 0$ so that the experimental washout function starts at 1.0.

15.5 A positive step change experiment is performed on a CSTR to determine $F(t)$ and, from it, the mean residence time. What is the effect of a variation in the inlet concentration C_0 during the course of the experiment? Consider a change from C_0 to $C_0 + \Delta C_0$ occurring at various times.

15.6 Compare Equation 15.11 to Equation 13.9. It is clear that $f(l)$ is the discrete analog of $f(t)$ and that summation over all possible chain lengths is equivalent to integration over the 0-to-∞ range on t. What is the analog of $W(t)$ for the chain length distribution.

15.7 What are the numerical values for the two time constants in the stagnancy model of Example 15.7? See Figure 15.8, but do not use a graphical method to determine them.

15.8 Apply the side capacity model of Figure 15.7 to bypassing. Calculate and plot $W(t)$ for the case where $Q = 8\ \text{m}^3\ \text{h}^{-1}$, $q = 7\ \text{m}^3\ \text{h}^{-1}$, $V_m = 1\ \text{m}^3$, and $V_s = 8$.

15.9 Suppose that the tracer fed to the reactor in Example 15.11 is not inert but decomposes according to first-order kinetics. Show that

$$|a_{out} - a_0|_{max} = \frac{\beta}{\sqrt{(1 + k\bar{t})^2 + \omega^2\bar{t}^2}}$$

15.10 Suppose a piston pump operating at 100 strokes per minute is used to meter one component into a reactant stream. The concentration of this component should not vary by more than 0.1%. Devise a method for achieving this.

15.11 Experimental conditions prevented the application of a good step change at the inlet to the reactor, but it was possible to monitor both C_{in} and C_{out} as functions of time:

Time, s	C_{in}	C_{out}
0	0	0
3	0.072	0
6	0.078	0
9	0.081	0.008
15	0.080	0.017
20	0.075	0.020
30	0.065	0.027
40	0.057	0.035
60	0.062	0.043
80	0.068	0.051
100	0.068	0.057
120	0.068	0.062

The reactor is a gas-fluidized bed for which the fractional tubularity model is usually appropriate.

(a) Write the model as $f(t) = \alpha \exp[-\alpha(t - \tau)]$ and estimate the parameters α and τ.

(b) Use this estimate and Equation 15.45 to predict $C_{\text{out}}(t)$ given the experimental values for $C_{\text{in}}(t)$. Can your estimates for α and τ be improved by this approach? Reasonable approximations to the input signal might be as follows:

t	C_{in}
0–20	0.078
20–40	0.066
40–60	0.060
60–80	0.065
80–100	0.068

15.12 Use the data in Problem 15.1 to estimate the conversion for an isothermal, first-order reaction with $k = 0.093\ \text{s}^{-1}$.

15.13 Apply the bounding theorem to the reversible, second-order reaction

$$A + B \underset{k_r}{\overset{k_f}{\rightleftarrows}} \text{C} + \text{D}$$

Assume A, B, C, and D have similar diffusivities so that local stoichiometry is preserved. Under what circumstances will conversion be maximized by complete segregation? By maximum mixedness?

15.14 Heterogeneous reactions are often modeled as if they were homogeneous. A frequently encountered rate expression is

$$\mathscr{R}_A = \frac{ka}{1 + K_A a}$$

Suppose $k = 2\ \text{s}^{-1}$ and $K_A = 0.8\ \text{m}^3\ \text{mol}^{-1}$. Determine bounds on the yield for a reactor having $\bar{t} = 3$ s and an inlet feed concentration of 2 mol m^{-3}.

15.15 Suppose the reactor in Problem 15.14 obeys the fractional tubularity model with $\tau_p = 0.5$. Use this information to calculate narrower bounds on the yield.

15.16 A typical power input for vigorous agitation is 10 hp per 1000 gallons in systems with waterlike physical properties.

(a) Calculate the Kolmogorov scale of turbulence.

(b) Assume that a spherical droplet with a diameter equal to the Kolmogorov size is placed in a large homogeneous mass of fluid. How long will it take for concentrations inside the drop to closely approach those in the homogeneous fluid? Use $\mathscr{D} = 2 \times 10^{-9}\ \text{m}^2\ \text{s}^{-1}$ and require a 95% response to the homogeneous phase concentration.

(c) Suppose a second-order reaction with unmixed feed streams is occurring in the agitated vessel. How large can the rate constant $a_{\text{in}}k$ be if mixing and diffusion times are to remain an order of magnitude smaller than reaction times?

Chapter 16

Reactor Design at Meso-, Micro-, and Nanoscales

Another title for this chapter might be "Size Effects in Reactor Design." A recurrent theme of the book is that chemical kinetics (i.e., rate equations) are combined with transport equations (i.e., convective diffusion equations) to produce reactor design equations. The resulting design equations are sometimes simple and sometimes complex, but they always combine kinetics with transport. Rate equations depend on chemical concentrations that are averages over volume and are essentially independent of sample size until well into the nanoscale. Even a picoliter of a one molar solution will sample nearly a trillion molecules. In contrast, transport phenomena are highly dependent on the scale. Figure 16.1 shows a stream of glacial runoff in contact with seawater. The two streams are completely compatible, but the distance scale is hundreds of meters, and homogenization by molecular diffusion would require geological time. See Problem 16.1.

Traditional chemical reaction engineering deals with smaller sizes, typically with tubing and pipe sizes ranging from about 1 mm to 10 m. This will be termed the macroscale. Table 16.1 provides definitions of three smaller scales: meso, micro, and nano. These terms have been used in a variety of ways in the literature. The term "microreactor" is sometimes used for systems defined here as mesoscale. The definitions in Table 16.1 are rational if somewhat arbitrary. They are based on the characteristic size of flow channels.

At the macro-scale, the characteristic size refers to the radius R of a pipe. Rectangular ducts are more common at the smaller scales, and the characteristic size refers to the half-height of the duct, H, $2H$ being the smaller of the cross-sectional dimensions. Design equations based on continuum mechanics are adequate for single-phase systems in all but the nanoscale. At the nanoscale, the molecular nature of matter must be explicitly addressed. The characteristic flow regimes, diffusion times, and heat transfer rates listed in Table 16.1 assume a waterlike fluid. Table 16.2 provides greater detail on flow regimes and diffusion times.

The new Tunnel 3 of the water supply system for New York City has a maximum diameter of 24 ft and at full capacity would have a Reynolds number above 10 million.

Chemical Reactor Design, Optimization, and Scaleup, Second Edition. By E. B. Nauman
Copyright © 2008 John Wiley & Sons, Inc.

Figure 16.1 Glacial Runoff (top) meets seawater (bottom). Homogenization by molecular diffusion would require geological time.

The results in Table 16.2 begin with a more modest pipe, 2 m in diameter that carries water at 1 m s^{-1}. This gives **Re** = 1,000,000. As the pipe size decreases, the results in Table 16.2 suppose that the axial velocity is decreased proportionally and that the length-to-diameter ratio, L/d_t or $L/(2H)$, is held constant upon scaledown. This is a scaledown with geometric similarity and gives constant ΔP for laminar flow. See Section 3.4. The diffusion times shown in Table 16.2 are the times needed for initially unmixed components to substantially equilibrate across the duct. The tabulated times assume a waterlike fluid with $\mathscr{D}_A \bar{t}/R^2 = 1$, which gives a reasonably close approach to complete radial mixing. A similar criterion applied to a slit of half-height H gives similar results.

The numerics in Table 16.2 make two points. One is that turbulence is difficult to achieve at the mesoscale and nearly impossible to achieve in micro- and nanoscale devices. The other point is that diffusion becomes so fast at the microscale that cross-channel (e.g., radial) mixing is essentially instantaneous for all but the very fastest reactions. Thus composition and temperature will be approximately uniform in the cross-channel direction. The solutions to the convective diffusion equations in

Table 16.1 Size Scales in Chemical Reaction Engineering

Scale	Size Range, m	Typical Flow Regime	Molecular Diffusion in Laminar Flow	Heat Transfer in Laminar Flow
Macro	10^{-3} and larger	Turbulent	Very slow	Moderate
Meso	10^{-5}–10^{-3}	Laminar	Slow	Fast
Micro	10^{-7}–10^{-5}	Laminar	Fast	Very fast
Nano	10^{-9}–10^{-7}	Laminar	Very fast	Nearly instantaneous

Table 16.2 Effects of Reactor Scale for Waterlike Fluids

Domain	Cross-Channel Dimension, m	Diffusion Time in Laminar Flow	Characteristic Reynolds Number
Macro	1	6 years	1,000,000
Macro	10^{-1}	23 days	10,000
Macro	10^{-2}	6 h	100
Macro–meso	10^{-3}	3 m	1
Meso	10^{-4}	2 s	0.01
Meso–micro	10^{-5}	20 ms	10^{-4}
Micro	10^{-6}	200 μs	10^{-6}
Micro–nano	10^{-7}	2 μs	10^{-8}
Nano	10^{-8}	20 ns	10^{-10}
Nano	10^{-9}	0.2 ns	10^{-12}

Chapter 8 ignored axial diffusion, and this approach would predict reactor performance like a PFR so that conversions would be generally better than in a laminar flow reactor without diffusion. However, in microscale devices, axial diffusion becomes important and must be retained in the convective diffusions equations. The method of lines ceases to be a good solution technique, and the method of false transients is preferred. Application of the false-transient technique to PDEs, both convective diffusion equations and hydrodynamic equations, is an important topic of this chapter.

16.1 MESOSCALE REACTORS

The mesoscale with characteristic dimensions around a tenth of a millimeter is an awkward region for reactor design. Reactors at this scale are often called microreactors, but this understates their size. Even so, flows will generally be laminar. An exception, the jet impingement reactor, is discussed in Section 16.1.3. In many mesoscale reactors, diffusion times remain large. Initially unmixed components are difficult to mix, but heat transfer to the channel walls is high. The good heat transfer has led to semiserious efforts to use mesoscale reactors for the production of bulk chemicals such as phthalic anhydride. The anticipated advantage is near-isothermal operation even with highly exothermic reactions, giving excellent selectivity. The difficulty is a problem of fabrication. How can narrow channels and associated means for heat transfer be plumbed together to give total reactor volumes measured in cubic meters while the flow passages have diameters on the order of a millimeter? Clever and economic designs may arise, but in the meantime, mesoscale reactors are finding use in diagnostic applications sometimes called “lab-on-a-chip.” They can also be used for combinatorial chemistry, kinetic studies, and the production of designer molecules. Reactors can be made from plastics by injection molding or by soft lithography. In soft lithography, a photopolymerizable material is selectively crosslinked by exposure to light.

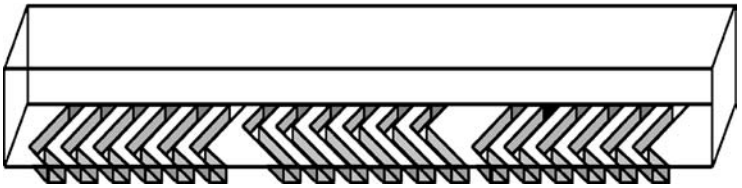

Figure 16.2 Bottom grooves to promote cross-channel mixing in a mesoscale duct. See Stroock and Whitesides (2003).

A solvent is used to dissolve the uncrosslinked areas. What remains are the walls of the reactor. Typical minimum dimensions for the flow channels are 10–100 μm. This scale reactor is used to study the chemistry of individual cells. The cell is introduced to the system, isolated, and lysed, and the effluent mixture is analyzed.

Radial mixing on the mesoscale can be enhanced using static mixers that have the mixing elements molded into the walls of the channel. A static mixer design consisting of diagonally oriented grooves on the floor of the channel is shown in Figure 16.2

Design techniques for mesoscale reactors are generally identical to those for laminar flow, macroscale reactors given in Chapter 8, although rectangular coordinates are better suited to channel flows than radial coordinates. The usual design intent is to approach piston flow with good radial or cross-channel mixing. Axial mixing remains negligible except near the side boundary with the microscale and when the L/H ratio is small.

16.1.1 Flow in Rectangular Geometries

The present section provides a brief introduction to the geometry of duct reactors and to laminar flow with negligible diffusion in such reactors. Consider a rectangular duct with width $2W$ and height $2H$ (defining W and H as the half-width and half-height is useful for the typical case where there are axes of symmetry). Equation 8.5 provides a general definition of the mixing-cup average concentration at position z. For flow in a duct it becomes

$$a_{\text{mix}}(z) = \frac{\int_{-W}^{W}\int_{-H}^{H} a(x,y,z)V_z(x,y,z)\,dy\,dx}{\int_{-W}^{W}\int_{-H}^{H} V_z(x,y,z)\,dy\,dx} = \frac{1}{4\bar{u}WH}\int_{-W}^{W}\int_{-H}^{H} aV_z\,dy\,dx \tag{16.1}$$

Note that $Q = 4\bar{u}WH$. If there is symmetry about $x = 0$ and $y = 0$, then

$$a_{\text{mix}}(z) == \frac{1}{\bar{u}WH}\int_{0}^{W}\int_{0}^{H} a(x,y,z)V_z(x,y,z)\,dy\,dx \tag{16.2}$$

The convective diffusion equation for flow in rectangular ducts is

$$\frac{\partial a}{\partial t} + \frac{\partial (V_z a)}{\partial z} = \mathscr{D}_A \left[\frac{\partial^2 a}{\partial x^2} + \frac{\partial^2 a}{\partial y^2} + \frac{\partial^2 a}{\partial z^2} \right] + \mathscr{R}_A \tag{16.3}$$

The associated boundary conditions are zero slope at the walls and at any planes of symmetry. The counterpart of Equation 16.3 for the convective diffusion of heat is

$$\rho C_p \frac{\partial T}{\partial t} + \frac{\partial (\rho C_p V_z T)}{\partial z} = \boldsymbol{\kappa} \left[\frac{\partial^2 T}{\partial x^2} + \frac{\partial^2 T}{\partial y^2} + \frac{\partial^2 T}{\partial z^2} \right] - \Delta H_R \mathscr{R} \tag{16.4}$$

The boundary conditions are specified temperatures or zero slope at the walls and zero slope at any planes of symmetry. Compare Equations 8.20 and 8.24. The major difference is that V_z is now a function of x and y rather than just r. Compare also Equations 8.50 and 8.51. Flows in the cross-channel directions that correspond to V_r have been ignored because cross-channel diffusion in microscale devices will largely eliminate the concentration and temperature gradients that drive these flows.

The velocity profile $V_z(x, y)$ must be determined. Suppose $W/H \gg 1$ so that side-wall effects at $x = \pm W$ can be ignored. This limiting case is known as slit flow or flow between parallel plates. The velocity profile within the slit is

$$V_z(y) = 1.5\bar{u} \left[1 - \frac{y^2}{H^2} \right] \tag{16.5}$$

The corresponding pressure drop is

$$\frac{dP}{dz} = \frac{-3\mu\bar{u}}{H^2} \tag{16.6}$$

The equation of motion for low-Reynolds-number channel flow is

$$\frac{\partial (\rho V_z)}{\partial t} = \frac{-dP}{dz} + \left[\frac{\partial}{\partial x} \left(\mu \frac{\partial V_z}{\partial x} \right) + \frac{\partial}{\partial y} \left(\mu \frac{\partial V_z}{\partial x} \right) \right]$$

This general form with variable viscosity applies to large slits and ducts. For the small reactors considered in this chapter, rapid diffusion will mitigate any variation of μ in the x and y directions, although μ could be a function of z. Thus,

$$\frac{\partial (\rho V_z)}{\mu \partial t} = \frac{1}{\mu} \frac{-dP}{dz} + \frac{\partial^2 V_z}{\partial z^2} + \frac{\partial^2 V_z}{\partial y^2} \tag{16.7}$$

The boundary conditions are zero velocity at the walls and zero slope at any planes of symmetry. Analytical solutions for the velocity profile in square and rectangular ducts are available but cumbersome, and a numerical solution is usually preferred. This is the reason for the transient term in Equation 16.7. A flat velocity profile is usually assumed as the initial condition. As in Chapter 8, V_z is assumed to vary slowly, if at all, in the axial direction. For single-phase flows, $\bar{u}$ can vary in the axial direction due to changes in mass density and possibly to changes in cross-sectional area. The continuity equation is just $A_c \bar{u} \rho =$ constant because the cross-channel velocity components are ignored.

16.1.2 False Transients Applied to PDEs

The method of false transients was used in Chapter 4 to solve the algebraic equations that govern a steady-state CSTR. Time derivatives were added to the algebraic equations to give ODEs. The ODEs were then integrated until a steady state was reached. The same approach can be used to solve PDEs. A time derivative has been included in Equation 16.7. The result remains a PDE with t as an additional, independent variable. Finite-difference approximations are written for the various spatial derivatives, converting the PDE into a set of ODEs with time (or false time) as the independent variable. The ODEs are integrated with respect to time until a steady state is achieved. Like the CSTR case, the method of false transients can sometimes model an actual transient, but its use here is to find the long-time solution that is the steady-state solution to the original PDE.

The method will be illustrated using Equation 16.7, with constant ρ and μ, to find the velocity profile in a rectangular duct. Equation 16.7 is converted to an ODE by using second-order approximations for the spatial derivatives. The result is

$$\frac{\rho}{\mu}\frac{dV_z}{dt} = \frac{1}{\mu}\frac{-dP}{dz} + \frac{V(x-\Delta x, y) + V(x+\Delta x, y)}{\Delta x^2} - \frac{2(\Delta x^2 + \Delta y^2)V(x, y)}{\Delta x^2\,\Delta y^2} + \frac{V(x, y-\Delta y) + V(x, y+\Delta y)}{\Delta y^2} \tag{16.8}$$

This set of ODEs can be solved by any convenient method. The computational template is shown in Figure 16.3. Five points, centered around (x, y, t) on the x–y plane, are used to project ahead to one point, $V_z(x, y, t + \Delta t)$, at the new time.

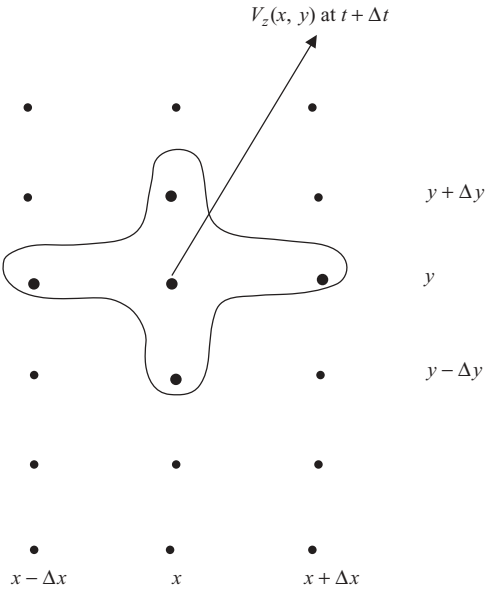

Figure 16.3 Computational template for the method of false transients.

Set $\Delta x = \Delta y$ (this does not imply a square duct with $W = H$). Then

$$\frac{dV_z}{d\theta} = \frac{\Delta y^2}{\mu}\left(\frac{-dP}{dz}\right) + V(x - \Delta x, y) + V(x + \Delta x, y) - 4V(x, y) + V(x, y - \Delta y) + V(x, y + \Delta y) \tag{16.9}$$

where θ is arbitrary since solution is by the method of false transients. Example 16.1 illustrates the solution for the velocity profile and the relationship between pressure drop and flow rate for a square duct. The example case is in the microscale rather than the mesoscale. It illustrates the applicability of the approach to both scales. The same technique can be used on the macroscale. It becomes problematic on the nanoscale due to wall effects.

EXAMPLE 16.1

Determine the axial velocity profile for laminar flow in a square duct. Also determine the pressure drop per unit length for water in a square duct with $H = 1$ μm (each side is 2 μm) when the average velocity is 10 μm s^{-1}.

SOLUTION: Code for Example 16.1 uses Euler's method for solution. Some results are as follows:

Grid Size, $I = J$	$\frac{-1}{\mu}\left(\frac{dP}{dz}\right)$	Mean Velocity, $\bar{u}$	Maximum Velocity, $V_z(0, 0)$	Normalized Maximum, $V(0, 0)/\bar{u}$
8	1	0.1388	0.2938	2.1164
16	1	0.1401	0.2945	2.1013
32	1	0.1405	0.2946	2.0975
64	1	0.1405	0.2947	2.0966

The analytical solution gives $V(0, 0)/\bar{u} = 2.0963$. As may be seen from Equation 16.6 or 16.8, the axial velocity is proportional to the pressure gradient. Setting $A = 1$ in the macro in Code for Example 16.1 gives $\bar{u} = 0.1405$. Setting $A = 7.114$ would give $\bar{u} = 1.0$. Thus,

$$\left(\frac{dP}{dz}\right) = \frac{-7.114\,\mu\bar{u}}{H^2} \tag{16.10}$$

The factor of H^2 in the denominator arises from computing the average velocity in a duct with $W = H$.

Equation 16.10 is the counterpart for a square duct of Equation 3.18 for a circular duct. The units are consistent. Using SI units for μ, $\bar{u}$, and H will give the pressure gradient in pascals per meter. The pressure drop for the example case is 71,100 Pa m^{-1}. A duct length of 1 cm would give $\bar{t} = 1000$ s and a pressure drop of about 700 Pa or 0.25 psi. Thus pressure drops are small for the envisioned use as a reactor.

Code for Example 16.1

```
Sub DuctVelocity()

' Laminar velocity profiles in a rectangular duct
Dim V(-1 To 256, -1 To 512)
Dim Vnew(-1 To 256, -1 To 512)

Iwall = 4
For jj = 1 To 4  'The main loop changes the grid size to test convergence
   Iwall = 2 * Iwall
   dx2 = 1 / Iwall ^ 2
   Jwall = Iwall  'This makes it a square duct
   A = 1          'Pressure drop constant
   dt = 0.00005  'Adequately small for Iwall = 64.

   For i = -1 To Iwall - 1   'Set initial condition
   For j = -1 To Jwall - 1
      V(i, j) = 1
   Next: Next
   For i = 0 To Iwall - 1    'Set wall BC
      V(i, Jwall) = 0
   Next
   For j = 0 To Jwall - 1    'Set wall BC
     V(Iwall, j) = 0
   Next
   t = 0

Do        'This loop preforms the false transient
   t = t + dt
   For i = 0 To Iwall - 1    'Take one step in time
```

```
   For j = 0 To Jwall - 1
      x = A * dx2 + V(i - 1, j) + V(i + 1, j) + V(i, j - 1) + V(i, j + 1) - 4 * V(i, j)
      Vnew(i, j) = V(i, j) + x * dt / dx2
   Next: Next
   For i = 0 To Iwall - 1
   For j = 0 To Jwall - 1
      V(i, j) = Vnew(i, j)
   Next: Next
   For i = 0 To Iwall - 1   'Set symmetry BC
      V(i, -1) = V(i, 1)
   Next
   For j = 0 To Jwall - 1   'Set symmetry BC
      V(-1, j) = V(1, j)
   Next j
Loop While t < 3   'Tested to closely approximate steady state

   Q = 0  'This starts a two-dimensional version of the trapizoidal rule
   For i = 1 To Iwall - 1
   For j = 1 To Jwall - 1
      Q = Q + V(i, j)
   Next: Next
   For i = 1 To Iwall - 1
      Q = Q + V(i, 0) / 2
   Next
   For j = 1 To Jwall - 1
      Q = Q + V(0, j) / 2
   Next
   Q = (Q + V(0, 0) / 4)
   ubar = Q / Iwall / Jwall
   Cells(jj, 1) = Iwall
   Cells(jj, 2) = ubar
   Cells(jj, 3) = V(0, 0)
   Cells(jj, 4) = V(0, 0) / ubar
Next jj

End Sub
```

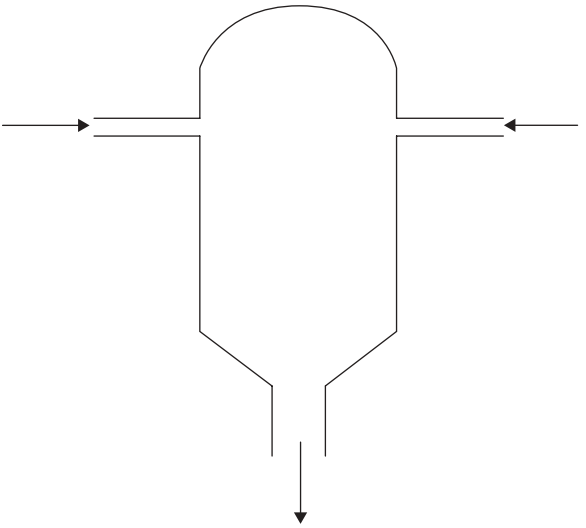

Figure 16.4 Impinging jet mixer/reactor.

16.1.3 Jet Impingement Mixers

A jet impingement mixer can be just a pipe tee. Two high-velocity streams enter the tee from opposite sides and leave through a relatively large side leg. Such devices have long been used to premix reactants. An example is reaction injection molding where the two components of polyurethane are mixed prior to entering a mold where the reaction occurs. For very fast reactions, the mixer becomes the reactor. Jet impingement mixers have been used to make ~50-nm particles of barium sulfate by the reaction of barium chloride with sulfuric acid. A mesoscale reactor with 0.5-mm-diameter inlet tubes was able to achieve such high power dissipations that the Kolmogorov scale was 1 μm, an order of magnitude lower than what is normally considered intensive mixing. Also, production rates of up to 4 kg h^{-1} are surprisingly large for a mesoscale reactor. Figure 16.4 shows a jet impingement reactor with a mixing chamber that surrounds the point of impingement. Computational fluid dynamics has aided in the optimization of such designs.

16.2 MICROSCALE REACTORS

The anticipated future designs on the microscale may use hard lithography where the reactor is formed by cutting channels in silicon using ion beams. These smaller designs have already been implemented to study protein folding. Both soft and hard lithography give rectangular channels that become ducts in a subsequent fabrication step that provides a cover for the channel. Thermal diffusivities are high enough that the reactors will be approximately isothermal at both the meso- and microscales, but they differ in the effects of molecular diffusion. The dimensionless diffusion number

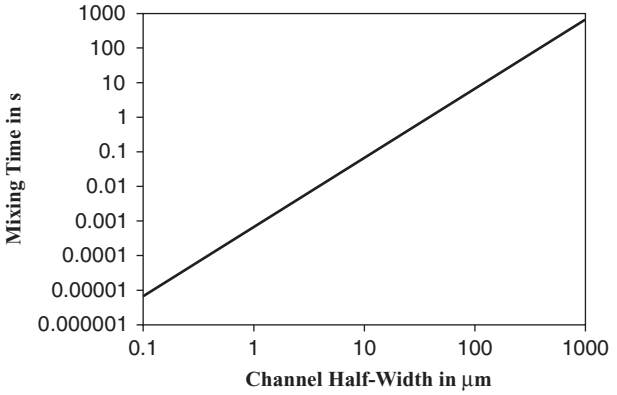

Figure 16.5 Mixing times for waterlike fluids in ducts.

$\mathscr{D}_A \bar{t}/R^2$ increases by a factor of 10^6 when R (or H) decreases by a factor of 10^3, which is the nominal difference between these scales. Thus even initially striated but compatible fluids will become uniform in very short times.

The use of microscale reactors is not confined to single-phase systems. Both striated and droplet flows of two-phase liquid mixtures have been studied, as have suspensions of solid particles. It seems that almost any chemistry can be used at the microscale. Effectiveness factors in heterogeneous catalysis will be nearly 1.0 since diffusion distances are so small. As pointed out below, rapid molecular diffusion gives nearly instantaneous cross-channel mixing and may cause significant axial mixing.

16.2.1 Mixing Times

Figure 16.5 allows estimates of the time required to achieve compositional uniformity when a minor component is injected along one wall. Equation 16.3 was simplified to

$$V_z(y)\frac{\partial a}{\partial z} = \mathscr{D}_A \frac{\partial^2 a}{\partial y^2}$$

with the velocity profile of Equation 16.5. The response of the system is governed by the initial distribution of components and a dimensionless diffusion number, $\mathscr{D}t_{\text{mix}}/H^2$. The mixing time is related to the mixing length by $L_{\text{mix}} = \bar{u}t_{\text{mix}}$.

The results in Figure 16.5 apply to waterlike fluids and to asymmetric injection of the minor component along one wall. Compositional uniformity is defined as a 99% response to the equilibrium concentration of the minor component at the opposite wall. The required value for $\mathscr{D}t_{\text{mix}}/H^2$ is a very weak function of the concentration ratio, and $\mathscr{D}t_{\text{mix}}/H^2 = 1.6$ is adequate for minor component concentrations in the range 0.1–50%. The key point is that radial mixing in microscale devices will be essentially instantaneous for all but the fastest reactions. An acid–base titration will go to completion in 67 milliseconds in a duct with half-width $H = 10$ μm and will go to completion in approximately 1 μs when $H = 0.1$ μm.

16.2.2 Radial or Cross-Channel Diffusion

The false-transient method can be applied to convective diffusion equations in a manner similar to that used for velocity profiles. Finite-difference approximations are written for the spatial derivatives. Second-order approximations can be used for first derivatives since they involve only the same five points needed for the second derivatives. The result is a set of simultaneous ODEs with (false) time as the independent variable. The computational template of Figure 16.3 is unchanged. The next two examples illustrate its application to problems where axial diffusion is negligible. Such problems are also readily solved by the method of lines as described in Chapter 8. Cases with significant axial diffusion are troublesome for the method of lines and require special boundary conditions for the method of false transients. They are treated in Section 16.2.4.

EXAMPLE 16.2

Use the method of false transients for the Graetz problem in Example 8.4. Specifically, solve the Graetz problem for $\alpha_T \bar{t}/R^2 = 0.4$ and report your results in terms of the dimensionless temperature

$$\mathcal{T} = \frac{T - T_{\text{in}}}{T_{\text{wall}} - T_{\text{in}}}$$

SOLUTION: The heat of reaction and axial diffusion terms are omitted from Equation 8.27 to give the governing PDE for the Graetz problem:

$$\frac{\partial \mathcal{T}}{\partial \theta} = -\mathcal{V}_z^o(\mathcal{r})\frac{\partial \mathcal{T}}{\partial \mathcal{z}} + \left(\frac{\alpha \bar{t}}{R^2}\right)\left[\frac{1}{\mathcal{r}}\frac{\partial \mathcal{T}}{\partial \mathcal{r}} + \frac{\partial^2 \mathcal{T}}{\partial \mathcal{r}^2}\right] \tag{16.11}$$

The velocity profile is parabolic. The inlet boundary condition is $\mathcal{T} = 0$ for all $\mathcal{r}$, the wall boundary condition is $\mathcal{T} = 1$ for all $\mathcal{z}$, and the problem is axisymmetric. Applying second-order difference approximations to the spatial derivatives gives

$$\begin{aligned}\frac{d\mathcal{T}}{d\theta} = &-\mathcal{V}_z^o(\mathcal{r})\frac{\mathcal{T}(\mathcal{z}+\Delta\mathcal{z},\mathcal{r}) - \mathcal{T}(\mathcal{z}-\Delta\mathcal{z},\mathcal{r})}{2\,\Delta\mathcal{z}} \\ &+\left(\frac{\alpha \bar{t}}{R^2}\right)\frac{\mathcal{T}(\mathcal{z},\mathcal{r}+\Delta\mathcal{r}) - \mathcal{T}(\mathcal{z},\mathcal{r}-\Delta\mathcal{r})}{2\mathcal{r}\Delta\mathcal{r}} \\ &+\left(\frac{\alpha \bar{t}}{R^2}\right)\frac{\mathcal{T}(\mathcal{z},\mathcal{r}+\Delta\mathcal{r}) - 2\mathcal{T}(\mathcal{z},\mathcal{r}) + \mathcal{T}(\mathcal{z},\mathcal{r}-\Delta\mathcal{r})}{\Delta\mathcal{r}^2}\end{aligned} \tag{16.12}$$

Code for Example 16.2 gives the macro that solves this set of ODEs. Recall that $\mathcal{r} = 0$ is a special case for cylindrical coordinates.

Unsurprisingly, converged results from this example are identical to converged results from the method of lines solution as generated by Code for Example 8.4.

16.2.3 False Transients Versus the Method of Lines

Codes for Examples 8.4 and 16.2 solve the same problem by different methods. The codes are roughly similar in complexity. In previous times, the method of lines had the advantage of requiring less memory, but this has ceased to be an important factor. The method of lines also offers the convenience of needing to consider only one spatial variable, Δr, when testing convergence since the other variable, Δz, is strictly limited in size by the stability criterion. The method of false transients allows the spatial variables to be sized independently so convergence must be tested independently as well. Additionally, the equilibration time needed to closely approximate a steady state must be determined on a case-by-case basis. These equilibration times can be long; for the same problem, the method of lines is probably faster, although the method of false transients is generally easier to program. In particular, it is easier to implement for problems with three spatial variables such as flow in a rectangular duct.

16.2.4 Axial Diffusion in Microscale Ducts

Figure 16.6 illustrates a possible microscale reactor. A photoinitiated reaction occurs in the region $0 < z < L$. The flow is laminar and isothermal. The operating fluid is incompressible and other physical properties are constant. The reaction is first order with respect to component A. The convective diffusion equation is Equation 16.3 but with zero reaction outside the reaction zone, $k = 0$ if $z < 0$ or $z > L$. The inlet boundary condition is that $a = a_{\text{in}}$ at $z = -\infty$ and the outlet boundary condition is that $\partial a/\partial z = 0$ at $z = +\infty$. Zero-slope boundary conditions are imposed at the walls and there is symmetry in the x and y directions. This model system contains two design parameters, W/H and L/H, and two operating parameters, $\mathscr{D}_A\bar{t}/H^2$ and $k\bar{t}$. When physical properties are constant, the velocity profile can be found by solving Equation 16.7 independently of 16.3. The solution is illustrated in Example 16.1. In the more general case, the method of false transients is used to solve Equations 16.3 and 16.7 simultaneously.

Reference is made to Example 9.2 and Figure 9.9. The microscale reactor shown in Figure 16.6 is an *open* system although the velocity profile is no longer flat. The solution theoretically requires integration from $-\infty < z < +\infty$, but practical results

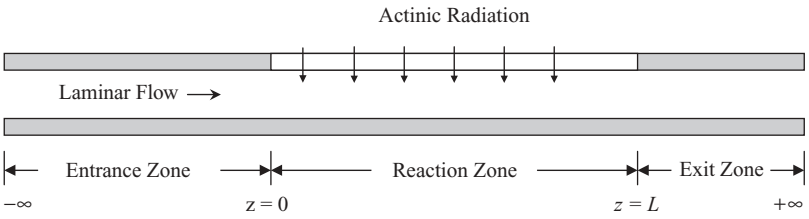

Figure 16.6 Slit flow, microscale reactor.

Code for Example 16.2

```
Sub Graetz()
'Solves Graetz proplem by the method of false transients
Dim T(-1 To 4097, -1 To 1023)
Dim Tnew(4097, 1023)
Dim Vz(4097)
Dim Cbz(4097), Cbr(4097), Cfr(4097), Crz(4097)

alpha = 0.4     'Thermal diffusion group

For jj = 2 To 5          'outer loop to test convergence
   Itotal = 2 ^ jj       'number of radial increments
   Jtotal = 4 * Itotal   'number of axial increments

   dr = 1 / Itotal     'radial increment size
   dz = 1 / Jtotal     'axial increment size
   dt = 0.0001

For i = 1 To Itotal - 1
   r = i * dr
   Vz(i) = 2 * (1 - r ^ 2)     'dimensionless velocity profile for a tube
   Cbz(i) = Vz(i) * dt / dz    'The time increment is build into the constants
   Cfr(i) = alpha * (1 / 2 / r / dr + 1 / dr ^ 2) * dt
   Cbr(i) = alpha * (-1 / 2 / r / dr + 1 / dr ^ 2) * dt
   Crz(i) = 1 - Cbz(i) - Cfr(i) - Cbr(i)
Next i
Vz(Itotal) = 0

Cbz(0) = 2 * dt / dz
Cfr(0) = 2 * alpha / dr ^ 2 * dt
Cbr(0) = Cfr(0)
Crz(0) = 1 - Cbz(0) - Cfr(0) - Cbr(0)

For i = -1 To Itotal - 1
   T(i, -1) = 0     'sets inlet temperature
Next i
```

```
For i = 0 To Itotal - 1
For j = 0 To Jtotal
   T(i, j) = 0      'sets initial temperature
Next: Next

For j = -1 To Jtotal
   T(Itotal, j) = 1   'this is the wall BC.
Next j

Do     'The false transient starts here
   For j = 0 To Jtotal
   For i = Itotal - 1 To 1 Step -1
      Tnew(i, j) = Crz(i) * T(i, j) + Cbz(i) * T(i, j - 1) + Cfr(i) * T(i + 1, j) + Cbr(i) * T(i - 1, j)
   Next i
      Tnew(0, j) = Crz(0) * T(0, j) + Cbz(0) * T(0, j - 1) + 2 * Cfr(0) * T(1, j)
   Next j
   For i = 0 To Itotal - 1
   For j = 0 To Jtotal
      T(i, j) = Tnew(i, j)
   Next j: Next i

   For j = 0 To Jtotal
       T(-1, j) = T(1, j) 'This is the centerline BC
   Next j
Ttime = Ttime + dt
Loop While Ttime < 3  'End of false transient
Ttime = 0
Sum = 0
Q = 0
For i = 1 To Itotal - 1
   Sum = Sum + 2 * dr * i * Vz(i) * T(i, Jtotal)
   Q = Q + 2 * dr * i * Vz(i)
Next i
Tbar = Sum / Q
    Cells(jj, 1) = Itotal
    Cells(jj, 2) = Tbar
Next jj
End Sub
```

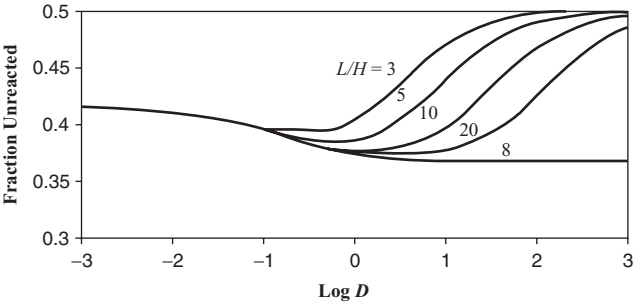

Figure 16.7 Combined effects of radial and axial diffusion on conversion for a first-order reaction with $k\bar{t} = 1$ and $D = \mathscr{D}_A\bar{t}/H^2$.

are obtained using finite values of the entrance and exit lengths. Selecting these lengths is another aspect of convergence testing.

It is desired to study the effect of cross-channel and axial diffusion, that is, the effects of varying $\mathscr{D}_A\bar{t}/H^2$, on reactor performance. In a reactor design problem, $\mathscr{D}_A$ will be fixed and $\bar{t}$ will be set to achieve some desired conversion. Thus the effective variable is H as it ranges from macro- to submicroscales. When H is large, the reactor will be a laminar flow reactor without diffusion. For smaller H, cross-channel diffusion causes reactor performance to approach that of piston flow. Still smaller H causes axial mixing and hurts performance. Reactor performance in this region is a strong function of L/H. Finally, at very small H, reactor performance approaches that of a CSTR. See Figure 16.7. These facts are obviously important to a lab-on-a-chip designer. In the examples that follow, they are illustrated for the case of $W/H \to \infty$ so that the velocity profile approximates slit flow. This assumption retains the essence of the duct flow problem but decreases the complexity of the code. Final design calculations should use the actual W/H.

EXAMPLE 16.3

Determine $a_{\text{out}}/a_{\text{in}}$ as a function of $\mathscr{D}_A\bar{t}/H^2$ for the slit flow reactor in Figure 16.6. The velocity profile is $V_z(y) = 1.5\,\bar{u}(1 - y^2/H^2)$. There is no dependence in the x direction. Assume a first-order reaction with $k\bar{t} = 1$.

SOLUTION: The equation to be solved is a simplified version of Equation 16.3 in which the x dependence is dropped and $V_z(y)$ is given by Equation 16.5. Set $\mathscr{z} = z/L$, $\mathscr{y} = y/H$, and $\tau = t/\bar{t}$. Then the equation to be solved is

$$\frac{\partial a}{\partial \tau} + \mathscr{V}_z(\mathscr{y})\frac{\partial a}{\partial \mathscr{z}} = \left(\frac{\mathscr{D}_A\bar{t}}{H^2}\right)\left(\frac{\partial^2 a}{\partial \mathscr{y}^2} + \frac{H^2}{L^2}\frac{\partial^2 a}{\partial \mathscr{z}^2}\right) - k\bar{t}a \tag{16.13}$$

Using finite-difference approximations for the spatial derivatives gives

$$\begin{aligned}\frac{da}{d\tau} &= -\mathscr{V}_z(y)\frac{a(y, z+\Delta z) - a(y, z-\Delta z)}{2\,\Delta z} - k\bar{t}a(y, z) \\ &+ \left(\frac{\mathscr{D}_A\bar{t}}{L^2}\right)\frac{a(y, z+\Delta z) - 2a(y, z) + a(y, z-\Delta z)}{\Delta z^2} \\ &+ \left(\frac{\mathscr{D}_A\bar{t}}{H^2}\right)\frac{a(y+\Delta y, z) - 2a(y, z) + a(y-\Delta y, z)}{\Delta y^2}\end{aligned} \tag{16.14}$$

A zero-slope condition is applied at the walls. The inlet boundary condition is that $a(y, -\infty) = a_{\text{in}} = 1$. Zero slope is also forced at the far upstream and downstream locations, $z = \pm\infty$. The entrance and exit lengths must be chosen large enough that an increase in size gives no significant change in a_{out}. The initial condition is somewhat arbitrary. Setting $a(y, z) = 0$ is a reasonable choice. Euler's method is used for integration with respect to time.

Code for Example 16.3 contains parameters chosen to allow a solution in a few minutes. Accurate calculations require a large number of cross-channel increments. This forces a small time step and running times of a few hours. The numerical solution of Equation 16.13 becomes ill conditioned at high values of $D = \mathscr{D}_A\bar{t}/H^2$. For first-order reactions, the analytical solution to the axial dispersion model, Equation 9.18, smoothly joins the numerical solution at the inflection points in Figure 16.7, for example, at $D = 100$ for $L/H = 20$, and was used to produce the high-D portions of Figure 16.7.

16.2.5 Second-Order Reactions with Unmixed Feed

Figure 16.8 shows a geometry where two feed streams merge into a combined stream and then react. The reaction is A + B $\xrightarrow{k}$ C. The components are mixed by diffusion in the cross-channel direction, but axial diffusion can also be important. Unlike Example 16.3, there is no fixed region where reaction occurs. It occurs everywhere that A and B are simultaneously present. The mean residence time in the reaction zone is undefined and thus cannot be used as a characteristic time. Problems of this type can be tackled by using the natural, physical variables and the natural dimensions as in Example 8.2. Alternatively, another characteristic time can be introduced to reduce the variables to dimensionless form. A reasonable choice is $t_c = H/\bar{u}$, where t_c has no physical interpretation but can be used to scale the diffusion and reaction groups $\mathscr{D}_A t_c/H^2$ and $t_c\mathscr{R}_A/a_{\text{in}}$. Figure 16.9 shows a sample result. Details are provided elsewhere (Nauman and Nigam 2005).

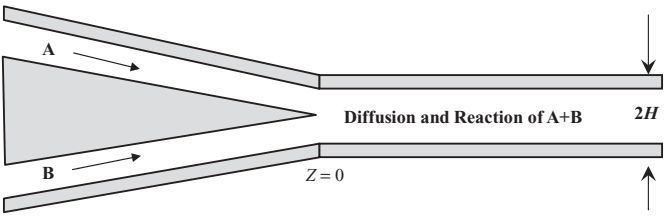

Figure 16.8 Geometry of open system suitable for second-order reaction.

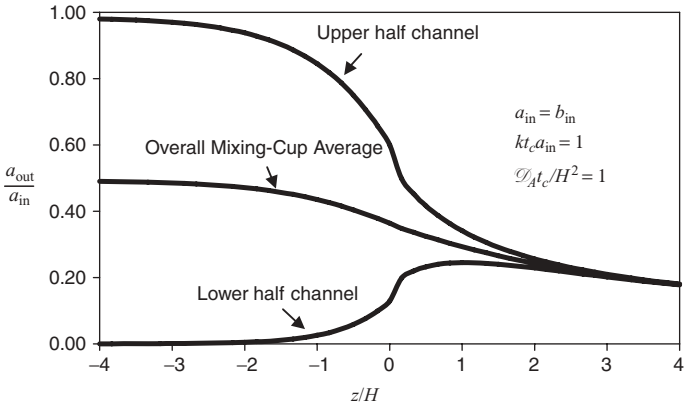

Figure 16.9 Mixing-cup average concentration profiles for a second-order reaction in the flat-plate geometry of Figure 16.8.

Code for Example 16.3

```
Sub FlatPlates()
Dim a(-1 To 128, -1024 To 8192)
Dim anew(128, -1024 To 8192), Vz(128)
Dim Dplus(128), Dminus(128), C(128)
' Laminar Flow between flat plates with radial and axial diffusion
' Open boundary conditions

Cells.Clear

ktbar = 1  'dimensionless first order rate constant
LW = 4     'reactor length to half-width ratio
ain = 1    'inlet concentration

iend = 8          'number of cross-channel increments
jend = 16         'number of axial increments in the reaction section
jin = -jend       'number of increments in inlet section
jout = 3 * jend   'number of increments in outlet section
dy = 1 / iend
dz = 1 / jend
Diff = 0.5
diffy = Diff / dy ^ 2
diffz = Diff / LW ^ 2 / dz ^ 2
dt = 0.01

For i = 0 To iend - 1
    y = i * dy
    Vz(i) = 1.5 * (1 - y ^ 2) 'Velocity profile in a slit
Next i

For j = jin + 1 To jout
For i = -1 To iend
   a(i, j) = 0       'sets initial concentration everywhere but at j = jin
Next: Next
```

```
For i = -1 To iend
   a(i, jin) = ain   'sets inlet concentration
Next

Do  'Main loop

For j = jin + 1 To jout - 1
For i = 0 To iend - 1
   del = -Vz(i) * (a(i, j) - a(i, j - 1)) / dz                    'convective term
   del = del + diffz * (a(i, j + 1) - 2 * a(i, j) + a(i, j - 1)) 'axial diffusion term
   del = del + diffy * (a(i + 1, j) - 2 * a(i, j) + a(i - 1, j)) 'radial diffusion term
   If j > 0 And j <= jend Then del = del - ktbar * a(i, j)       'reaction zone
   anew(i, j) = a(i, j) + del * dt 'Euler's method
Next: Next

For j = jin + 1 To jout - 1
For i = 0 To iend - 1
   a(i, j) = anew(i, j)
Next: Next

For i = 0 To iend - 1
   a(i, jin + 1) = a(i, jin)   ' zero slope far upstream, j = jin
   a(i, jout) = a(i, jout - 1) ' zero slope far downstream, j = jout
Next

For j = jin To jout
   a(iend, j) = a(iend - 1, j)
   a(-1, j) = a(1, j)
Next

For j = jin To jout
   Sum1 = Vz(0) * a(0, j) / 2   'Start trapezodial rule
   Sum2 = Vz(0) / 2
For i = 1 To iend - 1
  Sum1 = Sum1 + Vz(i) * a(i, j)
  Sum2 = Sum2 + Vz(i)
Next i
Cells(iend + 7, j - jin + 1) = Sum1 / Sum2 'Mixing cup average
Next j

For j = jin To jout   'entire matrix to spreadsheet
For i = 0 To iend
   Cells(1, j - jin + 1) = j
   Cells(iend + 6, j - jin + 1) = j
   Cells(i + 2, j - jin + 1) = a(i, j)
Next: Next

t = t + dt

Loop 'stop manually based on observing the outlet concentration on the spreadsheet

End Sub
```

16.2.6 Microelectronics

If renamed today, microelectronics would be called nanoelectronics since sizes have been pushed well below 1 μm. The fabrication of modern electronic devices, such as large-scale integrated circuits, involves an elaborate sequence of physical and chemical operations. As the size scale becomes smaller, it is increasingly necessary to recognize the molecular nature of matter. This and the next sections describe technology applicable to the microscale that is somewhat less than state-of-the art.

A chip fabrication process starts with a wafer of high-purity silicon that has been cut from a single crystal. Electronic functionality is achieved by creating a multilayer structure in and on the surface of the wafer in a precise geometric pattern. The pattern is laid down by a process known as ***photolithography*** using the following sequence of steps:

1. The surface is coated with a polymer, typically by spin coating
2. An image is formed on the surface using hard ultraviolet or soft x rays. If the polymer is a ***photoresist***, it crosslinks in those areas exposed to radiation. If the polymer is a ***negative photoresist***, it degrades in those areas exposed to radiation.
3. For the case of a photoresist, a solvent removes the polymer that is not crosslinked and thus exposes the underlying surface.
4. The freshly exposed surface is treated with a chemical agent, or ***dopant,*** to modify its electrical properties (e.g., to create transistors).
5. The remaining polymer is removed using a more aggressive solvent.

This procedure, with minor variations, is repeated dozens of times in the manufacture of a semiconductor chip. The chemical treatment can be done using reagents in a liquid phase, but gas phase treatment by a process known as ***chemical vapor deposition (CVD)*** has become more important as individual features in the integrated circuit become smaller.

Electrical connections are required between the various layers that are deposited on a wafer. One method for providing these connections is to pattern the surface using photolithography. Channels are then cut into the silicon substrate using ***chemical etching.*** A conductor such as copper will subsequently be deposited in the channels. Straight-sided channels having a width equal to the opening in the photoresist are desired, but experience shows that the channel will undercut the photoresist by an appreciable distance. See Figure 16.10. The reason for this is found in Equation 11.51. The etchant is an aggressive chemical that reacts with the solid. The reaction proceeds in a direction everywhere normal to the existing surface so that the walls of the channel will be attacked at the same rate as the base. Since there are two walls being attacked simultaneously, the width-to-depth ratio for a deep channel is 2. This limitation and the smaller sizes of modern devices have led to the replacement of chemical etching by more direct techniques such as ion beam etching.

From a reaction engineering viewpoint, semiconductor device fabrication is a sequence of semibatch reactions interspersed with mass transfer steps such as polymer

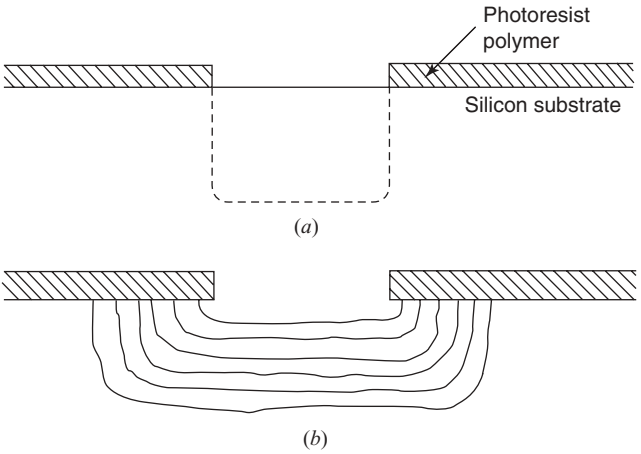

Figure 16.11 Etching of a silicon wafer to create interconnections: (*a*) desired profile achievable by ion bombardment; (*b*) profile obtained by chemical etching.

dissolution and physical vapor deposition (e.g., vacuum metallizing and sputtering). Similar sequences are used to manufacture still experimental devices known as ***NEMS*** (for ***nanoelectromechanical systems***).

16.2.7 Chemical Vapor Deposition

Chemical vapor deposition is distinguished from physical vapor deposition processes by the use of a chemical reaction, usually a decomposition, to create the chemical species that is deposited. An example important to the microelectronics industry is the formation of polycrystalline silicon by the decomposition of silane:

$$SiH_4 \rightarrow Si + 2H_2$$

The decomposition occurs on the surface and has an observed rate of the form (Claassen, 1982)

$$\mathscr{R} = \frac{k[SiH_4]}{1 + k_A[SiH_4] + k_B[H_2]^{1/2}}$$

This form suggests a Hougen and Watson mechanism in which silane and hydrogen atoms occupy sites that must also be used by the silicon being deposited. The primary disposition reaction can be complemented by dopant reactions involving compounds such as AsH_3, PH_3, and B_2H_6, which deposit trace amounts of the dopant metals in the silicon lattice.

A similar reaction is used in the diamond CVD process:

$$CH_4 \rightarrow C + 2H_2$$

The decomposition is accomplished using electrically heated filaments, microwave plasma discharge, or direct-current arc discharge. Polycrystalline diamond is deposited as a thin, hard film.

Organic coatings are also possible. The classic example is the ***paralene*** process where a cyclic dimer of *p*-xylene is thermally decomposed at about 850°C to form *p*-xylene free radicals that polymerize into a conformal film when deposited on a solid surface. Other examples of polymerization from a deposited vapor have been developed, and advocates believe this technology will replace spin coating of silicon wafers.

Manufacturing economics require that many devices be fabricated simultaneously in large reactors. Uniformity of treatment from point to point is extremely important, and the possibility of concentration gradients in the gas phase must be considered. For some reactor designs, standard models such as axial dispersion may be suitable for describing mixing in the gas phase. More typically, many vapor deposition reactors have such low L/R ratios that two-dimensional dispersion must be considered. A pseudo-steady model is

$$\bar{u}\frac{\partial a}{\partial z} = D_z\frac{\partial^2 a}{\partial z^2} + D_r\left(\frac{1}{r}\frac{\partial a}{\partial r} + \frac{\partial^2 a}{\partial r^2}\right) + \mathscr{R}_A \tag{16.15}$$

This model has been applied to vacuum coaters where the material being vapor deposited is evaporated from one or more point sources. Note that D_z and D_r are empirical parameters that account for both convection and diffusion. Rotary vacuum coaters avoid any dependence in the θ direction by rotating the substrate as it is coated. The false-transient method works here as in Section 16.2.4, but the axial and radial diffusivities are now separate and empirical.

16.3 NANOSCALE REACTORS

Continuum models are used almost exclusively in this book and are adequate down to the microscale. They fail on the nanoscale where it becomes necessary to directly address the particulate nature of matter. On the nanoscale, the diffusion times and Reynolds numbers shown in Table 16.1 become rather meaningless. Instead, the models must address the behavior of individual molecules. Thus, an alternative definition of the nanoscale is the scale at which continuum models must be replaced by molecular models.

The ultimate goal of synthetic chemistry is to produce designer molecules where the position of every atom and the stereo-orientation of every bond are predetermined. Achievement of this goal will most likely be done on the nanoscale. When achieved, the synthetic chemist can become an applications chemist who specifies the molecular design, and the chemical engineer will find ways to make the molecules in quantity.

Systems with structure pose problems for continuum models. Examples include surfactants, block copolymers, lipids, and amphiphilic molecules in general. Ad hoc models are used to predict surface packing and phase behavior, but the incorporation

of structure into transport equations is difficult. The structures formed by amphiphilic molecules typically have molecular dimensions and hence their study can be considered part of nanotechnology. These small structures can exert an influence over much large domains. An elephant is a self-assembled collection of much smaller domains (cells) that, in turn, depend on amphiphilic molecules at interfaces for their coherency. Thus the growth of an elephant—or perhaps even a woolly mammoth—can be considered a problem in nanoscale chemical reaction engineering, albeit a problem that is far from being solved. Tissue culture, particularly meristem culture discussed in Section 12.2.4, is an example of a self-assembled system. Carbon nanotubes self-assembled from CVD are another.

16.3.1 Self-Assembly

Chemical systems that arrange molecules in a specified structure are touted as providing the greatest advances in materials science and engineering. The touts are likely correct, but the area is still too young to be treated in a systematic fashion. A general observation is that the continuum mechanical models used in this book and as the basis for essentially all engineering designs do not hold at the molecular scale. Statistical mechanical methods such as molecular dynamics are being used as research tools. The conversion of these research tools into reliable design methodologies is a remaining challenge for the chemical reaction engineer.

Many examples of self-assembly do not involve reactions but involve merely the alignment of molecules among and between phases. Add a detergent to a mixture of oil and water. The detergent migrates to the oil–water interface. When the interface is saturated, the excess detergent forms nanoscale aggregates known as micelles. More complicated self-assembled structures can result when polymer mixtures are

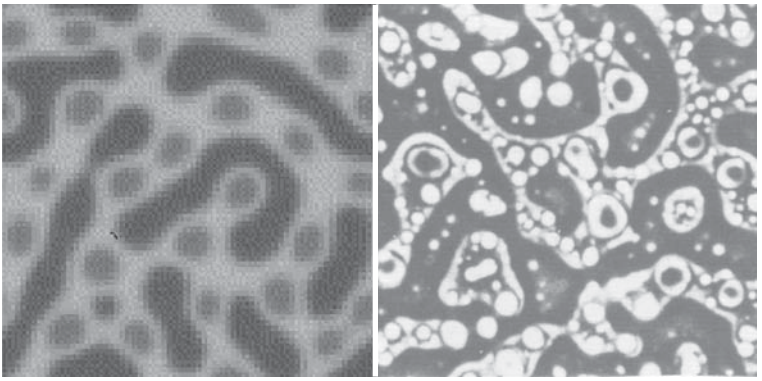

(*a*) (*b*)

Figure 16.12 Ternary polymer morphology resulting from spinodal decomposition: (*a*) simulation by fourth-order PDE; (*b*) experimental results.

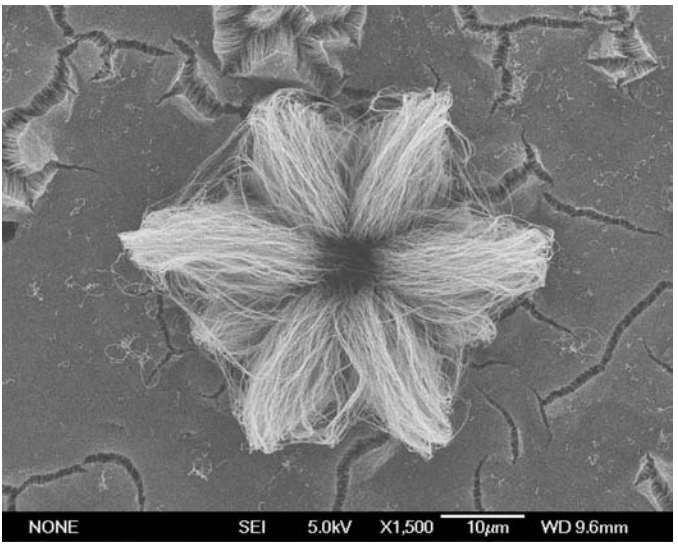

Figure 16.13 Nanoflower constructed from carbon nanotubes. (Courtesy of Zhengiun Zhang.) For additional pictures and details see Zhang et al. (2005).

rapidly displaced from equilibrium by a phase separation phenomenon known as spinodal decomposition. Figure 16.12 shows an elaborate structure formed from three incompatible polymers. The differences between the simulation and the experiment are attributed to the polydispersity of the polymers.

Figure 16.13 shows a marvelous example of self-assembly. The carbon nanotubes grew from seeded bases into a flower. The carbon source is from the gas phase, and the chemistry is complicated. A simplified model treats 14 species. Another model involves nearly 1000 species. Regardless of the model, the net result as shown in Figure 16.13 is that the individual tubes grow at approximately the same rate. It appears that the tube growth can be modeled as a living polymerization. See Section 13.4.1.

16.3.2 Molecular Dynamics

A numerical technique known as ***molecular dynamics*** treats the motion and interactions of individual molecules using Newtonian mechanics and a potential function between the molecules. These calculations have been extensively tested and calibrated against experimental results. They make believable predictions under circumstances where experimental measurements are difficult or impossible. Unfortunately, only a small number of molecules can be simulated at one time, and many simulations are needed to gather statistically significant results. "Massively parallel computing" usually just means running hundreds of simulations at once using separate CPUs. Days are required per run, and molecular dynamic simulations cannot yet be considered a means for engineering design. In this respect, they resemble computational fluid

mechanics. They remain limited by computer speeds and memory sizes and require validation when straying outside conventional applications.

16.4 SCALING, UP OR DOWN

To the limited extent that mesoscale and smaller reactors are used for production, the obvious approach is to scale in parallel. More conventional scaleups, that is, increasing reactor dimensions, could be needed when the small reactor is used to find the "perfect" molecule by means of combinatorial chemistry. With possible exceptions where the ultimate in mixing and heat transfer is required, scaleups to conventional macroscale reactors should be possible.

Scaledown to still smaller reactors seems to be mainly limited by fabrication techniques. Many valving, metering, and monitoring devices need to be designed and manufactured, and their fabrication is likely to be more challenging than making the reactor itself.

SUGGESTED FURTHER READINGS

Wall effects become important at or near the nanoscale. Above this scale, pressure drops all follow the same equations. See:

M. Bahrami, M. M. Yovanowich, and J. R. Culham, Pressure drop of fully-developed, laminar flow in microchannels of arbitrary cross-section, *J. Fluids Eng*, **120**, 1036–1044 (2006).

Diffusion can be slow at the mesoscale. Here is one approach to improving cross-channel mixing. See:

A. D. Stroock and G. M. Whitesides, Controlling flows in microchannels with patterned surface charge and topography, *Acc. Chem. Res*., **36**, 597–604 (2003).

Self-assembly permeates biology and is becoming increasingly important in materials science. Here is a text that surveys the field:

J. A. Pelesko, *Self Assembly: The Science of Things That Put Themselves Together*, Chapman and Hall/CRC, Boca Raton, FL, 2007, paperback edition.

PROBLEMS

16.1 The layer of glacial melt shown in Figure 16.1 will be near 0°C while the seawater in this location, a Chilean fjord, is several degrees warmer. Thermal diffusion in liquids is much faster than molecular diffusion, so temperatures near the interface will equilibrate much sooner than salinity. Use this fact to speculate as to the cause of the line of white froth in Figure 16.1.

16.2 Table 16.2 is based on the properties of water. Suppose that the fluid is air at 1 atm. Calculate the Reynolds number and the characteristic diffusion time for the various duct sizes. The velocity in the 2-m pipe remains 1 m s^{-1}.

16.3 The equation of motion for laminar flow in a slit is

$$0 = \frac{-dP}{dz} + \mu \frac{\partial^2 V_z}{\partial y^2}$$

(a) Assume symmetry about $y = 0$. List the simplifying assumptions needed to write the equation in this form.

(b) Integrate this equation twice with respect to y and apply appropriate boundary conditions to obtain $V_Z(y) = V_0(1 - y^2/H^2)$.

(c) Integrate again to obtain the volumetric flow rate per unit width of slit, q.

(d) Use $q = \bar{u}H$ to derive Equations 16.5 and 16.6. Why isn't it $q = \bar{u}H^2$? Should it be $q = 2\bar{u}H^2$?

16.4 Apply the logic of Problem 16.3, but with $q = \bar{u}H^2$ to derive Equation 16.9.

16.5 Plot $u_{\max}/\bar{u}$ as a function of aspect ratio, $q = H/W$, for laminar flow in rectangular ducts.

16.6 Perform the calculations for one of the L/H lines in Figure 16.7, but for a second-order reaction with rate $\bar{t}\mathcal{R}_A = -a_{\text{in}}k\bar{t}a^2$, where $a_{\text{in}}k\bar{t} = 1$.

References

Bermejo, M. D., et al., *Ind. Eng. Chem. Res.*, **44**, 3838–3845 (2005).
Blanch, H. W., and Clark, D. S., *Biochemical Engineering*, Marcel Dekker, New York, 1996.
Boyer, A., Niclause, M., and Letort, M., *J. Chim. Phys.*, **49**, 345 (1952).
Butt, J. C., *Reaction Kinetics and Reactor Design*, Prentice-Hall, Englewood Cliffs, NJ, 1980.
Chen, C. Y., Wu, C. W., and Hu, K. H., *Zhongguo Huanjing Gongcheng Xuekan*, **6**, 302–309 (1996).
Claassen, W. A. P., et al., *J. Crystal Growth*, **57**, 259 (1982).
Cropley, J. B., Burgess, L. M., and Loke, R. A., *ChemTech*, **June**, 374 (1984).
Cybulski, A., Eigenberger, G., and Stankiewicz, A., *Ind. Eng. Chem. Res.,* **36**, 3140–3148 (1977).
Danckwerts, *Chem. Eng. Sci.*, **2**, 1–18 (1953).
Dateo, C. E., Gokcen, O.T., and Meyyappan, M., *J. Nanosci. Nanotechnol.*, **2**, 523–534 (2002).
Dixon, A. G., and Cresswell, D. L., *AIChE J.*, **25**, 663 (1979).
Froment, G. F., and Bischoff, K. B., *Chemical Reaction Analysis and Design*, 2nd ed., Wiley, New York, 1990.
Gray, P., and Scott, S. K., *Chem. Eng. Sci.*, **39**, 1087 (1984).
Ham, G. E., *Copolymerization*, Interscience, New York, 1964.
Harnby, N., Edward, M. R., and Nienow, A. W., *Mixing in the Process Industries*, Butterworths, London, 1985.
Hinshelwood, C. N., and Green, T. W., *J. Chem. Soc.*, **1926**, 730 (1926).
Hogan, C. J., *Nature*, **408**, 48 (2000).
Hougen and Watson, *Chemical Process Principles,* Vol. III, Wiley, New York, 1947.
Hui and Hamielec, *J. Appl. Polym. Sci.*, **16**, 749 (1972).
Kice, J. L., and Bowers, K. W., *J. Am. Chem. Soc.*, **84**, 605 (1962).
Kim and Nauman, E. B., *J. Chem. Eng. Data*, **37**, 427 (1992).
Langmuir, I., *J. Am. Chem. Soc.*, **30**, 742 (1908).
Lee, H. H., *Homogeneous Reactor Design*, Butterworth, Boston, 1985.
Lewis, R. J., and Moodie, R. B., *J. Chem. Soc. Perkin Trans.*, **2**, 563 (1997).
Lindstedt, R. P., and Maurice, L. Q., *Combust. Sci. Technol.*, **120**, 119 (1996).
Martin, Y., and Vermette, P., *J. Biomater.* (2005).
Merrill and Hamrin, *AIChE J.*, **16**, 194 (1970).
Middleton, in N. Harnby, M. F. Edwards, and A.W. Nienow (Eds.), *Mixing in the Process Industries*, Butterworth, London, 1985, Chapter 17.
Milligan, B., Isomer distribution in mixed-acid nitration of toluene: Evidence for mass-transfer effects on selectivity, *Ind. Eng. Chem. Fund.*, **25**, 783–789 (1986).
Nauman, E. B., *Chem. Eng. Sci.*, **32**, 359–367 (1977).
Nauman, E. B., and Carter, K., *I&EC Proc. Des. Dev.*, **13**, 275 (1974).
Nauman, E. B., and Nigam, A., *I&EC Res.*, **44**, 5031–5035 (2005).
Nauman, E. B., and Savoca, *AIChE J.*, **47**, 1016 (2001).
Nigam, K. D. P., and Nauman, E. B., *Can. J. Chem. Eng.*, **63**, 519 (1985).
Nigam, K. D. P., and Saxena, A. K., *AlChE J.*, **30**, 363 (1984).
Norwood and Metzner, *AlChE J.*, **6**, 432 (1960).
Paul, E. L., et al., *Handbook of Industrial Mixing*, Wiley, New York, 2003.
Perry's Handbook, 7th Edition, McGraw-Hill, New York, 1997.

Chemical Reactor Design, Optimization, and Scaleup, Second Edition. By E. B. Nauman

Copyright © 2008 John Wiley & Sons, Inc.

Peters, V., Janssen, P. H., and Conrad, R., *FEMS Microbiol. Ecol*., **26**, 317 (1998).
Press, W. H., Teukolsky, S. A., Vetterling, W. T., and Flannery, B. P., *Numerical Recipes in Fortran 77: The Art of Scientific Computing*, Vol. 1, 2nd ed., Cambridge University Press, New York, 1992.
Pustelnik, P., and Nauman, E. B., *AIChE J*., **37**, 1589–592 (1991).
Roels, J. A., and Kossen, N. W. F., *Prog. Ind. Microbiol*., **14**, 95 (1978).
Rothfield, L. B., *AIChE J*., **9**, 19 (1963).
Smith, J. M., *Chemical Engineering Kinetics*, 1st ed., McGraw-Hill, New York, 1956.
Smith, J. M., Van Ness, H. C., and Abbott, M. M., *Introduction to Chemical Engineering Thermodynamics*, 6th ed., McGraw-Hill, New York, 2001.
Smith, J. M., Van Ness, H. C., and Abbott, M. M., *Introduction to Chemical Engineering Thermodynamics*, 7th ed., McGraw-Hill, New York, 2004.
Stokes, R. L., and Nauman, E. B., *Can, J. Chem. Eng*., **48**, 723 (1970).
Stroock, A. D., and Whitesides, G. M., *Acc. Chem. Res*., **36**, 597–604 (2003).
Thakur, R. K., et al., *Chem. Eng. Res. Des*., **81**, 787–826 (2003).
Treiling, E. C., Johnson, H. C., and Ogg, R. A., Jr., *J. Chem, Phys*., **20**, 327 (1952).
Tsukahara, H., Ishida, T. M., and Mitsufumi, M., *Nitric Oxide*, **3**, 191 (1999).
Vermeulen, D. P., and Fortuin, J. M. H., *Chem. Eng. Sci*., **41**, 1089 (1986).
Walling, C., and Metzger, G., *J. Am. Chem. Soc*., **81**, 5365 (1959).
Wang, D., et al., *Fermentation and Enzyme Technology*, Wiley Technology, Wiley, New York, 1979.
Weisz, P. B., and Hicks, J. S., *Chem. Eng. Sci*., **17**, 265 (1962).
Wenner, R. R., and Dybdal, F. C., *Chem. Eng. Prog*., **44**, 275 (1948).
Zhang, Z., Zhao, Y., and Zhou, Y., *Tsinghua Sci. Technol*., **10**, 741–744 (2005).

Index

Absorption, 182, 397, 403, 410, 414
Activation energy, 163, 195, 367, 373
Activation temperature, 164, 373, 459
Activation volume, 195
Activation, catalytic, 435
Activity coefficient, 254
Addition polymers, 461, 472, 478. *See also*, Chain growth polymers
Addition polymers, equilibrium, 467, 478
Adiabatic temperature change,173, 466
Adsorption, 357, 359, 437
Air-lift, 457. See Deep shaft
Arrhenius temperature dependence, 163, 438
Asymptotic property, 50
Autocatalytic, 62
Autorefrigerated reactors, 186
Axial diffusion, 288, 291, 587
Axial dispersion model, 336
Axial dispersion model, nonisothermal, 344
Axial dispersion model, utility of, 342
Axial dispersion, two-phase, 412, 419

Backward difference, 320
Batch reactor, 12
Bimolecular reactions, 366
Binary search, 158
Biochemical reactions, 433
Bounding theorem, 566
Bubbling fluidization, 418
Bypassing, 369, 548

Cell culture, 444
Central difference, 320
Chain growth polymers. See Addition polymers
Chain length, 463, 469
Chain reaction, 58, 64
Chain transfer, 61, 479
Chaos, chaotic, 132, 184
Chemostat, 238, 441, 537. *See also* CSTR
Closed system, 457
Cofactor, 438
Cold-flow models, 311
Collision, 5
Competitive reactions, 41
Complete segregation, 12, 560
Complex reactions, 10, 41. *See also* Multiple reactions
Component balance:
  axial dispersion, 412
  batch, 13
  CSTR, 21, 24
  differential, 21
  fed-batch, 71
  integral, 2, 21
  laminar flow reactors, 288
  matrix form for batch reactors, 173
  matrix form for CSTRs, 130
  matrix form for PFRs, 66
  multiple batch reactions, 43, 45
  packed beds, 324
  piston flow, 19, 90
  transpired wall reactor, 122
  two-phase CSTRs, 391, 410
  two-phase piston flow, 405, 410
  unsteady CSTR, 514
  unsteady piston flow, 526
Computation scheme for gas-phase PFRs, 99
Computation scheme for variable density CSTRs, 137, 584
Computational fluid dynamics, 366, 553
Condensation polymers, 462. *See also*, Step growth polymers
Condensation polymers, equilibrium, 464

Chemical Reactor Design, Optimization, and Scaleup, Second Edition. By E. B. Nauman

Copyright © 2008 John Wiley & Sons, Inc.

Condensation polymers, kinetics, 471
Condensation polymers, stoichiometry, 463
Confounded reactors, 241
Consecutive reactions, 41, 235
Contact time, 571
Control volume, 1
Convected-mean, 282. *See also*, Mixing cup average
Convective diffusion of heat, 290, 529. *See also*, Energy balances
Convective diffusion, of mass, 86, 288, 316. *See also*, Component balances
Convergence of ODE solvers, 46, 50
Convergence of optimization techniques, 222
Convergence of PDE solvers, 295, 587
Convergence order, trapezoidal rule, 284
Conversion, 15, 17
Copolymer composition distribution, 486, 488
Copolymerization, 465, 468
Core turbulence, 335
Creeping flow, 302
CSTRs, 12, 24
CSTRs, heat balance, 178
CSTRs, two-phase, 386
CSTRs, unsteady, 513

Danckwerts boundary conditions, 339
Deactivation, enzyme catalysis, 434, 438
Deactivation, in gas–solid catalysis, 363, 374
Dead polymer, 482
Dead time, 545
Debugging computer programs, 174, 502
Decoking, 375, 421
Delta function, 538
Density function, 538
Design of experiments, 239
Design variable, 31, 181
Desorption, 357
Differential distribution, of contact times, 570, 587
Differential distribution of residence times, 469, 537
Differential reactor, 238, 400, 413, 554
Diffusion:
  axial, 288, 291
  eddy, 115, 340
  Knudsen, 370
  multicomponent, 338
  product layer, 422
  radial, 280, 281
Diluents, 31, 185. *See also*, Inerts
Dilution rate, 441
Dimensionless rate constant, 32, 96, 135, 290
Dimensionless reaction time, 52, 471
Dimensionless variables, 31, 50
Dispersion polymerization, 508, 526
Dispersion, radial, 324, 325
Distributed system, 206, 308

Economy of scale, 157
Effectiveness, in enzyme reactions, 440
Effectiveness, general definition, 368
Effectiveness, nonisothermal, 372
Elementary reactions, 5, 262
Elephants, stampeding, 227, 367, 507
Eley–Rideal mechanism, 382
Emulsion polymerization, 185, 491
Emulsion, in fluidized bed reactors, 419
Endothermic reactions, 177, 185
Energy balance, two-phase CSTRs, 400
Energy balance for an unsteady CSTR, 244, 400, 523,
Energy balances, 170, 333, 513, 523
Enhancement factors, 414
Enthalpy, 170, 248
Enzyme catalysis, 434
Equal reactivity assumption, 471
Equilibrium compositions, single reactions, 257
Equilibrium constant, kinetic, 7, 252
Equilibrium constant, multiple reactions, 265
Equilibrium constant, reconciliation of types, 254
Equilibrium constant, reverse reaction rates, 256
Equilibrium constant, thermodynamic, 253
Ergun equation, 98
Etching, 422
Euler's method, 46, 50
Exotherm, 63, 174, 185
Exponential distribution, 414, 541
Exponential growth, 445

Exposure time, 413
Extent of reaction, 76. *See also*, Reaction coordinate

False transients, 131, 179
Fanning, 98
Fast fluidization, 420
Fast-fill-and-hold, 518
Fed-batch, 23, 65
Fermentation, 444
Fick's law, 371
Film mass transfer, 371
Finite difference approximations, 319
First appearance time, 457, 545
First-order ODEs, 46
First-order reaction, 8, 14, 420, 441, 486, 508
Flory distribution, 333, 342, 413, 475
Fluidized bed reactors, 66, 106, 135, 417, 419
Flux, 92, 317
Fraction unreacted, 14, 17
Fractional tank extension, 545
Fractional tubularity, 544
Free energy, 247, 253
Free radical polymers, 314, 478, 481, 486
Free radical reactions, 58, 478
Friction factor, 98
Froude number, 145
Fugacity, 253

Gamma function extension, 546
Gas scrubbing, 397
Gas–liquid reactors, 385
Gel effect, 483
Geometric similarity, 28
Graetz number, 191
Graetz problem, 296, 586
Grass, 54, 64, 154, 516

Half-integer kinetics, 60
Half-life, 15, 27
Heat balance. See Energy balance
Heat capacity, 171, 177
Heat generation, 171, 182
Heat of formation, 247
Heat of reaction, 171, 291
Heat of reaction, standard, 251, 318, 327, 344, 400
Heat removal curve, 182
Heat transfer coefficient, 172, 191
Henry's law, 388
Heterogeneous catalysis, biochemical, 436
Heterogeneous catalysis, gas–solid, 355, 377
Heterogeneous catalysis, polymerizations, 486, 493
Holdup, 94, 387, 416, 493
Homogeneous reaction, 5
Homopolymerization, 466, 487
Hotspot, 332
Hougen and Watson models, 366

Ideal gas law, flow systems, 94
Ideal reactors, 1, 12
Ill-conditioned computations, 141, 345
Immobilized cells, 457
Immobilized enzymes, 439
Impingement mixer, 584
Impulse, 537
Independent reactions, 42, 76, 294, 345, 564
Inerts, 94, 98, 487
Inhibition in enzyme catalysis, 434, 436
Initial value problem, 46, 90, 388, 405
Initiation, 58, 478
Integral reactor, 235
Interfacial area, 28, 112, 380, 386, 387
Interfacial mass transfer, 388
Intrinsic kinetics, 360, 368, 461, 574
Inventory, 1, 20

Kolmogorov scale of turbulence, 569

Laminar flow reactors, 279, 343
Langmuir, 339, 366
Laplace transforms, 542, 555
Least squares, 225
L'Hospital's rule, 16, 56
Limit cycle, 184, 525
Linear burn rate, 425
Liquid–liquid reactors, 385
Living polymer, 479
Lumped parameter systems, 24, 308
Lumping of chemical species, 367, 449
Lynx, 64, 516

Macromixing, 563, 569
Maintenance coefficients, 448
Marching, 46, 295
Mass balance, overall or integral, 1
Mass transfer coefficients, measurement, 401
Mass transfer coefficients, typical values, 401
Material balance closure, 239
Maximum mixedness, 536
Mean residence time, 20, 539
Mean residence time in a gas-phase tubular reactor, 101
Mean residence time, multiple of to achieve steady state, 526
Mean residence time, apparent in an open system, 556
Mechanism, 8, 9, 180
Membrane reactors, 123, 386
Mesoscale, 575
Metastable steady states, 132, 135
Michaelis constant, 436
Michaelis-Menten kinetics, 434
Microelectronics, 594
Micromixing, 536
Micromixing models, 563
Microscale, 575
Mixing cup average, 282, 284
Mixing space, 563
Mixing time, 26, 30
Molecular dynamics, 598
Molecular weight distributions, 468
Moments of molecular weight distribution, 469, 479
Moments of residence time distribution, 539
Mondispersedi, 470, 479
Monod kinetics, 445, 457
Monoliths, 332, 356
Motionless mixers, 308, 343
Moving solids reactors, 417
Multiphase reactors, 385
Multiple reactions, 41, 43
Multitubular reactor. See Shell-and-tube reactors

Nanoscale, 575, 596
Noncatalytic fluid–solid reactions, 417
Nonisothermal effectiveness, 372
Nonisothermal reactors, axial dispersiom, 344
Nonisothermal reactors:
  batch, 172, 242
  CSTRs, 178
  laminar, 312
  packed, 325
  piston flow, 175, 241
  reactors, scaleup, 185
*n*th order reactions, 52, 568
Numerical methods:
  binary search, 158
  Euler's method, 46, 50
  false transients, 131, 179
  linear regression, 274
  method of lines, 292
  Newton's method, 159
  optimization, 220
  Runge–Kutta, 84, 347
  shooting techniques, 344
  trapezoidal rule, 284

Objective function, 220
Occam's razor, 239
Open system, 341
Operating variable, 31
Optimization, 220
Oscillations in batch systems, 64
Oscillations in biological systems, 454
Oscillations in noisothermal CSTRs, 184, 516
Oscillations in polymerizations, 508

Packed bed reactors, scaleup, 118, 120
Packed beds, 98, 115
Parallel reactors, 113, 145
Parametric sensitivity, 332
Pathological behavior, 153, 353
Peclet number for the axial dispersion model, 338
Peclet number for the radial disperion model, 326
Pipeline flows, 342
Piston flow reactor, 89
Polydispersity, 470
Polymerization, 461
Polymerization kinetics, 471, 478

Population balance methods, 404
Pore diffusion, 368
Power in a stirred tank, 28, 29
Prandtl number, 191
Pressure gradient in laminar flow, 97
Pressure gradient in packed beds, 98
Pressure gradient in turbulent flow, 97
Product transitions, 521
Propagation, 58, 478
Pseudo-first order, 11, 54
Pseudohomogeneous, 138, 323, 324,
Pseudo-steady state, 50, 56, 442, 482. *See also*, Quasi-steady state

Quasi-steady state, 50, 56, 442, 482

Rabbits, 64, 516
Radial dispersion coefficient, 324
Radial velocities, 304, 501
Radioactive decay, 8, 54
Rate constant, 5, 6, 548
Rate constant, first-order, 8
Rate constant, pseudo-first order, 11
Rate constant, second-order, 8, 15
Rate-determining step, 363
Reaction coordinate for batch reactors, 74
Reaction equilibria, 252
Reaction front, 65, 376
Reaction order, 9
Reaction rate, 5, 43
Recycle reactors, 138, 150
Regression, linear, 274
Regression, nonlinear, 164
Residemce times, laminar flow, 552
Residence time distributions, 535
Reverse reaction rates, 256
Reverse shooting, 346
Runge–Kutta, 84, 347

Scale of turbulence, 569
Schmidt number, 327
Second order, 8, 9
Segregation, 494. *See also*, Complete segregation
Selectivity, 17
Self-assembly, 597
Semibatch, 71
Series reactors, 114, 116
Shooting, 344
Shutdown strategies, 517
Side capacity, 550
Single-train, 114
Site balance, 362
Site competition, 228, 367, 375
Slit flow, 279, 310, 576, 587
Slurry reactors, 416, 509
Space time, 103, 107
Spatial average, 282
Spouted bed reactors, 420, 457
Stability, numerical, 295, 327, 343
Stability, physical, 114, 494, 515, 526
Standard deviation, 50, 56
Startup strategies, 517
Static mixers, 308, 343. See Motionless mixers
Stiff equations, 50, 56
Stirred tank reactors. See CSTR
Stoichiometric coefficient, 5, 43, 75
Stoichiometric matrix, 75
Stoichiometry, global, 76
Streamlines, 281, 287, 306
Structured packing, 332
Substrate in biochemical reactions, 434
Sum of squares, 225, 274
Surface concentrations, 357
Surface renewal, 412
Suspending, 418, 419, 507

Tanks in series, 148, 545
Termination reactions, 58, 482
Thermal conductivity, 187, 318
Thermal initiation, 58, 183
Thermal time, 571
Thiele modulus, isothermal, 369
Thiele modulus, nonisothermal, 373
Third-order reactions, 9
Three-phase reactors, 404, 415
Throughput scaleup factor. See Scaleup factor
Transition metal catalysis, 478, 486
Transpired wall reactors, 122
Tray columns, 397
Trickle-bed reactors, 415
Tubular reactors, isothermal, 89
Tubular reactors, laminar flow, 279
Tubular reactors, turbulent flow, 323

Unimolecular, 8, 364
Unmixed feed streams, 27, 325
Unsteady reactors, 513

Vapor deposition, 73, 595
Variable cross-section, 90
Velocity profile in a packed bed, 324
Velocity profile, in laminar flow, 280
Velocity, superficial, 98
Void fraction, 98

Washout, 148, 453
Washout function, 536, 570
Working volume, 386

Yield, 17

Zero molecule, 7
Zero order reactions, 53
Zwietering's differential equation, 564